ACTA PHYSICA

ACADEMIAE SCIENTIARUM HUNGARICAE

TOMUS XLV FASCICULUS 1

AKADÉMIAI KIADÓ, BUDAPEST
1978

ACTA PHYS. HUNG. APAHAQ 45 (1) 1–86 (1978)

ACTA PHYSICA

ACADEMIAE SCIENTIARUM HUNGARICAE

SZERKESZTI

KOVÁCS ISTVÁN

Az *Acta Physica* angol, német, francia vagy orosz nyelven közöl értekezéseket. Évente két kötetben, kötetenként 4—4 füzetben jelenik meg. Kéziratok a szerkesztőség címére (1521 Budapest XI., Budafoki út 8.) küldendők.

Megrendelhető a belföld számára az Akadémiai Kiadónál (1363 Budapest Pf. 24. Bankszámla 215-11488), a külföld számára pedig a „Kultura" Külkereskedelmi Vállalatnál (1389 Budapest 62, P.O.B. 149. Bankszámla 217-10990), vagy annak külföldi képviseleteinél.

The *Acta Physica* publish papers on physics in English, German, French or Russian, in issues making up two volumes per year. Subscription: $ 36.00 per volume. Distributor: "Kultura" Foreign Trading Company (1389 Budapest 62, P.O. Box 149) or its representatives abroad.

Die *Acta Physica* veröffentlichen Abhandlungen aus dem Bereich der Physik in deutscher, englischer, französischer oder russischer Sprache, in Heften, die jährlich zwei Bände bilden.

Abonnementspreis pro Band: $ 36.00. Bestellbar bei »Kultura« Außenhandelsunternehmen (1389 Budapest 62, Postfach 149) oder seinen Auslandsvertretungen.

Les *Acta Physica* publient des travaux du domaine de la physique en français, anglais, allemand ou russe, en fascicules qui forment deux volumes par an.

Prix de l'abonnement: $ 36.00 par volume. On peut s'abonner à l'Entreprise du Commerce Extérieur «Kultura» (1389 Budapest 62, P.O.B. 149) ou chez représentants à l'étranger.

«*Acta Physica*» публикуют трактаты из области физических наук на русском, немецком, английском и французском языках.

«*Acta Physica*» выходят отдельными выпусками, составляющими два тома в год.

Подписная цена — $ 36.00 за том. Заказы принимает предприятие по внешней торговле «Kultura» (1389 Budapest 62, P.O.B. 149) или его заграничные представительства.

ACTA PHYSICA

ACADEMIAE SCIENTIARUM HUNGARICAE

TOMUS XLV

AKADÉMIAI KIADÓ, BUDAPEST
1978

ACTA PHYS. HUNG.

INDEX

Tomus 45

ACTA PHYSICA

ACADEMIAE SCIENTIARUM HUNGARICAE

TOMUS XLV FASCICULUS 1

AKADÉMIAI KIADÓ, BUDAPEST
1978

ACTA PHYS. HUNG.

INDEX

Acta Physica Academiae Scientiarum Hungaricae, Tomus 45 (1), pp. 3—8 (1978)

LATTICE DYNAMICS OF MAGNESIUM ON EXTENDED DE LAUNAY MODEL

By

R. CAVALHEIRO and M. M. SHUKLA*

INSTITUTO DE FISICA "GLEB WATAGHIN", UNIVERSIDADE ESTADUAL DE CAMPINAS
CAMPINAS – SP., BRASIL

(Received 9. VI. 1978)

The phonon dispersion relations in magnesium along the two principal symmetry directions i.e. | 000ξ | and |$0\xi\xi0$ | as well as lattice heat capacities of it are computed on extended de Launay model. Computed results show good agreement with experimental observations.

1. Introduction

While the lattice dynamics of cubic metals has been a subject of constant theoretical study for the past several decades, the hcp metals arouse such an interest quite recently. The probable reason behind this would be that the unit cell of hcp metals comprises of lattice with a basis giving rise to a complex dynamical matrix of higher order than that found in cubic metals. The earliest attempts to study theoretically hcp metals can be said to be those of SLUTSKY and GARLAND [1] and COLLINS [2]. These authors were not aware of the influence of the conduction electrons on the computed phonons. Probably GUPTA and DAYAL [3] were the earliest workers to take account of the conduction electrons in the lattice vibrational frequencies of hcp metals. Later on, SHARAN and BAJPAI [4], UPADHYAYA and VERMA [5], KING and CUTLER [6], BROVMAN et al. [7], SHUKLA and CLOSS [8], RAJPUT and KUSHWAHA [9] and several other workers have tried to propose models for hcp metals.

By now the experimental phonon dispersion relations in almost all hcp metals have been determined by neutron spectroscopy. The interpretation of the experimental data on the existing models has shown that none of them are capable of explaining with constant success the lattice vibrations in each and every hcp metal. It was also discovered that the effect of conduction electrons in the lattice vibrational frequencies in hcp metals has not so drastic an influence as those in cubic metals. This, however, indicated that a model taking account of the electron gas even in an approximate way, sometimes, gave better results in comparison to models where the influence of electron gas was considered more rigorously. In this connection we would

* On leave of absence from UNICAMP. Visiting Professor, Department of Electrica Engineering, University of Rhode Island, Kingston, R. I. 02881 (U.S.A.)

like to introduce here the extended de Launay model for hcp metals which has been found extremely successful in interpreting phonon dispersion relations in yttrium (CAVALHEIRO and SHUKLA [10]) and in terbium, holmium, thallium, zirconium and scandium (CAVALHEIRO and SHUKLA [11]). Such a success of extended de Launay model for six complicated metals of hcp structures has encouraged us to take up for the present study the lattice dynamics of magnesium, owing to the fact that for magnesium extensive experimental phonon and thermal data exist for comparison to our computed results.

2. Theory

The secular determinant to determine the phonon frequencies is given by

$$| D_{\alpha\beta}(q) - m\omega^2 I | = 0 , \tag{1}$$

where m is ionic mass, ω is angular frequency, I is a unit matrix of order 6, $D_{\alpha\beta}(q)$ is the dynamical matrix for the phonon wave vector $\mathbf{q}$.

The dynamical matrix D is further split up into two submatrices A and B of order 3×3 given by

$$D_{\alpha\beta}(q) = \begin{vmatrix} A_{\alpha\beta}(q) & B_{\alpha\beta}(q) \\ B^*_{\alpha\beta}(q) & A_{\alpha\beta}(q) \end{vmatrix} , \tag{2}$$

where $B^*_{\alpha\beta}(q)$ is complex conjugate of $B_{\alpha\beta}(q)$.

Let $A_{\alpha\beta}(q)$ and $B_{\alpha\beta}(q)$ denote dynamical matrices representing the bare ion-ion interaction. To calculate the electron-ion interaction we have followed our work on cubic metals (SHUKLA and CAVALHEIRO [12—13]). The matrices A and B are thus modified and given by (the details of the theory have been given elsewhere (CAVALHEIRO and SHUKLA [11]))

$$A_{\alpha\beta}(q) = \begin{vmatrix} A_{11} + pR_1 & A_{12} + qR_1 & A_{13} + rR_1 \\ A_{12} + pR_2 & A_{22} + qR_2 & A_{23} + rR_2 \\ A_{13} + pR_3 & A_{23} + qR_3 & A_{33} + rR_3 \end{vmatrix} \tag{3}$$

and

$$B_{\alpha\beta}(q) = \begin{vmatrix} B_{11} + pS_1 & B_{12} + qS_1 & B_{13} + rS_1 \\ B_{12} + pS_2 & B_{22} + qS_3 & B_{23} + rS_2 \\ B_{13} + pS_3 & B_{23} + qS_3 & B_{33} + rS_3 \end{vmatrix} , \tag{4}$$

where

$$R_1 = p(A'_{11} - A_{11}) + q(A'_{12} - A_{12}) + r(A'_{13} - A_{13}) , \tag{5.1}$$

$$R_2 = p(A'_{12} - A_{12}) + q(A_{22} - A_{22}) + r(A'_{23} - A_{23}) , \tag{5.2}$$

$$R_3 = p(A'_{13} - A_{13}) + q(A'_{23} - A_{23}) + r(A'_{33} - A_{33}) , \tag{5.3}$$

$$S_1 = p(B'_{11} - B_{11}) + q(B'_{12} - B_{12}) + r(B'_{13} - B_{13}), \tag{5.4}$$

$$S_2 = p(B'_{12} - B_{12}) + q(B'_{22} - B_{22}) + r(B'_{23} - B_{23}), \tag{5.5}$$

$$S_3 = p(B'_{13} - B_{13}) + q(B'_{23} - B_{23}) + r(B'_{33} - B_{33}), \tag{5.6}$$

where p, q and r are direction cosines of $\mathbf{q}$.

A'_{ii}, A'_{ij}, B'_{ii} and B'_{ij} are obtained from the corresponding unprimed elements of the dynamical matrices by replacing all the force constants by primed ones.

3. Numerical computations

We have confined the interionic interactions out to fourth neighbours only. The elements of dynamical matrices $A_{\alpha\beta}(q)$ and $B_{\alpha\beta}(q)$ are taken from the work of SCHMUNK et al. [4]. The seven disposable parameters of the model were determined from the experimental data, five elastic constants and two phonon frequencies from the boundary of the Brillouin zone. While elastic constants were taken from the work of SLUTSKY and GARLAND [15], phonon frequencies correspond to the measurements of IYENGER et al [16].

Table I

Input data to calculate force constants

Lattice parameter in (Å)	Elastic constants (in 10^{11} dyn cm^{-2})	Atomic mass (in 10^{-22} gm)	Phonon frequencies (in 10^{12} cs^{-1})
$a = 3.2028$ $c = 5.1960$	$C_{11} = 5.940$ $C_{12} = 2.561$ $C_{33} = 6.160$ $C_{44} = 1.640$ $C_{13} = 2.144$	4.036	$\nu_L \quad (0.001) = 5.20$ $\nu_{T0\perp} \; (01T0) = 6.12$

Table II

Output values of the force constants in 10^3 dyn cm^{-1}

$\alpha = 10.259$ $\beta = 3.779$	$\gamma = -0.040$ $\varepsilon = -0.239 = \varepsilon'$	$\alpha' = 10.137$ $\beta' = 3.583$ $\gamma' = 0.538$

While the input data to calculate the atomic force constants are given in Table I, output values of the force constants are given in Table II. Once the force parameters were determined, we calculated the phonon dispersion relations in $|\,000\xi\,|$ and $|\,0\xi\bar{\xi}0\,|$ directions. These results are shown in Fig. 1 together with experimental results shown for comparison. To have an independent check of the model, we also computed its lattice heat capacities.

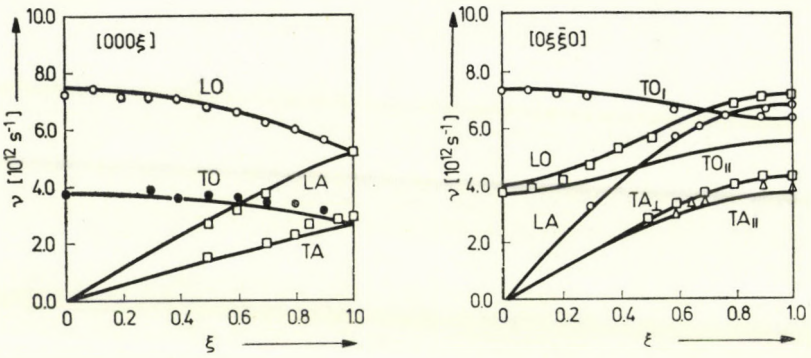

Fig. 1. Phonon dispersion relations in magnesium along | 000ξ | and | 0$\xi\bar{\xi}$0 | directions. Computed results are shown by continuous lines. Experimental points are shown by ○, ●, □ and △

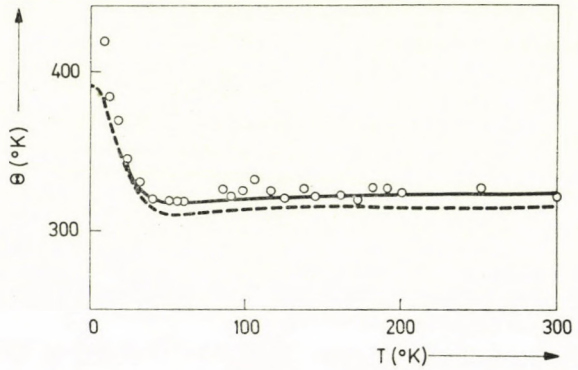

Fig. 2. (θ—T) curves of magnesium. Solid line shows present calculation. ○○○ are experimental result of CLUSIUS and VAUGHAN and – – – – experimental result of CRAIG et al.

To do that, the first Brillouin zone was divided into 1000 equivalent points. Lattice symmetry made it possible to solve the secular determinant for only 84 independent wave vectors including the origin. Heat capacities were computed by Blackman's sampling technique. A knowledge of lattice heat capacities, the deduction of its electronic contribution at that temperature, γT, was utilised to plot the (θ — T) curve of magnesium shown in Fig. 2. In Fig. 2 the experimental curves are also plotted for comparison. While the lattice heat capacities of magnesium correspond to the measurement of CLUSIUS and VAUGHAN [17] and CRAIG et al [18], the coefficient of the electronic heat capacity was taken from the measurement of MARTIN [19].

4. Discussion and conclusion

We have presented here the lattice dynamics and heat capacity of magnesium on the basis of extended de Launay model. The computed results have given very good agreement with the experimental ones as far as to say that the maximum deviation found between the calculated and experimental phonons was never found to be more than 10%. The maximum deviation found between the computed and experimental θ has never exceeded 5%. These kinds of results are quite superior to those found on other phenomenological models (e.g., UPADHYAYA and SINHA [20], SHARAN and BAJPAI [4], UPADHYAYA and VERMA [5], BOSE et al. [21] and on models on first principles (PINDORE and RYNN [22], KING and CUTLER [6], ROY and VENKETRAMAN [23] and BROVMAN and KAGAN [24]). The same kind of success was also obtained in the study of metals yttrium (CAVALHEIRO and SHUKLA [10]) and scandium, terbium, holmium, thallium and zirconium by us (CAVALHEIRO and SHUKLA [11]) on the extended de Launay model. We can, thus, conclude that the extended de Launay model applied to hcp metals gives a good description of their lattice dynamics.

Our model has some shortcomings, which are:

1. The electron gas does not keep the lattice periodic in the reciprocal space. But such an effect has some influence only in few frequencies near the zone boundaries.

2. We have assumed that the electron gas modifies the optical longitudinal branches in the very same way as the acoustical longitudinal branch. We do not have any theoretical justification for it.

3. The electron gas does not modify the transversal branches. This is responsible for the theory not being able to show as good an agreement as obtained for longitudinal branches. This defect can be found in several of the phenomenological models cited above.

Most probably, some of the above mentioned drawbacks of the theory might be minimized if we used the tensor forces to represent the ion-ion interaction part of the dynamical matrix. We are carrying out such studies which would be published in due course.

REFERENCES

1. L. J. SLUTSKY and C. W. GARLAND, J. Chem. Phys., **26,** 787, 1957.
2. M. F. COLLINS, Proc. Phys. Soc., (London), **80,** 362, 1962.
3. R. P. GUPTA and B. DAYAL, Phys. Stat. Sol., **8,** 115, 1965.
4. B. SHARAN and R. P. BAJPAI, Phys. Lett., **31A,** 120, 1970.
5. J. C. UPADYAYA and M. P. VERMA, Jr. Phys. F: Metal Physics, **3,** 640, 1973.
6. W. F. KING III and P. H. CUTLER, Phys. Rev., **B2,** 1733, 1970.
7. E. G. BROVMAN, Y. KAGAN and A. KHOLAS, Sov. Phys. Solid St., **11,** 733, 1969.
8. M. M. SHUKLA and H. CLOSS, Solid St. Commun., **13,** 803 1973.
9. J. S. RAJPUT and S. S. KUSHWAHA, Phys. Lett., **38A,** 497, 1972.

10. R. CAVALHEIRO and M. M. SHUKLA, Acta Physica Polonica, **49A**, 445, 1976.
11. R. CAVALHEIRO and M. M. SHUKLA, Il Nuovo Cimento, **30B**, 173, 1975.
12. M. M. SHUKLA and R. CAVALHEIRO, International Conference on Phonon, July 25 to 29, 1971, Rennes, France — Phonons, Editor Numovici, Flammarion, Paris, 1971.
13. M. M. SHUKLA and R. CAVALHEIRO, Il Nuovo Cimento, **16B**, 83, 1973.
14. R. E. SCHMUNK, R. M. BRUGGER, P. D. RANDOLPH and K. A. STRONG, Phys. Rev., **128**, 562, 1962.
15. S. J. SLUSTKY and C. W. GARLAND, Phys. Rev., **107**, 972, 1957.
16. P. K. IYENGER, G. VENKETRAMAN, G. VIJAYRAGHAVAN and A. P. ROY, Conference on Lattice Dynamics, edited by R. E. Wallis, Pergamon Press, N. Y. 1963.
17. K. CLUSIUS and J. V. VAUGHAN, Jr. Am. Chem. Soc., **52**, 4686, 1930.
18. K. S. CRAIG, C. A. KRIER, L. W. COFFER, E. A. BATES and W. E. WALLACE Jr. Am. Chem. Soc., **76**, 238, 1954.
19. D. L. MARTIN, Proc. Phys. Soc., **78**, 1482, 1961.
20. J. C. UPADHYAYA and H. P. SINHA, Jr. Phys. Chem. Solids, **36**, 975, 1975.
21. G. BOSE, H. C. GUPTA and B. B. TRIPATHI, Jr. Phys. Soc. Japan, **34**, 1006, 1973.
22. A. J. PINDORE and R. J. RYNN, J. Rhys. **C2**, 1037, 1969.
23. A. P. ROY and G. VENKETRAMAN, Phys. Rev., **156**, 769, 1969.
24. E. G. BROVMAN and Y. KAGAN, Sov. Phys. Doklady, **25**, 365, 1967.

Acta Physica Academiae Scientiarum Hungaricae, Tomus 45 (1), pp. 9—14 (1978)

PROPAGATION OF WEAK MHD DISCONTINUITIES IN AN OPTICALLY THIN MEDIUM

By

A. Rai, M. Gaur and R. Ram

APPLIED MATHEMATICS SECTION, INSTITUTE OF TECHNOLOGY,
B.H.U. VARANASI 221005, INDIA

(Received 15. VI. 1978)

The object of the present paper is to study the propagation of weak MHD discontinuities in an optically thin medium. The growth equation governing the growth and decay of MHD discontinuities and the behaviour of their amplitude has been studied. It is observed that expansion waves decay exponentially, while compressive waves may grow into shock waves. A critical value of the amplitudes of compressive waves is determined such that all waves with initial amplitude greater than the critical one will grow into shock waves, while those with amplitudes less than the critical one will decay out. The critical time for the formation of shock waves has also been determined.

I. Introduction

Thomas [1] studied the propagation of sonic waves in an ideal gas. Ram and Gaur [3] studied the problem of growth and decay of sonic discontinuities in dissociating gas flows. Ram and Srinivasan [4] studied the propagation of sonic waves in radiating gases. The problem of growth and decay of weak MHD discontinuities in a radiative medium has drawn a little attention. When the temperature of the gas is of order 10^4 °K, the radiative heat transfer terms of the radiation field are dominant, while radiation pressure and radiation energy terms are still negligible. In the present investigation, our main academic interest is to study the effects of radiative heat transfer on the behaviour of the amplitude of MHD discontinuities. We assume the existence of a moving surface $\Sigma(t)$ of a weak MHD discontinuity across which the flow parameters are continuous but their first and higher derivatives are discontinuous. The boundary conditions are

$$[\varrho] = 0\,, \quad [p] = 0\,, \quad [u] = 0\,, \quad [h] = 0\,, \tag{1.1a}$$

$$\left[\frac{\partial \varrho}{\partial r}\right] \neq 0\,, \quad \left[\frac{\partial p}{\partial r}\right] \neq 0\,, \quad \left[\frac{\partial u}{\partial r}\right] \neq 0\,, \quad \left[\frac{\partial h}{\partial r}\right] \neq 0\,, \tag{1.1b}$$

where $[Z]$ denotes the jump across a discontinuity surface $\Sigma(t)$. The geometrical and kinematical compatibility conditions of first order due to Thomas for sonic discontinuities are [2]

$$\left[\frac{\partial Z}{\partial r}\right] = B\,, \quad \left[\frac{\partial Z}{\partial t}\right] = -BG\,, \tag{1.2}$$

where Z stands for any of the flow variables and B is a scalar function defined over $\Sigma(t)$. G is the speed of propagation of the surface $\Sigma(t)$ into a medium at rest.

II. Propagation law

The basic equations governing the MHD flow in an optically thin medium are:

$$\frac{\partial \varrho}{\partial t} + \varrho \frac{\partial u}{\partial r} + u \frac{\partial \varrho}{\partial r} + \frac{\alpha \varrho u}{r} = 0, \tag{2.1}$$

$$\varrho \frac{\partial u}{\partial t} + \varrho u \frac{\partial u}{\partial r} + \frac{\partial p}{\partial r} + \frac{\partial h}{\partial r} + (1 - n) \frac{2h}{r} = 0, \tag{2.2}$$

$$\frac{\partial h}{\partial t} + u \frac{\partial h}{\partial r} + 2h \frac{\partial u}{\partial r} + \frac{2\alpha nhu}{r} = 0, \tag{2.3}$$

$$\frac{\partial p}{\partial t} + u \frac{\partial p}{\varrho r} + \gamma p \left\{ \frac{\partial u}{\partial r} + \frac{\alpha \varrho u}{r} \right\} + 4(\gamma - 1) D_R a_R T^4 = 0, \tag{2.4}$$

where v denotes the distance from the centre of symmetry. Here p, ϱ, u, h and v respectively represent the gas pressure, the density, the velocity of the gas, the magnetic pressure and the heat exponent of the gas. D_R, a_R and T respectively are the Planck mean absorption coefficient, the Stefan—Boltzmann constant and the temperature of the gas. $\alpha = 0, 1, 2$ for planar, cylindrical and spherical symmetry, respectively, and $n = 0, 1$ for azimuthal and axial magnetic field, respectively.

Taking jump in the Eqs. (2.1) to (2.4) and making use of (1.1) and (1.2) we get

$$(u - G)\zeta + \varrho\lambda = 0, \tag{2.5}$$

$$\varrho(u - G)\lambda + \xi + \eta = 0, \tag{2.6}$$

$$(u - G)\eta + 2h\lambda = 0, \tag{2.7}$$

$$(u - G)\xi + \gamma p \lambda = 0, \tag{2.8}$$

where $$\zeta = \left[\frac{\partial \varrho}{\partial r}\right], \quad \lambda = \left[\frac{\partial u}{\partial r}\right], \quad \xi = \left[\frac{\partial p}{\partial r}\right], \quad \eta = \left[\frac{\partial h}{\partial r}\right].$$

From Eqs. (2.5), (2.7) and (2.8) we get

$$\lambda = -\frac{(u - G)}{\varrho}\zeta = -\frac{(u - G)\eta}{2h} = -\frac{(u - G)}{\lambda p}\xi. \tag{2.9}$$

Substituting from (2.9) in (2.6), we get

$$\lambda\left\{(u-G)^2-\frac{\gamma p}{\varrho}-\frac{2h}{\varrho}\right\}=0. \tag{2.10}$$

The assumption that $\Sigma(t)$ is regular singular surface implies

$$\lambda \neq 0\,.$$

Hence we have

$$(u-G)^2=\frac{\gamma p}{\varrho}+\frac{2h}{\varrho}\,, \tag{2.11}$$

$$(u-G)^2=c^2+b^2\,, \tag{2.12}$$

where c is the local speed of sound and b is the Alfvén speed. If the medium ahead of $\Sigma(t)$ is uniform and at rest, u vanishes on $\Sigma(t)$. For this case the speed of propagation is a constant given by

$$G^2=c_0^2+b_0^2\,, \tag{2.13}$$

which is the effective speed of sound relative to the gas flow just ahead of the wave. The suffix 0 indicates the values evaluated in the constant state just ahead of the wave. Consequently, the relations (2.9) reduce to the forms:

$$\lambda=\frac{G}{\varrho}\zeta=\frac{G}{2h}\eta=\frac{G}{\gamma p}\xi\,. \tag{2.14}$$

III. Growth equation

Differentiating Eqs. (2.1) to (2.4) w.r. to r and taking jump across $\Sigma(t)$ and making use of the geometrical and kinematical compatibility conditions, we get:

$$-G\bar{\zeta}+\varrho\bar{\lambda}=-\left\{\frac{\delta\zeta}{\delta t}+2\zeta\lambda+\frac{\alpha\varrho\lambda}{R}\right\}, \tag{3.1}$$

$$-\varrho G\bar{\lambda}+\bar{\xi}+\bar{\eta}=G\zeta\lambda-\varrho\frac{\delta\lambda}{\delta t}-\varrho\lambda^2-\frac{(1-n)\,2\eta}{R}\,, \tag{3.2}$$

$$-G\bar{\eta}+2h\bar{\lambda}=-\left\{\frac{\delta\eta}{\delta t}+3\eta\lambda+\frac{2\alpha nh\lambda}{R}\right\}, \tag{3.3}$$

$$\gamma p\bar{\lambda}-G\bar{\xi}=-\left\{\frac{\delta\xi}{\delta t}+\lambda\xi+\frac{\alpha\gamma p}{R}+\gamma\xi\lambda+\frac{16(\gamma-1)\,D_R a_R T^3}{R_1\varrho}\left\{\xi-\frac{p}{\varrho}\zeta\right\}\right\}, \tag{3.4}$$

where

$$\lambda=\left[\frac{\partial^2 u}{\partial r^2}\right],\quad \bar{\zeta}=\left[\frac{\partial^2\varrho}{\partial r^2}\right],\quad \bar{\xi}=\left[\frac{\partial^2 p}{\partial r^2}\right],\quad \bar{\eta}=\left[\frac{\partial^2 h}{\partial r^2}\right].$$

Eliminating $\bar{\lambda}$, $\bar{\xi}$, $\bar{\zeta}$ and $\bar{\eta}$ and using the Eqs. (2.14) we have

$$\frac{\delta\lambda}{\delta t} = -\frac{\lambda^2}{2G^2}\{(\gamma+1)c^2+3b^2\} - \\ -\frac{\lambda}{2G}\left\{\frac{\alpha}{R}(c^2+nb^2)+\frac{2(1-n)b^2}{R}+\frac{16(\gamma-1)D_R a_R T^3 p}{R_1 \varrho^2 G}\right\}. \quad (3.5)$$

Let the configuration of the surface $\Sigma(t)$ at any time t be represented by $r = R(t)$ so that $G = dR/dt$. The scalars ξ, ζ, λ, and η are defined over $\Sigma(t)$ and can be regarded as functions of R. Hence we can write

$$\frac{\delta\lambda}{\delta t} = G\frac{d\lambda}{dR}, \quad \frac{\delta\zeta}{\delta t} = G\frac{d\zeta}{dR}, \quad \frac{\delta\xi}{\delta t} = G\frac{d\xi}{dR} \text{ and } \frac{\delta\eta}{\delta t} = G\frac{d\eta}{dR}. \quad (3.6)$$

Making use of Eqs. (3.6) in Eq. (3.5) we obtain

$$\frac{d\lambda}{dR} = -\frac{\lambda^2}{2G^3}\{(\gamma+1)c^2+3b^2\} - \\ -\frac{\lambda}{2G^2}\left\{\frac{\alpha}{R}(c^2+nb^2)+\frac{2(1-n)b^2}{R}+\frac{16(\gamma-1)D_R a_R T^3 p}{R_1 \varrho^2 G}\right\}. \quad (3.7)$$

Introducing the following dimensionless parameters

$$\delta = \frac{\lambda}{\lambda^*}, \quad \sigma = \frac{R-R^*}{2R^*} \text{ and } m_f = \frac{b_0}{c_0}, \quad (3.8)$$

where λ^* and R^* are the initial values of λ and R. The Eq. (3.7) assumes the form

$$\frac{d\delta}{d\sigma} = -\left[\left\{\frac{(1+nm_f^2)\alpha+2(1-n)m_f^2}{(1+2\sigma)(1+m_f^2)}+\beta\right\}\delta+\Phi\delta^2\right], \quad (3.9)$$

where

$$\beta = \frac{16(\gamma-1)D_R a_R T_0^3 R^*}{\gamma c_v \varrho_0 c_0 (1+m_f^2)^{3/2}} \text{ and } \Phi = \frac{\lambda^* R^*}{c_0}\left\{\frac{\gamma+1+3m_f^2}{(1+m^2)^{3/2}}\right\}. \quad (3.10)$$

IV. Particular cases of interest

Case I. Plane waves

For a plane wave ($\alpha = 0$, $n = 1$) the solution of (3.9) is of the form

$$\delta = \left\{e^{\beta\sigma}+\frac{\Phi}{\beta}(e^{\beta\sigma}-1)\right\}^{-1}. \quad (4.1)$$

The Eq. (4.1) shows that expansion waves ($\lambda > 0$) will exponentially decay, but compressive wave ($\lambda < 0$) will in general grow. If we define the amplitude of the wave by

$$a(t) = \left[\frac{\partial u}{\partial r}\right] = \lambda ,$$

we observe that there exists a critical value λ_c of the initial amplitude $\lambda(0)$ given by

$$\lambda_c = \frac{\beta c_0 (1 + m_f^2)^{3/2}}{R^*(\gamma + 1 + 3m_f^2)} ,$$

which is such that when $\lambda(0) < \lambda_c$, there will be no breakdown of a weak discontinuity after a finite time, but it will decay out ultimately. On the other hand when $\lambda(0) > \lambda_c$, a weak discontinuity will break down and consequently a shock wave will be formed after a finite critical time t_c given by

$$t_c = \frac{1}{\beta c_0} \log \left\{ \frac{\lambda(0)\, R^*(\gamma + 1 + 3m_f^2)}{\lambda(0)\, R^*(\gamma + 1 + 3m_f^2) - \beta c_0 (1 + m_f^2)^{3/2}} \right\} .$$

Case II. Cylindrical waves

For a cylindrical wave with azimuthal magnetic field we have $\alpha = 1$ and $n = 0$. For this case the Eq. (3.9) reduces to

$$\frac{d\sigma}{d\delta} + \left(\beta + \frac{1 + 2m_f^2}{(1 + m_f^2)(1 + 2\sigma)} \right) \delta + \Phi \delta^2 = 0 . \tag{4.2}$$

The solution of (4.2) is of the form

$$\frac{1}{\delta} = 1 + \Phi e^{\beta\sigma} (1 + 2\sigma)^{1 + 2m_f^2/2(1+m_f^2)} \int_0^\sigma e^{-\beta\sigma} (1 + 2\sigma)^{-(1+2m_f^2)/2(1+m_f^2)}\, d\sigma$$

which reduces to the following form in the case of non-radiating gases:

$$\delta = \frac{1}{(1 + 2\sigma)^{\mu/2} \left\{ 1 - \left(1 - (1 + 2\sigma)^{2-\mu/2}\right) \dfrac{\Phi}{2 - \mu} \right\}} , \tag{4.3}$$

where

$$\mu = (1 + 2m_f^2)/(1 + m_f^2) .$$

The solution (4.3) shows that the compressive acceleration waves ($\Phi < 0$) with initial amplitude greater than a certain critical value will terminate into shock waves after a finite time given by

$$t_c = -\frac{1}{2c_0} + \frac{1}{2c_0} \left\{ \frac{2 + |\Phi| - \mu}{|\Phi|} \right\}^{2/2-\mu} .$$

The expansion waves ($\Phi > 0$) will monotonically decay and will be damped out ultimately.

Case III. Spherical waves

For spherical wave we have $\alpha = 2$, $m_f = 0$ so that the Eq. (2.9) reduces to

$$\frac{d\delta}{d\sigma} + \left(\beta + \frac{2}{1+2\sigma}\right)\delta + \Phi\delta^2 = 0\,. \tag{4.4}$$

The solution of (4.4) for non-radiating gases is of the form

$$\delta = \frac{1}{(1+2\sigma)\left\{1 + \frac{\Phi}{2}\log(1+2\sigma)\right\}}\,. \tag{4.5}$$

The solution (4.5) shows that the compressive acceleration waves ($\Phi < 0$) with initial amplitude greater than a critical value will terminate into shock waves after a finite time given by

$$t_c = \frac{1}{2c_0}\left\{e^{2/|\Phi|} - 1\right\}.$$

The expansion waves ($\Phi > 0$) will monotonically decay and will be damped out ultimately.

REFERENCES

1. T. Y. Thomas, Jour. Math. Mech., **6**, 455, 1957.
2. T. Y. Thomas, Jour. Math. Mech., **6**, 311, 1957.
3. R. Ram and M. Gaur, Acta Phys. Hung., **40**, 85, 1976.
4. R. Ram and S. Srinivasan, ZAMM, **57**, 191, 1977.

Acta Physica Academiae Scientiarum Hungaricae, Tomus 45 (1), pp. 15—25 (1978)

SOME BOUNDARY VALUE PROBLEMS IN MAGNETO-ELASTODYNAMICS

By

A. Basu

UNIVERSITY OF WOLLONGONG, WOLLONGONG, N.S.W. AUSTRALIA

(Received 20. VI. 1978)

The interaction of magnetic fields and displacements in an elastic solid is considered as a mixed initial and boundary value problem in Magneto-elastodynamics. The solution is reduced to a system of Fredholm equations of the second kind, which in certain particular cases become Fredholm equations of the first kind. Some special cases are considered for a solid rectangular plate, and graphs are presented for forced vibrations of the plate.

1. Introduction

Primarily due to the successful merging of electromagnetic theory and fluid mechanics in magnetohydrodynamics, considerable attention has been given recently to the study of magneto-elastic solid interactions. Although there has been some progress in the study of magneto-elasticity the development of effective methods of solution for the general mixed initial and boundary value problem in magneto-elastodynamics remains a challenge.

On the basis of Nowacki's method [1] of solving problems of Elastodynamics with mixed boundary conditions, a complete and systematic mathematical formulation has been developed for mixed initial and boundary value problems in Magneto-elastodynamics with mixed boundary conditions [2].

As an application of this method we first consider a two-dimensional rectangular plate for which the displacements are given on some parts, and the loadings are prescribed on the remaining parts. We then reduce this problem to a number of special cases, such as an elastic foundation, and a plate with harmonic vibrations.

2. Basic equations and statement of the problem

Let R be the two dimensional region of the rectangular plate, (Fig. 1)

$$0 \leq x \leq a, \quad 0 \leq y \leq b,$$

where x and y are the usual cartesian coordinates.

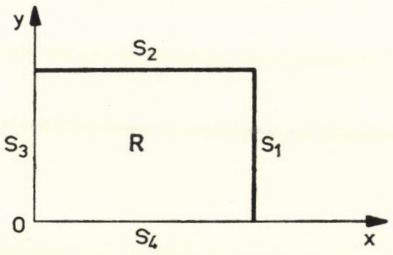

Fig. 1

The functions u, v representing the components of the displacement vector have to satisfy the motion equations. Using the facts that $H_3 = w = 0$ and $\partial \mathbf{u}/\partial Z = 0$, the magneto-elastodynamics equations of motion [2] can be written in the component forms:

$$\frac{\partial^2 u}{\partial t} = \left\{ c_2^2 \nabla^2 + R_H H_2^2 \nabla^2 + (c_1^2 - c_2^2) \frac{\partial^2}{\partial x^2} \right\} u + \\ + \left\{ (c_1^2 - c_2^2) \frac{\partial^2}{\partial x \, \partial y} - R_H H_1 H_2 \nabla^2 \right\} v + X,$$

$$\frac{\partial^2 v}{\partial t^2} = \left\{ (c_1^2 - c_2^2) \frac{\partial^2}{\partial x \, \partial y} - R_H H_1 H_2 \nabla^2 \right\} u + \\ + \left\{ (c_2^2 + R_H H_1^2) \nabla^2 + (c_1^2 - c_2^2) \frac{\partial^2}{\partial y^2} \right\} v + Y, \qquad (2.1)$$

where c_1 and c_2 are the longitudinal and shear wave velocities, H_1 and H_2 are the components in the x-direction and y-direction of the steady state magnetic field $\mathbf{H}$, R_H is Hartman's magnetic number, and $\nabla^2 \equiv \partial^2/\partial x^2 + \partial^2/\partial y^2$.

The conditions which must be satisfied at the plate-vacuum interfaces are:

(1) the continuity of the magnetic field vector,
(2) the continuity of the total normal and shear stresses across the surface S_2 on which the tractions are specifed, and
(3) the given boundary displacements on the surfaces S_1, S_3 and S_4.

As the magnetic field vector across the surface is continuous we can write the boundary conditions as:

$$q_i(\xi', t) = L[u_i(\xi', t)] = \mu(u_{j,i} + u_{i,j}) n_j + \lambda n_i \operatorname{div} \mathbf{u} \text{ on } S_2,$$
$$u_i(\xi', t) = f_i(\xi', t) \text{ on } S_1, S_3, \text{ and } S_4, \qquad (2.2)$$

where ξ' is a point on the boundary.

Applying the Laplace transform to equation (2.1) we get

$$\left\{(c \dot{+} R_H H_2^2)\nabla^2 + (c_1^2 - c_2^2)\frac{\partial^2}{\partial x^2} - p^2\right\}\bar{u} +$$

$$+\left\{(c_1^2 - c_2^2)\frac{\partial^2}{\partial x\,\partial y} - R_H H_1 H_2 \nabla^2\right\}\bar{v} + \bar{X} = 0,$$

$$\left\{(c_1^2 - c_2^2)\frac{\partial^2}{\partial x\,\partial y} - R_H H_1 H_2 \nabla^2\right\}\bar{u} +$$

$$\left\{(c_2^2 + R_H H_1^2)\nabla^2 + (c_1^2 - c_2^2)\frac{\partial^2}{\partial y^2} - p^2\right\}\bar{v} + \bar{Y} = 0. \tag{2.3}$$

The bar represents transformed space.

In order to find Green's functions $\bar{g}_{ij}(x, y;\ \xi, \eta;\ p)$ of the system (2.3) we replace the forces $\bar{X}$, $\bar{Y}$ by the δ-functions. Here (ξ, η) is the point of application of a unit concentrated force first applied parallel to the x-axis, and then parallel to the y-axis, respectively.

The Green's functions $\bar{g}_{ij}(x, y;\ \xi, \eta;\ p)$ satisfy the boundary conditions

$$\bar{g}_{ij}(x, y;\ \xi, \eta;\ p) = 0 \text{ on } \begin{cases} x = 0, a \\ y = 0, b \end{cases} \qquad (i, j = 1, 2). \tag{2.4}$$

Finding the solutions $\bar{g}_{11}, \bar{g}_{21}, \bar{g}_{12}, \bar{g}_{22}$ for (2.3) and (2.4) involves very complicated and cumbersome analysis. To facilitate analysis, we expand $\bar{g}_{ij}$ in terms of orthogonal sets $(\sin m\pi x/a,\ \cos m\pi x/a)$ $(m = 0, 1, 2, 3, \ldots)$ in the interval $(0, a)$. The differential equations (2.3) can be completely satisfied but the boundary conditions (2.4) can only be approximately satisfied. A subsequent paper, using the generalized function method, will show that the error so introduced is negligible. Proceeding with the present method we can now easily show that (with $H_2 = 0,\ R_H H_1^2 = R_x^2$)

$$\bar{g}_{11}(x, y;\ \xi, \eta;\ p) = \sum_\gamma F_1(\eta, y) \sin\gamma\xi\ \sin\gamma x,$$

$$\bar{g}_{21}(x, y;\ \xi, \eta;\ p) = \sum_\gamma F_2(\eta, y) \sin\gamma\xi \cos\gamma x,$$

$$\bar{g}_{12}(x, y;\ \xi, \eta;\ p) = \sum_\gamma F_3(\eta, y) \sin\gamma\xi \cos\gamma x,$$

$$\bar{g}_{22}(x, y;\ \xi, \eta;\ p) = \sum_\gamma F_4(\eta, y) \sin\gamma\xi \sin\gamma x, \tag{2.5}$$

where

$$\gamma = \frac{\pi m}{a}, \quad m = 0, 1, 2, 3, \ldots \tag{2.6}$$

$$F_1(\eta, y) = F'(0)\, C_1(y) + G'(0)\, D_1(y) - \frac{2}{ac_2^2} P_1(y, \eta) - \frac{2}{ac_2^2} H_7 P_2(y, \eta),$$

$$F_2(\eta, y) = F'(0)\, C_2(y) + G'(0)\, D_2(y) + \frac{2}{ac_2^2} H_8 P_3(y, \eta),$$

$$F_3(\eta, y) = R'(0)\, C_3(y) + S'(0)\, D_3(y) + \frac{2}{ac_2^2} H_8 P_3(y, \eta),$$

$$F_4(\eta, y) = R'(0)\, C_4(y) + S'(0)\, D_4(y) - \frac{2}{a(c_1^2 + R_x^2)} P_1(y, \eta) -$$

$$- \frac{2 H_9}{a(c_2^2 + R_x^2)} P_2(y, \eta). \tag{2.7}$$

Defining

$$k_1 = \frac{\alpha \sin h\alpha y - \beta \sin h\beta y}{\alpha^2 - \beta^2},$$

$$k_2 = \frac{\alpha \sin h\beta y - \beta \sin h\alpha y}{\alpha\beta(\alpha^2 - \beta^2)},$$

$$k_3 = \frac{\cos h\alpha y - \cos h\beta y}{\alpha^2 - \beta^2},$$

$$H_7 = \frac{(c_2^2 + R_x^2)\gamma^2 + p^2}{c_1^2 + R_x^2},$$

$$H_8 = \frac{(c_1^2 - c_2^2)\gamma}{c_1^2 + R_x^2},$$

$$H_9 = \frac{c_1^2\gamma^2 + p^2}{c_2^2}, \qquad H_{11} = \frac{(c_1^2 - c_2^2)\gamma}{c_2^2}, \tag{2.8}$$

where the quantities 'α' and 'β' are the roots of the equation:

$$c_2^2(c_1^2 + R_x^2)s^4 - s^2[R_x^2\{(c_1^2 + c_2^2)\gamma^2 + p^2\} + (c_1^2 + c_2^2)p^2 + 2c_1^2c_2^2\gamma^2] +$$
$$+ (c_1^2\gamma^2 + p^2)\{(c_2^2 + R_x^2)\gamma^2 + p^2\} = c_2(c_1^2 + R_x^2)(s^2 - \alpha^2)(s^2 - \beta^2).$$

We can write

$$C_1(y) = k_1 + H_7 \cdot k_2,$$

$$D_1(y) = H_{11} \cdot k_3, \quad C_2(y) = -H_8 \cdot k_3,$$

$$D_2(y) = k_1 + H_9 \cdot k_2,$$

$$C_3(y) = C_1(y), \qquad D_3(y) = -D_1(y),$$

$$C_4(y) = -C_2(y), \quad D_4(y) = D_2(y). \tag{2.9}$$

Also

$$A_1 = C_1(b), \quad B_1 = D_1(b), \quad A_2 = -C_2(b), \quad B_2 = D_2(b),$$

$$A_3 = A_1, \qquad B_3 = -B_1, \quad A_4 = -A_2, \qquad B_4 = B_2,$$

$$A_1 B_2 - A_2 B_1 = A\,, \qquad A_3 B_4 - A_4 B_3 = B \tag{2.10}$$

and

$$P_1(y,\eta) = H(y-\eta)\frac{\alpha \sin h\alpha(y-\eta) - \beta \sin h\beta(y-\eta)}{\alpha^2 - \beta^2}\,,$$

$$P_2(y,\eta) = H(y-\eta)\frac{\alpha \sin h\beta(y-\eta) - \beta \sin h\alpha(y-\eta)}{\alpha\beta(\alpha^2 - \beta^2)}\,,$$

$$P_3(y,\eta) = H(y-\eta)\frac{\cos h\alpha(y-\eta) - \cos h\beta(y-\eta)}{\alpha^2 - \beta^2}\,. \tag{2.11}$$

We also have

$$F'(0) = \frac{2}{Aac_2^2}\left[B_2\{P_1(b,\eta) + H_7 P_2(b,\eta)\} + B_1 \cdot H_8 P_3(b,\eta)\right] \sin\gamma\xi\,,$$

$$G'(0) = \frac{2}{Aac_2^2}\left[-A_1 \cdot H_8 P_3(b,\eta) - A_2\{P_1(b,\eta) + H_7 P_2(b,\eta)\}\right] \sin\gamma\xi\,,$$

$$R'(0) = \frac{2}{Bac_2^2}\Bigg[-B_4 \cdot H_8 \cdot P_3(b,\eta) - B_3\left\{\frac{c_2^2}{c_1^2 + R_x^2} P_1(b,\eta) + \frac{c_2^2}{c_1^2 + R_x^2} H_9 P_2(b,\eta)\right\}\Bigg] \cdot \sin\gamma\xi\,,$$

$$S'(0) = \frac{2}{Bac_2^2}\Bigg[A_3\left\{\frac{c_2^2}{c_1^2 + R_x^2} P_1(b,\eta) + \frac{c_2^2}{c_1^2 + R_x^2} H_9 P_2(b,\eta)\right\} + A_4 \cdot H_8 \cdot P_3(b,\eta)\Bigg] \sin\gamma\xi\,. \tag{2.12}$$

By using the symmetric property of the Green's functions we can re-write the Green's functions $\bar{g}_{ij}(x, y; \xi, \eta; p)$ as:

$$\bar{g}_{11}(x, y; \xi, \eta; p) = \sum_{\gamma} \bar{F}_1(y,\eta) \sin\gamma\xi \sin\gamma x\,,$$

$$\bar{g}_{21}(x, y; \xi, \eta; p) = \sum_{\gamma} \bar{F}_2(y,\eta) \sin\gamma x \cos\gamma\xi\,,$$

$$\bar{g}_{12}(x, y; \xi, \eta; p) = \sum_{\gamma} \bar{F}_3(y,\eta) \sin\gamma x \cos\gamma\xi\,,$$

$$\bar{g}_{22}(x, y; \xi, \eta; p) = \sum_{\gamma} \bar{F}_4(y,\eta) \sin\gamma x \sin\gamma\xi\,, \tag{2.13}$$

where $\bar{F}_1(y,\eta)$, $\bar{F}_2(y,\eta)$, $\bar{F}_3(y,\eta)$, and $\bar{F}_4(y,\eta)$ have been obtained from $F_1(\eta, y)$, $F_2(\eta, y)$, $F_3(y,\eta)$, and $F_4(y,\eta)$ respectively by interchanging η and y.

Now we consider the problem with mixed boundary conditions formulated earlier in (2.1) and (2.2).

Applying Betti's reciprocal theorem [1] we get

$$\bar{u}_k(\xi, \eta, p) = \bar{u}_k^0(\xi, \eta, p) - \int_{S_2(\xi)} [\bar{U}_i(\xi', p)]_2 \, L[\bar{g}_{ik}] \, dS_2(\xi') , \qquad (2.14)$$

where we have denoted by $[\bar{U}_i(\xi', p)]_2$ the unknown displacement functions on the surface S_2. Further,

$$\bar{u}_k^0(\xi, \eta, p) = \iint_B \bar{g}_{ik}(x, y; \xi, \eta; p) \, \bar{X}_i(x, y; p) \, dV -$$

$$- \int_{S_1+S_2+S_3} \bar{f}_i(\eta', p) \, L[\bar{g}_{ik}(\eta'; \xi, \eta; p)] \, dS(\eta') . \qquad (2.15)$$

In order to determine the unknown functions $\bar{U}_i(\xi', p)$ we perform on the expression (2.14) the operation $L'(\ldots)$ and obtain

$$L'[\bar{u}_k(\xi, \eta, p)] = L'[\bar{u}_k^0(\xi, \eta, p)] - \int_{S_2} [U_i]_2 L' L[\bar{g}_{ik}] \, dS_2 . \qquad (2.16)$$

The prime ($'$) on the operator L denotes that the operation refers to the point (ξ, η).

Now, we pass point (ξ, η) εB to the point (x', b) εS_2 and we use the boundary condition which states that the loading $\mathbf{q}$ is given on S_2. From (2.16), after passing the point (ξ, η) to the point (x', b) on the boundary, we arrive at the following system of integral equations of the first kind:

$$[\bar{q}_k(x', p)]_2 = [\bar{q}_k^0(x', p)]_2 - \int_{S_2(\xi')} [\bar{U}_i(\xi', p)]_2 \, [L' L(\bar{g}_{ik})] \, dS_2(\xi') . \qquad (2.17)$$

In Eq. (2.17) we know the transformed functions $\bar{q}_k$, $\bar{q}_k^0$, and $\bar{g}_{ik}$. Having determined the unknown functions $[U_i(\xi', p)]_2$ we return to the equations (2.14) from which we can obtain the transformed displacement $\bar{u}_k$ at the point (ξ, η) in the elastic body.

3. Some special cases

Case 1. We consider now the surfaces S_1, S_3, and S_4 to be fixed, while the boundary $y = b$ (i.e. the surface S_2) rests on an elastic Winklerian foundation, and thus satisfies the condition

$$q_k(x', t) = -\frac{1}{\chi_k} U_k(x', t) \qquad (k = 1, 2) , \qquad (3.1)$$

where χ_k is the Winklerian foundation constant.

When the relations (3.1) are used in (2.17) we obtain a system of integral equations:

$$\frac{\bar{U}_1(x', p)}{\chi_1} + \bar{q}_1^0(x', p) = \sum_\gamma \left\{ \int_0^a \bar{U}_1(\xi') \sin \gamma \xi' \, d\xi' \right\} p_{11} \sin \gamma x' ,$$

$$\frac{\bar{U}_2(x', p)}{\chi_2} + \bar{q}^0(x', p) = \sum_\gamma \left\{ \int_0^a \bar{U}_2(\xi') \sin \gamma \xi' \, d\xi' \right\} q_{11} \sin \gamma x' , \qquad (3.2)$$

where

$$p_{11} = c_2^4(\bar{F}_{1,22'} - 2\gamma\bar{F}_{2,2} - \gamma\bar{F}_{2,2'}) + c_2^2(c_1^2 - 2c_2^2)(-\gamma\bar{F}_{2,2'}),$$

$$q'_{11} = c_1^2 c_2^2(\bar{F}_{4,22'} + \bar{F}_{4,22}) + c_1^2(c_1^2 - 2c_2^2)(\bar{F}_{4,22'}) + c_2^2(c_1^2 - 2c_2^2) \cdot (-\gamma\bar{F}_{3,2} - \gamma^2\bar{F}_4). \tag{3.3}$$

As a solution to (3.2) we assume

$$\bar{U}_1(x', p) = \sum_l A_l \sin lx',$$

$$\bar{U}_2(x', p) = \sum_l B_l \sin lx'. \tag{3.4}$$

Substituting (3.4) into (3.2) we get

$$\sum_\gamma \frac{A_\gamma}{\chi_1} \sin \gamma x' + \bar{q}_1^0(x', p) = \sum_\gamma \left[\frac{a}{2} p_{11} A_\gamma\right] \sin \gamma x',$$

$$\sum_\gamma \frac{B_\gamma}{\chi_2} \sin \gamma x' + \bar{q}_2^0(x', p) = \sum_\gamma \left[\frac{a}{2} q'_{11} B_\gamma\right] \sin \gamma x'. \tag{3.5}$$

We also assume that

$$\bar{q}_1^0(x', p) = \sum_l a_l \sin lx',$$

$$\bar{q}_2^0(x', p) = \sum_l b_l \sin lx'. \tag{3.6}$$

Substituting (3.6) into (3.5) and equating coefficients of $\sin \gamma x'$ on both sides we get

$$\frac{A_\gamma}{\chi_1} + a_\gamma = \frac{a}{2} p_{11} A_\gamma,$$

$$\frac{B_\gamma}{\chi_2} + b_\gamma = \frac{a}{2} q'_{11} B_\gamma.$$

From the above we can easily determine A_γ and B_γ.

Case 2. We consider now the surfaces S_1, S_3, and S_4 to be fixed and the boundary $y = b$ (i.e. the surface S_2) to be subjected to a harmonic load $q_i(x')e^{iwt}$. Applying this boundary condition to Eq. (2.17) and assuming there are no body forces we get

$$q_1(x') = -\sum_\gamma \left\{\int_0^a U_1(\xi') \sin \gamma\xi' \, d\xi'\right\} p_{11} \sin \gamma x',$$

$$q_2(x') = -\sum_\gamma \left\{\int_0^a U_2(\xi') \sin \gamma\xi' \, d\xi'\right\} q'_{11} \sin \gamma x'. \tag{3.7}$$

Assume

$$U_1(\xi') = \sum_l A_l \sin l\xi' ,$$

$$U_2(\xi') = \sum_l B_l \sin l\xi' . \tag{3.8}$$

Using (3.8) in (3.7) we get

$$q_1(x') = -\sum_\gamma \frac{a}{2} A_\gamma p_{11} \sin \gamma x' ,$$

$$q_2(x') = -\sum_\gamma \frac{a}{2} B_\gamma q'_{11} \sin \gamma x' . \tag{3.9}$$

We assume that $q_l(x')$ can be expanded in the form

$$q_1(x') = \sum_\gamma Q_1^\gamma \sin \gamma x' ,$$

$$q_2(x') = \sum_\gamma Q_2^\gamma \sin \gamma x' , \tag{3.10}$$

where

$$Q_1^\gamma = \frac{2}{a}\int_0^a q_1(x') \sin \gamma x' \, dx' ,$$

$$Q_2^\gamma = \frac{2}{a}\int_0^a q_2(x') \sin \gamma x' \, dx' . \tag{3.11}$$

Using (3.10) in (3.9) and equating coefficients of $\sin \gamma x'$ we get

$$A_\gamma = -\frac{2}{a}\frac{Q_1^\gamma}{p_{11}} ,$$

$$B_\gamma = -\frac{2}{a}\frac{Q_2^\gamma}{q_{22}} . \tag{3.12}$$

Defining

$$N_{11} = c_2^2(\bar{F}_{1,2} - \gamma \bar{F}_2) ,$$

$$N_{12} = c_1^2 \bar{F}_{2,2} + (c_1^2 - 2c_2^2)\gamma \bar{F}_1 ,$$

$$N'_{11} = c_2^2(\bar{F}_{3,2} + \gamma \bar{F}_4) ,$$

$$N'_{12} = c_1^2 \bar{F}_{4,2} - (c_1^2 - 2c_2^2)\gamma \bar{F}_3 \tag{3.13}$$

and using (2.13) in (2.14) we get

$$u(\xi, \eta, t) = -\sum_\gamma \int_0^a [N_{11} U_1(\xi') \sin \gamma\xi' \sin \gamma\xi + N_{12} U_2(\xi') \cos \gamma\xi \sin \gamma\xi'] \, d\xi' \, e^{iwt} , \tag{3.14}$$

$$v(\xi, \eta, t) = -\sum_\gamma \int_0^a [N'_{11} U_1(\xi') \cos \gamma\xi \sin \gamma\xi' + N'_{12} U_2(\xi') \sin \gamma\xi' \sin \gamma\xi] \, d\xi' \, e^{iwt} .$$

Using (3.8) in (3.14) we get

$$u(\xi, \eta, t) = -\frac{a}{2} \sum_{\gamma} [N_{11} A_\gamma \sin \gamma\xi + N_{12} B_\gamma \cos \gamma\xi] \, e^{iwt},$$

$$v(\xi, \eta, t) = -\frac{a}{2} \sum_{\gamma} [N'_{11} A_\gamma \cos \gamma\xi + N'_{12} B_\gamma \sin \gamma\xi] \, e^{iwt}. \qquad (3.15)$$

Since all the quantities A_γ, B_γ and N_{11}, N_{12}, N'_{11}, and N'_{12} are known we can find the displacement at any point of the body considered.

As a special case, suppose the loading is in the y-direction, that is $q_1(x') = 0$ which means $Q_1^\gamma = 0$ for all γ and, hence $A_\gamma = 0$.

Using this condition in (3.15) we get

$$u(\xi, \eta, t) = -\sum_{\gamma} B_\gamma \cdot \frac{a}{2} \cdot N_{12} \cos \gamma\xi \, e^{iwt} = U(\xi, \eta, w) \, e^{iwt},$$

$$v(\xi, \eta, t) = -\sum_{\gamma} B_\gamma \cdot \frac{a}{2} \cdot N'_{12} \sin \gamma\xi \, e^{iwt} = V(\xi, \eta, w) \, e^{iwt}. \qquad (3.16)$$

Graphical results. Assuming a square plate $a = b = 1$, $D = R_x^2/c_2^2 = 0.1$, $c_1^2/c_2^2 = 3$, i.e. $\nu = 1/4$ we can draw the following graphs:

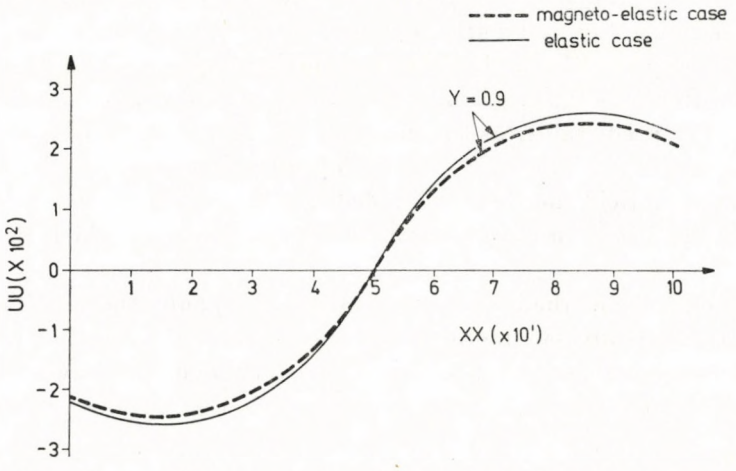

Fig. 2. Approximate solution: variation of horizontal displacement ω. γ. t. X-axis

4. Discussion

Figs. 2—3 show the solutions for both the magneto-elastic and the elastic cases. The curves are naturally steeper near the boundaries where the loads are applied than at points away from the loading region. The graphs

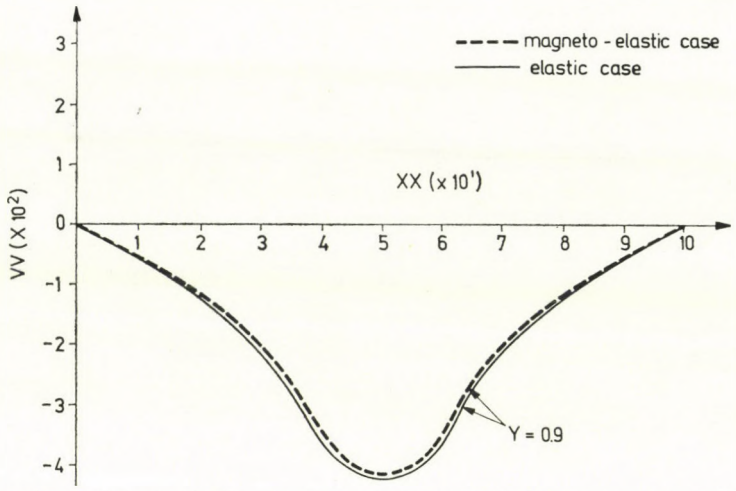

Fig. 3. Approximate solution: variation of vertical displacement ω. γ. t. X-axis

flatten out near the end $y = 0$, and ultimately coincide with the x-axis at this end. The accuracy of the horizontal displacement solution near the ends $x = 0$, a is reduced as the series solution is only less well satisfied at these boundaries. The graphs for the horizontal and vertical displacements, respectively, show symmetry and anti-symmetry with respect to the line $x = 0.5$; as would be expected from the fact that the loading is parallel to the y-axis.

The differences in the graphs between the elastic and the magneto-elastic cases are very predictable, as the effect of the magnetic field is to lower the amplitude of the vibrations. This lowering effect increases as the magnitude of the magnetic field increases, provided this magnitude is not large enough to destroy the Hookean nature of the elastic medium, on which the model is based.

Although the methods of MUSKHELISHVILI [6] and other familiar integral equation methods are satisfactory for two-dimensional problems, the method described here is not restricted to two dimensions, and it can also be extended to the case where thermal fields co-exist with the magneto-elastic effects.

Acknowledgement

The author is greatly indebted to Associate Professor W. W. RECKER, the State University of New York at Buffalo for his help and encouragement in preparing this manuscript.

REFERENCES

1. W. NOWACKI, Proc. Vibr. Prob., **3**, 161, 1964.
2. A. BASU, An Integral Equation Approach to Mixed Boundary Value Problems of Magneto-Elastodynamics, Ind. Sc. Congress, Jan. 3—7, 1979.
3. G. PARIA, Advances in Applied Mechanics, **10**, 73, 1967.
4. W. W. RECKER, Journal of Sound and Vibration, **23**, 41, 1972.
5. J. W. DUNKIN and A. C. ERINGEN, Int. Jour. Engg. Sci., **1**, 461, 1963.
6. N. I. MUSKHELISHVILI, Some Basic Problems of the Mathematical Theory of Elasticity, Noordhoff, Holland, 1953.
7. A. BASU, Acta Phys. Hung., **43**, 81, 1977.

Acta Physica Academiae Scientiarum Hungaricae, Tomus 45 (1), pp. 27—36 (1978)

BOND ORBITAL MODEL OF MOLECULES THE MODEL POTENTIAL APPROACH

By

R. GÁSPÁR

INSTITUTE OF THEORETICAL PHYSICS, KOSSUTH LAJOS UNIVERSITY, H—4010 DEBRECEN

and

R. GÁSPÁR Jr.

DEPARTMENT OF BIOPHYSICS, MEDICAL UNIVERSITY OF DEBRECEN, H—4012 DEBRECEN

(Received 27. VI. 1978)

Bond orbital model with the introduction of a model potential approach is suggested for the treatment of molecular systems. A Gaussian form of the model potential and the method of its parametrization is introduced. It is shown that this model potential is favourably applicable to the floating spherical Gaussian orbitals (FSGO) method, though its use is not restricted to any particular method. Using relatively primitive bond orbital basis sets molecular calculations with the pseudo-FSGO method on LiH and Li_2 molecules are discussed. Physical reasons for the good functioning of the model are given.

Introduction

In connection with the calculation of atomic and molecular properties pseudopotentials have been used for the description of the cores of many electron atoms for a long time [1]. Recently, detailed investigations have been carried out on the theoretical background of the pseudopotential approach and many ab initio and semiempirical pseudopotentials have been discussed [2], [3]. All these investigations show a common feature, namely that they reduce the all-electron problem to the problem of the valence electron.

There are two alternatives to choose from at the starting of the pseudo-method. One of them is to start with an all-electron theoretical method and make extensive use of the orbitals of the core electrons determined by the aid of this method. A straightforward consequence of this procedure is that the pseudo-method cannot go beyond the accuracy of the original method, and the net gain is only in computer time if the method is applied to more complicated atomic systems [4].

The other method starts with some empirical data and a simple model system (one electron ion in a model field etc.). By fitting the calculated and experimental data it determines a core electron effective potential field and the orbitals and energies of more complicated atomic systems in this field [5]. In principle, however, this approach may go beyond some of the more sophisticated all-electron theoretical methods. The main problem in connection with the latter approach is the consistent determination of the model parameters.

The first step towards this goal is presented in this paper. A variational method with double zeta basis set is used for the determination of the para-

meters in the pseudopotential. Further refinement of the method will be treated in forthcoming papers.

In the present article the theoretical basis of the model potential method is reviewed and it is extended in a direction which results in the simplest possible form of the model from the computational point of view. Moreover, the method is restricted here to Gaussian pseudopotentials and Gaussian lobe wavefunctions and the final results are gained by the pseudo-FSGO (floating spherical Gaussian orbital) method, the program of which has been developed by us through the modification of the original FSGO program of FROST [6].

A bond orbital model has been used extensively by HARRISON and PHILLIPS in the theory of bonding in molecules and solids [7]. Our method has a different theoretical basis and it does not make such an extensive use of empirical parameters as their method. In the calculation of molecular properties we do not introduce any new empirical parameter at all, and do not make any adjustment of the previously determined pseudopotential parameters.

Pseudopotential

The formal development of pseudopotentials has been reviewed in many articles and the treatment has been given in detail by SZÁSZ and BARDSLEY [3, 8]. Let us consider an atom or ion with a single valence electron. We assume at the beginning that the core is represented by a single determinant made up from N Hartree—Fock spin orbitals Φ_i, which satisfy the Hartree—Fock equation

$$\{h_{HF}(1) - \varepsilon_i\}\,\Phi_i(1) = 0\,, \tag{1}$$

where

$$h_{HF}(1) = -\frac{1}{2}\nabla_1^2 - \frac{Z}{r_1} \sum_{j=1}^{N+1} + \big(F_j(1) - G_j(1)\big) \tag{2}$$

and

$$F_j(1) = \int dx_2 \Phi_j^*(2) \frac{1}{r_{12}} \Phi_j(2) \tag{3}$$

and

$$G_j(1)\,\Phi(1) = \left[\int dx_2 \Phi_j^*(2) \frac{1}{r_{12}} \Phi(2)\right] \Phi_j(1)\,, \tag{4}$$

where the argument represents space and spin coordinates and the integration includes a summation on the spin variable, Z is the nuclear charge. The wave function for the $N + 1$ particle system is written as

$$\Psi(1, \ldots, N+1) = \left(\frac{1}{N+1}\right)^{1/2} A_p \left[\frac{1}{(N!)^{1/2}} \det\{\Phi_1(1) \ldots \Phi_N(N)\}\,\Phi_v(N+1)\right]. \tag{5}$$

Here A_p is the partial antisymmetrization operator which makes the wave function antisymmetric with respect to all $N + 1$ particles. Let us consider the equation

$$(h_p - \varepsilon)\Psi \equiv \left\{h_{HF} + \sum_c \alpha_c |\Phi_c\rangle\langle\Phi_c| - \varepsilon\right\}\Psi = 0\,. \tag{6}$$

All over the paper atomic units are used.

The wave functions Φ_v of the valence electron are solutions of Eq. (6) with the same eigenvalue ε_v and the core wave functions Φ_c are also eigenfunctions of Eq. (6), but the eigenvalues are changed from ε_c to $\varepsilon_c + \alpha_c$. Thus Eq. (6) preserves the valence spectrum of the Hartree—Fock equation but shifts the core energies.

For the valence electron Eq. (6) may be rearranged if one takes into account the spherical symmetry of the potential field of the closed shell of the core and the consequence of this, namely the core eigenfunctions being eigenfunctions of the total angular momentum. We gain this way for the pseudo-Hamiltonian

$$h_p = h_{HF} + \sum_{l_c} V_{l_c}^r(r) P_{l_c}\,, \tag{7}$$

where

$$V_{l_c}(r) = \sum_{c,\, l_c = \text{const.}} \alpha_c\, |R_c^{l_c}\rangle\langle R_c^{l_c}| \tag{8}$$

and $P_{l_c} = \sum_{m_{l_c}} |l_c, m_{l_c}\rangle\langle m_{l_c}, l_c|$ is a projection operator on the angular momentum eigenstates with quantum number l_c represented in the core and $|l, m_{l_c}\rangle$ are the eigenstates with magnetic quantum number $m_{l_c} = l_c, l_c - 1, \ldots, -l_c$. $|R_c^{l_c}\rangle$ are the eigenstates of the radial part of the core Hamiltonian i.e. $|\Phi_c\rangle = |R_c^{l_c}\rangle |l_c, m_{l_c}\rangle$. We may further rearrange the terms in Eq. (7) by writing the sum in Eq. (2) for $i = v$ in the form

$$\sum_{j=1}^{N} \big(F_j(1) - G_j(1)\big) = \frac{N}{r_1} + \sum_l V_l^e(r_1)\, P_l\,. \tag{9}$$

In Eq. (9) the sum over l_c represents the non-point-like coulombic, electrostatic potential field of the core electrons. By combining Eqs. (7), (8) and (9) and taking into account Eq. (2) we have

$$h_p = -\frac{1}{2}\nabla_1^2 - (Z - N)r^{-1} + \sum_l V_l(r)\, P_l\,, \tag{10}$$

where

$$V_l(r) = V_l^r(r) + V_l^e(r) \tag{11}$$

and $V_l^r(r) \equiv 0$ for l values not represented in the core.

In the subsequent steps we intend to use the above considerations to support the semiempirical procedure outlined below. The potential field acting on one of the valence electrons is assumed in the following form corresponding to Eq. (10):

$$V_p = -\frac{(Z-N)}{r} + \sum_l V_l(r)\, P_l\,, \tag{12}$$

where the actual analytical form of the radial factor of the noncoulombic part of the pseudopotential is

$$V_l(r) = \sum_{i=1} A_l^i e^{-\alpha_l^i r^2}\,. \tag{13}$$

This form of the factor in the pseudopotential is appropriate for the correct representation of it because both the noncoulombic part of the electrostatic potential and the repulsive potential are finite. The form described by Eq. (13), which has been suggested and used formely by SCHWARZ and BARDSLEY in a different way, is very appropriate from the computational point of view [3, 9, 10]. To begin with we simplify Eq. (13) by retaining the first term only with the linear parameter A_l^1 and the nonlinear parameter α_l^1. (In the future we drop the index 1.). The two parameters can be determined by selecting those parameter values which reproduce in the Schrödinger equation the energies of the ground and first excited states of the one electron with quantum number l outside the closed shell ion. Because of the Coulombic nature of the term values with $l \geq 2$ we have neglected the corresponding noncoulombic correction terms in Eq. (12) by setting $V_l(r) \equiv 0$ for $l \geq 2$. In the actual numerical calculations variational procedure with double ζ wave functions has been applied. Bearing in mind the fact that the parameters are determined with an approximate wave function of double ζ accuracy we name the parameters correspondingly. Double ζ parameters for the Li atom determined by the aid of this procedure will be given in the text later on.

Method of molecular calculations

In order to perform molecular calculations by the aid of the above defined pseudopotential the Hamiltonian of the valence electrons is defined in the form:

$$H_v = \sum_{j=1}^{n}\left\{-\frac{1}{2}\Delta_j - \sum_k \frac{Z_k - N_k}{r_{jk}} + \sum_l \sum_k A_l e^{-\alpha_l r_{jk}^2} P_l^k\right\} + \sum_{i>j=1}^{n} \frac{1}{r_{ij}} + \sum_{u,v} \frac{(Z_u - N_u)(Z_v - N_v)}{r_{uv}}\,. \tag{14}$$

A single determinental wave function

$$\Psi = \left[\frac{1}{\det|S|(2n)!}\right]^{1/2} \det|\Phi_1(1)\bar{\Phi}_1(2)\ldots\Phi_n(2n-1)\bar{\Phi}(2n)| \tag{15}$$

is employed in which $\det|S|$ is the determinant of the overlap matrix S with the elements

$$S_{ij} = \int \Phi_i^* \Phi_j \, dv \,. \tag{16}$$

Φ_i and $\bar{\Phi}_i$ are molecular orbitals with spin α and β. The energy expression is given by the aid of Eqs. (14) and (15) to be

$$E = 2\sum_{jk}(j|k)T_{jk} + \sum_{kl\,pq}(kl|pq)[2T_{kl}T_{pq} - T_{kq}T_{lp}] + \sum_{u,v}\frac{(Z_u - N_u)(Z_v - N_v)}{r_{u,v}}, \tag{17}$$

where

$$(j|k) = \int \Phi_j^* \left\{-\frac{1}{2}\Delta - \sum_u \left[\frac{Z_u - N_u}{r_{ju}} + \sum_l A_l^u e^{-\alpha_l^u r_{ju}^2} P_l^u\right]\right\} \Phi_k \, dv \tag{18}$$

and

$$(kl|pq) = \Phi_k^*(1)\Phi_l^*(2)\, r_{12}^{-1}\Phi_p(1)\Phi_q(2)\, dv \,. \tag{19}$$

The inverse matrix T of S is defined by

$$T_{kl} = (S^{-1})_{kl} \,. \tag{20}$$

In the formulae above P_l^u is a projection operator which projects onto the angular momentum eigenfunction subspace with centre at u. Matrix elements of the operators $e^{-\alpha_l^u r_{ju}^2} P_l$ have been calculated by us and independently by SCHWARZ using floating spherical Gaussian functions

$$\Phi_i(r_j) = \left(\frac{2}{\pi\varrho_i^2}\right)^{3/4} \exp(-r_{ji}^2/\varrho_i^2) \tag{21}$$

as one-electron functions where ϱ_i is the radius of the orbital i and $r_{ji} = |\bar{r}_j - \bar{R}_i|$ is the distance of the reference point from the centre at $\bar{R}_i$ [11]. By the aid of these matrix elements the FSGO method of FROST has been extended. We call the resulting method pseudo-FSGO method. The total valence energy of the molecule in the pseudo-FSGO approximation depends on the position of the centre of the Gaussian orbitals, the orbital radii and the position of the centres of the cores which coincide with the positions of the nuclei. These quantities may be obtained by minimizing E with respect to these quantities.

We would like to emphasize that the application of the Hamiltonian described by Eq. (14) is not necessarily connected with the FSGO method.

It may be applied in any theory for atomic systems. The application is especially very easy when the basis set of the method contains exclusively Gaussian functions owing to the possibility of giving explicitly all integrals in analytical form and the great reduction in computational requirements.

Results and discussion

Model systems containing Li have been studied for the Li atom is the smallest of the atoms to which the pseudo-FSGO method can be applied. The pseudopotential parameters for Li have been determined by performing a calculation on the neutral Li atom according to the previously outlined method. Their actual values are A_s=11.4701, α_s = 3.1113 and A_p = −5.2287, α_p = 1.4464.

The Li_2 and LiH molecules have been treated in a bond orbital approximation by the aid of the pseudo-FSGO method. One floating spherical Gaussian orbital per bond has been used to describe the molecules. The nonlinear parameter, the centre of the orbital as well as the separation of the nuclei have been varied during a direct search for the minimum of the valence only total

Table I

Parameters of the Li_2 molecule[a]

Gaussian parameters		
ϱ	Distance from Lithium atoms (R)	Comments
4.35437	2.29818	R_ϱ = freely varied
Internuclear distances		
	Calculated	Experimental[b]
Li—Li	4.59636	5.05035
Energies		
	Calculated	Experimental[c]
Dissociation energies	4.81429×10^{-2}	4.05574×10^{-2}
Valence only total energy	−0.44541	−0.43763
Contributions to the calculated valence only total energy		
Kinetic	0.15822	
Electron repulsion	0.25914	
Point core-electron attraction	−1.23374	
Core-core repulsion	0.21756	
Pseudo-core-electron repulsion	0.15340	

a) All lengths and energies are given in atomic units. See [12].
b) See [13].
c) Estimated value of valence only total energy using experimental ionization potentials and bond-energies. For experimental dissociation energy of Li_2 molecule see [14].

energy of the molecule under consideration. The results of the pseudo-FSGO calculations with the above presented pseudopotential parameters for Li_2 and LiH are summarized in Tables I and II.

Table II

Parameters of the LiH molecule[a]

	Gaussian parameters	
ϱ	Distance from Hydrogen atom (R)	Comments
1.74090	0.24180	R_ϱ = freely varied
	Internuclear distances	
	Calculated	Experimental[b]
Li—H	2.30285	3.10147
	Energies	
	Calculated	Experimental[c]
Valence only total energy	—0.88727	—0.79227
	Dipole moments	
	Calculated	Experimental[d]
Dipole moment[e]	4.62381	5.882
	Contributions to the valence only total energy	
Kinetic	0.98986	
Electron repulsion	0.64816	
Point core-electron attraction	—2.76298	
Core-core repulsion	0.43424	
Pseudo-core-electron repulsion	—0.19655	

a) All lengths and energies are given in atomic units.
b) See [13].
c) Estimated values of valence only total energy using experimental ionization potentials and bond energies.
d) See [15].
e) Dipole moments are presented in Debyes.

From Table I it can be seen that the bond orbital approximation gives good results for Li_2. The calculated valence only total energy and the resulting equilibrium internuclear separation are in fair agreement with experiment. The dissociation energy of the molecule may also be calculated in good agreement with experiment. This latter result is considered by us to occur only by chance and we mention it just to be complete.

Table II shows the results for LiH. The results of the bond orbital approximation for the LiH molecule are far from the experimental values though they are not unreasonable. The LiH molecule is highly asymmetrical and contains one atomic inner core the field of which is represented by a pseudopotential and a hydrogen core, a proton with pure coulombic field. The field on the proton is much stronger than the pseudopotential field for which a

cancellation theorem exists [16]. According to this theorem in the region of the core the average value of the pseudopotential with repulsive part (in our case $l = 0$) is zero to a good approximation. Because of this, the orbital of the valence electron need not have a node in the core region and the calculation becomes insensitive to the finer details of the orbital in this region. In the field of the proton, or in a pseudopotential field with attractive terms only the detailed form of the orbital in the core region is very important. E.g. the orbital with $l = 1$ must have a nodal plane going through the origin and the value of the orbital alternates in sign on the different sides of the plane. The contribution to the energy due to the noncoulombic part in an atom or ion is proportional to the quantity $|\langle Y_l^k(\vartheta, \varphi)|\Psi\rangle_{\vartheta,\varphi}$, where Ψ is the orbital of the valence electron and the matrix element is integrated on the angular polar coordinates ϑ and φ and $Y_l^k(\vartheta, \varphi)$ are cartesian spherical harmonics. If Ψ is spherically symmetrical this quantity for $l = 1$ is zero. For Ψ with $l = 1$ and $|m'| \leq 1$ this quantity is zero for $m \neq m'$ or has a nodal plane and the value of the integrand is as small as r^2 in the core region, r being the radial distance measured from the centre of the core. In molecular calculations, where there are no pure angular momentum eigenstates (as it is the case for ions with one valence electron outside the closed shell core), the problem of the pseudopotential calculations becomes slightly different. For molecular orbitals cross terms appear which tend to over-emphasize the importance of terms with $l > 0$ in the orbital. This can be seen in Tables III and IV where we present calculations for both Li_2 and LiH with variable

Table III

Variation of molecular parameters with the linear pseudopotential parameter A_p for the LiH molecule

A_p	Orbital radius ϱ	Distance of orbital centre from proton	Li—H internuclear distance	Valence only total energy	Dipole moment (Debyes)
—1.08310	2.25316	0.33151	2.88486	—0.68515	5.64705
—2.00000	2.12468	0.30668	2.74597	—0.72052	5.42022
—3.00000	1.99358	0.28349	2.59783	—0.76472	5.16158
—4.00000	1.87191	0.26227	2.45643	—0.81540	4.91009
—5.22869	1.74090	0.24180	2.30285	—0.88727	4.62381

noncoulombic part ($l = 1$). By diminishing the absolute value of A_p the results for Li_2 change only slightly but those of LiH tend to show better agreement with experiment. The results of calculations on symmetrical XH_n hydrides such as BeH_2, BH_3, CH_4 and on C_2H_4 have been published elsewhere [17]. In these calculations the same bond orbital model as described in this article has been used. It has been observed that the high symmetry of the molecules is reflected in the centres of the bond orbitals. Because of the ob-

Table IV

Variation of molecular parameters with the linear pseudopotential parameter A_p for the Li_2 molecule[a]

A_p	Orbital radius ϱ	Li—Li internuclear distance	Valence only total energy
—1.08310	4.42991	4.61113	—0.44231
—2.00000	4.41405	4.60809	—0.44297
—3.00000	4.39624	4.60471	—0.44371
—4.00000	4.37789	4.60125	—0.44446
—5.22869	4.35781	4.59792	—0.44541

a) The centre of the bond orbital is placed in the middle point of the Li—Li distance.

served symmetry of the bond orbitals in the core region of the atoms with a pseudo core, it is always possible to form linear combinations of the bond orbitals with appropriate symmetry e.g. simulate cartesian p orbitals with nodal planes. The energetic consequence of this fact has been a most regular behaviour over the whole domain of the nonlinear variational parameters, which are in conformity with the symmetry of the molecule.

We would like to mention here again the facts we consider important in connection with the good functioning of our bond orbital model. The pseudopotential approach gives us the possibility to concentrate only on the valence shell, the energy of which is much smaller than that of the whole molecule including the inner shells too. It is the exclusion of the inner shells with the cancellation theorem in the pseudo-core region that makes possible to obtain good results by the aid of a relatively primitive bond orbital basis set. The repulsive part ($l = 0$) of the pseudopotential in the core region combined with the attractive part of the potential in the bond region imitates a pseudo harmonic force field with the consequence that Gaussian functions for the bond orbitals are good approximations. This fact will be further analyzed in a subsequent article.

An interesting extension of the above deatiled bond orbital model has also been developed. On the basis of the present model pseudopotential molecular fragments have been defined and described in detail [18]. The pseudopotential molecular fragments may be used in the development of a theory which is able to treat large organic and biomolecules with presently available electronic computers.

REFERENCES

1. H. Hellmann, Acta Physico Chem., USSR, **1**, 913, 1935; P. Gombás, Z. Physik, **94**, 473, 1935; **118**, 164, 1941.
2. P. Gombás, Pseudopotentiale, Springer-Verlag, Wien, 1967; E. Schwartz, Theoret. Chim. Acta, **11**, 307, 1968.
3. J. N. Bardsley, Case Studies in Atomic Phys., **4**, 299, 1974.

4. See e.g.V. BONIFACIC and S. HUZINAGA, J. Chem. Phys., **64**, 956, 1976;
J. J. KAUFMAN, H. E. POPKIE and H. J. T. PRESTON, Int. J. Quant. Chem., **11**, 1005, 1977.
5. See e.g. K. LADÁNYI, Acta Phys. Hung., **5**, 361, 1956;
L. SZÁSZ and G. MCGINN, J. Chem. Phys., **42**, 2363, 1965;
H. A. POHL and D. R. FOWLER, Int. J. Quant. Chem., **8**, 435, 1974.
6. A. A. FROST, J. Chem. Phys., **47**, 3707, 1967; **47**, 3714, 1967.
7. See e.g. W. A. HARRISON, Phys. Rev. B, **8**, 4487, 1973;
J. C. PHILLIPS: Covalent Bonding in Crystals, Molecules and Polymers, The University of Chicago Press, Chicago.
8. L. SZÁSZ and G. MCGINN, J. Chem. Phys., **42**, 2363, 1965; **45**, 2898, 1966;
L. SZÁSZ, Z. Naturforsch., **32***a*, 252, 829, 1977.
9. T. C. CHANG, P. HABITZ and-W. H. E. SCHWARZ, Theoret. Chim. Acta (Berl.) **44**, 61, 1977.
10. S. TOPIOL, A. A. FROST, M. A. RATNER and J. W. MOSKOWITZ, J. Chem. Phys., **65**, 4467, 1976.
11. T. C. CHANG, P. HABITZ, B. PITTEL and W. H. E. SCHWARZ, Theoret. Chim. Acta (Berl.), **34**, 263, 1974.
12. H. SHULL and G. G. HALL, Nature, **184**, 1559, 1959.
13. L. E. SUTTON, Tables of Interatomic Distances and Configurations in Molecules and Ions, Spec. Publ. No. 11. The Chemical Society, London, 1958.
14. C. H. WU, J. Chem. Phys., **65**, 2040, 1976.
15. O. SINANOGLU and K. B. WIBERG, Sigma Molecular Orbital Theory, Yale Univ. Press, New Haven, 1970.
16. M. H. COHEN and V. HEINE, Phys. Rev., **122**, 1821, 1961.
17. R. GÁSPÁR and R. GÁSPÁR, Jr., Int. J. Quant. Chem., forthcoming.
18. R. GÁSPÁR Jr. and R. GÁSPÁR, Int. J. Quant. Chem., forthcoming.

Acta Physica Academiae Scientiarum Hungaricae, Tomus 45 (1), pp. 37—74 (1978)

LATTICE DYNAMICS AND STABILITY OF ANHARMONIC CRYSTALS

By

N. M. PLAKIDA

JOINT INSTITUTE FOR NUCLEAR RESEARCH, DUBNA
SU—101000 MOSCOW, HEAD POST OFFICE P.O.B. 79, USSR

and

T. SIKLÓS

CENTRAL RESEARCH INSTITUTE FOR PHYSICS
H—1525 BUDAPEST, P.O.B. 49, HUNGARY

(Received 27. VI. 1978)

The self-consistent phonon theory (SCPT) is formulated using Green's function method to describe both the dynamical and thermodynamical properties of highly anharmonic crystals and to investigate the dynamical stability of anharmonic lattices. The results of calculations for the phonon spectrum, elastic constants, PV-diagrams, etc., are presented for a simple model of the *fcc* lattice. The phenomenon of lattice instability due to the volume fluctuations at sufficiently high temperatures or as a consequence of a high zero-point energy is investigated. An application of the SCPT to structural (or ferroelectric) phase transitions (PT) is also discussed. In that case taking into account the fluctuations of the order parameter by the SCPT results in the renormalization of the Landau expansion and in a first order PT. A unified model for ferroelectric PT, where both the statistical disorder and the instability of lattice in the PT are taken into account, is shortly reviewed.

1. Introduction

In recent years the BORN—VON KÁRMÁN theory of lattice dynamics [1] has been reformulated in order to account for highly anharmonic crystals with so large vibrational motion that the conventional harmonic version of their theory is inapplicable. This generalised version, the so called self-consistent phonon theory (SCPT) of lattice dynamics has been reviewed in several papers [2]—[10] recently. Since in the SCPT anharmonic interactions are incorporated in the theory from the beginning the interesting phenomenon of anharmonic lattice instability can be investigated. With increasing temperature lattice vibrations in any solid become so intensive that the crystal as a bound state of atoms, can be destroyed. Though in reality the crystal will melt before this phenomenon could take place an upper bound of a given crystalline state can be estimated by the SCPT of lattice dynamics. Besides this instability of the lattice as a whole, there are a large number of examples of structural phase transitions driven by one (or several) unstable phonon mode. In this case the SCPT can also be applied to the investigation of the lattice dynamics of crystals with unstable modes and to get an estimation of the temperature of possible structural phase transitions.

One of the first investigations of the lattice stability was performed by BORN [11] in the so called quasiharmonic approximation. He has calculated the elastic constants for a model *bcc* lattice and found the temperature T_0 for which they vanish. Though T_0 appears to be close to the melting temperature, T_m, from this calculation one cannot find the latter, since melting is a first order phase transition and both crystalline and liquid phases should be considered (see, e.g. [12]). Furthermore the quasiharmonic approximation becomes unreliable at temperatures as high as T_m [4].

The SCPT, however, can be applied in the investigation of anharmonic lattice instability, since it can properly take into account the highly anharmonic vibrational motion near the instability point. At first the instability of the anharmonic one-dimensional linear chain was considered independently in [2] and [13] and later more general models were discussed [14]—[22]. Crystalline order and instability of highly anharmonic crystals on the basis of rigorous equations for the displacement-correlation function were discussed by MEISSNER [23]. Semiphenomenological theories of melting and lattice instability of anharmonic crystals, relevant to the present discussion, were given in [24]—[26].

Structural phase transitions were also investigated using the SCPT for simple models of ferroelectrics [9] and molecular crystals [27].

The present paper is devoted mainly to the discussion of lattice stability in highly anharmonic crystals. This problem, seemingly, has not yet found a proper formal and general presentation in the literature on the basis of the SCPT. In the next Section the Hamiltonian and the equilibrium conditions for an anharmonic crystal are discussed and the method of Green's functions is introduced. In Section 3 the SCPT is formulated in a rather simple but general way on the basis of Green's functions. The stability of certain models of anharmonic crystals is considered in Section 4 and the structural phase transition is described using the SCPT in Section 5. Conclusions are presented in the last Section.

2. Description of anharmonic crystals

2.1 *The Hamiltonian*

Let us consider a crystal in the adiabatic approximation [1] when it can be described by the Hamiltonian:

$$H = \sum_i \frac{p_i^2}{2M_i} + U(R_i) \tag{2.1}$$

with the local potential energy $U(R_i)$ depending only on the coordinates

$R_i = R_s^\alpha = R^\alpha \begin{pmatrix} l \\ \varkappa \end{pmatrix}$ of the atom of type $\varkappa = 1, 2, \ldots, r$ in the unit cell l; $\alpha = (x, y, z)$; $p_i = p_s^\alpha = -i\hbar\nabla_s^\alpha$ is the momentum operator and $M_i = M_\varkappa$ is the mass of the $\varkappa$-th type of atom. For the anharmonic crystal the equilibrium positions of atoms $x_i = \langle R_i \rangle = x^\alpha \begin{pmatrix} l \\ \varkappa \end{pmatrix}$ are temperature dependent and should be obtained from the equilibrium conditions. Let us apply an external static field with forces F_i acting on atoms at R_i

$$H_1 = -\sum_i F_i R_i = -\sum_{s\alpha} F_s^\alpha R_s^\alpha . \tag{2.2}$$

From the equation of motion for the momentum operator in the Heisenberg representation

$$p_i(t) = e^{i\mathcal{H}t} p_i e^{-i\mathcal{H}t} ; \qquad \mathcal{H} = H + H_1 , \tag{2.3}$$

one gets the equilibrium conditions in the form

$$\frac{d}{dt}\langle p_i(t)\rangle = \langle [\mathcal{H}, ip_i]\rangle = F_i - \left\langle \frac{\partial U}{\partial R_i} \right\rangle = 0 . \tag{2.4}$$

From thermodynamical considerations and Eq. (2.4) follows an equation for the stress tensor

$$\sigma_{\alpha\beta} = \frac{1}{V}\sum_s x_s^\alpha F_s^\beta = \frac{1}{V}\sum_s x_s^\alpha \langle \nabla_s^\beta U(R_i)\rangle \tag{2.5}$$

or for the pressure

$$P = -\frac{1}{3}\sum_\alpha \sigma_{\alpha\alpha} = -\frac{1}{3V}\sum_{\alpha s} x_s^\alpha \langle \nabla_s^\alpha U(R_i)\rangle , \tag{2.6}$$

where V is the volume of the crystal of N unit cells. The statistical average in Eqs. (2.4)—(2.6) is taken over the canonical ensemble:

$$\langle A\rangle = Tr\{e^{-\beta\mathcal{H}} A\}/Tr\{e^{-\beta\mathcal{H}}\} ; \qquad \beta = \frac{1}{kT} . \tag{2.7}$$

The lattice parameters can be obtained also directly from the partition function:

$$x_i = \langle R_i\rangle = \frac{1}{\beta}\frac{\partial}{\partial F_i} \ln Tr\{e^{-\beta\mathcal{H}}\} . \tag{2.8}$$

Now introducing the dynamical displacements of the atoms $u_i = R_i - x_i = u^\alpha \begin{pmatrix} l \\ \varkappa \end{pmatrix}$, the Hamiltonian (2.1) can be written as

$$H = \sum_i \frac{p_i^2}{2M_i} + U_0(x_i) + \sum_{n=1}^{\infty} \frac{1}{n!} \sum_{1\ldots n} \Phi_{1\ldots n} u_1 \ldots u_n , \tag{2.9}$$

where the coefficients of the Taylor expansion

$$\Phi_{1\ldots n} = \nabla_1 \ldots \nabla_n U_0(x_i) \equiv \Phi^{\alpha_1}_{l_1 \varkappa_1 \ldots l_n \varkappa_n}{}^{\alpha_n} \tag{2.9a}$$

are symmetric functions of the index $(1\ldots n)$ and satisfy several conditions which follow from the invariance of the lattice under translations and rotations [1].

2.2 *The Green's functions*

Various dynamical and thermodynamical properties of the anharmonic crystal can be discussed in terms of the Green's function (GF). Following [10], [13], [14] let us consider the thermodynamic GF [28]:

$$G_{ii'}(t - t') = \langle\langle u_i(t)\,;\; u_{i'}(t')\rangle\rangle = \int_{-\infty}^{\infty} \frac{d\omega}{2\pi} e^{-i\omega(t-t')} \langle\langle u_i | u_{i'}\rangle\rangle_\omega \tag{2.10}$$

in usual notations [29]. The spectral representation for it has the form

$$G_{ij}(\omega) = \frac{1}{2\pi} \int_{-\infty}^{\infty} \frac{d\omega'}{\omega - \omega'} (e^{\beta\omega'} - 1) J_{ij}(\omega')\,, \tag{2.11}$$

where the Fourier transform $J_{ij}(\omega)$ for the correlation function

$$\langle u_i(t)\, u_j\rangle = \int_{-\infty}^{\infty} \frac{d\omega}{2\pi} e^{i\omega t} J_{ij}(\omega) \tag{2.12}$$

is real and has the properties

$$J_{ij}(\omega) = J_{ji}(\omega) = e^{-\beta\omega} J_{ij}(-\omega) = (e^{\beta\omega} - 1)^{-1}[-2\,Im\, G_{ij}(\omega + i\varepsilon)]\,, \tag{2.13}$$
$$\varepsilon \to 0^+$$

since the displacement operators u_i are hermitian. The GF (2.11) obeys the sum rules [29]:

$$\int_{-\infty}^{\infty} \omega\, d\omega \left[-\frac{1}{\pi} Im\, G_{ij}(\omega + i\varepsilon)\right] = \frac{1}{M_i}\,\delta_{ij}\,, \tag{2.14}$$

$$\int_{-\infty}^{\infty} \omega^3\, d\omega \left[-\frac{1}{\pi} Im\, G_{ij}(\omega + i\varepsilon)\right] = \frac{1}{M_i M_j} \langle \nabla_i \nabla_j U(R_i)\rangle\,. \tag{2.15}$$

In the discussion of the anharmonic properties of the lattice an (n, n')-point GF of the type $\langle\langle A_n(t); A_{n'}(t')\rangle\rangle$, where $A_n(t) = \{u_1(t) \ldots u_n(t) - \langle u_1 \ldots u_n\rangle\}$ and $A_{n'}(t') = \{u_{1'}(t') \ldots u_{n'}(t') - \langle u_{1'}, \ldots u_{n'}\rangle\}$ will appear for which the representations similar to Eqs. (2.11)—(2.13) hold.

In the translationally invariant lattice the GF (2.10) depends only on the difference of the coordinates and the Fourier transformation for it can be written in the form:

$$\langle\langle u_s^\alpha \,|\, u_{s'}^\beta \rangle\rangle_\omega = \frac{1}{N} \sum_{\mathbf{q}jj'} \frac{e_{\mathbf{q}j}^{*\alpha}(\varkappa)\, e_{\mathbf{q}j'}^{\beta}(\varkappa')}{\sqrt{M_\varkappa M_{\varkappa'}}}\, e^{-i\mathbf{q}(\mathbf{x}_s - \mathbf{x}_{s'})} G_{jj'}(\mathbf{q}, \omega)\,. \tag{2.16}$$

Here for each wave vector $\mathbf{q} = \langle \mathbf{q}_1, \ldots, \mathbf{q}_N \rangle$ the set of polarization vectors $\mathbf{e}_{\mathbf{q}j'}(\varkappa)$; $j = \langle 1 \ldots 3r \rangle$ satisfying the orthonormality and closure conditions:

$$\begin{aligned} \sum_{\varkappa,\alpha} e_{\mathbf{q}j}^{*\alpha}(\varkappa)\, e_{\mathbf{q}j'}^{\alpha}(\varkappa) &= \delta_{jj'}\,, \\ \sum_{j} e_{\mathbf{q}j}^{*\alpha}(\varkappa)\, e_{\mathbf{q}j}^{\beta}(\varkappa') &= \delta_{\alpha\beta}\, \delta_{\varkappa\varkappa'} \end{aligned} \tag{2.17}$$

are introduced.

The physical meaning of the retarded GF (2.16) follows from linear response theory [29]: the energy of phonon-like excitations at given $(\mathbf{q}, j)$ measured by inelastic neutron scattering, are defined by the imaginary part of the GF:

$$q_{j=j'}(\mathbf{q}, \omega) = -\frac{1}{\pi}\, Im\, G_{j=j'}(\mathbf{q}, \omega + i\varepsilon)\,. \tag{2.18}$$

The position and the width of the maximum of (2.18) give the energy and the inverse life-time of the excitations, respectively. The long-wavelength ($\mathbf{q} \to 0$) limit of the static ($\omega = 0$) self-energy of the GF defines the isothermal elastic constants [30].

Therefore the dynamical properties of the lattice are well defined by the GF (2.16) and a direct comparison between theory and experiment is possible.

2.3 *The free energy and the internal energy of the anharmonic crystal*

To discuss the thermodynamical properties of the anharmonic crystal its free energy should be calculated. The most elegant way for doing this is to integrate the GF over the formal coupling constant λ [31]. For the anharmonic lattice Hamiltonian, Eq. (2.9) λ can be introduced in the form:

$$H(\lambda) = H_0 + H_1(\lambda)\,, \tag{2.19}$$

$$H_0 = \sum_i \frac{p_i^2}{2M_i} + U_0(x_i) + \frac{1}{2} \sum_{ij} \Phi_{ij}^0\, u_i\, u_j\,, \tag{2.19a}$$

$$H_1(\lambda) = \sum_{n=1}^{\infty} \frac{\lambda^n}{n!} \sum_{1\ldots n} \Phi_{1\ldots n}\, u_1 \ldots u_n - \frac{\lambda^2}{2} \sum_{ij} \Phi_{ij}^0\, u_i\, u_j\,. \tag{2.19b}$$

Then for the free energy

$$F(\lambda) = -\frac{1}{\beta} \ln Tr\{e^{-\beta H(\lambda)}\} = -\frac{1}{\beta} \ln Z(\lambda) \tag{2.20}$$

one obtains the equation

$$\frac{\partial F(\lambda)}{\partial \lambda} = \frac{1}{Z(\lambda)} Tr\left\{e^{-\beta H(\lambda)} \frac{\partial H_1(\lambda)}{\partial \lambda}\right\} \equiv \left\langle \frac{\partial H_1(\lambda)}{\partial \lambda} \right\rangle_\lambda , \tag{2.21}$$

To express F in terms of GF, Eq. (2.10), consider an equation of motion for the GF with the Hamiltonian (2.19)

$$\sum_j \{M_i \omega^2 \delta_{ij} - \Phi^0_{ij}\} G_{ji'}(\omega) = \delta_{ii'} +$$

$$+ \sum_{n=2}^{\infty} \frac{\lambda^n}{(n-1)!} \sum_{2\ldots n} \Phi_{i2\ldots n} \langle\langle u_2 \ldots u_n | u_{i'} \rangle\rangle_\omega - \lambda^2 \sum_j \Phi^0_{ij} G_{ji'}(\omega) \equiv$$

$$\equiv \delta_{ii'} + \sum_j \Pi_{ij}(\lambda, \omega) G_{ji'}(\omega) . \tag{2.22}$$

After integrating its imaginary part using Eqs. (2.12) and (2.13) one gets the right hand side of (2.21) and the free energy in the form

$$F - F_0(\lambda = 0) = \int_0^1 d\lambda \left\langle \frac{\partial H_1}{\partial \lambda} \right\rangle_\lambda =$$

$$= \int_0^1 \frac{d\lambda}{\lambda} \frac{1}{2\pi} \int_{-\infty}^{\infty} \frac{d\omega}{e^{\beta\omega} - 1} \sum_{ij} (M_i \omega^2 \delta_{ij} - \Phi^0_{ij}) [-2 Im G_{ij}(\omega + i\varepsilon)] =$$

$$= \int_0^1 \frac{d\lambda}{\lambda} \frac{i}{2\pi} \int_C \frac{dz}{e^{\beta z} - 1} \sum_{ij} \Pi_{ij}(\lambda z) G_{ij}(z) , \tag{2.23}$$

where in the last line the integration over the complex variable z is performed along the contour C of two straight lines: $(-\infty + i\varepsilon) \to (\infty + i\varepsilon)$ and $(\infty - i\varepsilon) \to (-\infty - i\varepsilon)$. Deforming the contour C to circle the imaginary axes of z one obtains, by counting the residues from the poles of $(e^{\beta z} - 1)^{-1}$ at $z_n = (2\pi i n/\beta)$, the same result as in [32] based on the imaginary time GF [31].

The internal energy of the anharmonic crystal apart from being calculated thermodynamically from the free energy (2.23) can be obtained in a more direct way by writing it in the form

$$E = \langle H \rangle = \langle T \rangle + \langle U(x_i + u_i) \rangle , \tag{2.24}$$

where the average kinetic energy is easily expressed in terms of GF with the help of Eqs. (2.12), (2.13) as:

$$\langle T \rangle = \sum_i \frac{1}{2M_i} \langle p_i^2 \rangle = \int_0^\infty \omega^2 d\omega \coth \frac{\beta\omega}{2} \sum_i \frac{M_i}{2} \left[-\frac{1}{\pi} Im G_{ii}(\omega + i\varepsilon) \right]. \tag{2.25}$$

The average potential energy can be written in the form of a cumulant expansion:

$$\langle U(x_i + u_i)\rangle = \langle \exp\{\Sigma\, u_i \nabla_i\}\rangle\; U_0(x_i) =$$

$$= \exp\left\{\sum_{n=2}^{\infty} \frac{1}{n!} \sum_{1\ldots n}^{\infty} \langle u_1 \ldots u_n\rangle^c \nabla_1 \ldots \nabla_n\right\} U_0(x_i)\,, \tag{2.26}$$

where the cumulants $\langle u_1 \ldots u_n\rangle^c$ can also be defined from the GF as it will be shown in the next Section. Then from a given approximation for the self-energy $\Pi_{ij}(\omega)$ and GF in (2.23), (2.25) and (2.26) one obtains a corresponding approximate value for the thermodynamical functions.

Therefore the dynamical as well as the thermodynamical properties of anharmonic crystals can be investigated by means of GF. This procedure greatly simplifies the calculations and allows one to perform them in a unified self-consistent manner.

3. Self-consistent phonon theory

3.1 *Irreducible GF*

Consider an equation of motion for the GF (2.10) by differentiating it twice with respect to the time t and performing the necessary commutations. Then for the Fourier transform of the GF one gets

$$M_i \omega^2 G_{ii'}(\omega) = \delta_{ii'} + \sum_{n=1}^{\infty} \frac{1}{n!} \sum_{1\ldots n} \Phi_{i1\ldots n} \langle\langle u_1 \ldots u_n \,|\, u_{i'}\rangle\rangle_\omega\,, \tag{3.1}$$

where the symmetry properties of (2.9a) were taken into account. There is a large class of n-point (multi-phonon) GF in (3.1) that describes an uncorrelated propagation of phonons in an averaged phonon field. This class should be summed up not only for the simplification of further calculations but also for physical reasons: in highly anharmonic crystals atoms do not move in a static field but rather in the dynamic potential of their vibrating neighbours and this renormalization should be taken into account from the beginning. Therefore we introduce the irreducible (or cumulant) GF [33] that have no disconnected parts of average field renormalization

$$\langle\langle u_1 \ldots u_n \,|\, u_{i'}\rangle\rangle^{\mathrm{irr}} = \langle\langle u_1 \ldots u_n \,|\, u_{i'}\rangle\rangle -$$

$$- \sum_{m=1}^{n-1} C_n^{n-m} \langle u_{m+1} \ldots u_n\rangle \langle\langle u_1 \ldots u_m \,|\, u_{i'}\rangle\rangle^{\mathrm{irr}}\,. \tag{3.2}$$

Here the symmetry with respect to permutations of the commuting operators $u_1 \ldots u_n$ has been taken into account and the corresponding coefficient

$C_n^{n-m} = C_n^m = n!/m!(n-m)!$ was introduced. The GF (3.2) cannot be reduced to lower order ones by the usual decoupling procedure [29] and so it describes the correlations between n-particle vibrations. The definition (3.2) can be rewritten in the form of the decomposition for the n-point GF as the sum of the irreducible ones:

$$\langle\langle u_1 \dots u_n | u_{i'} \rangle\rangle = \sum_{m=1}^{n} C_n^m \langle u_{m+1} \dots u_n \rangle \langle\langle u_1 \dots u_m | u_{i'} \rangle\rangle^{\text{irr}}. \tag{3.2a}$$

By using a spectral representation of the type given in Eqs. (2.12), (2.13) one gets from (3.2a) the decomposition for the n-point correlation functions in terms of the irreducible (or cumulant) ones:

$$\langle u_1 \dots u_n \rangle = \sum_{m=1}^{n-1} C_{n-1}^m \langle u_{m+2} \dots u_n \rangle (\langle u_1 \dots u_{m+1} \rangle^c). \tag{3.3}$$

In obtaining Eq. (3.3) some obvious changes of indices have been performed in Eq. (3.2a).

Substituting now (3.2a) into the equation (3.1) and performing the summation at first over n for each m-particle irreducible GF and then over all m, one obtains:

$$\sum_j (M_i \omega^2 \delta_{ij} - \tilde{\Phi}_{ij}) G_{ij'}(\omega) = \delta_{ii'} + \sum_{n=2}^{\infty} \frac{1}{n!} \sum_{1 \dots n} \tilde{\Phi}_{i1 \dots n} \langle\langle u_1 \dots u_n | u_{i'} \rangle\rangle^{\text{irr}}, \tag{3.4}$$

where the renormalized interaction has the form:

$$\begin{aligned} \tilde{\Phi}_{1 \dots n} &= \sum_{n'=0}^{\infty} \frac{1}{n'!} \sum_{1' \dots n'} \Phi_{1 \dots n, 1' \dots n'} \langle u_{1'} \dots u_{n'} \rangle = \langle \nabla_1 \dots \nabla_n U(x_i + u_i) \rangle = \\ &= \nabla_1 \dots \nabla_n \exp \left\{ \sum_{n'=2}^{\infty} \frac{1}{n'!} \sum_{1' \dots n'} \langle u_{1'} \dots u_{n'} \rangle^c \nabla_{1'} \dots \nabla_{n'} \right\} U_0(x_i). \end{aligned} \tag{3.5}$$

The cumulant expansion in the last line (as well as in (2.26)) follows from the equation [34]:

$$\frac{\partial}{\partial \lambda} \langle U(\lambda) \rangle = \frac{\partial}{\partial \lambda} \sum_{n=0}^{\infty} \frac{\lambda}{n!} \sum_{1 \dots n} \Phi_{1 \dots n} \langle u_1 \dots u_n \rangle \tag{3.6}$$

that can be easily solved in the form (2.26) by introducing the expansion (3.3) and performing the summation over n and m in the same manner as in (3.4).

To obtain the equation of motion for the n-point irreducible GF in Eq. (3.4) let us differentiate the operator $u_{i'}(t')$ with respect to t'. Then taking into account the identity

$$\langle [u_1 \dots u_n, i p_{i'}] \rangle^{\text{irr}} = 0 \qquad (n \geq 2)$$

that follows from the definition (3.2), and introducing the same decomposition as in Eq. (3.2a) for the operators $\langle u_{1'}(t') \dots u_{n'}(t') \rangle$ on the right hand side of the (n, n')-point GF, one gets

$$\sum_{j'} \{M_{i'} \omega^2 \delta_{i'j'} - \tilde{\Phi}_{i'j'}\} \langle\langle u_1 \dots u_n \,|\, u_{j'} \rangle\rangle_\omega^{\text{irr}} = \sum_{n'=2}^{\infty} \frac{1}{n'!} \sum_{1' \dots n'} \tilde{\Phi}_{i'1' \dots n'} G^{\text{irr}}_{1 \dots n, 1' \dots n'}(\omega), \tag{3.7}$$

where

$$G^{\text{irr}}_{1 \dots n, 1' \dots n'}(\omega) = \langle\langle u_1 \dots u_n \,|\, u_{1'} \dots u_{n'} \rangle\rangle^{\text{irr}}_\omega$$

is the (n, n')-point GF irreducible both in the n-point and n'-point parts of it.

Now it is convenient to define the zero order GF by the equation

$$\sum_j (M_i \omega^2 \delta_{ij} - \tilde{\Phi}_{ij}) G^0_{ji'}(\omega) = \delta_{ii'}, \tag{3.8}$$

which describes the undamped vibrations (or one-phonon propagation) in an average phonon field. Then solving the matrix equations (3.4) and (3.7) with the help of Eq. (3.8) one gets for the GF:

$$G_{ii'}(\omega) = G^0_{ii'}(\omega) + \sum_{jj'} G^0_{ij} P_{jj'}(\omega) G^0_{j'i'}(\omega), \tag{3.9}$$

where the scattering matrix is defined by

$$P_{jj'}(\omega) = \sum_{n,n'=2}^{\infty} \frac{1}{n!\, n'!} \sum_{\substack{1 \dots n \\ 1' \dots n'}} \Phi_{j1 \dots n} G^{\text{irr}}_{1 \dots n, 1' \dots n'}(\omega) \tilde{\Phi}_{j'1' \dots n'}. \tag{3.10}$$

Then the one-phonon GF can be written in the form of the Dyson equation

$$G_{ii'}(\omega) = \{M_i \omega^2 \delta_{ii'} - \tilde{\Phi}_{ii'} - \Pi_{ii'}(\omega)\}^{-1}, \tag{3.11}$$

where the self-energy operator $\Pi_{ii'}(\omega)$ is given by the proper part (p) of the scattering matrix (3.10): $\Pi_{ii'}(\omega) = P^{(p)}_{ii'}(\omega)$. According to Eqs. (3.9) and (3.11) $\Pi_{ii'}$ satisfies the equation:

$$P_{ii'}(\omega) = \Pi_{ii'}(\omega) + \sum_{jj'} \Pi_{ij}(\omega) G^0_{jj'}(\omega) P_{j'i'}(\omega). \tag{3.12}$$

Hence, the self-energy operator $\Pi_{ii'}(\omega)$ has the same form as Eq. (3.10) where the (n, n')-point GF is replaced by its proper part $K_{1 \dots n, 1' \dots n'}(\omega) = G^{(\text{irr}, p)}_{1 \dots n, 1' \dots n'}(\omega)$. $K(\omega)$ according to Eq. (3.12) cannot be cut into two pieces by cutting only one G^0-line; G^0 is defined by Eq. (3.8).

The n-point irreducible GF in (3.7) can also be written in terms of $K_{1\ldots n,1'\ldots n'}(\omega)$ if one uses Eqs. (3.8)—(3.12):

$$\langle\langle u_1 \ldots u_n \,|\, u_{i'}\rangle\rangle_\omega^{\mathrm{irr}} = \sum_{j'} G^0_{i'j'}(\omega) \sum_{n'=2}^{\infty} \frac{1}{n'!} \sum_{1'\ldots n'} \tilde{\Phi}_{j'1'\ldots n'} G^{\mathrm{irr}}_{1\ldots n,1'\ldots n'}(\omega) =$$

$$= \sum_{j'} G_{i'j'}(\omega) \sum_{n'=2}^{\infty} \frac{1}{n'!} \sum_{1'\ldots n'} \tilde{\Phi}_{j'1'\ldots n'} K_{1\ldots n,1'\ldots n'}(\omega)\,. \quad (3.13)$$

Then from the spectral representation, Eqs. (2.11)—(2.13) for the cumulant part of the correlation functions one gets:

$$\langle u_1 \ldots u_n\rangle^c = \int_{-\infty}^{\infty} \frac{d\omega}{e^{\beta\omega} - 1} \left[-\frac{1}{\pi} Im \langle\langle u_2 \ldots u_n \,|\, u_1\rangle\rangle^{\mathrm{irr}}_{\omega + i\varepsilon} \right] =$$

$$= 2\, Im \int_0^{\infty} dt \sum_{n'=3}^{\infty} \frac{1}{(n'-1)!} \sum_{1'\ldots n'} \tilde{\Phi}_{1'\ldots n'} \langle u_1(t)\, u_{1'}\rangle \langle u_2(t) \ldots u_n(t) \,|\, u_{2'} \ldots u_{n'}\rangle^{\mathrm{irr},p}, \quad (3.14)$$

where a two-time proper irreducible correlation function, corresponding to $K_{2\ldots n,2'\ldots n'}(t)$, has been introduced.

Thus the one-phonon GF Eq. (3.11) as well as the cumulants (3.14) in the renormalized interaction (3.5) are written in terms of the (n, n')-point GF $K_{1\ldots n,1'\ldots n'}(\omega) = \langle\langle u_1 \ldots u_n \,|\, u_{1'} \ldots u_{n'}\rangle\rangle^{\mathrm{irr},p}_\omega$. The equations obtained are exact but unclosed and therefore some approximations to the $K_{1\ldots n,1'\ldots n'}(\omega)$ should be considered in order to obtain a self-consistent system of equations.

3.2 *First order or renormalized harmonic approximation*

In the first order of the SCPT (SCl) only the renormalization of phonons in the self-consistent field is taken into account. Thus the SCl is obtained by neglecting all the terms which contribute to the damping (or correlations) of phonons. In that case the self-energy operator $\Pi_{ii'}(\omega)$ in the GF (3.11) and the cumulants (3.14) for $n \geq 3$ should be put equal to zero. Therefore the SCl GF is equal to the zero order one (3.8) with the renormalized pseudo-harmonic force-constant matrix

$$\tilde{\Phi}^{(1)}_{ij} = \nabla_1 \nabla_2 \exp\left\{ \frac{1}{2} \sum_{1,2} \langle u_1\, u_2\rangle \nabla_1 \nabla_2 \right\} U_0(x_i) \equiv \nabla_i \nabla_j \tilde{U}_1(x_i)\,. \quad (3.15)$$

The system of equations gets closed by the equation for the pair-correlation function in (3.15). From the spectral representation Eqs. (2.12), (2.13) and (2.16), one gets

$$\langle u^\alpha_s u^\beta_{s'}\rangle = \sum_{qj} \frac{1}{N} \frac{e^{*\alpha}_{qj}(\varkappa)\, e^\beta_{qj}(\varkappa')}{\sqrt{M_\varkappa M_{\varkappa'}}} \frac{1}{2\omega_{qj}} \coth \frac{\beta\omega_{qj}}{2}\, e^{-iq(x_s - x_{s'})}\,, \quad (3.16)$$

where the frequencies ω_{qj} and the polarization vectors $\mathbf{e}_{qj}(\varkappa)$ are defined by the equation

$$\omega_{qj}^2 e_{qj}^{\alpha}(\varkappa) = \sum_{\beta s'} e_{qj}^{\beta}(\varkappa') \frac{1}{\sqrt{M_{\varkappa} M_{\varkappa'}}} \tilde{\Phi}_{ss'}^{(1)\alpha\beta} e^{-iq(\mathbf{x}_s - \mathbf{x}_{s'})} . \tag{3.17}$$

The free energy (2.23) in SCl is obtained by using the mean-field self-energy operator (2.22):

$$\Pi_{ij}^{(1)}(\lambda) = \lambda^2 \{\tilde{\Phi}_{ij}^{(1)}(\lambda) - \Phi_{ij}^0\} = \lambda^2 \left\{ \nabla_i \nabla_j \exp\left(\frac{\lambda^2}{2} \sum_{1,2} \langle u_1 u_2 \rangle \nabla_1 \nabla_2 \right) U_0(x_i) - \Phi_{ij}^0 \right\} . \tag{3.18}$$

So one finds

$$F_1 = F_0 + \int_0^1 \frac{d\lambda}{\lambda} \sum_{ij} \Pi_{ij}^{(1)}(\lambda) \langle u_i u_j \rangle_0 = F_0 + \tilde{U}_1(x_i) - U_0(x_i) - \frac{1}{2} \sum_{ij} \Phi_{ij}^0 \langle u_i u_j \rangle_0 . \tag{3.19}$$

The trial force-constant matrix Φ_{ij}^0 in (2.19) has not been specified yet. From the self-consistency condition Φ_{ij}^0 should be put equal to $\tilde{\Phi}_{ij}^{(1)}$ in (3.15) since the latter one defines the spectrum of excitations in SCl according to (3.17). Then for the free energy one gets

$$F_1 = \tilde{U}_1(x_i) + \frac{1}{\beta} \sum_{qj} \ln \left(2 \sinh \frac{\beta \omega_{qj}}{2} \right) - \frac{1}{4} \sum_{qj} \omega_{qj} \coth \frac{\beta \omega_{qj}}{2} , \tag{3.19a}$$

which coincides with that obtained from the variational approach:

$$\frac{\delta F_1}{\delta \Phi_{ij}^0} = 0, \qquad \Phi_{ij}^0 = \tilde{\Phi}_{ij}^{(1)} .$$

For the internal energy (2.24) one easily obtains from Eqs. (2.25) and (2.26) in the SCl

$$E_1 = \frac{1}{4} \sum_{qj} \omega_{qj} \coth \frac{\beta \omega_{qj}}{2} + \tilde{U}_1(x_i) . \tag{3.20}$$

Therefore in the SCl approximation one treats the vibrations of an anharmonic crystal as a system of noninteracting pseudoharmonic phonons with the δ-function type behaviour for the phonon spectrum (2.18). This approximation simplifies the calculations; but due to this approximation all the odd terms in the anharmonic interaction (2.9a) are missing. One should not hope to obtain a quantitative description in SCl: even in the limit of weak anharmonicity the results do not coincide with those of the ordinary perturbation theory (see, e.g. [4]).

3.3 *Second order of SCPT*

Since the self-energy operator $\Pi_{ii'}(\omega)$ in the GF (3.11) on account of (3.10) is proportional to the second order of the renormalized anharmonic interaction (3.5) one should calculate the (n, n')-point GF in the lowest order. This is done by taking in account only the uncorrelated propagation of $n = n'$ "dressed" phonons and results in the following approximation for the (n, n')-point two-time correlation function ($n \geq 2$):

$$\langle u_1(t) \ldots u_n(t) \,|\, u_{1'} \ldots u_{n'} \rangle^{\mathrm{irr},\, p} \approx n!\, \delta_{nn'} \prod_{i=1}^{n} \langle u_i(t)\, u_{i'} \rangle \,. \tag{3.21}$$

Now employing the spectral representation for the (n, n')-point GF one obtains for the self-energy operator in the second order of the SCPT (SC2)

$$\Pi^{(2)}_{ii'}(\omega) = \int_{-\infty}^{\infty} \frac{d\omega'}{\omega - \omega'} (e^{\beta\omega'} - 1) \int_{-\infty}^{\infty} \frac{dt}{2\pi} e^{-i\omega' t} \times$$

$$\times\, !\sum_{n=2}^{\infty} \frac{1}{n!} \left(\sum_{jj'} \langle u_j(t)\, u_{j'} \rangle \nabla_j \nabla_{j'} \right)^n \langle \nabla_i U(x_i + u_i) \rangle \langle \nabla_{i'} U(x_{i'} + u_{i'}) \rangle, \tag{3.22}$$

where $\nabla_j = \partial/\partial x_j$ and $\nabla_{j'} = \partial/\partial x_{j'}$ are acting on $U(x_i)$ and $U(x_{i'})$, respectively. For the cumulants (3.14) one gets in the same SC2 approximation (3.21):

$$\langle u_1 \ldots u_n \rangle^c \approx 2\, Im \int_0^{\infty} dt \prod_{i=1}^{n} \left\{ \sum_{i'} \langle u_i(t)\, u_{i'} \rangle \nabla_{i'} \right\} \langle U(x_{i'} + u_{i'}) \rangle. \tag{3.23}$$

The equation for the pair correlation function

$$\langle u_i(t)\, u_j \rangle = \int_{-\infty}^{\infty} \frac{d\omega}{e^{\beta\omega} - 1} e^{i\omega t} \left[-\frac{1}{\pi} Im \{ \omega^2 M_i \delta_{ij} - \tilde{\Phi}_{ij} - \Pi^{(2)}_{ij}(\omega + i\varepsilon) \}^{-1} \right] \tag{3.24}$$

closes the system of self-consistent equations (3.5), (3.22)—(3.24). In the present form the SC2 system of equations can be applied for anharmonic crystals with strong repulsive interactions since only fully renormalized vertices $\tilde{\Phi}_{1\ldots n}$ (3.5) appear in the Eqs. (3.22), (3.23), as in the HORNER theory [6]. But just due to the full renormalization of the vertices the system of equations is rather untractable. To solve it one should either introduce a trial short-range correlation function $\hat{g}_{\mathrm{sr}}(x_i)$ in Eq. (3.5):

$$\langle U(x_i + u_i) \rangle = \exp \left\{ \sum_{n=3}^{\infty} \frac{1}{n!} \sum_{1\ldots n} \langle u_1 \ldots u_n \rangle^c \nabla_1 \ldots \nabla_n \right\} \tilde{U}_1(x_i) \equiv \hat{g}_{\mathrm{sr}}(x_i)\, \tilde{U}_1(x_i) \,, \tag{3.25}$$

or, employing some cut-off procedure for the strong repulsive part of the interaction expand (3.25) in powers of cumulants:

$$\langle U(x_i + u_i)\rangle \approx \left\{1 + \sum_{n=3}^{\infty} \frac{1}{n!} \sum_{1\ldots n} \langle u_1 \ldots u_n\rangle^c \nabla_1 \ldots \nabla_n + \ldots\right\} \widetilde{U}_1(x_i) =$$

$$= \widetilde{U}_1(x_i) + \Delta\widetilde{U}_2(x_i) + \ldots . \tag{3.26}$$

The renormalized potential energy in the pseudoharmonic approximation

$$\widetilde{U}_1(x_i) = \exp\left\{\frac{1}{2} \sum_{ij} \langle u_i u_j\rangle \nabla_i \nabla_j\right\} U_0(x_i) \tag{3.26a}$$

is calculated by integration with a Gaussian function.

We shall not discuss the problem of hard core interaction here since an elegant presentation of it is given by HORNER [6] and consider only the cumulant expansion in Eq. (3.26) up to second order in $\Delta\widetilde{U}_2(x_i)$. In this approximation the renormalized vertices (3.15)

$$\tilde{\Phi}^{(2)}_{1\ldots n} = \nabla_1 \ldots \nabla_n \{\widetilde{U}_1(x_i) + \Delta\widetilde{U}_2(x_i)\} \tag{3.27}$$

can be calculated on account of Eqs. (3.23), (3.26) by iteration. In the classical limit of high temperatures, $\beta\omega_{\max} \ll 1$, the integration over time in cumulants (3.23) using the spectral representation can easily be done with the result

$$\langle u_1 \ldots u_n\rangle^c \approx -\beta \prod_{i=1}^{n} \left(\sum_{i'} \langle u_i u_{i'}\rangle \nabla_{i'}\right) \langle U(x_i + u_i)\rangle , \tag{3.28}$$

and

$$\Delta\widetilde{U}_2(x_i) \approx -\beta \sum_{n=3}^{\infty} \frac{1}{n!} \left(\sum_{ii'} \langle u_i u_{i'}\rangle \nabla_i \nabla_{i'}\right)^n \widetilde{U}_1(x_i) . \tag{3.29}$$

The thermodynamical properties in the SC2 approximation can be obtained from the internal energy (2.24), where the average kinetic energy (2.25) is calculated by using GF (3.11) with the self-energy operator (3.22) and the average potential energy (2.26) is given by (3.26). To calculate the second order correction to the free energy in (2.23) one should introduce first the irreducible GF in (2.22) as done in Section 3.1. Then by integration over frequencies using Eq. (3.14) one gets:

$$\Delta F_2 = \int_0^1 \frac{d\lambda}{\lambda} \left\{\lambda^2 \sum_{ij} \langle u_i u_j\rangle \nabla_i \nabla_j \Delta\widetilde{U}_2(\lambda, x_i) +\right.$$

$$\left. + \sum_{n=3}^{\infty} \frac{\lambda^n}{(n-1)!} \sum_{1\ldots n} \langle u_1 \ldots u\rangle^c_\lambda \nabla_1 \ldots \nabla_n \widetilde{U}_1(\lambda, x_i)\rangle\right\},$$

where the first term is due to the second order correction to the renormalized pseudoharmonic matrix $\tilde{\Phi}_{ij}^{(2)}(\lambda)$ as in (3.27). The λ-dependent functions $\langle u_1 \ldots u_n \rangle_\lambda^c$, $\Delta\tilde{U}_2(\lambda, x_i)$ and $\tilde{U}_1(\lambda, x_i)$ are given by (3.23), (3.26), and (3.26a), respectively with every power of u_i multiplied by λ. After the integration over λ with $\langle u_i u_j \rangle$, $\langle u_i(t) u_j \rangle$ being independent of λ, one gets

$$\Delta F_2 = Im \int_0^\infty dt \sum_{n=3}^{\infty} \frac{1}{n!} \left(\sum_{ii'} \langle u_i(t)\, u_{i'} \rangle \nabla_i \nabla_{i'} \right)^n \tilde{U}_1(x_i)\, \tilde{U}_1(x_i') =$$

$$= \frac{1}{2} \sum_{n=3}^{\infty} \frac{1}{n!} \sum_{1 \ldots n} \langle u_1 \ldots u_n \rangle^c \nabla_1 \ldots \nabla_n \tilde{U}_1(x_i) = \frac{1}{2} \Delta\tilde{U}_2(x_i). \quad (3.30)$$

In the calculation of the first two terms $F_0 + \Delta F_1$ in the free energy expansion one should employ (3.19) with the SC1 frequencies ω_{qj} being replaced by the SC2 frequencies Ω_{qj} defined as the maxima of the imaginary part of the GF in the SC2 approximation according to (2.18).

The proposed cumulant expansions for the average potential energy (3.26) and the free energy (3.30) with the GF (3.11) and Eqs. (3.22)—(3.24) give the same results as other methods based on diagrammatic techniques or on the variational approach proposed by WERTHAMER [3] (see e.g. [4]).

4. Stability conditions for simple lattices

Formally one can distinguish between the thermodynamical stability conditions (the free energy of the lattice should have a minimum with respect to small variations, mechanical or otherwise) and the dynamical ones (the phonon spectrum of the lattice should be positively defined). From the first one, apart from the trivial inequalities for any stable thermodynamical system

$$c_p < 0\,, \qquad \left(\frac{\partial P}{\partial V}\right)_T < 0 \quad (4.1)$$

follows that some elastic constants should be positive [1] e.g. for the cubic lattice,

$$c_{11} > 0\,, \qquad c_{44} > 0\,, \qquad c_{11} - c_{12} > 0 \quad (4.2)$$

that really means that the acoustic spectrum should be stable. Therefore the dynamical conditions seem to be more general and should be used for the investigation of crystal stability. These conditions are easily formulated in terms of the GF (2.10): for the stable lattice there should be no poles in the upper half-plane of the complex variable ω for the retarded GF $G_{ii'}(\omega)$. The temperature T_s (or any other relevant quantity, e.g. mean-squared displace-

ment of atoms), at which the dynamical conditions are violated defines the upper limit for the stability of a given crystalline phase. For a simple Bravais lattice T_s just defines the temperature at which the bound crystalline state of atoms vanishes and therefore it can be used as an upper estimate for the melting temperature. But for non-primitive lattices some optical mode can become unstable and a structural phase transition, driven by this "soft" optical mode, from one to some other crystalline state can occur.

In the present Section the SCPT of a simple model crystal considered in our papers [17]—[19], [22], will be presented briefly, while a general discussion of the structural phase transition on the basis of the SCPT will be given in the next Section.

4.1 *Simple model of anharmonic crystals*

To consider qualitatively the physical properties of a real highly anharmonic crystal and to discuss the physical reason for the lattice instability at large vibrational motions it would be quite reasonable to investigate a simple model of a three-dimensional lattice, namely a *fcc* one with nearest neighbour (NN) interactions. Though this model is rather simple, it can be used for the description of rare gas solids and due to this fact it has been investigated extensively in recent years (see, e.g. [4], [5]).

For the potential energy of the lattice

$$U(\mathbf{R}_l) = \frac{1}{2} \sum_{l \neq m}{}' \varphi(\mathbf{R}_l - \mathbf{R}_m), \tag{4.3}$$

where the prime means the sum only over nearest neighbours, one gets the pseudoharmonic renormalization in the form (3.26a):

$$\widetilde{U}_1(\mathbf{l}) = \frac{1}{2} \sum_{l \neq m}{}' \tilde{\varphi}(\mathbf{l} - \mathbf{m}) = \frac{1}{2} \sum_{l \neq m}{}' \exp\left\{\frac{1}{2} \langle (\mathbf{u}_{lm} \cdot \nabla_l)^2 \rangle\right\} \varphi(\mathbf{l} - \mathbf{m}), \tag{4.4}$$

where $\mathbf{l} = \langle \mathbf{R}_l \rangle$ are the equilibrium positions of atoms and $\mathbf{u}_{lm} = \mathbf{u}_l - \mathbf{u}_m$ is the relative displacement of the neighbours.

To define the pseudoharmonic frequencies $\omega_{\mathbf{q}j}$ and polarization vectors $\mathbf{e}_{\mathbf{q}j}$ for the model one should consider Eq. (3.17) that can be written in the form

$$\omega_{\mathbf{q}j}^2 = \frac{f(l, T)}{M} \sum_{l}{}' \frac{(\mathbf{l} \cdot \mathbf{e}_{\mathbf{q}j})}{l^2} (1 - \cos \mathbf{q}\mathbf{l}) \equiv \frac{f(l, T)}{f} \omega_{0\mathbf{q}j}^2. \tag{4.5}$$

For the model with NN interaction the pseudoharmonic renormalization is reduced to the renormalization of one force constant $f(l, T) = \tilde{\varphi}^{(2)}(l)$ and so

the harmonic frequencies $\omega^2_{0\mathbf{q}j}$, corresponding to the force constant f, can be introduced.

Adopting the leading term approximation for the derivatives of the potential:

$$\nabla_l^{\alpha_1} \dots \nabla_l^{\alpha_n} \varphi(l) \approx \frac{l_{\alpha_1} \dots l_{\alpha_n}}{l^n} \varphi^{(n)}(l)$$

one can greatly simplify the equation for the renormalized potential (4.4):

$$\tilde{\varphi}(l) = \sum_{n=0}^{\infty} \frac{1}{n!} \left(\frac{1}{2} \overline{u^2(l)} \right)^n \varphi^{(2n)}(l) , \tag{4.6}$$

where only one projection $\overline{u^2(l)} = \langle (\mathbf{l} \cdot \mathbf{u}_{l0})^2 \rangle / l^2$ of the displacement correlation function appears. Since the latter depends only on the distance l between neighbours ($\mathbf{m} = 0$), one can write it using Eqs. (2.12), (2.16) and (4.5) in the form

$$f(l, T) \frac{z}{2} \overline{u^2(l)} = \frac{f(l, T)}{2} \sum_l{}' \frac{1}{l^2} \langle \{ \mathbf{l}(\mathbf{u}_l - \mathbf{u}_0) \}^2 \rangle =$$

$$= \sum_{\mathbf{q}j} \omega^2_{\mathbf{q}j} \int_0^{\infty} d\omega \coth \frac{\beta\omega}{2} \left[-\frac{1}{\pi} Im\, G_j(\mathbf{q}, \omega) \right], \tag{4.7}$$

where $z = 12$ is the number of nearest neighbours for an *fcc* lattice. The Fourier transform $G_j(\mathbf{q}, \omega)$ of the GF in (2.16) by ignoring the polarization mixing can be written in the form:

$$G_{j=j'}(\mathbf{q}, \omega) = \frac{1}{\omega^2 - \omega^2_{\mathbf{q}j} - 2\omega_{\mathbf{q}j} \Pi_{\mathbf{q}j}(\omega)} . \tag{4.8}$$

The Fourier transform $\Pi_{\mathbf{q}j}(\omega)$ of the self-energy operator in SC2 approximation can be obtained from (3.22), but as in [17] only its lowest order term will be taken into account

$$\Pi_q(\omega) =$$

$$= -\sum_{1,2} |\tilde{V}_3(-\mathbf{q}j, q_1, q_2)|^2 \left\{ \frac{(n_1 + n_2 + 1)(\omega_1 + \omega_2)}{(\omega_1 + \omega_2)^2 - \omega^2} - \frac{(n_1 - n_2)(\omega_1 - \omega_2)}{(\omega_1 - \omega_2)^2 - \omega^2} \right\} \equiv$$

$$\equiv -\frac{g^2(l, T)}{f^3(l, T)} S_{\mathbf{q}j}(T, \omega) . \tag{4.9}$$

Here the renormalized cubic anharmonic interaction $\tilde{V}_3 \to \tilde{\varphi}^3$ $(l) \equiv g(l, T)$ is introduced and the time-dependent correlation function $\langle u_i(t) u_{i'} \rangle$ in Eq. (3.22) is calculated in pseudoharmonic approximation; $\omega_{q_1} = \omega_{1_1}$, $q_1 = (\mathbf{q}_1 j_1)$, $n_1 = [\exp(\beta\omega_{q_1}) - 1]^{-1}$ etc.

However, it should be pointed out here that in the self-consistency equation (4.7) the second order term, namely $\Pi_q(\omega)$ in Eq. (4.8), is taken into account; usually it is neglected, as in the ISC (Improved Self-Consistent) theory (see, e.g. [4]). As in the ordinary perturbation theory the second order cubic anharmonic interaction in SC2 gives a contribution comparable with the SC1 terms in the denominator of Eq. (4.8). As will be shown later, if one neglects the former some unphysical results may be obtained.

For the lattice under constant external pressure the lattice constant is obtained from the equation (2.6) which can be written as

$$P = -\frac{1}{3V}\sum_{l,\alpha} l_\alpha \nabla_l^\alpha \tilde{U}_1(l) = -\frac{zl}{6v}\tilde{\varphi}'(l), \tag{4.10}$$

where $v = V/N = l^3/\sqrt{2}$. To discuss the thermodynamics of the model one should calculate the free energy (3.30) or the internal energy (2.24)—(2.26). By taking into account only the renormalized cubic anharmonic interaction one obtains the same expression for the free energy as in the conventional perturbation theory but with renormalized frequencies ω_{qj}, and vertices $\tilde{\varphi}^3(\omega) = g(l, T)$ as in (4.9) (see [17]). In the following we shall call this set of equations (4.5)—(4.10) the reduced second order self-consistent phonon approximation (RSC2). This RSC2 scheme was used in [17]—[19], [22] for the investigation of physical properties of the model: the phonon spectrum $\varepsilon_q \approx \omega_q + Re\,\Pi_q(\varepsilon_q)$, the phonon width $\Gamma_q = -Im\,\Pi_q(\varepsilon_q + i\varepsilon)$, PV-diagram (4.10), elastic constants, etc. to be discussed below.

4.2 *Results of numerical calculations*

The main problem in solving the system of self-consistent equations is the ω-integration in Eq. (4.7). To obtain analytical expressions the integration was done in an approximate manner in [17] in the high and low temperature limits using the explicit forms of the self-energy operator (4.9).

In the high temperature limit ($\beta^{-1} = kT \gg \omega_D$) by employing the dispersion relations for the GF and sum rules (2.14) the equation (4.7) can be written in the form:

$$\frac{z}{2} f(l, T)\,\overline{u^2(l)} \approx \frac{T}{N}\sum_{qj}\omega_{qj}^2\left\{-Re\,G_j(\mathbf{q}, \omega = 0) + \frac{1}{12\,T^2}\right\} \approx$$

$$\approx 3T\left\{\left[1 - \mu T\frac{g^2(l, T)}{f^3(l, T)}\right]^{-1} + \frac{\omega_L^2}{24\,T^2}\right\}, \tag{4.11}$$

where $\omega_L^2 = 8f(l, T)/M$. In the low temperature limit ($T \ll \omega_D$) Eq. (4.7) can be approximated in the same manner as

$$\frac{z}{2} f(l, T)\,\overline{u^2(l)} \approx \varepsilon_0\left[1 - \nu_0\varepsilon_0\frac{g^2(l, T)}{f^3(l, T)}\right]^{-1} + \frac{3\pi^4}{5}\frac{T^4}{\omega_D^3}\left[1 + \nu_1\varepsilon_0\frac{g^2(l, T)}{f^3(l, T)}\right], \tag{4.12}$$

where the zero-point energy $\varepsilon_0 \approx 1.02\omega_L$; $\omega_D \approx 1.05\omega_L$ for the *fcc* lattice. The numerical coefficient μ in (4.11) as well as v_0 and v_1 in (4.12) account for the contribution coming from $\Pi_{qj}(\omega)$ in (4.8) after some averaging over $(\mathbf{q}, j)$ and ω-integration in (4.12). The estimations found for them in [17], based on the numerical calculations for the cubic anharmonic corrections to the free energy, are:

$$\mu \approx 0.11\,, \qquad v_0 \approx 7.3 \cdot 10^{-3}\,, \qquad v_1 \approx 0.10\,.$$

Then employing the model Morse potential in Eq. (4.6) one gets the renormalized potential in the form

$$\tilde{\varphi}(l) = D\{e^{-2a(l-r_0)}e^{2y} - 2e^{-a(l-r_0)}e^{y/2}\}\,. \tag{4.13}$$

The renormalization parameter $y = a^2\overline{u^2(l)}$ is defined by Eq. (4.11) or (4.12) with $f(l, T) = \tilde{\varphi}^{(2)}(l)$ and $g(l, T) = \tilde{\varphi}^{(3)}(l)$ and Eq. (4.10) for the lattice constant l.

Therefore one gets the self-consistent (SC) equation for the parameter $y(l, T)$, which is the dimensionless displacement correlation function. The results of the solution for this SC equation and some thermodynamical functions at different pressures are shown in Figs. 1—4. By choosing $ar_0 = 6$

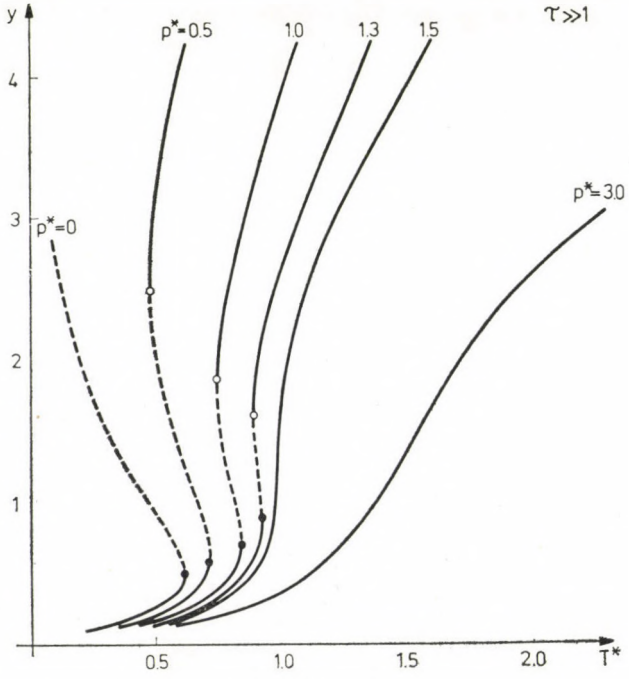

Fig. 1. Real solution of the self-consistent equation for $\tau \gg 1$

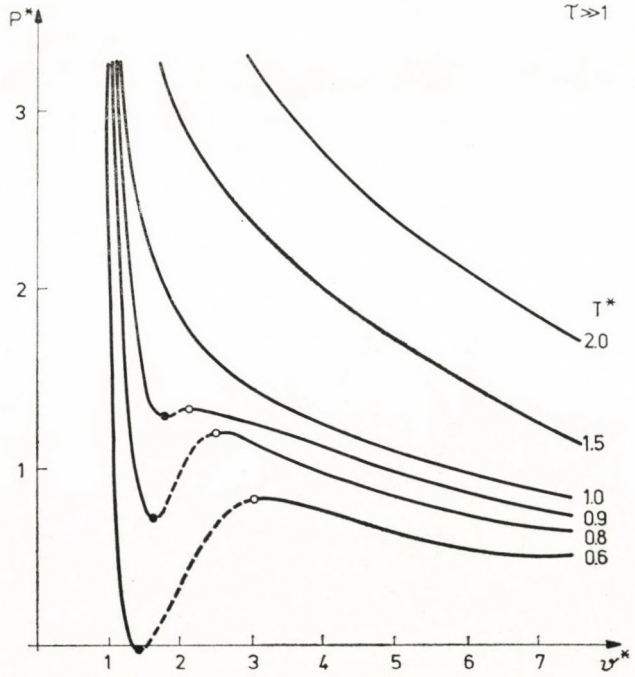

Fig. 2. The PV-diagram of the anharmonic crystals for $\tau \gg 1$

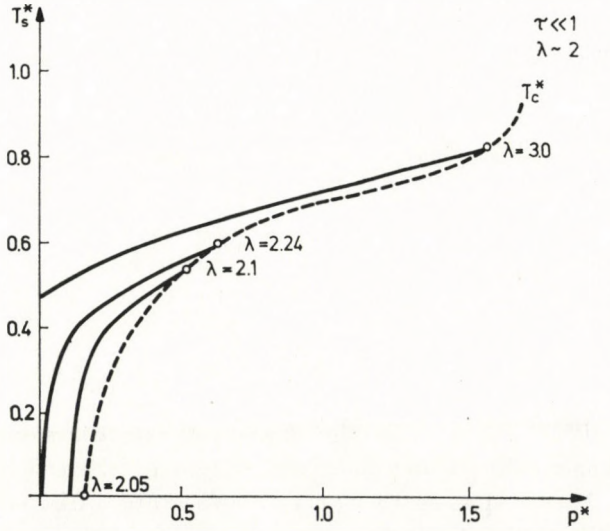

Fig. 3. The dependence of the instability temperature T_s^* of a crystal with weak coupling of atoms ($\lambda \approx \lambda_0 \approx 2.2$) on the reduced pressure P^*

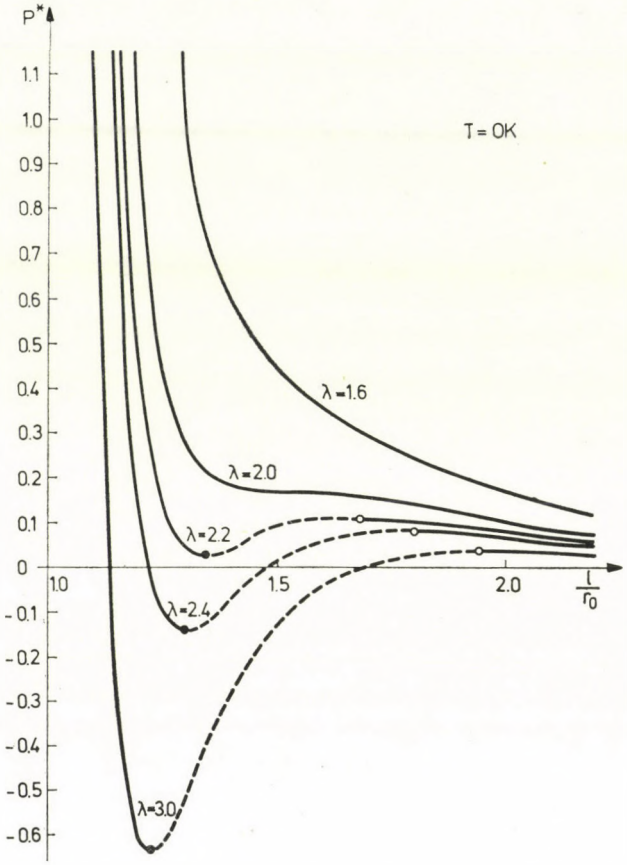

Fig. 4. The PV-diagram of a crystal with weak coupling of atoms at $T=0$ °K

in Eq. (4.13) the following dimensionless quantities are introduced: temperature $T^* = T/D$ and $\tau = T/\omega_{0L} = \lambda T^*/11.76$; pressure $P^* = P(r_0^3/D\sqrt{2})$ and coupling constant $\lambda = zD/\varepsilon_0^{(0)}$ ($\varepsilon_0^{(0)} \approx 1.02\omega_{0L}$; $\omega_{0L} = \sqrt{8f/M}$; $f = 2Da^2 = 72D/r_0^2$).

In the high temperature limit ($\tau \gg 1$) the solutions of the SC equation (4.11) for $y(T)$ are shown in Fig. 1. At sufficiently low temperature

$$T^* < T_c^* \approx 0.98$$

(or pressure $P^* < P_c^* \approx 1.35$) there are several real solutions for $y(T)$, the thermodynamically stable ones are shown by the full lines. The lowest line, $y_1(T) \leq 1$ corresponds to a crystalline state with small vibrational motions. In the limit of small anharmonicity (or lower temperature), this solution gives the harmonic correlation function. But as $T^* \to T_s^*(P)$ (denoted

by the full dots in Fig. 1) $y_1(T)$ becomes unstable since the poles of the retarded GF (4.8) given by the renormalized phonon frequency

$$\varepsilon_{\mathbf{q}j} \approx 0.77\omega_{0\mathbf{q}j}\{1 + 0.4\sqrt{1 - T^*/T_s^*} + \dots\} \tag{4.14}$$

shift to the upper half-plane at $T^* > T_s^*(P)$ for any $(\mathbf{q}, j)$ value. Physically it means that the lattice as a bound state of atoms with given interatomic forces becomes unstable at $T_s^*(P)$ with respect to the propagation of the collective excitations i.e. phonons. The specific heat at constant pressure c_P and the thermal expansion coefficient $\alpha_T \approx (\partial V/\partial T)_P$ become divergent as $(1 - T^*/T_s^*)^{-1/2}$ when $T^* \to T_s^*(P)$. As can be seen from Fig. 1 and from the PV diagram corresponding to Eq. (4.10), shown in Fig. 2, at $T^* = T_s^*(P)$ there is a first order phase transition that drives the lattice from the crystalline state with $y = y_1(T)$ to some other state with $y = y_2(T)$, shown by the upper full line in Fig. 1. The latter is also a crystalline state (due to the restrictions imposed by the theory) that should be considered as a lattice gas state. The vibrations of the atoms are rather large, $y_2(T) \gg 1$ and are defined by the external pressure: in the limit $P \to 0$ the solution $y_2(T) \to \infty$. In reality this state has no physical meaning since at some lower temperature, $T_m < T_s$, the crystal should melt. It is worth-while to point out now that the instability temperature $T_s^* \approx 0.6(1 + 0.3\, P^*)$ [17] lies close to the reduced melting curves of rare gas solids: $T_m^* \approx 0.5(1 + 0.2\, P^*)$ and the mean square displacement is constant for the given model potential at the instability point:

$$\left(\overline{u^2(l)}\right)^{1/2}/l \approx 0.10(\tau_s \gg 1) \div 0.14(\tau_s \ll 1)$$

(compare with [24]—[26]). Therefore it seems natural that the vibrational instability of the anharmonic crystals plays some role in the melting phenomenon as was proposed by LINDEMAN. But one should distinguish between these two physically different phenomena as was discussed in the Introduction.

At sufficiently high pressure, $P^* > P_c^*$ or corresponding high temperature, $T^* > T_c^*$ this type of vibrational instability disappears. The two solutions at P_c^* coincide and there is only one stable solution for the correlation function $y(T)$ for $P^* > P_c^*$. Physically it means that the external forces become more efficient than the interatomic ones and the former define the lattice dynamics: they are strong enough to localise the atomic vibrations.

At low temperatures ($\tau = T/\omega_{0L} \ll 1$) the solution of the SC equation (4.12) for the correlation function $y(\lambda, T)$ leads to the same result as in the high temperature limit. The only difference is that at low temperature the amplitude of atomic vibrations is given mostly by zero-point energy, proportional to λ^{-1}. As a result, highly anharmonic crystals with small coupling constant λ can be unstable even at $T = 0$ K. In Fig. 3 the dependence of the

instability temperature on the pressure, $T_s^*(P^*)$ for some values of λ is shown; $T_s^* = 0$ for $\lambda < \lambda_0 \approx 2.24$. There are also critical values for the pressure P_c^* for any given $\lambda > \lambda_c \approx 2.05$ denoted by the dashed line in Fig. 3. The effect of lattice stabilization at $P^* > P_c^* > 0$ or $\lambda < \lambda_c \approx 2.05$ at $T = 0$ is quite analogous to that discussed above for high temperatures. The PV diagram at $T = 0$ is shown in Fig. 4. It has the same Van der Waals character as the curves in Fig. 2, only the temperature being replaced by the coupling constant λ that defines the zero-point energy.

4.3 *Elastic constants and lattice stability*

It is of interest to compare now for the discussed model the thermodynamical stability conditions (4.1), (4.2) with the dynamical ones obtained from the solutions of the SC equation (4.7) for $\overline{u^2(l)}$. To perform the comparison one should calculate the elastic constants c_{11}, c_{44} and $c_{11} - c_{12}$ of the *fcc* lattice. They can be obtained from the static long-wavelength limit of the self-energy operator of the GF (4.8) in the form

$$\frac{c_{\alpha\beta}(T)}{c_{\alpha\beta}^{(0)}} = \frac{r_0}{l(T)} \frac{f(l, T)}{f} \left[1 - 2 \frac{g^2(l, T)}{f^3(l, T)} S_{\mathbf{K}j}(T)\right]. \tag{4.15}$$

Here $c_{\alpha\beta}^{(0)}$ is the corresponding harmonic elastic constant and the function

$$S_{\mathbf{K}j} = \lim_{q \to 0} \left[\frac{1}{\omega_{\mathbf{q}j}} Re\ S_{\mathbf{q}j}(T, \omega = 0)\right]$$

is defined by the appropriate choice of the type of the mode j and the direction $\mathbf{K} = \mathbf{q}/|q|$ of the wave vector yielding the corresponding elastic constants c_{11}, c_{44} and $c_{11} - c_{12}$ [22].

It should be pointed out here that though the elastic constants defined by the static limit of an exact self-energy operator are equal to those defined by the strain derivatives of an exact free energy [30] in approximate calculations this theorem does not hold. For instance the SC1 self-energy (3.15) yields only the first term in the elastic constants obtained from the strain derivatives of the SC1 free energy (3.19). One should take into account higher order terms in the SC2 self-energy, namely an infinite number of bubble diagrams produced by cubic and quartic anharmonic interactions, to obtain the same expression as from the SC1 free energy [35]. In our approximation (4.15) only the first bubble diagram given by Eq. (4.9) is taken into account. Though for quantitative estimations all other bubble diagrams should be taken into account [35], in the present qualitative discussions they can be neglected. Apart from these explicit approximations the results of the calculations in the SCPT depend

also on the implicit approximations adopted for the SC equation (4.7). In the SC1 and ISC approximations all second order terms are neglected in the SC equation (formally, $\mu = 0$ in (4.11) and $v = v_0 = 0$ in (4.12)). But in the above proposed RSC2 approximation the leading second order terms given by Eq. (4.9) are taken into account in Eq. (4.7). As was discussed earlier, they are quite compatible with the first order one in SC1 approximation and therefore the results of calculations based on the SC equation in SC1 or RSC2 approximations should be different. For instance, the instability temperature defined via Eq. (4.11) is equal to $T_s^* \approx 0.6$ at $P = 0$ (see Fig. 1), while in SC1 approximation ($\mu = 0$ in Eq. (4.11)) it is much higher $T_s^*(\mathrm{SC1}) \approx 1.5$ [15].

Taking into account these general remarks we discuss now the results of the numerical calculations for the elastic constants (4.15). They are shown in Fig. 5 at $P = 0$ for high temperatures, $\tau \gg 1$. The elastic constants are shown by the solid lines when the full form of Eq. (4.11) was used for $y(T)$ and by the dashed lines when SC1 approximation was used in Eq. (4.11) ($\mu = 0$). For comparison the elastic constants for solid Xe obtained in [35] are also shown in Fig. 5: by dots, when only the first bubble diagram (as in Eqs. (4.9), (4.15)) is taken into account (the so called HORNER approximation),

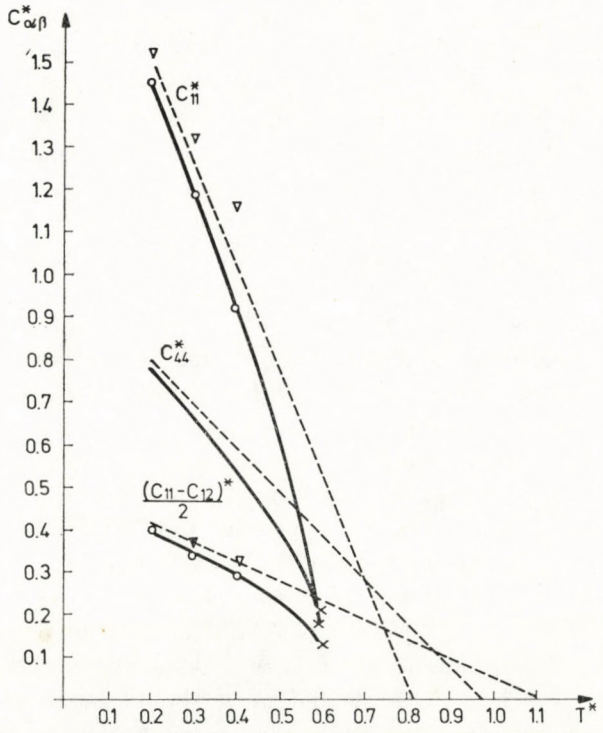

Fig. 5. The dependence of the reduced elastic constants $C^*_{\alpha\beta} = C_{\alpha\beta}/C^{(0)}_{44}$ on the reduced temperature T^*

and by triangles, when the sum of bubble diagrams was considered. The SC equation was solved in [35] in the SC1 approximation, i.e. neglecting second order terms. Though the results of different types of approximations are close to each other at low temperatures, $T^* \leq 0.3$, they show quite a different behaviour near the instability temperature $T_s^* \approx 0.6$. Since at this point in the RSC2 approximation the whole phonon spectrum becomes unstable, as given by Eq. (4.14), the elastic constants also show this instability by taking complex values. But in the SC1 or ISC approximations the instability temperature is much higher, $T_s^*(\mathrm{SC1}) \approx 1.5$, and the elastic constants may vanish at some lower temperature, as e.g. $c_{11}(T^* \approx 0.8) = 0$, producing a spurious soft-mode behaviour [21]. As follows from (4.15), it occurs due to the negative contribution from the same second order term which is neglected in the SC1 approximation for the SC equation, $\mu = 0$ in (4.11). A consistent approximation both for the elastic constants (4.15) and for the SC equation (4.7) in the RSC2 approximation excludes the above mentioned type of discrepancy.

Considering now the PV diagram in Fig. 2, it can be seen that the bulk modulus, $B_T = -(1/V)\,(\partial P/\partial V)_{T'}$ vanishes as $T^* \to T_s^*$. Since in our calculations Eq. (4.10) was used for $P(T)$, as in the SC1 approximation, this bulk modulus should be close to that one obtained from Eq. (4.15): $B(T) = c_{11} - (2/3)\,(c_{11} - c_{12})$.

As seen from Fig. 5, it also vanishes at $T^* \to T_s^*$. Therefore the dynamical instability discussed here is driven by the fluctuations of the volume and the "breathing" mode is the soft one though all sound velocities are nonzero at $T^* \to T_s^*$. In reality this dynamical instability may be unobservable for real crystals since they would melt at some lower temperature.

The same kind of behaviour for elastic constants (4.15) is obtained at low temperature, $\tau \ll 1$ for quantum crystals [22], and therefore they will not be discussed here.

From these model calculations one may claim that the SCPT can be applied to the investigation of the range of stability of anharmonic crystals. For primitive Bravais lattice the instability temperature defines the upper limit for the stability of a given crystalline structure with respect to the propagation of collective excitations. The numerical estimations would depend on the adopted approximations but they should not change considerably from those obtained here in RSC2 approximation. The corrections from the higher order terms are of the order $(T^*)^n$ at $\tau \gg 1$ or $(1/\lambda)^n$ at $\tau \ll 1$ where $n \geq 2$ and since T^* or $(1/\lambda)$ are small enough even at the instability point: $T_s^* \approx 0.6$; $1/\lambda_c \approx 0.5$ these corrections should be also small. But for a more realistic model of anharmonic crystals with strongly repulsive interactions the short-range correlations, neglected here, should be properly taken into account. They are of importance not only for quantum crystals [6], [8], but for other rare gas crystals as well at high temperatures, as shown by a recent

calculation [36]. Then a consistent consideration for the short-range correlations in the framework of the SCPT would give one a possibility for quantitative calculation of range of stability of anharmonic solids.

5. Structural phase transitions

5.1 *Soft modes and free energy expansion*

The structural phase transition (PT) can be described microscopically as an appearance of some finite displacements of atoms $\eta_i(T)$ below the temperature T_c of the PT. For the second order PT the $\eta_i(T)$ change smoothly from zero value at $T = T_c$ while for the first order PT they change discontinuously to some finite value at $T \leq T_c$. But in both cases the displacements $\eta_i(T)$ are rather small in comparison to the lattice spacing, at least not far from the transition temperature T_c. Therefore it is convenient to write the equilibrium positions of atoms in Eq. (2.8) as

$$\langle R_i \rangle = x_i = x_i^0 + \eta_i \equiv \mathbf{x}_s^0 + \boldsymbol{\eta}_s \equiv \mathbf{x}^0 \begin{pmatrix} l \\ \varkappa \end{pmatrix} + \boldsymbol{\eta} \begin{pmatrix} l \\ \varkappa \end{pmatrix}, \tag{5.1}$$

where x_i^0 is the equilibrium position in the high-temperature phase, $T > T_c$ (by definition, the PT is assumed to occur below T_c). Considering now η_i as a small virtual atomic displacement near the PT point, one can write the Fourier transformation for it in the same form, as for the dynamical displacement u_i:

$$\eta_i \equiv \eta^\alpha \begin{pmatrix} l \\ \varkappa \end{pmatrix} = \frac{1}{\sqrt{NM_\varkappa}} \sum_{\mathbf{q}j} e^\alpha_{\mathbf{q}j}(\varkappa)\, e^{i\mathbf{q}\mathbf{x}_s^0} \eta(\mathbf{q}, j) \equiv \sum_q W_i(q)\, \eta(q). \tag{5.2}$$

The appearance of finite displacements η_i in the framework of lattice dynamics can be described as a condensation or "freezing" of some unstable phonon mode, the so called soft mode, the frequency of which tends to zero as $T \to T_c$ [37], [38]:

$$\Omega_c(T_c) = 0, \tag{5.3}$$

where c denotes the particular mode j_c and wave vector $\mathbf{q}_c$ of the unstable mode.

From the phenomenological point of view the structural PT is usually described by the LANDAU-type expansion for the free energy [39]:

$$F(\eta) = F_0 + A(T)\,\eta^2 + \frac{1}{2} B\eta^4 + D\eta^6, \tag{5.4}$$

where we assumed for simplicity that only even powers of the order parameter η are essential for a given type of PT. The order parameter η at the structural PT should be a linear combination of atomic displacements η_i and in the simplest case of one soft mode $(\mathbf{q}_c j_c)$ it is just equal to the Fourier transform of the displacements in Eq. (5.2): $\eta = \eta(\mathbf{q}_c j_c)$. The first coefficient in Eq. (5.3) defines the temperature of the second order PT:

$$A(T_c) = 0 \tag{5.5}$$

provided that

$$B(T_c) > 0 .$$

Though the LANDAU theory is a mean-field theory (actually it is better since $A(T)$ and $B(T)$ can be renormalized) and does not describe properly the critical region in the vicinity of T_c it still appears useful for phenomenological considerations. Now employing the results of Section 3.1, the equivalence of the dynamical and thermodynamical conditions for the structural PT, Eqs. (5.3) and (5.5), respectively, will be proven.

The phonon frequency spectrum $\Omega_{\mathbf{q}j}$ for a lattice is defined by the poles of the GF (3.11) and can be written in the general form as

$$\Omega^2_{\mathbf{q}j} = \frac{1}{N} \sum_{ss'} \sum_{\alpha\beta} \frac{1}{\sqrt{M_\varkappa M_{\varkappa'}}} e^{*\alpha}_{\mathbf{q}j}(\varkappa)\, e^{\beta}_{\mathbf{q}j}(\varkappa')\, e^{-i\mathbf{q}(\mathbf{x}_s - \mathbf{x}_{s'})} \{\tilde{\Phi}^{\alpha\beta}_{ss'} + Re\, \Pi^{\alpha\beta}_{ss'}(\omega = \Omega_{\mathbf{q}j})\} , \tag{5.6}$$

where the force-constant matrix is given by Eq. (3.5):

$$\tilde{\Phi}^{\alpha\beta}_{ss'} = \langle \nabla^\alpha_s \nabla^\beta_{s'} U(\boldsymbol{x}_i + \boldsymbol{u}_i) \rangle \tag{5.6a}$$

and the self-energy operator according to Eqs. (3.10), (3.12) is equal to

$$\Pi^{\alpha\beta}_{ss'}(\omega) =$$

$$= \sum_{n,n'=2}^{\infty} \frac{1}{n!} \frac{1}{n'!} \left\langle \left\langle \left(\sum_j \boldsymbol{u}_j \nabla_j \right)^n \middle| \left(\sum_{j'} \boldsymbol{u}_{j'} \nabla_{j'} \right)^{n'} \right\rangle \right\rangle_\omega \langle \nabla^\alpha_s U(\boldsymbol{x}_i + \boldsymbol{u}_i) \rangle \langle \nabla^\beta_{s'} U(\boldsymbol{x}'_i + \boldsymbol{u}'_i) \rangle =$$

$$= \langle \langle \nabla^\alpha_s U(\boldsymbol{x}_i + \boldsymbol{u}_i) \,|\, \nabla^\beta_{s'} U(\boldsymbol{x}_{i'} + \boldsymbol{u}_{i'}) \rangle \rangle^{\mathbf{P}}_w . \tag{5.6b}$$

In the last line the definition of the irreducible GF (3.2) was used and the self-energy operator was written in terms of the proper (p) part of the usual GF. At $T = T_c$ the frequency of the soft mode $\Omega_c(T_c) = 0$ and the dynamical condition (5.3) can be written as an equation for the self-energy operator:

$$\sum_{ij} W^*_i(q_c) \{\tilde{\Phi}_{ij} + Re\, \Pi_{ij}(\omega = 0)\} W_j(q_c) = 0 , \tag{5.7}$$

where the polarization vectors for the soft mode defined in Eq. (5.2) were introduced.

The free energy as a function of small displacements can be written in the form:

$$F(T, \eta_i) = -\frac{1}{\beta} \ln Tr \exp\left\{-\beta\left(H_0 + U'(\eta_i)\right)\right\} =$$

$$= F_0(\eta_i = 0) + \frac{1}{\beta}\int_0^\beta d\tau \langle U'(\tau)\rangle_0^c - \frac{1}{2\beta}\int_0^\beta\int_0^\beta d\tau_1 d\tau_2 \langle U'(\tau_1)U'(\tau_2)\rangle_0^c + \ldots, \quad (5.8)$$

where $H_0 = H(\eta_i = 0)$ and the perturbation

$$U'(\eta_i) = U(x_i^0 + \eta_i + u_i) - U(x_i^0 + u_i) = \left\{\exp\left(\sum_i \eta_i \nabla_i\right) - 1\right\} U(x_i^0 + u_i). \quad (5.9)$$

The linked-cluster expansion [31] was used and imaginary time $\tau = it$ correlation functions, only the connected ones, were introduced. Taking into account only quadratic terms in the displacement η_i in Eqs. (5.8) and (5.9) the free energy is obtained as

$$F(\eta_i) = F_0 + \frac{1}{2}\sum_{ij} A_{ij}(T)\eta_i \eta_j, \quad (5.10)$$

where

$$A_{ij}(T) = \langle \nabla_i \nabla_j U(x_i + u_i)\rangle_0^c - \int_0^\beta d\tau \langle \nabla_i U\big(x_i + u_i(\tau)\big) \nabla_j U(x_j + u_j)\rangle_0^c. \quad (5.11)$$

To compare Eq. (5.10) with the more general representation (5.4) the order parameter should be introduced which is essentially the Fourier transform of the displacements $\eta(\mathbf{q}_c j_c)$ in Eq. (5.2). Therefore for the coefficient $A(T)$ in Eq. (5.4) we get an explicit form:

$$A(T) = \frac{1}{2}\sum_{ij} W_i^*(q_c)\, A_{ij}(T) W_j(q_c)\,. \quad (5.12)$$

Now employing the identity for the retarded GF

$$Re\langle\langle a \,|\, b\rangle\rangle_{\omega = i\varepsilon} = -\int_0^\beta d\tau \,\langle a(\tau)\, b\rangle\,, \quad (5.13)$$

$$A(T_c) = \frac{1}{2}\Omega_c^2\,(T, \eta = 0) \quad (5.14)$$

is obtained, that proves the equivalence of Eqs. (5.3) and (5.5).

If the structural PT is described by homogeneous deformation the soft mode behaviour occurs for the elastic constant. Since the latter can be obtained either as a static long-wavelength limit of the self-energy operator in (5.6) [30], or as the second derivative of the free energy with respect to the stress

tensor $u_{\alpha\beta}$ which is the order parameter in this case, the equivalence of the dynamical and thermodynamical conditions for the PT is apparent. Therefore in discussing the structural PT one can take into account only the dynamics of the lattice and obtain the temperature of the PT from the equation (5.7) for the soft mode.

Though the connection between the soft mode behaviour at the structural PT and the thermodynamical stability condition for the free energy in Eq. (5.4), is now widely accepted (see e.g. [9], [40]) the discussion presented here seems to be the most rigorous one since it is based on the explicit nonperturbative forms for the soft mode frequency (5.6) and for the coefficient A, Eq. (5.12).

5.2 *Self-consistent phonon approximation and fluctuation effects*

To obtain numerical results from the rigorous but untractable explicit form for the soft mode (5.6) or the coefficient A (5.11) one should employ some method of approximations. Mainly two different approaches have been used. Curie—Weiss type mean field approximation (MFA), as in the theory of magnetism, and the SCPT. In the MFA the one-particle character of the atomic motion is emphasized by neglecting the correlations between atomic displacements on different lattice sites, while in the SCPT the collective picture of the atomic motion is adopted by taking into account the correlation of dynamical displacements. The advantages of both methods are now discussed in the literature in some detail (see [9] and e.g., [41]) and here we only point out that the MFA seems to be more preferable for the order-disorder PT while the SCPT is much better for the description of lattice dynamics in the displacive structural PT.

Now we consider the first order of the SCPT, as it was given in Section 3.2, with a more general definition (5.1) for the equilibrium positions of the atoms. The renormalized harmonic approximation, or SC1, was mainly used in the calculations due to its simplicity [9]. The free energy in this approximation according to (3.19) has the form:

$$F_1 = \frac{1}{\beta} \sum_q ln \left(2\, sh \frac{\beta \Omega_q}{2} \right) - \sum_q \frac{\Omega_q}{4} \coth \frac{\beta \Omega_q}{2} + \widetilde{U}(x_i)\,, \tag{5.15}$$

where $\Omega_q = \Omega_{qj}(x_i^0 + \eta_i)$ is given by the Eq. (3.17) using Eqs. (3.15), (3.16). The renormalized potential energy in the SC1 approximation is equal to

$$\widetilde{U}(x_i^0 + \eta_i) = \exp \left\{ \frac{1}{2} \sum_{ij} \langle u_i u_j \rangle \nabla_i \nabla_j \right\} U_0(x_i^0 + \eta_i)\,. \tag{5.16}$$

To discuss the structural PT by the SCPT we start with the LANDAU-type expansion (5.4) for the free energy (5.15). For simplicity we assume that there is only one soft mode, $\Omega_{\mathbf{q}_c j_c}(T_c, \eta_i = 0) = 0$ and that the symmetry of the crystal lattice allows only even powers of η as in Eq. (5.4). Then for the first coefficient in Eq. (5.4) one gets

$$A(T) = \left(\frac{dF_1}{d\eta^2}\right)_{\eta=0} = \exp\left\{\frac{1}{2}\sum_{ij}\langle u_i u_j\rangle \nabla_i \nabla_j\right\} \frac{dU_0(x_i)}{d\eta^2} \equiv \frac{\partial \widetilde{U}(x_i^0 + \eta_i)}{\partial \eta^2}\bigg|_{\eta=0}. \quad (5.17)$$

In deriving (5.17) the self-consistent condition imposed upon the frequency Ω_{qj} by Eqs. (3.15)—(3.17) was used that results in strong cancellation of terms [2]. Now assuming $\eta = \eta(\mathbf{q}_c j_c)$ in (5.2), as discussed earlier, the first coefficient can be written in the equivalent form

$$A(T) = \frac{1}{2}\sum_{ij}\frac{\partial^2 \widetilde{U}}{\partial \eta_i \partial \eta_j} W_i^*(q_c) W_j(q_c) = \frac{1}{2}\Omega_{q_c}^2(\eta_i = 0). \quad (5.17a)$$

Therefore the general theorem of the previous Section holds for the SC1 approximation and the temperature of PT can be obtained from the equation $\Omega_c^2(T_c) = 0$. In the case of small anharmonicity, using Eq. (3.17), Ω_c^2 can be written in the form:

$$\Omega_c^2(T_c) \approx \omega_{q_c}^2 + \frac{1}{2}\sum_q V_4(q_c, q)\frac{1}{2\Omega_q}\coth\frac{\Omega_q}{2T_c} = 0, \quad (5.18)$$

where $\omega_q^2 = \sum_{ij} W_i^*(q)\{\nabla_i \nabla_j U_0(x_i^0)\} W_j(q)$ is the harmonic phonon frequency at $\eta_i = 0$ and

$$V_4(q, q') = \sum_{ijkl} W_i^*(q) W_j(q) W_k^*(q') W_l(q') \nabla_i \nabla_j \nabla_k \nabla_l U_0(x_i^0)$$

is the quartic anharmonic interaction. Since usually the second term in (5.18) is positive $V_4(q, q') > 0$, Eq. (5.18) can hold only for $\omega_{q_c}^2(\eta_i = 0) < 0$. Therefore the structural PT can occur at $T_c > 0$ only when the harmonic lattice is unstable for $\eta_i = 0$. In the classical high temperature limit, $T \gg \Omega_{\max}$ the temperature of PT can be defined explicitly by the equation:

$$T_c = -\omega_{q_c}^2(\eta_i = 0)\left[\frac{1}{2}\sum_q V_4(q_c, q)\frac{1}{\Omega_q^2}\right]^{-1}. \quad (5.18a)$$

These results for small anharmonicity have been obtained previously by ANDERSON [37], COCHRAN [38] and others and are well discussed in the literature (see, e.g. [9]).

For further consideration of the character of PT one should obtain the second coefficient in Eq. (5.4):

$$B(T) = \left[\frac{d^2 F_1}{d(\eta^2)^2}\right]_{\eta=0} = \frac{d}{d\eta^2}\left\{\exp\left(\frac{1}{2}\sum_{ij}\langle u_i u_j\rangle \nabla_i \nabla_j\right)\frac{dU_0(x_i)}{d\eta^2}\right\}. \quad (5.19)$$

It is convenient to write Eq. (5.19) as a sum of two terms,

$$B(T) = B_0(T) + B_1(T) = \left[\frac{\partial^2}{\partial(\eta^2)^2}\tilde{U}(x^0 + \eta_i)\right]_{\eta=0} + \frac{1}{2}\sum_{ij}\left[\frac{\partial\tilde{\Phi}_{ij}}{\partial\eta^2}\frac{d\langle u_i u_j\rangle}{d\eta^2}\right]_{\eta=0}, \quad (5.19a)$$

where an explicit dependence of $\tilde{U}(x_i^0 + \eta_i)$ on η_i is taken into account by $B_0(T)$ and an implicit one occurring through the correlation function, by $B_1(T)$. As in the calculations of second-order elastic constants in the SCPT [30], [35], the equation for the correlation function $d\langle u_i u_j\rangle/d\eta^2$ takes the form of an integral equation. By introducing the matrix

$$\hat{C}(q|q') \equiv C(\mathbf{q}j_1 j_2|\mathbf{q}'j_1'j_2') = -\frac{1}{2}\tilde{V}_4(\mathbf{q}j_1 j_2|\mathbf{q}'j_1'j_2')\frac{E_{\mathbf{q}'j_1'} - E_{\mathbf{q}'j_2'}}{\Omega^2_{\mathbf{q}'j_1'} - \Omega^2_{\mathbf{q}'j_2'}} \quad (5.20)$$

with $E_q = 1/\Omega_q \coth(\beta\Omega_q/2)$, it can be formally solved and the second term in Eq. (5.19a) takes the form:

$$B_1(T) = -\frac{1}{4}\sum_{\mathbf{q}j_1 j_2} C(\mathbf{q}_c j_c j_c|\mathbf{q}j_1 j_2)\sum_{\mathbf{q}'j_1'j_2'}[1 + \hat{C}(q|q')]^{-1}\tilde{V}_4(\mathbf{q}'j_1'j_2'|\mathbf{q}_c j_c j_c). \quad (5.21)$$

The renormalized quartic anharmonic interaction is defined as

$$\tilde{V}_4(q, q') = \tilde{V}_4(\mathbf{q}j_1 j_2|\mathbf{q}'j_1'j_2') = \sum_{iklm} W_i^*(\mathbf{q}j_1)W_k(\mathbf{q}j_2)W_l^*(\mathbf{q}'j_1')W_m(\mathbf{q}'j_2')\tilde{\Phi}_{iklm}, \quad (5.22)$$

where the notation of Eq. (5.2) was used.

To estimate $B_1(T)$ near the transition temperature we assume that the vertex (5.22) depends weakly on $\mathbf{q}$ and $\mathbf{q}'$, and can be approximated by a constant for the critical mode:

$$\tilde{V}_4(q, q') \approx \tilde{V}_4(\mathbf{q}_c j_c j_c|\mathbf{q}_c j_c j_c) = \left[\frac{\partial^4\tilde{U}(x_i^0 + \eta_i)}{\partial\eta_i^4}\right]_{\eta_i=0} = \tilde{V}_4(q_c).$$

(This approximation is reasonable for optic modes but not for acoustic ones, where $V_4(q, q') \approx q^2 \cdot q'^2$ for small $\mathbf{q}$, $\mathbf{q}'$.) Then the matrix (5.20) can be factorized and Eq. (5.21) takes the form:

$$B_1(T) \approx -\frac{1}{4}\tilde{V}_4(q_c)\frac{\xi(T)}{1+\xi(T)}, \tag{5.23}$$

where

$$\xi(T) = -\frac{1}{2}\tilde{V}_4(q_c)\sum_{\mathbf{q}}\frac{\partial}{\partial\Omega^2_{\mathbf{q}j_c}}\left[\frac{1}{2\Omega_{\mathbf{q}j_c}}\coth\frac{\beta\Omega_{\mathbf{q}j_c}}{2}\right] \tag{5.24}$$

is the correlation parameter. It diverges for $\tau = |T - T_c|/T_c \to 0$ due to the critical fluctuations, as the usual estimation shows:

$$-\frac{1}{N}\sum_{\mathbf{q}}\frac{\partial}{\partial\Omega^2_{\mathbf{q}j_c}}\left[\frac{1}{2\Omega_{\mathbf{q}j_c}}\coth\frac{\Omega_{\mathbf{q}j_c}}{2T}\right] \approx \frac{T}{N}\sum_{\mathbf{q}}\frac{1}{\Omega^4_{\mathbf{q}j_c}} \approx \frac{T}{4\pi\sqrt{2}\,\omega_0^4}\frac{1}{r_0^3\sqrt{\tau}}. \tag{5.25}$$

Here the soft mode frequency was approximated by the equation $\Omega^2_{\mathbf{q}j_c} \approx$ $\approx \omega_0^2\tau + s^2q^2$ and the dimensionless radius r_0 of interatomic interaction was defined by the dispersion of the soft mode: $s^2 \approx r_0^2\omega_0^2a^2$, a is the lattice constant. Therefore for the whole coefficient (5.19) near the PT point one gets:

$$B(T) = \frac{1}{12}\tilde{V}_4(q_c) - \frac{1}{4}\tilde{V}_4(q_c)\frac{\xi(T)}{1+\xi(T)} \approx -\frac{1}{6}\tilde{V}_4(q_c). \tag{5.26}$$

Since $B(T \to T_c) < 0$ the structural PT should be of the first order. (The same arguments show that $D(T \to T_c) > 0$ in Eq. (5.4).) This quite general result is due to a certain renormalization of the phenomenological expansion (5.4) by taking into account fluctuations. As seen from (5.21), or (5.23), an effective summation of all bubble diagrams (Fig. 6) divergent at $\tau \to 0$ is done for the fluctuation term $B_1(T)$.

Fig. 6. The sum of bubble diagrams for the fluctuations term $B_1(T)$ in Eq. (5.21)

The first order PT in the SC1 approximation was first obtained by GILLIS and KOEHLER for a model calculation and then discussed in several papers (see [9] and e.g. [42], [43]). It is obvious that the first order PT is a consequence of the adopted approximations in SC1 and higher order corrections may change the result. It is well known now in the theory of PT (see e.g. [39], [44]) that the average field approximations do not work near the transition point. Therefore the order of PT cannot be defined by the SCPT, based on the average phonon field approximation. The region of strong fluctuation effects depends on the range of interatomic interactions: $\xi(\tau) > 1$ for $\tau < r_0^{-6}$. The second order PT in MFA is explained by the complete supression of the critical fluctuations since in MFA $r_0 \to \infty$. In the SC1 approximation one also gets a second order PT in the limit $r_0 \to \infty$ as it can be easily deduced from

Eq. (5.23) using Eq. (5.25): $B(\tau \neq 0, r_0 \to \infty) = B_0 > 0$. The latter result was pointed out by GILLIS [45] in a model calculation. In a real structural PT an interaction between the soft optic mode and acoustic ones should be taken into account. This striction interaction is usually the reason for the first order of PT [46].

Corrections up to second order in $\xi(\tau)$ in the framework of SCPT were considered in [43] for a simple continuum model of displacive ferroelectrics. However, the case of a weak quartic anharmonic interaction was discussed in [43] and the conventional perturbation theory, as in [47], was applied. Practically it leads to the expansion of (5.21), or (5.23) in powers of $\xi(\tau)$ taking into account some second order corrections. But since the SCPT is based on the variational approach without assuming that the anharmonicity is small, this expansion of $B_1(T)$ in powers of the divergent parameter seems to be inappropriate. Much better results can be obtained with the reduced SC2 approximation scheme considered in Section 4. In that case the SC1 approximation taking into account the leading second order terms in the equation for the correlation function is used as the zero approximation. Corrections to this nondivergent approximation are then obtained by some approximation procedure for the higher order terms [48].

Therefore the SCPT can be used as an interpolation method for the investigation of structural phase transitions and lattice dynamics of crystals with unstable modes. Contrary to the MFA in the SCPT the critical fluctuations of the order parameter are taken into account in some reasonable approximation that results in the renormalization of the phenomenological Landau expansion.

5.3 *Unified theory of ferroelectric phase transitions*

It is generally assumed that there are two basic kinds of PT in ferroelectrics, the order-disorder type PT and displacive type PT (see, e.g. [47] chapter 1). In the former case the PT results from a statistical disorder of active atoms among several (in the simplest case between two) equilibrium positions, while in the latter case the PT is caused by a lattice instability as discussed in the previous Section. Nevertheless it was shown in the last years that both types of ferroelectric PT can be described within a single model and that there are no essential differences (see, e.g. [9]) between them. Since the SCPT can be applied with some success only for the displacive PT it is of interest to consider a more general approximation that should simultaneously account for both the statistical fluctuations of active atoms into their equivalent equilibrium positions and for the dynamical correlations of atomic displacements. A unified approach of this type was proposed in [49] and we briefly consider it below.

As a simple model for the ferroelectric (or more generally structural) PT one can consider a system of active atoms moving in the static field of the remaining nonactive atoms. This model can be described by the Hamiltonian:

$$H = \sum_i \left\{ \frac{\mathbf{P}_i^2}{2M} + V(\mathbf{R}_i) \right\} + \frac{1}{2} \sum_{i \neq j} \varphi(\mathbf{R}_i - \mathbf{R}_j) \,. \tag{5.27}$$

Here $\mathbf{P}_i$ and $\mathbf{R}_i$ denote the momentum and coordinate referring to the active atoms, $V(\mathbf{R}_i)$ is a single-particle potential due to the remaining atoms, whereas $\varphi(\mathbf{R}_i - \mathbf{R}_j)$ is the pair interaction between active atoms in different cells. The potential $V(\mathbf{R}_i)$ may have two or more minima which provide the possibility for the active atoms to occupy those states in the unit cell. We assume for simplicity that there are only two such states (denote by $\lambda = \pm 1$) in each cell, so the atomic coordinate can be represented as follows:

$$\mathbf{R}_i = \mathbf{x}_i^0 + \sum_\lambda \sigma_i^\lambda \mathbf{S}_i^\lambda \,. \tag{5.28}$$

Here $\mathbf{x}_i^0$ denotes the centre of the cell, $\sigma_i^+ = 1(0)$ and $\sigma_i^- = 0, (1)$ if the atom occupies the state $\lambda = +1\ (-1)$. The projection operator σ_i^λ itself can be expressed by the pseudospin operator $\sigma_i = \pm 1$:

$$\sigma_i^\lambda = \frac{1}{2}(1 + \lambda\sigma_i) \,, \qquad (\lambda = \pm 1)$$

which is introduced as an independent variable, commuting with the atomic displacement ($\mathbf{S}_i^\lambda$) and the momentum ($\mathbf{P}_i^\lambda$) operators. To elucidate such additional pseudo-spin degree of freedom one has to take explicitly into account the tunnelling effect being described by the x-component of the pseudo-spin operator [50].

If the atomic displacement is in the state λ, $\mathbf{S}_i^\lambda$ can be written as a sum of a static displacement $\mathbf{b}_i^\lambda$ and a thermal fluctuation $\mathbf{u}_i^\lambda$:

$$\mathbf{S}_i^\lambda = \mathbf{b}_i^\lambda + \mathbf{u}_i^\lambda \,; \qquad \mathbf{b}_i^\lambda = \langle \mathbf{S}_i^\lambda \rangle = \mathbf{b}_\lambda \,. \tag{5.29}$$

Therefore this representation of atomic coordinates enables one to take into account, first, the atomic random distribution over two equilibrium positions in the cell, using the operator σ_i^λ and, secondly, the thermal atomic fluctuation $\mathbf{u}_i^\lambda$ in the neighbourhood of a given equilibrium position. In describing order-disorder phase transitions the latter variables are usually neglected, whereas in describing displacive phase transitions it is assumed that all atoms have identical equilibrium positions in the cells ($\lambda = +1$ or $\lambda = -1$) thus the operator σ_i^λ takes the same value at each site i. In this generalized model

we will be able to study both types of phase transitions using the full representation. Such a physical picture is in agreement with recent computer simulations and is also appealing for resons of universality [51].

Having inserted the definition (5.28), (5.29) in the Hamiltonian (5.27), it can be written in the form

$$H = \sum_{i\lambda} \sigma_i^\lambda \left\{ \frac{1}{2M} (\mathbf{P}_i^\lambda)^2 + V(\mathbf{x}_i^0 + \mathbf{S}_i^\lambda) + \frac{1}{2} \sum_{ij} \sum_{\lambda\varkappa} \sigma_i^\lambda \sigma_j^\varkappa \varphi(\mathbf{x}_i^0 - x_j^0 + \mathbf{S}_i^\lambda - \mathbf{S}_j^\varkappa) \right\}. \tag{5.30}$$

The lattice dynamics of the model can be considered within the framework of the SCPT, as was discussed earlier. Dealing with the pseudo-spin subsystem an effective Hamiltonian can be introduced:

$$\widetilde{H}_s = \sum_i h_i \sigma_i - \frac{1}{2} \sum_{i \neq j} I_{ij} \sigma_i \sigma_j . \tag{5.31}$$

Here the effective single particle "field" h_i and the effective "exchange energy" I_{ij} can be written on the basis of variational approach [52] in the form:

$$h_i = \sum_\lambda \frac{\lambda}{2} \left\langle \frac{1}{2M} (\mathbf{P}_i^\lambda)^2 + V(\mathbf{x}_i^0 + \mathbf{S}_i^\lambda) \right\rangle_0 + \sum_{\lambda\varkappa} \sum_j \frac{\lambda}{4} \langle \varphi(\mathbf{x}_i^0 - \mathbf{x}_j^0 + \mathbf{S}_i^\lambda - \mathbf{S}_j^\varkappa) \rangle_0 ; \tag{5.32}$$

$$I_{ij} = -\frac{1}{4} \sum_{\lambda\varkappa} \frac{\lambda\varkappa}{4} \langle \varphi(\mathbf{x}_i^0 - \mathbf{x}_j^0 + \mathbf{S}_i^\lambda - \mathbf{S}_j^\varkappa) \rangle_0 , \tag{5.33}$$

where the statistical averaging $\langle \ldots \rangle_0$ is performed over phonon variables.

The general model was considered in [49] for the one particle potential having a double-minimum form

$$V(\mathbf{x}_i^0 + \mathbf{S}_i) = V(\mathbf{x}_i^0) - \frac{A}{2} (\mathbf{S}_i)^2 + \frac{B}{4} (\mathbf{S}_i)^4 , \tag{5.34}$$

and for the pair interaction in the harmonic approximation:

$$\varphi(\mathbf{x}_i^0 - \mathbf{x}_j^0 + \mathbf{S}_i - \mathbf{S}_j) = \varphi(\mathbf{x}_i^0 - \mathbf{x}_j^0) + \frac{1}{2} \varphi_{ij} (\mathbf{S}_i - \mathbf{S}_j)^2 . \tag{5.35}$$

It was also assumed that the critical vibrations occur only along one crystalline axis $\mathbf{S}_i = (S_i, 0, 0)$ but the interaction (5.35) acts isotropically between the atoms in the 3-dimensional lattice. Employing the pseudoharmonic approximation for the phonon subsystem, as given in Section 3.2, and MFA for the pseudo-spin subsystem with the effective Hamiltonian (5.31) a closed system of equations was obtained for the equilibrium displacements η_λ:

$$\eta_\lambda^3 - (1 - 3y_\lambda)\eta_\lambda + (\eta_+ + \eta_-) f_0 \sigma_{-\lambda} = 0 , \tag{5.36}$$

for the average quadratic displacement y_λ of an atom in state λ:

$$y_\lambda = \frac{B}{A}\langle (u_i^\lambda)^2\rangle = \frac{B}{A}\int_0^\infty d\omega \coth\frac{\beta\omega}{2}\left[-\frac{1}{\pi} Im\,\langle\langle u_i^\lambda \mid u_i\rangle\rangle_{\omega+i\varepsilon}\right] \tag{5.37}$$

and for the order parameter $\sigma_\lambda = \langle\sigma_i^\lambda\rangle$ or $\sigma = \langle\sigma_i\rangle = 2\sigma_+ - 1$:

$$\sigma = th\,\beta(I\sigma - h)\,, \qquad I = \sum_j I_{ij}. \tag{5.38}$$

In (5.36) the dimensionless displacement $\eta_\lambda \to \sqrt{B/A}\, b_\lambda$ and the coupling constant $f_0 = (1/A)\sum_j \varphi_{ij}$ were introduced.

By analysing only the equilibrium conditions (5.36) one finds that in addition to the solutions $\eta_+ = \eta_- = 0$ corresponding to the paraelectric phase (with $I_{ij} \equiv 0$), nonzero solutions, $\eta_\lambda \neq 0$ are also possible. In the case of weak coupling, $f_0 \ll 1$ an order-disorder PT can occur since there are two equilibrium positions η_+ and η_- in the cell ($\eta_+ - \eta_- \approx \sigma f_0 \ll 1$) while for sufficiently strong coupling, $f_0 \geq 0.25$ only one nonzero solution may exist, e.g. $\eta_+ \neq 0$, and therefore only the displacive PT is possible. A numerical calculation for the whole system of equations in [49] shows that the mixed type PT occurs in a small range of the coupling constant, $f_0 \approx 0.1$, when the lattice instability prevents the statistical disordering of the atoms. For $f_0 \ll \ll 0.1$, there is order-disorder PT with negligible effect from the lattice vibra-

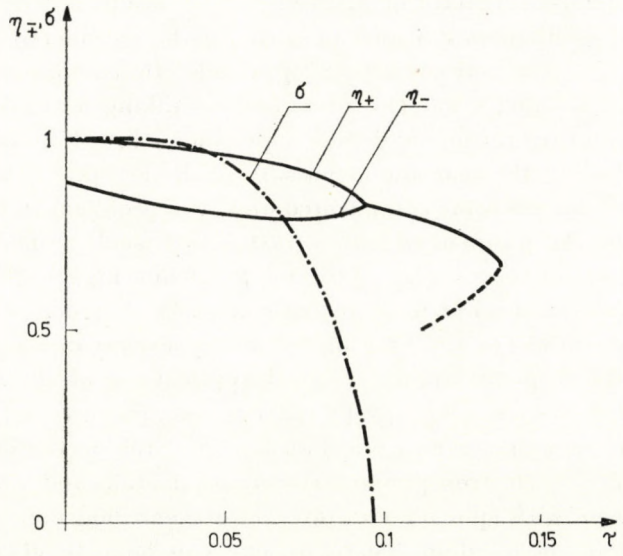

Fig. 7. The temperature dependences of the order parameters: η-average displacement, and σ-average pseudo-spin value, for the value $f_0 = 0.10$ of the dimensionless coupling parameter

tions while for $f_0 \gtrsim 0.15$ there is only displacive PT described by one order parameter, say $\eta = \eta_+$ at $\sigma = 1$. In Fig. 7 the temperature dependence of the three order parameters σ, η_+ and η_- is shown for $f_0 = 0.1$ where $\tau = T/(A^2/B)$ is the dimensionless temperature. These features are also obtained by a more sophisticated calculation [53] based on the coherent potential approximation for the disordered lattice.

Therefore the proposed unified model can describe both types of the ferroelectric PT in the limiting cases and interpolate between them. Nevertheless a real picture of PT in the vicinity of T_c cannot be obtained from this model. Besides both MFA and SCPT being inapplicable in the critical region, the basic representation (5.28) for the atomic coordinate as a static displacement η_l^λ and a dynamical one $\mathbf{u}_l^\lambda$ cannot be proved as $T \to T_c$, when excitations with large amplitude of the soliton type become of importance. The latter problem has been discussed recently from numerical and from purely theoretical points of view in several papers (see, e.g. [54], [55]).

6. Conclusions

A general treatment of the lattice instability of anharmonic crystals and estimations for some simple models presented here on the basis of the SCPT show that this theory can be applied for the investigation of this important problem of the theory of solid state. Practically there are no phase transitions in solids, magnetic or otherwise, that would not involve to some extent the lattice dynamics, which in turn can be considered properly only on the basis of some self-consistent approach. In comparison with other approximations the SCPT has the advantage of taking into account the correlations of atomic vibrations and thus it produces the self-consistent phonon spectrum as close to the real one as possible at the accepted level of approximations. There are still some complicated unsolved problems in the application of the SCPT to the problem of lattice instability, such as hard core effects correlation effects in the vicinity of the PT point and higher order corrections to the SC1 approximation in more realistic models — much work should be done in these directions on the basis of the theory already developed [6]—[10]. It is worth-while to point out also several applications of the SCPT to more complicated systems (see, e.g. [56]—[62]) where the interaction of lattice vibration with other subsystems plays an essential role in the lattice instability, as e.g. in the electron-phonon system of metals and semiconductors, magnetic systems with spin-phonon interaction, and molecular crystals with rotational degrees of freedom. Therefore one can hope to obtain some new results in the application of the SCPT to the problem of phase transitions in solids and to lattice instabilities driven by anharmonicities.

Acknowledgements

The authors are greatly indebted to Prof. Dr. W. GÖTZE and Dr. NÓRA MENYHÁRD for helpful discussions and critical reading of the manuscript. One of the authors (N. P.) wishes to express his gratitude to the Central Research Institute for Physics, Budapest, for hospitality.

REFERENCES

1. M. BORN and K. HUANG, Dynamical Theory of Crystal Lattices, Oxford Univ. Press, (Clarendon) London and New York, 1967.
2. PH. F. CHOQUARD, The Anharmonic Crystal, W. A. Benjamin Inc. New York, 1967.
3. N. R. WERTHAMER, Am. J. Phys. **37**, 763, 1969.
4. H. R. GLYDE and M. L. KLEIN, Critical Review in Solid St. Sc. **2**, 181, 1971.
5. G. K. HORTON, Rare Gas Solids — A Century of Excitement and Progress, in "Rare Gas Solids" (M. L. Klein and J. A. Venables, Ed.) Vol. 1., Chap. 1, p. 1—121, Academic Press, London—New York—San Francisco, 1976.
6. H. HORNER, Strongly Anharmonic Crystals With Hard Core Interaction, in "Dynamical Properties of Solids" (G. K. Horton and A. A. Maradudin, Ed.) Vol. 1, Ch. 8. p. 451—498, North-Holland Publ. Comp. Amsterdam, 1974.
7. W. GÖTZE and K. H. MICHEL, Self-Consistent Phonons, ibid, Vol. 1, Ch. 9, p. 499—540, 1974.
8. T. R. KOEHLER, Lattice Dynamics of Quantum Crystals, ibid., Vol. 2, Ch. 1, p. 1—104, 1975.
9. N. S. GILLIS, Lattice Dynamics of Ferroelectricity, ibid., Vol. 2. Ch. 2. p. 105—150, 1975.
10. N. M. PLAKIDA, The Method of Green Function in the Theory of Anharmonic Crystals, in "Statistical Physics and Quantum Field Theory" (N. N. Bogoliubov, Ed.) p. 205—240, Nauka, Moscow, 1973 (in Russian).
11. M. BORN, J. Chem. Phys. **7**, 591, 1939.
12. A. R. UBBELOHDE, Melting and Crystal Structure, Clarendon Press, Oxford, 1965.
13. N. M. PLAKIDA and T. SIKLÓS, Phys. Lett. **26A**, 342, 1968. Acta Phys. Hung., **26**, 387, 1969.
14. N. M. PLAKIDA and T. SIKLÓS, phys. stat. sol. **33**, 103, 1969, ibid., 113.
15. N. M. PLAKIDA, Fiz. tv. tela **11**, 700, 1969.
16. T. SIKLÓS, Acta Phys. Hung., **30**, 181. 1971. ibid., 193; ibid., 301.
17. N. M. PLAKIDA and T. SIKLÓS, phys. stat. sol. **39**, 171, 1970.
18. T. SIKLÓS and V. L. AKSIENOV, Acta Phys. Hung., **31**, 335 1972. ibid., 345; phys. stat sol. **50**, 171 1972.
19. T. SIKLÓS and I. TÜTTŐ, Acta Phys. Hung. **39**, 275, 1975.
20. V. L. AKSIENOV, Fiz. tv. tela **14**, 1986, 1972.
21. P. S. ZIRYANOV, V. V. KONDRATYEV and I. G. KULIEV, Fiz. met. i met. **34**, 263, 1972, ibid. **35**, 233 1973.
22. N. M. PLAKIDA and V. L. AKSIENOV, Fiz. tv. tela, **15**, 2575, 1973; phys. stat. sol. (b), **62**, 261, 1974.
23. G. MEISSNER, Phys. Rev. **B1**, 1822, 1970; Fiz. nizk. temp. (Low Temp. Phys., USSR) **1**, 697. 1975.
24. Y. IDA, Phys. Rev., **187**, 951, 1969; ibid. **B1**,, 2488, 1970.
25. K. ISHIZAKI, P. BOLSAITIS and I. L. SPAIN, Phys. Rev. **B7**, 5412, 1973.
26. J. N. SHAPIRO, Phys. Rev. **B1**, 3982, 1970.
27. J. C. RAICH and R. D. ETTERS ,J. Chem. Phys. **55**, 3901, 1971.
28. N. N. BOGOLIUBOV and S. V. TYABLIKOV, Dokl. Akad. Nauk SSSR, **126**, 53, 1959.
29. D. N. ZUBAREV, Sov. Phys. Uspekhi **3**, 320, 1960. Non-equilibrium Statistical Mechanics § 16, Plenum Prses, New York, 1974.
30. W. GÖTZE and K. H. MICHEL, Z. Phys. **217**, 170, 1968.
31. A. A. ABRIKOSOV, L. P. GORKOV and I. E. DZYALOSHINSKI, Methods of Quantum Field Theory in Statistical Physics, Prentice-Hall, Inc., Englewood Cliffs, New York, 1963.
32. L. J. SHAM, Phys. Rev., **139**, A 1189, 1965.
33. N. M. PLAKIDA, Theor. i mat. fiz. **5**, 147, 1970.
34. N. M. PLAKIDA, Theor. i mat. fiz. **12**, 135, 1972.

35. M. L. KLEIN, G. K. HORTON and V. V. GOLDMAN, Phys. Rev. **B2**, 4995, 1970.
36. L. B. KANNEY and G. K. HORTON, Phys. Rev. Lett. **34**, 1565, 1975.
37. P. W. ANDERSON, in: Fizika Dielektrikov, (G. L. Skanavi, Ed.) p. 290—296, Akad. Nauk SSSR, Moscow, 1960.
38. W. COHRAN, Adv. in Phys. **9**, 387, 1960.
39. L. D. LANDAU and E. M. LIFSHITZ, Statistical Physics Third Edition, Ch. 14, § 145—146, Nauka, Moscow, 1976 (in Russian).
40. T. SCHNEIDER, G. SRINIVASAN and C. P. ENZ, Phys. Rev. **A5**, 1528, 1972.
41. E. EISENRIEGLER, Phys. Rev. **B9**, 1029, 1974.
42. R. CONTE, Jour. de Phys. **35**, 67, 1974.
43. A. I. SOKOLOV, Fiz. tv. tela **16**, 733 1974. Journ. teor. i exp. fiz. **68**, 1137, 1975.
44. L. P. KADANOFF, et al. Rev. Mod. Phys. **39**, 395, 1967.
45. N. S. GILLIS, Phys. Rev. **B11**, 309, 1975.
46. A. I. LARKIN and S. A. PIKIN, Journ teor i exp. fiz. **56**, 1664, 1969.
47. V. G. VAKS, "Introduction to Microscopic Theory of Ferroelectrics", Ch. 1, and §§ 44 –42, Nauka, Moscow, 1973, (in Russian).
48. N. M. PLAKIDA and V. L. AKSIENOV, Teor i mat. fiz. **34**, 353, 1978; ibid. **35**, 104, 1978.
49. S. STAMENKOVIC', N. M. PLAKIDA, V. L. AKSIENOV and T. SIKLÓS, Phys. Rev. **B14**, 5080, 1976.
50. S. STAMENKOVIC', N. M. PLAKIDA, V. L. AKSIENOV and T. SIKLÓS, Acta Phys. Hung. **42**, 265, 1977; Report KFKI—1987—68, Budapest, 1978.
51. H. BECK, J. Phys. C. Solid St. Phys. **9**, 33, 1976.
52. N. M. PLAKIDA, Phys. Lett. **32A**, 134, 1970.
53. V. L. AKSIENOV, H. BRETER, J. M. KOVALSKI, N. M. PLAKIDA and V. B. PRIEZZHEV, Fiz. tv. tela **18**, 2920, 1976.
54. S. AUBRY, J. Chem. Phys. **62**, 3217, 1975. These, Université Paris VI., 1975.
55. J. A. KRUMHANSL and J. R. SCHRIEFFER, Phys. Rev. **B11**, 3535, 1975.
A. R. BISHOP and J. A. KRUMHANSL, Phys. Rev. **B12**, 2824 1975.
A. R. BISHOP, E. DOMANY and J. A. KRUMHANSL, Phys. Rev. **B14**, 2966, 1976.
56. N. S. GILLIS, Phys. Rev. Lett. **22** 1251, 1969, Phys. Rev. **B1**, 1872, 1970.
57. G. MEISSNER, Zs. Phys. **235**, 85, 1970. Zs. Phys. **247**, 203, 1971.
59. H. KONWENT and N. M. PLAKIDA, The Spin-Phonon Interaction in Anharmonic Ferromagnetic Crystals in: "Magnetism in Metals and Metallic Compounds" (J. Lopuszanski, A. Pekalski and J. Przystawa, Ed.) p. 543—572, Plenum Press, New York and London, 1976.
60. G. MEISSNER, Zs. Phys. **237**, 272, 1970.
61. J. C. RAICH, N. S. GILLIS and A. B. ANDERSON, J. Chem. Phys. **61**, 1399, 1974.
A. B. ANDERSON, J. C. RAICH and R. D. ETTERS, Phys. Rev. **B14**, 814, 1976.
62. T. WASIUTYNSKI, phys. stat. sol. (b) **76**, 175, 1976.

Acta Physica Academiae Scientiarum Hungaricae, Tomus 45 (1), pp. 75—80 (1978)

LATTICE DYNAMICS OF CHROMIUM ON EXTENDED DE LAUNAY MODEL

By

R. CAVALHEIRO and M. M. SHUKLA*

INSTITUTO DE FISICA "GLEB WATAGHIN", UNIVERSIDADE ESTADUAL DE CAMPINAS
CAMPINAS – SP. BRASIL

(Received 29. VI. 1978)

Phonon dispersion relations along the principal symmetry directions and lattice heat capacities of chromium have been calculated on the basis of extended de Launay model. Theoretical results are found to exhibit good reproduction of experimental ones.

1. Introduction

The original model of DE LAUNAY [1] happened to be one of the earliest successful phenomenological models of metals. It has been applied extensively to compute the thermal properties of almost all cubic metals (JOSHI and RAJGOPAL [2]). It was discovered by us that DE LAUNAY's model was a complete failure as far as the reproduction of the experimental phonon dispersion relations in most of the metals was concerned. We attributed this failure of DE LAUNAY's model to its termination of the interatomic interactions out to second neighbors only. We have thus extended dE LAUNAY's model (SHUKLA and CAVALHEIRO [3]) to consider the interatomic interactions beyond the second nearest neighbor. Our scheme has been very successful in explaining the experimental phonon dispersion relations and the lattice heat capacities of copper, silver, nickel, platinum and palladium (SHUKLA and CAVALHEIRO [4]), lead (CAVALHEIRO and SHUKLA [5]), alkali metals (CAVALHEIRO and SHUKLA [6]), b.c.c. transition metals, α-iron, molybdenum and tungsten (CAVALHEIRO and SHUKLA [7]), and gold (CAVALHEIRO and SHUKLA [8]).

The success of extended DE LAUNAY model for the study of several f.c.c. and b.c.c. metals has encouraged us to take up also the study of chromium on the same basis. An independent motive to consider chromium for the present study was that this metal is a favorite metal as far as the study of experimental phonon dispersion curves is concerned. While MÖLLER and MACKINTOSH [9] carried out such measurements a few years ago, recently SHAW and MUHLENSTEIN [10] have also done an extensive measurement of phonon frequencies of chromium. The existence of experimental thermal and elastic data of chromium has also facilitated its resent lattice dynamical studies.

* On leave of absence from UNICAMP. Visiting Professor, Department of Electrical Engineering, University of Rhode Island, Kingston, Rhode Island, 02881 (U.S.A.).

2. Theory

The secular determinant by which the frequency of vibration is determined (see SHUKLA and CAVALHEIRO [3]) is given by

$$\begin{vmatrix} D_{11} - m\omega^2 + pR_1 & D_{12} + qR_1 & D_{13}\, rR_1 \\ D_{21} + pR_2 & D_{22} - m\omega^2 + qR_2 & D_{23} + rR_2 \\ D_{31} + pR_3 & D_{32} + qR_3 & D_{33} - m\omega^2 + rR_3 \end{vmatrix} = 0\,, \tag{1}$$

where

$$R_1 = (D'_{11} - D_{11})\,p + (D'_{12} - D_{12})\,q + (D'_{13} - D_{13})\,r\,, \tag{2.1}$$

$$R_2 = (D'_{21} - D_{21})\,p + (D'_{22} - D_{22})\,q + (D'_{23} - D_{23})\,r\,, \tag{2.2}$$

$$R_3 = (D'_{31} - D_{31})\,p + (D'_{32} - D_{32})\,q + (D'_{33} - D_{33})\,r\,. \tag{2.3}$$

When the interionic interactions are taken up to fourth neighbors, the typical diagonal and non-diagonal elements of the dynamical matrix are given by:

$$D_{ii} = \frac{8}{3}\alpha(1 - C_iC_jC_k) + 4\beta S_i^2 + 4\gamma[1 - (2C_i^2 - 1)\cdot(C_j^2 + C_k^2 - 1)]$$

$$+ \frac{8}{3}\varepsilon[11 - 9(1 - 4S_i^2)\,C_iC_jC_k - 2(1 - 2s_j^2 - S_k^2)\,C_iC_jC_k]\,, \tag{3.1}$$

$$D_{ij} = \frac{8}{3}aC_kS_iS_j + 8\gamma C_kS_iS_j + \frac{8}{11}\varepsilon[6(2C_i^2 + 2C_j^2 - 1) + (1 - 4S_k^2)]\,C_kS_iS_j, \tag{3.2}$$

$$S = \sin a\,K_i\,,$$

$$C = \cos a\,K_i\,.$$

a = lattice parameter and K_i ($i = 1, 2, 3$) are Cartesian components of the wave vector $\bar{k}$.

By changing $\alpha, \beta, \gamma, \varepsilon$ to $\alpha', \beta', \gamma', \varepsilon'$, the elements D'_{ii} and D'_{ij} are obtained from (3.1) and (3.2).

By expanding the secular determinant in long wavelength limits ($k \to 0$) the relations obtained between the elastic constants and force constants are the following:

$$aC_{11} = \left(2\alpha + 3\gamma + \frac{57}{11}\varepsilon - \frac{4}{3}\alpha' + 2\beta' + \gamma' + \frac{109}{11}\varepsilon'\right) + aK_e\,,$$

$$aC_{12} = \left(\frac{2}{3}\alpha - \gamma - \frac{19}{11}\varepsilon + 3\gamma' + \frac{57}{11}\varepsilon'\right) + aK_e\,,$$

$$aC_{44} = \frac{2}{3}\alpha + 2\gamma + \frac{38}{11}\varepsilon\,,$$

where the bulk modulus of the electron gas is given by

$$aK_e = \frac{2}{a}\left[(\alpha' - \alpha) + 3(\gamma' - \gamma) + \frac{57}{11}(\varepsilon' - \varepsilon)\right].$$

3. Numerical computations

Before the calculation of phonon frequencies, we needed numerical values of the seven free parameters of the model. To evaluate them uniquely we have employed seven independent equations, three relating the elastic constants and four between phonon frequencies from the boundary of the Brillouin zone and the force constants. We made several choices to select these four frequencies and found that zone boundary frequencies from [ξ 00] and [$\xi\xi$ 0] directions gave the best fit with the experimental result. Care was taken to use the elastic constants at the same temperature at which phonons were determined. The phonon frequencies of chromium were determined at room temperature. We took room temperature values of the elastic constants of chromium from the measurements of SUMER and SMITH [11]. The input data to calculate force constants are given in Table I. In Table II we have given the output values of the force constants. The computed phonon dispersion curves of chromium along all the three principal symmetry directions are shown in Figs. 1 and 2; the experimental results are also shown for comparison purposes. While the calculated curves are shown by solid lines, the experimental points are demonstrated by the different symbols given in the captions.

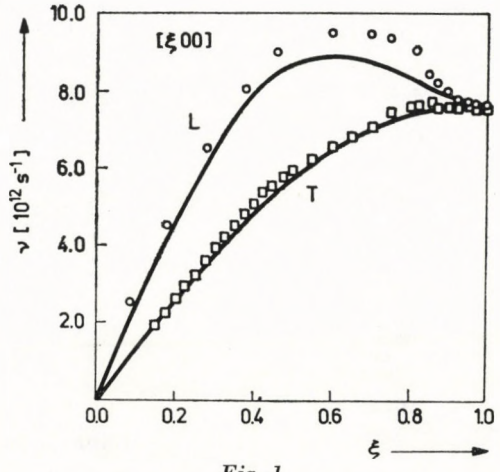

Fig. 1

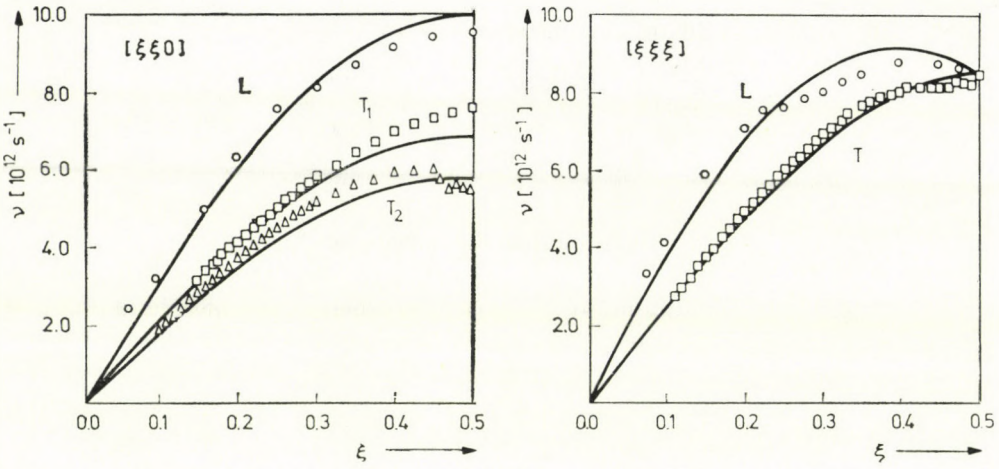

Fig. 2

In order to afford an independent check of the model we have also calculated the $(\Theta - T)$ curve of chromium. In order to accomplish such calculations, the first Brillouin zone of chromium was divided into 8000 miniature cells, and lattice heat capacities at different temperatures were calculated by Blackman's sampling technique. The resulting C_v was used to calculate Θ. Calculated $(\Theta - T)$ curve of chromium is shown in Fig. 3 together with the experimental points also shown for comparison purposes. The value of Θ for chromium was estimated from the experimental values of C_v from the measurements of CLUSIUS and FRANZOSINI [12] and the electronic heat capacity from the measurement of HEINIGER [13].

4. Comparison with experimental results

A critical study of Figs. 1 and 2 reveals that the calculated phonon dispersion curves of chromium along all the three principal symmetry directions, $[\xi\,00]$, $[\xi\xi\,0]$, and $[\xi\xi\xi]$, have given a good account of the experimental curves. At low wave vectors the calculated and experimental phonons are found to coincide. A little discrepancy of the order of 4 to 8% exists between the calculated and experimental phonons near the zone boundaries of the longitudinal branch of $[\xi\,00]$ and in all three branches in $[\xi\xi\,0]$. The experimental observations of the lowering of the longitudinal frequencies near $k = 0.2$ to $k = 0.4$ seemed quite strange.

A study of Fig. 3 shows that the $(\Theta - T)$ curve of chromium has been found to reproduce the entire course of the experimental curves. The calculated curve is found to lie 3% below the experimental results.

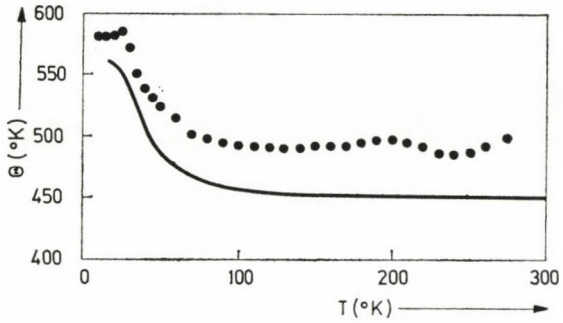

Fig. 3

5. Conclusion

The present study of lattice dynamics and heat capacities of chromium has given a fair account of the experimental results. It should be borne in mind that the extended DE LAUNAY model has been designed for metals whose conduction electrons form a sea of free electron gas, which also implies that those metals have spherical Fermi surfaces. A critical study of the electronic properties of chromium may reveal that this is a quite complicated metal. The Fermi surface of chromium is not at all spherical. The conduction electrons of this metal do not behave like free electrons. Also they are found to lie in hybrid orbits. These considerations guarantee that the extended de Launay model has only a limited application to this metal. Chromium is the only metal of cubic structure whose experimental value of C_{44} is found to be greater than C_{12}. This indicates that the bulk modulus of electron gas is negative for this metal. Our calculations have shown that this kind of behavior has no peculiar effect on the calculated phonons. A negative K_e theoretically predicts lower values of longitudinal frequency along $[\xi 00]$ and $[\xi\xi 0]$ directions.

Here, it is worthwhile to compare our theoretical predictions for this metal with those of other workers. The people who have carried out such studies are PAL [14], FELDMANN [15], and GUPTA and HEMKAR [16]. A critical study of their results would reveal that our theoretical predictions have been better. The model employed by these workers is not superior to that used by us. FELDMANN [15] has ignored electron-ion interaction. PAL [13] applied the original model of SHARMA and JOSHI [17]; he used $K_e = 0$ in the model of SHARMA and JOSHI for the calculation of longitudinal branches; this has no physical justification. GUPTA and HEMKAR [16] used the model of SHUKLA and SALZBERG [18]. Results reported by them are superior to our calculations, due to the fact that GUPTA and HEMKAR [16] used the crystal equilibrium condition and the Cauchy deviation to calculate bulk modulus of electron gas from the relation $(C_{12} - C_{44}) = 2.2K_e$, which has been proved by one of us

(SHUKLA [19]) to be an incorrect procedure. The work of GUPTA and HEMKAR [16] has no physical significance.

While a sophisticated model study of chromium does not emerge, our result should serve as an early attempt to tackle the problem.

REFERENCES

1. J. DE LAUNAY, Solid State Physics edited by Seitz and Turnbull, Academic Press, New York, Vol. 2, 220, 1956.
2. S. K. JOSHI and A. K. RAJAGOPAL, Solid State Physics edited by Seitz and Turnbull, Academic Press, New York, Vol. 22, 159 1968.
3. M. M. SHUKLA and R. CAVALHEIRO, Phonons edited by Nucimovici, Flammarion, Paris, 313, 1971.
4. M. M. SHUKLA and R. CAVALHEIRO, Il Nuovo Cimento, **16B,** 63, 1973.
5. R. CAVALHEIRO and M. M. SHUKLA, J. Phys. Soc. Japan, **34,** 1002, 1973.
6. R. CAVALHEIRO and M. M. SHUKLA, Acta Phys. Hung., **37,** 187, 1974.
7. R. CAVALHEIRO and M. M. SHUKLA, Acta Physica Polonica, **49A,** 27, 1976.
8. R. CAVALHEIRO and M. M. SHUKLA, Physica Status Solidi, **76B,** 371, 1976.
9. H. B. MÖLLER and A. R. MACKINTOSH, Inelastic Scattering of Neutrons (I. A. E. A, Vienna), Vol. 1, 95, 1965.
10. W. M. SHAW and L. D. MUHLENSTEIN, Phys. Rev., **B4,** 969, 1971.
11. A. SUMER and J. F. SMITH, J. Appl. Phys., **34,** 2691, 1963.
12. C. K. CLUSIUS and P. FRANZOSINI, Z. Naturforsch, **A17,** 522, 1962.
13. F. HEINIGER, Phys. Kon. Mat., **5,** 285, 1966.
14. S. PAL, Phys. Rev., **B9,** 5144, 1974.
15. J. L. FELDMAN, Phys. Rev., **B1,** 448, 1970.
16. O. P. GUPTA and M. P. HEMKAR, Z. Naturforsch., **329,** 1495, 1977.
17. P. K. SHARMA and S. K. JOSHI, J. Chem. Phys., **40,** 662, 1970.
18. M. M. SHUKLA and J. B. SALZBERG, J. Phys., **F3L,** 1973.
19. M. M. SHUKLA, Physical Review (submitted for publication).

Acta Physica Academiae Scientiarum Hungaricae, Tomus 45 (1), pp. 81—86 (1978)

APPLICATION OF G.P.D.P. TO THERMAL BOUNDARY LAYER

By

P. SINGH* and D. K. BHATTACHARYA

DEPARTMENT OF MATHEMATICS, INDIAN INSTITUTE OF TECHNOLOGY, KHARAGPUR, INDIA

(Received 4. VII. 1978)

The governing principle of dissipative processes is applied to study the steady state thermal boundary layer along a semi-infinite flat plate when plate temperature differs from that of free stream. The thermal boundary—layer thickness is obtained using a third degree profile. It is found that the rate of heat transfer from the plate to the fluid computed for various Prandtl numbers using present variational method is quite close to the already known exact results. The results of the present investigation are fairly better than those of well-known Karman-Pohlhausen solution.

Introduction

In the present investigation our main aim is to study the applicability of the governing principle of dissipative processes to thermal boundary layer along a semi-infinite flat plate when an incompressible viscous fluid flows over it. The temperature of the plate T_w is uniform and it differs from free stream temperature T_w ($T_\infty > T_w$). It is well known that in the formulation of GYARMATI's variational principle the various balance equations play a basic role [1, 2]. In the present case the energy balance with convective term is required to study the temperature distribution inside the boundary layer if the viscous boundary layer is already known. If T denotes the temperature the energy balance equation without viscous dissipation is

$$\varrho c_v \frac{\partial T}{\partial t} + \varrho c_v \cdot (\boldsymbol{v} T) + \nabla I_q = 0, \tag{1}$$

where v denotes the velocity vector and I_q is the heat current density. ϱ and c_v are density and the specific heat of the fluid, respectively. We shall formulate GYARMATI's variational principle in the energy picture. The energy dissipation for the system in the energy picture is [2, 3]

$$T\sigma = -I_q \cdot \nabla \ln T. \tag{2}$$

* Present address: Department of Mathematics, Indian Institute of Technology, Kanpur, India.

Here the state variable $\ln T$ is used for T. The linear constitutive relation in energy picture is given by

$$I_q = -L_{\lambda\lambda} \nabla(\ln T), \tag{3}$$

where $L_{\lambda\lambda}$ is the phenomenological coefficient and represents the conductivity in the linear Onsager theory. In the present formulation $L_{\lambda\lambda}$ is given by

$$L_{\lambda\lambda} = KT, \tag{4}$$

where K is the coefficient of thermal conductivity of the fluid. The dissipation potentials can now be defined in the energy picture as

$$\Psi^* = \frac{1}{2} L_{\lambda\lambda} (\nabla \ln T)^2, \quad \Phi^* = \frac{1}{2L_{\lambda\lambda}} I_q^2. \tag{5}$$

Finally, the GYARMATI's principle in energy picture

$$\delta \int_V (T\sigma - \Psi^* - \Phi^*) \, dV = 0 \tag{6}$$

takes the following form for the system under consideration

$$\delta \int_V \left[-I_q \cdot \nabla \ln T - \frac{L_{\lambda\lambda}}{2} (\nabla \ln T)^2 - \frac{1}{2 L_{\lambda\lambda}} I_q^2 \right] dV = 0, \tag{7}$$

where dV denotes the element of the volume V of the system.

Solution of two dimensional thermal boundary layer

Consider the two dimensional steady flow of an incompressible fluid along a flat plate. The essence of boundary layer theory is to presume that irreversible processes of heat and momentum transfer are confined in very thin layer adjacent to the plate. If x measures the distance along the plate from $x = 0$ to $x = \infty$ and y normal to it and u and v are velocity components along x and y directions respectively, the Eq. (1) reduces to

$$\varrho c_v \left(u \cdot \frac{\partial T}{\partial x} + v \frac{\partial T}{\partial y} \right) + \nabla \cdot I_q = 0. \tag{8}$$

This equation describes the steady state temperature distribution inside the boundary layer region. The constitutive equation in this particular case has the form

$$I_{q1} = -L_{\lambda\lambda} \frac{\partial \ln T}{\partial y} \tag{9}$$

in the energy picture. The principle (7) takes now the simple form

$$\delta \int_0^{\infty} \int_0^{d_T} \left[-I_{q1} \frac{\partial \ln T}{\partial y} - \frac{L_{\lambda\lambda}}{2} \left(\frac{\partial \ln T}{\partial y} \right)^2 - \frac{1}{2 L_{\lambda\lambda}} I_{q1}^2 \right] dx\, dy = 0 , \tag{10}$$

where d_T denotes the thermal boundary layer thickness.

The principle (10) contains two unknown I_{q1}, and T which are connected by the exact constitutive relation (9). In the dual field method we assume the thermodynamic current I_{q1} in term of an approximate constitutive relation [4, 5, 6]

$$I_{q1} = -\alpha \frac{\partial \ln T^*}{\partial y} , \tag{11}$$

where T^* is an approximate temperature field and satisfies the same conditions as T. In the exact theory $T = T^*$ and the Lagrangian density is zero. Introducing (11) in (8) and (10), we get

$$u \frac{\partial T}{\partial x} + v \frac{\partial T}{\partial y} = \alpha \frac{\partial^2 T^*}{\partial y^2} , \tag{12}$$

$$\delta \int_0^{\infty} \int_0^{d_T} \left[\frac{\partial T^*}{\partial y} \frac{\partial T}{\partial y} - \frac{1}{2} \left(\frac{\partial T}{\partial y} \right)^2 - \frac{1}{2} \left(\frac{\partial T^*}{\partial y} \right)^2 \right] dx\, dy = 0 , \tag{13}$$

where α denotes the thermal diffusivity of fluid.

Using similarity transformations

$$\eta = y \sqrt{\frac{u_\infty}{\nu x}}$$

$$u = u_\infty f'(\eta) , \quad v = \frac{1}{2} \sqrt{\frac{\nu u_\infty}{x}} (\eta f' - f) \tag{14}$$

the equation (12) and principle (13) yields

$$\frac{d^2 T^*}{d\eta^2} + \frac{Pr}{2} f \frac{dT}{d\eta} = 0 , \tag{15}$$

$$\delta \int_0^{\infty} \frac{dx}{\sqrt{x}} \int_0^{d_T} \left[\frac{dT}{d\eta} \frac{dT^*}{d\eta} - \frac{1}{2} \left(\frac{dT}{d\eta} \right)^2 - \frac{1}{2} \left(\frac{dT^*}{d\eta} \right)^2 \right] d\eta = 0 , \tag{16}$$

where P_r is Prandtl number.

To determine T^* we need the velocity profile inside the boundary layer over a flat plate. We have already obtained a variational solution of viscous

boundary layer with the help of GYARMATI's principle (see SINGH and BHATTACHARYA [7]). The third degree polynomial for velocity profile is

$$\frac{u}{u_\infty} = f' = \frac{3\eta}{2d} - \frac{1}{2}\frac{\eta^3}{d^3} \tag{17}$$

where d denotes the viscous boundary layer thickness. Its value is

$$d = 4 \cdot 696 \,. \tag{18}$$

We shall use the expression (17) in the calculation of thermal boundary layer thickness from the present variational formulation.

To determine d_T the thermal boundary layer thickness we assume the following third degree polynomial for

$$\frac{T - T_\infty}{T_w - T_\infty} = 1 - \frac{3}{2}\frac{\eta}{d_T} + \frac{1}{2}\frac{\eta^3}{d_T^3} \tag{19}$$

which satisfies the boundary conditions

at
$$\eta = 0, \quad T = T_w, \quad \frac{d^2T}{d\eta^2} = 0,$$

$$\eta = d_T, \quad T = T_\infty, \quad \frac{dT}{d\eta} = 0 \,. \tag{20}$$

In (19) d_T is the variational parameter which is to be determined from the principle (16). From Eq. (15) with (17) and (19) we get

$$\frac{dT^*}{d\eta} = \frac{3}{16}\frac{P}{d_T}\left[\frac{1}{14}\frac{\eta^7}{d^3 d_T^2} - \frac{3\eta^5}{5d\,d_T^2} - \frac{1}{10}\frac{\eta^5}{d^3} + \frac{\eta^3}{d} + \frac{1}{35}\frac{d_T^5}{d^3} - \frac{2}{5}\frac{d_T^3}{d}\right], \tag{21}$$

which satisfies the condition $dT^*/d\eta = 0$ at the edge of thermal boundary layer.

Substitution of (21) and (19) in principle (16) and partial integration w.r. to η gives

$$\delta \int_0^\infty \frac{dx}{\sqrt{x}}\left[P_r\left(117 \cdot 18\frac{d_T^2}{d} - 9 \cdot 37\frac{d_T^4}{d^3}\right) - \frac{1200}{d_T} - \right.$$

$$\left. - P_r^2\left(0 \cdot 018\frac{d_{T^9}}{d^6} - 0 \cdot 457\frac{d_{T^7}}{d^4} + 2 \cdot 84\frac{d_{T^5}}{d^2}\right)\right] = 0 \,. \tag{22}$$

The Euler—Lagrange's equation of (22) is

$$\Delta^{10} - 19 \cdot 753\Delta^8 + 89 \cdot 228\Delta^6 + \frac{11 \cdot 475}{P_r}\Delta^5 - \frac{65 \cdot 487}{P_r}\Delta^3 - \frac{15 \cdot 179}{P_r^2} = 0\,, \tag{23}$$

where

$$\Delta = \frac{d_T}{d}\,.$$

Equation (23) is solved using the Newton—Raphson method to get its roots. The value of thermal boundary layer thickness depends on Prandtl number P_r.

We can now calculate the heat transfer at the plate which is an important physical characteristic of the problem. The nondimensional heat transfer obtained with the help of the formula

$$q = -K\left(\frac{\partial T}{\partial y}\right) y = 0$$

is

$$q^* = -K\sqrt{\frac{u_\infty}{\nu x}}\left(\frac{dT}{d\eta}\right)\eta = 0\,.$$

This approximate value of q^* is quite close to exact values [8] as can be seen from Table I. The heat transfer obtained with the help of Karman—Pohlhausen technique is also compared with the present values and it is found that the present method which is based on sound physical reality can be used as approximate variational technique for this type of problems.

Table I

Heat transfer at the plate

Pr	Approximate value from G. P. D. P.	Exact value	Karman—Pohlhausen method
0.6	0.266	0.276	0.266
0.8	0.295	0.307	0.295
1.0	0.319	0.332	0.319
1.1	0.330	0.344	0.330
7.0	0.623	0.645	0.621
10.0	0.705	0.730	0.701
15.0	0.806	0.835	0.803

The difference between the approximate and the exact values of heat transfer at the plate is less than 4%. The results can be improved by taking more variational parameters in the temperature profile and performing first varia-

tions of each of the parameters independently. Forcing all these variations to vanish simultaneously provides us a set of equations

$$\frac{\partial F}{\partial c_i} = 0, \qquad (i = 1, 2, \ldots n),$$

where c_i are n variational parameters. These equations can be solved to obtain temperature profile. In more complicated flow field such analysis may be very helpful in approaching the exact result which is not known a priori.

Acknowledgement

One of the authors (P.S.) is thankful to Prof. I. GYARMATI, Hungarian Academy of Sciences, Budapest, for his valuable suggestions in the preparation of this paper. D. K. BHATTACHARYA is thankful to C.S.I.R., New Delhi, for financial assistance.

REFERENCES

1. I. GYARMATI, Ann. Phys., **23**, 353, 1969.
2. I. GYARMATI, Non Equilibrium Thermodynamics Field Theory and Variational Principles, Springer, Berlin, 1970.
3. H. FARKAS, Z. Phys. Chem., **239**, 124, 1968.
4. A. STARK, Ann. Phys., **27**, 53, 1974.
5. P. SINGH, Int. J. Heat and Mass Transfer, **19**, 571, 1976.
6. P. SINGH, J. Non-Equilib. Thermodynamics, **1**, 105, 1976.
7. P. SINGH and D. K. BHATTACHARYA, Application of Gyarmati Principle to Boundary Layer Flow, Acta Mech., 1977 (in press).
8. H. SCHLICHTING, Boundary Layer Theory, Mc-Graw Hill Co., New York, 1968.

Printed in Hungary

A kiadásért felel az Akadémiai Kiadó igazgatója — Műszaki szerkesztő: Botyánszky Pá

A kézirat a kiadóba érkezett: 1978. VII. 28. A kézirat nyomdába érkezett: 1978. VII. 31.

Terjedelem: 7,5 (A/5) ív, 15 ábra

79.6155 Akadémiai Nyomda, Budapest — Felelős vezető: Bernát György

NOTES TO CONTRIBUTORS

I. PAPERS will be considered for publication in Acta Physica Hungarica, only if they have not previously been published or submitted for publication elsewhere. They may be written in English, French, German or Russian.

Papers should be submitted to

Prof. I. Kovács, Editor
Department of Atomic Physics, Technical University
1521 Budapest, Budafoki út 8, Hungary

Papers may be either articles with abstracts or short communications. Both should be as concise as possible, articles in general not exceeding 25 typed pages, short communications 8 typed pages.

II. MANUSCRIPTS

1. Papers should be submitted in five copies.

2. The text of papers must be of high stylistic standard, requiring minor corrections only.

3. Manuscripts should be typed in double spacing on good quality paper, with generous margins.

4. The name of the author(s) and of the institutes where the work was carried out should appear on the first page of the manuscript.

5. Particular care should be taken with mathematical expressions. The following should be clearly distinguished, e.g. by underlining in different colours: special founts (italics, script, bold type, Greek, Gothic, etc.); capital and small letters; subscripts and superscripts, e.g. x_2, x^3; small l and 1; zero and capital O; in expressions written by hand: e and l, n and u, v and v, etc.

6. References should be numbered serially and listed at the end of the paper in the following form: J. Ise and W. D. Fretter, Phys. Rev., *76*, 933, 1949.

For books, please give the initials and family name of the author(s), title, name of publisher, place and year of publication, e.g.: J. C. Slater, Quantum Theory of Atomic Structures, I. McGraw-Hill Book Company, Inc., New York, 1960.

References should be given in the text in the following forms: Heisenberg [5] or [5].

7. Captions to illustrations should be listed on a separate sheet, not inserted in the text.

III. ILLUSTRATIONS AND TABLES

1. Each paper should be accompanied by five sets of illustrations, one of which must be ready for the blockmaker. The other sets attached to the copies of the manuscript may be rough drawings in pencil or photocopies.

2. Illustrations must not be inserted in the text.

3. All illustrations should be identified in blue pencil by the author's name, abbreviated title of the paper and figure number.

4. Tables should be typed on separate pages and have captions describing their content. Clear wording of column heads is advisable. Tables should be numbered in Roman numerals (I, II, III, etc.).

IV. MANUSCRIPTS not in conformity with the above Notes will immediately be returned to authors for revision. The date of receipt to be shown on the paper will in such cases be that of the receipt of the revised manuscript.

Reviews of the Hungarian Academy of Sciences are obtainable at the following addresses:

AUSTRALIA
C.B.D. LIBRARY AND SUBSCRIPTION SERVICE, Box 4886, G.P.O., *Sydney N.S.W.2001*
COSMOS BOOKSHOP, 145 Ackland Street, *St Kilda (Melbourne), Victoria 3182*

AUSTRIA
GLOBUS, Höchstädtplatz 3, *1200 Wien XX*

BELGIUM
OFFICE INTERNATIONAL DE LIBRAIRIE, 30 Avenue Marnix, *1050 Bruxelles*
LIBRAIRIE DU MONDE ENTIER, 162 Rue du Midi, *1000 Bruxelles*

BULGARIA
HEMUS, Bulvar Ruszki 6, *Sofia*

CANADA
PANNONIA BOOKS, P.O. Box 1017, Postal Station "B", *Toronto, Ontario M5T 2T8*

CHINA
CNPICOR, Periodical Department, P.O. Box 50, *Peking*

CZECHOSLOVAKIA
MAD'ARSKÁ KULTURA, Národní třida 22, *115 66 Praha*
PNS DOVOZ TISKU, Vinohradská 46, *Praha 2*
PNS DOVOZ TLAČE, *Bratislava 2*

DENMARK
EJNAR MUNKSGAARD, Norregade 6, *1165 Copenhagen*

FINLAND
AKATEEMINEN KIRJAKAUPPA, P.O. Box 128, *SF-00101 Helsinki 10*

FRANCE
EUROPERIODIQUES S. A., 31 Avenue de Versailles, *78170 La Celle St.-Cloud*
LIBRAIRIE LAVOISIER, 11 rue Lavoisier, *75008 Paris*
OFFICE INTERNATIONAL DE DOCUMENTATION ET LIBRAIRIE, 48 rue Gay-Lussac, *75240 Paris Cedex 05*

GERMAN DEMOCRATIC REPUBLIC
HAUS DER UNGARISCHEN KULTUR, Karl-Liebknecht-Strasse 9, *DDR-102 Berlin*
DEUTSCHE POST ZEITUNGSVERTRIEBSAMT, Strasse der Pariser Kommüne 3—4, *DDR-104 Berlin*

GERMAN FEDERAL REPUBLIC
KUNST UND WISSEN ERICH BIEBER, Postfach 46, *7000 Stuttgart 1*

GREAT BRITAIN
BLACKWELL'S PERIODICALS DIVISION, Hythe Bridge Street, *Oxford OX1 2ET*
BUMPUS, HALDANE AND MAXWELL LTD., Cowper Works, *Olney, Bucks MK46 4BN*
COLLET'S HOLDINGS LTD., Denington Estate, *Wellingborough, Northants NN8 2QT*
W.M. DAWSON AND SONS LTD., Cannon House, *Folkestone, Kent CT19 5EE*
H. K. LEWIS AND CO., 136 Gower Street, *London WC1E 6BS*

GREECE
KOSTARAKIS BROTHERS, International Booksellers, 2 Hippokratous Street, *Athens-143*

HOLLAND
MEULENHOFF-BRUNA B.V., Beulingstraat 2, *Amsterdam*
MARTINUS NIJHOFF B.V., Lange Voorhout 9—11, *Den Haag*
SWETS SUBSCRIPTION SERVICE, 347b Heereweg, *Lisse*

INDIA
ALLIED PUBLISHING PRIVATE LTD., 13/14 Asaf Ali Road, *New Delhi 110001*
150 B-6 Mount Road, *Madras 600002*
INTERNATIONAL BOOK HOUSE PVT. LTD., Madame Cama Road, *Bombay 400039*
THE STATE TRADING CORPORATION OF INDIA LTD., Books Import Division, Chandralok, 36 Janpath, *New Delhi 110001*

ITALY
EUGENIO CARLUCCI, P.O. Box 252, *70100 Bari*
INTERSCIENTIA, Via Mazzé 28, *10149 Torino*
LIBRERIA COMMISSIONARIA SANSONI, Via Lamarmora 45, *50121 Firenze*
SANTO VANASIA, Via M. Macchi 58, *20124 Milano*
D. E. A., Via Lima 28, *00198 Roma*

JAPAN
KINOKUNIYA BOOK-STORE CO. LTD., 17-7 Shinjuku-ku 3 chome, Shinjuku-ku, *Tokyo 160-91*
MARUZEN COMPANY LTD., Book Department, P.O. Box 5050 Tokyo International, *Tokyo 100-31*
NAUKA LTD. IMPORT DEPARTMENT, 2-30-19 Minami Ikebukuro, Toshima-ku, *Tokyo 171*

KOREA
CHULPANMUL, *Phenjan*

NORWAY
TANUM-CAMMERMEYER, Karl Johansgatan 41—43, *1000 Oslo*

POLAND
WĘGIERSKI INSTYTUT KULTURY, Marszalkowska 80, *Warszawa*
CKP I W ul. Towarowa 28 *00-958 Warsaw*

ROMANIA
D. E. P., *Bucureşti*
ROMLIBRI, Str. Biserica Amzei 7, *Bucureşti*

SOVIET UNION
SOJUZPETCHATI — IMPORT, *Moscow* and the post offices in each town
MEZHDUNARODNAYA KNIGA, *Moscow G-200*

SPAIN
DIAZ DE SANTOS, Lagasca 95, *Madrid 6*

SWEDEN
ALMQVIST AND WIKSELL, Gamla Brogatan 26, *101 20 Stockholm*
GUMPERTS UNIVERSITETSBOKHANDEL AB, Box 346, *401 25 Göteborg 1*

SWITZERLAND
KARGER LIBRI AG, Petersgraben 31, *4011 Basel*

USA
EBSCO SUBSCRIPTION SERVICES, P.O. Box 1943, *Birmingham*, Alabama 35201
F. W. FAXON COMPANY, INC., 15 Southwest Park, *Westwood*, Mass. 02090
THE MOORE-COTTRELL SUBSCRIPTION AGENCIES, *North Cohocton, N. Y. 14868*
READ-MORE PUBLICATIONS, INC., 140 Cedar Street, *New York, N. Y. 10006*
STECHERT-MACMILLAN, INC., 7250 Westfield Avenue, *Pennsauken* N. J. 08110

VIETNAM
XUNHASABA, 32, Hai Ba Trung, *Hanoi*

YUGOSLAVIA
JUGOSLAVENSKA KNJIGA, Terazije 27, *Beograd*
FORUM, Vojvode Mišiča 1, *21000 Novi Sad*

Index: 26.025
Acta Phys. Hung. Tom. 45. No. 1. Budapest, 10. IV. 1979 HU-ISSN 0001-6705

ACTA PHYSICA

ACADEMIAE SCIENTIARUM HUNGARICAE

TOMUS XLV FASCICULUS 2

AKADÉMIAI KIADÓ, BUDAPEST

1978

ACTA PHYS. HUNG. APAHAQ 45 (2) 87—152 (1978)

ACTA PHYSICA

ACADEMIAE SCIENTIARUM HUNGARICAE

SZERKESZTI

KOVÁCS ISTVÁN

Az *Acta Physica* angol, német, francia vagy orosz nyelven közöl értekezéseket. Évente két kötetben, kötetenként 4—4 füzetben jelenik meg. Kéziratok a szerkesztőség címére (1521 Budapest XI., Budafoki út 8.) küldendők.

Megrendelhető a belföld számára az Akadémiai Kiadónál (1363 Budapest Pf. 24. Bankszámla 215-11488), a külföld számára pedig a „Kultura" Külkereskedelmi Vállalatnál (1389 Budapest 62, P.O.B. 149. Bankszámla 217-10990), vagy annak külföldi képviseleteinél.

The *Acta Physica* publish papers on physics in English, German, French or Russian, in issues making up two volumes per year. Subscription: $ 36.00 per volume. Distributor: "Kultura" Foreign Trading Company (1389 Budapest 62, P.O. Box 149) or its representatives abroad.

Die *Acta Physica* veröffentlichen Abhandlungen aus dem Bereich der Physik in deutscher, englischer, französischer oder russischer Sprache, in Heften, die jährlich zwei Bände bilden.

Abonnementspreis pro Band: $ 36.00. Bestellbar bei »Kultura« Außenhandelsunternehmen (1389 Budapest 62, Postfach 149) oder seinen Auslandsvertretungen.

Les *Acta Physica* publient des travaux du domaine de la physique en français, anglais, allemand ou russe, en fascicules qui forment deux volumes par an.

Prix de l'abonnement: $ 36.00 par volume. On peut s'abonner à l'Entreprise du Commerce Extérieur «Kultura» (1389 Budapest 62, P.O.B. 149) ou chez représentants à l'étranger.

«*Acta Physica*» публикуют трактаты из области физических наук на русском, немецком, английском и французском языках.

«*Acta Physica*» выходят отдельными выпусками, составляющими два тома в год.

Подписная цена — $ 36.00 за том. Заказы принимает предприятие по внешней торговле «Kultura» (1389 Budapest 62, P.O.B. 149) или его заграничные представительства.

ACTA PHYSICA
ACADEMIAE SCIENTIARUM HUNGARICAE

TOMUS XLV FASCICULUS 2

AKADÉMIAI KIADÓ, BUDAPEST
1978

ACTA PHYS. HUNG.

INDEX

COMMUNICATIO BREVIS

Acta Physica Academiae Scientiarum Hungaricae, Tomus 45 (2), pp. 87—96 (1978)

О ДВИЖЕНИИ И КИНЕТИЧЕСКИХ ФОРМАХ ПОР В ДИФФУЗИОННОЙ ЗОНЕ СИСТЕМЫ KCl-KBr

Д. Л. БЕКЕ, Ф. РЕВЕС, Ф. Й. КЕДВЕШ, И. ГЕДЕНЬ и Й. ФЕЛСЕРФАЛВИ
КАФЕДРА ПРИКЛАДНОЙ ФИЗИКИ УНИВЕРСИТЕТА им. Л. КОШУТА
Н-4010 ДЕБРЕЦЕН, ВНР

(Поступило 20. VI. 1978)

Излагаются результаты экспериментальных исследований температурной зависимости процесса развития, перемещения и кинетической формы пор, образующихся в диффузионной зоне системы KCl—KBr. Из начального участка роста пор на основании температурной зависимости времени τ, в течение которого поры достигают определенного размера $R^x \simeq 1\mu$, определена эффективная энергия роста пор Q_D, которая хорошо согласуется с энергией активации самодиффузии ионов Br в кристалле KBr. Наши данные усреднённые на совокупности пор, подтверждают, что поры смещаются от границы контакта по закону $v' \sim t^{-1/2}$. Установлено, что это движение ограничивается поверхностными диффузионными потоками, и в этом случае $Q_K \sim Q_S - 1/2\ Q_D$, где Q_S эффективная энергия процесса поверхностной диффузии, ограничивающей движение поры. На основании темтературной зависимости скорости движения пор, определена эффективная энергия смещения $Q_K = 0{,}3$ eV. Установлено, что стрела погиба выпуклого участка поверхности поры λ, линейно зависит от линейного размера поры R, $\lambda = m(T)R$. На основании полуколичественных оценок величины λ/R, показано, что температурная зависимость $m(T)$ определяется законом $\ln m \sim (Q_D - Q_S)/3kT$. Значение Q_S определенное из этого соотношения хорошо согласуется со значением Q_S, полученним из температурной зависимости скорости пор.

1. Введение

При взаимной диффузии — естественными следствиями неравенства парциальных коэффициентов диффузии — являются два эффекта, один из которых заключается в смещении плоскости исходного контакта (еффект Киркендалла), а другой — в возникновении макроскопических пор в том веществе (эффект Френкеля), из которого диффузионный поток определяется большим из парциальных коэффициентов диффузии. Поры, образующиеся вследствие возникновения избыточных вакансий в диффузионной зоне, в системах щелочногалоидных кристаллов имеют отчетливо выраженную огранку («отрицательный кристалл»), определяемую анизотропией поверхностной энергии.

Ранее [1] было показанно, что обращенная к фронту диффузии поверхность отрицательного кристалла, имеющего кубическую огранку, несколько выпукла, т. е. кинетические формы пор оказываются удалёнными от равновесия. Известно также [1], что поры, формирующиеся в диффузионной зоне, со временем не только возрастают, но и находяясь в поле градиента концентрации перемешаются как целое. Оба эти эффекта изучены недостаточно. Между тем каждый из них может быть использован для получения важных

сведений, характеризующих диффузионные потоки в зоне, примыкающей к границе раздела между диффундирующими веществами.

В данной статье излагаются результаты экспериментального исследования температурной зависимости процесса перемещения и кинетических форм пор, образующихся в диффузионной зоне системы **KCl—KBr**.

2. Методика эксперимента

Опыты проводились на трёхслойных образцах **KCl—KBr—KCl** составленных из монокристаллов **KCl** и **KBr** с маркой «Топа» и «Воска» соответственно. Высокотемпературному отжигу предшествовал предварительный отжиг образцов, под одноосьным давлением 0,1 kg/cm^2 при 300 °C в течение 2—3 ч., для создания лучшего контакта на границах **KCl—KBr**. Основные диффузионные отжиги проводились при $T = 721, 708, 697, 681, 664$ °C. Время отжига изменялось в пределах 0,5 мин. — 6 ч. Колебание температуры в печи при этом не превышало ± 2 °C. При коротких временах отжига учитывалось время выгода на T и охлаждение печи.

Благодаря оптической прозрачности кристалла **KBr**, для наблудения за порой возникающейся в нём, использовался следующий приём. В окуляре оптического микроскопа натягивался волосок, который совмещался с границей раздела **KCl—KBr** при фокусировке оптики на поверхность образца. Затем оптика дефокусировалась так, чтобы в фокусе оказалась наблюдаемая пора и при измерении смещения пор волосок играл роль реперной линии.

Наблюдаемые параметры движущихся пор схематически показаны на рис. 1. При данной температуре и времени отжига измерились параметры 50—100 пор в разных образцах и на разных местах образцов. Параметр характеризующий смещение пор от границы раздела был получен путём усреднения величины $d = (x + y)/2$. При каждой температуре были определены времена (τ), в течение которых растущие поры достигли определённого линейного размера

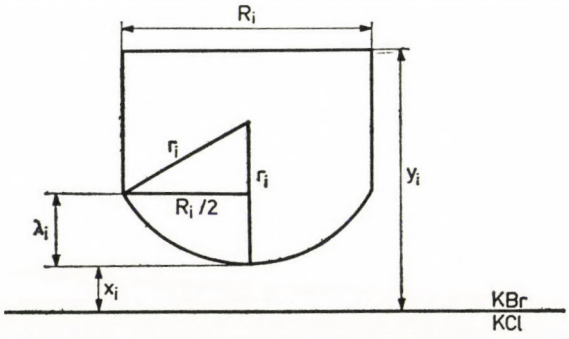

Рис. 1. Наблюдаемые параметры поры

$R^x = 1\ \mu$. Изучалась связь между параметром характеризующим степень отклонения истинной формы поры от разновесной (λ) и линейным размером поры (R). Усреднённые значения кривизны пор ($\bar{\lambda}$), относящиеся к определённому размеру (R) рассчитаны не меньше чем для 50 поры для каждой температуры.

3. Экспериментальные результаты и их обсуждения

Известно [2, 3], что характер роста поры в диффузионной зоне со временем отжига меняется. Можно предположить, что значения τ определенные как время, в течение которого поры достигают размера $R^x \simeq 1\mu$, соответствуют начальному участку роста определенный законом [2]:

$$R \sim \left(\frac{\Delta\xi}{\xi_0}\right)^{1/2} (\tilde{D}t)^{1/2}, \tag{1}$$

где $\Delta\xi/\xi_0$ пересыщение вакансий в диффузионной зоне. В работе [3] было показано, что пересыщение на этой стадии остается практически постоянным. Можно ожидать что значение $\tau \sim R^{x2}/\tilde{D}$ следующим образом зависит от температуры:

$$\ln \tau \sim -Q_{\tilde{D}}/kT. \tag{2}$$

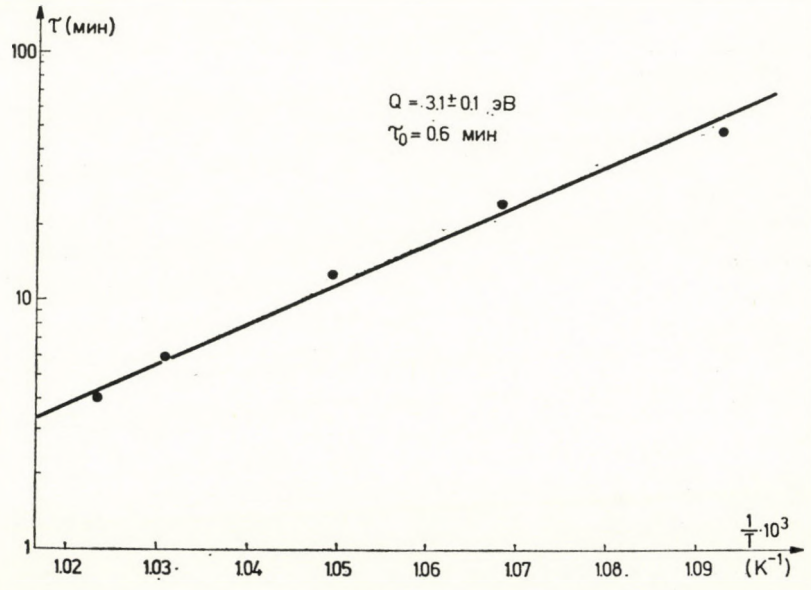

Рис. 2. Зависимость $\ln \tau$ от $1/T$, где τ время, в течение которого поры достигают размера $R^x \sim 1\ \mu$

На рис. 2 изображена величина $\ln \tau$ в зависимости от $1/T$ и по наклону этой прямой определена $Q_{\tilde{D}} = (3{,}1 \pm 0{,}1)$ эВ. Найденную таким образом энергию активации можно интерпретировать как эффективную энергию роста пор в диффузионной зоне. Хотя такие эффективные величины, как «энергия активации» коэффициента взаимной диффузии, обычно не имеют наглядного физического смысла (см. напр. [1]), полученное значение $Q_{\tilde{D}}$ в этом случае хорошо согласуется с энергией активации самодиффузии ионов Br^- ($Q = 3{,}06$ эВ [4]) в кристалле KBr.

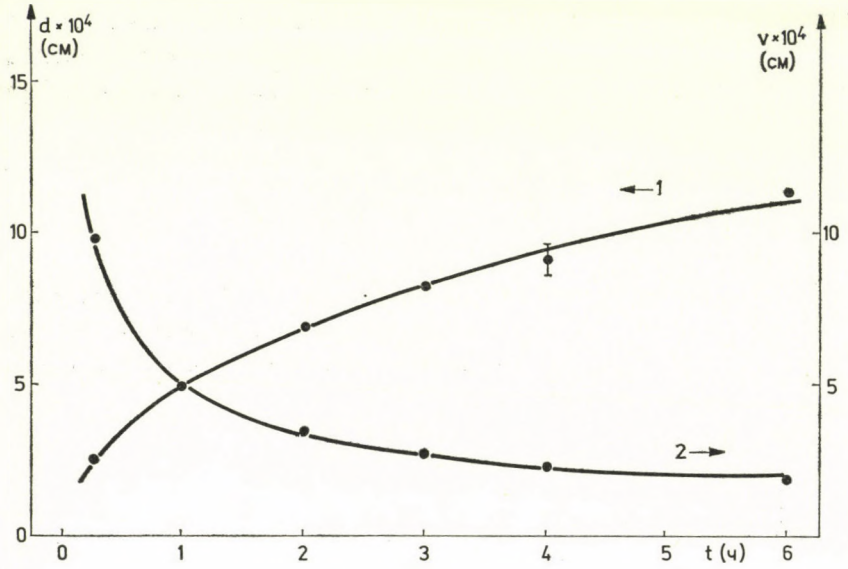

Рис. 3. Зависимость величины смещения (1) и скорость движения пор (2) в диффузионной зоне от времени изотермического отжига при 721°C

В работе [5] было показано, что поры возникающиеся в диффузионной зоне, как целые смещаются от границы контакта по закону $v \sim t^{-1/2}$. Как видно на рис. 3 наши данные усреднённые на совокупности пор подтверждают этот результат. Экспериментальная температурная зависимость смещения пор подчиняется уравнению (рис. 4)

$$d = K\sqrt{t} + d_0. \tag{3}$$

Коэффициент K зависит от температуры по закону Аррениуса (рис. 5). Энергия активации, определяющая температурную зависимость этой величины, равна $Q_K = 0{,}3 \pm 0{,}1$ эВ.

В работе [1] было показано, что скорость движения поры в поле градиента концентрации атомов относительно кристаллической решетки матрицы

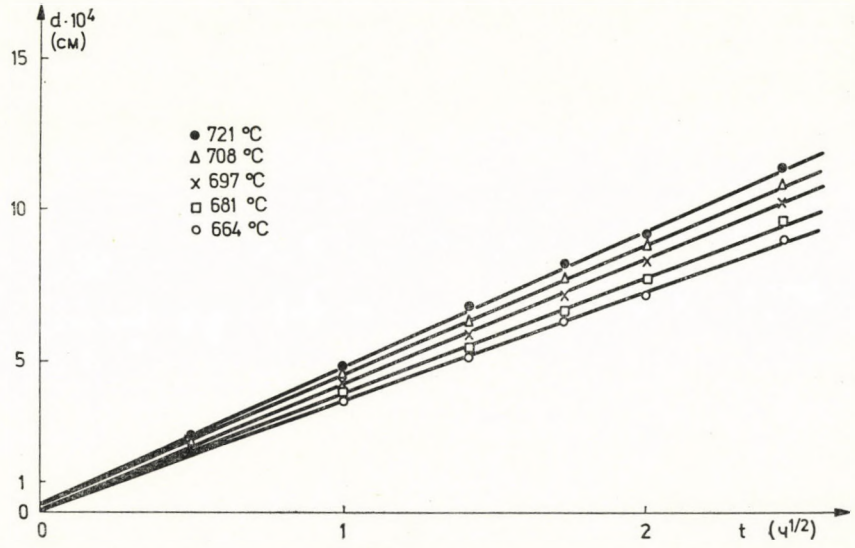

Рис. 4. Смещение поры (d) от границы раздела в зависимости от времени отжига при разных температурах

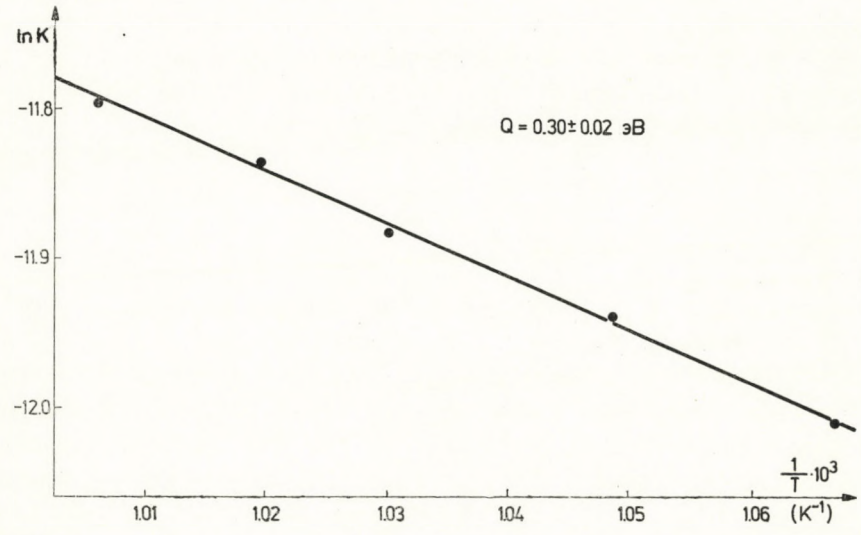

Рис. 5. Температурная зависимость коэффициентов K, характеризующих смещение пор от границы раздела диффузионной зоны

определяется соотношением

$$v' = \frac{3a}{R}\,\chi\,\frac{D_{s1}\bar{D}_2 - D_{s2}\bar{D}_1}{\tilde{D} + \frac{a}{R}\chi\tilde{D}_s}\,\nabla c_\infty\ , \tag{4}$$

где $\bar{D}_1$ и $\bar{D}_2$ обёмные парциальные диффузионные коэффициенты, D_{s1} и D_{s2} коэффициенты поверхностной химической диффузии, a толщина одноатомного слоя на поверхности, R линейный размер поры, χ параметр, который показывает, как отличаются концентрации атомов на поверхности и в обьёме кристалла ($c_s = \chi c$), и

$$\tilde{D} = c_1\bar{D}_2 + c_2\bar{D}_1,$$
$$\tilde{D}_s = c_1\bar{D}_{s2} + c_2\bar{D}_{s1}.$$

Если предположим, как в работах [1] и [5] что а $\chi_s\tilde{D} \gg R\tilde{D}$ тогда при заметном различии $\bar{D}_1$ и $\bar{D}_2$ (или $\bar{D}_{s1}$ и $\bar{D}_{s2}$), из формулы (4) [1]:

$$v' \sim \tilde{D}\nabla c \tag{5}$$

или так как $\nabla c \sim (\tilde{D}t)^{-1/2}$,

$$v' \sim (\tilde{D}/t)^{1/2}. \tag{6}$$

Из экспериментально найденного значения $Q_K = 0{,}3$ эВ, получается, что $Q_{\tilde{D}} = 2Q_K = 0{,}6$ эВ, которая не совпадает $Q_{\tilde{D}}$, полученной из температурной зависимости значений τ. Если предположим, что вместо условия $a\chi\,\tilde{D}_s \gg R_{\tilde{D}}$ выполняется противоположное условие, т. е. поверхностные потоки ограничивают движение поры, тогда из формулы (4) имеем

$$v' \sim \frac{3a}{R}\chi D_s\tilde{D}^{1/2}t^{-1/2}. \tag{7}$$

В этом случае $Q_K \simeq Q_s - 1/2\,Q_{\tilde{D}}$, и с учётом что $Q_{\tilde{D}} = 3{,}1$ эВ, $Q_s = 1{,}8$ эВ.

К сожалению в литературе нет данных по энергии активации поверхностной диффузии в области температур близких к температуре плавления, и поэтому нет возможности сравнения полученного результата с прямым измерением. Следует отметить, что в работе [6] методом меченых атомов была определена энергия активации процесса поверхностной диффузионной миграции адатомов Br($Q_{s\mathrm{Br}} = 0{,}41$ эВ) в интервалле 250—550 °C. Однако перенос массы по поверхности не всегда происходит в меру поверхностного диффузионного коэффициента, определенного техникой меченых атомов при низких температурах. На основании большинства литературных данных с температурной зависимости поверхностного диффузионного коэффициента, можно предположить что изменением температуры изменяется механизм поверхностной диффузии (см. напр. [7]), т. е. с увеличением температуры в переносе массы кроме одиночных адатомов участвуют и их разные комплексы. Этот факт выражается в том, что график Аррениуса не прямая линия, а имеет узел;

при температурах, близких к температуре плавления, энергия активации выше, близка к энергии активации объемной самодиффузии.

На рис. 6 изображены прямые, иллустрирующие связь между величиной λ и линейным размером поры R. Из соотношения

$$\lambda = mR + R_0 \tag{8}$$

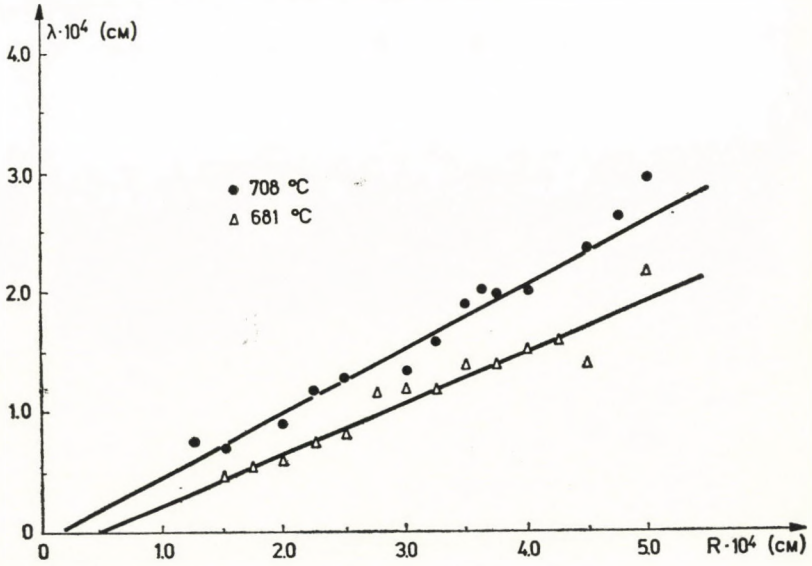

Рис. 6. Зависимость стрели погиба выпуклого участка поверхности (λ) от линейного размера поры (R)

были рассчитаны данные, приведенные в табл. I. Хорошо видно, что значение R_0 практически равно нулю ($\Delta R_0 \simeq \pm 0{,}5 \cdot 10^{-4}$ см) и не зависит от температуры в то время, как величина m систематически меняется с температурой.

Таблица I

T[°C]	$R_0 \times 10^4$ [см]	m
721	0,268	0,507
708	0,153	0,541
697	0,048	0,463
681	0,469	0,424
664	0,384	0,374

Если предположить что форма искривленной, движущейся поры обусловлена только потоком вакансий, который направлен к поре от границы контакта [1, 5], можно сделать элементарную оценку величины λ/R. В этом слу-

чае обьемный поток вакансий через цилиндрическую поверхность, вигнутую по направлению к границе раздела, будет равен поверхностной дивергенции поверхностного потока вакансий, т. е.

$$\frac{2r\pi \cdot R}{4} D_v \nabla \xi_v = \mathrm{div}_s J_s = D_{sv} aR \cdot \mathrm{div}_s \nabla_s \xi_s, \tag{9}$$

где $\nabla \xi_v$ и $\nabla_s \xi_s$ градиенты концентраций вакансий в объеме матрицы вблизи от поры и на поверхности соответственно. При вычислении объёмного потока вакансий предполагалось, что площадь цилиндрической изгнутой поверхности поры равна четверти поверхности цилиндра с радиусом r (рис. 1).

Градиент концентрации вакансий в объёме можно записать в виде:

$$\nabla \xi_v = \frac{\Delta \xi}{L} \approx \xi_0 \frac{\alpha\omega}{kTrL} \approx \xi_0 \frac{\alpha\omega}{kTr(\tilde{D}t)^{1/2}}, \tag{10}$$

где α — коэффициент поверхностного натяжения, ω — атомной объем, k — постоянная Больцмана, L — характерное расстояние от поверхности поры до границы раздела, пропорциональное ширину диффузионной зоны $(\tilde{D}t)^{1/2}$.

Считая, что после начального участка роста пор, линейный размер поры определяется законом [3];

$$R \approx \left(\frac{D_A - D_B}{\tilde{D}^{1/2}}\right)^{1/3} t^{1/6} \approx (\tilde{D}t)^{1/6},$$

$$\nabla \xi_v \approx \xi_0 \frac{\alpha\omega}{kTr\, R^3}. \tag{11}$$

Следует отметить, что мы экспериментально убедились в том, что при исследованных временах отжига ($t > \tau$), размеры пор изменялись значительно медленнее, чем при временах $t \sim \tau$.

Из формулы (9) с учётом (11), считая, что

$$\mathrm{div}_s \nabla_s \xi_s \approx \xi_{s0} \frac{\alpha\omega}{kTr^3},$$

и из геометрии формы поры (см. рис. 1);

$$r^2 = (r - \lambda)^2 + R^2/4 \approx r^2 - 2r\lambda + R^2/4,$$

т. е.

$$r \approx R^2/8\lambda,$$

связь между λ и R определяется соотношением

$$\lambda \approx \left(\frac{D_v \xi_0}{D_{sv}\, \xi_{s0} a}\right)^{1/3} R\,, \tag{12}$$

что совпадает с экспериментально наблюдаемой линейной зависимостью. По этой формуле величина m следующим образом зависит от температуры:

$$\ln m \approx -\frac{Q_a - Q_s}{3\, kT}\,, \tag{13}$$

где Q_a и Q_s энергии активации объемной и поверхностной самодиффузии атомов. Легко видеть, что характер формулы (13) не меняется если учесть тот факт, что в ионных кристаллах наблюдаемое искривление связано с диффузионным движением ионов двух знаков. В этом случае в выражении (12) вместо коэффициентов $D_a = D_v \xi_0$ и, $D_{sa} = D_{sv}\, \xi_{s0}$, входят эффективные коэффициенты [1]:

$$D_{s\,\text{эфф}} = \frac{D_{1a} \cdot D_{2a}}{D_{1a} + D_{2a}} \quad \text{и} \quad D_{sa\,\text{эфф}} = \frac{D_{sa1} \cdot D_{sa2}}{D_{sa1} + D_{sa2}}\,.$$

Допустив те же упрощающие предположения, как при анализе температурной зависимости движения пор, из (12) получаем выражение (13).

На рис. 7 видно, что знак температурной зависимости величин согласу-

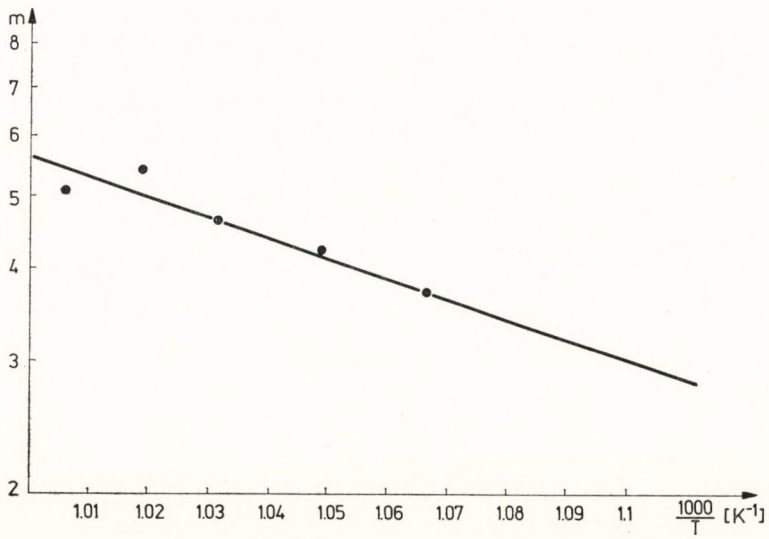

Рис. 7. Температурная зависимость величин m, характеризующих линейную связь между параметрах λ и R поры

ется с знаком, полученным из (13). Из наклона приведенного графикона: $(Q_a - Q_s)/3 = 0{,}5$ эВ и с учётом, что $Q_a \approx Q_{\tilde{D}} = 3{,}1$ эВ, $Q_s \approx 1{,}6$ эВ. Эта величина хорошо согласуется с значением Q_s, полученным из температурной зависимости скорости пор.

В заключение авторы выражают благодарность Проф. Я. Е. Гегузину и Ю. С. Кагановскому за полезные консультации. Авторы тоже выражают благодарность Ш. Месарошу за участие в подготовке образцов и в экспериментах.

ЛИТЕРАТУРА

1. Я. Е. Гегузин, М. А. Кривоглаз, Движение махроскопических включений в твёрдых телах. Изд. «Металлургия» Москва, 1971.
2. Я. Е. Гегузин, В. И. Солунский, Ф. Т. Т., **6,** 30, 1964.
3. Я. Е. Гегузин, Ю. И. Бойко, Ф. Т. Т., **9,** 1375, 1967.
4. C. P. Flynn, **Point defects and diffusion, Clarendon Press, Oxford,** 1972, p. 595.
5. Я. Е. Гегузин, Ю. И. Бойко, Л. Н. Парицкая, Ф. М. М., **24,** 418, 1967. изд. «Наука», 1969, стр. 81.
6. H. P. Bonzel, **Surf. Science, 21,** 45, 1970.

Acta Physica Academiae Scientiarum Hungaricae, Tomus 45 (2), pp. 97—106 (1978)

UNSTEADY COMBINED FREE AND FORCED CONVECTION EFFECTS ON THE FLOW IN A HORIZONTAL CHANNEL

By

K. S. SHIRKOT and S. SINGH

DEPARTMENT OF MATHEMATICS, HIMACHAL PRADESH UNIVERSITY, SIMLA-5, INDIA

(Received 27. VI. 1978)

An exact solution of the problem of an unsteady combined free and forced convection flow of a viscous incompressible fluid between two horizontal parallel walls with a linear axial temperature variation has been solved. It is found that the velocity and temperature profiles are asymmetric. The skin friction at the upper wall is always negative for cooling there, so that no reversal flow takes place while heating the upper wall leads to incipient reversed flow thus increasing the tendency of instability. Also more and more cooling at the lower wall induces reversal flow there.

1. Introduction

It is well known that forced and free convection play a predominant role in determining the rate of heat transfer from a surface to fluid moving past it. To date, however, the theoretical and experimental studies on this subject have been limited, with a few exceptions, to cases where either, but not both, of the two mehanisms is taken into account. These investigations have been very successful, particularly in regions where the flow is laminar and have resulted in experimentally verified theoretical predictions. In general, however, heat is transferred by both mechanisms acting simultaneously. It is, therefore, of some interest and importance to be able to predict how the rate of heat transfer is affected by the combined action of both forced and free convections and to know under what conditions it is permissible to neglect one mode of transfer or the other. A few studies have been made in this direction. By including free convection effects a few researchers have investigated the velocity and temperature distribution in vertical pipes and channels with low Reynold's numbers. ACRIVOS [1] has given a theoretical treatment of combined laminar free and forced convection heat trasnfer in external flows.

This paper will present a theoretical investigation of unsteady combined free and forced convection flow of a viscous incompressible fluid between two horizontal parallel walls with a linear axial temperature variation. Initially the walls and the fluid are at the same temperature T_0 and there is no flow. The temperature of both the walls of the channel changes with the law $T_0 + N\bar{x}$ and a constant pressure gradient is impressed upon the system. An exact

solution of the governing equations has been obtained. The effect of the dimensionless physical parameters characterizing the flow on the velocity, the skin friction and the temperature distribution have been discussed in detail.

2. Equations of motion and their solution

We choose a Cartesian coordinate system such that the x-axis is in the direction of the flow. Then the governing equations for unsteady combined free and forced convection flow can be writen as

$$\varrho \frac{\partial \bar{u}}{\partial \bar{t}} = -\frac{\partial \bar{p}}{\partial \bar{x}} + \mu \frac{\partial^2 \bar{u}}{\partial \bar{y}^2}, \tag{1}$$

$$0 = -\frac{\partial \bar{p}}{\partial \bar{y}} - \varrho g , \tag{2}$$

when the y-axis is perpendicular to the walls $\bar{y} = \pm h$.

The equation of state under the Boussinesq approximation is assumed to be

$$\varrho = \varrho_0[1 - \beta(T - T_0)], \tag{3}$$

where T is the temperature, β is the coefficient of the thermal expansion and σ_0, T_0 are respectively the density and temperature in the reference state.

The boundary conditions are

$$\bar{t} = 0;\ \bar{u} = 0,\ T = T_0 \text{ for al } \bar{y} \in [-h, h],$$
$$\bar{t} > 0;\ \bar{u} = 0,\ T = T_0 + N\bar{x} \text{ at } \bar{y} = \pm h.$$

Using (3), Eq. (2) can be written as

$$\frac{\partial \bar{p}}{\partial \bar{y}} = -\varrho_0 g[1 - \beta(T - T_0)] . \tag{4}$$

Assuming that the wall temperature has a uniform gradient along the $\bar{x}$-axis the temperature of the fluid can be assumed as

$$T - T_0 = N\bar{x} + \bar{\Phi}(\bar{y}, \bar{t}). \tag{5}$$

Now Eq. (4) becomes

$$\frac{\partial \bar{p}}{\partial \bar{y}} = -\varrho_0 g + \varrho_0 g \beta N \bar{x} + \varrho_0 g \bar{\Phi}(\bar{y}, \bar{t}) .$$

which gives

$$\left.\begin{aligned} &\bar{p} = -\varrho_0 g\bar{y} + \varrho_0 g\beta N\bar{x}\bar{y} + \varrho_0 g\beta \int \bar{\Phi}(\bar{y}, \bar{t})\, d\bar{y} + \bar{F}(\bar{x}, \bar{t}) \\ \text{and} \quad &\frac{\partial \bar{p}}{\partial \bar{x}} = \varrho_0 g\beta\, N\bar{y} + \frac{\partial \bar{F}}{\partial \bar{x}}\,. \end{aligned}\right] \tag{6}$$

Using (6) Eq. (1) can be written as

$$\frac{\partial \bar{u}}{\partial \bar{t}} = -g\beta N\bar{y} - \frac{1}{\varrho_0}\frac{\partial \bar{F}}{\partial \bar{x}} + \nu \frac{\partial^2 \bar{u}}{\partial \bar{y}^2}, \tag{7}$$

where

$$\nu = \frac{\mu}{\varrho_0}.$$

We define the following dimensionless quantities:

$$u = \frac{h\bar{u}}{\nu}, \quad t = \frac{\nu\bar{t}}{h^2}, \quad F = \frac{\bar{F}h^2}{\varrho_0\nu^2}, \quad y = \frac{\bar{y}}{h}, \quad x = \frac{\bar{x}}{h}.$$

Eq. (7) then becomes

$$\frac{\partial u}{\partial t} = c - Gy + \frac{\partial^2 u}{\partial y^2}, \tag{8}$$

where

$$-\frac{\partial F}{\partial x} = c(t > 0), \quad G = \frac{g\beta N h^4}{\nu^2}.$$

The boundary conditions are

$$\left.\begin{aligned} &t = 0,\ u = 0\ \forall\ y \in [-1, 1]\ , \\ &t > 0,\ u = 0 \text{ at } y = \pm 1\ . \end{aligned}\right] \tag{9}$$

Eq. (5) shows that positive and negative values of N correspond to heating and cooling, respectively, along the walls of the channel. Therefore $G \gtrless 0$ according as the channel walls are heated or cooled in the axial direction.

Let $L = \int_0^\infty e^{-st} u\,dt$ be the Laplace transform of u, then the expression (8) takes the form

$$\frac{d^2L}{dy^2} - sL = \frac{Gy}{s} - \frac{c}{s}. \tag{10}$$

The solution of (10) under the boundary conditions (9) is

$$L = G\frac{\sinh\sqrt{s}\,y}{s^2\sinh\sqrt{s}} - c\frac{\cosh\sqrt{s}\,y}{s^2\cosh\sqrt{s}} + \frac{c - Gy}{s^2}\,. \tag{11}$$

On inversion we get

$$\left.\begin{aligned} u = {} & \frac{c}{2}(1-y^2) - \frac{1}{6}Gy(1-y^2) - \frac{2G}{\pi^3}\sum_{n=1}^{\infty}\frac{(-1)^n}{n^3}\exp(-n^2\pi^2 t)\sin(n\pi y) \\ & - \frac{16c}{\pi^3}\sum_{n=0}^{\infty}\frac{(-1)^n}{(2n+1)^3}\exp\left[-\frac{(2n+1)^2\pi^2}{4}t\right]\cos\left(\frac{2n+1}{2}\right)\pi y\,. \end{aligned}\right] \tag{12}$$

The energy equation is

$$\frac{\partial}{\partial t}(T - T_0) + \bar{u}\frac{\partial}{\partial \bar{x}}(T - T_0) = \alpha\frac{\partial^2}{\partial y^2}(T - T_0)\,, \tag{13}$$

where α is the thermal diffusivity of the fluid.

Using (5), Eq. (13) becomes

$$\frac{\partial\bar{\Phi}}{\partial\bar{t}} + N\bar{u} = \alpha\frac{\partial^2\bar{\Phi}}{\partial\bar{y}^2}\,. \tag{14}$$

Introducing the dimensionless variables as given before, the above equation becomes

$$\frac{\partial^2\theta}{\partial y^2} = p\left(u + \frac{\partial\theta}{\partial t}\right)\,, \tag{15}$$

where

$$p = \frac{\nu}{\alpha}\,, \quad \theta = \frac{\bar{\Phi}}{Nh}\,. \tag{16}$$

Obviously the boundary conditions for θ are

$$\left.\begin{aligned} & t = 0;\ \theta = 0\ \forall\ y \in [-1, 1]\,, \\ & t > 0,\ \theta = 0 \text{ at } y = \pm 1\,. \end{aligned}\right] \tag{17}$$

Let $\theta = \int_0^{\infty} e^{-st}\,\theta dt$ be the Laplace transform of θ, then using this and the condition (17), Eq. (15) gives

$$\frac{d^2\bar{\theta}}{dy^2} - ps\,\theta = pL\,. \tag{18}$$

Using (11) the solution of (18) under the boundary conditions (17) is

$$\bar{\theta} = \frac{c}{1-p}\frac{\cosh y\sqrt{ps}}{s^3\cosh\sqrt{ps}} - \frac{G}{1-p}\frac{\sinh y\sqrt{ps}}{s^3\sinh\sqrt{ps}} - \frac{Gy-c}{s^3} + \frac{pG}{1-p}\frac{\sinh y\sqrt{s}}{s^3\sinh\sqrt{s}} - \frac{pc}{1-p}\frac{\cosh y\sqrt{s}}{s^3\cosh\sqrt{s}}, \tag{19}$$

where $p \neq 1$.

Inverting (19), we get

$$\begin{aligned}\theta = &-\frac{cp}{24}(1-y^2)(5-y^2) + \frac{Gpy}{360}(1-y^2)(7-3y^2)\\ &-\frac{64cp^2}{(1-p)\pi^5}\sum_{n=0}^{\infty}\frac{(-1)^n}{(2n+1)^5}\exp\left[-\frac{(2n+1)^2\pi^2}{4p}t\right]\cos\frac{2n+1}{2}\pi y\\ &+\frac{64cp}{(1-p)\pi^5}\sum_{n=0}^{\infty}\frac{(-1)^n}{(2n+1)^5}\exp\left[-\frac{(2n+1)^2\pi^2}{4}t\right]\cos\frac{2n+1}{2}\pi y\\ &-\frac{2Gp^2}{(1-p)\pi^5}\sum_{n=1}^{\infty}\frac{(-1)^n}{n^5}\exp\left[-\frac{n^2\pi^2}{p}t\right]\sin n\pi y\\ &+\frac{2Gp}{(1-p)\pi^5}\sum_{n=1}^{\infty}\frac{(-1)^n}{n^5}\exp\left[-n^2\pi^2 t\right]\sin n\pi y. \end{aligned}\tag{20}$$

The non-dimensional shear stresses at the walls $y = 1$ and $y = -1$ are given by

$$\tau_1 = \left(\frac{du}{dy}\right)_{y=1} = -c + \frac{8c}{\pi^2}\sum_{n=0}^{\infty}\frac{1}{(2n+1)^2}\exp\left[-\frac{(2n+1)^2\pi^2}{4}t\right] + \frac{G}{3} - \frac{2G}{\pi^2}\sum_{n=1}^{\infty}\frac{1}{n^2}\exp\left[-n^2\pi^2 t\right], \tag{21}$$

$$\tau_2 = \left(\frac{du}{dy}\right)_{y=-1} = c - \frac{8c}{\pi^2}\sum_{n=0}^{\infty}\frac{1}{(2n+1)^2}\exp\left[-\frac{(2n+1)^2\pi^2}{4}t\right] + \frac{G}{3} - \frac{2G}{\pi^2}\sum_{n=1}^{\infty}\frac{1}{n^2}\exp\left[-n^2\pi^2 t\right]. \tag{22}$$

3. Results and discussion

The velocity profiles have been plotted against y for $c = 1$ and for various values of G and t in Figs. 1 to 3. It is found from these Figures that with the increase of the magnitude of $G(G > 0)$ the velocity increases in the lower

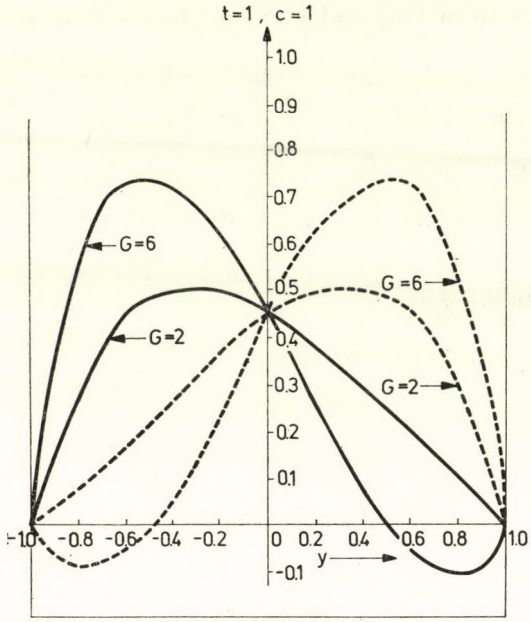
t=1, c=1
1.0
0.9
0.8
0.7
0.6
0.5
0.4
0.3
0.2
0.1
-0.1
G=6
G=2
G=6
G=2
-1.0 -0.8 -0.6 -0.4 -0.2 0 0.2 0.4 0.6 0.8 1.0
y

Fig. 1

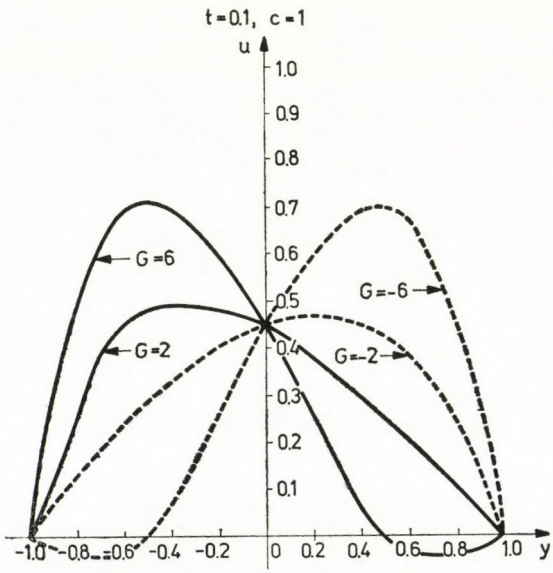
t=0.1, c=1
u
1.0
0.9
0.8
0.7
0.6
0.5
0.4
0.3
0.2
0.1
G=6
G=2
G=-6
G=-2
-1.0 -0.8 -0.6 -0.4 -0.2 0 0.2 0.4 0.6 0.8 1.0 y

Fig. 2

half while it decreases in the upper half of the channel. The position is reversed for negative values of G. The velocity profiles are asymmetric due to the presence of buoyancy force $G(G \neq 0)$.

The temperature profiles have been plotted against y for $c = 1$, $p = 0.5$ and various values of G and t in Figs. 4 to 6. From Fig. 4 we observe the oscillations in the temperature profiles for small values of t and clearly as time t increases the temperature at any point in the channel becomes steady. It is

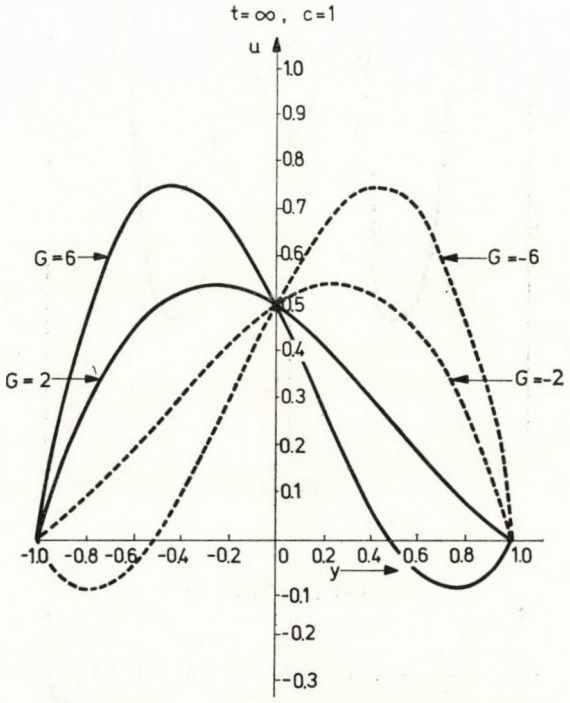

Fig. 3

found from Figs. 5 and 6 that with the increase of the magnitude of $G(G > 0)$, the temperature increases in the upper half while it decreases in the lower half of the channel. The position is reversed for $G(G < 0)$. These Figures depict that the temperature profiles are also asymmetric.

When the buoyancy forces are absent $(G = 0)$, the Eq. (22) shows that the skin friction at the lower plate is always positive for $t = \infty$ since $c > 0$. There is thus no flow separation in this case. On the other hand more and more cooling at the lower plate (which corresponds to the negative value of G mentioned before) causes progressive decrease in the values of the skin friction there. From Fig. 7 we observe that τ_1 is always negative for cooling at the upper wall

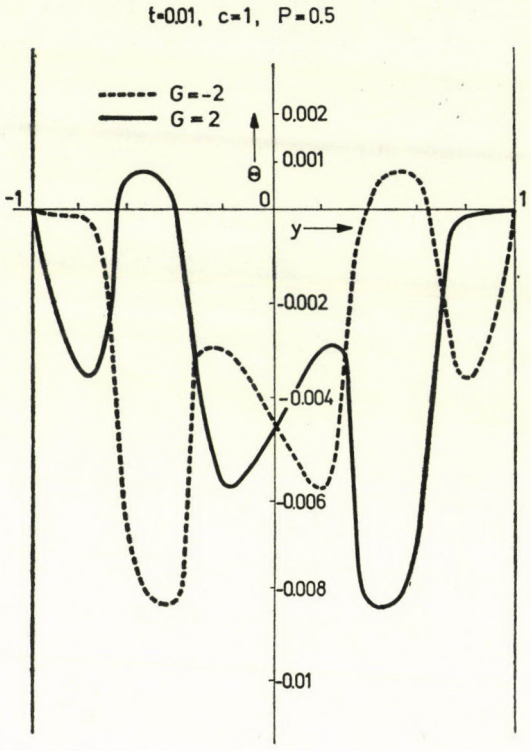
t=0.01, c=1, P=0.5
G=-2
G=2
θ
y
-1
0
1
0.002
0.001
-0.002
-0.004
-0.006
-0.008
-0.01

Fig. 4

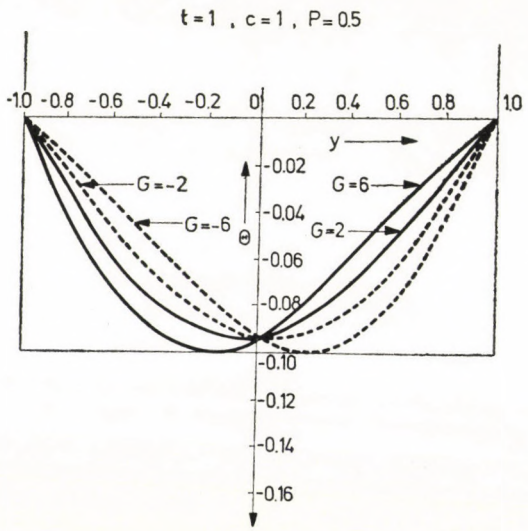
t=1 , c=1 , P=0.5
-1.0 -0.8 -0.6 -0.4 -0.2 0 0.2 0.4 0.6 0.8 1.0
y
G=-2
G=-6
θ
G=6
G=2
-0.02
-0.04
-0.06
-0.08
-0.10
-0.12
-0.14
-0.16

Fig. 5

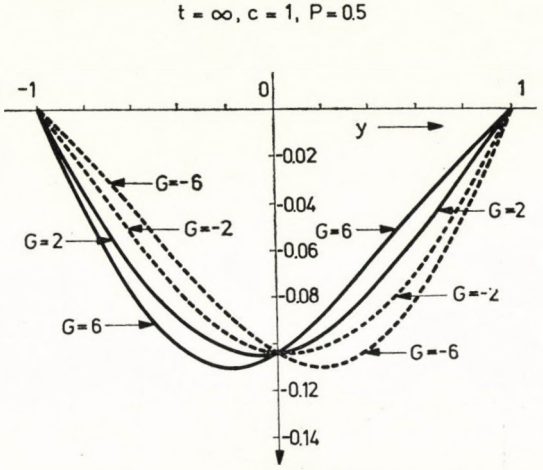

Fig. 6

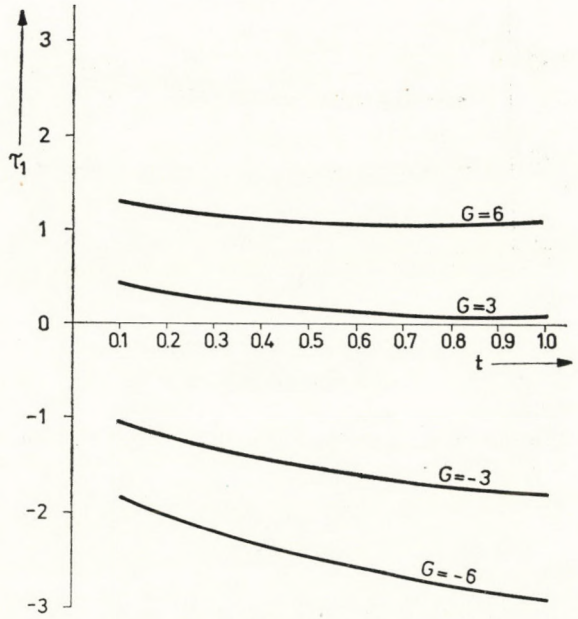

Fig. 7

so that incipient reversed flow does not take place. This Figure also shows that heating the upper wall leads to incipient reversed flow there and thus increases the tendency of instability.

Fig. 8 shows that there is an incipient reversal flow at the lower wall when the temperature of the lower wall decreases. Thus more and more cooling at the lower wall induces reversal flow there. From this Figure we also observe that τ_2 increases with increase of time.

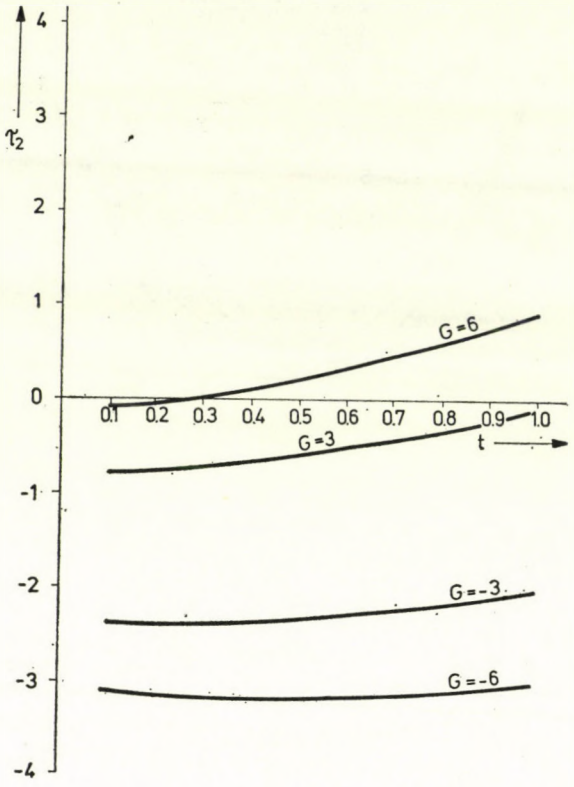

Fig. 8

Acknowledgement

The authors wish to express their sincere thanks to Dr. S. N. DUBE for the suggestions in the preparation of this paper.

REFERENCES

1. A. ACRIVOS, A. I. Ch. E. Journal, **4**, No. 3, 285 1958.

Acta Physica Academiae Scientiarum Hungaricae, Tomus 45 (2), pp. 107—112 (1978)

CYLINDRICALLY SYMMETRIC SELF-GRAVITATING FLUIDS WITH PRESSURE EQUAL TO ENERGY DENSITY

By

T. SINGH and R. B. S. YADAV

APPLIED MATHEMATICS SECTION, INSTITUTE OF TECHNOLOGY, BANARAS HINDU UNIVERSITY
VARANASI 221005, INDIA

(Received 6. VII. 1978)

Solutions of EINSTEIN's field equations are obtained under the assumption that (1) the source of the gravitational field is a perfect fluid with pressure p, equal to energy density ϱ, (2) the space time is cylindrically symmetric with two degrees of freedom, and (3) the metric is given by three functions of two variables. The co-ordinate transformation to comoving co-ordinate is discussed. The HAWKING—PENROSE energy conditions and THORNE's C-energy are also studied. Some physically interesting solutions are obtained. The relation of the present work to EINSTEIN—ROSEN waves is also investigated.

1. Introduction

In a recent paper TABENSKY and TAUB [1] have found that EINSTEIN's field equations for self-gravitating perfect fluid with pressure p equal to rest energy density ϱ and four-velocity u_i is equivalent to the field equations

$$R_{ij} = -2\sigma_{,i};\ \sigma_{,j}, \tag{1.a}$$

$$\Box\sigma = \left((-g)^{1/2}\ \sigma_{,i}\ g^{ij}\right)_{,j} = 0, \tag{1.b}$$

when irrotationality is imposed, viz.

$$u_i = \sigma_{,i}/(\sigma_{,k}\ \sigma^{,k}). \tag{2}$$

The pressure p and energy momentum tensor T_{ij} are related to σ by

$$p = \varrho = \sigma_{,k}\ \sigma^{,k}, \tag{3}$$

$$T_{ij} = 2\sigma_{,i}\ \sigma_{,j} - g_{ij}\ \sigma_{,k}\ \sigma^{,k}. \tag{4}$$

The units are chosen so that the velocity of light $C = 1$ and Newton's constant of gravitation $G = 1/8\pi$. A comma means partial derivative with respect to the index.

Further LETELIER [2] and LETELIER and TABENSKY [3] have obtained cylindrically symmetric solutions of the field equations (1). It is the purpose

of this paper to discuss the solution of Eqs. (1) in a cylindrically symmetric space time with two degrees of freedom (STACHEL [4]) expressed as

$$ds^2 = e^{2A-2B}(dt^2 - dr^2) - (C^2e^{2B} + r^2e^{-2B})\,d\varphi^2 - e^{2B}\,dz^2 - 2Ce^{2B}\,d\varphi\,dz, \qquad (5)$$

where A, B and C are functions of r and t only, and r, Φ, z, t correspond respectively to x^1, x^2, x^3, x^4 coordinates. When $C = 0$ the metric (5) reduces to EINSTEIN—ROSEN metric (EINSTEIN and ROSEN [5] and ROSEN [6]) with one degree of freedom.

In Section 2 we find the solution of Eqs. (1) for the metric (5). In Section 3 the coordinate transformation that enables us to write the solution in comoving coordinates is discussed. In Section 4, the HAWKING—PENROSE energy conditions [7] are verified. In Section 5, some special solutions corresponding to monochromatic and pulse wave solution for σ are obtained and THORNE's C-energy is discussed. Also the relation of the present work to EINSTEIN—ROSEN waves is pointed out.

2. The solution of field equation

For the metric (5) the field equations (1) and the pressure p are

$$B_{11} - B_{44} + \frac{B_1}{r} - (e^{2B}/2r^2)\,(C_1^2 - C_4^2) = 0\,, \qquad (6)$$

$$C_{11} - C_{44} - \frac{C_1}{r} + 4(B_1C_1 - B_4C_4) = 0\,, \qquad (7)$$

$$A_1 = r(B_1^2 + B_4^2) + (e^{4B}/4r)\,(C_1^2 + C_4^2) + \frac{1}{2r}(\sigma_1^2 + \sigma_4^2), \qquad (8)$$

$$A_4 = 2rB_1B_4 + (e^{4B}/2r)C_1C_4 + r\sigma_1\sigma_4, \qquad (9)$$

$$A_{11} - A_{44} + B_1^2 - B_4^2 - (e^{4B}/4r^2)\,(C_1^2 - C_4^2) = -\frac{1}{2}(\sigma_1^2 - \sigma_4^2), \qquad (10)$$

$$\sigma_{11} - \sigma_{44} + \frac{\sigma_1}{r} = 0\,, \qquad (11)$$

$$p = \varrho = e^{-2A+2B}(\sigma_4^2 - \sigma_1^2), \qquad (12)$$

where the indices 1 and 4 indicate partial derivatives with respect to r and t, respectively.

The Eqs. (6) and (7) which determine B and C are identical to those of the empty space for the metric (5). Eq. (10) can be obtained from (6)—(9)

and (11). When B and C are known from (6) and (7) and σ from Eq. (11) Eqs. (8) and (9) give A as an integral

$$A = \int\Big[\Big\{r(B_1^2 + B_4^2) + (e^{4B}/4r)\,(C_1^2 + C_4^2) + \frac{1}{2}\,r(\sigma_1^2 + \sigma_4^2)\Big\}\,dr + \\ + \{2rB_1B_4 + (e^{4B}/2r)\,C_1C_4 + r\sigma_1\sigma_4\}\,dt\Big]\,. \tag{13}$$

The integrability conditions for A are satisfied by virtue of Eqs. (6), (7) and (11). One can always add a constant to A. Further if (g_{ij}, σ) is any solution $(\lambda g_{ij}, \sigma)$ is also a solution whenever λ is a constant. So from now onwards all line elements can be multiplied by a constant conformal factor.

3. Comoving coordinates

Now we shall discuss how to transform the solution to comoving coordinates which are usually used in hydrodynamics and they are important for physical interpretation.

We can choose σ as the comoving time T. It can be easily seen that the coordinate R defined by

$$dR = r(\sigma_4 dr + \sigma_1 dt) \tag{14}$$

and $T = \sigma$ transform the four-velocity u_i to $U_i = (0, 0, 0, U_4)$ and therefore R is comoving. Eq. (11) ensures the exactness of the differential (14) defining R.

The required transformation formulae are

$$\begin{cases} T = \sigma(r, t), \quad R = R(r, t) \\ \Phi = \varphi, \quad Z = z, \end{cases} \tag{15}$$

where T, R, Φ and Z are comoving coordinates. The Jacobian of (15) is

$$\frac{\partial(R, \Phi, Z, T)}{\partial(r, \varphi, z, t)} = r(\sigma_4^2 - \sigma_1^2),$$

which can vanish where $p = \varrho = 0$ in the nonsingular regions of space time. In comoving coordinates the line element (5) is transformed to

$$ds^2 = \{e^{2A-2B}/(\sigma_4^2 - \sigma_1^2)\}\left(dT^2 - \frac{1}{r^2}\,dR^2\right) - (C^2e^{2B} + r^2e^{-2B}) \times \\ \times d\Phi^2 - e^{2B}\,dZ^2 - 2Ce^{2B}\,d\Phi\,dZ\,. \tag{16}$$

The line element (16) has a singularity at $r = 0$.

4. The reality conditions

In irrotational fluids with the limiting form of the equation of state $p = \varrho$, the energy condition $T_{ij}u^iu^j \geq 0$ and the HAWKING—PENROSE condition [7]

$$\left(T_{ij} - \frac{1}{2} g_{ij} T\right) u^i u^j \geq 0$$

both reduce to

$$\varrho = \frac{1}{2} e^{-2A+2B}(\sigma_4^2 - \sigma_1^2) \geq 0 .$$

Thus it is possible that ϱ may be negative in some regions of the space-time. The metric does not have necessarily a pathological behaviour when this happens. The way of solving this problem is to fill the region where the energy density is negative with a different kind of fluid, whose energy tensor we prescribe as follows.

From (14) we find that $R_{,i}$ is orthogonal to $\sigma_{,i}$, $\Phi_{,i}$ and $Z_{,i}$. In this region, $R_{,i}$ is a timelike vector and $\hat{\sigma}_{,i}$ is spacelike. Now let $\hat{R}_{,i}$, $\hat{\Phi}_{,i}$, $\hat{Z}_{,i}$, $\hat{\sigma}_{,i}$ denote the corresponding unit vector fields. If we use the fact that

$$g_{ij} = \hat{R}_{,i}\,\hat{R}_{,j} - \hat{\sigma}_{,i}\,\hat{\sigma}_{,j} - \hat{\Phi}_{,i}\,\hat{\Phi}_{,j} - \hat{Z}_{,i}\,\hat{Z}_{,j}$$

the stress energy tensor (4) can be written as

$$T_{ij} = (-\sigma_{,k}\,\sigma^{,k})\,[\hat{R}_{,i}\,\hat{R}_{,j} + \hat{\sigma}_{,i}\,\hat{\sigma}_{,j} - \hat{\Phi}_{,i}\,\hat{\Phi}_{,j} - \hat{Z}_{,i}\,\hat{Z}_{,j}].$$

This stress energy tensor is that of an anisotropic fluid with positive rest energy density $(-\sigma_{,k}, \sigma^{,k})$ and vanishing heat flow vector. In this case both the reality conditions are satisfied.

5. Some special solutions and Thorne's C-energy

The Eqs. (6)—(9) are a set of coupled, second order non-linear partial differential equations and it is difficult to obtain a general solution of these equations. As Eqs. (6) and (7) which determine B and C are the same as those in the case of empty space, following STACHEL [4] we try some special solutions. STACHEL has mentioned two particular cases (i) $B = 0$ and $B = (1/4)\log r + b$, where b is a constant. When $B = 0$, Eqs. (6) and (7) lead to $C =$ constant which can be eliminated with the help of a coordinate transformation $z' = z + C\varphi$, where C is a constant. When $B = (1/4)\log r + b$, from Eqs. (6) and (7) it follows that C is a function of $t - r$ or $t + r$, but not their sum, because of the nonlinearity of the equations.

The Eq. (11) is the Euclidean wave equation in cylindrical coordinates from which σ can be obtained by the well known method. A typical solution of this equation may be written in the form

$$\sigma = MJ_0(kr)\cos kt, \tag{17}$$

where M and k are constants and $J_0(kr)$ is Bessel's function of first kind and of order zero. As suggested by WEBER and WHEELER [8] a physically more interesting case is that of a pulse formed by linear superposition of monochromatic waves with σ of the form (17). One can superpose such waves with an amplitude factor $M = 2Ne^{-ak}$ and thus

$$\sigma = 2N\int_0^\infty e^{-ak} J_0(kr)\cos kt\, dk = N\left[\{(a-it)^2 + r^2\}^{-1/2} + \{(a+it)^2 + r^2\}^{-1/2}\right]. \tag{18}$$

For monochromatic outgoing waves, we have $C = C(t-r)$, $B = (1/4)\log r + b$, σ given by (17) and

$$A = \frac{1}{16}\log r - \frac{1}{2}e^{4b}\int (\bar{c})^2\, du + \frac{1}{2}(L^2kr)\, J_0(kr)\, J_0''(kr)\cos 2kt + \\ + \frac{1}{2}(L^2k^2r^2)\left\{[J_0'(kr)]^2 - J_0(kr)\, J_0''(kr)\right\}, \tag{19}$$

where $u = t - r$ and a bar over a function means differentiation with respect to its argument.

For monochromatic incoming waves, we have $C = C(t+r)$, $B = (1/4)\log r + b$, σ given by (17) and

$$A = \frac{1}{16}\log r + \frac{1}{2}e^{4b}\int (\bar{c})^2\, dv + \frac{1}{2}(L^2kr)\, J_0(kr)\, J_0''(kr)\cos 2kt + \\ + \frac{1}{2}(L^2k^2r^2)\left\{[J_0'(kr)]^2 - J_0(kr)\, J_0''(kr)\right\}, \tag{20}$$

where $v = t + r$.

In the case of the pulse wave also one can write down the expression for A, when $B = (1/4)\log r + b$, $C = C(t+r)$ and σ is given by (18).

Further THORNE [9] has given a definition of energy for cylindrically symmetric systems termed as C-energy. His definition has been adapted by one of the present authors [10] to cylindrical systems in a scalar-tensor theory.

In this definition of C-energy a quantity $E(r, t)$ expressed in terms of the generators of the system acts as a potential function from which C-energy

flux vector p^i is calculated for the metric (5). The function E is

$$E(r, t) = (1/4G)\, A(r, t) = 2A(r, t), \tag{21}$$

where we have taken $G = 1/8\pi$, G being the usual universal gravitational constant. Thus the use of the expression for A in (21) will give E consisting of two parts, one corresponding to g_{ij} and the other to σ, both contributing positively to the C-energy density.

When $C = 0$, the matrix (5) reduces to the EINSTEIN—ROSEN metric [5], [6] in which case the field equations have already been investigated by LAL and SINGH [11] and LETELIER [2]. The cylindrical gravitational waves are related to a special class of spherical and toroidal waves [12], [13] and therefore the solutions can easily be related to these waves.

Remarks

It is interesting to remark that the solutions found in this paper can be transformed to solutions of BRANS—DICKE theory in the vacuum (DICKE [14]).

The solutions can also be interpreted as the solutions of EINSTEIN's equation with a massless scalar field source, since such a source has the same stress-energy tensor as an irrotational fluid with $p = \varrho$ (TABENSKY and TAUB [1]).

REFERENCES

1. R. TABENSKY and A. H. TAUB, Commun. Math. Phys., **29,** 61, 1973.
2. P. S. LETELIER, J. Math. Pyhs., **16,** 1488, 1975.
3. P. S. LETELIER and R. R. TABENSKY, Il Nuovo, Cimento, **28M,** 408, 1975.
4. J. J. STACHEL, J. Math. Phys. **7,** 1321, 1966.
5. A. EINSTEIN and N. ROSEN, J. Franklin Inst., **223,** 43, 1937.
6. N. ROSEN, Bull. Res. Counc. Israel, **3,** 328, 1954.
7. S. W. HAWKING and R. PENROSE, Proc. Roy. Soc., **A312,** 529, 1970.
8. J. WEBER and J. A. WHEELER, Rev. Mod. Phys., **29,** 509, 1957.
9. K. S. THORNE, Phys. Rev., **138,** B251, 1965.
10. T. SINGH, Proc. Indian Acad. Sci., **85A,** 90, 1977.
11. K. B. LAL and T. SINGH, Tensor, N. S., **27,** 211, 1973.
12. L. MARDER, Proc. Roy. Soc., **A313,** 83, 1969.
13. L. MARDER, Proc. Roy. Soc., **A327,** 123, 1972.
14. R. H. DICKE, Phys. Rev., **125,** 2163, 1962.

Acta Physica Academiae Scientiarum Hungaricae, Tomus 45 (2), pp. 113—121 (1978)

FORMATION OF SHOCK WAVES IN DISSOCIATING GASES

By

R. SHANKAR and S. K. JAIN

DEPARTMENT OF MATHEMATICS, INDIAN INSTITUTE OF TECHNOLOGY, NEW DELHI-110029, INDIA

(Received 6. VII. 1978)

Using singular surface theory the phenomena associating with the non-uniform propagation of weak discontinuities through dissociating gases are studied. The fundamental differential equations governing the growth and decay of these discontinuities are formulated and these equations are solved completely. The criteria for decay or "blow up" of these discontinuities are obtained. It turns out that the dissociating character of the gas allows the existence of a singular surface carrying a weak discontinuity into a non-uniform medium, this weak discontinuity may grow into a shock, and the role of mass-fraction variable is to contribute to possible damping in the formation of the shock.

1. Introduction

Recently, a great deal of interest has arisen in the problems associated with the formation of shock waves in compressible fluids. Several research papers have been published on the formation of shock waves in gases with thermodynamically relaxed state. (BECKER [1], BURGER [2], [3], SCHMITT [4], RAMA SHANKAR [11] [12], RISHI RAM [13], etc.) The purpose of the present work is to apply singular surface theory to provide a mathematical description of the propagation of sonic discontinuities existing into a non-uniform dissociative gaseous medium. Such a study in an ideal uniform gas flow has its origin in the work of THOMAS [8]. He showed that the discontinuity in a gradient of any of the field variables grows indefinitely and becomes infinite for a finite time. Many applications of his method followed. (RAMA SHANKAR [10, 11, 12], RISHI RAM [13], KAUL [5], NARIBOLI [6, 7]).

If the medium ahead is moving, then it can be shown [12] that the wave propagation is anisotropic. In order to study anisotropic wave propagation, LIGHTHILL [15] has developed an elegant method which essentially involves the evaluation of the Fourier integrals by the stationary phase method and gives the asymptotic features of the solution. Numerous applications of this method followed. LUDWIG [16] and DUFF [17] further generalized and developed this technique.

The mathematical theory of geometric optics (ray theory) of LUNEBERG [18] was found useful by BAZER [19] in the investigation of weak discontinuities. NARIBOLI [6, 7] combined the theory of singular surfaces and ray theory

to study the propagation of weak discontinuities in nonlinear anisotropic media. Using this combination the integrated the equation of growth of discontinuities in a simple and straightforward manner. Following NARIBOLI, UPADHYAY [20] obtained the growth equation for sonic discontinuities propagating through thermally conducting gases, but did not discuss the growing or decaying tendency.

Recently, ELCRAT [21] studied the non-uniform propagation of sonic discontinuities in an unsteady flow of a perfect gas. In order to integrate the growth equations, he transformed them to an equation along the bicharacteristic curve in the characteristic manifold. While doing so, he arrived at an ordinary differential equation which was solved completely, and the criteria for decay or "blow up" was obtained. In the present paper following ELCRAT we shall derive and discuss the solutions of fundamental differential equations for the nonuniform propagation of sonic discontinuities through dissociating gases. We shall also find the criteria for "blow up" for sonic discontinuities.

2. Non-uniform propagation of weak discontinuities

The basic equations governing the three-dimensional unsteady flow of an ideal dissociating gas referred to a rectangular coordinate system are (RAMA SHANKAR [11])

$$\frac{\partial \varrho}{\partial t} + v_i \varrho_{,i} + \varrho v_{i,i} = 0, \tag{1}$$

$$\varrho \frac{\partial v_i}{\partial t} + \varrho v_k \, v_{i,k} + p_{,i} = 0, \tag{2}$$

$$\varrho \frac{dh}{dt} - \frac{dp}{dt} = 0, \tag{3}$$

$$\frac{dq}{dt} = c\varrho\theta^{-n}\left[(1-q)\, e^{-D/R\theta} - \frac{\varrho}{\varrho_D} q^2\right], \tag{4}$$

$$p = \varrho R\theta(1+q), \tag{5}$$

$$h = R\theta(4+q) + qD, \tag{6}$$

where $\varrho, v_i, p, h, q, \theta, D, \varrho_D$ and t are respectively, the density, components of flow velocity, pressure, enthalpy, mass-fraction variable, temperature, dissociation energy per unit mass, characteristic density and time. R is the gas constant, c is a constant with the dimension of time and d/dt $\left(\equiv \partial/\partial t + v_i(\partial/\partial x_i)\right)$ is the mobile operator.

Using the above equations we can always write

$$\frac{\partial p}{\partial t} + \varrho a_f^2 v_{i,i} - \varrho v_i \frac{\partial v_i}{\partial t} - \varrho v_i v_k v_{i,k} + \\ + \left\{ D\varrho \sqrt{\gamma(q) - 1} - \frac{p}{3\sqrt{\gamma(q) - 1}} \right\} \frac{dq}{dt} = 0, \tag{7}$$

where a_f is the frozen speed of sound defined by

$$a_f^2 = \gamma(q) \frac{p}{\varrho} \quad \text{and} \quad \gamma(q) = \frac{4 + q}{3}.$$

We consider a moving singularity surface $S(t)$ across which the flow quantities are continuous with possible discontinuities in their first and second order derivatives.

Suppose that the moving singularity surface $S(t)$ is given by $\varphi(x_i, t) = 0$, and that we denote by n_i the components of the unit normal vector $\varphi_{,i}/|\operatorname{grad}\varphi|$, and by $G = -(\partial\varphi/\partial t)/|\operatorname{grad}\varphi|$, the normal speed of advance of this surface. We consider the surface as having two sides denoted by ① and ② and n_i points into ②. The relative speed of advance of $S(t)$ in the fluid, $G - v_i n_i$, is denoted by U. A square bracket denotes the jump in the quantity enclosed. Let the discontinuities be denoted by THOMAS [8]:

$$[v_{i,j}] = \lambda n_i n_j; \quad \left[\frac{\partial v_i}{\partial t}\right] = -G\lambda n_i,$$

$$[p_{,i}] = \xi n_i; \quad \left[\frac{\partial p}{\partial t}\right] = -G\xi,$$

$$[\varrho_{,i}] = \zeta n_i; \quad \left[\frac{\partial \varrho}{\partial t}\right] = -G\zeta,$$

$$[h_{,i}] = \eta n_i; \quad \left[\frac{\partial h}{\partial t}\right] = -G\eta,$$

where λ, ξ, ζ and η are the scalars corresponding to velocity, pressure, density and enthalpy, respectively, on $S(t)$.

Using the first order compatibility conditions in Eqs. (1)—(3) and (7), we get:

$$U\zeta = \varrho\lambda, \tag{8}$$

$$\varrho U\lambda = \xi, \tag{9}$$

$$\varrho\eta = \xi, \tag{10}$$

and

$$\varrho U\lambda_i v_i - G\xi + \varrho a_f^2 \lambda = 0. \tag{11}$$

From Eqs. (8), (9) and (11), we get

$$\xi = \varrho U\lambda = U^2\zeta = a_f^2\zeta,$$

i.e. $U^2 = a_f^2$, which indicates that the weak discontinuities in non-uniform gaseous medium propagate with the frozen speed of sound.

Differentiating Eqs. (1) and (2) with respect to x_j we get after taking jump across $S(t)$:

$$\left[\frac{\partial^2\varrho}{\partial x_j\,\partial t}\right] + v_i[\varrho_{,ij}] + [v_{i,j}\,\varrho_{,i}] + [\varrho_{,j}\,v_{i,i}] + \varrho[v_{i,ij}] = 0 \tag{12}$$

and

$$\varrho\left[\frac{\partial^2 v_i}{\partial x_j\,\partial t}\right] + \left[\varrho_{,j}\frac{\partial v_i}{\partial t}\right] + \varrho[v_{k,j}\,v_{i,k}] + \varrho v_k[v_{i,kj}] + v_k[\varrho_{,j}\,v_{i,k}] + [p_{,ij}] = 0. \tag{13}$$

Now following ELCRAT [21], we get

$$U\frac{\delta\zeta}{\delta t} - (U^2\bar{\zeta} - \varrho U\bar{\lambda}_i\,n_i) + 2U\zeta(v_{i,j}\,n_i\,n_j)_2 +$$

$$+ 2U\lambda\left\{\left(\frac{\partial\varrho}{\partial n}\right)_2 - \varrho\Omega\right\} - 2U\zeta\lambda + Ug^{\alpha\beta}\,\zeta_{,\alpha}\,v_i\,x_{i,\beta} = 0 \tag{14}$$

and

$$\varrho\frac{\delta\lambda}{\delta t} + (\bar{\xi} - \varrho U\bar{\lambda}_i\,n_i) - U\lambda\left(\frac{\partial\varrho}{\partial n}\right)_2 + \left(\frac{\partial v_i}{\partial t} + v_k\,v_{i,k}\right)_2 n_i\zeta +$$

$$U\zeta\left(\frac{\partial v_i}{\partial n}\right)_2 n_i + U\zeta(v_{i,j}\,n_i\,n_j)_2 + \varrho g^{\alpha\beta}\,\lambda_{,\alpha}\,v_k\,x_{k,\beta} = 0, \tag{15}$$

where $\bar{\xi} = [p_{,ij}]n_i n_j \ldots$ etc. and $\delta/\delta t$ is a differentiation along an orthogonal trajectory of the surface $S(t)$, which is given by $x_i = x_i(u_\alpha)$, $(\alpha = 1, 2)$, Ω the mean curvature of $S(t)$ defined by $2\Omega = g^{\alpha\beta}b_{\alpha\beta}$, $g^{\alpha\beta}$ and $b_{\alpha\beta}$ are first and second fundamental forms of $S(t)$, respectively, and the remaining symbols have their usual meanings.

Elimination of λ_i between (14) and (15) leads to the following equation:

$$U\left(\frac{\delta\zeta}{\delta t} + v_i\,g^{\alpha\beta}\,\zeta_{,\alpha}\,x_{i,\beta}\right) + \varrho\left(\frac{\delta\lambda}{\delta t} + v_k\,g^{\alpha\beta}\,\lambda_{,\alpha}\,x_{k,\beta}\right) +$$

$$(\bar{\xi} - U^2\bar{\zeta}) + 3U\zeta(v_{i,j}\,n_i\,n_j)_2 + \left(\frac{\partial v_i}{\partial n}\right)_2 n_i\,U\zeta + U\lambda\left(\frac{\partial\varrho}{\partial n}\right)_2 -$$

$$2\varrho U\lambda\Omega - 2U\zeta\lambda + \left(\frac{\partial v_i}{\partial t} + v_k\,v_{i,k}\right)_2 n_i\zeta = 0. \tag{16}$$

Now our aim is the elimination of $(\bar{\xi} - U^2\bar{\zeta})$ from Eq. (16). For this, we proceed as follows:

Differentiating $p = \varrho R\theta(1 + q)$ and evaluating across $S(t)$, we get

$$[p_{,i}] = \varrho R\theta[q_{,i}] + \varrho R(1 + q)\,[\theta_{,i}] + R\theta(1 + q)\,[\varrho_{,i}],$$

or

$$[\theta_{,i}] = \frac{\theta}{p}\{\xi - R\theta(1 + q)\,\zeta\}\,n_i. \tag{17}$$

Once again differentiating $p_{,i}$ with respect to x_l and taking jump, we have

$$\begin{aligned}\bar{\xi} = [p_{,ii}] = {} & \varrho R\theta[q_{,ii}] + 2\varrho R(q_{,i})_2\,[\theta_{,i}] + 2R\theta(q_{,i})_2\,\zeta n_i \\ & + \varrho R(1 + q)\,[\theta_{,ii}] + R\theta(1 + q)\,\bar{\zeta} + 2R(1 + q) \\ & \{(\theta_{,i})_2\,\zeta n_i + (\varrho_{,i})_2\,[\theta_{,i}] - \zeta[\theta_{,i}]\,n_i\}\,.\end{aligned} \tag{18}$$

In order to find out $[\theta_{,ii}]$, differentiate the equation $h = R\theta(4 + q) + qD$ twice and making use of second order compatibility conditions of THOMAS [8, 9], we have

$$[\theta_{,ii}] = \frac{1}{R(4 + q)}\{[h_{,ii}] - 2R(q_{,i})_2\,[\theta_{i,}] - (D + R\theta)\,[q_{,ii}]\}\,. \tag{19}$$

For $[h_{,ii}]$ we differentiate the Eq. (3) with respect to x_j, multiply by n_j, take summation over j and taking jump, we get

$$\begin{aligned}[h_{,ii}] = \bar{\eta} = \frac{1}{\varrho U}\Bigg[& \varrho\,\frac{\delta\eta}{\delta t} - U\eta\left(\frac{\partial\varrho}{\partial n}\right)_2 + \left(\frac{\partial h}{\partial t}\right)_2 \zeta + U\zeta\eta + \\ & \varrho(h_{,i})_2\,\lambda_i - \varrho\lambda\eta + v_i(h_{,i})_2\,\zeta + U\bar{\xi} - \frac{\delta\xi}{\delta t} - v_i\,g^{\alpha\beta}\,\xi_{,\alpha}\,x_{i,\beta} + \\ & \varrho v_i\,g^{\alpha\beta}\,\eta_{,\alpha}\,x_{i,\beta} - (p_{,i})_2\,\lambda_i + \xi\lambda\Bigg].\end{aligned} \tag{20}$$

Differentiation of the rate equation (4) with respect to x_j and taking jump across $S(t)$ yields $[q_{,ii}]$:

$$[q_{,ii}] = \frac{\lambda}{U}(q_{,i})_2\,n_i + \frac{c\zeta\theta^{-n}}{U}\left\{\frac{2\varrho}{\varrho_D}q^2 - (1 - q)\,e^{-D/R\theta}\right\} +$$

$$\frac{c\theta^{-n}}{pU}\{\xi - R\theta(1 + q)\,\zeta\}\,\{n(1 - q)\,e^{-D/R\theta} - \frac{n\varrho}{\varrho_D}q^2 - \frac{D\varrho}{R\theta}(1 - q)\,e^{-D/R\theta}. \tag{21}$$

Now making use of Eqs (17), (20) and (21) in Eq. (19) we yield:

$$[\theta_{,ii}] = \frac{1}{(4+q)\,R}\left[\frac{1}{\varrho U}\left\{\varrho\,\frac{\delta\eta}{\delta t} - U\eta\left(\frac{\partial\varrho}{\partial n}\right)_2 + \left(\frac{\partial h}{\partial t}\right)_2\zeta + U\zeta\eta + \varrho(h_{,i})_2\,\lambda_i - \varrho\lambda\eta + v_i(h_{,i})_2\,\zeta + \varrho v_i\,g^{\alpha\beta}\,x_{i,\beta}\,\eta_{,\alpha} + U\bar{\xi} - \frac{\delta\xi}{\delta t} - v_i\,g^{\alpha\beta}\,\xi_{,\alpha}\,x_{i,\beta} + \xi\lambda - (p_{,i})_2\,\lambda_i\right\} - \right. \tag{22}$$

$$2R(q_{,i})_2\,\frac{\theta}{p}\left\{\xi - R\theta(1+q)\,\zeta\right\}n_i - (D+R\theta)\left\{\frac{\lambda}{U}(q_{,i})_2\,n_i + \frac{c\zeta\theta^{-n}}{U}\left(\frac{2\varrho}{\varrho_D}q^2(1-q)\,e^{-D/R\theta}\right)\right\} - (D+R\theta)\,\frac{c\theta^{-n}}{pU}\{\xi -$$

$$\left. R\theta(1+q)\,\zeta\right\}\left\{n(1-q)\,e^{-D/R\theta} - \frac{n\varrho}{\varrho_D}q^2 - \frac{D\varrho}{R\theta}(1-q)\,e^{-D/R\theta}\right\}\Bigg] .$$

Now with the help of Eqs. (17), (18), (21) and (22) we get

$$\bar{\xi} - U^2\bar{\zeta} = \frac{1}{U}E\gamma(q)\,\varrho(q_{,i})_2\,n_i\lambda + \frac{\gamma(q)}{U}AE\varrho e\theta^{-n}\zeta +$$

$$\frac{\gamma(q)EP^*c\theta^{-n}}{pU}\{\xi - R\theta(1+q)\,\zeta\} + \gamma(q)\,\frac{\varrho}{U}\left(\frac{1+q}{4+q}\right)\frac{\delta\eta}{\delta t} -$$

$$\gamma(q)\left(\frac{1+q}{4+q}\right)\left(\frac{\partial\varrho}{\partial n}\right)_2\eta + \frac{\gamma(q)}{U}\left(\frac{1+q}{4+q}\right)\left[\left(\frac{\partial h}{\partial t}\right)_2\zeta + U\zeta\eta +$$

$$\varrho(h_{,i})_2\,\lambda_i - \varrho\lambda\eta + v_i(h_{,i})\,\zeta - \frac{\delta\xi}{\delta t} - \left(\frac{\partial p}{\partial n}\right)_2\lambda +$$

$$\xi\lambda + \varrho v_i\,g^{\alpha\beta}\,x_{i,\beta}\,\eta_{,\alpha} - v_i\,g^{\alpha\beta}\,x_{i,\beta}\,\xi_{,\alpha}\Big] +$$

$$\frac{2R\theta}{p}\,\gamma(q)\left\{\frac{\varrho}{\gamma(q)}(q_{,i})_2 + (1+q)\left((\varrho_{,i})_2 - \zeta n_i\right)\right\}\times$$

$$\{\xi - R\theta(1+q)\,\zeta\}\,n_i + 2R\theta + \gamma(q)\,(q_{,i})_2\,n_i\zeta +$$

$$2\gamma(q)\,R(1+q)\,(\theta_{,i})_2\,n_i\zeta\,, \tag{23}$$

where

$$A = \frac{2\varrho}{\varrho_D}q^2 - (1-q)\,e^{-D/R\theta}\,,$$

$$E = 3R\theta - D(1+q)\,,$$

and

$$P^* = \left(n - \frac{\varrho D}{R\theta}\right)(1-q)\,e^{-D/R\theta} - \frac{n\varrho}{\varrho_D}q^2\,.$$

Now eliminating $(\bar{\xi} - U^2\bar{\zeta})$ between Eqs (16) and (23), we get

$$U\left(\frac{\partial\xi}{\partial t} + g^{\alpha\beta}v_i\, x_{i,\beta}\,\zeta_{,\alpha}\right) + \varrho\left(\frac{\delta\lambda}{\delta t} + g^{\alpha\beta}v_k\, x_{k,\beta}\,\lambda_{,\alpha}\right) +$$

$$\frac{\gamma(q)\,E\varrho}{U}(q_{,i})_2\, n_i\,\lambda + \frac{\gamma(q)\,AE\varrho c\theta^{-n}}{U}\zeta + \frac{\varrho}{U}\left(\frac{1+q}{4+q}\right)\gamma(q)\,\frac{\delta\eta}{\delta t} +$$

$$\frac{\gamma(q)\,EP^*c\theta^{-n}\varrho}{pU}\{\xi - R\theta(1+q)\,\zeta\} - \gamma(q)\left(\frac{1+q}{4+q}\right)\left(\frac{\partial\varrho}{\partial n}\right)_2\eta +$$

$$\frac{\gamma(q)}{U}\left(\frac{1+q}{4+q}\right)\left[\left\{\frac{\partial h}{\partial t}\right\}_2\zeta + U\zeta\eta + \varrho\left(\frac{\partial h}{\partial n}\right)_2\lambda - \varrho\lambda\eta + v_i(h_{,i})_2\,\zeta -\right.$$

$$\left.\frac{\delta\xi}{\delta t} - \left(\frac{\partial p}{\partial n}\right)_2\lambda + \xi\lambda + \varrho v_i\, g^{\alpha\beta}x_{i,\beta}\,\eta_{,\alpha} - v_i\, g^{\alpha\beta}x_{i,\beta}\,\xi_{,\alpha}\right] +$$

$$\frac{2\gamma(q)\,R\theta}{p}\left\{\frac{\varrho}{\gamma(q)}(q_{,i})_2 + (1+q)\left((\varrho_{,i})_2 - \zeta n_i\right)\right\}\{\xi - R\theta\times$$

$$(1+q)\,\zeta\}\,n_i + 2R\theta\gamma(q)\,(q_{,i})_2\,n_i\zeta + 2R\gamma(q)\,(1+q)\,(\theta_{,i})_2\,n_i\zeta +$$

$$3U\zeta(v_{i,j}\,n_i\,n_j)_2 + U\zeta\left(\frac{\partial v_i}{\partial n}\right)_2 n_i\zeta + U\lambda\left(\frac{\partial\varrho}{\partial n}\right)_2 - 2\varrho U\lambda\Omega -$$

$$2U\zeta\lambda + \left(\frac{\partial v_i}{\partial t} + v_k\, v_{i,k}\right)_2 n_i\zeta = 0. \tag{24}$$

Eq. (24) is a differential equation for ζ ($U\zeta = \varrho\lambda$, $\xi = U^2\zeta$ and $\varrho\eta = \zeta$) and therefore, one for ζ and one for λ, along the orthogonal trajectories of $S(t)$. Since it is a Riccatti differential equation, it is amenable to analysis, at least in certain special cases. However, the "inhomogeneous terms" arising from the surface derivatives cause some difficulty in interpretation, and if we transform Eq. (24) into a differential equation along bicharacteristic curves in the characteristic manifold $\Sigma = U_t S(t)$, this difficulty disappears because while doing so, we will arrive at an ordinary differential equation (26).

Following ELGRAT [21], we write

$$\frac{d\zeta}{dt} = \frac{\delta\zeta}{\delta t} + g^{\alpha\beta}v_i\, x_{i,\beta}\,\zeta_{,\alpha}\,,$$

$$\frac{d\xi}{dt} = \frac{\delta\xi}{\delta t} + g^{\alpha\beta}v_i\, x_{i,\beta}\,\xi_{,\alpha}\,, \tag{25}$$

$$\frac{d\lambda}{dt} = \frac{\delta\lambda}{\delta t} + g^{\alpha\beta}v_i\, x_{i,\beta}\,\lambda_{,\alpha}\,,$$

where the symbols have their usual meaning.

Now using Eqs. (8)—(10) and (25) in Eq. (24), we get

$$\frac{d\zeta}{dt} + \zeta\left[\frac{1}{2}\frac{d}{dt}\log\left(\frac{U}{\varrho}\right) - \frac{1+q}{\sigma}\frac{d}{dt}(\log\varrho) + Q\right] - \{\gamma(q)+1\}\frac{U\zeta^2}{2\varrho} = 0, \quad (26)$$

where

$$Q = \left\{E\gamma(q) + \frac{2}{3}\frac{p}{\varrho} + 2R\theta\right\}(q_{,i})_2\, n_i + \frac{\gamma(q)}{U} AE\varrho c\theta^{-n} \times$$

$$\frac{1}{3\varrho U}\{(1+q)\,\gamma(q)EP^* c\theta^{-n}\} + \frac{1}{3U}(1+q)\left(\frac{\partial h}{\partial t} + v_i\, h_{,i}\right)_2 +$$

$$\frac{(1+q)}{3}\left(\frac{\partial h}{\partial n}\right)_2 + \left\{\frac{U^2}{\varrho}\gamma(q)\right\}\left(\frac{\partial \varrho}{\partial n}\right)_2 - \frac{1+q}{3\varrho}\left(\frac{\partial p}{\partial n}\right)_2 +$$

$$2R\gamma(q)\,(1+q)\,(\theta_{,i})_2\, n_i + 3U(v_{i,j}\, n_i\, n_j)_2 +$$

$$U\left(\frac{\partial v_i}{\partial n}\right)_2 n_i - 2U^2\Omega + \left(\frac{\partial v_i}{\partial t} + v_k\, v_{l,k}\right)_2 n_i\,.$$

Eq. (26) is the basic differential equation for the growth and decay of weak discontinuities associated with the wave surface $S(t)$.

Integration of Eq. (26) yields:

$$\zeta = \left[\zeta_0\left(\frac{U}{U_0}\right)^{-1/2}\left(\frac{\varrho}{\varrho_0}\right)^{3/2}\exp\left(\frac{q-q_0}{6} - \int_0^t \frac{1}{2U}Q d\tau\right)\right] \Big/ \left[1 -\right.$$

$$\frac{1}{2}\zeta_0\, U_0^{1/2}\,\varrho_0^{-3/2}\exp\left(-\frac{1+q_0}{6}\right)\int_0^t \{\gamma(q)+1\}\,(\varrho U)^{1/2} \times$$

$$\left.\exp\left(\frac{1+q}{6} - \frac{1}{2U}\int_0^t Q d\tau\right) d\tau\right],$$

where $S(t) = S_0$, $\lambda = \lambda_0$, $\xi = \xi_0$, $\zeta = \zeta_0$, $U = U_0$, $q = q_0$ at $t = 0$.

If $\zeta_0 > 0$, we have the criteria

$$\int_0^T \{\gamma(q)+1\}\,(\varrho U)^{1/2}\exp\left(\frac{1+q}{6} - \int_0^t \frac{1}{2U}Q d\tau\right) d\tau = \frac{2\varrho_0^{3/2}\, e^{(1+q_0)/6}}{\zeta_0\, U_0^{1/2}}$$

for "blow up" at a finite time T.

If we associate $\zeta \to \infty$, with the formation of a shock, these remarks may be thought of as a generalization of the corresponding statement in RAM [13] and RAMA SHANKAR [12] (if we consider q of [12] as a mass-fraction variable) where the surfaces $S(t)$ are planes. Thus, the dissociating character

of the gas allows the existence of singular surface carrying a weak discontinuity into a non-uniform medium. This weak discontinuity may grow into a shock and the role of mass-fraction variable is to contribute to possible damping in the formation of the shock.

Acknowledgement

The authors are grateful to Professor O. P. BHUTANI for his constant encouragement and valuable suggestions in the presentation of this work and CSIR, Government of India, for financial help,

REFERENCES

1. E. BECKER and H. SCHMITT, Arch., **36**, 335, 1968.
2. W. BURGER, ZAMM, **46**, 149, 1966.
3. W. BURGER, Dissertation, Darmstadt, 1967.
4. H. SCHMITT, ZAMM, **48**, 241, 1968
5. C. N. KAUL, Journ. Math. Mech., **10**, 393, 1961.
6. G. A. NARIBOLI, Journ. Math. Mech., **12**, 141, 1963.
7. G. A. NARIBOLI and B. B. SECREST, Tensor (N. S.), **18** (1), 22, 1967.
8. T. Y. THOMAS, Journ. Math. Mech., **6**, 455, 1957.
9. T. Y. THOMAS, Journ. Math. Mech., **6**, 311, 1957.
10. RAMA SHANKAR, General Theory of Discontinuities in Non-equilibrium Gasdynamics, Ph. D. Thesis, Chapter 4, Indian Institute of Technology, Delhi, New Delhi, India, 1970.
11. RAMA SHANKAR, Int. Journ. of Engg. Science, **9**, 1157, 1971.
12. RAMA SHANKAR and P. CHANDRAN, Journ. Math. and Physical Sciences, **11**, 237, 1977.
13. R. RAM and M. GAUR, Acta Phys. Hung., **40**, 85, 1976.
14. L. D. LANDAU and E. M. LIFSHITZ, Fluid Mechanics, Pergamon Press, Oxford, p. 259, 1959.
15. M. J. LIGHTHILL, Philosophical Trans. of Roy. Soc. of London **252A**, 397, 1960.
16. D. A. LUDWIG, A. E. C. Rept., NYO-9351, 1961.
17. G. F. D. DUFF, Comm. of Pure and Applied Mathematics, **17**, 189, 1964.
18. R. K. LUNCBERG, Mathematical Theory of Optics, 1964.
19. J. BAZER and O. FLEISCHMAN, The Physics of Fluids, **2**, 366, 1959.
20. K. S. UPADHYAY, Tensor (N. S.), **21**, 296, 1970.
21. A. R. ELCRAT, Int. Journ. of Engg. Sci., **15**, 29, 1977.

Acta Physica Academiae Scientiarum Hungaricae, Tomus 45 (2), pp. 123—131 (1978)

CALCULATIONS IN A MODEL POTENTIAL FIELD FOR THE ISOELECTRONIC SERIES OF THE Li ATOM

By

R. GÁSPÁR and I. KOÓS

INSTITUTE OF THEORETICAL PHYSICS, KOSSUTH LAJOS UNIVERSITY, H-4010 DEBRECEN

(Received 25. VII. 1978)

The pseudopotential method is used to calculate the ground states and excited states of the Li atom and those of the ions of its isoelectronic series in the first row of the periodic system. The energy eigenvalues and the pseudowavefunctions were computed numerically. The agreement between the calculated and empirical energies is good. The method is appropriate to consider the effect of the inner orbitals of many-electronic systems on the valency electrons.

Introduction

The solution of the Hartree—Fock equations causes great difficulties in the computations of atomic, molecular and solid state properties. There are a number of attempts to simplify either the methods of solution or the structure of the equations. One of the possibilities is the introduction of the pseudopotentials, which means to take into account the orthogonality of the valence states to the core states with a repulsive term [1]. In the Hartree—Fock equations one may try to substitute the sum of the terms of the nucleus-electron interaction, the Coulomb and the exchange-interaction with a Coulomb like and a non-local repulsive potential. In this way we can attain so considerable a reduction on the computational effort that the calculations may be carried out for the atomic systems with small or medium size computers [2]. There are further possibilities of the applications of this method in the molecular and the solid state field.

We have tried to substitute the non local potential with a linear combination of a local radial part multiplied by projection operators in the angular momentum space. The local radial part is a Gauss-type term, which contains some adjustable parameters. The values of these parameters have been obtained numerically with a semiempirical procedure. Substituting these values of parameters into the Gaussian term, we have calculated some energy eigenvalues and pseudowavefunctions of the Li atom and its isoelectronic series, numerically too.

The pseudopotential

Let us consider the Hartree—Fock equations of an atom with N electrons in the form

$$\left[H(1) + \sum_{j=1}^{N} \langle \psi_j | \, r_{12}^{-1}(1 - P_{12}) \, | \psi_j \rangle\right] \psi_i(1) = E_i \, \psi_i(1) \, , \tag{1}$$

where

$$H(1) = -\frac{1}{2} \Delta_1 - \frac{z}{r_1} , \tag{2}$$

z the atomic number, $\mathbf{P}_{12}$ the permutation operator and the quantities are measured in atomic units.

If we use the Eq. (1) the wavefunction of the atom is

$$\psi = N^{-\frac{1}{2}} \begin{vmatrix} \psi_1(1) & \psi_1(2) & \dots & \psi_1(N) \\ \psi_2(1) & \psi_2(2) & \dots & \psi_2(N) \\ \psi_N(1) & \psi_N(2) & \dots & \psi_N(N) \end{vmatrix} , \tag{3}$$

where ψ_N is the wavefunction of the valence electron and the ψ_i functions are assumed to be orthogonal ones. Let us write ψ_N in the following form:

$$\psi_N = \psi_0 - \sum_{i=1}^{N-1} c_i \, \psi_i, \quad c_i = \langle \psi_i \, | \, \psi_0 \rangle \, , \tag{4}$$

where ψ_0 is *not* orthogonal to the core functions ψ_i. We can substitute (4) into the determinant (3), and we get the Hartree—Fock equations (1) in the form

$$(H_F + V_R) \, \psi_0 = E_N \, \psi_0, \tag{5}$$

where

$$H_F = H(1) + \sum_{j=1}^{N-1} \langle \psi_j \, | \, r_{12}^{-1}(1 - P_{12}) \, | \, \psi_j \rangle , \tag{6}$$

and

$$V_R = \sum_{j=1}^{N-1} (E_N - E_j) \, | \, \psi_j \rangle \, \langle \psi_j \, | \, . \tag{7}$$

V_R is called the pseudopotential.

HELLMANN suggested [3] that the total interaction potential should be written in the form

$$V_H = -\frac{Z}{r} + A \exp \{-ar\}/r \, . \tag{8}$$

We can discover other forms such as $-Z/r + A \, e/r^{-ar}$, $-Z/r + A \, e/r^{-r^2}$ and so on used before. The latter form has been employed by RAY and SWITALSKI [4].

With this potential we have also calculated numerically some energy eigenvalues and the eigenfunctions using the parameteres obtained by RAY and SWITALSKI.

Let the form of the pseudopotential be

$$V(r) = -\frac{Z}{r} + \sum_l A_l \, e^{-a_l r^2} \, P_l \,, \tag{9}$$

where Z is the nuclear charge minus the number of core electrons and A_l and a_l the parameters of the pseudopotential for the state with quantum number l, respectively, P_l projection operator. The potential consists of two terms: the first is a Coulombic term and the second has Gaussian form. The latter will be used for the description of an electron, moving in the field of an $(1s)^2$ closed shell ion excluding the Coulomb term, but including all other interactions e.g. correlation, polarization, etc.

There are a number of ways to determine the parameters of (9). At the first trial a variational method with doublezeta wave functions has been used. The computed energy-values were fitted to the $2s$, $3s$ and $2p$, $3p$ terms of the Li atom and the ions of its isoelectronic series, resp. [5].

Here the parameters A_l and a_l have been determined by a numerical procedure. Let us consider the one-electron wavefunctions in the form

$$\psi_{nlm}(r, \vartheta, \chi) = \frac{1}{r} \, P_{nl}(r) \; Y_{lm}(\vartheta, \chi) \,, \tag{10}$$

where Y_{lm} are spherical harmonics. Because the computations have been carried out for atoms containing one valency electron, the dependence of one-electron wavefunctions upon the spin coordinates has been neglected.

By inserting the function (10) into the equation

$$\left[-\frac{1}{2} \Delta_{r\vartheta\chi} + V(r) \right] \psi_{nlm} = E_{nl} \; \psi_{nlm} \tag{11}$$

obtained from the Eqs. (5) and (6), and multiplying the Eq. (11) from left by the $\langle Y_{lm} |$, we obtain the radial Schrödinger equation

$$\frac{1}{2} \frac{d^2 P_{nl}}{dr^2} + \left(E_{nl} - \frac{l(l+1)}{r^2} - V_l(r) \right) P_{nl} = 0 \,. \tag{12}$$

To simplify the form of Eq. (12), it is convenient to introduce Rydberg units for the energy and the potential. Then Eq. (12) becomes

$$\frac{d^2 P_{nl}}{dr^2} + \left(E_{nl} - \frac{2l(l+1)}{r^2} - 2V_l(r) \right) P_{nl} = 0 \,. \tag{13}$$

The numerical solution of this equation has been obtained by a subroutine suggested by HERMAN and SKILLMAN [6]. The pontential $V_l(r)$ in Eq. (13) has to satisfy the conditions

$$\lim_{r\to 0} rV_l(r) = -Z \tag{14a}$$

and

$$\lim_{r\to\infty} V_l(r) = 0, \tag{14b}$$

which is in agreement with the form (9) selected by us. The parameters A_l and a_l in (9) have been determined by the requirement that the energy value for the ground state and the energy value for the first excited state (if $l = 0$), the energy values of the first and second excited states (if $l = 1$) computed from (13) agree with the experimental values, respectively. This requirement means that we have to solve the equations

$$E^c_{nl}(A_l, a_l) = E^{\exp}_{nl}, \quad n = n_1, n_2, \tag{15}$$

where $E^c_{nl}(A_l, a_l)$ are the computed energy values at some parameter values and $E^{\exp}_{nl}$ is the experimental value.

The solution of the system of equations (15) has been obtained by determining the roots of the nonlinear equation

$$f(A_l, a_l) = \left| \frac{E^c_{n_1 l}(A_l, a_l) - E^{\exp}_{n_1 l}}{E^{\exp}_{n_1 l}} \right| + \left| \frac{E^c_{n_2 l}(A_l, a_l) - E^{\exp}_{n_2 l}}{E^{\exp}_{n_2 l}} \right|. \tag{16}$$

The Gauss—Seidel method and/or a random-search method has been suitable for this purpose. The convergence of both methods has been nearly the same.

The function $f(A_l, a_l)$ in Eq. (16) has been regarded to be zero, if the $|f| < \varepsilon$ condition has been satisfied, where $\varepsilon = 0.01$ has been selected in our case.

Discussion of results

The calculations with the Gaussian pseudopotential (9) were performed on the Li atom and the ions of its isoelectronic series. The parameters have been determined for the $l = 0$ and $l = 1$ states. The reference energy levels have been the lowest experimental states $2s$, $3s$ and $2p$, $3p$, respectively.

In Table I the parameter values determined with the double-zeta wavefunction and the numerical one are presented. We may observe considerable agreement between the parameters a_l, computed with different wavefunctions. In the calculational process more roots of function (16) have been obtained at some elements. In this case the values lying nearest to the values obtained by the double-zeta wavefunction method have been chosen.

Table Ia

Parameters of the potential $V_l(r)$ determined with the double-zeta wavefunction variationally and with the numerical method ($l = 0$)

Z	A_0		a_0	
	Double zeta	Numerical	Double zeta	Numerical
1	11.470	53.528	3.1113	3.0881
2	20.345	77.185	5.2933	5.2939
3	30.408	32.178	7.7567	5.2173
4	31.690	52.458	8.0076	8.0076
5	39.390	55.590	9.6892	9.6891
6	54.942	76.330	13.318	13.320
7	78.083	123.12	18.813	18.810

Table Ib

Parameters of the potential $V_l(r)$ determined with the double-zeta wavefunction and with the numerical method ($l = 1$)

Z	A_1		a_1	
	Double zeta	Numerical	Double zeta	Numerical
1	— 5.2287	— 1.0831	1.4464	1.4464
2	— 8.2100	— 8.2080	7.0004	7.0110
3	—11.894	—11.894	13.504	13.504
4	—15.271	—15.083	20.631	20.631
5	—16.603	—16.604	29.156	29.156
6	—17.090	—20.490	37.860	37.860
7	—17.522	—17.980	47.228	47.090

Table IIa

Energy eigenvalues computed by numerical integration for the Li atom at $l = 0$ with different pseudopotentials

	$-E$ (in Rydberg units)		$Z = 1$	
n	Experimental	Numerical $A = 53.5287$ $a = 3.08811$	Double zeta $A = 11.47005$ $a = 3.11307$	Ray—Switalski
1	0.39643	0.40210	0.48554	0.39894
2	0.14842	0.14806	0.16510	0.15054
3	0.077262	0.076172	0.082517	0.077467
4	0.047293	0.046383	0.049580	0.047064
5	0.031911	0.031131	0.032776	0.031527

In Tables II—III we present the energy eigenvalues computed by the numerical integration procedure outlined before with the pseudopotential field (9) with the numerical and the double-zeta parameter values, respectively, the RAY—SWITALSKI potential and the experimental energy values [7].

Table IIb

Energy eigenvalues computed by numerical integration for the Li atom at $l = 1$ with different pseudopotentials

	$-E$ (in Rydberg units)		$Z = 1$	
n	Experimental	Numerical $A = -1.0831$ $a = -1.44637$	Double zeta $A = -5.22868$ $a = 1.44637$	RAY—SWITALSKI
2	0.26056	0.26095	0.53752	
3	0.11450	0.11287	0.16369	
4	0.063980	0.062729	0.081915	
5	0.040783	0.039842	0.048676	
6	0.028253	0.027489	0.032501	

Table IIIa

Energy eigenvalues computed by numerical integration for the O^{5+} ion at $l = 0$ with different pseudopotentials

	$-E$ (in Rydberg units)		$Z = 6$	
n	Experimental	Numerical $A = 76.3259$ $a = 13.32$	Double zeta $A = 54.94254$ $a = 13.318322$	RAY—SWITALSKI
1	10.155	10.244	11.283	10.212
2	4.3208	4.2799	4.6143	4.8958
3	2.3822	2.3340	2.4938	2.6383
4	—	1.4745	1.5502	1.6328
5	—	1.0165	1.0563	1.1066

For saving space the Tables contain the energy values for the Li atom and the O^{5+} ion only. The energy eigenvalues computed with the numerical parameters are in agreement with the experimental ones within the precision of the accuracy of the fitting criterion (16) at the excited states, too. The agreement between the energies calculated by the numerical and the experimental parameters is better than the agreement of the energies with the double-zeta parameters; these latter are sometimes even lower than the experimental ones. This fact can be easily explained, when we observe that the potential (9) with the double-zeta parameters is less repulsive, than the potential with the numerical parameters.

Table IIIb

Energy eigenvalues computed by numerical integration for the O^{5+} ion at $l = 1$ with different pseudopotentials

$-E$ (in Rydberg units)			$Z = 6$	
n	Experimental	Numerical $A = -20.4903$ $a = 37.8607$	Double zeta $A = -17.0903$ $a = 37.8607$	RAY—SWITALSKI
2	9.2770	9.3049	9.3563	9.3531
3	4.0831	4.0684	4.0483	4.0404
4	2.2852	2.2588	2.2617	2.2368
5	—	1.4340	1.4255	1.4271
6	—	0.99093	0.98557	0.98158

The radial pseudowavefunctions with the different parameter values in the potential (9), those of the RAY—SWITALSKI potential and the wavefunction for the Li obtained from the Hartre—Fock calculations [8] are exhibited in Figs. 1, 2, 3 and 4. The wavefunctions are plotted for the states $l = 0$ and $l = 1$ respectively and for the Li atom and O^{5+} ion only. In the Figures it may be seen that the maxima of the numerical wavefunctions are always farther from the origin than those computed with the double-zeta parameters by the same method. This is due to the more powerful repulsion of the poten-

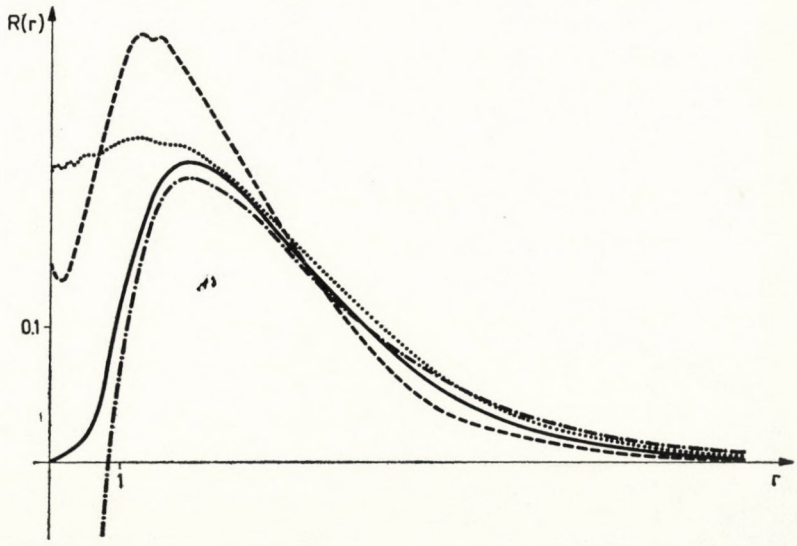

Fig. 1. Radial part of the wavefunctions computed with different parameter sets and different pseudopotentials, and the Hartree—Fock wavefunction for the Li atom at $n = 2$, $l = 0$
——— numerical; - - - - double-zeta; .... RAY—SWITALSKI, —•—•—•— HARTREE—FOCK

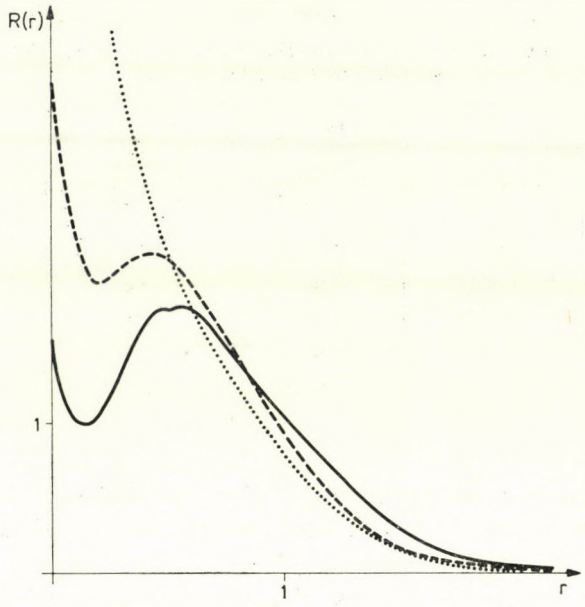

Fig. 2. Radial part of the wavefunctions computed with different parameter sets and different pseudopotentials for the Li atom at $n = 2$, $l = 1$. ——— numerical; - - - - double-zeta; .... RAY—SWITALSKI

tials obtained by the numerical method, as compared with the other ones. Although the pseudowavefunctions are nodeless (in the ground state) they have some oscillations close to the origin, which is more conspicuous for wavefunctions for the ions with higher atomic number.

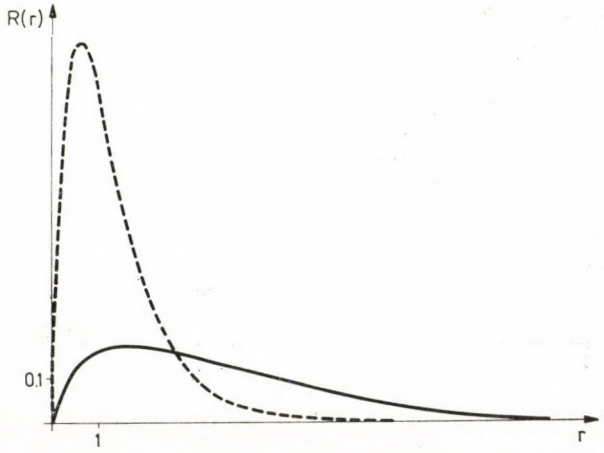

Fig. 3. Radial part of the wavefunctions computed with different parameter sets and different pseudopotentials for the O^{5+} ion at $n = 2$, $l = 0$. ——— numerical; - - - - double-zeta

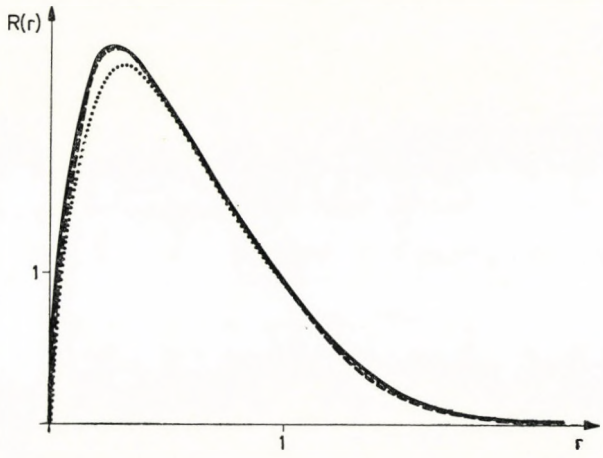

Fig. 4. Radial part of the wavefunctions computed with different parameter sets and different pseudopotentials for the O^{5+} ion at $n = 2$, $l = 1$. ——— numerical, - - - - double-zeta; .... Ray—Switalski

REFERENCES

1. See e.g.: P. Gombás, Pseudopotentiale, Springer Verlag, Wien—New York, 1967; J. C. Philips and L. Kleinman, Phys. Rev., **116,** 287, 1959.
2. L. Szász and G. McGinn, J. of Chem. Phys., **45,** 2898, 1966.
3. H. Hellmann, J. Chem. Phys., **3,** 61, 1935.
4. N. K. Ray and J. D. Switalski, J. of Chem. Phys., **63,** 5053, 1975.
5. R. Gáspár and R. Gáspár Jr., to be published.
6. F. Herman and S. Skillman, Atomic Structure Calculations, Prentice Hall, Inc., Englewood Cliffs, New-Jersey, 1963.
7. Landolt—Börnstein, Zahlenwerte und Funktionen, 6. Auflage, Springer Verlag, Berlin—Göttingen—Heidelberg, 1950.
8. Ch. F. Fischer, Atomic Data, **4,** 301, 1972.

Acta Physica Academiae Scientiarum Hungaricae, Tomus 45 (2), pp. 133—147 (1978)

THE ANALYSIS OF THE HERZBERG SYSTEM IN THE $^{13}C^{16}O$ AND PARTLY IN THE $^{12}C^{16}O$ MOLECULES

By

R. KĘPA

ATOMIC AND MOLECULAR PHYSICS LABORATORY, PEDAGOGICAL COLLEGE, RZESZÓW, POLAND

(Received 25. VII. 1978)

In the emission spectrum of the carbon monoxide isotopic molecules the Herzberg bands at a 0.6 Å/mm dispersion have been obtained. For the $^{13}C^{16}O$ molecule all the seven bands of this system have been obtained and for the $^{12}C^{16}O$ molecule the 0—2 and 0—3 bands only. A rotational analysis of these bands has been performed and the following constants were determined: the rotational constants of the $C^1\Sigma^+$ and $A^1\Pi$ states, the band origins for the $C^1\Sigma^+ - A^1\Pi$ transition, and the new vibrational constants for the $C^1\Sigma^+$ state.

Introduction

The $C^1\Sigma^+$ state was the subject of many studies in new systematic investigations of the electronic levels of the CO molecule, performed in recent years. Possibility for its explorations is given in the absorption as well as in the emission spectrum. In the absorption spectrum the $C^1\Sigma^+$ state can be investigated from the Hopfield—Birge band system ($C^1\Sigma^+ - X^1\Sigma^+$ transition) situated in the vacuum ultraviolet region. In emission, C state can be investigated from the Herzberg bands ($C^1\Sigma^+ - A^1\Pi$ transition) situated in the visible and near ultraviolet region. An intercombination $C^1\Sigma^+ - a'^3\Sigma^+$ emission bands, only once mentioned [12], does not give any further possibility for studies, than the one derived from the above transitions.

Up to now most of the information about the C state has been derived from the high resolution studies of the $C - X$ transition, reported by TILFORD and VANDERSLICE [22]. The 0—0 and 1—0 bands obtained in $^{12}C^{16}O$ and $^{13}C^{16}O$ molecules by these authors have made the calculation of the main molecular constants in this state possible. After detailed considerations, however, it seems that the constants obtained are doubtful. The same situation occurs for the constants of the $B^1\Sigma^+$ state, derived in this paper from the analysis of the bands of the $B - X$ system. Namely, in the calculations of the vibrational constants the authors have omitted the electronic isotope effect, what would not have been necessary, if both obtained vibrational quanta had been used.

Such an assumption has a significant effect upon the constant values (as can be seen from the detailed considerations) and consequently these values are very deformed. For example the $\omega_e x_e$ constant values of both the

Table I

0—0 band lines of $^{13}C^{16}O$ (in cm^{-1})

J	R		Q		P	
1			27168.695**		27164.557*	
2	27181.209		169.910		162.529	
3	187.049		171.975		160.874*	
4	193.425		174.734*		159.931	
5	200.920		178.569		159.931	
6	209.800		182.542	27154.610	161.488	
7	220.305*	27208.190*	187.659	163.210	164.557	27152.493
8	234.040	220.305*	193.807	172.760	170.800	157.104
9		231.424	201.186	183.028		160.874*
10		242.590	210.461	192.720**		164.557*
11		254.099	222.102	203.435		168.695**
12		266.373	235.950**	213.032*		173.526
13	265.280	279.668		222.590	164.910	179.423
14	294.750	282.774		232.389	175.120	187.049
15	299.446	312.673*		242.590	184.383	197.611
16	315.138			253.374	192.720	
17	330.778			264.711	200.920	
18	346.693			276.665	209.437	
19	363.125			289.262	218.489	
20	380.149			302.509	228.140	
21	397.817			316.435*	239.433	
22	416.250*			331.138	249.490	
23			340.391*	347.374		262.086
24				361.591		272.630
25				378.823		286.183
26				397.308		301.028

C and *B* states obtained under this assumption are only about half of the real values.

Other papers published on the *C* state were concerned with the Herzberg bands, but as they were based upon either fragmentary or insufficiently accurate analyses they did not give any further information about this state [5, 9]. Therefore the author attempts to give complete studies of the *C* state by means of analyses of the Herzberg bands in isotopic molecules. In this way, due to the advantageous location of these bands and by the use of molecules

Table II

0—1 band lines of $^{13}C^{16}O$ (in cm^{-1})

J	R	Q		P	
1	25722.794**	25715.389		25711.659	
2	727.941	716.791		709.373	
3	733.753	718.877		707.743	
4	740.251	721.681*		706.814	
5	747.462	725.176		706.603	
6	755.367	729.363		707.065	
7	763.969	734.257		708.204*	
8	773.268	739.843		710.113	
9	783.271	746.126		712.690	
10	793.949	753.119		715.955	
11	805.347	760.832*		719.930	
12	817.436	769.324		724.615	
13	830.258	779.482	25774.940	730.009	
14	843.864		787.448	736.215	
15	858.620		798.100	743.573	
16	25871.180		809.325		25748.727
17	887.450		821.241		757.632
18	903.876		833.972		766.634
19	920.858	845.671	850.365		776.205*
20	938.497	860.486			786.493
21	956.826	875.227			797.439
22	975.827	890.604			809.100
23		906.630			821.419
24		923.375			834.471
25		940.822			848.243
26		959.053			862.785
27		976.313			876.398
28					893.364
29					910.004
30					927.294
31					945.290
32					963.953

Table III

0—2 band lines of $^{13}C^{16}O$ (in cm^{-1})

J	R	Q		P	
1		24300.013		24296.035*	
2	24312.659*	301.489		293.873*	
3	318.563	303.690		292.446*	
4	325.227	306.645		291.747*	
5	332.618	310.344		291.747*	
6	340.774	314.767		292.446*	
7	349.615	320.029		293.873*	
8	359.212	325.631		296.035*	
9	369.553	332.348		298.967	
10	380.628	339.730		302.629	
11	392.442	347.847		307.029	
12	404.984	356.690		312.163	
13	418.287	366.274		318.041	
14	432.300	376.594		324.662	
15	447.068	387.651		332.029	
16	462.569	399.459		340.136	
17	478.824	412.012		348.990	
18	495.817	425.300		358.599	
19	513.566	439.343		368.952	
20	532.057	454.131		380.074	
21	551.335	469.679		391.976	
22	571.418	485.984		404.681	
23	592.392	503.052		418.287	
24		520.946		433 381	
25		539.660		455.138	
26		559.385			24461.107
27		580.727			476.840
28		607.423	24592.392		

more enriched with ^{13}C isotope, the determination of the line wave numbers may be performed with greater accuracy than in vacuum ultraviolet studies.

The Herzberg bands in the $^{12}C^{18}O$ molecule have been the subject of previous analyses [15]. In this paper the analysis of this system in $^{13}C^{16}O$ and partly in $^{12}C^{16}O$ molecules is presented.

Table IV

0—3 band lines of $^{13}C^{16}O$ (in cm^{-1})

J	*R*	*Q*	*P*
1	22923.907**	22916.454**	22912.754*
2	929.129**	918.040	910.606
3	935.244	920.377	909.236
4	942.072	923.493	908.644
5	949.684	927.403	908.809
6	958.088	932.043*	909.783
7	967.210*	937.546	911.532
8	977.216	943.786	914.060
9	987.948	950.806	917.373
10	999.458	958.605	921.464
11	23011.760	967.205	926.341
12	024.828	976.563	932.043*
13	038.677	986.715	938.434
14	053.313	997.646	945.670
15	068.740	23009.368	953.686
16	084.935	021.878	962.491
17	101.921	035.176	972.082
18	119.703	049.281	982.465
19	138.278	064.224	993.653
20	157.656	080.205	23005.654
21	177.876*	102.586 23094.658	018.502
22	199.091	112.861	032.358
23	23222.922	131.029	048.801 23039.996
24		149.939	059.954
25		169.696	076.356
26			093.218

Experimental procedure

The emission spectrum of the Herzberg bands has been obtained from a hollow-cathode type lamp. This type of lamp, although many other discharge tubes were tried, provided the highest intensity of the Herzberg bands relative to other "blending" systems. To obtain the spectrum of the $^{12}C^{16}O$ molecule, a lamp was filled with gaseous carbon dioxide of spectral purity. The spectrum of the $^{13}C^{16}O$ molecule was obtained from a lamp filled with gaseous carbon

Table V

0—4 band lines of $^{13}C^{16}O$ (in cm^{-1})

J	R	Q	P
1		21566.514*	
2	21579.186*	568.173	21560.697
3	585.365*	570.643	559.462
4	592.361*	573.867*	559.065*
5	600.218*	578.039	559.462
6	608.933*	582.977	560.697
7	618.430*	588.739	562.744
8	628.699*	595.328	565.586
9	639.846*	602.742	569.310
10	651.816*	610.976	573.867*
11	664.563*	620.029	579.186*
12	678.229*	629.919	585.365*
13	692.620	640.630	592.361*
14	707.861	652.163	600.218*
15	723.924	664.563*	608.858*
16	740.819	677.717	618.354*
17	758.535	691.739	628.699*
18	777.079	706.593	639.846*
19	796.437	722.261	651.816*
20	816.628	738.779	664.563*
21	837.595*	756.112	678.229*
22	859.493	774.294	692.729*
23	882.163	793.366	708.044
24		813.031	724.213
25		833.732	741.062
26		855.250	758.993
27		877.804*	777.715

dioxide enriched in 95% isotope ^{13}C. Pressure in both types of the lamps was 3 mmHg. The lamps were supplied by 600 V d.c. generator with current about 50 mA. Photographs were made in the 5th, 6th and 7th orders of the plane-grating PGS-2 spectrograph (VEB Carl Zeiss, Jena) with a reciprocal linear dispersion from 0.38 Å/mm to 0.83 Å/mm. Expositions were made on ORWO UV1-type plates for shorter wavelength bands and on Agfa-Gevaert 68A56 plates for the longer wavelength i.e. for the 0—4, 0—5 and 0—6 bands. The

Table VI

0—5 band lines of $^{13}C^{16}O$ (in cm^{-1})

J	*R*	*Q*	*P*
2	20262.840**	20251.664*	20244.219**
3	269.084*	254.292	243.098
4	276.308	257.753	242.870
5	284.364	262.063	243.495
6	293.284	267.273	244.976
7	303.062	273.353	247.341
8	313.729	280.257	250.560
9	325.252	288.122	254.654
10	337.640	296.767	259.632
11	350.897	306.331	265.465
12	365.004	316.747	272.170
13	380.023	328.020	279.762
14	395.871	340.188	288.167*
15	412.591	353.216	297.556
16	430.180	367.121	307.754
17	448.666	381.893	318.837
18	468.018	397.542	330.791
19	488.252	414.069	343.625
20	509.339*	431.482	357.344
21		449.764	371.919
22		468.900	387.427
23		489.034	

exposure time of bands ranged from 2.5 to 7 hours. For the wavelength calibration Fe and Kr standard lines from the hollow-cathode type lamp and ordinary Geissler lamp were employed. The measurements of the lines with an accuracy (1 μm) were performed using Abbé-type comparator. As a result of the deviations analysis of the calibration spectrum lines, the accuracy of band lines was estimated. The absolute accuracy is about 0.005—0.010 cm^{-1} and 0.003—0.005 cm^{-1} is the internal one. The lines marked by one or two asterisks for various reasons, small intensity, blending, etc. are respectively less accurate. Calculated values of the wave numbers of the lines for the 0—0, 0—1 up to the 0—6 band in the $^{13}C^{16}O$ molecule are listed in Tables I to VII. Wave numbers of lines for the 0—2 and 0—3 bands in the $^{12}C^{16}O$ molecule are given in Tables VIII and IX.

Table VII

0—6 band lines of $^{13}C^{16}O$ (in cm^{-1})

J	R	Q	P
2		18964.676*	
3		967.852	
4		971.879	18957.460**
5	18999.051	976.768	958.200**
6	19008.390	982.517	960.207
7	018.881	989.149	963.132
8	030.105	996.656	966.937
9	042.209	19005.057	971.683*
10	055.192*	014.319*	977.199
11	069.067	024.498	983.646
12	083.844	035.550	990.995
13	099.503	047.514	999.245
14	116.007	060.370	19008.390
15	133.541	074.141	018.468
16	151.863	088,805	029.440
17	171.277	104.459	041.427
18	191.270*	120.817	054.056
19	212.382**	138.218	067.777
20		156.522*	082.423
21			097.939

Results and discussion

The B_0 and D_0 rotational constants for the C state were determined from $R(J)$ and $P(J)$ branch lines, by means of $\Delta_2 F'(J)$ term differences. For this purpose, average values of these differences were determined from all the seven bands in the $^{13}C^{16}O$ molecule, and from both analysed bands in the $^{12}C^{16}O$ molecule. Using the least-squares method, by means of the equation:

$$\Delta_2 F'(J) = (4B_0 - 6D_0)(J + 1/2) - 8D_0(J + 1/2)^3, \tag{1}$$

the following constants were calculated:

$$B_{01}^C = (1.85847 \pm 0.00015)\ cm^{-1},$$
$$D_0^C = (5.67 \pm 0.19) \cdot 10^{-6}\ cm^{-1}$$

for the $^{13}C^{16}O$ molecule and

Table VIII

0—2 band lines of $^{12}C^{16}O$ (in cm^{-1})

J	R		Q		P	
1			24244.041		24239.958	
2	24257.236		245.593		237.768*	
3	263.400**		247.900		236.170*	
4	270.414		250.984		235.419	
5	278.154		254.859		235.419	
6	286.667		259.519		236.170*	
7	295.955		265.128		237.664	
8	306.011		270.912		239.958	
9	316.843		277.918		243.021	
10	328.435		285.657		246.860	
11	340.798		294.158		251.473	
12	353.936		303.430		256.863	
13	367.865		313.475		263.029	
14	382.537		324.287		269.973	
15	398.000		335.877		277.695	
16	414.234		438.231		286.194	
17	431.250		361.381		295.479	
18	449.033		375.306		305.546	
19	467.610		390.007		316.402	
20	486.973		405.496		328.045	
21	507.117		421.773		340.490	
22	528.079		438.840		353.755	
23	549.916		456.701		367.865	
24	572.897		475.386		383.080	
25		24598.350*	494.919		400.948	24389.451
26			515.369			414.234
27			537.002			430.266
28			561.294	24544.412		448.465
29						467.357

$$B_o^C = (1.94345 \pm 0.00007)\ cm^{-1},$$
$$D_o^C = (6.28 \pm 0.07) \cdot 10^{-6}\ cm^{-1}$$

for the $^{12}C^{16}O$ molecule. On the basis of these B_o^C constant values and the constant obtained in the $^{12}C^{18}O$ molecule [15], including also the B_0 and B_1 constants determined from the analysis of the Hopfield—Birge bands [22],

Table IX

0—3 band lines of $^{12}C^{16}O$ (in cm^{-1})

J	R	Q	P
1	228 39.020**	22831.317	22827.426*
2	844.605	832.951	825.177
3	850.957	835.410	823.744
4	858.117	838.686	823.139
5	866.092	842.782	823.343
6	874.886	847.714**	824.369
7	884.522	853.423	826.216
8	894.930	859.972	828.883
9	22906.175	867.338	832.367
10	918.234	875.520	836.676
11	931.120	884.522	841.802
12	944.817	894.352	847.714**
13	959.334	22904.994	854.513
14	974.667	916.453	862.109
15	990.820	928.731	870.519
16	23007.789	941.843	879.761
17	025.583	955.767	889.816
18	044.167	970.491	22900.678
19	063.623	986.086	912.410
20	083.831**	23002.484	924.948
21	23104.973	019.708	938.318
22	126.812	037.708	952.473
23	149.527	056.631	067.532
24	173.103	076.340	983.390
25	197.478*	096.884	23000.072
26	23222.646*	23118.223	017.562
27		140.589	035.985

a set of seven equations for the constants B_e and α_e in the C state was established.* Its solution after using the Dunham isotope relations [1] gives the following constant for the $^{12}C^{16}O$ molecule:

$$B_c^C = (1.95381 \pm 0.00036)\ cm^{-1},$$

$$\alpha_c^C = (0.02005 \pm 0.00039)\ cm^{-1}.$$

* Taking primarly the constants B_e, α_e and γ_e for the fitting of this set of data, the constant value γ_e was found in limits of its standard error; therefore further the constant γ_e was omitted.

Table X

Rotational constants of the $C^1\Sigma^+$ state for the $^{13}C^{16}O$ and $^{12}C^{16}O$ molecules (in cm^{-1})

Molecule	$^{13}C^{16}O$		$^{12}C^{16}O$		
Constant	Present results	After TILFORD and VANDERSLICE [22]	Present results	After SCHMID and GERŐ [18]	After TILFORD and VANDERSLICE [22]
B_0	1.85847 ± 0.00015	1.8590	1.94345 ± 0.00007	1.9422	1.9435
B_1	—	1.8389	—	—	1.9239
D_0	$(5.67 \pm 0.19) \cdot 10^{-6}$	$7.6 \cdot 10^{-6}$	$(6.28 \pm 0.07) \cdot 10^{-6}$	$5.7 \cdot 10^{-6}$	$6.3 \cdot 10^{-6}$
D_1	—	$6.1 \cdot 10^{-6}$	—	—	$6.1 \cdot 10^{-6}$
B_e	—	—	1.95381 ± 0.00036*	—	—
α_e	—	—	0.02005 ± 0.00039*	—	—

* — calculated with the assumption $\gamma_e = 0$.

Table XI

Rotational constants B_v of the $A^1\Pi$ state in $^{13}C^{16}O$ and $^{12}C^{16}O$ molecules (in cm^{-1})

Molecule	$^{13}C^{16}O$			$^{12}C^{16}O$			
Constant	Present results	After MCCULLOH and GLOCKLER [14]	After JANJIĆ et al. [6]	Present results	After SCHMID and GERŐ [19]	After SIMMONS et al. [20]	After KEPA and RYTEL [11]
B_0	—	—	—	—	1.6001	1.6001	—
B_1	1.5092 (4)	1.509	—	—	1.5775	1.5788	—
B_2	1.4895 (2)	1.489	—	1.5568 (3)	1.5561	1.5576	1.5582
B_3	1.4679 (6)	1.468	—	1.5340 (3)	1.5329	1.5346	1.5344
B_4	1.4463 (4)	1.446	1.4460 (6)	—	1.5089	1.5108	1.5116
B_5	1.4241 (4)	1.424	1.4238 (6)	—	1.4861	1.4877	1.4884
B_6	1.3988 (6)	—	—	—	1.4616	1.4630	—

The uncertainty given in parentheses corresponds to a standard deviation.

Present and earlier data for the values of the rotational constants are listed in Table X. Using the Kovács's functions $f_Q(J)$, $f_{PR}(J)$ and $f_{\overline{PR}}(J)$ [2], the differences of the rotational constants for both combining states were determined. The average values computed from all the band lines are respectively:

$$B_o^C = B_1^A = (0.3490 \pm 0.0006)\ \text{cm}^{-1},$$
$$B_o^C - B_2^A = (0.3687 \pm 0.0002)\ \text{cm}^{-1},$$
$$B_o^C - B_3^A = (0.3902 \pm 0.0004)\ \text{cm}^{-1},$$
$$B_o^C - B_4^A = (0.4120 \pm 0.0004)\ \text{cm}^{-1},$$
$$B_o^C - B_5^A = (0.4341 \pm 0.0004)\ \text{cm}^{-1},$$
$$B_o^C - B_6^A = (0.4593 \pm 0.0006)\ \text{cm}^{-1}$$

for the $^{13}C^{16}O$ molecule and

$$B_o^C - B_2^A = (0.3863 \pm 0.0002)\ \text{cm}^{-1},$$
$$B_o^C - B_3^A = (0.4094 \pm 0.0001)\ \text{cm}^{-1}$$

for the $^{12}C^{16}O$ molecule. From these values and the constants B_o^C determined previously the rotational constants of the $A^1\Pi$ state have been calculated. The results are listed in Table XI. For the calculation of band origins two methods were applied; the first one for the regular bands and the second for the bands with perturbation in initial rotational levels.

For the perturbed i.e. the 0—0, 0—1 and 0—6 bands the band origins have been determined by extrapolation of $Q(J)$ branch lines and by $R(J-1) + P(J)$ lines combinations [1]. In the remaining bands, the band origins have been found by means of $g_Q(J)$, $g_{PR}(J)$ and $g_{\overline{PR}}(J)$ functions [2]. The results obtained by use of both methods are listed in Table XII. Further, using the constants B_v listed in Table XI, it was possible to recalculate the σ_{ov}^{CA} band origins to the c_{ov}^{CA} values i.e. "reduced" band origins. These values simply contain the differences of the electronic and vibrational terms for both combining states. Using the c_{ov}^{CA} values determined in the $^{13}C^{16}O$ and $^{12}C^{16}O$ molecules as well as in $^{13}C^{18}O$ (on the basis of earlier data [15]), and including the vibrational quanta $\Delta G_{1/2}^C$ of the C state in the $^{13}C^{16}O$ and $^{12}C^{16}O$ molecules [22] one can obtain the following equations for the vibrational constants of the C state:

$$c_{ov}^{CA} + G^A(v) = \sigma_e^{CA} + \frac{1}{2}\omega_e^C - \frac{1}{4}\omega_e x_e^C,$$
$$\Delta G_{\frac{1}{2}}^C = \omega_e^C - 2\omega_e x_e^C$$

for the $^{12}C^{16}O$ molecule,

Table XII

Band origins of the $C^1\Sigma^+ - A^1\Pi$ system in $^{13}C^{16}O$ and $^{12}C^{16}O$ molecules (in cm^{-1})

Molecule	$^{13}C^{16}O$		$^{12}C^{16}O$		
Band	Present results	After [9]	Present results	After JOHNSON and ASUNDI [7]	After [9]
0—0	27168.0 ± 0.2				
0—1	25714.691 ± 0.016			25686.1	
0—2	24299.217 ± 0.018	24299.4	24243.264 ± 0.019	24243.2	24243.3
0—3	22915.679 ± 0.021	22915.8	22830.499 ± 0.016	22830.5	22830.6
0—4	21565.641 ± 0.028	21565.7			
0—5	20249.066 ± 0.025	20249.1			
0—6	18962.32 ± 0.03				

$$c_{ov(1)}^{CA} + G_{(1)}^{A}(v) = \sigma_{e(1)}^{CA} + \frac{1}{2}\varrho_1 \omega_e^C - \frac{1}{4}\varrho_1^2 \omega_e x_e^C ,$$

$$\Delta G_{\frac{1}{2}(1)}^{C} = \varrho_1 \omega_e^C - 2\varrho_1^2 \omega_e x_e^C$$

for the $^{13}C^{16}O$ molecule and

$$c_{ov(2)}^{CA} + G_{(2)}^{A}(v) = \sigma_{e(2)}^{CA} + \frac{1}{2}\varrho_2 \omega_e^C - \frac{1}{4}\varrho_2^2 \omega_e x_e^C$$

for the $^{13}C^{18}O$ molecule, where ϱ_1^2 and ϱ_2^2 are the ratios of the reduced masses of the $^{13}C^{16}O$ and $^{12}C^{18}O$ molecules, relative to the $^{12}C^{16}O$ molecule. The values of $G^A(v)$ vibrational terms in the $A^1\Pi$ state were found using Dunham isotopic relations and the following constants of this state:*

$$\omega_e^A = 1518.398 \text{ cm}^{-1},$$

$$\omega_e x_e^A = 17.678 \text{ cm}^{-1},$$

$$\omega_e y_e^A = 0.0146 \text{ cm}^{-1}.$$

For the $c_{ov}^{CA} + G^A(v)$ values on the left side of Eqs. (2) average values, determined from all regular bands have been used. In the solution of this set of equations, which permits avoiding the influence of the error of experimental data on the calculated constants (impossible in the direct method of solution), some simplifications can also be employed. Namely, the σ_e^{CA}, $\sigma_{e(1)}^{CA}$ and $\sigma_{e(2)}^{CA}$ system origin values on the right side of equations may differ only by differences of the electronic isotope effects of C and A states.

* The constants were determined from reduced band origins obtained from RYTEL data [11, 16, 17] and isotopic relations.

The fact that the $C^1\Sigma^+$ and $B^1\Sigma^+$ states are Rydberg states and belong to the same electronic configuration: $(1\sigma)^2(2\sigma)^2(3\sigma)^2(4\sigma)^2(1\pi)^4(5\sigma)(m\sigma)$, where $m = 7$ for the $B^1\Sigma^+$ states and $m = 9$ for the $C^1\Sigma^+$ [13, 21] was also taken into consideration. Therefore, it was assumed that the behaviour of both the B and C states is similar and they have the same electronic isotope effects. As the exact values of the differences of electronic isotope effects in $B^1\Sigma^+$ and $A^1\Pi$ states are known [16]**

$$\sigma_e^{BA}(^{12}C^{16}O) - \sigma_{e(1)}^{BA}(^{13}CO^{16}) = -0.590 \text{ cm}^{-1},$$

and

$$\sigma_e^{BA}(^{12}C^{16}O) - \sigma_{e(2)}^{BA}(^{12}C^{18}O) = -0.489 \text{ cm}^{-1},$$

the same values, as differences of the electronic isotope effects in $C^1\Sigma^+$ and $A^1\Pi$ states were used. Under such assumption the set of equations (2) was solved yielding the following constant values:

$$\omega_e^C = (2220.2 \pm 1.3) \text{ cm}^{-1},$$
$$\omega_e x_e^C = (37.09 \pm 0.84) \text{ cm}^{-1},$$
$$\sigma_e^{CA} = (26826.6 \pm 1.6) \text{ cm}^{-1}.$$

The confrontation of these results with the vibrational constants of other Rydberg states is presented in Table XIII. The fact that the constant values are quite similar proves the earlier hypothesis that the constants of all Rydberg states may be very similar [13], as well as the correctness of our assumptions.

Table XIII

Vibrational constants $\omega_e, i, \omega_e X_e$ of the known Rydberg states in the $^{12}C^{16}O$ molecule (in cm^{-1})

State \ Constant		ω_e	$\omega_e x_e$
$C^1\Sigma^+$	Present results	2220.2 ± 1.3 (2175.92)*	37.09 ± 0.84 (14.76)*
$B^1\Sigma^+$	After RYTEL [16]	2153.929	35.879
	After MCCULLOH and GLOCKLER [14]	2160.7 (2112.70)*	39.3 (15.22)*
$E^1\Pi$	After KĘPA et al. [10]	2246.85	46.53
$c^3\Pi$	After DANIELAK et al. [8]	2246	—
$j^3\Sigma^+$	After TILFORD and VANDERSLICE [22]	(2196)*	(15.0)*

( )* TILFORD and VANDERSLICE results [22].

** The values were recalculated using the reduced band origins and new vibrational constants of the $A^1\Pi$ state, presented earlier.

Acknowledgement

The author is greatly indebted to Dr. M. RYTEL for his inspiration to carry out this work, many discussions and constant help during all the time it was in progress.

REFERENCES

1. G. HERZBERG, Spectra of Diatomic Molecules, Van Nostrand, Princeton, 1950.
2. I. KOVÁCS, Rotational Structure in the Spectra of Diatomic Molecules, Akadémiai Kiadó, Budapest and Adam Hilger Ltd, London, 1969.
3. P. H. KRUPENIE, The Band Spectrum of Carbon Monoxide, Nat. Stand. Ref. Data. Ser., Nat. Bur. Stand. 5, 1966.
4. B. ROSEN, Selected Constants Spectroscopic Data Relative to Diatomic Molecules, Pergamon Press, Oxford, 1970.
5. R. K. ASUNDI, R. K. DHUMWAD and A. B. PATWARDHAN, J. Mol. Spectrosc., **34,** 528, 1970.
6. J. JANJIĆ, J. DANIELAK, R. KEPA and M. RYTEL, Acta Phys., Pol., A**41,** 757, 1972.
7. R. C. JOHNSON and R. K. ASUNDI, Proc. Roy. Soc. London, Ser. A: **123,** 560, 1929.
8. J. DANIELAK, M. RYTEL and T. SIWIEC, Acta Phys. Pol., A**47,** 561, 1975.
9. R. KĘPA, Acta Phys. Pol., **36,** 1109, 1969.
10. R. KĘPA, M. RYTEL and Z. RZESZUT, Acta Phys. Pol. A**54,** 355, 1978.
11. R. KĘPA and M. RYTEL, Acta Phys. Pol., A**37,** 585, 1970.
12. H. P. KNAUSS, Phys. Rev., **37,** 471, 1931.
13. H. LEFEBVRE-BRION, C. M. MOSER and R. K. NESBET, J. Mol. Spectrosc., **13,** 418, 1964.
14. K. E. MCCULLOH and, G. GLOCKLER, Phys. Rev., **89,** 145, 1953.
15. D. S. PESIĆ, J. D. JANJIC, R. KĘPA, M. RYTEL and Lj. U. ČONKIĆ, J. Mol. Spectrosc., **72,** 297, 1978.
16. M. RYTEL, Acta Phys. Pol., A**38,** 299, 1970.
17. M. RYTEL, Acta Phys. Pol., A**37,** 559, 1970.
18. R. SCHMID and L. GERŐ, Z. Physik, **93,** 656, 1935.
19. R. SCHMID and L. GERŐ, Z. Physik **101,** 343, 1936.
20. J. D. SIMMONS, A. M. BASS and S. G. TILFORD, Astrophys. J., **155,** 345, 1969.
21. J. D. SIMMONS and S. G. TILFORD, J. Chem. Phys., **45,** 2965, 1966.
22. S. G. TILFORD and J. T. VANDERSLICE, J. Mol. Spectrosc., **26,** 419, 1968.

Acta Physica Academiae Scientiarum Hungaricae, Tomus 45 (2), pp. 149—151 (1978)

COMMUNICATIO BREVIS

BOUND FOR THE HARMONIC OSCILLATOR GREENS FUNCTION

By

L. B. RÉDEI

DEPARTMENT OF THEORETICAL PHYSICS, UMEÅ UNIVERSITY, S-901 87 UMEÅ, SWEDEN

(Received 5. IX. 1978)

We derive a bound for the harmonic oscillator resolvent kernel $R(x, x', z)$ defined as

$$R(x, x'; z) = \sum_{n=0}^{\infty} \frac{u_n(x)\, u_n(x')}{n - z}, \quad z \neq 0, 1, 2, \ldots, \tag{1}$$

where $u_n(x)$ are standard harmonic oscillator eigenfunctions.

Case I. $\operatorname{Re} z < 0$

This is simple. We use the well-known integral representation [1]

$$R(x, x'; z) = \pi^{-1/2} \int_0^1 d\tau\, \tau^{-(z+1)} (1 - \tau^2)^{-1/2}\, L(x, x', \tau), \tag{2}$$

$$\operatorname{Re} z < 0,$$

where

$$L(x, x'; \tau) = \exp\left(-\frac{1}{2}\,\frac{1 + \tau^2}{1 - \tau^2}\,(x^2 + x'^2) + \frac{2\tau}{1 - \tau^2}\, xx'\right). \tag{3}$$

Since $|L(x, x;, \tau)| \leq 1$ for $\operatorname{Im} \tau = 0$, $0 \leq \tau \leq 1$, x and x' real one has that

$$|R(x, x'; z)| \leq \pi^{-1/2} \int_0^1 d\tau\, \tau^{-(\operatorname{Re} z+1)} (1 - \tau^2)^{-1/2}, \tag{4}$$

giving the bound

$$|R(x, x; z)| \leq \frac{1}{2}\pi^{-1/2}\, B\left(-\frac{1}{2}\operatorname{Re} z, 1/2\right), \quad \operatorname{Re} z < 0,$$

where

$$B(\alpha, \beta) = \frac{\Gamma(\alpha)\, \Gamma(\beta)}{\Gamma(\alpha + \beta)}$$

is the Riemann beta function.

Case II. $\operatorname{Re} z \geq 0,\ z \neq 0, 1, 2, \ldots$

First of all we need an integral representation of $R(x, x'; z)$ which is valid even if $\operatorname{Re} z \geq 0$. This can be obtained by distorting the path of integration in the right-hand side of Eq. (2). In fact one has that

$$R(x, x'; z) = \frac{1}{2} \frac{\pi^{-1/2}}{\sinh(i\pi z)} \int_C d\tau (-\tau)^{-(z+1)} (1 - \tau^2)^{-1/2} L(x, x'; \tau),$$
$$z \neq 0, 1, 2, \ldots, \quad |\arg(-\tau)| \leq \pi,$$

where the integration path C in the complex τ-plane can be taken to consist of a line from $\tau = 1$ to $\tau = \varrho$ ($\operatorname{Im} \varrho = 0,\ 0 < \varrho < 1$) just above the cut drawn between 0 and 1, an anti-clockwise circle of radius ϱ around the origin and finally to close to contour a straight line just below the cut from $\tau = 1$ to $\tau = \varrho$.

This representation is useful only for obtaining a bound if ϱ is such that $L(x, x'; \tau)$ is uniformly bounded in all its variables as long as $\tau \in C$. A straightforward computation shows that in fact

$$|L(x, x'; \tau)| \leq 1,$$

if

$$0 < \varrho < \sqrt{2} - 1$$

for all $\tau \in C$ and x, x' real. From this it follows that

$$|R(x, x'; \tau)| \leq \pi^{-1/2} (1 - \varrho^2)^{-1/2} \varrho^{-\operatorname{Re} z}$$
$$\left(\pi \frac{e^{\pi |\operatorname{Im} z|}}{|\sinh(i\pi z)|} + 2(\varrho^{-2} - 1) \right)$$

for $\operatorname{Re} z \geq 0$ and any $0 < \varrho \leq \sqrt{2} - 1$. Taking $\varrho = \sqrt{2} - 1$ we obtain our final result that

$$|R(x, x'; z)| \leq \left(2(\sqrt{2} - 1)\right)^{-1/2} \pi^{-1/2} e^{-\ln(\sqrt{2}-1) \operatorname{Re} z}$$
$$\left(\pi \frac{e^{\pi |\operatorname{Im} z|}}{|\sinh i\pi z|} + 4 \frac{\sqrt{2} - 1}{3 - 2\sqrt{2}} \right)$$

valid for $\operatorname{Re} z \geq 0,\ z \neq 0, 1, 2, \ldots$

Remark

We have derived a bound for the harmonic oscillator Greens function. Such a bound can be used for estimating the rate of convergence of the Fredholm solution for a perturbed harmonic oscillator resolvent kernel. (The Fredholm solution converges provided that the perturbating potential is absolutely integrable.) In fact a simple application of Hadamard's theorem [2] for determinants gives the following estimate for the nth order term I_n in the series expansion of the Fredholm denominator

$$| I_n | \leq g^n \frac{n^{1/2\,n}}{n!} A^n \left(\int_{-\infty}^{\infty} dx \, | V(x) | \right)^n ,$$

where g is the coupling constant, V is the perturbing potential and A is a bound for the unperturbed harmonic oscillator Greens function.

REFERENCES

1. See e.g. R. P. FEYNMAN and A. R. HIBBS, Quantum Mechanics and Path Integrals, McGraw-Hill. Co., New York, 1965 or Bateman Manuscript Project, McGraw-Hill Co., New York, 1953.
2. See e.g. F. G. TRICOMI, Integral Equations, Interscience Publishers Inc. New York, 1965.

Printed in Hungary

A kiadásért felel az Akadémiai Kiadó igazgatója. Műszaki szerkesztő: Botyánszky Pál
A kézirat a kiadóba érkezett: 1978. IX. 13. — A kézirat nyomdába érkezett: 1978. IX. 18. — Terjedelem: 5,75 (A/5) ív, 19 ábra

79.6328 Akadémiai Nyomda, Budapest — Felelős vezető: Bernát György

NOTES TO CONTRIBUTORS

I. PAPERS will be considered for publication in Acta Physica Hungarica, only if they have not previously been published or submitted for publication elsewhere. They may be written in English, French, German or Russian.

Papers should be submitted to

Prof. I. Kovács, Editor
Department of Atomic Physics, Technical University
1521 Budapest, Budafoki út 8, Hungary

Papers may be either articles with abstracts or short communications. Both should be as concise as possible, articles in general not exceeding 25 typed pages, short communications 8 typed pages.

II. MANUSCRIPTS

1. Papers should be submitted in five copies.

2. The text of papers must be of high stylistic standard, requiring minor corrections only.

3. Manuscripts should be typed in double spacing on good quality paper, with generous margins.

4. The name of the author(s) and of the institutes where the work was carried out should appear on the first page of the manuscript.

5. Particular care should be taken with mathematical expressions. The following should be clearly distinguished, e.g. by underlining in different colours: special founts (italics, script, bold type, Greek, Gothic, etc.); capital and small letters; subscripts and superscripts, e.g. x^2, x_3; small l and 1; zero and capital O; in expressions written by hand: e and l, n and u, v and v, etc.

6. References should be numbered serially and listed at the end of the paper in the following form: J. Ise and W. D. Fretter, Phys. Rev., *76*, 933, 1949.

For books, please give the initials and family name of the author(s), title, name of publisher, place and year of publication, e.g.: J. C. Slater, Quantum Theory of Atomic Structures, I. McGraw-Hill Book Company, Inc., New York, 1960.

References should be given in the text in the following forms: Heisenberg [5] or [5].

7. Captions to illustrations should be listed on a separate sheet, not inserted in the text.

III. ILLUSTRATIONS AND TABLES

1. Each paper should be accompanied by five sets of illustrations, one of which must be ready for the blockmaker. The other sets attached to the copies of the manuscript may be rough drawings in pencil or photocopies.

2. Illustrations must not be inserted in the text.

3. All illustrations should be identified in blue pencil by the author's name, abbreviated title of the paper and figure number.

4. Tables should be typed on separate pages and have captions describing their content. Clear wording of column heads is advisable. Tables should be numbered in Roman numerals. (I, II, III, etc.).

IV. MANUSCRIPTS not in conformity with the above Notes will immediately be returned to authors for revision. The date of receipt to be shown on the paper will in such cases be that of the receipt of the revised manuscript.

Reviews of the Hungarian Academy of Sciences are obtainable at the following addresses:

AUSTRALIA
C.B.D. LIBRARY AND SUBSCRIPTION SERVICE, Box 4886, G.P.O., *Sydney N.S.W. 2001*
COSMOS BOOKSHOP, 145 Acland Street, *St. Kilda (Melbourne), Victoria 3182*

AUSTRIA
GLOBUS, Höchstädtplatz 3, *1200 Wien XX*

BELGIUM
OFFICE INTERNATIONAL DE LIBRAIRIE, 30 Avenue Marnix, *1050 Bruxelles*
LIBRAIRIE DU MONDE ENTIER, 162 Rue du Midi, *1000 Bruxelles*

BULGARIA
HEMUS, Bulvar Ruszki 6, *Sofia*

CANADA
PANNONIA BOOKS, P.O. Box 1017, Postal Station "B", *Toronto, Ontario M5T 2T8*

CHINA
CNPICOR, Periodical Department, P.O. Box 50, *Peking*

CZECHOSLOVAKIA
MAD'ARSKÁ KULTURA, Národní třida 22, *115 66 Praha*
PNS DOVOZ TISKU, Vinohradská 46, *Praha 2*
PNS DOVOZ TLAČE, *Bratislava 2*

DENMARK
EJNAR MUNKSGAARD, Norregade 6, *1165 Copenhagen*

FINLAND
AKATEEMINEN KIRJAKAUPPA, P.O. Box 128, *SF-00101 Helsinki 10*

FRANCE
EUROPERIODIQUES S. A., 31 Avenue de Versailles, *78170 La Celle St.-Cloud*
LIBRAIRIE LAVOISIER, 11 rue Lavoisier, *75008 Paris*
OFFICE INTERNATIONAL DE DOCUMENTATION ET LIBRAIRIE, 48 rue Gay-Lussac, *75240 Paris Cedex 05*

GERMAN DEMOCRATIC REPUBLIC
HAUS DER UNGARISCHEN KULTUR, Karl-Liebknecht-Strasse 9, *DDR-102 Berlin*
DEUTSCHE POST ZEITUNGSVERTRIEBSAMT, Strasse der Pariser Kommüne 3—4, *DDR-104 Berlin*

GERMAN FEDERAL REPUBLIC
KUNST UND WISSEN ERICH BIEBER, Postfach 46, *7000 Stuttgart 1*

GREAT BRITAIN
BLACKWELL'S PERIODICALS DIVISION, Hythe Bridge Street, *Oxford OX1 2ET*
BUMPUS, HALDANE AND MAXWELL LTD., Cowper Works, *Olney*, Bucks *MK46 4BN*
COLLET'S HOLDINGS LTD., Denington Estate, *Wellingborough*, Northants *NN8 2QT*
W.M. DAWSON AND SONS LTD., Cannon House *Folkestone, Kent CT19 5EE*
H. K. LEWIS AND CO., 136 Gower Street, *London WC1E 6BS*

GREECE
KOSTARAKIS BROTHERS, International Booksellers, 2 Hippokratous Street, *Athens-143*

HOLLAND
MEULENHOFF-BRUNA B.V., Beulingstraat 2, *Amsterdam*
MARTINUS NIJHOFF B.V., Lange Voorhout 9—11, *Den Haag*
SWETS SUBSCRIPTION SERVICE, 347b Heereweg, *Lisse*

INDIA
ALLIED PUBLISHING PRIVATE LTD., 13/14 Asaf Ali Road, *New Delhi 110001*
150 B-6 Mount Road, *Madras 600002*
INTERNATIONAL BOOK HOUSE PVT. LTD., Madame Cama Road, *Bombay 400039*
THE STATE TRADING CORPORATION OF INDIA LTS, Books Import Division, Chandralok, 36 Janpath, *New Delhi 110001*

ITALY
EUGENIO CARLUCCI, P.O. Box 252, *70100 Bari*
INTERSCIENTIA, Via Mazzé 28, *10149 Torino*
LIBRERIA COMMISSIONARIA SANSONI, Via Lamarmora 45, *50121 Firenze*
SANTO VANASIA, Via M. Macchi 58, *20124 Milano*
D. E. A., Via Lima 28, *00198 Roma*

JAPAN
KINOKUNIYA BOOK-STORE CO. LTD., 17-7 Shinjuku-ku 3 chome, Shinjuku-ku, *Tokyo 160-91*
MARUZEN COMPANY LTD., Book Department, P.O. Box 5050 Tokyo International, *Tokyo 100-31*
NAUKA LTD. IMPORT DEPARTMENT, 2-30-19 Minami Ikebukuro, Toshima-ku, *Tokyo 171*

KOREA
CHULPANMUL, *Phenjan*

NORWAY
TANUM-CAMMERMEYER, Karl Johansgatan 41—43, *1000 Oslo*

POLAND
WĘGIERSKI INSTYTUT KULTURY, Marszałkowska 80, *Warszawa*
CKP I W ul. Towarowa 28 *00-958 Warsaw*

ROUMANIA
D. E. P., *Bucureşti*
ROMLIBRI, Str. Biserica Amzei 7, *Bucureşti*

SOVIET UNION
SOJUZPETCHATJ — IMPORT, *Moscow*
and the post offices in each town
MEZHDUNARODNAYA KNIGA, *Moscow G-200*

SPAIN
DIAZ DE SANTOS, Lagasca 95, *Madrid 6*

SWEDEN
ALMQVIST AND WIKSELL, Gamla Brogatan 26, *101 20 Stockholm*
GUMPERTS UNIVERSITETSBOKHANDEL AB, Box 346, *401 25 Göteborg 1*

SWITZERLAND
KARGER LIBRI AG, Petersgraben 31, *4011 Basel*

USA
EBSCO SUBSCRIPTION SERVICES, P.O. Box 1943, *Birmingham, Alabama 35201*
F. W. FAXON COMPANY, INC., 15 Southwest Park, *Westwood, Mass. 02090*
THE MOORE-COTTRELL SUBSCRIPTION AGENCIES, *North Cohocton, N. Y. 14868*
READ-MORE PUBLICATIONS, INC., 140 Cedar Street, *New York, N. Y. 10006*
STECHERT-MACMILLAN, INC., 7250 Westfield Avenue, *Pennsauken* N. J. 08110

VIETNAM
YXUNHASABA, 32, Hai Ba Trung, *Hanoi*

YUGOSLAVIA
JUGOSLAVENSKA KNJIGA, Terazije 27, *Beograd*
FORUM, Vojvode Mišiča 1, *21000 Novi Sad*

Index: 26.025
Acta Phys. Hung. Tom. 45. No. 2. Budapest, 10. IV. 1979 HU-ISSN 0001-6705

ACTA PHYSICA

ACADEMIAE SCIENTIARUM HUNGARICAE

REDIGIT
I. KOVÁCS

TOMUS XLV FASCICULUS 3

AKADÉMIAI KIADÓ, BUDAPEST
1978

ACTA PHYS. HUNG. APAHAQ 45 (3) 153—282 1978

ACTA PHYSICA

ACADEMIAE SCIENTIARUM HUNGARICAE

SZERKESZTI

KOVÁCS ISTVÁN

Az *Acta Physica* angol, német, francia vagy orosz nyelven közöl értekezéseket. Évente két kötetben, kötetenként 4—4 füzetben jelenik meg. Kéziratok a szerkesztőség címére (1521 Budapest XI., Budafoki út 8.) küldendők.

Megrendelhető a belföld számára az Akadémiai Kiadónál (1363 Budapest Pf. 24. Bankszámla 215-11488), a külföld számára pedig a „Kultura" Külkereskedelmi Vállalatnál (1389 Budapest 62, P.O.B. 149. Bankszámla 217-10990), vagy annak külföldi képviseleteinél.

The *Acta Physica* publish papers on physics in English, German, French or Russian, in issues making up two volumes per year. Subscription: $ 36.00 per volume. Distributor: "Kultura" Foreign Trading Company (1389 Budapest 62, P.O. Box 149) or its representatives abroad.

Die *Acta Physica* veröffentlichen Abhandlungen aus dem Bereich der Physik in deutscher, englischer, französischer oder russischer Sprache, in Heften, die jährlich zwei Bände bilden.

Abonnementspreis pro Band: $ 36.00. Bestellbar bei »Kultura« Außenhandelsunternehmen (1389 Budapest 62, Postfach 149) oder seinen Auslandsvertretungen.

Les *Acta Physica* publient des travaux du domaine de la physique en français, anglais, allemand ou russe, en fascicules qui forment deux volumes par an.

Prix de l'abonnement: $ 36.00 par volume. On peut s'abonner à l'Entreprise du Commerce Extérieur «Kultura» (1389 Budapest 62, P.O.B. 149) ou chez représentants à l'étranger.

«*Acta Physica*» публикуют трактаты из области физических наук на русском, немецком, английском и французском языках.

«*Acta Physica*» выходят отдельными выпусками, составляющими два тома в год.

Подписная цена — $ 36.00 за том. Заказы принимает предприятие по внешней торговле «Kultura» (1389 Budapest 62, P.O.B. 149) или его заграничные представительства.

ACTA PHYSICA

ACADEMIAE SCIENTIARUM HUNGARICAE

TOMUS XLV FASCICULUS 3

AKADÉMIAI KIADÓ, BUDAPEST
1978

ACTA PHYS. HUNG.

INDEX

Acta Physica Academiae Scientiarum Hungaricae, Tomus 45 (3), pp. 153—161 (1978)

EFFECT OF Bi ON THE ANNEALING KINETICS OF AMORPHOUS As_2Se_3

By

M. K. EL-MOUSLY, M. F. KOTKATA and S. A. MAZEN

PHYSICS DEPARTMENT, FACULTY OF SCIENCE, AIN-SHAMS UNIVERSITY, CAIRO, EGYPT

(Received 29. VI. 1978)

The characteristic properties of As_2Se_3: density d, activation energy for conduction E_σ and dc conductivity σ with the addition of 1.96—2.72 at % Bi has been determined for the amorphous state and for the crystalline state. The effect of Bi impurity on the thermally induced phase transformation of As_2Se_3 has been followed by measuring these quantities for all intermediate stages during the annealing at three isotherms higher than T_g. The calculated energy of activation for crystallization declears the addition effect of Bi in stimulating the devitrification of the native phase As_2Se_3.

Introduction

An important group of amorphous semiconductors can be prepared in massive form by quenching the liquid. The As_2Se_3 composition, which is characterised by a very stable glass structure, is a typical representative of this group. Amorphous As_2Se_3 are widely used in electrophotographic processes because of their high photosensitivity, thermostability and time-stability of properties.

The transport measurements on amorphous As_2Se_3 have been studied by many authors [1—5]. FINKMAN [6] has studied the influence of temperature, laser beam intensity and sample history on the rate of crystallisation of As_2Se_3. Microscopic observations on surface crystallisation of As_2Se_3 films induced by organic substances have been recently investigated by SHELKOV [7]. LEZAL [8] has carried out theoretical studies of impurities in amorphous As_2Se_3 and their experimental verifications. According to SHKOLNIKOV [9], glass formation of $AsSe_{1.5}Bi_x$ may be obtained up to 3.7 at % Bi ($x \leq 0.1$).

In this paper, the effect of addition of bismuth on the crystallization of amorphous arsenic-selenide conducted at different isothermal annealing, between T_g and T_c, has been investigated by means of density and dc conductivity measurements. The experimental data have been used to determine the kinetic parameters and activation energy of the crystallization process.

Experimental

Two $AsSe_{1.5}Bi_x$ amorphous samples ($x = 0.05$ and 0.07) were prepared by reacting and homogenizing the appropriate amounts of the elements, whose purities were 4—9's or better, under vacuum in precleaned quartz ampoules at 950 $\pm$ 20 °C for 16 h and subsequently quenched in air at room temperature. The resulting samples were cut in the form of discs having two parallel faces about 1.2 cm in diameter and 3—5 mm thick, within 0.003 mm error. The dc conductivity was measured accurately under isothermal conditions. The accuracy of density was $\pm 0.1\%$.

For studying the amorphous—crystal transformation each sample was subjected to isothermal annealing in a preheated oven adjusted to the required temperature. The process of annealing was conducted step by step. This implies that after each step the sample was removed from the oven, rapidly quenched in air, and the characteristic properties d and $\sigma(T)$ were then measured. The electric conductivity σ was measured in the temperature range below T_g ($\sim$ 170 °C) to preserve quenching of the transformation process at each step of annealing.

Diffraction model for amorphous $AsSe_{1.5}$ Bi_x

The amorphous state is a structural concept and generally loosely defined by its lack of long-range order. The scale of what is long-range is determined by the practical resolution limit of X-ray or electron diffraction. Diffraction patterns with broad halos rather than sharp lines or spots can imply no long-range order beyond about 20 Å. The X-ray work carried out by VAIPOLIN [10] and RENNINGER [11] on bulk As—Se glasses showed that the local order in the As_2Se_3 composition was similar to that in the crystalline form.

In this respect, the amorphous character of the Bi-doped and free As_2Se_3 samples was achieved by X-ray diffraction using a modern Philips diffractometer. In Fig. 1 traces (b, c & d) are typical X-ray diffraction patterns taken for powdered samples, as initially prepared by quenching the melt, using copper K_α radiation. Within the amorphous phase there is no continuous narrowing of the halos, with addition of bismuth to 2.72% that would be indicative of a gradual increase in long-range order. So, the patterns are characterized by what is called the "stepped-hump", which differs greatly from the ideal amorphous hump pattern known for a proper glass. Similar patterns were observed for glassy As_2Se_3—As_2S_3 [12], $(As_2Se_3)_{1-x}(Tl_2Se_3)_x$ [13], and for As_2Se_3—As_2Te_3 components [14].

The introduction of bismuth into the arsenic-selenide system and the replacement of some As ($4S^24P^3$) by Bi($6S^26P^3$) caused no considerable change in the structure of the As_2Se_3 amorphous matrix. However, it gives greater

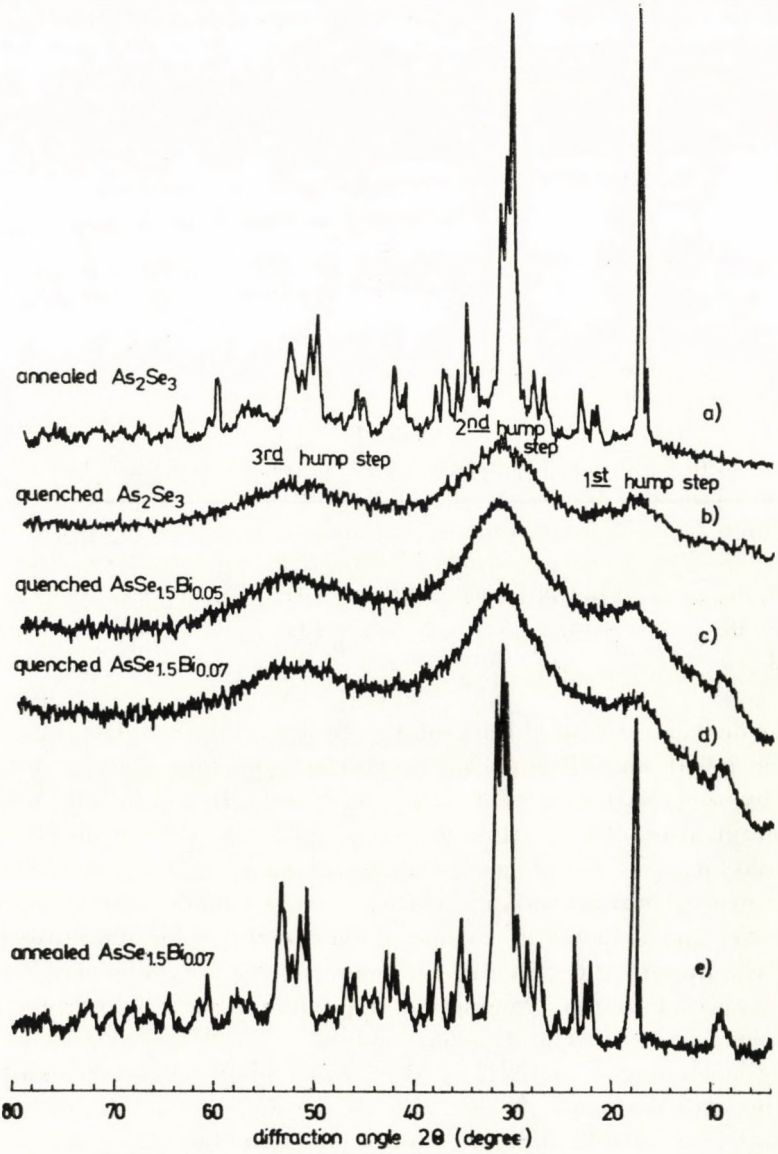

Fig. 1. X-ray diffraction patterns of amorphous and polycrystalline As_2Se_3 and $AsSe_{1.5}Bi_x$ samples

structural stability of Bi—Se in comparison with As—Se where the values of energy of the single chemical bond are, respectively, 67 and 23 kcal/mole [15]. In Fig. 1 the second step is the biggest and has the highest intensity maxima in the three traces (b, c & d). The relative areas under the observed steps roughly occupy the angular ranges: (12—21), (21—44) and (44—60)

degrees (2θ) for the first, second and third step, respectively. These angular ranges correspond to numerous lattice directions or atomic planes of high scattering power in the respective crystalline forms, see traces (a & e) in Fig. 1.

Properties of amorphous samples $AsSe_{1.5}\,Bi_x$

The initial values of the characteristic properties, the logarithm of specific conductivity at 20 °C $\log \sigma_{20\,°C}$ (σ in $\text{ohm}^{-1}\,\text{cm}^{-1}$), activation energy of the conduction process E_σ (eV), and density d (g/c.c.) were nearly the same for four discs of the same sample indicating the homogeneity of samples. Table I gives the mean numerical values of these properties with those of As_2Se_3 [5].

Table I

Mean values of the characteristic properties for the amorphous As_2Se_3 and $AsSe_{1.5}Bi_x$ samples

Sample	d(g/c.c.)	$-\log \sigma_{20}$	$\log \sigma_0$	E_σ (eV)
$AsSe_{1.5}Bi_{0.05}$	4.78 ± 0.00	11.60 ± 0.00	4.20 ± 0.6	1.86 ± 0.01
$AsSe_{1.5}Bi_{0.07}$	4.82 ± 0.01	10.66 ± 0.05	5.48 ± 0.9	1.88 ± 0.02
As_2Se_3	4.49	13.70	2.20	1.87

The dc electric conductivity of the Bi-doped As_2Se_3 glasses is exponentially dependent on $1/T$ and can be satisfactorily described between 16 °C and T_g by the relation: $\sigma = \sigma_0 \exp(-E_\sigma/2\,KT)$. However, the addition of such concentration of bismuth (1.96—2.72%) increases the room-temperature conductivity $\sigma_{20\,°C}$ of the prototype As_2Se_3 by more than might be expected from the nearly constant activation energy for the conduction process (Table I). The preexponential factor σ_0 changes from about 10^2 for As_2Se_3 to 10^5—10^6 $\text{ohm}^{-1}\text{cm}^{-1}$ due to the presence of Bi. The relative lower value of σ_0 for As_2Se_3 is mainly related to that conduction is predominantely by carriers hopping between localized states at the band edge.

The constancy of both E_σ ($\sim$1.87 eV) and σ_0 (10^5—10^6 $\text{ohm}^{-1}\,\text{cm}^{-1}$) for the present Bi-doped glasses leads to the conclusion that the variation of the electric conductivity with composition is due to the variation of mobility rather than carrier density. UPHOFF et al [16] reported that the equations of the carrier concentration and mobility which hold for crystalline semiconductors can also be applied to vitreous ones. This can account for an estimation of the carrier mobility in terms of the thermal activation energy E_σ to be of the order of 10^{-4}—10^{-3} $\text{cm}^2/\text{V}\cdot\text{sec}$ with an increase with Bi. However, it is probable that Bi replaces As isomorphously leading to no significant short-range structural changes. That is, the current model of the density of states and the mobility in an amorphous semiconductor is preserved.

Annealing kinetics of amorphous $AsSe_{1.5}Bi_x$

Isothermal crystallization has been carried out for both $AsSe_{1.5}Bi_{0.05}$ and $AsSe_{1.5}Bi_{0.07}$ at three different temperatures higher than T_g, namely 225, 240 and 260 °C. The changes in the characteristic quantities: d, $\log \sigma_{20°C}$ and E_σ with the annealing time for $AsSe_{1.5}Bi_{0.05}$ conducted at 240 °C are given in Fig. 2. All these properties change from values corresponding to the amorphous state to some limiting values corresponding to the complete crystallized samples. In Fig. 2, it is clear that the quantities $\log \sigma_{20°}$ and E_σ need nearly the same value of total crystallization time. In spite of this the density d reaches its limit value in a much shorter time than that necessary for complete crystallization indicating that it is more sensitive to the beginning of the process.

A behaviour similar to that shown in Fig. 2 has been observed for the other two annealing temperatures, but with different durations depending on the crystallization temperature. Increasing the temperature from 225 to 260 °C decreased the time required for crystallization of $AsSe_{1.5}Bi_{0.05}$ from 95 h to 16 h. Also, the increase of Bi-content in As_2Se_3 from 1.96 to 2.72% corresponds to a decrease in the crystallization time of about 35%.

The observed values characterizing each property at the end of the amorphous — crystalline transformation process were, to a good approximation, temperature-independent over the considered temperature range of annealing, 225—260 °C. Table II gives the mean values for the characteristic properties at the end of the annealing process.

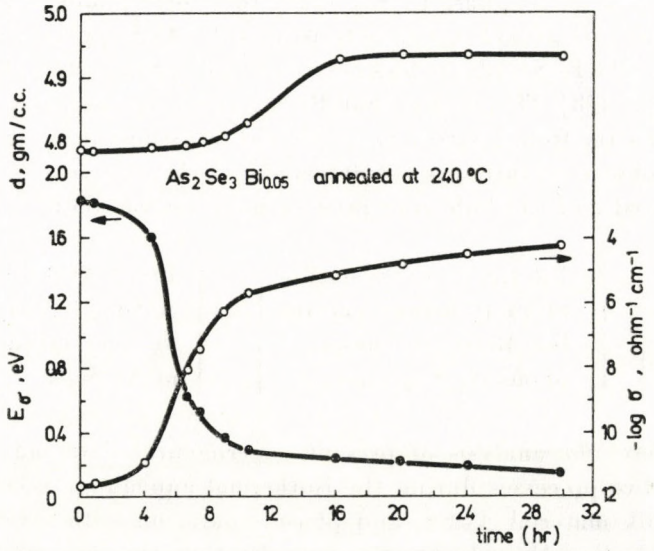

Fig. 2. The annealing time dependence of d, E_σ and $\log \sigma_{20°C}$ for $As_2Se_3Bi_{0.05}$ samples aged at 240 °C

Table II

Mean values of the characteristic properties at the end of the transformation process

Sample	d(g/c.c.)	E_σ (eV)	$-\log \sigma_{20}$
$AsSe_{1.5}Bi_{0.05}$	4.93 ± 0.02	0.12 ± 0.03	4.64 ± 0.3
$AsSe_{1.5}Bi_{0.07}$	5.07 ± 0.02	0.17 ± 0.05	2.10 ± 0.2

MYULLER [17] has indicated that the process of crystallization may separate into two successive processes: diffusion redistribution of structural units and local transformation of chemical bonds. However, the two processes have an overlapping, just as there is evidently an overlapping between the process of appearance of centres of crystallization and their growth. All these processes are limited to a definite degree by the same activation energy of the transformation of covalent bonds. Accordingly, the observed changes of the present characteristic quantities can be explained by the process of structural ordering occurring during the thermal treatment and, as a consequence, the crystallization of the sample. This, however, may include phase separation and/or crystallization. X-ray examination of the materials after finishing the annealing process indicates the presence of two crystalline phases: As_2Se_3 and Bi_2Se_3, note traces (a & e) in Fig. 1.

SHKOLNIKOV [9] has observed from the analysis of the thermogram of $AsSe_{1.5}Bi_{0.05}$ the presence of a weak exothermic peak at 245 °C related to crystallization of a first phase Bi_2Se_3 beside that corresponds to the maximum crystallization rate at 330 °C characteristic of the As_2Se_3 phase. However, the appearance of the Bi_2Se_3 phase does not represent any more than 8% by weight in the material [18]. This means that Bi_2Se_3 acts as an impurity in a massive crystalline matrix from As_2Se_3. So, a simple transition from the amorphous to the crystalline structure was not detected, but the existence of intermediate stages occurred and the following process could be written:

$$\left\{\begin{array}{l}\text{Amorphous}\\ \text{single phase}\rightarrow\\ (AsSe_{1.5}Bi_x)\end{array}\right\} \left\{\begin{array}{l}\text{Intermediate crystalline}\\ \text{phase (partially crystal-}\\ \text{line } Bi_2Se_3 \text{ in amor-}\\ \text{phous } As_2Se_3 \text{ matrix)}\end{array}\right\} \rightarrow \left\{\begin{array}{l}\text{Final crystalline}\\ AsSe_{1.5}Bi_x\ (Bi_2Se_3 \text{ crystal}\\ \text{in a crystalline matrix}\\ \text{of } As_2Se_3).\end{array}\right\}$$

Therefore, the analysis of present experimental data may include the presence of two processes during the isothermal annealing: crystallization of the main bulk material As_2Se_3 and phase separation with crystallization of minor phase Bi_2Se_3. According to this consideration, the changes in the density that accompany the changes in specific volume during the isothermal annealing

process depend essentially on the crystallization of the native component As_2Se_3. Alternatively, the changes of electric conductivity as well as the activation energy of conduction are controlled to a large extent by the existence of the impurities Bi_2Se_3. This idea could be checked in the present article by studying the annealing kinetics using the changes in density following the crystallisation process.

To determine the kinetics order, or the activation energy of crystallization at isothermal annealing, we apply the AVRAMI equation [19] which gives the volume fraction α of the transformed material at any time t

$$\alpha = 1 - \exp(-kt^n).$$

The fraction α can be calculated on the basis of changes in the density d during the crystallization process using the relation [20]

$$1 - \alpha = \frac{d(t) - d(\text{crystal})}{d(\text{amorphous}) - d(\text{crystal})} .$$

A plot of the volume transformed versus annealing time gives the experimental curves of crystallisation kinetics. This is shown for $AsSe_{1.5}Bi_{0.07}$ in Fig. 3. From this we can construct the curves of:

$$\log\log[1/(1-\alpha)] = n\log(t) + \log(k) - \log 2.3 .$$

The resulting values for the kinetic constants n and k which we obtain over the temperature range 225—260 °C are listed in Table III.

The activation energy of crystallisation for As_2Se_3 has been reported by CHKOLNIKOV [21] to be 34 kcal/mole as deduced from the slope of a plot of $\log(\tau_f)$ versus $1/T$, where f is a fraction of the total time of complete crystal-

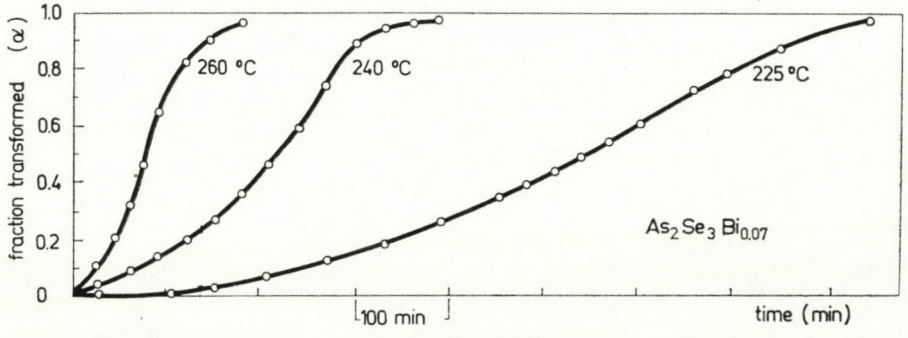

Fig. 3. The volume transformed vs time for both Bi-doped As_2Se_3 samples annealed at 225, 240 and 260 °C

Table III

The experimentally determined parameters n and k from a fit to the AVRAMI's kinetic equation

Temperature °C	$AsSe_{1.5}Bi_{0.05}$		$AsSe_{1.5}Bi_{0.07}$	
	n	$\bar{K}$	n	$\bar{K}$
225	3.4	$7.6 \times 10^{-19} \pm 0.3$	3.0	$2.0 \times 10^{-14} \pm 0.8$
240	3.3	$3.7 \times 10^{-16} \pm 0.4$	2.9	$1.3 \times 10^{-12} \pm 0.5$
260	2.8	$2.1 \times 10^{-13} \pm 0.1$	2.7	$3.4 \times 10^{-11} \pm 0.4$

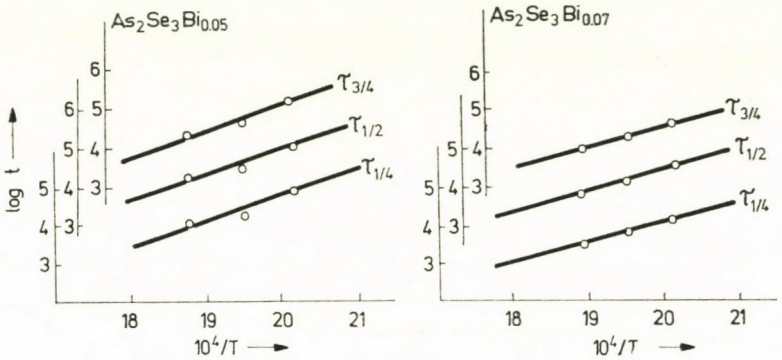

Fig. 4. The function log log $[1/(1-\alpha)]$ vs log (t) for both Bi-doped As_2Se_3 samples

lisation τ. Fig. 4 shows such relation for our Bi-doped As_2Se_3 samples at three different fractions, namely $\tau_{1/4}$, $\tau_{1/2}$ and $\tau_{3/4}$. The results of the activation energy of crystallization for $AsSe_{1\cdot5}Bi_{0\cdot05}$ and $AsSe_{1.5}Bi_{0.07}$, respectively are 32.0 and 23.7 kcal/mole which declears the effect of addition of Bi in stimulating the devitrification of the native phase As_2Se_3.

REFERENCES

1. B. T. KOLOMIETS, Phys. Stat. Solidi, **7,** 359 and 713, 1964.
2. J. T. EDMOND, J.-Non-Cryst. Solids, **1,** 39, 1968.
3. B. T. KOLOMIETS and E. M. RASPOPOVA, J. Non-cryst. Solids, **11,** 350, 1973.
4. F. D. FISHER, J. M. MARSHALL and A. E. OWEN, Phil. Mag., **33,** 261, 1976.
5. M. K. EL-MOUSLY and M. F. KOTKATA, Indian J. of Technology, **15,** 296, 1977.
6. E. FINKMAN, A. P. DEFONZO and J. TAUC, Proc. of 12th Int. Conf. on Physics of S.C., 1022—1026, Stuttgart, 1974.
7. A. F. SHELKOV, S. A. TAURAJITENE and G. Z. VINOGRADOVA, Proc. of Int. Conf. on Amorphous S.C., Balatonfüred, Hungary, 1976.
8. D. LEZAL and I. SRB, Proc. of Int. Conf. on Amorphous S.C., Balatonfüred, Hungary, 1976.
9. E. V. SHKOLNIKOV, Z. U. BORISOVA and A. Y. BESSONOVA, J. Inorganic Material (USSR), **11,** 1574, 1975.
10. A. A. VAIPOLIN and E. A. PORAI-KOSHITS, Soviet Phys. — Solid State, **2,** 1500, 1960.
11. A. L. RENNINGER and B. L. AVERBACH, Acta Crystall, *B* **29,** 8, 1583, 1973.
12. E. S. RONALD, J. Non-cryst. Solids, **8—10,** 598, 1972.

13. C. A. MAJID, P. R. PRAGER, N. H. FLETCHER and J. M. BRETTELL, J. Non-Cryst. Solids, **16,** 365, 1974.
14. S. A. SALEH, M. F. KOTKATA and M. K. EL-MOUSLY, Proc. of Math. and Phys. Soc. of Egypt, **42,** 73, 1976.
15. O. M. VY and J. DROWART, Trans. Farad. Soc., **65,** 3221, 1969.
16. H. L. UPHOFF and J. H. HEALY, J. Appl. Phys., **32,** 950, 1961.
17. R. L. MYULLER, Chemistry of Solid state, Izd. Leningrad State Univ., 1965, p. 9.
18. G. OFFERGELD and VAN CAKENBERH, J. Phys. Chem. Sol., **11,** 310, 1959.
19. M. AVRAMI, J. Chem. Phys., **8,** 212, 1940.
20. M. K. EL-MOUSLY and M. F. KOTKATA, Acta Phys. Hung., **43,** 117, 1977.
21. E. V. CHKOLNIKOV, Chemistry of Solid State, Izd. Leningrad State Univ., 1965. p. 184.

Acta Physica Academiae Scientiarum Hungaricae, Tomus 45 (3), pp. 163—170 (1978)

ON UNSTEADY VISCOUS MHD FLOW THROUGH A POROUS CHANNEL WITH CONSTANT SUCTION

By

L. M. SRIVASTAVA and R. P. AGARWAL

DEPARTMENT OF APPLIED MATHEMATICS, MOTILAL NEHRU REGIONAL ENGINEERING COLLEGE
ALLAHABAD, 211004 INDIA

(Received 15. VIII. 1978)

The problem of incompressible laminar viscous electrically conducting flow under the influence of time-varying pressure gradient in a channel with two parallel porous walls with uniform suction and injection at the walls is studied The exact solution of the problem has been obtained when pressure gradient (i) varying linearly with time (ii) varying exponentially with time (iii) varying harmonically with time (iv) varying impulsively with time.

1. Introduction

PRAKASH [1] discussed the problem of unsteady incompressible viscous flow under a time-varying pressure gradient in a straight channel with two parallel porous walls with uniform suction and injection at the walls. He obtained the exact solution of the problem for a special case by considering pressure gradient to be a constant quantity. SRIVASTAVA [2] extended the same problem for an electrically conducting fluid in the presence of magnetic field. The present paper is concerned with the study of unsteady flow of an electrically conducting viscous fluid through a straight channel with two parallel porous flat plates under a time-varying pressure gradient when there is equal and uniform suction and injection on the walls. The exact solution of the problem has been obtained when pressure gradient (i) varying linearly with time (ii) varying exponentially with time (iii) varying harmonically with time (iv) varying impulsively with time. The flow takes place in the presence of a uniform vertical magnetic field.

2. Formulation of the problem and its solution

Consider an unsteady electrically conducting incompressible flow through a straight channel with two parallel porous flat plates situated at a distance h apart. We take x and y values along and transverse to the parallel plates and assume a uniform magnetic field H_0 acting along y-axes. The fluid is being injected into the channel through the wall at $y = 0$ and is being sucked

through the wall at $y = h$ with a uniform velocity V_0. Electric field E is assumed to be zero. The induced magnetic field due to electrical current flow in the fluid is assumed to be very small and the electric conductivity σ of the fluid is sufficiently large.

At a sufficiently large distance from the origin the flow is fully developed and the physical quantities depend on y and t only. Then the governing equation of the problem are [2].

$$\frac{\partial u}{\partial t} + V_0 \frac{\partial u}{\partial y} = -\frac{1}{\varrho}\frac{\partial p}{\partial x} + v\frac{\partial^2 u}{\partial y^2} - \frac{\sigma}{\varrho} B_u^2 , \tag{1}$$

$$0 = \frac{\partial p}{\partial y} , \tag{2}$$

with the initial and boundary conditions

$$\left.\begin{aligned} &0 \leq y \leq h : u = 0,\ v = 0 \quad \text{for} \quad t \leq 0, \\ &y = 0 : u = 0,\ v = V_0 \\ &y = h : u = 0,\ v = V \end{aligned}\right\} \rightarrow \text{for } t > 0. \tag{3}$$

Introducing non-dimensional quantities as

$$u_1 = \frac{u}{V_0},\ x_1 = \frac{x}{h},$$

$$y_1 = \frac{y}{h},\ p_1 = \frac{p}{\varrho V_0^2},\ t_1 = \frac{t}{h/V_0} \tag{4}$$

into Eq. (1)—(3), which reduce to

$$\frac{\partial u_1}{\partial t_1} + \frac{\partial u_1}{\partial y_1} = -\frac{\partial p_1}{\partial x_1} + \frac{1}{R_s}\frac{\partial^2 u_1}{\partial y_1^2} - m_1 u_1, \tag{5}$$

$$0 = \frac{\partial p_1}{\partial y_1} , \tag{6}$$

$$\begin{aligned} &0 \leq y_1 \leq 1 : u_1 = 0 \text{ for } t_1 \leq 0, \\ &y_1 = 0, 1 : u_1 = 0 \text{ for } t_1 > 0 , \end{aligned} \tag{7}$$

where $R_s = V_0 h/v$ = suction and injection Reynolds number,

$$m_1^{1/2} = \left(\frac{h}{V_0} \cdot \frac{\sigma}{\varrho}\mu e^2 H_0^2\right)^{1/2} = R_M = \text{magnetic paremeter},$$

$$m_1 = \frac{M^2}{R_s},\ M = \left(\frac{\sigma}{\mu}\mu e^2\, H_0^2 h^2\right) = \text{Hartmann number}.$$

Now assuming $\partial p_1/\partial x_1 = -f(t_1)$, thus (5) reduces to

$$\frac{\partial u_1}{\partial t_1} + \frac{\partial u_1}{\partial y} = f(t_1) + \frac{1}{R_s}\frac{\partial^2 u_1}{\partial y_1^2} - m_1 u_1. \tag{8}$$

To obtain the solution of (8), we will apply Laplace transformation which is defined for velocity u_1, as

$$\bar{u}_1 = \int_0^\infty u_1 e^{\lambda t_1} dt_1 . \tag{9}$$

Thus (8) and (7) transform to

$$\frac{d^2\bar{u}_1}{dy_1^2} - R_s\frac{d\bar{u}_1}{dy_1} - R_s(\lambda + m_1)\bar{u}_1 = -R_s\bar{f}(\lambda), \tag{10}$$

$$\bar{u}_1 = 0 \text{ at } y_1 = 0, 1, \tag{11}$$

where

$$\bar{f}(\lambda) = \int_0^\infty f(t_1) e^{-\lambda t_1} dt_1 . \tag{12}$$

The solution of (10) subject to the boundary condition (11) is

$$\bar{u}_1 = \frac{\bar{f}(\lambda)}{(\lambda + m_1)\sin h\sqrt{\beta}}\left[-\exp\left[(y_1 - 1)\frac{R_s}{2}\right]\sin h\left(\sqrt{\beta}\, y_1\right) - \right.$$
$$\left. - \exp\left[y_1\frac{R_s}{2}\right]\sin h\left[(1 - y_1)\sqrt{\beta}\right]\right] + \frac{\bar{f}(\lambda)}{\lambda + m_1}, \tag{13}$$

where

$$\beta = \frac{R_s^2 + 4R_s(\lambda + m_1)}{4} .$$

Thus by applying inversion formula

$$u_1 = \frac{1}{2\pi i}\int_{\nu - i\infty}^{\nu + i\infty}\left[\frac{\bar{f}(\lambda)}{(\lambda + m_1)\sin h\sqrt{\beta}}\left[-\exp\left((y_1 - 1)\frac{R_s}{2}\right)\sin h\left(\sqrt{\beta}\, y_1\right) - \right.\right.$$
$$\left.\left. - \exp\left(y_1\frac{R_s}{2}\right)\sin h\left((1 - y_1)\sqrt{\beta}\right)\right] + \frac{\bar{f}(\lambda)}{(\lambda + m_1)}\right] e^{\lambda t_1} d\lambda . \tag{14}$$

3. Exact solutions for different variations of pressure gradient

Case I: Pressure gradient varies linearly with time

We now assume that

$$-\frac{\partial p_1}{\partial x_1} = f(t_1) = a_0 + a t_1 . \tag{15}$$

Therefore

$$\bar{f}(\lambda) = \int_0^\infty (a_0 + a t_1)\, \bar{e}^{\lambda t_1} dt_1 = \frac{a_0}{\lambda} + \frac{a}{\lambda^2} . \tag{16}$$

Eq. (14) then reduces to

$$v_1 = \frac{1}{2\pi i} \int_{\nu - i\infty}^{\nu + i\infty} \left[\frac{e^{\lambda t_1}}{(\lambda + m_1)} \left(\frac{a_0}{\lambda} + \frac{a}{\lambda^2} \right) \left[\frac{1}{\sin h \sqrt{\beta}} \left(- \exp\left\{ (y_1 - 1) \frac{R_s}{2} \right\} \times \right. \right. \right.$$
$$\left. \left. \left. \times \sin h \left(\sqrt{\beta}\, y_1 \right) - \exp\left(\frac{y_1 R_s}{2} \right) \sin h \left[(1 - y_1) \sqrt{\beta} \right] \right) + 1 \right] \right] d\lambda . \tag{17}$$

Therefore the solution, when the pressure gradient varies linearly with time, with the help of poles and residue method is given by

$$u_1 = \frac{e^{\frac{y_1 R_s}{2}}}{m_1} \left[\frac{e^{-\frac{R_s}{2}} \sin h \left(y_1 \sqrt{\beta_0} \right) + \sin h \left[(1 - y_1) \sqrt{\beta_0} \right]}{\sin h \left(\sqrt{\beta_0} \right)} \right] \times$$
$$\times \left[- a_0 + a \left(-t + \frac{1}{m_1} + \frac{R_s \coth \sqrt{\beta_0}}{2 \sqrt{\beta_0}} \right) \right] +$$
$$+ \frac{1}{m} \left[a_0 + a \left[t - \frac{1}{m_1} - \frac{R_s\, e^{\frac{y_1 R_s}{2}}}{2 \sqrt{\beta_0} \sin h \sqrt{\beta_0}} \times \right. \right. \tag{18}$$
$$\left. \left. \times \left[y_1 e^{-\frac{R_s}{2}} \cosh \left(y_1 \sqrt{\beta_0} \right) + (1 - y_1) \cos h \left((1 - y_1) \sqrt{\beta_0} \right) \right] \right] \right] +$$
$$+ \sum_{n=0}^{\infty} \left[\frac{32\, n\pi R_s \sin(\pi n y_1) [4R_s(a - m_1 a_0) - a_0 (R_s^2 + 4\pi^2 n^2)] \left[1 - (-1)^n e^{-\frac{R_s}{2}} \right]}{(R_s^2 + 4\pi^2 n^2)(4 m_1 R_s + R_s^2 + 4\pi^2 n^2)^2} \times \right.$$
$$\left. \times \exp\left[\frac{y_1 R_s}{2} - t_1 \left(m_1 + \frac{R_s^2 + 4\pi^2 n^2}{4 R_s} \right) \right] \right] ,$$

where

$$\beta_0 = \frac{R_s^2 + 4 R_s m_1}{4} .$$

Case II: Pressure gradient varies exponentially with time

We assume that

$$-\frac{\partial p_1}{\partial x_1} = f(t_1) = a_0 + \sum_{n=1}^{\infty} a_n e^{-nt_1}. \tag{19}$$

Therefore

$$\bar{f}(\lambda) = \int_0^{\infty} \left[a_0 + \sum_{n=1}^{\infty} a_n e^{-nt_1}\right] e^{-\lambda t_1} dt_1 = \sum_{k=0}^{\infty} \frac{a_k}{(k+\lambda)}. \tag{20}$$

Eq. (14) then reduces to

$$u_1 = \frac{1}{2\pi i} \int_{\nu-i\infty}^{\nu+i\infty} \left[\sum_{k=0}^{\infty} \frac{a_k e^{\lambda t_1}}{(k+\lambda)(\lambda+m_1)} \left[\frac{1}{\sin h \sqrt{\beta}} \left[-\exp\left((y_1-1)\frac{R_s}{2}\right) \times \right.\right.\right.$$
$$\left.\left.\left. \times \sin h\left(\sqrt{\beta}\, y_1\right) - \exp\left(\frac{y_1 R_s}{2}\right) \sin h\left((1-y_1)\sqrt{\beta}\right)\right] + 1\right]\right] d\lambda. \tag{21}$$

Therefore the solution in this case, with the help of poles and residue method, is given by

$$u_1 = -\sum_{k=0}^{\infty} \frac{a_k e^{-kt}}{(k+m)} \left[\frac{\exp\left(\frac{y_1 R_s}{2}\right)}{\sin h \sqrt{\frac{R_s^2 + 4R_s(m_1-k)}{4}}} \times \right.$$
$$\times \left[\exp\left(-\frac{R_s}{2}\right) \sin h \left(y_1 \sqrt{\frac{R_s^2 + 4R_s(m_1-k)}{4}}\right) + \right.$$
$$\left. + \sin h \left[(1-y_1)\sqrt{\frac{R_s^2 + 4R_s(m_1-k)}{4}}\right]\right] + 1 \Bigg] +$$
$$+ \sum_{n=0}^{\infty} \left[32\, n\pi R_s \sin(n\pi y_1) \left((-1)^n e^{-\left(\frac{R_s}{2}\right)} - 1\right) \times \right.$$
$$\times \exp\left\{\frac{y_1 R_s}{2} - \left(m + \frac{R_s^2 + 4\pi^2 n^2}{4R_s}\right) t_1\right\} \times$$
$$\left. \times \sum_{k=0}^{\infty} \left[\frac{a_k}{[4R_s(m_1-k) + (R_s^2 + 4\pi^2 n^2)][R_s^2 + 4\pi^2 n^2]}\right]\right]. \tag{22}$$

Case III: Pressure gradient varies harmonically with time

We assume that

$$-\frac{\partial p_1}{\partial x_1} = f(t_1) = B_1 \sin \omega t_1 . \tag{23}$$

Therefore

$$\bar{f}(\lambda) = \int_0^\infty B \sin \omega t_1 \, e^{-\lambda t_1} \, dt_1 = \frac{B\omega}{\lambda^2 + \omega^2} . \tag{24}$$

Eq. (14) then reduces to

$$u_1 = \frac{1}{2\pi i} \int_{\nu - i\infty}^{\nu + i\infty} \frac{B_1 \omega e^{\lambda t_1}}{(\lambda + m_1)(\lambda^2 + \omega^2)} \left[\frac{1}{\sin h \sqrt{\beta}} \left[- \exp\left((y_1 - 1) \frac{R_s}{2} \right) \times \right. \right.$$
$$\left. \left. \times \sin h \left(\sqrt{\beta} \, y_1 \right) - \exp\left(\frac{y_1 R_s}{2} \right) \sin h \left((1 - y_1) \sqrt{\beta} \right) \right] + 1 \right] d\lambda . \tag{25}$$

Therefore the solution in this case is given by

$$u_1 = \frac{B_1}{(m_1^2 + \omega^2)} \left[m \sin \omega t - \omega \cos \omega t \right] +$$
$$+ \sum_{n=0}^{\infty} \left[\frac{128 \pi n \, B_1 \omega R_s^2 \sin (\pi n y_1) \left[1 - (-1)^n \exp\left(-\frac{R_s}{2} \right) \right] \times}{(R_s^2 + 4\pi^2 n^2) \left[16 R_s^2 \omega^2 + (R_s^2 + 4\pi^2 n^2 + 4 R_s m_1)^2 \right]} \right.$$
$$\left. \times \exp\left[\frac{y_1 R_s}{2} - t_1 \left(m_1 + \left[\frac{R_s^2 + 4\pi^2 n^2}{4 R_s} \right] \right) \right] \right] +$$
$$+ \frac{B_1 e^{\frac{y_1 R_s}{2}}}{(m_1^2 + \omega^2)(C^2 + S^2)} \left[(m_1 \cos \omega t_1 + \omega \sin \omega t_1) \left[\exp\left(-\frac{R_s}{2} \right) \times \right. \right. \tag{26}$$
$$\left. \times (CSy - SCy) - A \left[(CSy - SCy) - B(SSy + CCy) + Fy(S^2 + C^2) \right] \right] +$$
$$+ (\omega \cos \omega t_1 - m_1 \sin \omega t_1) \left[\exp\left(-\frac{R_s}{2} \right) (SSy - CCy) - \right.$$
$$\left. \left. - \left(B(CSy - SCy) + A(SSy + CCy) - Ey(S^2 + C^2) \right) \right] \right] ,$$

where

$$S = \sin h \sqrt{X} \cos \sqrt{Y}, \qquad E_y = \cos h\left(y\sqrt{X}\right)\cos y\sqrt{Y},$$

$$Sy = \sin h\left(y_1\sqrt{X}\right)\cos\left(y_1\sqrt{Y}\right), \qquad F_y = \sin h\left(y\sqrt{X}\right)\sin\left(y\sqrt{Y}\right),$$

$$C = \cos h\left(\sqrt{X}\right)\sin\sqrt{Y}, \qquad A = \cos h\sqrt{X}\cos\sqrt{Y},$$

$$Cy = \cos h\left(y_1\sqrt{X}\right)\sin\left(y_1\sqrt{Y}\right), \qquad B = \sin h\sqrt{X}\sin\sqrt{Y},$$

$$X = \frac{1}{2}\left[x \pm \sqrt{x^2 + z^2}\right], \quad x = \frac{R_s^2 + 4R_s m_1}{4},$$

$$Y = \frac{1}{2}\left[\frac{z^2}{x \pm \sqrt{x^2 + z^2}}\right], \quad z = \omega R_s .$$

Case IV: Pressure gradient varies impulsively with time

We assume that

$$-\frac{\partial p_1}{\partial x_1} = f(t_1) = A\delta(t_1), \tag{27}$$

where $\delta(t_1)$ is the Dirac Delta.

Therefore

$$\bar{f}(\lambda) = \int_0^\infty A\delta(t_1)\, e^{-\lambda t_1}\, dt_1 = A. \tag{28}$$

Eq. (14) then reduces to

$$u_1 = \frac{1}{2\pi i}\int_{\nu-i\infty}^{\nu+i\infty} e^{\lambda t_1}\left[\frac{A}{(\lambda + m_1)\sin h\sqrt{\beta}}\left[-\exp\left((y_1 - 1)\frac{R_s}{2}\right)\times\right.\right.$$
$$\left.\left.\times \sin h\left(\sqrt{\beta}\, y_1\right) - \exp\frac{y_1 R_s}{2}\sin h\left((1 - y_1)\sqrt{\beta}\right)\right] + \frac{A}{\lambda + m_1}\right] d\lambda . \tag{29}$$

Therefore the solution in this case is given by

$$u_1 = -\sum_{n=0}^{\infty}\left[\frac{8A\pi n \sin(\pi n y_1)\exp\left[\frac{y_1 R_s}{2} - t_1\left[\left(\frac{R_s^2 + 4\pi^2 n^2}{4R_s}\right) + m_1\right]\right]}{(R_s^2 + 4\pi^2 n^2)}\cdot\right.$$
$$\left.\cdot\left[(-1)^n \exp\left(-\frac{R_s}{2}\right) - 1\right]\right]. \tag{30}$$

Acknowledgement

One of us (R.P.A.) is grateful to the State Council of Science and Technology U.P. for a scholarship.

REFERENCES

1. S. PRAKASH, Proc. Nat. Inst. Sci. India, **35**(A), 123, 1969.
2. L. M. SRIVASTAVA, Acta Phys. Hung., **41**, 63, 1976.

Acta Physica Academiae Scientiarum Hungaricae, Tomus 45 (3), pp. 171—178 (1978)

ON STATIONARY SPHERICALLY SYMMETRIC CLUSTER OF PARTICLES

By

T. M. KARADE

DEPARTMENT OF MATHEMATICS, NAGPUR UNIVERSITY, NAGPUR-440010, INDIA

(Received in revised form 22. VIII. 1978)

In this paper various relativistic models representing the Einstein stationary spherically symmetric clusters of gravitating particles have been constructed. The motion of an individual particle is studied by employing the analogy of Killing vector. The Kretschmann curvature invariant, the gravitational mass and the boundary for each cluster model have been calculated.

I. Introduction

For the first time EINSTEIN [1] ingeniously contemplated a stationary symmetric cluster of particles revolving in a circular orbit about the centre of symmetry. There, on physical grounds, EINSTEIN could get rid of the Schwarzschild singularity for such a distribution. The different aspects of the EINSTEIN stationary spherically symmetric clusters (ESSSC) were later on investigated by GILBERT [2] in his extraordinary way. The possibility of the two types of clusters ('A' and 'B') was suspected. According to GILBERT [2] the cluster 'A' is characterized by

(a) e^h is monotonic increasing;

(b) On the boundary $r = b$, $q > 0$;

(c) The velocities of the particles increase with increasing distance from the centre in such a way that the particles at the boundary have the velocity less than half that of light. (The meanings of h and q are clarified in the next section.)

For the cluster B we have

(a) e^h increases sharply to a maximum $<3/2$ near $r = 0$ and then decreases to the boundary;

(b) $q > 0$ for $r < b$ and $q = 0$ for $r = b$;

(c) The central region particles have the highest velocities.

The special cases considered by EINSTEIN [1] and by SEN and ROY [3] come out as the examples of 'A' clusters. Further it was speculated that 'B' clusters would give a better approximation to the clusters of stars in reality. Very recently HOGAN [4] brought out a new derivation of the energy tensor for ESSSC and studied the emission of neutrinos in the above field. TEIXEIRA

and SOM [5] obtained a solution corresponding to ESSSC under a particular constraint of motion.

Motivated with an intention to study the problem of ESSSC in greater detail than has been done till now, we in this paper constructed the various solutions by adopting a procedure analogous to those of TOLMAN [6]. One of the solutions, discussed in case (g), is free from singularity. It has been seen that the solution obtained by TEIXEIRA and SOM [3] emerges as a particular example of our case (c). To have a comprehensive study of the distributions so obtained the Kertschmann curvature invariant $L = R_{abcd}R^{abcd}$ for each model has been calculated to know the singularity aspects: the Killing vector analogy (ANDERSON [7]) has been freely used to draw the information regarding the motion of the particle and finally the expressions for the gravitational mass and the boundary of the cluster have been deduced. A comparison of these predictions with our observational knowledge would provide a test of the validity of the model.

II. The field equations

Consider a cluster of particles having a spherical symmetry in which an individual particle is moving in a circular orbit about the centre of symmetry in the gravitational field of the cluster. The gravitational field within the cluster is given by

$$ds^2 = -e^h\,dr^2 - r^2(d\theta^2 + \sin^2\theta d\Phi^2) + e^k\,dt^2, \tag{1}$$

where h and k are functions of r alone. Denoting $r = b$ as the boundary of the cluster, it is obvious that for the region $r > b$ the space-time will be depicted in the well known Schwarzschild exterior solution

$$ds^2 = -(1-2m/r)^{-1}\,dr^2 - r^2(d\theta^2 + \sin^2\theta d\Phi^2)]+ (1 - 2m/r)\,dt^2, \tag{2}$$

where m can now be treated as the gravitational mass of the cluster as measured by its external gravitational field. Also on the boundary $r = b$, fields given by (1) and (2) must match together.

In the usual notation the field equations of general relativity, without a cosmical term, are

$$R_n^m - (R/2)\delta_n^m = -8\pi\,T_n^m\,. \tag{3}$$

The left hand side of the above equation is the geometrical part whereas the right hand side is the physical part which in our case, following GILBERT [2], can be written as

$$T_2^2 = T_3^3 = -(q/2)V^2 e^{-k}, \quad T_4^4 = q\,. \tag{4}$$

The quantity V appearing in (4) has a physical significance. It is not simply the velocity but that measured in proper time. It denotes the speed of the particle P moving at right angles to OP where O is the centre of the symmetry of the cluster. The quantity q is the density of energy referred to axes fixed at P.

The field equations (3) alongwith (1) and (3) yield

$$e^{-h}(k_1/r + 1/r^2) - 1/r^2 = 0, \tag{5}$$

$$e^{-h}(k_{11}/2 - h_1 k_1/4 + k_1^2/4 + (k_1 - h_1)/2r) = 4\pi q V^2 e^{-k}, \tag{6}$$

$$e^{-h}(-h_1/r + 1/r^2) - 1/r^2 = -8\pi q \tag{7}$$

and from the energy conservation law, we get

$$rk_1 = 2V^2 e^{-k} \quad \text{with} \quad h_1 = dh/dr \text{ etc.} \tag{8}$$

One can easily derive Eq. (8) from Eq. (5)—(7). Therefore we are left with three independent field equations while the number of unknowns (h, k, q, V) is four. The problem is indeterminate and in order to have a unique solution it is necessary to presume one more relation arbitrarily to make the system determinate. TOLMAN [6] and KUCHOWICZ [8] have freely used this methodology to obtain the different solutions of the fluid sphere in general relativity. However, this method is not so safe as it stands. It may happen that the mathematical solution thus obtained may not be of any physical importance. The physical interest of such models will, however, depend on whether they exhibit positive energy density. Another alternative is to introduce one more relation which is related to some physical condition of the distribution. Such type of procedure has some serious drawbacks because very often by introducing an auxiliary condition the problem becomes highly complicated. We, in this paper, have preferred the first methodology to the latter.

It is noteworthy that the gravitational field defined by the metric (1) possesses an everywhere timelike vector K^i (ANDERSON [7]) which satisfies

$$K_{i,j} + K_{j,i} = 0\,.$$

We can always find a mapping such that in finite region of space-time

$$K^i = (0,\ 0,\ 0,\ 1) \tag{9}$$

and hence

$$K_i = (0,\ 0,\ 0,\ e^k).$$

The projection operator B^i_j onto the hyperplane normal to K^i is then given by

$$B^i_j = \text{diag}\,(1,\ 1,\ 1,\ 0)\,. \tag{10}$$

If we suppose

$$u^i = dx^i/ds = (0,\ 0,\ u^3,\ u^4)^*$$

as the four velocity of the member, in the equatorial motion, of the cluster following the geodesic in the field of (1), we get

$$(u^3)^2\,(2r/k_1) = e^k\,(u^4)^2 = (1 - rk_1/2)^{-1}\,. \tag{11}$$

From equations (9)—(11) we obtain the magnitude of the covariant normal velocity, which corresponds to the classical velocity of the particle, and is given by

$$2v^2 = rk_1. \tag{12}$$

We shall employ this result in the next Section.

III. A set of various solutions

(a) *Supposition*: $e^k =$ constant.

With the above condition, equations (5)—(8) yield

$$h = V = q = v = 0$$

and then we have

$$ds^2 = -dr^2 - r^2(d\theta^2 + \sin^2\theta d\Phi^2) + c^2dt^2,$$

with $e^k = c^2$.

This line-element corresponds to that of special relativity and is devoid of any physical importance in the context of our paper.

(b) *Supposition*: $e^{h+k} = \text{const.} = B^2$.

Now Eqs. (5)—(8) give

$$e^{-h} = 1 - A/r, \quad e^k = B^2\,e^{-h},$$
$$V^2 = AB^2/2r, \quad v^2 = A/2(r - A),$$
$$q = 0, \quad L = 12\ A^2/r^6\,,$$

where A is a constant of integration.

It is amazing to note that the solution corresponds to $T^m_n = 0$ and is nothing else than Schwarzschild's exterior solution as it stands. The gravitational mass of the cluster ($= m$) is $A/2$.

* This choice of u^i is in conformity with that of EINSTEIN [1].

(c) *Supposition*: $e^k k_1/2r = \text{const.} = (B/A)^2$. (13)

We obtain the following :

$$e^h = (A^2 + 3r^2)/(A^2 + r^2), \quad e^k = B^2(1 + r^2/A^2),$$
$$V = Br/A, \; v^2 = (1 + A^2/r^2)^{-1},$$
$$4\pi q = 3(A^2 + r^2)(A^2 + 3r^2)^{-2}, \; b^2 = (A^2/3B^2)(1 - B^2),$$
$$m = (A/B)\big((1 - B^2)/3\big)^{3/2},$$
$$L = 12(18r^4 + 12A^2r^2 + 5A^4)(A^2 + 3r^2)^{-4}.$$

Here the field is free from singularity. The functions e^h and v are increasing with r. The stability of the circular orbits ($A^2 > 0$) is trivially satisfied for real values of A. The density at the centre of the cluster is finite and the particles thereat will be at rest. No member of this cluster will attain the velocity of light. The interesting feature of V is that it is proportional to the distance from the centre. Denoting B/A by H, we write $V = Hr$ which is similar to Hubble's law for the velocity of recession of the galaxies. Of course we are aware of the fact that V in our case has a different significance. The gravitational field can then be written as

$$ds^2 = -\frac{1+3H^2(r^2 - b^2)}{1+H^2(r^2 - 3b^2)}dr^2 - r^2(d\theta^2 + \sin^2\theta d\Phi^2) + \\ + \big(1 + H^2(r^2 - 3b^2)\big)dt^2.$$

If we replace A by $1/\omega$ and B^2 by A, the result of TEIXEIRA and SOM [5] are reclaimed with $c = 1$. The quantity ϱ (proper density of matter used by them) is connected to q by the equation

$$\varrho = q(1 - e^k V^2).$$

Furthermore if we restrict the size of the cluster such that $v = 1/2$ at the boundary, we get

$$3b^2 = A^2, \; 2B^2 = 1$$

and

$$q_c = 3q_b\,,$$

where the suffix c stands for centre.

As a matter of fact Eq. (13) has the solution

$$e^k = B^2(\varepsilon + r^2/A^2) \text{ with } \varepsilon = 0 \text{ or } \pm 1.$$

The situation already discussed corresponds to $\varepsilon = 1$. The case $\varepsilon = -1$ has no physical meaning because $v > 1$, but the case $\varepsilon = 0$ seems to be good and then we obtain

$$e^k = (B/A)^2 r^2, \quad e^h = 3, \quad v = 1 \text{ etc.}$$

This is strange but probably not physical.

(d) *Supposition*: $e^h = \text{constant} = c$.

The field equations yield

$$e^k = Ar^{c-1}, \; 2V^2 = A(c-1)r^{c-1},$$
$$2v^2 = c - 1, \; 8\pi q = (c-1)/cr^2,$$
$$2m = b(c-1)/c, \quad b = (Ac)^{-1/(c-1)},$$
$$L = (1/4c^2 r^4)(c-1)^2(c^2 - 6c + 33).$$

The field has intrinsic singularity at $r = 0$. The density is inversely proportional to the square of the distance and becomes infinite at the centre. On physical grounds $c > 1$. The condition for the stability of the orbits further restricts c such that $1 < c < 3$. Choosing $c = 2$, the line-element can be written as

$$ds^2 = -2dr^2 - r^2(d\theta^2 + \sin^2\theta d\Phi^2) + Ardt^2.$$

Also as v does not depend upon r, in the above context all particles will be moving at constant speed which is $1/\sqrt{2}$ times the speed of light which is not a very pleasing situation. The above cluster does not belong to GILBERT's classification.

(e) *Supposition*: $e^{-h} = c/r$.

We find that

$$e^k = (A/r)e^{r/c}, \; V^2 = (A/2r)(r/c - 1)e^{r/c},$$
$$v^2 = (r-c)/2c, \; 8\pi q = 1/r^2,$$
$$b = c \log (c/A), \; m = (c/2) \log (c/eA),$$
$$L = 2c^2/r^6 + 6(c-r)^2/r^6 + (1/2r^3 c)^2(r^2 - 3rc + 4c^2)^2.$$

The stability of the orbits corresponds to

$$r^2 - 5rc + 3c^2 < 0.$$

Physical grounds that the particles at the boundary should not approach the velocity of light, impose a condition given by

$$1 < \log (c/A) < 3.$$

We find that the particles at the centre move with imaginary velocities. To avoid this situation we suppose that the space-time is valid for the region $r \geq c$. The particles on the surface $r = c$ have zero velocities and the condition for stability is satisfied trivially thereat. As our solution stands for the restricted region, it does not reveal anything about $0 \leq r < c$. One may imagine that the inner regions are devoid of any particle.

The model we arrived at, has EINSTEIN's [1] cluster shell analogue replacing his thin shell S by the region $c \leq r \leq b$. The field inside the region $0 \leq r \leq c$ will be Minkowskian if the number of particles in the shell is large enough so that the exterior gravitational field is completely screened off from the inner region. If the number of particles is smaller enough, the field will not be screened off entirely and then the arguments similar to that of EINSTEIN [1] may be applied for the inner field.

This model cannot be accommodated in GILBERT's [2] classification.

(f) *Supposition*: $e^{-h} = c/r^2$.

In this case we get

$$e^k = (A/r)e^{(r^2/2c)},\ V^2 = (A/2r)(r^2/c - 1)\, e^{r^2/2c},$$
$$v^2 = (1/2c)(r^2 - c),\ 8\pi q = (c + r^2)/r^4,$$
$$be^{(b^2/2c)} = c/A,\ m = (b/2)(1 - c/b^2),$$
$$L = 8c^2/r^8 + 6(r^2 - c)^2/r^8 + (2r^2 + (r^2 - c)^2/2c)/r^8 .$$

Stability condition of the orbits gives

$$r^4 - 6r^2c + 3c^2 < 0.$$

In this case the space-time is valid for $r \geq \sqrt{c}$. The arguments for the case (e) are also applicable here.

(g) *Supposition*: $e^{-h} = 1 - r^2/R^2$.

In this case we obtain a solution which is free from singularity.

$$e^k = (B/R)e^{h/2},\ V^2 = (Br^2/2)(R^2 - r^2)^{-3/2},$$
$$v^2 = (r^2/2)/(R^2 - r^2),\ 8\pi q = 3/R^2 = \text{constant},$$
$$m = b^3/2R^2,\ b^2 = R^2(1 - (B/R)^{2/3}),$$
$$L = 14/R^4 + (1 + r^2/2R^2)^2(R^2 - r^2)^{-2},$$

with B and R as constants.

The velocity v approaches the velocity of light at $r = R\sqrt{2/3}$ and on physical grounds the boundary of the cluster must be restricted according to

$$b^2 < 2R^2/3. \tag{14}$$

The space-time outside this boundary corresponds to Schwarzschild's exterior solution. As $0 \leq r \leq b < R$, this model is free from singularity and satisfies the condition for the stability of the circular orbits $3r^2 < 4R^2$.

For real values of b we must have

$$(B/R)^2 < 1. \tag{15}$$

From (14), (15) and the expression of b^2, we get

$$1/27 < (B/R)^2 < 1. \tag{16}$$

The boundary of the cluster can further be restricted so that the outermost particle moves with a velocity less than half the velocity of light. The model will be an example of cluster A. In this case

$$b^2 < R^2/3$$

and

$$8/27 < (B/R)^2 < 1.$$

IV. Conclusion

Our investigation suspects that one of the solutions belongs to class B and only two of them may belong to class A, if the boundary is chosen suitably.

Acknowledgement

The author is extremely grateful to the Referees for their kind and helpful suggestions.

REFERENCES

1. A. Einstein, Ann. Math., **40,** 922, 1939.
2. C. Gilbert, Mon. Not. Roy. Astr. Soc., **114,** 628, 1954.
3. N. R. Sen and T. C. Roy, Zs. für Astrophysik, **34,** 84, 1954.
4. P. A. Hogan, Proc. Roy. Irish. Acad., **A73,** 91, 1973.
5. A. F. Daf Teixeira and M. M. Som, J. Phys., **A7,** 838, 1974.
6. R. C. Tolman, Phys. Rev., **55,** 364, 1939.
7. J. L. Anderson, Principles of Relativity Physics, Academic Press, New York, London, pp. 350—54, 1967.
8. B. Kuchowicz, Acta Phys. Pol., **33,** 541, 1968.

Acta Physica Academiae Scientiarum Hungaricae, Tomus 45 (3), pp. 179—189 (1978)

HEAT TRANSFER THROUGH A ROTATING CHANNEL IN POROUS MEDIUM

By

V. VIDYANIDHI and V. DHANANJAYA RAO

DEPARTMENT OF ENGINEERING MATHEMATICS, ANDHRA UNIVERSITY, WALTAIR, INDIA

(Received 24. VIII. 1978)

A theoretical analysis of the hydrodynamic flow and its temperature distribution in a porous medium is presented for an incompressible viscous fluid in a rotating channel, bounded by two impermeable infinite parallel plates at a constant temperature, under the action of a uniform pressure gradient in the direction of the flow. An exact solution of the governing equations is obtained. The flow is governed by the Darcy's number σ dependent on the permeability k of the medium and the Taylor number T. The primary and the secondary flows, the temperature distribution, the shear stresses and the Nusselt number at the plates are studied in detail for various values of σ and T. In general, σ is found to have a stronger influence in reducing the mass flux and the temperature of the flow compared to rotation. For large values of σ ($\sigma > 10$), there is no appreciable change in temperature and Nusselt number with rotation. When σ and T are large, the flow is confined to a boundary layer in the vicinity of the plates.

1. Introduction

Many interesting flows through porous media have been studied on the basis of Darcy's empirical law (see SCHEIDEGGER [1], BEAR [2], YIH [3]) which expresses the fact that the pressure gradient pushes the fluid in the porous medium against the body force exerted on it by the fluid. Darcy's law is found to be inadequate to describe the flows, more particularly in situations with high speeds or near the surface inside the porous body. A non-Darcy description for the viscous flows in porous media, is as such warranted. To this extent, the equations of motion of a fluid in porous medium were proposed by a number of authors (BRINCKMAN [4], TAM [5] and LUNDGREN [6]). YAMAMOTO and YOSHIDA [7] incorporated the convective terms in the basic equations and later YAMAMOTO and IWAMURE [8] and PATTABHI RAMACHARYULU [9] investigated a class of flows in porous media employing a more general field equation taking into account the fluid inertia and the viscous stresses as well.

It is assumed here that the medium is completely saturated with the viscous fluid, which, when set in motion generates viscous stresses in the same way as it does in a pure fluid medium. The fundamental equations, characterising the flow of a viscous incompressible fluid in such a saturated porous medium

(see [8], [9]) can thus be written as

$$\nabla \cdot \mathbf{v} = 0, \tag{1}$$

$$\frac{D\mathbf{v}}{D\tau} = -\nabla p - \frac{\mu}{k}\mathbf{v} + \mu\nabla^2\mathbf{v}^2\,, \tag{2}$$

$$\varrho c_p \frac{D\theta}{D\tau} = K\nabla^2\theta + \mu\left[\Phi + \frac{1}{k}\mathbf{v}\cdot\mathbf{v}\right], \tag{3}$$

where $\mathbf{v}$ is the fluid velocity, θ the temperature, p the pressure, Φ the viscous dissipation term, ϱ the fluid density, K the thermal conductivity, c_p the specific heat at constant pressure of the fluid, μ the viscous coefficient of the fluid and k the permeability of the medium. Eq. (2) is the same as the Navier-Stokes equations, when the flow is influenced by a special type of body force 'Darcy force' equal to $-\mu v/k$. In the limit, as $k \to \infty$, this reduces to the Navier-Stokes equation of motion, which is valid for a pure fluid medium.

We consider here the flow of an infinite expanse of an incompressible viscous fluid in a porous medium through a rotating channel formed by two infinite impermeable horizontal parallel plates $Z = \pm h$. The fluid and the plates are assumed to be in a state of rigid body rotation with constant angular velocity Ω about the Z-axis while the fluid is driven by a uniform pressure gradient $-\partial p/\partial X$ in the direction of the X-axis. For a pure fluid medium, this problem was solved by VIDYANIDHI and NIGAM [10]. VIDYANIDHI [11] and NANDA and MOHANTY [12] extended it in the framework of hydromagnetics. The effect of suction and injection on this flow was investigated by VIDYANIDHI et al [13]. The corresponding problems of heat transfer by RAMANA RAO and BALA PRASAD [14] and MOHAN [15] are equally important. In these problems on rotating fluids, a strong interaction occurs due to the interplay of the uniform pressure gradient and the Coriolis forces. An attempt has been made here to seek the influence of the Darcy's number σ on these flows in porous medium.

Flows of this type occur in geothermal situations, ground water movement, squeeze film performance and lubrication theory. As a matter of fact, we ought to include the buoyancy force which is of some special significance in the parallel flow in geothermal situations, but the mathematical expressions become cumbersome. So the results are presented for a simple geometry. We assume further that both the lower and upper plates are maintained at fixed temperatures θ_0 and θ_1.

2. Mathematical formulation

The relevant equations of motion, relative to the rotating frame of reference, are

$$-2\varrho\Omega V = -\frac{\partial p}{\partial X} + \mu\frac{d^2U}{dZ^2} - \frac{\mu}{k}U\,, \tag{4}$$

$$2\varrho\Omega U = \mu\frac{d^2V}{dZ^2} - \frac{\mu}{k}V, \tag{5}$$

$$0 = K\frac{d^2\theta}{dZ^2} + \mu\left[\left(\frac{dU}{dZ^2}\right)^2 + \left(\frac{dV}{dZ}\right)^2\right] + \frac{\mu}{k}(U^2 + V^2)\,. \tag{6}$$

Here U and V are the primary and secondary velocity components of the velocity vector $\mathbf{v}$ in X and Y directions.

In terms of the quantities defined by

$$z = \frac{Z}{h}\,,\quad c = -\frac{1}{\mu}\frac{\partial p}{\partial X}\,,\quad (u, v) = \frac{1}{ch^2}(U, V),\quad t = \frac{\theta - \theta_0}{\theta_1 - \theta_0}\,,$$

$$\sigma = \frac{h}{\sqrt{k}}\ \text{(Darcy number)},\quad T = \frac{2\varrho\Omega h^2}{\mu}\ \text{(Taylor number)}, \tag{7}$$

$$P_r = \frac{\mu c_p}{K}\ \text{(Prandtl numer)},\quad E = \frac{c^2h^4}{c_p\cdot(\theta_1 - \theta_0)}\ \text{(Eckert number)}$$

the Eqs. (4), (5) and (6) become

$$\frac{d^2q}{dz^2} - (\sigma^2 + iT)q = -1\,,$$

$$\frac{d^2t}{dz^2} = -P_rE\left(\frac{dq}{dz}\,\frac{d\bar{q}}{dz} + \sigma^2q\bar{q}\right),$$

where $q = u + iv$ and bar denotes complex conjugate. The solutions of these equations are sought subject to $q = 0$ at $z = \pm 1$ (no slip at the plates), $t = 0$ at $z = -1$ and $t = 1$ at $z = 1$. The primary velocity u and the secondary velocity v are found to be

$$u = \frac{2\sigma^2(1 - P) - TQ}{L(\sigma^4 + T^2)}\,, \tag{8}$$

$$v = -\frac{2\sigma^2Q + T(1 - P)}{L(\sigma^4 + T^2),}\,, \tag{9}$$

wherein

$$P = \cosh \alpha z \cdot \cos \beta z \cdot \cosh \alpha \cdot \cos \beta + \sinh \alpha z \cdot \sin \beta z \cdot \sinh \alpha \cdot \sin \beta,$$

$$Q = \sinh \alpha z \cdot \sin \beta z \cdot \cosh \alpha \cdot \cos \beta - \cosh \alpha z \cdot \cos \beta z \cdot \sinh \alpha \cdot \sin \beta,$$

$$L = \cosh 2\alpha + \cos 2\beta,$$

$$\alpha, \beta = \left[\frac{\sqrt{\sigma^4 + T^2} \pm \sigma^2}{2}\right]^{1/2}. \tag{10}$$

The solution for temperature t is

$$t = \frac{1}{2} + \frac{1}{2} z - P_r E [F(z) - F(1)], \tag{11}$$

where

$$F(z) = A(z) + \sigma^2 B(z),$$

$$A(z) = \frac{1}{4L(\alpha^2 + \beta^2)} \left[\frac{\cosh 2\alpha z}{\alpha^2} + \frac{\cos 2\beta z}{\beta^2}\right],$$

$$B(z) = \frac{1}{\sigma^4 + T^2} \left[\frac{1}{2} - \frac{4(\sigma^2 P + TQ)}{L(\sigma^4 + T^2)} + \frac{1}{4L} \left[\frac{\cosh 2\alpha}{\alpha^2} - \frac{\cos 2\beta}{\beta^2}\right]\right].$$

The primary and the secondary shear stresses τ_X and τ_Y at $z = \pm 1$ are

$$\tau_X = \left(\frac{du}{dz}\right)_{z=\pm 1} = \mp \frac{\alpha \sinh 2\alpha + \beta \sin 2\beta}{L(\alpha^2 + \beta^2)}, \tag{12}$$

$$\tau_Y = \left(\frac{dv}{dz}\right)_{z=\pm 1} = \mp \frac{\alpha \sin 2\beta - \beta \sinh 2\alpha}{L(\alpha^2 + \beta^2)}. \tag{13}$$

The Nusselt number, which is the local dimensionless coefficient of heat transfer, is

$$Nu_{\pm 1} = \left(\frac{dt}{dz}\right)_{z=\mp 1} = \frac{1}{2} \pm P_r E \left[\frac{1}{L(\alpha^2 + \beta^2)} \left(\frac{\sinh 2\alpha}{2\alpha} - \frac{\sin 2\beta}{2\beta}\right) + \right. \tag{14}$$

$$\left. + \frac{\sigma^2}{\sigma^4 + T^2} \left[1 + 2\tau_{X|z=+1} + \frac{1}{L} \left(\frac{\sinh 2\alpha}{2\alpha} + \frac{\sin 2\beta}{2\beta}\right)\right]\right].$$

Particular cases:

(i) When $T = 0$, $\sigma = 0$, we obtain the usual Poiseuille flow

$$u = \frac{1}{2}(1 - z^2),\ v = 0,\ t = \frac{1}{2} + \frac{1}{2}z = P_r E(1 - z^4)\ ,$$

$$\tau_X = \mp 1,\ \tau_Y = 0,\ Nu = \frac{1}{2} \pm \frac{1}{3} P_r E\ .$$

(ii) When $T = 0$, $\sigma \neq 0$ (non-rotating liquid in porous medium [9])

$$u = \frac{1}{\sigma^2}\left(1 - \frac{\cosh \sigma z}{\cosh \sigma}\right),\ v = 0\ ,$$

$$\tau_X = \mp \frac{\tanh \sigma}{\sigma},\ \tau = 0,$$

$$t = \frac{1}{2} + \frac{1}{2}z + \frac{P_r E}{\sigma^2 \cosh^2 \sigma}\left[\frac{1}{4\sigma^2}\left[2(\sigma^2 - 3)\cosh^2 \sigma - 1\right] + \right.$$

$$\left. + \frac{2 \cosh \sigma \cdot \cosh \sigma z}{\sigma^2} - \frac{\cosh 2\sigma z}{4\sigma^2} - \frac{z^2}{2} \cosh^2 \sigma\right],$$

$$Nu = \frac{1}{2} \mp \frac{P_r E}{\sigma^3 \cosh \sigma}(\sigma \cosh \sigma - \sinh \sigma).$$

The effect of the permeability k of the flow is analogous to that of the magnetic field on the conducting flow in magnetohydrodynamics.

(iii) When $T \neq 0$, $\sigma = 0$, we recover the flow through a rotating straight channel for the pure fluid medium [10].

3. Discussion and conclusions

The primary and the secondary velocity profiles u and v are shown in Figs. 1 and 2 for typical values of σ and T. They are symmetric about $z = 0$. Figs. 1 (a) and (b) show that, for a fixed σ, as T increases, the velocity component u decreases, the maximum value occurring at the centre as long as $T < T_1$. When $T > T_1$, the maximum of u is shifted towards the plates. With further rise in $T(T > T_2)$, the u-profile turns intermittently positive and negative for $-1 \leq z \leq 1$ cutting the Z-axis more often for larger T. When $\sigma = 0, 2, 5$ and 10, T_1 is found to be 5.5, 9, 20 and 50, respectively, while for $\sigma = 0$ and 1, T_2 is estimated to be about 18 and 80, respectively. T_1 and T_2 increase with σ.

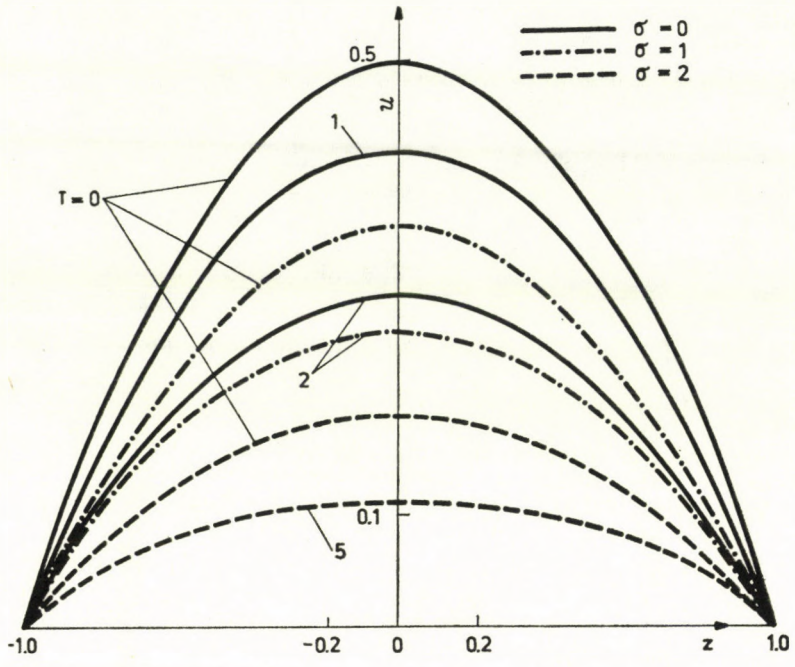

Fig. 1a. Primary flow ($T < T_1$)

When $T = 0$, $v = 0$ for all σ. As T increases, v becomes negative. Fig. 2 shows that v in the negative direction of the Y-axis increases till $T = T^*$ and then decreases. T^* is calculated to be 2.45, 3.6, 6.3 and 25.6 when $\sigma = 0$, 1, 2 and 5, respectively. The corresponding values for the maximum of v, occurring at the centre of the flow, are -0.25602, -0.20116, -0.09503 and -0.02007. When $T > T^*$, the v-profile decreases. The maximum of v is shifted towards the plates from the centre and with further increase in T, v-profile behaves just as that of u with the difference that it does not cut the Z-axis. In Fig. 1 (b) a steep fall may be observed in the velocity near the plates. For large T and σ, there arises in the vicinity of the plates a thin boundary layer whose thickness can be shown to be of $0(1/\alpha)$. This thickness diminishes as σ increases for a fixed T and vice versa. The velocity outside the layers falls off rapidly to zero and most of the flow takes place through the boundary layers.

When $T < T^*$, the mass flow rate m_y due to the secondary motion is less than m_x due to the primary flow. However, m_y dominates m_x when $T > T^*$. Fig. 3 shows the resultant flow $m = \sqrt{m_x^2 + m_y^2}$ decreases with increase in T for a fixed σ and vice versa. In Fig. 3 m_0 represents the mass flow rate for the Poiseuille flow. The permeability of the medium has, however, stronger influence in reducing mass flow rate compared to rotation. To give a quanti-

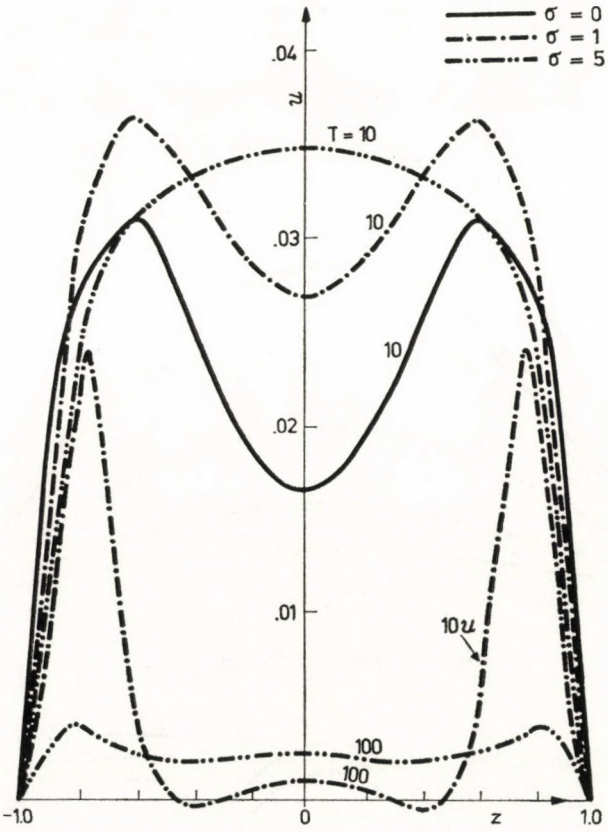

Fig. 1b. Primary flow ($T > T_1$)

tative estimate, there is a reduction of 25.7% in the mass flux as σ increases from 0 to 1, for $T = 1$, while this reduction is relatively less being 5.4%, as T increases from 0 to 1 for $\sigma = 1$.

Fig. 4. shows the plot of the primary and the secondary shear stresses at the lower plate $z = -1$ (that at the upper plate is just opposite in sign). The effect of increasing σ is to reduce both the shear stresses for a fixed T. For a fixed σ, the primary stress steadily decreases with T, while the secondary stress is observed to increase till $T = T^*$ and then decreases.

Fig. 5 shows that the effect of rotation for a fixed σ is, in general, to decrease the temperature at any point of the flow, this decrease diminishing with increase in σ. For large $\sigma(\sigma > 10)$, there is no appreciable change in temperature with rotation. When $\sigma \to \infty$, the temperature distribution assumes the linear form $t = 0.5\ (1 + z)$ and is independent of P_rE.

Fig. 6 illustrates the dependence of the Nusselt number at both the plates on T for different values of σ. When $\sigma \to \infty$, it is 0.5 for both the plates and remians the same practically for all T.

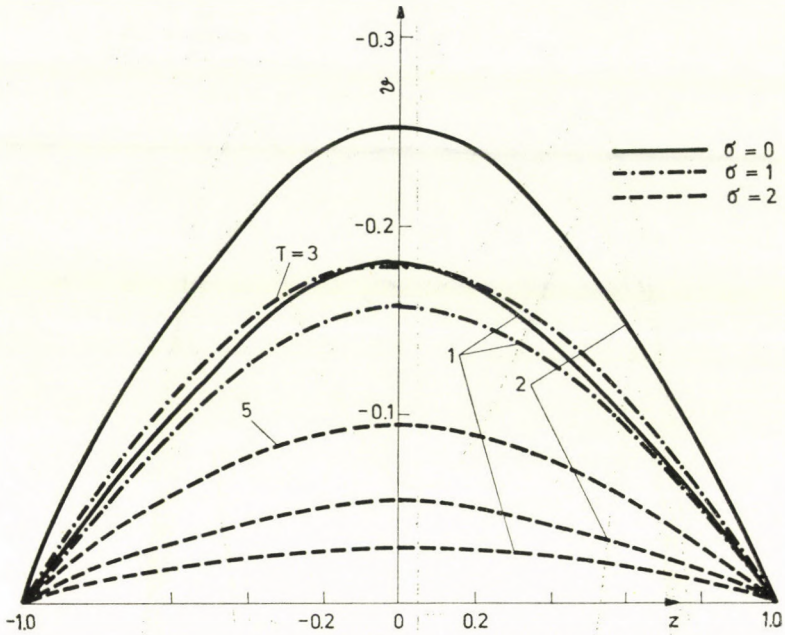

Fig. 2a. Secondary flow ($T < T^*$)

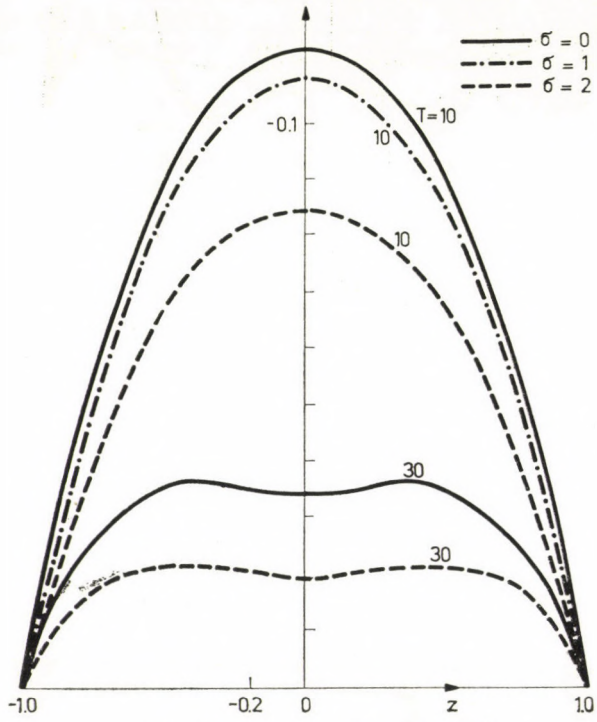

Fig. 2b. Secondary flow ($T > T^*$)

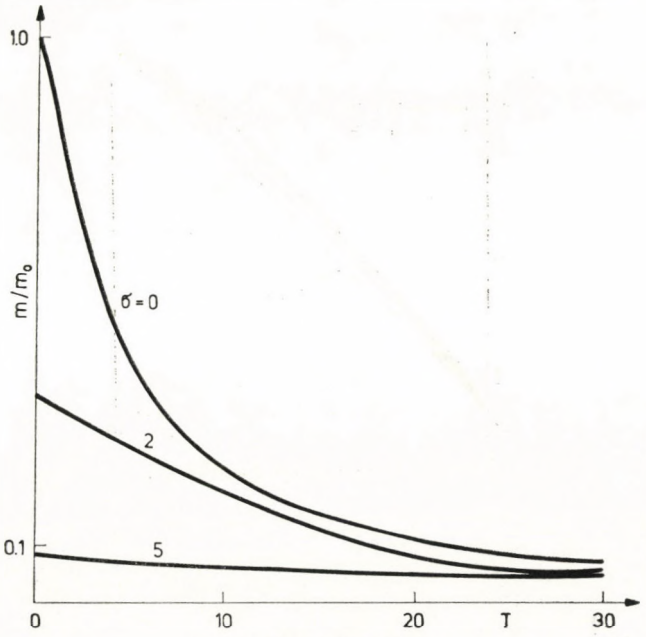

Fig. 3. Normalised flux

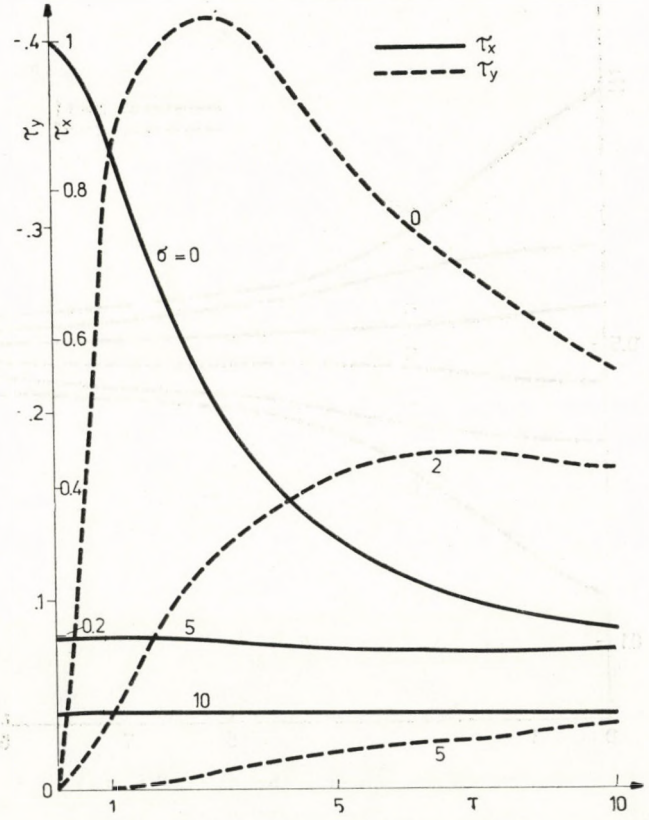

Fig. 4. Shear stresses at the lower plate

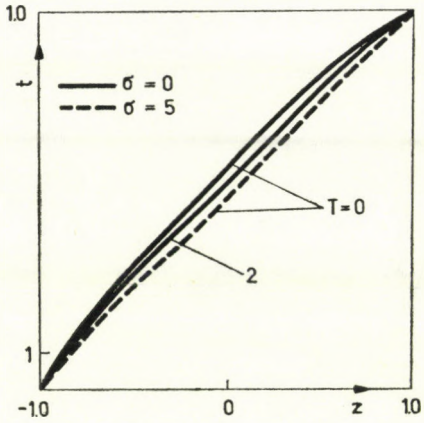

Fig. 5. Temperature distribution

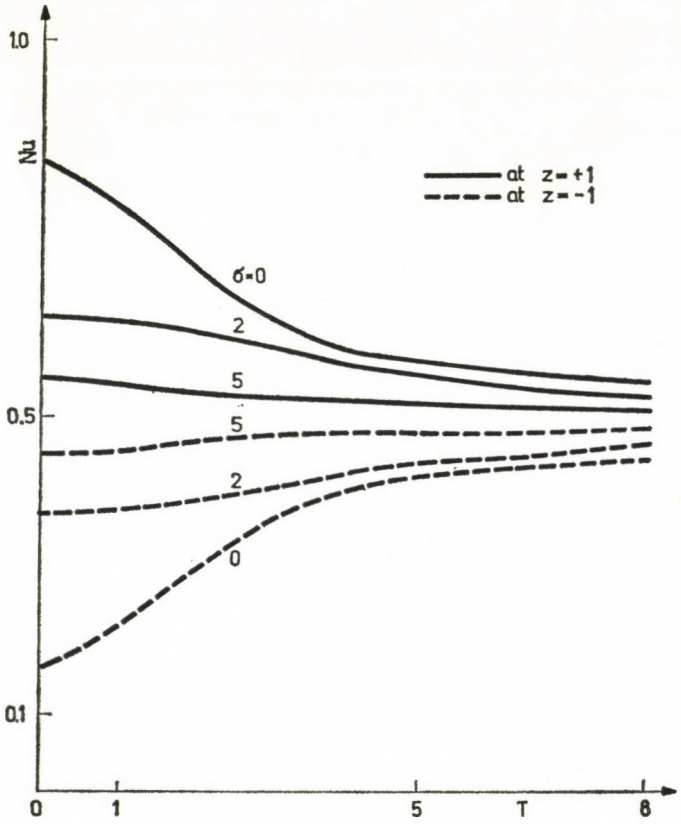

Fig. 6. Nusselt number at the plates ($P_rE = 1$)

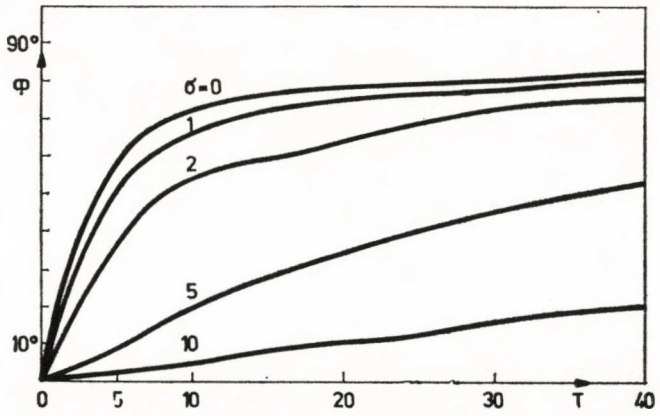

Fig. 7. The angle Φ as a function of T

Following [10], wherein suggestions were given for experimental verification, we can determine the angle $-\Phi$, at which the side plates are to be inclined to the X-axis in order that there is no total flow across them. Fig. 7 gives the angle $-\Phi$ versus T for different values of σ. We conclude from this that the angle Φ for any T decreases as σ increases. The effect of the permeability of the medium (increasing σ) is thus to inhibit the secondary flow through the side plates.

REFERENCES

1. A. E. Scheidegger, The Physics of Flow through Porous Media, University of Toronto Press, 1957.
2. J. Bear, Dynamics of Fluids in Porous Media, American Elsevier Publ. Co., New York, 1972.
3. C. S. Yih, Dynamics of Non-homogeneous Fluids, Macmillan Co., New York, 1965.
4. H. C. Brinckman, Appl. Sci. Res. A1, **27,** 81, 1947.
5. C. W. Tam, J. Fluid. Mech., **38,** 537, 1969.
6. T. S. Lundgren, J. Fluid. Mech., **51,** 273, 1972.
7. K. Yamamoto and Z. Yoshida, J. Phys. Soc. Japan, **37,** 774, 1974.
8. K. Yamamoto and N. Iwamure, J. Engg. Maths., **10,** 41, 1976.
9. N. Ch. Pattabhi Ramacharyulu, Int. Report No. 122. ICTP., Trieste, 1976.
10. V. Vidyanidhi and S. D. Nigam, J. Math. Phy Sci., **1,** 85, 1967.
11. V. Vidyanidhi, J. Math. Phy. Sci., **3,** 193, 1969.
12. R. S. Nanda and H. K. Mohanty, Appl. Sci. Res., **24,** 65, 1970.
13. V. Vidyanidhi, V. Bala Prasad and V. V. Ramana Rao, J. Phy. Soc. Japan, **39,** 1077, 1975.
14. V. V. Ramana Rao and V. Bala Prasad, Acta Phys. Hung., **42,** 143, 1977.
15. M. Mohan, Proc. Ind. Acad. Sci., **85,** 383, 1977.

Acta Physica Academiae Scientiarum Hungaricae, Tomus 45 (3), pp. 191—200 (1978)

SUR L'EQUIVALENCE DES THEORIES DE GRÜNEISEN ET DE BRILLOUIN POUR LA DILATATION THERMIQUE DES SOLIDES

Par

Y. THOMAS

INSTITUT DE RECHERCHES SCIENTIFIQUES ET TECHNIQUES
49045 ANGERS CEDEX, FRANCE

et

P. SIX

LABORATOIRE DE BIO-MATHÉMATIQUE, U.E.R. DES SCIENCES MÉDICALES ET PHARMACEUTIQUES
ANGERS, FRANCE

(Reçu 1. IX. 1978)

Une équivalence mathématique est établie entre les formules de GRÜNEISEN et BRILLOUIN pour la dilatation thermique des solides. dans l'approximation du continuum de Debye.

Le coefficient de dilatation linéaire d'un solide est alors calculé à l'aide de ces deux théories.

L'application des deux expressions dégagées à des solides ioniques et à des métaux conduit en effet a des résultats identiques en bon accord avec les mesures experimentales.

Equivalence mathématique

L'énergie libre peut s'écrire [1]:

$$F(V, T) = U_0(V) + F^*(T, V) = E(a) + \\ + \sum_i \frac{hvi}{2} + \sum_i + KT \log\left[1 - \exp\left(-\frac{hvi}{KT}\right)\right],$$

où $U_0(V)$ est l'énergie cohésive et $F^*(T, V)$ l'énergie vibrationnelle des oscillateurs.

La pression extérieure s'exerçant sur la surface du solide s'écrit:

$$P(T, V) = -\left(\frac{\partial F}{\partial V}\right)_T = P_0(V) + P^*(T, V).$$

$P_0(V)$ la pression interne statique et $P^*(T, V)$ la pression interne dynamique liée à l'agitation thermique équilibrent $P(T, V)$.

Naturellement seule $P^*(T, V)$, fonction du nombre de phonons naissant par élévation de température, participe à la dilatation thermique.

Dans l'approximation quasi-harmonique:

$$P^*(T, V) = -\left(\frac{\partial F^*}{\partial V}\right)_T = \sum_i h\left(\exp \cdot \frac{hvi}{KT} - 1\right)^{-1}\left(\frac{\partial v}{\partial V}\right)_T,$$

$U^*(T, V)$ étant l'énergie interne de vibration on retrouve l'équation d'état thermique du solide:

$$P^*(T, V) = \frac{U^* \gamma}{V}$$

si tous les coefficients $\gamma_i = -\frac{\partial \log \nu_i}{\partial \log V}$ sont égaux et constants quelque soit le mode dans "approximation de GRÜNEISEN ou, ce qui est plus logique, si on définit la moyenne:

$$\gamma = \frac{\sum_i h\nu_i \gamma_i}{\sum_i h\nu_i} .$$

Dans le cas d'un solide harmonique la fréquence est constante, P^* est nulle, le solide ne se dilate pas.

D'après la relation thermodynamique:

$$\frac{3\alpha}{X} = \left(\frac{\partial P}{\partial T}\right)_V = \left(\frac{\partial P^*}{\partial T}\right)_V$$

on a par exemple:

$$P^* = \int_0^T \left(\frac{3\alpha}{X}\right)_{P=0} dT .$$

La pression P^* est celle qu'il serait nécessaire d'appliquer sur la surface d'un solide, initialement à $P = 0$ et T, pour ramener son volume à celui du zéro absolu. On retrouve le résultat de BRILLOUIN [2] à l'aide des tenseurs correspondants: dans une transformation isochore un solide chauffé voit se développer sur ses faces un ensemble de contraintes hydrostatiques — appelées pressions thermiques — donnant naissance à une pression, égale à la pression extérieure à une constante près, et seule responsable de la dilatation thermique (sans doute grâce aux impulsions des phonons cédées aux parois).

BRILLOUIN a calculé les pressions de radiation exercées de l'intérieur vers l'extérieur par les ondes élastiques se propageant dans le solide lorsqu'elles se réfléchissent sur ses parois:

$$P_{m'} = \frac{U^*_{m'}}{V}\left(\frac{1}{3} - \frac{V}{v_{m'}}\frac{\partial v_{m'}}{\partial V}\right)$$

où v est la vitesse de groupe et m' le mode de polarisation des ondes. Evaluons le terme $\frac{\partial \log v_{m'}}{\partial \log V}$ qui rend compte du fait que les phonons ne peuvent être considérés comme un gaz indépendant des parois du solide.

Dans l'approximation du continuum de Debye, on peut écrire:

$$v_{m'} = \frac{\partial \omega_{m'}}{\partial \mathbf{K}} \simeq \frac{\omega_{m'}}{\mathbf{K}},$$

$\mathbf{K}$ est le vecteur d'onde dans l'espace réciproque (où le volume est $V' = \mathbf{K}^3$) et $\omega_{m'}$ la pulsation des ondes de polarisation m'.

$$\frac{\partial \log \frac{\omega_{m'}}{\mathbf{K}}}{\partial \log V} = \frac{\partial \log \omega_{m'} - \partial \log \mathbf{K}}{\partial \log V},$$

or

$$\frac{\partial V'}{V'} = -\frac{\partial V}{V} = 3\frac{\partial \mathbf{K}}{\mathbf{K}} \quad \text{d'ou} \quad \frac{1}{3} = -\frac{\partial \log \mathbf{K}}{\partial \log V}$$

et selon GRÜNEISEN:

$$\frac{\partial \log \omega_{m'}}{\partial \log V} = -\gamma_{m'}.$$

Soit:

$$P_{m'} = \frac{U^*_{m'}}{V}\left(\frac{1}{3} + \gamma_{m'} - \frac{1}{3}\right) = P^*.$$

On retrouve l'expression obtenue dans l'approximation quasi-harmonique. Les théories de MIE—GRÜNEISEN—DEBYE et de BRILLOUIN sont équivalentes dans l'approximation du continuum de DEBYE.

Calcul du coefficient de dilatation linéaire

Considérons ω atomes constituant la cellule de base d'un solide cristallin à une température de référence T_0 quelconque. Son volume est alors V_0 et a_0 le paramètre du réseau. Ce paramètre devient à une température voisine T par dilatation thermique de façon à ce que l'énergie libre F de la cellule soit minimale:

$$F = E(a) - KT \cdot \log f,$$

où $E(a)$ est l'énergie potentielle non thermique à l'équilibre (les atomes étant fixés dans leurs positions moyennes), K la constante de Boltzmann et f la fonction de partition des vibrations atomiques ν_i:

$$f = \prod_{i=1}^{3\omega}\left(\sum_{n=0,1,2\ldots} \exp -\left(n + \frac{1}{2}\right)\frac{h\nu_i}{KT}\right).$$

D'où à T donnée:

$$F = E(a) + \sum_{i=1}^{3\omega} \left[\frac{h\nu_i}{2} + KT \cdot \log \left(1 - e^{-\frac{h\nu_i}{KT}} \right) \right]$$

où l'on peut négliger l'énergie résiduelle quantique à OK: $\left(\sum_i \frac{h\nu_i}{2} \right)$ sans inconvénient par la suite.

En développant $E(a)$ en série de Taylor autour de a_0:

$$E(a) = E_{(a_0)} + \left[\frac{\partial E(a)}{\partial a} \right]_{a_0} (a - a_0) + \frac{1}{2} \left[\frac{\partial^2 E(a)}{\partial a^2} \right]_{a_0} (a - a_0)^2 + \ldots$$

que l'on écrit:

$$E(a) = E(a_0) + \eta(a - a_0) + \mu(a - a_0)^2 + \ldots$$

Si T varie, les atomes vibrent, l'amplitude des vibrations augmente ainsi que a. Les longueurs d'ondes λ_i pouvant se propager dans le solide varient. Les fréquences ν_i sont donc fonction de a (approximation quasi-harmonique) ce qui entraîne une variation du terme de l'énergie thermique $KT \cdot \log f$.

Cherchons pour quelle valeur de a l'énergie F est minimale à une température T donnée:

$$\frac{\partial F}{\partial a} = \eta + 2\mu(a - a_0) + \sum_{i=1}^{3\omega} KT \frac{\frac{h}{KT} e^{-\frac{h\nu_i}{KT}}}{1 - e^{-\frac{h\nu_i}{KT}}} \cdot \frac{d\nu_i}{da} = 0,$$

$$a - a_0 = -\frac{\eta}{2\mu} - \frac{h}{2\mu} \sum_{i=1}^{3\omega} \frac{1}{e^{\frac{h\nu_i}{KT}} - 1} \cdot \frac{d\nu_i}{da},$$

on en déduit le coefficient de dilatation linéaire isotrope près de T_0:

$$\alpha = \frac{1}{a_0} \frac{d}{dT} (a - a_0) = -\frac{h}{2\mu a_0} \sum_{i=1}^{3\omega} \frac{\frac{h\nu_i}{KT^2} e^{\frac{h\nu_i}{KT}}}{\left[e^{\frac{h\nu_i}{KT}} - 1 \right]^2} \cdot \frac{d\nu_i}{da},$$

$d\nu_i/da$ étant indépendant de ν_i, si on pose C_v, la chaleur spécifique, égale à la somme des fonctions d'Einstein:

$$\boxed{\alpha = -\frac{1}{2a_0\mu} \cdot \frac{d \log \nu}{da} \cdot C_v} \qquad (1)$$

en accord avec un résultat précédent [3]. Si a_0 est supposé constant, on retrouve α proportionnel à C_v selon une dépendance déjà mise en évidence par GRÜNEISEN.

A T_0, les atomes vibrant de part de d'autre de leurs positions moyennes d'équilibre a_0, l'écart interatomique instantané devient r. En posant $x = r - a_0$, l'énergie potentielle de la cellule développée en série de Taylor autour du minimum a_0 est à la constante $E(a_0)$ près:

$$E(r) = \frac{1}{2}\left[\frac{\partial^2 E(r)}{\partial r^2}\right]_{a_0} x^2 + \frac{1}{6}\left[\frac{\partial^3 E(r)}{\partial r^3}\right]_{a_0} x^3 + \dots$$

que l'on écrit:

$$E(r) = \frac{f}{2} x^2 - \frac{g}{3} x^3 + \dots$$

La force exercée par une particule sur les autres est au second ordre:

$$F(x) = -\frac{\partial E(r)}{\partial x} = -fx + gx^2$$

d'où sa valeur moyenne (l'écart x par rapport à la position d'équilibre étant en moyenne nul):

$$\bar{F}(x) = g\bar{x}^2 .$$

La force résultante s'exerçant sur la surface $S = 4\pi R^2$ de la cellule est $\omega . \bar{F}(x)$ où R est le rayon moyen de la cellule. En effet, on envisagera des champs de force à symétrie sphérique dans des solides ayant une structure cubique ou hexagonale compacte dans lesquels un atome est entouré d'un certain nombre d'autres atomes jouant tous des rôles identiques et placés à la distance $R = \frac{a_0}{\sqrt{2}}$ de l'atome considéré placé au centre d'une sphère .

La force avec laquelle une particule vibrant thermiquement agit sur l'aire unité est une pression thermique:

$$P_T = \frac{\omega \cdot \bar{F}(x)}{S} .$$

Lors de la dilatation de la cellule, ses atomes se comportent comme une sorte de gaz, la pression P_T est équilibrée par une pression élastique statique [2]:

$$P_E = -\frac{1}{X_0}\frac{dV}{V_0}$$

où X_0 est la compréssibilité à T_0. D'où:

$$\frac{1}{X_0}\frac{dV}{V_0} = \frac{\omega g \bar{x}^2}{2\pi a_0^2},$$

C_v étant la chaleur spécifique d'une mole et N le nombre d'Avogadro, chaque oscillateur a en moyenne l'énergie:

$$\bar{E}_{(r)} = \frac{f}{2}\bar{x}^2 = \int_0^T \frac{C_v}{N} dT.$$

D'après la définition du coefficient de dilatation linéaire $\alpha = \frac{1}{3V_0}\frac{dV}{dT}$:

$$\frac{dV}{3V_0} = \int \alpha dT = \frac{P_T X_0}{3} = \frac{\omega g \bar{E}_{(r)} X_0}{3\pi a_0^2 f}$$

d'où au voisinage de T_0:

$$\boxed{\alpha = \frac{\frac{\omega}{N}}{3\pi} \cdot \frac{g}{f} \cdot \frac{X_0}{a_0} \cdot C_v} \qquad (2)$$

Si on suppose X_0 et a_0 constants quelque soit T, on retrouve la dépendance de GRÜNEISEN.

Application aux solides ioniques

L'énergie potentielle d'équilibre d'un cristal représentant la chaleur de formation par mole est [4]:

$$E(a_0) = \frac{NMe^2}{a_0}\left(1 - \frac{1}{n}\right)$$

où M est la constante de Madelung, e la charge de l'électron et n la constante de Born.

Appliquons la formule (1):

$$\mu = \frac{NMe^2}{2a_0^3}(n-1) = \frac{nE(a_0)}{2a},$$

d'où

$$\alpha = -\frac{1}{n}\frac{a_0}{E(a_0)} \cdot \frac{d \log v}{da} \cdot C_v.$$

Pour les oscillations linéaires harmoniques des ions de masse m on a en première approximation:

$$\nu = \frac{1}{2\pi}\sqrt{\frac{2\mu}{m}} = \frac{1}{2\pi}\left[\frac{NMe^2}{ma_0^3}(n-1)\right]^{1/2},$$

$$\frac{d\nu}{da} = -\frac{n+4}{4\pi}\left[\frac{NMe^2}{na_0^5}(n-1)\right]^{1/2},$$

$$\frac{d\log\nu}{da} = -\frac{n+4}{2a_0}, \tag{1'}$$

d'où

$$\alpha = \frac{n+4}{2nE(a_0)} \cdot C_v.$$

A T_0, le potentiel interatomique est [4]:

$$E(r) = -\frac{Me^2}{r} + \frac{Me^2 a_0^{n-1}}{nr^n}.$$

Appliquons la formule (2):

$$f = \frac{(n-1)Me^2}{a_0^3} \quad \text{et} \quad g = \frac{(n+4)(n-1)Me^2}{2a_0^4}.$$

Si $\pi \simeq 3$ et si $a_0^3/\omega \cdot N = v_0$ (volume d'un atome gramme à T_0) on a:

$$\alpha = \frac{(n+4)}{18} \cdot \frac{X_0}{v_0} \cdot C_v.$$

Si $W_0' = NMe/a_0$ est l'énergie électrostatique de Madelung d'un atome gramme:

$$X_0 = \frac{9v_0}{(n-1)W_0'}$$

et

$$\alpha = \frac{n+4}{2(n-1)W_0'} C_v \tag{2'}$$

or $E(\alpha_0) = W_0'\left(1 - \frac{1}{n}\right)$: les formules (1') et (2') sont équivalentes. Le tableau I donne quelques examples.

Tableau I

Application à des solides ioniques

Solides ioniques $T^0 = 300$ K [7]	n	$E(a_0)$ $10^{-8} \cdot$ cal $\cdot$ mole^{-1}	C_v cal $\cdot$ K^{-1} $\cdot$ mole^{-1}	$\alpha(1')(2')$ $10^5 \cdot$ K^{-1}	α expérimental $10^5 \cdot$ K^{-1}	Différence %
NaCl	8	201	11.1	41,4	40	3,5
NaBr	8,5	171	12,5	43,1	43	0,3
NaF	7	215	10,1	36,6	36	1,7
LiF	6	240	9,6	33	34	2,9
LiCl	7	198	11,4	45,2	44	2,7
AgCl	9,5	204	12,2	31,5	32,8	4,2
MgO	7	940	11,5	9,7	10	3

Application aux métaux

Adoptons entre les ions adjacents d'un métal le potentiel central [5]:

$$E(a) = -\frac{A}{a} + \frac{Aa_0}{2a^2}$$

où A est une constante.

Appliquons la formule (1):

Des calculs analogues à ceux développées pour les solides ioniques conduisent à:

$$\alpha = \frac{2}{3E(a_0)} C_v \qquad (1'')$$

(c'est la fonction précédente [4] où $n = 2$).

Avec ce même potentiel à T_0 en fonction de r:

$$E_{(r)} = -\frac{A}{r} + \frac{Aa_0}{2r^2} .$$

Appliquons la formule (2):

$$f = \frac{A}{a_0^3} \text{ et } g = \frac{3A}{a_0^4}$$

d'où

$$\alpha = \frac{X_0}{3v_0} \cdot C_v$$

Tableau II

Application à des métaux

Métaux $T_0 = 300$ K [7]	a_0(Å) Constant	W_0 $10^{-8} \cdot$ cal $\cdot$ mole^{-1}	C_v cal $\cdot$ K$^{-1} \cdot$ mole^{-1}	$\alpha(1'')(2'')$ $10^5 \cdot$ K^{-1}	α expérimental $10^6 \cdot$ K^{-1}	K' (3) $10^{-4} \cdot$ cal$^{-1} \cdot$ m$^{-1} \cdot$ mole	K'' (4) $10^{-4} \cdot$ K$^{-1} \cdot$ m^{-1}
Li	3,46	160	5,85	55	57	2,7	16,4
Na	4,24	141	6,85	72	72	2,4	16,8
K	5,25	120	6,90	86	84	2,3	16,1
Be	2,28	702	3,78	8	9,2	1	4,2
Mg	3,20	552	6,02	16,3	20,1	0,8	5,1
Cu	3,61	539	6,0	16,4	16,1	0,78	4,5
TK 400			6,29	16,9	17,1	0,77	
TK 700			6,68	18,8	19,3	0,80	
TK 900			6,95	19,9	20,9	0,82	
Al	4,04	420	6,62	23,5	23,1	0,86	5,6
TK 400			7,0	24,8	25,0	0,88	
TK 500			7,41	27,0	26,6	0,88	
TK 600			7,83	28,1	27,6	0,87	
TK 700			8,31	30,0	29,2	0,87	

or l'énergie potentielle totale d'un atome gramme peut se mettre sous la forme [6]:

$$W_0 = -\frac{A'}{v_0^{1/3}} + \frac{A' a_0}{2 v_0^{2/3}}$$

ou A' est une constante et

$$X_0 = \frac{9}{2} \cdot \frac{v_0}{|W_0|} .$$

d'où

$$\alpha = \frac{3}{2|W_0|} \cdot C_v . \qquad (2'')$$

Les formules (1″) et (2″) sont aussi équivalentes.

Remarquons que $W_0 = \frac{(\text{constante}\, K_1)}{a_0}$ où K_1 dépend de la forme du potentiel et de la structure du réseau. Pour des corps de même structure:

$$\alpha = \frac{2}{3K_1} a_0 C_v = K' a_0 C_v . \qquad (3)$$

A haute température quand C_v est pratiquement constante:

$$\alpha = K'' a_0 \qquad (4)$$

(K' et K'' sont des constantes).

Le tableau II donne quelques exemples.

BIBLIOGRAPHIE

1. C. A. SWENSSON, J. Phys. Chem. Solids, **29**, 1337, 1968.
2. L. BRILLOUIN, Les tenseurs en mécanique et en élasticité, Masson, Paris, 1960.
3. Y. THOMAS, C. R. Acad. Sci. Paris, **265**, 1339, 1967.
4. L. V. AZÁROFF, Introduction to Solids, Mc. Graw-Hill, New York, 1960.
5. IA. I. FRENKEL, Introduction to the Theory of Metal, State Techn. and Theor. Lit. Press, 1950.
6. J. K. ROBERTS and A. R. MILLER, Heat and Thermodynamics, Blackie and Son, London, 1960.
7. F. SEITZ, Théorie moderne des solides, Masson, Paris, 1949.
J. C. SLATER, Introduction to Chemical Physics, Mc. Graw-Hill, New York, 1939.

Acta Physica Academiae Scientiarum Hungaricae, Tomus 45 (3), pp. 201–211 (1978)

VARIATIONAL SOLUTION OF HEAT CONVECTION IN THE CHANNEL FLOW WITH THE HELP OF GPDP

By

P. SINGH and K. K. SRIVASTAVA

DEPARTMENT OF MATHEMATICS, INDIAN INSTITUTE OF TECHNOLOGY, KANPUR-208016, INDIA

(Received 7. IX. 1978)

The Governing Principle of Dissipative Processes is applied to study the temperature distribution in the fluid flow inside two parallel semi-infinite plates. It is found that the flux representation of the principle yields exactly the same result as obtained with the help of Lagrangian thermodynamics of BIOT. The results obtained in the present analysis compare well with the exact ones.

Introduction

The aim of the present analysis is two-fold: firstly, to develop a variational method to get the temperature distribution in the fluid flow inside a channel and secondly, to show that the result obtained with the help of flux representation of GPDP is equivalent to that of Lagrangian thermodynamics of BIOT. The present variational method is based on the governing principle of dissipative processes which describes the evolution of dissipative transport processes in space and time [1, 2]. The principle is

$$\delta \int_V (\sigma - \psi - \Phi)\, dV = 0\,, \tag{1}$$

where σ denotes the rate of entropy production and ψ, Φ are the dissipation potentials which are obtained from entropy production with the help of linear constitutive relations given by ONSAGER in 1931 [3]. It is well known that GPDP results into two partial forms known as force and flux representations. It has been already proved by GYARMATI and his co-workers [2] that the force representation is equivalent to the local potential method of GLANSDORFF and PRIGOGINE [4]. This fact has also been proved recently for particular problems in viscuous flows and heat transfer by SINGH [5, 6, 7, 8].

Recently, SINGH [9] has proved that the Lagrangian thermodynamics of BIOT is equivalent to the flux representation of GYARMATI's principle. In this paper we have established this fact by investigating the temperature distribution in the fluid flowing laminarly inside two semi-infinite parallel plates. The analytical expression for the temperature distribution is obtained when

the fluid is flowing with a uniform velocity U. The result obtained with the help of GPDP is quite close to the exact result. It is found that the flux representation gives exactly the same result as obtained by NIGAM and AGARWAL [10] with the help of Lagrangian thermodynamics of BIOT [11].

Formulation of the problem

Let us consider the flow of an incompressible fluid in a channel which is assumed to be uniform and semi-infinite that is $0 \leq x \leq \infty$, the x-axis is taken along the length of the channel. For the sake of simplicity the entry conditions are neglected and the flow is assumed to be a fully developed laminar flow, $U = U(y, z)$. It has been shown by many workers that for Peclet number > 100 the effect of axial conduction is almost negligible (SCHNEIDER [12], MILLSAPES and POHLHAUSEN [13], SINGH [14]). The equation for steady heat convection with axial conduction and viscous dissipation neglected is given by

$$\frac{\partial}{\partial y}\left(k\frac{\partial \theta}{\partial y}\right) + \frac{\partial}{\partial z}\left(k\frac{\partial \theta}{\partial z}\right) = CU\frac{\partial \theta}{\partial x}\,, \tag{2}$$

where $k(y, z)$ is the thermal conductivity, $C(y, z)$ the heat capacity per unit volume of the fluid and $U(y, z)$ is the fully developed laminar velocity in the channel. For the slug flow (U is constant) between two semi-infinite parallel plates, Eq. (2) reduces to

$$k\frac{\partial^2 \theta}{\partial y^2} = CU\frac{\partial \theta}{\partial x}\,, \tag{3}$$

where k and C are kept constant. The boundary conditions are

$$\begin{aligned} &\theta = 0 \quad \text{at } x = 0\text{: } 0 < y < 2l; \\ &\theta = \theta_0 \quad \text{at } x > 0\text{: } y = 0, 2l\,. \end{aligned} \tag{4}$$

Therefore

$$\frac{\partial \theta}{\partial y} = 0 \quad \text{at } y = l\,. \tag{5}$$

Considering only the region between $y = 0$, $y = l$; the temperature distribution is assumed to be represented by a parabola and the phenomenon is considered in two phases. In the first phase which extends up to x_1 the effect of wall temperature penetrates only up to a depth q_1 (Fig. 1), the temperature in the shaded part being that of the incident fluid.

In the formulation of governing principle, it is well-known that the basic requirement is the balance equation of the system. Here writing the equation of energy (3) as energy balance, we have

$$\frac{\partial \theta}{\partial x} + \frac{\partial}{\partial y} J_q = 0 \,, \tag{6}$$

where J_q denotes the heat current density and it is given, here, by the following linear constitutive law

$$J_q = -L \frac{\partial \theta}{\partial y} \,. \tag{7}$$

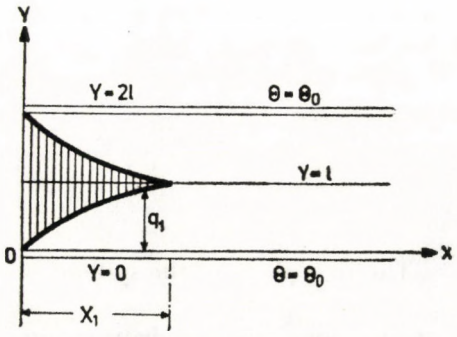

Fig. 1. Fluid flow between parallel walls

Here $L = k/CU$ is constant. The alternative form of the constitutive equation can be written as

$$\frac{\partial \theta}{\partial y} = -\frac{1}{L} J_q \,. \tag{8}$$

The entropy production σ of the system is given by

$$\sigma = -J_q \frac{\partial \theta}{\partial y} \tag{9}$$

and the dissipation potentials are given by

$$\psi = \frac{L}{2} \left(\frac{\partial \theta}{\partial y} \right)^2, \quad \Phi = \frac{1}{2L} J_q^2 \,. \tag{10}$$

Finally GYARMATI's principle (1) takes the form

$$\delta \int_V \left[-J_q \frac{\partial \theta}{\partial y} - \frac{L}{2} \left(\frac{\partial \theta}{\partial y} \right)^2 - \frac{1}{2L} J_q^2 \right] dV = 0 \,, \tag{11}$$

where dV denotes the elementary volume of the system. It is clear that (11) contains two independent variables J_q and θ. The driving force of the system is $\partial\theta/\partial y$ and hence we take θ as the basic quantity and J_q is substituted by another temperature θ^* which is related with J_q through the following approximate constitutive law

$$J_q = -L\frac{\partial\theta^*}{\partial y}. \tag{12}$$

It should be noted that θ^* satisfies the same conditions as θ. Using (12), the principle (11) and the balance equation (6) become

$$\delta\int_V\left[\frac{\partial\theta}{\partial y}\frac{\partial\theta^*}{\partial y}-\frac{1}{2}\left(\frac{\partial\theta}{\partial y}\right)^2-\frac{1}{2}\left(\frac{\partial\theta^*}{\partial y}\right)^2\right]dV=0, \tag{13}$$

$$\frac{\partial^2\theta^*}{\partial y^2}=\frac{CU}{k}\frac{\partial\theta}{\partial x}. \tag{14}$$

The first phase of the system

In the first phase, the temperature distribution is approximated by

$$\theta=\theta_0\left(1-\frac{y}{q_1}\right)^2 \quad \text{for} \quad y<q_1, \tag{15}$$

$$\theta=0 \quad \text{for} \quad y>q_1.$$

This profile (15) satisfies the conditions (4) and (5). Using (15) in (14), and integrating, we get

$$\frac{\partial\theta^*}{\partial y}=\frac{CU}{k}\theta_0 q_1'\left(\frac{y^2}{q_1^2}-\frac{2}{3}\frac{y^3}{q_1^3}-\frac{1}{3}\right). \tag{16}$$

In getting (16) we have used the condition

$$\frac{\partial\theta^*}{\partial y}=0 \quad \text{at} \quad y=q_1. \tag{17}$$

The principle (13) for first phase becomes

$$\delta\int_0^\infty\int_0^{q_1}\left[\frac{\partial\theta}{\partial y}\frac{\partial\theta^*}{\partial y}-\frac{1}{2}\left(\frac{\partial\theta}{\partial y}\right)^2-\frac{1}{2}\left(\frac{\partial\theta^*}{\partial y}\right)^2\right]dy\,dx=0. \tag{18}$$

The use of (15) and (16) in principle (18) gives

$$\delta \int_0^{\infty} \left(q_1' - \frac{13}{147} \frac{q_1}{L} q_1'^2 - \frac{20}{7} \frac{L}{q_1} \right) dx = 0 \,, \tag{19}$$

where prime denotes derivative with respect to x. The Euler-Lagrange equation of (19) is obtained as

$$2q_1^3 q_1'' + q_1^2 q_1'^2 + \frac{420}{13} L^2 = 0 \,. \tag{20}$$

The solution of this equation is easily found to be

$$q_1 = q x^{1/2}, \tag{21}$$

where q is given by

$$q = 3.3716 \left(\frac{k}{CU} \right)^{1/2} . \tag{22}$$

Finally q_1 may be written in the form

$$q_1 = 2l(3.3716) \left(\frac{\varkappa}{2lPe} \right)^{1/2} , \tag{23}$$

where $Pe = 2lCU/k$ is the Peclet number. The temperature distribution θ_1 in the first phase is thus obtained as

$$\theta_1 = \theta_0 \left[1 - \frac{y}{2l(3.3716) \left(\frac{x}{2lPe} \right)^{1/2}} \right]^2 . \tag{24}$$

Defining the mean mixed temperature in this phase by

$$T_{m1} = \int_0^{q_1} U\theta_0 \left(1 - \frac{y}{q_1} \right)^2 dy \Big/ \int_0^{l} U dy \,,$$

we get it as

$$\bar{\theta}_1 = - \frac{T_{m1} - \theta_0}{\theta_0} = \left[1 - 2.247 \left(\frac{x}{2lPe} \right)^{1/2} \right] . \tag{25}$$

The first phase of the system ends at a distance $x = x_1$ where the effect of wall temperature penetrates upto the half of the channel width. Thus x_1 is obtained from (23) by putting $q_l = l$

$$x_1 = (0.02199)\, 2lPe \,. \tag{26}$$

The second phase of the system

Let us assume that in the second phase the temperature θ at $y = l$ is denoted by $q_2(x)$. In this region, the temperature distribution may be approximated as

$$\theta = (\theta_0 - q_2)\left(1 - \frac{y}{l}\right)^2 + q_2\,, \tag{27}$$

which satisfies the conditions

$$\begin{aligned} &\theta = \theta_0 \quad \text{at} \quad y = 0 \\ &\theta = q_2, \frac{\partial\theta}{\partial y} = 0 \quad \text{at} \quad y = l. \end{aligned} \tag{28}$$

The balance equation (14) using (27) gives

$$\frac{\partial\theta^*}{\partial y} = \frac{CUl}{k} q_2' \left(\frac{y^2}{l^2} - \frac{y^3}{3l^3} - \frac{2}{3}\right) \tag{29}$$

which satisfies the condition $\partial\theta^*/\partial y = 0$ at $y = l$. The principle (13) in this case becomes

$$\delta \int_0^\infty \int_0^l \left[\frac{\partial\theta}{\partial y}\frac{\partial\theta^*}{\partial y} - \frac{1}{2}\left(\frac{\partial\theta}{\partial y}\right)^2 - \frac{1}{2}\left(\frac{\partial\theta^*}{\partial y}\right)^2\right] dy\,dx = 0. \tag{30}$$

Using expressions (27) and (29) and integrating with respect to y, principle (30) becomes

$$\delta \int_0^\infty \left[\frac{4}{15} l q_2'(\theta_0 - q_2) - \frac{17}{105} q_2'^2 \frac{l^3}{L} - \frac{L}{l}(\theta_0 - q_2)^2\right] dx = 0. \tag{31}$$

The Euler-Lagrange equation of the principle is

$$q_2'' - \frac{105}{17}\frac{L^2}{l^4}(q_2 - \theta_0) = 0\,. \tag{32}$$

The solution of (32) is easily obtained as

$$q_2 - \theta_0 = -\exp\left[-0.2185\left(\frac{x}{x_1} - 1\right)\right], \tag{33}$$

which satisfies the conditions

$$\begin{aligned} &q_2 \to \theta_0 \quad \text{as} \quad x \to \infty \\ &q_2 = 0 \quad \text{at} \quad x = x_1. \end{aligned} \tag{34}$$

The temperature distribution θ_2 in the second phase is

$$\theta_2 = \theta_0 \left[1 + \left\{ \left(1 - \frac{y}{l} \right)^2 - 1 \right\} \left\{ \exp \left[-0.2185 \left(\frac{x}{2l\, Pe(0.02199)} - 1 \right) \right] \right\} \right] . \quad (35)$$

The mean mixed temperature in the second phase is

$$\bar{\theta}_2 = \frac{2}{3} \exp \left[-0.2185 \left(\frac{x}{2l\, Pe\, (0.02199)} - 1 \right) \right] . \quad (36)$$

The exact solution for the temperature distribution obtained by SCHNEIDER [12] and DOEST–SCHENK [15] is

$$\theta = \theta_0 \left[1 - \frac{4}{\pi} \sum_{n=1}^{\infty} \frac{1}{2n-1} \sin \frac{\pi}{2l} y\,(2n-1) \exp \left(- \frac{(2n-1)^2 \pi^2 x^2}{2l\, Pe} \right) \right] . \quad (37)$$

Table I

	θ/θ_0 (present solution)					θ/θ_0 (exact solution)				
$\downarrow \frac{y}{2l} \Big/ \frac{x}{2l\,Pe} \rightarrow$	0.005	0.01	0.1	0.2	1	0.005	0.01	0.1	0.2	1
0	1	1	1	1	1	1	1	1	1	1
0.05	0.6245	0.7253	0.9126	0.9677	0.99999	0.62	0.724	0.915	0.97	0.00000
0.10	0.337	0.4947	0.8434	0.9388	0.99998	0.32	0.48	0.833	0.94	0.99998
0.20	0.0259	0.1654	0.7056	0.8912	0.99995	0.043	0.168	0.72	0.89	0.99996
0.30	0	0.0121	0.6136	0.8572	0.99994	0	0.021	0.61	0.852	0.99994
0.50	0	0	0.54	0.83	0.99993	0	0	0.526	0.823	0.99993

Table II

$x/2l\,Pe$	$\bar{\theta}$ 1,2	
	present solution	exact solution
0.0	1.0	1.0
0.005	0.8427	0.840
0.01	0.7753	0.774
0.05	0.5407	0.496
0.1	0.3067	0.306
0.2	0.1133	0.117
0.5	0.0057	0.0058
1	0.0001	0.00005
∞	0	0

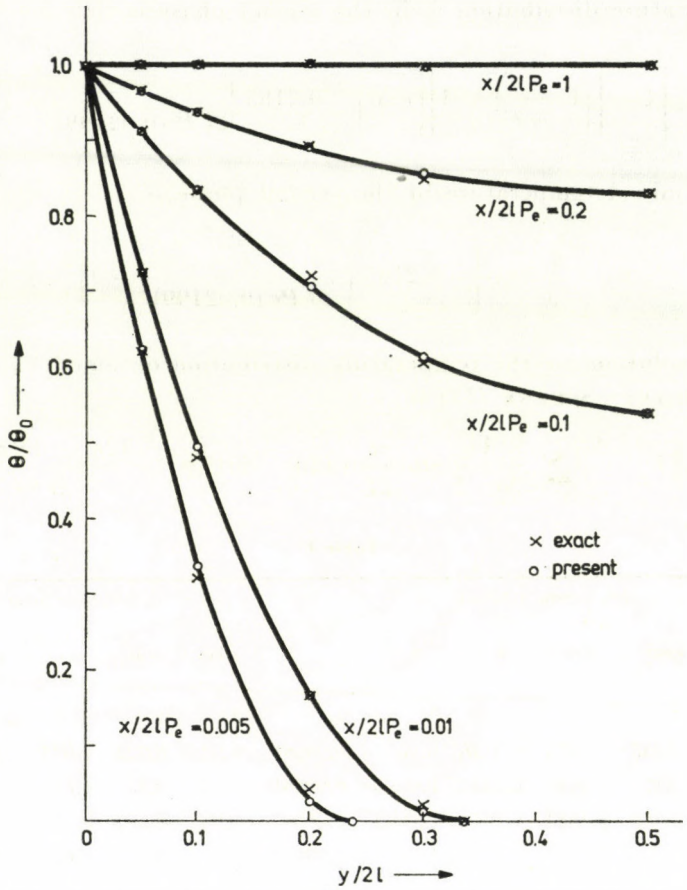

Fig. 2. The temperature distribution θ/θ_0 against $y/2l$ for various values of $x/2l\ P_e$

Table I shows the variation of θ/θ_0 with $y/2l$ for various values of $x/2lPe$. The comparison of the temperature distribution of the present method with the exact result is clearly predicted in Fig. 2. The variation of mean mixed temperature from exact and present method is shown in Table II and Fig. 3. The agreement between the present and the exact solution is seen to be quite satisfactory.

Flux representation and comparison with Biot's method

In the flux representation, GYARMATI's principle (13) takes the form

$$\delta \int_V \left[\frac{\partial \theta}{\partial y} \frac{\partial \theta^*}{\partial y} - \frac{1}{2} \left(\frac{\partial \theta^*}{\partial y} \right)^2 \right] dV = 0 \tag{38}$$

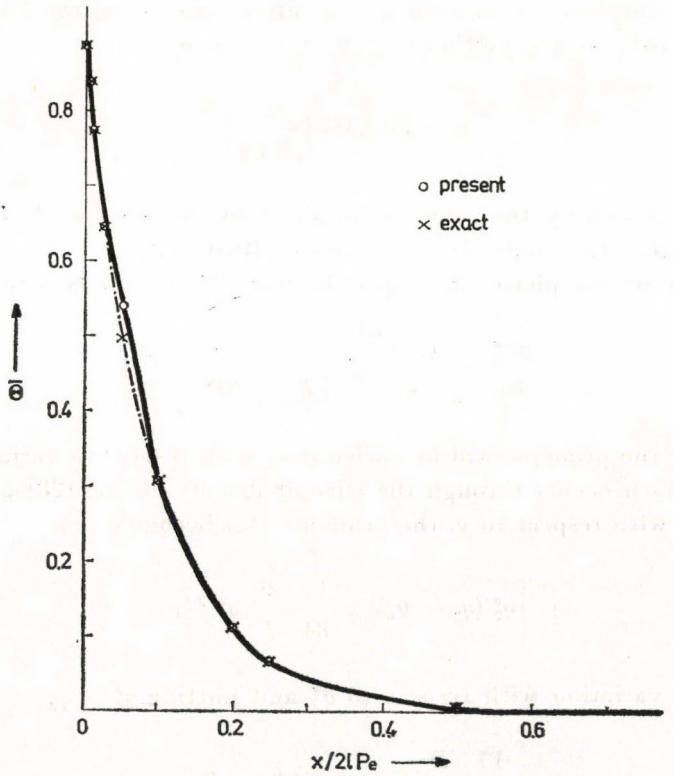

Fig. 3. Mean temperature $\bar{\theta}_{1,2}$ against $x/2lP_e$

and the variation is taken only with respect to stared quantities. To distinguish the variational parameter q_1 occurring in θ and θ^*, we write from (16) as

$$\frac{\partial\theta^*}{\partial y} = \frac{CU}{k}\,\theta_0 q_1^{*\prime}\left(\frac{y^2}{q_1^{*2}} - \frac{2y^3}{3q_1^{*3}} - \frac{1}{3}\right). \tag{39}$$

By putting the value of θ and θ^* from (15) and (39) into (38), we get the principle in first phase as

$$\delta\int_0^\infty \left[\frac{13}{630}\frac{q_1^*}{L}q_1^{*\prime 2} + \frac{1}{10}\frac{q_1^*}{q_1^2}q_1^{*\prime} - \frac{1}{3}\frac{q_1^*}{q_1}q_1^{*\prime}\right]dx = 0\,. \tag{40}$$

Taking the variation with respect to stared quantities, we get Euler-Lagrange equation of (40) as

$$q_1 q_1' - \frac{147}{26}L = 0\,. \tag{41}$$

This Eq. is obtained by putting $q_1 = q_1^*$ after considering the variation. The solution of (41) with condition $q_1 = 0$ at $x = 0$, is

$$q_1 = 2l(3.36)\left(\frac{x}{2l\,Pe}\right)^{1/2}. \tag{42}$$

This result is exactly the same as obtained by NIGAM and AGARWAL using the Lagrangian thermodynamic method of BIOT [10].

In the second phase, the expression for $\partial\theta^*/\partial y$ may be written as

$$\frac{\partial\theta^*}{\partial y} = \frac{CUl}{k} q_2^{*\prime}\left(\frac{y^2}{l^2} - \frac{y^3}{3l^3} - \frac{2}{3}\right). \tag{43}$$

In this case the principle will be varied only with respect to variational parameter q_2^* which occurs through the current density. Using (28) and (43) and integrating with respect to y, the principle (38) becomes

$$\delta\int_0^\infty \left[q_2^{*\prime}(q_2 - \theta_0) + \frac{17}{84}\frac{l^2}{L} q_2^{*\prime 2}\right] dx = 0\,. \tag{44}$$

Taking the variation with respect to q_2^* and putting $q_2^* = q_2$

$$\frac{17}{42}\frac{l^2}{L} q_2' + q_2 - \theta_0 = 0\,. \tag{45}$$

The solution of (45) with $q_2 = 0$ at $x = x_1$ is

$$q_2 = \theta_0\left[1 - \exp\left\{-0.2186\left(\frac{x}{x_1} - 1\right)\right\}\right]. \tag{46}$$

To get this form we have used relation (42) with $q_1 = l$ at $x = x_1$. This is exactly the same as obtained by NIGAM and AGARWAL [10]. Thus it is proved that BIOT's method is equivalent to the flux representation of GYARMATI's principle.

Acknowledgement

The authors are thankful to Prof. I. GYARMATI for his encouragement.

REFERENCES

1. I. GYARMATI, Ann. Phys., **23,** 353, 1969.
2. I. GYARMATI, Non-equilibrium Thermodynamics, Springer, Berlin, 1970.
3. L. ONSAGER, Phys. Rev., **37,** 405, 1931: **37,** 2265, 1931.
4. P. GLANSDORFF and I. PRIGOGINE, Thermodynamic Theory of Structure, Stability and Fluctuations, Wiley Interscience, New York, 1971.
5. P. SINGH, Int. J. Heat Mass Transfer, **19,** 581, 1976.
6. P. SINGH, J. Non-Equilib. Thermodyn., **1,** 105, 1976.
7. P. SINGH, Acta Phys. Hung., **43,** 59, 1977.
8. P. SINGH, Acta Mech. **30,** 137, 1978.
9. P. SINGH, Acta Phys., **43,** 133, 1977.
10. S. D. NIGAM and H. C. AGARWAL, J. Math. and Mech., **9,** 689, 1960.
11. M. A. BIOT, Variational Principle in Heat Transfer, Oxford, 1970.
12. P. J. SCHNEIDER, Trans. A. S. M. E., **79,** 765, 1957.
13. K. MILLSAPES and K. POHLHAUSEN, Proceedings of the Conference on Differential Equations, University of Maryland, 271, 1956.
14. S. N. SINGH, Appl. Sci. Res., **A7,** 325, 1958.
15. V. D. DOES and J. SCHENK, Appl. Sci. Res., **3,** 308, 1953.

Acta Physica Academiae Scientiarum Hungaricae, Tomus 45 (3), pp. 213—220 (1978)

RAYLEIGH-TAYLOR INSTABILITY OF TWO VISCOELASTIC SUPERPOSED FLUIDS

By

R. C. SHARMA and K. C. SHARMA

DEPARTMENT OF MATHEMATICS, HIMACHAL PRADESH UNIVERSITY, SIMLA-171005, INDIA

(Received 8. IX. 1978)

The stability of the plane interface separating two viscoelastic superposed fluids of uniform densities has been studied. The stability analysis has been carried out, for mathematical simplicity, for two highly viscous fluids of equal kinematic viscosities. It is found that the system is stable for stable configuration and unstable for unstable configuration. The behaviour of growth rates with respect to stress relaxation time and strain retardation time parameters are examined analytically.

1. Introduction

The instability of the plane interface between two incompressible and viscous fluids of different densities when the lighter is accelerated into the heavier has been discussed by CHANDRASEKHAR [2]. The influence of viscosity on the stability of the plane interface separating two incompressible superposed fluids of uniform densities, when the whole system is immersed in a uniform horizontal magnetic field, is studied by BHATIA [1]. He has carried out the stability analysis for two fluids of equal kinematic viscosities and different uniform densities.

SHARMA [4] studied the thermal instability of a layer of viscoelastic (OLDROYD) fluid acted on by a uniform rotation. The rotation is found to have a destabilizing as well as a stabilizing effect under certain conditions in contrast to that of a Maxwell fluid where it always has a destabilizing effect. The stability of a layer of Oldroyd fluid heated from below and subject to a magnetic field has been studied by SHARMA [5].

It may be of some interest to study the stability of the plane interface separating two incompressible superposed viscoelastic fluids of uniform densities. This aspect forms the subject matter of the present paper wherein we have carried out the stability analysis for two fluids of equal kinematic viscosities and different uniform densities.

2. Perturbation equations

Consider a static state, in which an incompressible viscoelastic fluid of variable density is arranged in horizontal strata and the pressure p and the density ϱ are functions of the vertical coordinate z only. The character of the equilibrium of this initial static state is determined, as usual, by supposing that the system is slightly disturbed and then by following its further evolution. The fluid is assumed to have a viscoelastic nature described by the OLDROYD constitutive relation.

The constitutive relation for the fluid, as proposed by OLDROYD [3], is

$$\left.\begin{aligned} T'_{ij} &= T_{ij} - \delta_{ij} p, \\ \left(1 + \lambda \frac{d}{dt}\right) T_{ij} &= 2\mu \left(1 + \lambda_0 \frac{d}{dt}\right) e_{ij}, \\ e_{ij} &= \frac{1}{2}\left(\frac{\partial u_i}{\partial x_j} + \frac{\partial u_j}{\partial x_i}\right), \end{aligned}\right\} \tag{1}$$

where T_{ij}, e_{ij}, μ, λ and λ_0 ($<\lambda$) denote respectively the shear stress tensor, the rate of strain tensor, the viscosity, the stress relaxation time and the strain retardation time. p is the isotropic pressure, δ_{ij} the Kronecker delta, d/dt the mobile operator while u_i and x_i are the velocity and position vector, respectively.

Let $\mathbf{u}(u, v, w)$, $\delta\varrho$ and δp denote the perturbations in velocity, density ϱ and pressure p, respectively. Then the linearized perturbation equations relevant to the problem are

$$\left(1 + \lambda \frac{\partial}{\partial t}\right) \varrho \frac{\partial \mathbf{u}}{\partial t} = \left(1 + \lambda \frac{\partial}{\partial t}\right) [-\nabla \delta p + \mathbf{g}\delta\varrho] + \varrho\nu \left(1 + \lambda_0 \frac{\partial}{\partial t}\right) \nabla^2 \mathbf{u} + \\ + \left(1 + \lambda_0 \frac{\partial}{\partial t}\right) \left(\frac{\partial w}{\partial \bar{x}} + \frac{\partial \mathbf{u}}{\partial z}\right) \frac{d\mu}{dz}, \tag{2}$$

$$\nabla \cdot \mathbf{u} = 0, \tag{3}$$

$$\frac{\partial}{\partial t} \delta\varrho = -wD\varrho, \tag{4}$$

where $\nu (= \mu/\varrho)$ denotes the kinematic viscosity of the fluid, $\mathbf{g}(0, 0, -g)$ the acceleration due to gravity, $\bar{x} = (x, y, z)$ and $D = d/dz$. Eq. (4) ensures that the density of every particle remains unchanged as we follow it with its motion. Analyzing the disturbances into normal modes, we assume that the perturbed quantities have the space and time dependence of the form

$$f(z) \exp (ik_x x + ik_y y + nt), \tag{5}$$

where n is the growth rate of the harmonic disturbance, k_x and k_y are the horizontal wave numbers ($k^2 = k_x^2 + k_y^2$) and $f(z)$ is some function of z.

For perturbations of the form (5), Eqs. (2)—(4) become

$$(1 + \lambda n)\,\varrho n u = (1 + \lambda n)(-ik_x\,\delta p) + \varrho\nu(1 + \lambda_0 n)\,(D^2 - k^2)u + \\ + (1 + \lambda_0 n)(ik_x w + Du)D\mu, \tag{6}$$

$$(1 + \lambda n)\,\varrho\, nv = (1 + \lambda n)\,(-ik_y\,\delta p) + \varrho\nu(1 + \lambda_0 n)(D^2 - k^2)v + \\ + (1 + \lambda_0 n)\,(ik_y\, w + Dv)\,D\mu\,, \tag{7}$$

$$(1 + \lambda n)\,\varrho n w = (1 + \lambda n)[-\,D\delta p - g\delta\varrho] + \\ + \varrho\nu(1 + \lambda_0\, n)\,(D^2 - k^2)w + 2(1 + \lambda_0 n)\,DwD\mu\,, \tag{8}$$

$$ik_x\, u + ik_y\, v + Dw = 0, \tag{9}$$

and

$$n\delta\varrho = -w(D\varrho), \tag{10}$$

where

$$D = d/dz\,.$$

Multiplying Eqs. (6) and (7) by $-ik_x$ and $-ik_y$, respectively, adding the resultant equations and using Eq. (9) in it, we obtain

$$(1 + \lambda n)\varrho n Dw = (1 + \lambda n)(-k^2\delta p) + \\ + \varrho\nu(1 + \lambda_0 n)(D^2 - k^2)\,Dw + (1 + \lambda_0 n)(D\mu)(D^2 + k^2)w\,. \tag{11}$$

Substituting for $\delta\varrho$ from (10) in Eq. (8) and eliminating δp between Eqs. (8) and (11), we obtain the equation in w

$$n(1 + \lambda n)\,[D(\varrho Dw) - k^2\,\varrho w] - (1 + \lambda_0 n)\,[D\{\varrho\nu\,(D^2 - k^2)\,Dw\} - \\ k^2\,\varrho\nu\,(D^2 - k^2)w] + \frac{gk^2}{n}(1 + \lambda n)(D\varrho)w - (1 + \lambda_0\, n) \times \\ \times\,[D\{(D\mu)(D^2 + k^2)w\} - 2k^2(D\mu)(Dw)] = 0\,. \tag{12}$$

3. Two superposed viscoelastic fluids of uniform densities

We consider the case when two superposed fluids of uniform densities ϱ_1 and ϱ_2 and uniform viscosities μ_1 and μ_2 are separated by a horizontal boundary at $z = 0$. The subscripts 1 and 2 distinguish the lower and the upper fluids, respectively. Then, in each region of constant ϱ and constant μ, Eq. (12) becomes

$$(D^2 - k^2)(D^2 - q^2)w = 0, \tag{13}$$

where

$$q^2 = k^2 + \frac{n}{\nu}\left(\frac{1+\lambda n}{1+\lambda_0 n}\right).$$

Since w must vanish both when $z \to +\infty$ (in the upper fluid) and $z \to -\infty$ (in the lower fluid), the general solution of Eq. (13) can be written as

$$w_1 = A_1 e^{+kz} + B_1 e^{+q_1 z}, (z < 0) \tag{14}$$

$$w_2 = A_2 e^{-kz} + B_2 e^{-q_2 z}, \quad (z > 0) \tag{15}$$

where A_1, B_1, A_2, B_2 are constants of integration,

$$q_1 = \sqrt{k^2 + \frac{n}{\nu_1}\left(\frac{1+\lambda n}{1+\lambda_0 n}\right)} \quad \text{and} \quad q_2 = \sqrt{k^2 + \frac{n}{\nu_2}\left(\frac{1+\lambda n}{1+\lambda_0 n}\right)}. \tag{16}$$

In writing the solutions (14) and (15) it is assumed that q_1 and q_2 are so defined that their real parts are positive.

4. Boundary conditions

The solutions (14) and (15) must satisfy certain boundary conditions. The boundary conditions to be satisfied at the interface $z = 0$ are (CHANDRASEKHAR [2], p. 432)

$$w, \tag{17}$$

$$Dw, \tag{18}$$

and

$$\mu(D^2 + k^2)w \tag{19}$$

must be continuous.

Integrating Eq. (12) across the interface $z = 0$, we obtain another condition

$$\begin{aligned}(1+\lambda n)[\varrho_2 Dw_2 - \varrho_1 Dw_1]_{z=0} - (1+\lambda_0 n) \times \\ \times \left[\frac{\mu_2}{n}(D^2 - k^2) Dw_2 - \frac{\mu_1}{n}(D^2 - k^2) Dw_1\right]_{z=0} = \\ = -\frac{gk^2}{n^2}(1+\lambda n)[\varrho_2 - \varrho_1]w_0 - \frac{2k^2}{n}(\mu_2 - \mu_1)(1+\lambda_0 n)(Dw)_0,\end{aligned} \tag{20}$$

where w_0 is the common value of w_1 and w_2 at $z = 0$.

5. Dispersion relation and discussion

Applying the boundary conditions (17)—(20) to the solutions (14) and (15), we obtain

$$A_1 + B_1 = A_2 + B_2 \quad (= w_0)\,, \tag{21}$$

$$kA_1 + q_1 B_1 = -kA_2 - q_2 B_2 \ (= Dw_0)\,, \tag{22}$$

$$\begin{aligned} \mu_1 [2\,k^2\,A_1 + (q_1^2 + k^2)\,B_1] &= \mu_2 [2\,k^2\,A_2 + (q_2^2 + k^2)\,B_2] \\ &(= \mu(D^2 + k^2)\,w_0)\,, \end{aligned} \tag{23}$$

$$\begin{aligned} &(1 + \lambda n)\,[-k\,\varrho_2\,A_2 - \varrho_2 q_2\,B_2 - k\varrho_1 A_1 - \varrho_1 q_1\,B_1] - (1 + \lambda_0\,n) \times \\ &\quad \times \left[\frac{\mu_2}{n}\,(-q_2)(q_2^2 - k^2)\,B_2 - \frac{\mu_1}{n}\,q_1\,(q_1^2 - k^2)\,B_1\right] + \\ &\quad + \frac{gk^2}{2n^2}\,(1 + \lambda n)(\varrho_2 - \varrho_1)(A_1 + B_1 + A_2 + B_2) + \\ &\quad + \frac{k^2}{n}\,(1 + \lambda_0\,n)(\mu_2 - \mu_1)(kA_1 + q_1\,B_1 - kA_2 - q_2\,B_2) = 0\,. \end{aligned} \tag{24}$$

Eliminating the constants A_1, B_1, A_2, B_2 from Eqs. (21)—(24), we obtain

$$\begin{vmatrix} 1 & 1 & -1 & -1 \\ k & q_1 & k & q_2 \\ 2k^2\,\mu_1 & \mu_1\,(q_1^2 + k^2) & -2k^2\,\mu_2 & -\mu_2(q_2^2 + k^2) \\ \left[-\alpha_1(1 + \lambda n) + \right. & \left[\frac{R}{2}\,(1 + \lambda n) - \right. & \left[-\alpha_2(1 + \lambda\,n) + \right. & \left[\frac{R}{2}\,(1 + \lambda n) + \right. \\ + \frac{R}{2}\,(1 + \lambda n) - & - C\,\frac{q_1}{k} \times & + \frac{R}{2}\,(1 + \lambda\,n) + & + C\,\frac{q_2}{k} \times \\ \left. -C(1 + \lambda_0\,n)\right] & \left. \times (1 + \lambda_0\,n)\right] - & \left. +C(1 + \lambda_0\,n)\right] & \left. \times (1 + \lambda_0\,n)\right] \end{vmatrix} = 0 \tag{25}$$

where

$$\alpha_1 = \frac{\varrho_1}{\varrho_1 + \varrho_2}\,,\ \alpha_2 = \frac{\varrho_2}{\varrho_1 + \varrho_2}\,,\ R = \frac{gk}{n^2}\,(\alpha_2 - \alpha_1)$$

$$C = \frac{k^2}{n}\,\frac{\mu_1 - \mu_2}{\varrho_1 + \varrho_2} = \frac{k^2}{n}\,(\alpha_1 \nu_1 - \alpha_2\,\nu_2)\,.$$

The determinant can be reduced by subtracting the first column from the second, the third column from the fourth and adding the first column to

the third. By this procedure we obtain

$$\begin{vmatrix} q_1-k & 2k & q_2-k \\ \alpha_1 n\left(\dfrac{1+\lambda n}{1+\lambda_0 n}\right) & 2k^2(\alpha_1 v_1-\alpha_2 v_2) & -\alpha_2 n\left(\dfrac{1+\lambda n}{1+\lambda_0 n}\right) \\ \left[-\dfrac{C}{k}(1+\lambda_0 n)(q_1-k)+\right. & (R-1)(1+\lambda n) & \left[\dfrac{C}{k}(1+\lambda_0 n)(q_2-k)+\right. \\ \left.+\alpha_1(1+\lambda n)\right] & & \left.+\alpha_2(1+\lambda n)\right] \end{vmatrix} = 0. \tag{26}$$

Evaluating the determinant (26), we obtain the following characteristic equation:

$$\begin{aligned} &(q_1-k)\left[2k^2(\alpha_1 v_1-\alpha_2 v_2)\left\{\frac{C}{k}(1+\lambda_0 n)(q_2-k)+\alpha_2(1+\lambda n)+\right.\right. \\ &\left.\left.+(R-1)(1+\lambda n)\,\alpha_2 n\left(\frac{1+\lambda n}{1+\lambda_0 n}\right)\right\}\right]- \\ &-2k\left[\alpha_1 n\left(\frac{1+\lambda n}{1+\lambda_0 n}\right)\left\{\frac{C}{k}(1+\lambda_0 n)(q_2-k)+\alpha_2(1+\lambda n)\right\}+\right. \\ &\left.+\alpha_2 n\left(\frac{1+\lambda n}{1+\lambda_0 n}\right)\left\{-\frac{C}{k}(1+\lambda_0 n)(q_1-k)+\alpha_1(1+\lambda n)\right\}\right]+ \\ &+(q_2-k)\left[(R-1)(1+\lambda n)\,\alpha_1 n\left(\frac{1+\lambda n}{1+\lambda_0 n}\right)-2k^2(\alpha_1 v_1-\alpha_2 v_2)\times\right. \\ &\left.\times\left\{-\frac{C}{k}(1+\lambda_0 n)\cdot(q_1-k)+\alpha_1(1+\lambda n)\right\}\right]=0. \end{aligned} \tag{27}$$

The dispersion relation (27) is quite complicated as the values of q_1 and q_2 involve square roots. We therefore make the assumption that the two fluids are highly viscous. Under this assumption, we have

$$q=k\left[1+\frac{n}{vk^2}\left(\frac{1+\lambda n}{1+\lambda_0 n}\right)\right]^{1/2}=k+\frac{n}{2vk}\left(\frac{1+\lambda n}{1+\lambda_0 n}\right), \tag{28}$$

so that

$$q_1-k=\frac{n}{2v_1 k}\left(\frac{1+\lambda n}{1+\lambda_0 n}\right) \quad \text{and} \quad q_2-k=\frac{n}{2v_2 k}\left(\frac{1+\lambda n}{1+\lambda_0 n}\right). \tag{29}$$

Substituting the values of q_1-k and q_2-k from (29) in Eq. (27) and putting $v_1=v_2=v$ (the case of equal kinematic viscosities, for mathematical simp-

licity, as in CHANDRASEKHAR [2]), we obtain the following dispersion relation:

$$\lambda^3 n^5 + \lambda^2 (3 + 2k^2 \nu\lambda_0) n^4 + [3\lambda + gk\lambda^3 (\alpha_1 - \alpha_2) + 2k^2 \nu\lambda \times \\ \times (\lambda + 2\lambda_0)] n^3 + [1 + 3\lambda^2 gk (\alpha_1 - \alpha_2) + 2k^2 \nu(2\lambda + \lambda_0)] n^2 + \\ + [3\lambda gk(\alpha_1 - \alpha_2) + 2k^2\nu] n + gk(\alpha_1 - \alpha_2) = 0 . \tag{30}$$

For the potentially stable arrangement $\alpha_1 > \alpha_2$, we find that all the coefficients in (30) are positive and so all the roots of n are either real and negative or there are two complex roots with negative real parts and three real, negative roots or there are four complex roots with negative real parts and one real, negative root. The system is therefore stable in each case. Thus the potentially stable configuration remains stable whether the fluid is viscoelastic or not.

For the unstable configuration $\alpha_2 > \alpha_1$, there is at least one change of sign in Eq. (30) and so Eq. (30) has one positive root. The occurrence of positive root implies that the system is unstable. The potentially unstable arrangement, therefore, remains unstable for the viscoelastic fluid described by the OLDROYD constitutive relation.

We now wish to examine the behaviour of growth rates with respect to stress relaxation time and strain retardation time parameters analytically. Since for $\alpha_2 > \alpha_1$, Eq. (30) has one positive root, let n_0 denote the positive root. Then

$$\lambda^3 n_0^5 + \lambda^2(3 + 2k^2 \nu\lambda_0)n_0^4 + [3\lambda - gk\lambda^3 (\alpha_2 - \alpha_1) + 2k^2 \nu\lambda(\lambda + 2\lambda_0)] n_0^3 + \\ + [1 - 3\lambda^2 gk(\alpha_2 - \alpha_1) + 2k^2 \nu(2\lambda + \lambda_0)] n_0^2 + \\ + [2k^2\nu - 3\lambda gk(\alpha_2 - \alpha_1)] n_0 - gk(\alpha_2 - \alpha_1) = 0 . \tag{31}$$

Letting

$$x = \frac{n_0}{k^2 \nu} , \quad F = \nu k^2 \lambda, \quad \Gamma = \nu k^2 \lambda_0 \quad \text{and} \quad Q = \frac{g}{k^3 \nu^2} . \tag{32}$$

Eq. (31), in nondimensional form, transforms to

$$F^3 x^5 + F^2(3 + 2\Gamma) x^4 + [3F - QF^3(\alpha_2 - \alpha_1) + \\ + 2F(F + \Gamma)] x^3 + [1 - 3F^2 Q(\alpha_2 - \alpha_1) + 2 (2F + \Gamma)]x^2 \\ + [2 - 3FQ(\alpha_2 - \alpha_1)]x - Q(\alpha_2 - \alpha_1) = 0. \tag{33}$$

To study the behaviour of growth rates with respect to stress relaxation time and strain retardation time parameters, we examine the nature of $\frac{dx}{dF}$ and $\frac{dx}{d\Gamma}$.

It follows from Eq. (33) that

$$\frac{dx}{d\Gamma} = -\frac{2x^2(F^2x^2 + Fx + 1)}{[5F^3x^4 + 4F^2(3 + 2\Gamma)x^3 + 3F\{3 - QF^2(\alpha_2 - \alpha_1) + 2(F + \Gamma)\}x^2 + + 2\{1 - 3F^2Q(\alpha_2 - \alpha_1) + 2(2F + \Gamma)\}x + \{2 - 3FQ(\alpha_2 - \alpha_1)\}]}. \tag{34}$$

If

$$2 > 3FQ(\alpha_2 - \alpha_1), \tag{35}$$

the denominator in Eq. (34) is positive and so $dx/d\Gamma$ is negative. Thus with the increase in strain retardation time parameter the growth rate decreases showing the stabilizing effect of strain retardation time parameter.

Also $dx/d\Gamma$ is positive and Γ has a destabilizing effect if

$$5F^3x^4 + 4F^2(3 + 2\Gamma)x^3 + 3F[3 + 2(F + \Gamma)]x^2 + + 2[1 + 2(2F + \Gamma)]x + 2 < 3FQ(\alpha_2 - \alpha_1)(Fx + 1)^2. \tag{36}$$

From Eq. (33), it follows that

$$\frac{dx}{dF} = -\frac{x[3F^2x^4 + 2F(3 + 2\Gamma)x^3 + \{3 + 2(2F + \Gamma)\}x^2 + 4x] - - 3Q(\alpha_2 - \alpha_1)(Fx + 1)^2}{[5F^3x^4 + 4F^2(3 + 2\Gamma)x^3 + 3\{3F + 2F(F + \Gamma)\}x^2 + + 2\{1 + 2(2F + \Gamma)\}x + 2 - 3QF(\alpha_2 - \alpha_1)(Fx + 1)^2]}. \tag{37}$$

Consider the inequalities

$$3F^2x^5 + 2F(3 + 2\Gamma)x^4 + \{3 + 2(2F + \Gamma)\}x^3 + + 4x^2 \gtreqless 3Q(\alpha_2 - \alpha_1)(Fx + 1)^2 \tag{38a, 38b}$$

and

$$5F^3x^4 + 4F^2(3 + 2\Gamma)x^3 + 3\{3F + 2F(F + \Gamma)\}x^2 + + 2\{1 + 2(2F + \Gamma)\}x + 2 \gtreqless 3QF(\alpha_2 - \alpha_1)(Fx + 1)^2, \tag{39a, 39b}$$

where (38a), (39a) correspond to the 'greater than' sign and (38b), (39b) correspond to the 'less than' sign in Eq. (38) and (39). If (38a), (39a) or (38b), (39b) are satisfied simultaneously, dx/dF is negative. The stress relaxation time parameter F has, therefore, the stabilizing effect. If (38b) and (39a) or (38a) and (39b) are satisfied simultaneously, then dx/dF is positive meaning thereby the destabilizing effect of the stress relaxation time parameter F.

REFERENCES

1. P. K. Bhatia, Nuovo Cimento, **19B,** 161, 1974.
2. S. Chandrasekhar, "Hydrodynamic and Hydromagnetic Stability" Oxford University Press, 1961, Chap. 10.
3. J. G. Oldroyd, Proc. Roy. Soc. (London), **A245,** 278, 1958.
4. R. C. Sharma, Acta Phys. Hung., **40,** 11, 1976.
5. R. C. Sharma, Acta Phys. Hung., **38,** 293, 1975.

Acta Physica Academiae Scientiarum Hungaricae, Tomus 45 (3), pp. 221—232 (1978)

POTENTIAL ENERGY PARAMETERS FROM CRYSTALLINE STATE PROPERTIES

By

C. MALINOWSKA-ADAMSKA

STATE UNIVERSITY OF NEW YORK AT BINGHAMTON,
DEPARTMENT OF CHEMISTRY, BINGHAMTON, NEW YORK 13901, USA*

(Received 12. IX. 1978)

The parameters of the potential functions suggested by MORSE, RYDBERG and VARSHNI in the higher approximation with respect to the number of nearest-neighbours are determined using experimental values for the energy of sublimation, the compressibility, the lattice constant, the distance between nearest-neighbours in the crystal lattice at any given temperature.

The calculated force constants for some metals, in the pseudoharmonic approximation, compared with experimental data show a properly chosen shape of the functions in question and confirm the self-consistency of the present method.

1. Introduction

Pairwise additive central potential functions are widely applied to various problems related to the description of the solid state [1]. Usually, the pair potential functions contain two or more adjustable parameters [2, 3] determined by experiment. In the case of metals the potential energy parameters are generally calculated from crystalline state physical properties as cohesive energy, compressibility or lattice constants extrapolated to 0 K [4—6]. Thus, the accuracy of the parameters obtained in this way is often questionable [1, 7].

Morever, when only the first shell of nearest-neighbours is taken into account [6] one cannot obtain the correct results in the case of the interactions considered in crystals. So far the effect of various shapes of the potential functions have been considered but only in terms of parameters determined in the nearest-neighbour approximation. We intend, in this paper, to determine the parameters of the potential functions suggested by MORSE, RYDBERG and VARSHNI as they depend on the number of shells of nearest neighbours having their influence on the pair interaction.

In order to assure the accuracy of the present calculations, we use experimental data for sublimation energy, compressibility, lattice constants taken at room temperature. But instead of the extrapolation procedure we consider

* Permanent address: Institute of Physics, Technical University of Łódz, ul. Wolczanska 219, 93—005 Łódz, Poland.

the potential function in its pseudoharmonic approximation [8] which allows us to discuss properties of the crystal at arbitrary temperatures [8—11].

Taking into account the conditions for potential functions required by their real behaviour the force constants can be expressed by means of the parameters appearing in these functions. The calculated pseudoharmonic force constants compared with experimental data show a properly chosen shape of the functions near r_e in question and justify the self-consistency method here applied.

2. Theoretical assumptions

If $U(r)$ is the energy of interactions of two atoms embedded in a crystal with a distance r, and it satisfies the following conditions [5, 13]:

1) the force $-\partial U/\partial r$ is attractive at large r and repulsive at small r, respectively, i.e. $U(r)$ has a minimum at a point $r = r_e$,

2) the magnitude of U decreases more rapidly with r than r^{-3},

3) all elastic constants are positive,

4) $C_{11} - C_{12} > 0$, where C_{11} and C_{12} are elastic constants,

then $U(r)$ represents the interatomic potential of two atoms in a stable state of a crystal.

Conditions (1) and (2) result from simply physical considerations. Namely, the first arises from the existence of condensed phases, and the second is equivalent to requiring that the cohesive energy should be finite. These two conditions taken together guarantee that a crystal is stable with respect to infinitesimal homogeneous expansions and contractions of the lattice. The conditions (3) and (4) guarantee that a cubic crystal is stable with respect to infinitesimal shear deformations [13]. In the light of our recent paper [6] the condition (3) is not trivial because force constants corresponding to some potential functions can be negative for certain ranges of temperature. For this reason it seems to be very important to analyze the force constants as dependent on temperature, which is very convenient in the case of pseudoharmonic approximation, and to check their behaviour with respect to condition (3). The analysis of this behaviour can eliminate some class of the potential functions as being unphysical ones.

The interaction potential energy $U(r_{ij})$ of two atoms, i and j, separated by a distance r_{ij} is given in terms of the RYDBERG, MORSE and VARSHNI functions by:

$$U_R(r_{ij}) = -D_e\{[1 + \alpha(r_{ij} - r_e)] \exp[-\alpha(r_{ij} - r_e)]\}, \tag{1}$$

$$U_M(r_{ij}) = D_e\{\exp[-2\alpha(r_{ij} - r_e)] - 2\exp[-\alpha(r_{ij} - r_e)]\}, \tag{2}$$

and

$$U_V(r_{ij}) = D_e\{\exp[-2\alpha(r_{ij}^2 - r_e^2)] - 2\exp[-\alpha(r_{ij}^2 - r_e^2)]\}, \tag{3}$$

where α and D_e are constants with dimensions of reciprocal distance and energy of approach of the two atoms. Since $U(r_e) = -D_e$, D_e is the dissociation energy.

In order to obtain the potential energy of a large crystal whose atoms are at rest it is necessary to sum the above equations over the entire crystal. This is most easily done by choosing one atom in the lattice as an origin calculating its interaction with all n_j other atoms in the crystal, and then multiplying by $1/2\ N$ where N is the total number of atoms in the crystal [5, 14]. Thus, for functions (1), (2) and (3), the total energy is respectively equal to:

$$\Phi_R = -L\beta\alpha\left[\left(\frac{1}{\alpha} - r_e\right)\sum_j n_j\gamma_j + \sum_j n_j r_j \gamma_j\right], \tag{4}$$

$$\Phi_M = -L\beta\left(\beta\sum_j n_j\gamma_j^2 - 2\sum_j \gamma_j n_j\right) \tag{5}$$

and

$$\Phi_V = L\beta_e\left[\beta_e\sum_j n_j(\gamma_j)^{2r_j} - 2\sum_j n_j(\gamma_j)^{r_j}\right], \tag{6}$$

where r_j is the distance from the origin to the j-th atom, $L = 1/2\ ND_e$, $\beta = \exp(\alpha r_e)$, $\gamma_j = \exp(-\alpha r_j)$ and $\beta_e = (\beta)^{r_e}$. For the f.c.c. lattice, the separation r_j is [4, 14]:

$$r_j = d_0\sqrt{j},$$

where d_0 is the separation between nearest lattice points in the crystal.

If a_0 is the value of the lattice constant a for which the lattice is in equilibrium, then:

$$\Phi(a_0) + K_0 \tag{7}$$

gives the energy of sublimation U_0,

$$\frac{d}{da}(\Phi + K_0) = 0, \tag{8}$$

and $[d^2\Phi/da^2]_{a_0}$ is related to the compressibility $\varkappa$ [5]:

$$\left[\frac{d^2\Phi}{da^2}\right]_{a_0} = \frac{9c\,Na_0}{2\varkappa} \tag{9}$$

where $c = 2$ for face-centred crystals and $c = 4$ for body-centred crystals.

The zero point energy K_0 is given approximately in terms of the Debye characteristic temperature θ_D by [4, 14]:

$$K_0 = \frac{9}{8}Nk_B\theta_D, \tag{10}$$

where k_B is Boltzmann's constant. (It should be noted that for temperatures other than 0 K $\Phi = 5/2\,RT - \Delta H - E_1 - PV$ [1], where ΔH is the amount of enthalpy required to transfer N atoms from the crystalline state to the vapour phase, E_1 represents the vibrational energy of the crystal including the zero point energy).

Using (7), (8) and (9) in (4)—(6) we get the systems of equations (A), (B) and (C) (Appendix A) for the parameters α, D_e and r_e of respective potentials. These equations were numerically solved using experimental values of the energy of sublimation [15], the compressibility [1], the lattice constant [15], the distance between nearest-neighbours in the crystal lattice at 298 K and the Debye characteristic temperature determined at low temperature [1].

Numerical values of the above constants for some metals are collected in Table I.

Table I

Experimental data of some metals used in calculations of potential energy parameters

Metal	$(U_0 - K_0) \cdot 10^{-19}$ $\left[\frac{J}{\text{atom}}\right]$	$\varkappa \cdot 10^{-11}$ $\left[\frac{m^2}{N}\right]$	$a_0 \cdot 10^{-10}$ [m]	$d_0 \cdot 10^{-10}$ [m]
Au	6.371210	0.562540	4.070	2.870
Ag	4.695416	1.018500	4.080	2.880
Cu	5.626504	0.723410	3.610	2.550
K	1.551255	39.77300	5.330	4.620

The equations (A) and (B) derived assuming the RYDBERG and MORSE potentials, respectively, were solved using the iteration method [16]. The convergence of solution was so rapid that about 20 iterations were sufficient to obtain a result with the relative error of solutions less than $10^{-8}\%$. The iteration method, however, appears to be divergent in the case of VARSHNI potential and the steepest method was chosen to solve the equations (C) [16].

Numerical solutions depend on the number of the nearest neighbours taken into account in the series (A)—(C). In the cases of f.c.c. and b.c.c. structure the consecutive neighbours up to $n_{\max} = 12$ and 13, respectively, were taken in the calculations. The solutions for MORSE potential constants are tabulated as function of the number n for copper (as an example). RYDBERG, MORSE and VARSHNI potential constants for $n = \infty$ are collected for some cubic metals in Table III. Graphical analyses of these constants as functions $1/n$ are given in Figs. 1—3. The obtained functions $y = y(n)$, where y is one of the quantities D_e, α, r_e, were fitted to the expressions:

$$y(n) = y(\infty) + B\left(n + \frac{2\sqrt{n}}{\alpha d_0}\right) \exp\left(-\alpha d_0 \sqrt{n}\right) \tag{11}$$

Table II

MORSE potential constants for copper as functions of the number n

n	$D_e \cdot 10^{-20}$ [J]	$\alpha \cdot 10^{10}$ [m^{-1}]	$r_e \cdot 10^{-10}$ [m]
1	9.292800000	1.420547333	2.550000000
2	7.676418255	1.388398667	2.632239490
3	5.969460801	1.350144666	2.779030978
4	5.699542813	1.345944112	2.811667618
5	5.500857015	1.347431851	2.840995551
6	5.475971283	1.348704701	2.845430401
7	5.422054121	1.356075937	2.857403336
8	5.419988797	1.356810638	2.858065604
9	5.417796885	1.360096924	2.859342858
10	5.418773797	1.361673265	2.860336202
11	5.420396296	1.362796727	2.860517636
12	5.422003294	1.363594107	2.860559381

Table III

RYDBERG, MORSE and VARSHNI potential constants for the pairwise atomic interaction in cubic metals ($n = \infty$)

Potential model	Metal	$D_e \cdot 10^{-20}$ [J]	$\alpha \cdot 10^{10}$ [m^{-1}]	$r_e \cdot 10^{-10}$ [m]
RYDBERG	Au	8.113146	22.340757	2.9794647
	Ag	5.6052340	1.965701	3.0903540
	Cu	6.0962740	2.002727	2.8162580
	K	1.0544520	0.767954	6.0615100
MORSE	Au	7.5833990	1.6243880	2.9998380
	Ag	5.0911600	1.3501210	3.1262460
	Cu	5.42409900	1.3649220	2.8607390
	K	0.6462303	0.4257647	7.1577160
VARSHNI	Au	8.9092239	$2.9177307 \cdot \alpha_1$	2.9438268
	Ag	6.5845508	$2.4789801 \cdot \alpha_1$	3.0136351
	Cu	7.5719697	$2.8943859 \cdot \alpha_1$	2.7109734
	K	1.6460100	$0.6133440 \cdot \alpha_1$	5.50126670
			$\alpha_1 = 10^9$ m^{-1}	

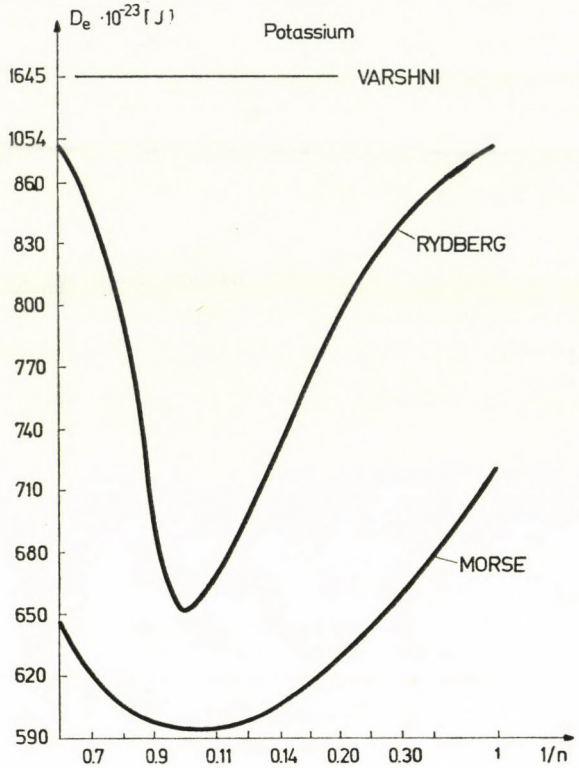

Fig. 1. The parameter D_e for potassium as a function of $1/n$

in the case of RYDBERG and MORSE potentials and

$$y(n) = y(\infty) + Bn \exp(-\alpha d_0^2 n) \tag{12}$$

in the case of VARSHNI potential. The form of the above analytical approximations was derived retaining the leading terms of the respective potentials integrated over space in continuous approximation. The parameters α and d_0 are assumed as $\alpha(n_{\max})$ and $d_0(n_{\max})$, the coefficient $y(\infty)$ and B are calculated by the least-squares method. The former coefficient represents the limit of the quantity y for $n \to \infty$.

3. Strength constant in the pseudoharmonic approximation

A test of suitability of the RYDBERG, MORSE and VARSHNI potentials as interatomic potential models in cubic metals are their abilities to reproduce the temperature dependence of the strength constant $f(T)$ [17]. In our consi-

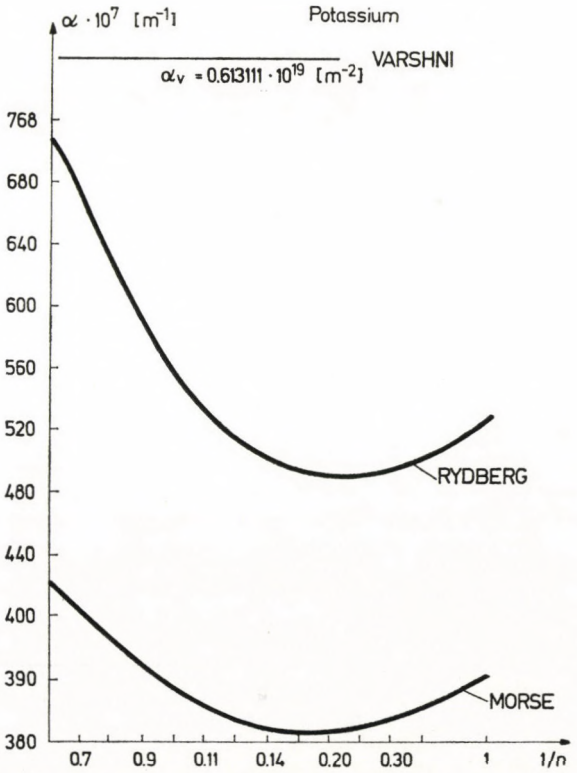

Fig. 2. The parameter α for potassium as a function of $1/n$

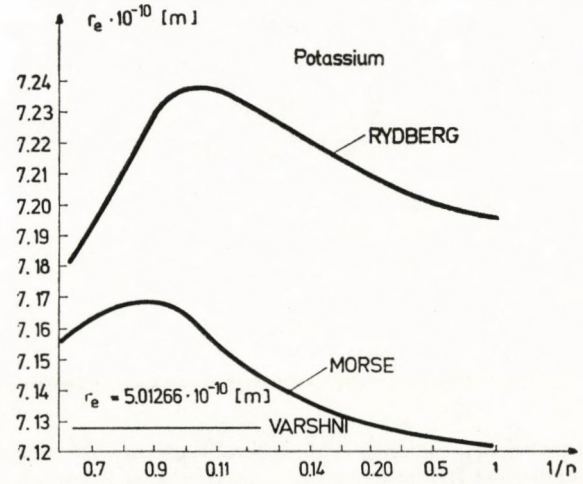

Fig. 3. The parameter r_e for potassium as a function of $1/n$

derations we choose the expressions for $f(T)$ obtained in pseudoharmonic approximation [6, 8, 18]. In terms of the above theory, the strength constant is related to that f found in the harmonic approximation as [8]:

$$f(T) = f\alpha(T) . \tag{13}$$

Analytical expressions for the renormalized factor $\alpha(T)$ in terms of the potentials discussed here (Eqs. (4), (5) and (6)) are given in Appendix B (Eqs. (R), (M) and (V)). The harmonic strength constants, in the notation of VARSHNI [2, 3] are respectively:

$$f_R = D_e \alpha^2 , \tag{14}$$

$$f_M = 2D_e \alpha^2 , \tag{15}$$

$$f_V = 8D_e \alpha^2 r_e^2 . \tag{16}$$

The numerical results for f in the case $n = \infty$ (at room temperature) are listed in Table IV. In Table V we have several numerical results for the

Table IV

Values of the harmonic strength constants at room temperature ($n = \infty$)

Potential model	f [N/m]			
	Au	Ag	Cu	K
RYDBERG	44.453112	21.658514	24.451452	0.621866
MORSE	40.019660	18.560604	20.210323	0.234291
VARSHI	52.582897	29.404201	37.295998	1.499188

Table V

Comparison of the values reported in the literature for the strength constants used for calculating the RYDBERG, MORSE and VARSHNI potential models in pseudoharmonic approximation (at $T = 298$ K)

Metal	$f(T)$ [N/m]			
	Other calcul.	Our results ($n = \infty$)		
		RYDBERG	MORSE	VARSHNI
Au	33.646[a]	34.150214	29.124855	43.482900
Ag	24.110[a]	18.787713	15.631236	25.945970
Cu	29.231[a]: 36.16[b]	21.521256	17.241229	26.712512
K	$6.015 \cdot 10^{-3}$ [c]	$5.976 \cdot 10^{-3}$	$4.812 \cdot 10^{-3}$	$6.991 \cdot 10^{-3}$

[a] References [19] (The evaluation of these force constants has been made with the help of three elastic constants and five zone boundary experimental frequencies.)
[b] Experimental results [17].
[c] Values reported in [20] for $a_0 = 5.233 \cdot 10^{-3}$ [m] (in the notation of VARSHNI.)

renormalized strength constants $f(T)$ for cubic metals. For comparison, some values reported in the literature for the above constants are given too [17, 19—20].

For those metals that are included in our calculation the values of α, D_e, r_e are found to be dependent on the number of the nearest neighbours taken into account (Tables II, III and Figs. 1—3). The parameters α and r_e of the MORSE potential for various metals do not satisfy the condition $\alpha r_e = 6$ (Table III). (This condition was used in some papers related to the solid state [9—11]). In fact, αr_e is only 3.05 for potassium and in no case considered here is αr_e as large as 5. This result is to be expected on the basis of some findings by KONOWALOW [22]. Even for the rare gases whose potential curves surely correspond more closely than those for the metals considered here, the relation $\alpha r_e = 6$ fails to hold.

The present results, which account for the pairwise interaction of a central atom with essentially an infinite number of shells of nearest-neighbours are expected to be much more reliable than those which account for only a single shell of neighbours. Furthermore, the present approach allows the use of crystal data taken at any temperature; thus avoiding the need for extrapolations to 0 K. Thus the present approach is expected to be more useful than those previously used.

Appendix A

In terms of the Rydberg potential, Eqs. (7), (8) and (9) may be written as:

$$\begin{aligned} &D_e \cdot \beta \left[(\ln \beta - 1) \sum_j \beta_j - \alpha \sum_j r_j \beta_j \right] = 2(U_0 - K_0) , \\ &\alpha \sum_j r_j^2 \beta_j - \ln \beta \sum_j r_j \beta_j = 0 , \\ &D_e \cdot \beta \alpha^2 \left[(\ln \beta + 1) \sum_j r_j^2 \beta_j - \alpha \sum_j r_j^3 \beta_j \right] = \frac{9 c a_0^3}{4 \varkappa} . \end{aligned} \tag{A}$$

For the MORSE function the Eqs. (7)—(9) are respectively:

$$\begin{aligned} &D_e \cdot \beta \left[\beta \sum_j \gamma_j \beta_j - 2 \sum_j \beta_j \right] = 2(U_0 - K_0) , \\ &\sum_j r_j \beta_j - \beta \sum_j r_j \gamma_j \beta_j = 0 , \\ &D_e \alpha^2 \beta \left[2\beta \sum_j r_j^2 \gamma_j \beta_j - \sum_j r_j^2 \beta_j \right] = \frac{9 c a_0^3}{8 \varkappa} . \end{aligned} \tag{B}$$

Using (6) in (7), (8) and (9) we get the following equations for the parameters of the VARSHNI potential energy functions:

$$D_e\beta_e\left[\beta_e\sum_j\frac{1}{n_j}\delta_j^2-2\sum_j\delta_j\right]=2(U_0-K_0),$$

$$\sum_j r_j^2\,\delta_j-\beta_e\sum_j\frac{r_j}{n_j}\delta_j^2=0, \tag{C}$$

$$2D_e\beta_e\alpha\left[\sum_j r_j^2\cdot\delta_j-2\alpha\sum_j r_j^4\cdot\delta_j-\beta_e\sum_j\frac{r_j^2}{n_j}\delta_j^2+\right.$$

$$\left.+4\alpha\beta_e\sum_j\frac{r_j^4}{n_j}\delta_j^2\right]=\frac{9ca_0^3}{8\varkappa}.$$

The symbols β_j and δ_j used in Eqs. (A)—(C) have the following meaning:

$$\beta_j=n_j\gamma_j,$$

$$\delta_j=n_j\cdot\exp(-\alpha r_j^2).$$

Appendix B

By applying the theory of anharmonic crystals in the pseudoharmonic approximation given by PLAKIDA and SIKLÓS [8] we get (Table B) the following analytical expression for the parameter $\alpha(T)$.

Table B

Analytical expression for $\alpha(T)$ in terms of the RYDBERG (Eq. (R)), MORSE (Eq. (M)) and VARSHNI (Eq. (V)) potentials in high temperature limit

Position	$\alpha(T)$	Literature
1. Eq. (R)	$\alpha(T)=\frac{3\theta B^2}{2C^2}\left(1+\sqrt{1+\frac{2AC}{3B^2}}\right)^2$	[6]
2. Eq. (M)	$\alpha(T)=\frac{1}{12}p_0+\frac{1}{2}e^{-y}\left(1+\sqrt{1+\frac{p_0}{6}e^y}\right)$	[8]
2. Eq. (V)	$\alpha(T)=\left[\frac{\sqrt{2}p\alpha r_e^3}{f}-2\left(\alpha r^2-1+42\frac{\alpha\theta}{f}\right)+\right.$ $\left.+\frac{2}{3}\frac{K}{fH}\left(1+\frac{K}{12H^3}\right)\right]^2$	[17]

The symbols used in this Table have the following meaning:

$$\theta = k_B \cdot T\,;$$

$$B = D_e C_r \left[D_K(6D_K + 1) + \alpha r_e \left(4D_K^2 + \frac{1}{\sqrt{\pi}\, D_K}\right) - \frac{3}{\sqrt{\pi}\, D_K}\right];$$

$$C_r = \alpha \exp(\alpha r_r)\,, \quad D_K = 0.1\sqrt{3 + \alpha r_e}\,,$$

$$C = D_e\left[\frac{C_r D_K}{\alpha} + B_r\left(D_K - \frac{1}{\sqrt{\pi}\, D_K}\right)\right] + \frac{p r_e^3}{2\sqrt{2}};$$

$$B_r = (\alpha r_e - 1)\exp(\alpha r_e)\,,$$

$$A = 12\, D_e \alpha C_r\, D_K\, [D_K(3D_K + 2) + \alpha r_e + 1]\,.$$

$$p_0 = \frac{p r_e l_e^2}{\sqrt{2}\, D_e}\,, \quad l_e = r_e\left(1 + \frac{3y}{3\alpha r_e}\right),$$

$$y = \frac{\theta}{D_e}\left[1 + \frac{\theta}{D_e} + \frac{f\hbar^2}{6m\theta^2}\left(1 - \frac{7\theta}{2D_e}\right)\right]$$

and

$$K = 2g^3 + 9gh + 27j\,,$$

$$K = g^2 + 3h,\ g = 42\alpha\theta - \frac{1}{\sqrt{2}} p\alpha r_e^3 + f(\alpha r_e^2 + 1)\,,$$

$$h = 72\alpha\theta\,[0.4\, p\alpha r_e^3 - f(\alpha r_e^2 - 1)]\,,$$

$$j = 576\alpha^2 f\theta^2(\alpha r_e^2 - 1)\,,$$

where: k_B is the Boltzmann constant, h the Planck constant, p pressure and m is the mass of the atom.

Acknowledgement

The author wishes to thank Professor D. D. KONOWALOW for helpful discussions connected with this paper as well as for the possibility to visit the Department of Chemistry, State University of New York at Binghamton.

Warm thanks are due to Professor L. WOJTCZAK, Head of the Department of Solid State Physics, University of Łódz, for reading the manuscript.

REFERENCES

1. T. HALICIOGLU and G. M. POUND, phys. stat. sol. (a) **30,** 619, 1975.
2. Y. P. VARSHNI, Trans. Faraday Soc., **53,** 132, 1957; **57,** 537, 1961.
3. Y. P. VARSHNI, Revs. Modern Phys., **29,** 664, 1957.
4. J. O. HIRSCHFELDER, C. F. CURTISS and R. B. BIRD, The Molecular Theory of Gases and Liquids, J. Wiley and Sons, New York, 1954.
5. L. A. GIRIFALCO and V. G. WEIZER, Phys. Rev., **114,** 687, 1959.
6. C. MALINOWSKA-ADAMSKA, Acta Phys. Hung., **42,** 295, 1977.
7. F. O. GOODMAN, Phys. Rev., **164,** 1113, 1967.

8. N. M. PLAKIDA and T. SIKLÓS, phys. stat. sol., **33,** 103, 1069; **33,** 113, 1969; **39,** 171, 1970.
9. T. SIKLÓS, Acta Phys. Hung., **30,** 193, 1971.
10. T. SIKLÓS and V. L. AKSIENOV, Acta Phys. Hung., **31,** 335, 1972; phys. stat. sol., (b) **50,** 171, 1972.
11. T. SIKLÓS, Acta Phys. Hung., **34,** 327, 1973.
12. L. WOJTCZAK and K. STACHULEC, phys. stat. sol., (b) **70,** K165, 1975.
13. M. BORN, Proc. Cambridge Phil. Soc., **36,** 160, 1940.
14. D. D. KONOWALOW and J. O. HIRSCHFELDER, Phys. Fluids, **4,** 629, 1961.
15. CH. KITTEL, Introduction to Solid State Physics, J. Wiley and Sons, New York, 1967.
16. A. RALSTON, A First Course in Numerical Analysis, Mc Graw-Hill, New York, 1965.
17. P. S. YUEN and Y. P. VARSHNI, Phys. Rev., **164,** 895, 1967.
18. C. MALINOWSKA-ADAMSKA and L. WOJTCZAK, Acta Phys. Hung. (in print).
19. S. KUMAR, Indian J. Phys., **49,** 615, 1975.
20. R. A. COWLAY, A. D. B. WOODS and G. DOLLING, Phys. Rev., **150,** 487, 1966.
21. R. C. SHULKA and R. TAYLOR, J. Phys. (F), **6,** 531, 1976.
22. D. D. KONOWALOW, J. Chem. Phys., **42,** 818, 1967.

Acta Physica Academiae Scientiarum Hungaricae, Tomus 45 (3), pp. 233—241 (1978)

ELECTRON AND HOLE GENERATION IN ANTHRACENE UNDER ELECTRON BOMBARDMENT

By

M. SALEH

DEPARTMENT OF PHYSICS, UNIVERSITY OF SANA'A, SANA'A, YEMEN ARAB REPUBLIC

and

M. S. ZAFAR

DEPARTMENT OF PHYSICS, UNIVERSITY OF THE PUNJAB, NEW CAMPUS, LAHORE, PAKISTAN*

(Received in revised form 9. X. 1978)

In order to study the effect of trapping and release of carriers in anthracene, short electron pulses of energy up to 50 KeV and dose 2.5×10^{-14} C per pulse were used to excite the anthracene crystals and the induced charge transferred was measured for a series of increasing bias voltages of either sign at room temperature. It is found that the hole charge collected at transit time is only half of the total hole charge eventually collected which always equalled the electron charge. An interpretation is given in terms of a trap release mechanism. Shallow hole traps with an activation energy of the order of 0.13 eV are estimated in anthracene crystals at room temperature. The electron mobility normal to '*ab*' crystallographic plane is 0.38 ± 0.02 cm^2 V^{-1} s^{-1} and agrees well with other published values.

1. Introduction

Experimental results regarding electron and hole production in anthracene crystals are discussed with emphasis on the relevance of the mechanism of trapping and release of carriers in such low mobility crystals. KOKADO and SCHNEIDER [1] using a conductivity "glow curve" technique, have observed hole traps about 0.8 eV above the valence band. In these experiments irradiation at low temperatures was performed with highly absorbed light, so that it is probable that the traps are characteristic of the surface only. BREE and KYDD [2] have suggested that adsorbed oxygen is responsible for them, and such traps appear also to play an important role in electron bombardment experiments (see Sections 3 and 4).

The method adopted for studying trapping and release of carriers in anthracene crystals is the drift method essentially pioneered by SPEAR [3]. This method has been used for studying many different materials [3] and in particular for anthracene [4, 5].

* Present address: Physics Department, University of Multan, Multan, Pakistan

2. Experimental

2.1. *Preparation of specimens*

Single crystals of anthracene were grown from the melt, following extensive purification in specially designed crystal growing tubes [6]. The growth vessel was cut open to tip out the ingot and all further operations were carried out within an N_2-filled dry glove box. The plates cleaved from the crystal boule had surfaces of 5 mm $\times$ 5 mm, which were "*ab*" planes,* and thicknesses varying between 0.35 and 0.5 mm.

Specimens were prepared for electron bombardment by evaporating circular semi-transparent metal electrodes, onto each face in turn. The plates were placed in the vacuum system (pressure $\leq 10^{-5}$ torr) for about half an hour prior to evaporation in order to ensure fresh surface by sublimation. Aluminium was then flash evaporated from a 3-strand tungsten helix covered by a radiation shield with a hole 4 mm in diameter, and at a distance of about 150 mm from the crystal specimen placed on a brass mask. The layers produced were highly opaque and conductive and when viewed against the light had a mirror-like finish. Such layers were estimated to be about 200 Å thick. The specimen was mounted behind an aperture of 1—2 mm in diameter in the copper lid of the specimen chamber, which could be heated or cooled from outside. Electric contact was made by sandwiching the crystal, painted with Aquadag rings on the aluminium, between a washer of platinum foil and a copper disc. The front (bombarded) electrode was connected to the bias supply, the rear (collecting) electrode to the current integrator as described below.

2.2. *Apparatus*

The electron bombardment apparatus** was based on that developed by SPEAR [3]. The crystals were equipped with evaporated aluminium electrodes (see Section 2.1) on two opposite faces. Carriers were generated at one electrode by the incident single electron pulses (typically 90 ns long, of energy between 20 and 50 KeV and carrying 2.5 $\times$ 10^{-14} C total charge Q_b) and drifted through the crystal under an applied field to be colledted at the other electrode. The resulting pulse was displayed on 85 MHz oscilloscope (Tektronix type 581 with 86 preamplifier) as an integrated charge pulse and recorded photographically from which the transit time was determined. Positive or negative

* The orientation of the cleavage planes was kindly checked by Professor J. W. JEFFERY of the Crystallography Department, Birkbeck College, University of London.

** Fuller details of the apparatus and experimental technique are given by M. SALEH Ph. D. thesis, University of London 1972.

carriers could be caused to move through the crystal bulk by applying a field of the appropriate polarity. Any space charge accumulated during the "setting-up" procedure was removed by applying a few bombarding pulses to the short-circuited specimen.

3. Results

A study of the total quantity of charge collected as a function of applied bias was made at room temperature. The specimens were unpolished and prepared as described by SALEH [6]. A short pulse of electrons of energy between 20 and 50 KeV (carrying 2.5×10^{-14} C total charge) was used to excite the specimen. Occasionally the sample was short-circuited and bombarded to check for trapped space charge. The electron induced charge, when the bombarded electrode was at a negative potential with respect to the collecting electrode, was calculated from the following equation:

$$Q_0 = Q_T \pm Q_b ,$$

where Q_0 = total secondary charge of one sign produced, Q_b = total electron charge deposited by the beam and Q_T = total charge collected at the transit time T.

However, in the case of holes, with trapping present, the charge was calculated by using the final steady signal height in the above equation.

With the bombardment electrode at a negative potential with respect to the collecting electrode (electrons collected at the back electrode) the induced charge signal exhibited ramp i.e. an almost constant rate of change of charge collected, culminating in a "knee" after which no further increase in charge was observed. Careful study revealed that the duration of the ramp varied inversely with the applied field. The ramps are identifiable with the drift of electrons in a uniform field and the drift-mobility can be immediately deduced. The value of the electron drift-mobility normal to the "*ab*" crystallographic plane at room temperature for the specimen No. 13.01 (representative of a group of specimens) was found to be 0.38 ± 0.02 cm^2 V^{-1}s^{-1}.

In contrast to this with positive applied bias (holes drawn to the back electrode), strong trapping was inferred from the rounded transits. However, when the temperature was increased from 293 to 323 K, the hole signals also developed ramps and knees. It is believed that shallow hole traps with an activation energy of the order of 0.13 eV are responsible for the trapping at room temperature.

The induced charge vs bias voltage curves at various bombarding energies for the specimen No. 13.01 (representative of a group of specimens) are shown in Figs. 1 and 2.

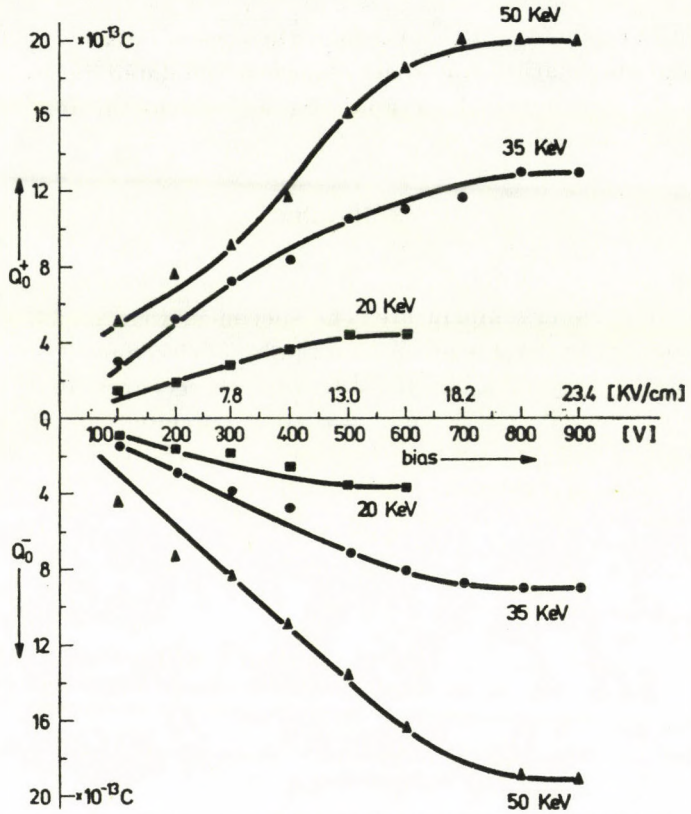

Fig. 1. Field dependence of electron and hole induced charge at 293 K. Specimen No. 13.01. Thickness 380 μm. $Q_b = 2.5 \times 10^{-14}$ C/pulse

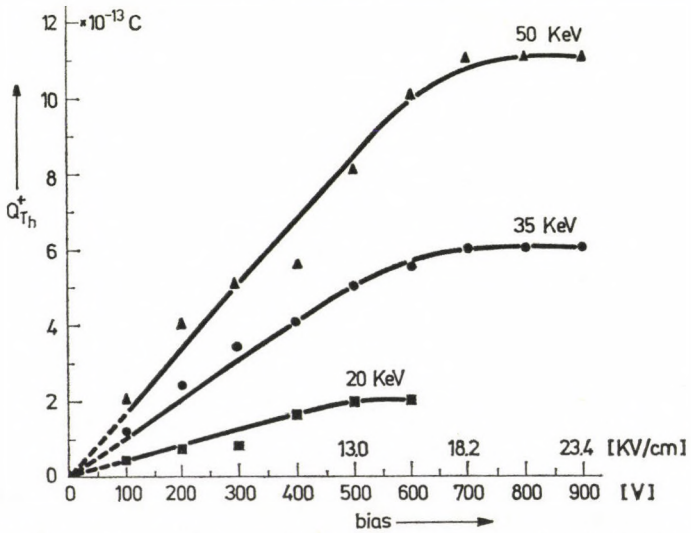

Fig. 2. Charge collected at transit time vs bias at 293 K. Specimen No. 13.01. Thickness 380 μm, $Q_b = 2.5 \times 10^{-14}$ C/pulse. Transit time calculated from $\mu_h = 1.0$ cm^2 V^{-1} s^{-1}

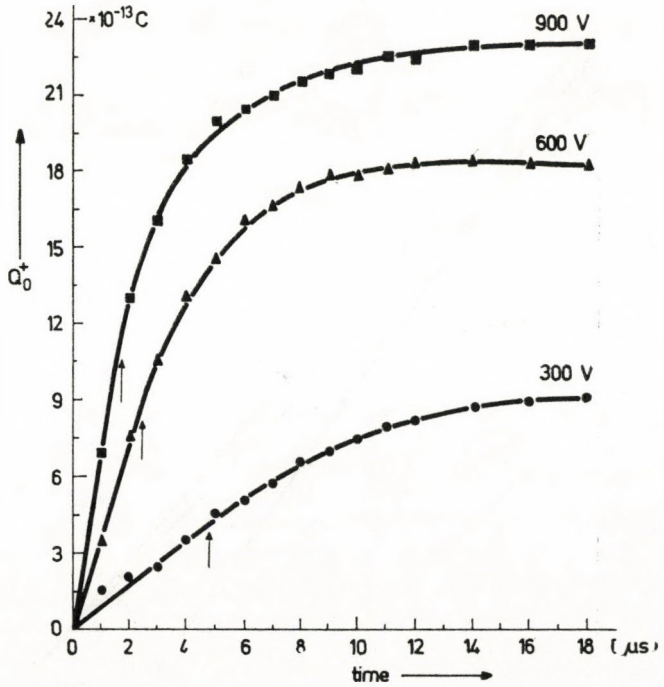

Fig. 3. Hole charge Q_0^+, collected as a function of time at different bias voltages. Arrows indicated end of transit time T_h, if $\mu_h = 1.0\ \mathrm{cm^2\,V^{-1}\,s^{-1}}$. Specimen No. 13.01, Thickness 380 μm, temperature 293 K

The electron and hole induced charge saturate at lower applied bias when the beam voltage V_b was low than when V_b was high. It was found that the applied bias could not be increased beyond the saturation value at low V_b without risking a breakdown of the insulation resistance of the specimen. Fig. 1 also shows that the hole-induced charge vs voltage curve exhibits superlinear dependence on bombarding voltage of the hole charge collected at saturation. Comparison of the two diagrams (1 and 2) shows that the hole charge collected at transit time accounts for only $\simeq$ half of the total hole charge eventually collected, which always equalled the electron charge.

In Fig. 3, the hole transits photographed at three bias voltages for the specimen No. 13.01 have been replotted. The arrows indicate the end of the transit period T_h calculated on the assumption that the field is uniform and $\mu_h = 1.0\ \mathrm{cm^2\,V^{-1}s^{-1}}$. In each case the charge collection is seen to continue long after the first sheet of carriers has traversed the sample. In Fig. 4, the difference between the final value of charge collected and that collected at various times is replotted against time after T_h, and is seen to follow an approximately exponential law in each case. As will be explained below (Section 4), this behaviour is compatible with trapping.

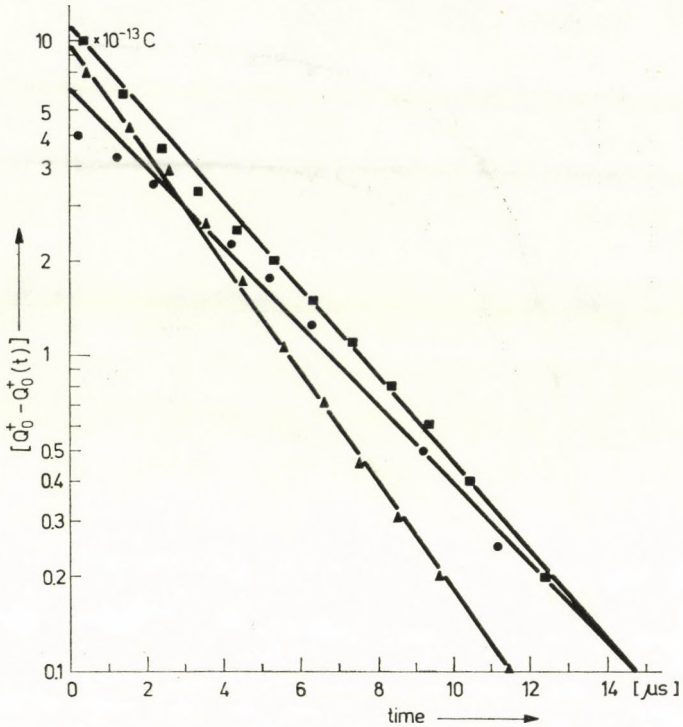

Fig. 4. (Total hole charge — hole charge collected at t) vs time counted from end of transit

4. Discussion and conclusions

4.1. *Drift of "thick sheet" of charge*

In the presence of shallow hole trapping and release, let charge generation be described by

$$\dot{Q} = Q_0/\tau e^{-t/\tau}$$

so that total charge in pulse

$$Q_0 = \int_0^\infty \dot{Q}\, dt\,,$$

where τ is the decay time due to shallow hole trapping and release.

Two time regions can be distinguished when a charge sheet travels with velocity v towards the back electrode of the crystal specimen thickness L, (Fig. 5).

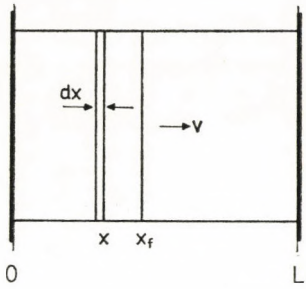

Fig. 5. Drift of 'thick sheet' of charge through crystal bulk

Case 1. *Drift during* $t \leq T$.

The charge in a sheet of thickness dx, at x at time t is

$$\frac{Q_0}{\tau} e^{-(t-x/v)/\tau} \frac{dx}{v} .$$

The current induced by the sheet is

$$v/L \frac{Q_0}{\tau} e^{-(t-x/v)/\tau} \frac{dx}{v}$$

and that by all the sheets $0 \ldots x \ldots x_f$, $x_f = vt$

$$I = (Q_0/L\tau) \int_0^{x_f} e^{-(t-x/v)/\tau} \, dx .$$

Therefore,

$$I_t \leqq T = \frac{Q_0}{T} (1 - e^{-t/\tau}) .$$

The total charge induced at back electrode is then (see Fig. 6)

$$q = \frac{Q_0}{T} \int_0^t (1 - e^{-t/\tau}) \, dt .$$

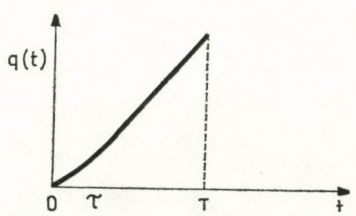

Fig. 6. Charge induced at back electrode of specimen up to $t = T$

Therefore,

$$q_t \leq T = \frac{Q_0}{T}\left[t - \tau\left(1 - e^{-t/\tau}\right)\right].$$

N.B. for $t \ll \tau$, initially,

$$q \to \frac{Q_0}{T} t^2/2\tau .$$

At $t = T$

$$q_T = Q_0\left[1 - \frac{\tau}{T}\left(1 - e^{-T/\tau}\right)\right],$$

Case 2. *Drift during* $t \geq T$

Since the sheet is thick, charge continues to arrive after the front surface of the sheet, i.e. after T. This gives rise to a current

$$I_{t \geq T} = (Q_0/L\tau)\int_0^L e^{-(t-x/v)/\tau}\, dx$$

$$= \frac{Q_0}{T}\left(1 - e^{-T/t}\right) e^{-(t-T)/\tau}.$$

It is convenient to let $t - T = \theta$, so that

$$I_\theta = \frac{Q_0}{T}\left(1 - e^{-T/\tau}\right) e^{-\theta/\tau}.$$

Therefore, the charge induced at the back electrode becomes:

$$q_{t \geq T} = \int_0^t I dt = \int_0^T I_{t \leq T}\, dt + \int_0^\theta I_\theta\, d\theta = q_T + q_\theta, \quad \text{say}$$

$$q_\theta = \frac{Q_0}{T}\left(1 - e^{-T/\tau}\right)\int_0^\theta e^{-\theta/\tau}\, d\theta =$$

$$= \frac{Q_0}{T}\tau(1 - e^{-T/\tau})(1 - e^{-\theta/\tau}) .$$

Therefore,

$$q_{t \geq T} = Q_0\left[1 - \frac{\tau}{T}\left(1 - e^{-\theta/\tau}\right) e^{-T/\tau}\right].$$

This shows that the higher the drift field (i.e., the smaller T), the more pronounced is the "hump" following the ramp, but the time constant is always τ, (Fig. 7).

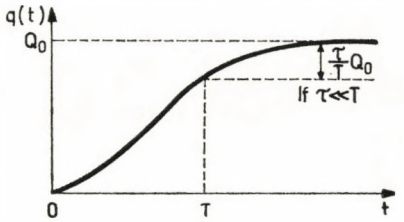

Fig. 7. Charge induced at back electrode

It is, therefore, concluded that shallow hole traps with an activation energy of the order of 0.13 eV are responsible for the trapping in anthracene crystals at room temperature. However, no electron traps were observed in these crystals at room temperature. The electron mobility normal to the "*ab*" crystallographic plane is 0.38 ± 0.02 cm^2 V^{-1}s^{-1} and agrees well with other published values. It is, of course, conceivable that the short hole lifetime is an intrinsic property of narrow band conduction, but it is rather more obvious to suspect structural defects such as dislocations, or impurities, especially oxygen as being responsible for the trapping.

Acknowledgement

Dr. M. SALEH wishes to thank Dr. J. HIRSCH of Birkbeck College, University of London for his valuable discussions.

REFERENCES

1. H. KOKADO and W. G. SCHNEIDER, J. Chem. Phys., **40**, 2937, 1964.
2. A. BREE and R. A. KYDD, J. Chem. Phys., **40**, 1775, 1957.
3. W. E. SPEAR, Proc. Phys. Soc., **B70**, 669, 1957; J. Non. Cryst. Solids, **1**, 197, 1969.
4. J. L. DELANY and J. HIRSCH, J. Chem. Phys., **48**, 4717, 1968.
5. M. SALEH, J. Phys. C.: Solid State Phys., **9**, 4165, 1976.
6. M. SALEH, Japanese Journal of Applied Phys., **17**, No. 6 (June), 1978.

Acta Physica Academiae Scientiarum Hungaricae, Tomus 45 (3), pp. 243—275 (1978)

ON THE DIURNAL VARIATION COEFFICIENTS OF THE NUCLEONIC COMPONENT OF COSMIC RAYS

By

M. F. TOLBA, S. A. WAHAB and A. M. SALEM
COSMIC RAY GROUP, PHYSICS DEPARTMENT,
FACULTY OF SCIENCE, AIN SHAMS UNIVERSITY, CAIRO, EGYPT

(Received in revised form 24. X. 1978)

The expected amplitudes, as well as the time shift due to geomagnetic bending, of the diurnal waves have been calculated for 27 cosmic ray neutron monitors for the recent shapes of the diurnal, semidiurnal and tridiurnal anisotropies. The calculations are performed for latitude dependence of the form, $\cos^n \lambda$ and rigidity dependence of the form $R^\beta \exp[(1-R)/R_0]$ where λ is the asymptotic latitude, R is the rigidity in GV, and n, β and R_0 are constants. For the diurnal anisotropy, the calculations are given for $n = 1$, $\beta = -0.4, 0.0, +0.4, +0.8$, $R_0 = \infty$ and maximum cutoff rigidity = 90 GV, while for semidiurnal and tridiurnal anisotropies the results are given for $n = 1, 2$, $\beta = 1, 2$ and $R_0 = 50, 90$ GV. Moreover, the calculation of the attenuation due to the latitude effect, the smoothing effect, and the mean latitude and mean cone broadening are given for the different concerned anisotropies. The presently calculated coefficients for diurnal variation are significantly smaller than those calculated previously due to the careful selection of the used parameters. A considerable increase in the time shift due to geomagnetic bending is only found in the wide cone stations. The relation between the mean latitude, the cone broadening, the time shift, and the expected amplitude for all diurnal components and the minimum cutoff rigidity of the different stations are discussed.

1. Introduction

The information about the different modulation mechanisms of cosmic rays in the interplanetary space can be obtained by the investigation of the different components of solar diurnal variations. However, the accurate characteristics of the anisotropies that produce these variations can only be obtained by a careful calculation of the coefficients transforming the shape of the variations recorded on the surface of the earth to the corresponding free space anisotropy. Several calculations have been carried out by different authors for the coefficients of the first and second components of diurnal variation using different methods of calculation and shapes of anisotropy [1, 2, 3, 4, 5].

MCCRACKEN et al [2] have calculated the coefficients and the shift in the asymptotic time due to geomagnetic bending for both dirunal and semidiurnal anisotropies, where the rigidity dependence of the anisotropy is used in the form R_β up to rigidity 500 GV and latitude dependence of the form $\cos \lambda$. In later investigation, FUJII et al [5] and NAGASHIMA et al [6] showed that the semidiurnal anisotropy is reasonably assumed to have the rigidity dependence of the form $R^\beta \exp(-R/R_0)$, where R is the rigidity in GV, β

and R_0 are constants controlling the gradual increase and decrease of the anisotropy with rigidity. Theoretical and experimental investigations of semidiurnal variation show a latitude dependence of the form $\cos^2 \lambda$ rather than $\cos \lambda$ as given by LIETTI and QUENBY [7] and RAO and AGRAWAL [8]. For the diurnal variation, SUBRAMANIAN [9] suggested that the consideration of accurate value of maximum cutoff rigidity, variability of the spectral exponent of the differential primary spectrum, the contribution of high rigidity particles to the counting rate, and the proper selection of the coupling constants would considerably change the expected diurnal waves from those calculated by MCCRACKEN et al [2]. On the other hand, the existence of the tridiurnal anisotropy is discovered by MORI et al [10], FUJIMOTO et al [11] and found to be of almost similar characteristics to those obtained for semidiurnal variation (e.g. KUDO and WADA [12], and GIRGIS et al [13]).

The change of the predicted characteristics of diurnal and semidiurnal anisotropy from those assumed by MCCRACKEN et al [2] together with the discovery of the tridiurnal anisotropy show the great requirement of recent theoretical calculations to the diurnal variation coefficients for the three components of diurnal variation and different cosmic ray stations. In the present work, the expected amplitudes and time shift due to geomagnetic bending are calculated for 27 cosmic ray stations for the diurnal, semidiurnal and tridiurnal anisotropies taking into consideration the different shapes of the rigidity and latitude dependences. Moreover, the mean latitude, mean longitude mean deflection and mean cone broadening of cosmic ray trajectories are approximately calculated for the same stations and for the specified shapes of anisotropy.

2. The expected diurnal waves

The general form of the fractional change in the counting rate $\Delta N(t)/N$ at time t arising from any diurnal anisotropy with harmonic h, and amplitude A may be expressed by:

$$\Delta N(t)/N = A \int_{R_{\min}}^{R_{\max}} W(R) \cdot F(R) \cdot T[\lambda(R, a)] \cdot G[\psi(R, a), t, h] \cdot dR \,, \quad (1)$$

where $W(R)$ is the coupling constant as defined by DORMAN [4], $F(R)$ is the function describing the rigidity distribution of the anisotropy, $T[\lambda(R, a)]$ is the declination dependence function of the solar ecliptic latitude $\lambda(R, a)$ for a particle with rigidity R and direction of arrival (a), and $G[\psi(R, a), t,h]$ is the longitude dependence function for solar ecliptic longitude $\psi(R, a)$ at time t for anisotropy of component h. $R_{\min}$ and $R_{\max}$ are the minimum and maximum cutoff rigidity of the anisotropy, respectively. The functions $F(R)$,

$T[\lambda(R, a)]$ and $G[\psi(R, a), t, h]$ can generally be taken, for all diurnal components as follows:

$$F(R) = R^{\beta} \exp\left(\frac{1 - R}{R_0}\right), \tag{2}$$

$$T[\lambda(R, a)] = \cos^n \lambda(R, a), \tag{3}$$

$$G[\psi(R, a), t, h] = \cos h\,[\psi(R, a) + 15t - C_h], \tag{4}$$

where β, R_0 and n are constants, C_h is the angle of the free space anisotropy measured eastward from antisolar direction and t is the universal time in hours. The constant 1 appearing in the rigidity dependence function $F(R)$ stands for the rigidity of 1 GV to achieve the normalization so that the anisotropies with different shapes will have the same value at rigidity = 1 GV as suggested by GIRGIS et al [13].

The diurnal wave of certain harmonic h arising from an anisotropy in the outer space and observed at certain direction of arrival (a) may be obtained by calculating $\Delta N(t)/N$ at different times t using equation (1). The resultant diurnal wave observed at any location can be calculated by adding all diurnal waves observed at all possible directions of arrival, and from which the expected amplitude A_{ex} and time of maximum T_{max} are calculated by harmonic analysis.

The observed amplitude of the diurnal wave with any component at a given location is, certainly, expected to be less than the mean value of the corresponding free space anisotropy. The attenuation of the amplitude arises from the smoothing effect of the asymptotic cone of acceptance due to its longitudinal broadening, as well as from its inclination to the solar ecliptic plane where the anisotropies exist. Generally, the expected amplitude at a given cosmic ray station A_{ex} may be written in the form:

$$A_{ex} = \bar{A} \cdot S \cdot L \tag{5}$$

where $\bar{A}$ is the mean value of the anisotropy in the outer space as seen by a certain station, S is the coefficient representing the attenuation of the anisotropy due to the cone broadening only, and L is the coefficient representing the attenuation due to the cone inclination. $\bar{A}$ can be calculated in percentage of A using the normalized values of $W(R)$ as follows:

$$\bar{A} = \int_{R_{min}}^{R_{max}} W(R)\, F(R)\, dR. \tag{6}$$

Usually, it is very useful to have the values of S and L for all harmonics when studying the characteristics of the different free space anisotropies. However, it is impossible, analytically, to separate the total attenuation coeffi-

cient calculated by equation (1) into two coefficients depending on the longitudinal broadening and inclination of the station's cone. Approximate values of S and L, S_{ap} and L_{ap} respectively, can be obtained using the following equations:

$$S_{ap} = \int_{R_{\min}}^{R_{\max}} W(R)\, F(R) \cos\{h[\bar{\psi} - \psi(R, a)]\}\, dR \Big/ \int_{R_{\min}}^{R_{\max}} W(R) F(R) dR, \tag{7}$$

$$L_{ap} = \int_{R_{\min}}^{R_{\max}} W(R) F(R) \cos^n [\lambda(R, a)]\, dR \Big/ \int_{R_{\min}}^{R_{\max}} W(R)\, F(R) dR\,, \tag{8}$$

where $\bar{\psi}$ is given by:

$$\bar{\psi} = \frac{1}{h} \tan^{-1} \left\{ \int_{R_{\min}}^{R_{\max}} W(R)\, F(R) \sin [h\psi(R, a)]\, dR \Big/ \Big/ \int_{R_{\min}}^{R_{\max}} W(R)\, F(R) \cos [h\psi(R, a)]\, dR \right\}. \tag{9}$$

The approximated values of S_{ap} and L_{ap} approach the exact values only if all asymptotic directions either have common latitude or common longitude. In other words, the error in the determined attenuation coefficients will be considerably small for asymptotic cones with either latitudinal or longitudinal broadening, while for cones having both types of broadening, the error increases effectively. An estimation of the percentage error E, that is dependent on the accuracy of the calculated values of S_{ap} and L_{ap}, is obtained tained by:

$$E = \frac{A_{ap} - A_{ex}}{A_{ex}} \times 100\,, \tag{10}$$

where A_{ex} is the expected amplitude calculated using equation (1), and A_{ap} is the approximated amplitude calculated by $A_{ap} = \bar{A} \cdot S_{ap} \cdot L_{ap}$.

From the values of S_{ap} and L_{ap}, the mean cone broadening $\bar{\Phi}$ which is the longitudinal angle between two cosmic ray trajectories having equivalent smoothing effect of the station's asymptotic cone of acceptance, and the mean latitude $\bar{\lambda}$, which is the latitude of the cosmic ray trajectory having the latitude attenuation of the investigated cone, are calculated using the following equations:

$$\bar{\Phi} = \frac{2}{h} \cos^{-1} (S_{ap}) \tag{11}$$

and

$$|\,\bar{\lambda}\,| = \cos^{-1} [(L_{ap})^{1/n}]\,. \tag{12}$$

The mean time shift due to geomagnetic bending G(hrs), is computed by $G = [(C_h - \Psi)/15] - T_{\max}$, where Ψ is the geographic longitude.

In the present calculations the inclination of the earth's axis to the ecliptic plane is neglected. However, it is expected that this effect will reduce the observed amplitude of the ecliptic plane anisotropies by a coefficient depending on the season of detection. On the other hand, anisotropies perpendicular to the ecliptic plane, will be detected as a sidereal variation due to the inclination of the axis. The diurnal variation coefficients at the different seasons can be calculated after considering the inclination effect using the present coefficients by direct multiplication with the coefficients given by TOLBA and LINDGREN [15], EL-BEDEWI et al [16].

3. Method of calculation

For calculating the expected diurnal waves, the appropriate values of the used parameters are adopted as follows:

1) The asymptotic directions (λ, ψ) calculated for most of the worldwide cosmic ray stations by MCCRACKEN et al [2] for different rigidities and for 9 directions of arrival, are used in the present calculations. $R_{\min}$ at a given direction of arrival is, therefore, determined by the minimum representative rigidity of the arriving asymptotic direction. For Cairo station, the asymptotic directions were calculated by GONED and SALEM [17].

2) The coupling constants $W(R)$ are used as calculated by MATHEW and KODAMA (1964) for maximum solar activity and normalized so that:

$$\int_{R_{\min}}^{\infty} W(R)dR = 100\% \,. \tag{13}$$

This normalization is practically performed by taking the maximum limit of the integration as 500 GV instead of infinity and $W(R)$ is normalized to 91% for low cutoff rigidity stations and to 83% for high cutoff rigidity stations as stated by SUBRAMANIAN [5]. The use of recent values of $W(R)$ did not show any significiant change in the calculated coefficients.

3) The parameters β and R_0 in the rigidity dependence function (Eq. (2)) express the increase and decrease of the anisotropy with rigidity respectively. For diurnal variation, R_0 is taken as infinity where the expression is reduced to R^{β} and the integration is carried out up to $R_{\max} = 90$ GV [9] for different values of β. For the second and third harmonics of diurnal variation the calculations are performed for $\beta = 1$, 2 and $R_0 = 50$, 90 GV. The calculated amplitudes for both cases are not sensitive to $R_{\max}$ for values greater than 500 GV since $F(R)$, for the used values of β and R_0, is considerably small, and hence the integration is carried out up to 500 GV.

4) The effect of variable spectral exponent of the differential rigidity spectrum of primary cosmic rays $\gamma(R)$ at different values of R on the expected

Table I

Diurnal variation

Station	Geographic coordinates, and cutoff rigidity	β	L_{ap}	S_{ap}	$\bar{A}$	A_{ap}	A_{ex}	G	$\lvert\bar{\lambda}\rvert$	$\bar{\Phi}$	E
Ahmadabad, India	Lat. = 23.02	−0.4	0.97	0.63	15.14	9.29	9.25	5.61	13.43	101.84	0.34
	Long. = 72.60	0.0	0.97	0.66	59.86	38.13	37.88	5.01	14.69	97.62	0.65
	R_c = 15.94	+0.4	0.96	0.69	246.60	164.70	163.30	4.45	15.97	91.96	0.87
		+0.8	0.96	0.76	1059.00	744.90	737.80	3.95	17.20	85.23	0.97
Alert, Canada	Lat. = 82.52	−0.4	0.20	0.58	22.34	2.58	2.31	2.41	78.42	109.75	11.62
	Long. = 297.40	0.0	0.23	0.50	68.77	7.80	6.88	2.22	76.90	119.90	13.40
	R_c = 0.00	+0.4	0.25	0.43	233.30	25.34	22.47	2.00	75.29	129.35	12.77
		+0.8	0.28	0.36	870.90	88.71	80.84	1.76	73.75	137.30	9.74
Berkeley, USA	Lat. = 37.87	−0.4	0.90	0.86	21.85	17.03	16.95	3.47	25.28	60.93	0.46
	Long. = 237.70	0.0	0.91	0.88	69.09	55.30	55.26	3.08	25.11	55.74	0.07
	R_c = 4.54	+0.4	0.91	0.90	238.10	194.50	194.90	2.72	25.12	51.06	−0.20
		+0.8	0.90	0.92	895.30	741.10	743.70	2.41	25.41	47.86	−0.35
Cairo, Egypt	Lat. = 29.36	−0.4	0.96	0.58	17.47	9.74	9.80	5.45	16.52	108.89	−0.64
	Long. = 31.18	0.0	0.95	0.63	64.46	38.57	38.63	4.83	17.94	102.05	−0.15
	R_c = 12.35	+0.4	0.94	0.68	250.50	160.80	160.40	4.25	19.47	94.13	0.25
		+0.8	0.93	0.73	1027.00	703.80	700.30	3.75	21.02	85.57	0.50
Calgary, Canada	Lat. = 51.08	−0.4	0.93	0.98	22.41	20.36	20.42	1.53	21.92	23.51	−0.29
	Long. = 245.87	0.0	0.90	0.97	68.93	60.59	60.86	1.48	24.33	26.95	−0.45
	R_c = 1.09	+0.4	0.88	0.96	233.50	197.10	198.40	1.43	28.86	30.95	−0.63
		+0.8	0.85	0 95	870.20	702.60	708.30	1.39	32.16	34.94	−0.79
Chicago, USA	Lat. = 41.83	−0.4	0.94	0.96	22.41	20.25	20.29	2.52	19.30	33.62	−0.20
	Long. = 272.33	0.0	0.93	0.96	68.93	61.37	61.54	2.33	21.62	33.40	−0.27
	R_c = 1.72	+0.4	0.91	0.95	233.50	203.10	203.70	2.15	24.38	34.63	−0.32
		+0.8	0.89	0.95	870.20	735.00	737.60	1.99	27.16	36.61	−0.34

Churchill, Canada	Lat. = 58.75	−0.4	0.78	0.97	22.41	17.03	17.15	1.30	38.34	28.79	−0.72
	Long. = 265.92	0.0	0.75	0.95	68.93	49.64	50.18	1.29	41.01	34.72	−1.07
	R_c = 0.21	+0.4	0.72	0.94	233.50	158.60	160.90	1.27	43.57	40.73	−1.46
		+0.8	0.70	0.92	870.20	557.00	567.50	1.24	45.86	46.36	−1.83
Dallas, USA	Lat. = 32.98	−0.4	0.91	0.84	21.94	16.87	16.77	3.82	24.19	65.08	0.60
	Long. = 263.27	0.0	0.91	0.87	69.10	54.92	54.79	3.40	23.96	59.14	0.22
	R_c = 4.35	+0.4	0.91	0.89	237.40	193.40	193.50	3.00	23.86	54.02	−0.05
		+0.8	0.91	0.91	891.30	738.40	739.90	2.65	23.99	49.86	−0.20
Deep River, Canada	Lat. = 46.10	−0.4	0.93	0.97	22.41	20.19	20.27	2.37	21.96	27.49	−0.34
	Long. = 282.50	0.0	0.90	0.96	68.93	59.93	60.26	2.24	25.52	31.04	−0.54
	R_c = 1.02	+0.4	0.87	0.95	233.50	194.60	195.90	2.11	29.09	34.99	−0.67
		+0.8	0.84	0.94	870.20	693.40	698.80	1.97	32.35	38.74	−0.76
Denver, USA	Lat. = 39.67	−0.4	0.93	0.91	22.34	18.89	18.92	2.83	21.65	49.01	−0.12
	Long. = 255.03	0.0	0.93	0.93	68.98	59 21	59.36	2.54	22.32	43.76	−0.24
	R_c = 2.91	+0.4	0.92	0.94	234.20	201.60	202.20	2.29	23.53	40.32	−0.32
		+0.8	0.91	0.94	873.50	746.30	749.20	2.07	25.08	38.73	−0.38
Goose Bay, Canada	Lat. = 53.27	−0.4	0.85	0.97	22.41	18.47	18.61	2.51	31.47	29.77	−0.74
	Long. = 299.60	0.0	0.82	0.95	68.93	53.74	54.33	2.40	35.08	35.34	−1.07
	R_c = 0.52	+0.4	0.78	0.94	233.50	171.10	173.50	2.28	38.56	40.92	−1.40
		+0.8	0.75	0.92	870.20	598.50	608.60	2.14	41.66	45.96	−1.66
Inuvik, Canada	Lat. = 68.35	−0.4	0.70	0.96	22.41	15.07	15.28	0.57	45.35	33.92	−1.37
	Long. = 226.28	0.0	0.67	0.94	68.93	43.44	44.36	0.63	47.71	41.02	−2.08
	R_c = 0.18	+0.4	0.64	0.91	233.50	136.90	141.10	0.69	50.00	48.30	−2.97
		+0.8	0.61	0.89	870.20	473.90	493.40	0.74	52.07	55.23	−3.94
Kampala, Uganda	Lat. = 0.33	−0.4	0.98	0.64	15.68	9.83	9.78	4.93	11.86	100.33	0.54
	Long. = 32.56	0.0	0.98	0.67	61.05	40.11	39.87	4.41	12.36	95.47	0.58
	R_c = 14.98	+0.4	0.98	0.71	248.10	171.70	170.70	3.91	12.82	89.52	0.58
		+0.8	0.97	0.75	1054.00	770.10	765.80	3.47	13.28	82.73	0.56

Table I (contd.)

Station	Geographic coordinates, and cutoff rigidity	β	L_{ap}	S_{ap}	$\bar{A}$	A_{ap}	A_{ex}	G	$\lvert\bar{\lambda}\rvert$	$\bar{\Phi}$	E
Kiel, FRG	Lat. = 54.30	−0.4	0.91	0.93	22.40	18.91	19.02	3.57	24.65	43.50	−0.54
	Long. = 10.10	0.0	0.87	0.93	68.93	56.12	56.55	3.31	28.98	42.99	−0.76
	R_c = 2.29	+0.4	0.84	0.93	233.60	181.10	182.80	3.06	33.25	44.08	−0.96
		+0.8	0.80	0.92	870.50	638.30	645.40	2.82	37.13	46.23	−1.10
Kiruna, Sweden	Lat. = 67.83	−0.4	0.73	0.95	22.41	15.43	15.72	2.61	43.34	37.56	−1.84
	Long. = 20.43	0.0	0.69	0.92	68.93	43.85	45.10	2.55	46.39	45.45	−2.76
	R_c = 0.54	+0.4	0.65	0.89	233.50	135.90	141.20	2.47	49.32	53.58	−3.79
		+0.8	0.62	0.86	870.20	461.50	484.80	2.39	51.94	61.26	−4.80
Leeds, England	Lat. = 53.83	−0.4	0.91	0.93	22.40	18.84	18.93	3.60	25.13	43.54	−0.50
	Long. = 358.42	0.0	0.87	0.93	68.93	55.83	56.27	3.34	29.47	43.03	−0.77
	R_c = 2.20	+0.4	0.83	0.93	233.60	179.80	181.60	3.10	33.74	44.50	−1.02
		+0.8	0.79	0.92	870.50	632.40	640.20	2.86	37.61	46.97	−1.20
Lindau, FRG	Lat. = 51.60	−0.4	0.92	0.89	22.31	18.36	18.44	3.92	22.66	53.77	−0.40
	Long. = 10.10	0.0	0.89	0.91	68.99	55.77	56.06	3.59	26.79	50.18	−0.51
	R_c = 3.00	+0.4	0.86	0.91	234.40	183.30	184.50	3.27	30.92	48.50	−0.63
		+0.8	0.82	0.91	874.60	655.90	660.60	2.98	34.72	48.34	−0.71
London, England	Lat. = 51.53	−0.4	0.92	0.90	22.36	18.58	18.65	3.79	23.20	50.59	−0.39
	Long. = 359.90	0.0	0.89	0.91	68.97	55.91	56.21	3.45	27.42	48.08	−0.53
	R_c = 2.73	+0.4	0.85	0.92	234.00	182.50	183.70	3.15	31.61	47.43	−0.66
		+0.8	0.81	0.91	872.70	649.40	654.20	2.87	35.44	48.07	−0.73
McMurdo, Antartica	Lat. = −77.85	−0.4	0.24	0.59	22.41	3.23	2.95	6.85	75.92	107.27	9.52
	Long. = 166.72	0.0	0.25	0.47	68.93	8.23	6.96	6.53	75.25	124.05	18.21
	R_c = 0.01	+0.4	0.27	0.34	233.50	21.69	16.87	5.81	74.32	139.81	18.57
		+0.8	0.29	0.24	870.20	59.10	45.40	4.29	73.25	152.74	10.17
Mt. Wellington, Australia	Lat. = −42.92	−0.4	0.94	0.94	22.41	19.88	19.99	3.15	19.64	39.20	−0.50
	Long. = 147.23	0.0	0.92	0.94	68.93	59.91	60.24	2.89	23.08	38.26	−0.55
	R_c = 1.89	+0.4	0.89	0.94	233.50	196.90	198.10	2.64	26.61	38.78	−0.59
		+0.8	0.87	0.94	870.20	708.70	713.20	2.41	29.88	40.12	−0.62

Munich, FRG	Lat. = 48.20	−0.4	0.93	0.84	22.05	17.27	17.30	4.30	21.16	65.76	−0.14
	Long. = 11.60	0.0	0.91	0.87	69.08	54.32	54.42	3.90	24.81	59.93	−0.18
	R_c = 4.14	+0.4	0.88	0.88	236.60	183.80	184.20	3.52	28.55	55.59	−0.19
		+0.8	0.85	0.90	886.40	673.20	674.30	3.17	32.05	52.70	−0.15
Ottawa, Canada	Lat. = 45.40	−0.4	0.93	0.97	22.41	20.21	20.29	2.46	21.53	28.43	−0.38
	Long. = 284.40	0.0	0.91	0.96	68.93	60.07	6 0.39	2.32	25.06	31.69	−0.53
	R_c = 1.08	+0.4	0.88	0.95	233.50	195.30	196.60	2.18	28.61	35.42	−0.68
		+0.8	0.85	0.94	870.20	696.60	702.20	2.03	31.87	38.99	−0.80
Oulu, Finland	Lat. = 65.02	−0.4	0.79	0.95	22.41	16.86	17.11	2.68	38.01	34.65	−1.50
	Long. = 25.50	0.0	0.75	0.94	68.93	48.24	49.35	2.59	41.56	41.43	−2.25
	R_c = 0.81	+0.4	0.71	0.91	233.50	150.50	155.30	2.50	44.99	48.59	−3.10
		+0.8	0.67	0.89	870.20	514.60	535.80	2.41	48.08	55.46	−3.95
Resolute, Canada	Lat. = 74.72	−0.4	0.40	0.87	22.41	7.85	8.05	0.62	66.24	59.19	−2.43
	Long. = 265.02	0.0	0.40	0.82	68.93	22.71	23.55	0.64	66.33	69.66	−3.58
	R_c = 0.00	+0.4	0.40	0.77	233.50	71.91	75.75	0.65	66.33	79.87	−5.06
		+0.8	0.40	0.71	870.20	249.90	268.10	0.65	66.24	89.04	−6.79
Rome, Italy	Lat. = 41.90	−0.4	0.94	0.73	21.30	14.71	14.76	5.32	19.54	85.73	−0.34
	Long. = 12.52	0.0	0.93	0.76	68.98	48.79	48.81	4.73	22.23	80.31	−0.05
	R_c = 6.32	+0.4	0.91	0.80	241.60	174.30	173.80	4.16	25.15	74.33	0.28
		+0.8	0.88	0.83	918.10	671.90	668.10	3.64	27.97	68.08	0.57
Thule, Greenland	Lat. = 76.58	−0.4	0.33	0.81	22.41	6.06	6.21	1.80	70.54	71.50	−2.38
	Long. = 291.58	0.0	0.34	0.75	68.93	17.47	18.06	1.73	70.18	83.24	−3.29
	R_c = 0.00	+0.4	0.35	0.68	233.50	55.00	57.66	1.64	69.70	94.49	−4.60
		+0.8	0.36	0.61	870.20	189.60	202.40	1.52	69.17	104.39	−6.34
Uppsala, Sweden	Lat. = 59.85	−0.4	0.86	0.96	22.41	18.46	18.62	3.03	30.44	34.27	−0.82
	Long. = 17.58	0.0	0.82	0.94	68.93	53.58	54.26	2.87	34.62	38.31	−1.25
	R_c = 1.43	+0.4	0.78	0.93	233.50	169.40	172.40	2.72	38.68	43.29	−1.69
		+0.8	0.74	0.91	870.20	586.70	599.20	2.57	42.34	48.98	−2.08

anisotropy, is considered in the present calculations. This is achieved by multiplying the function $F(R)$ by $[\gamma(R) + 2]/[\gamma_{max} + 2]$, where γ_{max} is the maximum value of $\gamma(R)$. The consideration of this effect reduces the coefficients of diurnal variation by a small factor ($\approx 10\%$ for Deep River station), while it has a negligible effect for semidiurnal variation as well as for tridiurnal variation as stated by GIRGIS et al [13].

5) The parameter n which represents the steepness of the variation of the anisotropy with the latitude is taken as 1 for the diurnal variation, while for other diurnal components, the calculations were performed using $n = 1, 2$. The coefficients A_{ex} of the tridiurnal variation for $n = 3$ are important from the theoretical point of view. Their values can approximately be predicted from the corresponding coefficients for $n = 2$ using equation (5). Under the assumption that $\bar{\lambda}$ is slightly dependent on n, the ratio between the coefficients for $n = 2$ to those for $n = 3$ is simply $1/\cos \bar{\lambda}$.

4. Results and discussion

The calculation result of the latitude effect L_{ap}, smoothing effect S_{ap}, mean anisotropy $\bar{A}(\%)$, the approximated amplitude $A_{ap}(\%)$, the expected amplitude $A_{ex}(\%)$, the mean shift in the asymptotic time due to geomagnetic bending G (hrs), the mean latitude $|\bar{\lambda}|$ (degrees), the mean cone broadening $\bar{\Phi}$ (degrees) and the percentage error $E(\%)$ are given for the different diurnal components and for 27 cosmic ray neutron monitors. $\bar{A}$, A_{ap} and A_{ex} are given in percentage of the amplitude of the free space anisotropy A at rigidity 1 GV. The results are given in the following tables;

i) Table I: gives the results of the diurnal anisotropy for $\beta = -0.4$, 0.0, $+0.4$ and $+0.8$ together with the station's geographic coordinates (Λ, Ψ) and minimum cutoff rigidity R_c.

ii) Tables II and III: give the results of the semidiurnal anisotropy for $n = 1$ and 2, respectively. In each Table, the computations are performed for $R_0 = 50$ and 90 GV and $\beta = 1$ and 2.

iii) Tables IV and V: give the results of the tridiurnal anisotropy for $n = 1$ and 2, respectively. Also, the computed values are given for $R_0 = 50$ and 90 GV and $\beta = 1$ and 2.

The computed results are represented in Figs. 1—7 which summarize their relation to the characteristics of the different cosmic ray stations, and therefore they are useful in predicting the required coefficients for other stations if they have almost the same characteristics to those selected in the present work. The results show that the response of the station to any anisotropy in the ecliptic plane is mainly dependent on the geographic coordinates of the asymptotic directions. However, the shape of the asymptotic cone of

Table II

Semidiurnal variation, $n = 1$
$R_0 = 50$ GV

Station	β	L_{ap}	S_{ap}	$\bar{A}(\times 10^3)$	$A_{ap}(\times 10^3)$	$A_{ex}(\times 10^3)$	G	$\lvert\bar{\lambda}\rvert$	$\bar{\Phi}$	E
Ahmadabad	1	0.95	0.41	1.14	0.44	0.42	3.10	17.37	66.08	4.18
	2	0.93	0.56	59.66	31.33	30.41	2.21	21.41	55.66	3.00
Alert	1	0.27	0.20	0.98	0.05	0.03	2.91	74.26	78.53	115.65
	2	0.33	0.08	41.12	1.09	0.50	2.88	70.66	85.39	119.28
Berkeley	1	0.90	0.72	1.01	0.65	0.66	2.43	25.93	44.29	−1.89
	2	0.87	0.73	42.43	26.99	27.52	1.70	29.17	43.24	−1.94
Cairo	1	0.93	0.42	1.12	0.44	0.44	3.36	20.94	65.05	1.53
	2	0.90	0.56	54.06	27.39	26.71	2.22	25.86	55.72	2.54
Calgary	1	0.85	0.83	0.98	0.70	0.72	1.39	31.37	33.42	−3.28
	2	0.77	0.72	40.95	22.55	23.87	1.18	39.66	44.32	−5.54
Chicago	1	0.90	0.82	0.98	0.71	0.73	2.04	26.46	35.27	−1.77
	2	0.83	0.74	40.95	25.17	25.77	1.54	33.82	42.26	−2.31
Churchill	1	0.70	0.74	0.98	0.51	0.55	1.25	45.21	42.10	−6.60
	2	0.64	0.57	40.95	14.87	16.91	1.05	50.40	55.25	−12.05
Dallas	1	0.91	0.69	1.00	0.63	0.64	2.71	24.47	46.26	−1.17
	2	0.89	0.71	42.18	26.62	26.86	1.82	27.05	44.86	−0.89
Deep River	1	0.85	0.80	0.98	0.67	0.69	2.04	31.42	36.66	−2.96
	2	0.78	0.70	40.95	22.25	22.98	1.56	39.12	45.54	−3.18
Denver	1	0.91	0.80	0.98	0.71	0.72	2.10	24.99	36.84	−1.56
	2	0.86	0.76	41.13	26.69	27.15	1.56	30.82	40.91	−1.69
Goose Bay	1	0.76	0.74	0.98	0.55	0.59	2.24	40.69	42.00	−5.91
	2	0.68	0.60	40.95	16.61	18.16	1.70	47.52	53.06	−8.54
Inuvik	1	0.62	0.68	0.98	0.42	0.46	0.69	51.47	46.76	−9.79
	2	0.56	0.48	40.95	10.83	13.31	0.79	56.25	61.56	−18.60
Kampala	1	0.97	0.37	1.14	0.41	0.40	2.81	13.22	68.27	3.66
	2	0.97	0.57	58.39	32.39	31.69	1.85	14.65	55.01	2.19
Kiel	1	0.81	0.73	0.98	0.58	0.61	2.95	36.08	43.01	−4.55
	2	0.70	0.62	40.97	17.97	18.79	2.24	45.30	51.42	−4.38
Kiruna	1	0.63	0.66	0.98	0.40	0.45	2.44	51.20	49.02	−10.66
	2	0.54	0.48	40.95	10.70	11.94	2.30	57.18	61.16	−10.37
Leeds	1	0.80	0.73	0.98	0.57	0.60	3.00	36.52	43.48	−4.74
	2	0.70	0.61	40.97	17.52	18.30	2.27	45.59	52.30	−4.21
Lindau	1	0.83	0.71	0.98	0.58	0.60	3.10	33.70	44.71	−3.36
	2	0.73	0.63	41.19	19.14	19.58	2.29	42.89	50.63	−2.26

Table II (contd.)

Station	β	L_{ap}	S_{ap}	$\bar{A}(\times 10^3)$	$A_{ap}(\times 10^3)$	$A_{ex}(\times 10^3)$	G	$\lvert\bar{\lambda}\rvert$	$\bar{\Phi}$	E
London	1	0.83	0.71	0.98	0.58	0.60	3.00	34.36	44.70	−3.60
	2	0.73	0.63	41.09	18.66	19.16	2.17	43.47	51.24	−2.59
McMurdo	1	0.28	0.19	0.98	0.05	0.04	7.50	73.58	79.27	39.80
	2	0.34	0.06	40.95	0.86	0.61	8.41	70.37	86.40	41.09
Mt. Wellington	1	0.87	0.78	0.98	0.67	0.69	2.40	28.97	38.31	−2.36
	2	0.80	0.72	40.95	23.47	23.69	1.83	36.91	44.19	−0.93
Munich	1	0.86	0.67	1.00	0.57	0.59	3.30	31.14	47.77	−2.45
	2	0.77	0.64	41.88	20.45	20.49	2.33	39.95	50.44	−0.23
Ottawa	1	0.86	0.80	0.98	0.67	0.69	2.11	30.94	36.96	−2.73
	2	0.78	0.70	40.95	22.42	23.12	1.58	38.65	45.48	−3.04
Oulu	1	0.68	0.69	0.98	0.46	0.51	2.47	47.22	46.71	−10.55
	2	0.58	0.52	40.95	12.31	14.06	2.08	54.34	58.93	−12.40
Resolute	1	0.40	0.47	0.98	0.18	0.19	0.59	66.24	62.28	−5.86
	2	0.41	0.27	40.95	4.47	5.40	0.54	65.72	74.61	−17.31
Rome	1	0.89	0.49	1.03	0.45	0.44	3.60	27.32	60.81	0.94
	2	0.82	0.59	43.94	21.31	20.55	2.34	34.99	53.70	3.65
Thule	1	0.35	0.33	0.98	0.11	0.12	1.77	69.36	70.57	−6.09
	2	0.38	0.15	40.95	2.36	2.79	1.11	67.86	81.20	−15.50
Uppsala	1	0.75	0.72	0.98	0.53	0.57	2.67	41.36	43.81	−7.52
	2	0.64	0.56	40.95	14.86	16.47	2.15	49.94	55.67	−9.79

Table II (contd.)

Semidiurnal variation, $n = 1$
$R_0 = 90$ GV

Station	β	L_{ap}	S_{ap}	$\bar{A}(\times 10^3)$	$A_{ap}(\times 10^3)$	$A_{ex}(\times 10^3)$	G	$\lvert\bar{\lambda}\rvert$	$\bar{\Phi}$	E
Ahmadabad	1	0.94	0.46	1.96	0.85	0.82	2.45	19.84	62.35	4.04
	2	0.91	0.64	148.40	86.81	84.62	1.57	23.83	50.25	2.57
Alert	1	0.30	0.14	1.53	0.07	0.04	2.84	72.69	81.71	83.88
	2	0.35	0.04	98.42	1.53	0.57	1.14	69.37	87.47	174.57
Berkeley	1	0.88	0.69	1.57	0.97	0.99	2.09	27.83	45.99	−2.04
	2	0.85	0.72	101.50	61.41	62.25	1.27	32.28	44.31	−1.34
Cairo	1	0.92	0.46	1.86	0.78	0.75	2.64	23.73	62.81	3.16
	2	0.88	0.63	131.90	72.99	71.35	1.54	28.61	50.92	2.29
Calgary	1	0.81	0.78	1.53	0.96	1.01	1.29	35.46	39.15	−4.74
	2	0.73	0.65	97.93	46.24	49.68	0.95	43.33	49.51	−6.91
Chicago	1	0.87	0.77	1.53	1.02	1.04	1.82	30.06	39.62	−2.26
	2	0.80	0.71	97.93	55.72	57.17	1.17	36.84	44.68	−2.52
Churchill	1	0.67	0.66	1.53	0.68	0.75	1.16	47.59	48.66	−9.53
	2	0.61	0.49	97.93	29.11	34.62	0.83	52.41	60.82	−15.89
Dallas	1	0.90	0.66	1.57	0.94	0.95	2.30	26.01	48.32	−1.17
	2	0.87	0.70	100.90	61.68	61.91	1.32	29.68	45.28	−0.36
Deep River	1	0.82	0.75	1.53	0.93	0.97	1.84	35.11	41.62	−3.27
	2	0.74	0.67	97.93	48.47	49.56	1.18	42.12	48.14	−2.20
Denver	1	0.88	0.76	1.53	1.03	1.05	1.86	28.06	40.18	−1.73
	2	0.83	0.73	98.36	59.00	59.72	1.19	34.31	43.42	−1.19
Goose Bay	1	0.72	0.67	1.53	0.74	0.80	2.02	43.82	47.77	−7.10
	2	0.64	0.56	97.93	35.40	38.59	1.24	49.88	55.86	−8.25
Inuvik	1	0.59	0.59	1.53	0.53	0.62	0.71	53.65	54.19	−14.26
	2	0.53	0.36	97.93	18.55	24.70	0.74	58.14	68.96	−15.19
Kampala	1	0.97	0.45	1.94	0.85	0.82	2.10	14.04	63.24	2.99
	2	0.96	0.66	144.50	92.64	91.17	1.28	15.44	48.32	1.60
Kiel	1	0.76	0.66	1.53	0.77	0.81	2.68	40.49	48.75	−5.52
	2	0.66	0.56	97.98	36.39	38.27	1.67	48.87	55.61	−4.90
Kiruna	1	0.59	0.57	1.53	0.52	0.58	2.31	53.91	54.97	−11.56
	2	0.51	0.43	97.93	21.60	22.47	1.67	59.35	64.36	−3.86
Leeds	1	0.76	0.65	1.53	0.75	0.80	2.72	40.82	49.44	−5.58
	2	0.66	0.56	97.98	35.78	37.21	1.67	48.99	56.17	−3.81
Lindau	1	0.79	0.65	1.54	0.78	0.81	2.78	38.14	49.67	−3.72
	2	0.69	0.59	98.52	40.29	40.84	1.68	46.52	53.52	−1.33

Table II (contd.)

Station	β	L_{ap}	S_{ap}	$\bar{A}(\times 10^3)$	$A_{ap}(\times 10^3)$	$A_{ex}(\times 10^3)$	G	$\lvert\bar{\lambda}\rvert$	$\bar{\Phi}$	E
London	1	0.78	0.64	1.53	0.77	0.80	2.63	38.72	49.93	−4.01
	2	0.68	0.59	98.26	39.29	39.77	1.54	46.96	54.14	−1.22
McMurdo	1	0.31	0.14	1.53	0.06	0.04	7.66	72.11	82.14	73.07
	2	0.36	0.06	97.93	2.01	2.27	8.61	68.83	86.74	−11.85
Mt. Wellington	1	0.84	0.73	1.53	0.94	0.96	2.10	32.82	42.74	−1.85
	2	0.77	0.69	97.93	52.04	51.46	1.33	40.04	46.04	1.11
Munich	1	0.81	0.62	1.56	0.79	0.80	2.90	35.46	51.75	−1.98
	2	0.72	0.62	100.10	44.77	44.38	1.67	43.59	51.90	0.88
Ottawa	1	0.82	0.74	1.53	0.94	0.96	1.88	34.63	41.85	−2.98
	2	0.75	0.67	97.93	49.01	50.10	1.17	41.64	47.95	−2.17
Oulu	1	0.64	0.61	1.53	0.59	0.67	2.32	50.50	52.76	−11.99
	2	0.54	0.47	97.93	25.26	26.91	1.67	57.00	61.72	−6.14
Resolute	1	0.41	0.37	1.53	0.23	0.26	0.57	65.98	68.05	−10.25
	2	0.42	0.17	97.93	7.13	10.48	0.49	65.36	79.93	−31.97
Rome	1	0.86	0.49	1.62	0.67	0.65	2.97	31.19	60.84	3.43
	2	0.78	0.62	105.20	51.21	49.21	1.61	38.44	51.58	4.08
Thule	1	0.36	0.26	1.53	0.14	0.15	1.55	68.67	75.09	−7.22
	2	0.39	0.19	97.93	7.23	6.42	0.55	67.19	79.03	12.49
Uppsala	1	0.70	0.64	1.53	0.69	0.76	2.47	45.39	50.23	−9.29
	2	0.60	0.50	97.93	29.51	32.26	1.66	53.22	59.77	−8.51

Table III

Semidiurnal variation, $n = 2$
$R_0 = 50$ GV

Station	β	L_{ap}	S_{ap}	$\bar{A}(\times 10^3)$	$A_{ap}(\times 10^3)$	$A_{ex}(\times 10^3)$	G	$\lvert\bar{\lambda}\rvert$	$\bar{\Phi}$	E
Ahmadabad	1	0.92	0.41	1.14	0.42	0.40	3.18	16.84	66.08	6.57
	2	0.88	0.56	59.66	29.45	27.94	2.25	20.69	55.66	5.38
Alert	1	0.10	0.20	0.98	0.02	0.01	3.19	71.83	70.53	153.85
	2	0.14	0.08	41.12	0.45	0.13	2.57	68.43	85.39	247.69
Berkeley	1	0.82	0.72	1.01	0.59	0.61	2.42	25.24	44.29	−3.22
	2	0.78	0.73	42.43	24.03	24.89	1.73	28.15	43.24	−3.42
Cairo	1	0.88	0.42	1.12	0.42	0.41	3.46	20.27	65.05	2.14
	2	0.82	0.56	54.06	25.02	23.97	2.29	24.96	55.72	4.39
Calgary	1	0.76	0.83	0.98	0.62	0.65	1.40	29.65	33.42	−5.39
	2	0.63	0.72	40.95	18.31	20.20	1.20	37.74	44.32	−8.32
Chicago	1	0.82	0.82	0.98	0.65	0.68	2.08	25.21	35.27	−3.40
	2	0.71	0.74	40.95	21.64	22.59	1.58	32.33	42.26	−4.23
Churchill	1	0.53	0.74	0.98	0.38	0.43	1.26	43.46	42.10	−10.30
	2	0.44	0.57	40.95	10.32	12.69	1.06	48.32	55.26	−18.69
Dallas	1	0.84	0.69	1.00	0.58	0.59	2.71	23.69	46.26	−2.31
	2	0.81	0.71	42.18	24.09	24.54	1.85	26.19	44.86	−1.81
Deep River	1	0.75	0.80	0.98	0.59	0.62	2.09	29.81	36.66	−5.18
	2	0.63	0.70	40.95	18.14	19.29	1.61	37.31	45.54	−5.94
Denver	1	0.83	0.80	0.98	0.65	0.67	2.13	24.11	36.84	−2.81
	2	0.76	0.76	41.13	23.50	24.27	1.60	29.58	40.91	−3.16
Goose Bay	1	0.61	0.74	0.98	0.44	0.49	2.30	38.69	42.00	−9.38
	2	0.50	0.60	40.95	12.18	14.00	1.76	45.27	53.06	−12.99
Inuvik	1	0.42	0.68	0.98	0.28	0.33	0.65	49.33	46.76	−14.18
	2	0.35	0.48	40.95	6.84	9.34	0.73	53.69	61.55	−16.77
Kampala	1	0.95	0.37	1.14	0.40	0.38	2.82	13.03	68.27	3.34
	2	0.94	0.57	58.39	31.41	30.43	1.85	14.40	55.01	3.22
Kiel	1	0.69	0.73	0.98	0.50	0.54	3.05	33.66	43.01	−7.94
	2	0.54	0.62	40.97	13.86	15.06	2.36	42.55	51.42	−7.95
Kiruna	1	0.43	0.66	0.98	0.28	0.33	2.48	48.87	49.02	−16.66
	2	0.54	0.48	40.95	6.67	8.25	2.17	54.46	61.16	−19.08
Leeds	1	0.69	0.73	0.98	0.49	0.53	3.10	34.08	43.48	−8.39
	2	0.54	0.61	40.97	13.46	14.67	2.39	42.85	52.30	−8.25
Lindau	1	0.75	0.71	0.98	0.51	0.54	3.21	31.48	44.71	−6.35
	2	0.58	0.63	41.19	15.18	15.95	2.41	40.34	50.63	−4.84

Table III (contd.)

Station	β	L_{ap}	S_{ap}	$\bar{A}(\times 10^3)$	$A_{ap}(\times 10^3)$	$A_{ex}(\times 10^3)$	G	$\lvert\bar{\lambda}\rvert$	$\bar{\Phi}$	E
London	1	0.72	0.71	0.98	0.50	0.54	3.00	32.10	44.70	−6.80
	2	0.57	0.63	41.09	14.69	15.52	2.17	40.90	51.24	−5.35
McMurdo	1	0.10	0.19	0.98	0.02	0.01	7.50	71.54	79.27	143.99
	2	0.14	0.06	40.95	0.35	0.45	6.41	68.19	86.40	−22.09
Mt. Wellington	1	0.79	0.78	0.98	0.60	0.63	2.40	27.42	38.31	−4.17
	2	0.67	0.72	40.95	19.85	20.12	1.90	35.09	44.19	−2.31
Munich	1	0.76	0.67	1.00	0.51	0.54	3.42	29.24	47.77	−4.94
	2	0.63	0.64	41.88	16.70	16.96	2.46	37.68	50.44	−1.49
Ottawa	1	0.76	0.80	0.98	0.59	0.62	2.15	29.34	36.96	−4.89
	2	0.64	0.70	40.95	18.38	19.46	1.62	36.86	45.48	−5.57
Oulu	1	0.50	0.69	0.98	0.34	0.40	2.52	44.78	46.71	−15.81
	2	0.39	0.52	40.95	8.19	10.23	2.18	51.51	58.93	−20.03
Resolute	1	0.18	0.47	0.98	0.08	0.09	0.56	64.53	62.28	−7.95
	2	0.20	0.27	40.95	2.17	2.90	0.42	63.46	74.61	−13.36
Rome	1	0.81	0.49	1.03	0.41	0.41	3.76	25.93	60.81	0.02
	2	0.70	0.59	43.94	18.21	17.30	2.46	33.21	53.70	5.22
Thule	1	0.15	0.33	0.98	0.05	0.05	1.76	67.59	70.57	−6.84
	2	0.17	0.15	40.95	1.06	1.46	1.22	65.68	81.20	−20.10
Uppsala	1	0.61	0.72	0.98	0.43	0.49	2.73	38.77	43.81	−11.90
	2	0.47	0.56	40.95	10.75	12.75	2.24	46.97	55.67	−15.70

Table III (contd.)

Semidiurnal variation, $n = 2$
$R_0 = 90$ GV

Station	β	L_{ap}	S_{ap}	$\bar{A}(\times 10^3)$	$A_{ap}(\times 10^3)$	$A_{ex}(\times 10^3)$	G	$\lvert\bar{\lambda}\rvert$	$\bar{\Phi}$	E
Ahmadabad	1	0.89	0.46	1.96	0.81	0.76	2.51	19.16	62.35	7.10
	2	0.85	0.64	148.40	80.45	76.85	1.85	22.96	50.25	4.68
Alert	1	0.11	0.14	1.53	0.03	0.01	2.89	70.25	81.71	197.32
	2	0.15	0.04	98.42	0.65	0.35	0.63	67.20	87.47	85.26
Berkeley	1	0.79	0.69	1.57	0.87	0.90	2.10	26.94	45.99	−3.65
	2	0.73	0.72	101.50	53.32	54.78	1.30	31.04	44.31	−2.65
Cairo	1	0.85	0.46	1.86	0.72	0.68	2.75	22.88	62.81	5.38
	2	0.79	0.63	131.90	65.38	62.75	1.58	27.53	50.92	4.18
Calgary	1	0.70	0.78	1.53	0.82	0.89	1.32	33.50	39.15	−7.87
	2	0.56	0.65	97.93	35.87	40.58	0.97	41.31	49.51	−11.62
Chicago	1	0.77	0.77	1.53	0.91	0.95	1.87	28.60	39.62	−4.19
	2	0.67	0.71	97.93	46.50	48.55	1.20	35.19	44.68	−4.21
Churchill	1	0.49	0.66	1.53	0.49	0.58	1.17	45.61	48.66	−14.75
	2	0.41	0.49	97.93	19.57	25.77	0.84	50.18	60.82	−24.05
Dallas	1	0.82	0.66	1.57	0.85	0.87	2.32	25.12	48.32	−2.39
	2	0.77	0.70	100.90	54.76	55.22	1.35	28.57	45.28	−0.83
Deep River	1	0.70	0.75	1.53	0.80	0.85	1.90	33.27	41.62	−5.96
	2	0.58	0.67	97.93	38.20	40.03	1.21	40.13	48.14	−4.57
Denver	1	0.79	0.76	1.53	0.93	0.96	1.90	26.93	40.18	−3.24
	2	0.71	0.73	98.36	50.39	51.72	1.22	32.87	43.42	−2.57
Goose Bay	1	0.56	0.67	1.53	0.57	0.65	2.09	41.55	47.77	−11.28
	2	0.46	0.56	97.93	25.21	28.72	1.28	47.36	55.86	−12.19
Inuvik	1	0.39	0.59	1.53	0.35	0.44	0.66	51.29	54.19	−20.73
	2	0.32	0.36	97.93	11.21	17.65	0.67	55.61	68.96	−36.48
Kampala	1	0.94	0.45	1.94	0.82	0.79	2.10	13.81	63.24	4.42
	2	0.93	0.66	144.50	89.53	87.40	1.28	15.16	48.32	2.43
Kiel	1	0.63	0.66	1.53	0.63	0.70	2.80	37.70	48.75	−9.27
	2	0.48	0.56	97.98	26.80	28.88	1.79	45.89	55.61	−7.20
Kiruna	1	0.39	0.57	1.53	0.34	0.42	2.37	51.29	54.97	−18.96
	2	0.30	0.43	97.93	12.90	14.59	1.78	56.50	64.36	−11.56
Leeds	1	0.62	0.65	1.53	0.62	0.68	2.85	38.04	49.44	−10.05
	2	0.48	0.56	97.98	26.28	28.15	1.79	46.03	56.17	−6.64
Lindau	1	0.66	0.65	1.54	0.66	0.71	2.92	35.57	49.67	−7.13
	2	0.52	0.59	98.52	30.55	31.33	1.80	43.76	53.52	−2.49

Table III (contd.)

Station	β	L_{ap}	S_{ap}	$\bar{A}(\times 10^3)$	$A_{ap}(\times 10^3)$	$A_{ex}(\times 10^3)$	G	$\lvert\bar{\lambda}\rvert$	$\bar{\Phi}$	E
London	1	0.65	0.64	1.53	0.64	0.70	2.63	36.13	49.93	−7.66
	2	0.51	0.59	98.26	29.61	30.36	1.54	44.18	54.14	−2.48
McMurdo	1	0.12	0.14	1.53	0.02	0.01	7.66	69.92	82.14	134.13
	2	0.16	0.06	97.93	0.87	1.76	8.61	66.64	86.74	−50.29
Mt. Wellington	1	0.73	0.73	1.53	0.82	0.86	2.10	31.01	42.74	−3.76
	2	0.62	0.69	97.93	42.19	41.87	1.39	38.02	46.04	0.75
Munich	1	0.70	0.62	1.56	0.67	0.71	3.06	33.22	51.75	−4.50
	2	0.57	0.62	100.10	35.10	34.69	1.79	41.10	51.90	1.16
Ottawa	1	0.71	0.74	1.53	0.80	0.85	1.94	32.81	41.85	−5.54
	2	0.59	0.67	97.93	38.85	40.58	1.20	39.68	47.95	−4.27
Oulu	1	0.45	0.61	1.53	0.42	0.51	2.40	47.72	42.76	−18.60
	2	0.35	0.47	97.93	16.01	18.40	1.78	54.02	61.72	−12.98
Resolute	1	0.19	0.37	1.53	0.11	0.13	0.50	64.05	68.05	−14.54
	2	0.21	0.17	97.93	3.52	6.30	0.29	63.03	79.93	−44.12
Rome	1	0.76	0.49	1.62	0.60	0.57	3.16	29.49	60.84	4.21
	2	0.65	0.62	105.20	42.32	39.73	1.71	36.44	51.58	6.51
Thule	1	0.16	0.26	1.53	0.06	0.07	1.55	66.70	75.09	−9.84
	2	0.18	0.19	97.93	3.37	3.28	0.76	64.84	79.03	2.69
Uppsala	1	0.54	0.64	1.53	0.53	0.62	2.56	42.42	50.23	−14.81
	2	0.41	0.50	97.93	20.34	23.53	1.76	50.03	59.77	−13.55

Table IV

Tridiurnal variation, $n = 1$
$R_0 = 50$ GV

Station	β	L_{ap}	S_{ap}	$\bar{A}(\times 10^3)$	$A_{ap}(\times 10^3)$	$A_{ex}(\times 10^3)$	G	$\lvert\bar{\lambda}\rvert$	$\bar{\Phi}$	E
Ahmadabad	1	0.95	0.21	1.14	0.23	0.22	2.90	17.37	51.79	6.99
	2	0.93	0.34	59.66	18.88	18.05	2.04	21.41	46.74	4.59
Alert	1	0.27	0.16	0.98	0.04	0.02	1.56	74.26	54.81	116.17
	2	0.33	0.20	41.12	2.72	1.30	0.38	70.66	52.31	109.91
Berkeley	1	0.90	0.51	1.01	0.46	0.48	2.46	25.93	39.57	−4.72
	2	0.87	0.49	42.43	17.98	18.91	1.77	29.17	40.64	−4.88
Cairo	1	0.93	0.19	1.12	0.20	0.19	2.82	20.94	52.77	5.65
	2	0.90	0.33	54.06	15.97	15.27	1.98	25.86	47.21	4.63
Calgary	1	0.85	0.68	0.98	0.57	0.61	1.41	31.37	31.21	−6.61
	2	0.77	0.48	40.95	15.03	17.19	1.24	39.66	41.01	−12.54
Chicago	1	0.90	0.65	0.98	0.57	0.59	2.12	26.46	32.92	−3.81
	2	0.83	0.50	40.95	17.14	18.20	1.64	33.82	39.82	−5.80
Churchill	1	0.70	0.56	0.98	0.39	0.44	1.28	45.21	37.11	−11.13
	2	0.64	0.32	40.95	8.42	10.77	1.13	50.40	47.44	−21.85
Dallas	1	0.91	0.46	1.00	0.42	0.43	2.76	24.47	41.64	−2.96
	2	0.89	0.45	42.18	16.98	17.33	1.87	27.05	42.08	−1.99
Deep River	1	0.85	0.63	0.98	0.53	0.56	2.13	31.43	33.93	−6.47
	2	0.78	0.45	40.95	14.19	15.53	1.70	39.12	42.30	−8.57
Denver	1	0.91	0.64	0.98	0.57	0.59	2.15	24.99	33.64	−3.21
	2	0.86	0.53	41.13	18.67	19.44	1.65	30.82	38.71	−3.92
Goose Bay	1	0.76	0.56	0.98	0.42	0.47	2.37	40.69	37.29	−10.98
	2	0.68	0.33	40.95	9.08	11.25	1.91	47.52	47.22	−19.32
Inuvik	1	0.62	0.53	0.98	0.33	0.37	0.77	51.47	38.44	−10.73
	2	0.56	0.32	40.95	7.30	8.69	0.75	56.25	47.52	−15.99
Kampala	1	0.97	0.24	1.14	0.27	0.26	2.20	13.22	50.55	4.75
	2	0.97	0.39	58.39	22.16	21.27	1.64	14.65	44.60	4.14
Kiel	1	0.81	0.54	0.98	0.43	0.47	3.08	36.08	38.09	−9.45
	2	0.70	0.35	40.97	10.16	11.54	2.50	45.30	46.23	−11.96
Kiruna	1	0.63	0.51	0.98	0.31	0.36	2.54	51.20	39.74	−14.25
	2	0.54	0.26	40.95	5.66	7.21	2.42	57.18	50.14	−21.52
Leeds	1	0.80	0.54	0.98	0.42	0.47	3.16	36.52	38.38	−10.20
	2	0.70	0.33	40.97	9.59	11.05	2.58	45.59	46.96	−13.06
Lindau	1	0.83	0.52	0.98	0.42	0.46	3.26	33.70	39.32	−7.43
	2	0.73	0.36	41.19	10.73	11.60	2.54	42.89	46.11	−7.49

Table IV (contd.)

Station	β	L_{ap}	S_{ap}	$\bar{A}(\times 10^3)$	$A_{ap}(\times 10^3)$	$A_{ex}(\times 10^3)$	G	$\lvert\bar{\lambda}\rvert$	$\bar{\Phi}$	E
London	1	0.83	0.52	0.98	0.42	0.45	3.20	34.26	39.25	—7.72
	2	0.73	0.35	41.09	10.31	11.26	2.46	43.47	46.50	—8.44
McMurdo	1	0.28	0.34	0.98	0.09	0.06	7.07	73.58	46.86	40.50
	2	0.34	0.31	40.95	4.20	2.57	7.37	70.37	48.16	62.95
Mt. Wellington	1	0.87	0.61	0.98	0.52	0.55	2.47	28.97	35.04	—5.35
	2	0.80	0.47	40.95	15.46	15.98	1.89	36.91	41.21	—5.28
Munich	1	0.86	0.45	1.00	0.38	0.41	3.47	31.14	42.11	—6.12
	2	0.77	0.35	41.88	11.33	11.49	2.54	39.95	46.21	—1.35
Ottawa	1	0.86	0.63	0.98	0.52	0.55	2.21	30.94	34.19	—5.43
	2	0.78	0.45	40.95	14.30	15.33	1.71	38.65	42.28	—6.69
Oulu	1	0.68	0.53	0.98	0.35	0.41	2.57	47.22	38.68	—14.92
	2	0.58	0.29	40.95	6.92	8.86	2.38	54.34	48.76	—21.86
Resolute	1	0.40	0.24	0.98	0.09	0.11	0.44	66.24	50.85	—11.60
	2	0.41	0.06	40.95	1.08	2.11	0.46	65.72	57.53	—48.49
Rome	1	0.89	0.25	1.03	0.23	0.23	3.56	27.32	50.18	0.59
	2	0.82	0.32	43.94	11.55	10.59	2.33	34.99	47.52	9.03
Thule	1	0.35	0.27	0.98	0.09	0.09	1.94	69.36	49.42	5.88
	2	0.38	0.17	40.95	2.68	2.24	2.19	67.86	53.33	19.47
Uppsala	1	0.75	0.54	0.98	0.40	0.46	2.79	41.36	38.27	—13.66
	2	0.64	0.29	40.95	7.72	9.99	2.39	49.94	48.65	—12.80

Table IV (contd.)

Tridiurnal variation, $n = 1$
$R_0 = 90$ GV

Station	β	L_{ap}	S_{ap}	$\bar{A}(\times 10^3)$	$A_{ap}(\times 10^3)$	$A_{ex}(\times 10^3)$	G	$\lvert\bar{\lambda}\rvert$	$\bar{\Phi}$	E
Ahmadabad	1	0.94	0.25	1.96	0.47	0.44	2.21	19.84	50.22	6.21
	2	0.91	0.42	148.40	56.56	54.21	1.44	23.83	43.58	4.34
Alert	1	0.30	0.16	1.53	0.07	0.04	0.95	72.69	53.90	103.58
	2	0.35	0.27	98.42	9.25	4.54	0.64	69.37	49.68	103.89
Berkeley	1	0.88	0.46	1.57	0.64	0.68	2.16	27.83	41.62	−5.25
	2	0.85	0.46	101.50	39.38	40.81	1.33	32.28	41.79	−3.50
Cairo	1	0.92	0.24	1.86	0.40	0.37	2.16	23.73	50.91	7.59
	2	0.88	0.40	131.90	46.14	44.42	1.39	28.61	44.34	3.86
Calgary	1	0.81	0.59	1.53	0.73	0.81	1.34	35.96	36.12	−9.87
	2	0.73	0.37	97.93	26.54	31.95	1.04	43.33	45.41	−16.91
Chicago	1	0.87	0.57	1.53	0.75	0.79	1.94	30.06	36.88	−5.16
	2	0.80	0.45	97.93	35.40	37.98	1.26	36.84	42.09	−6.79
Churchill	1	0.67	0.45	1.53	0.47	0.56	1.22	47.65	41.96	−18.04
	2	0.61	0.23	97.93	13.93	19.60	0.93	52.41	51.00	−28.90
Dallas	1	0.90	0.41	1.57	0.58	0.59	2.37	26.01	43.88	−3.05
	2	0.87	0.45	100.90	39.36	39.58	1.32	29.68	42.21	−0.53
Deep River	1	0.82	0.54	1.53	0.67	0.73	1.98	35.11	38.29	−7.79
	2	0.74	0.39	97.93	28.36	30.35	1.32	42.12	44.68	−6.58
Denver	1	0.88	0.57	1.53	0.77	0.80	1.95	28.06	36.99	−3.82
	2	0.83	0.48	98.36	38.62	39.81	1.28	34.31	41.07	−2.99
Goose Bay	1	0.72	0.45	1.53	0.50	0.58	2.22	43.82	42.14	−14.17
	2	0.64	0.26	97.93	16.46	20.62	1.43	49.88	49.91	−20.20
Inuvik	1	0.59	0.44	1.53	0.40	0.46	0.76	53.65	42.66	−14.02
	2	0.53	0.23	97.93	11.93	14.92	0.76	58.14	51.09	−20.02
Kampala	1	0.97	0.31	1.94	0.58	0.55	1.73	14.04	48.09	4.09
	2	0.96	0.47	144.50	66.00	63.91	1.15	15.44	41.14	3.27
Kiel	1	0.76	0.43	1.53	0.50	0.58	2.91	40.49	42.87	−12.50
	2	0.66	0.26	97.98	16.81	19.31	1.92	48.87	49.91	−12.90
Kiruna	1	0.59	0.38	1.53	0.34	0.43	2.51	53.91	44.98	−19.73
	2	0.51	0.10	97.93	5.23	8.94	2.18	59.35	55.99	−41.50
Leeds	1	0.76	0.42	1.53	0.49	0.56	2.99	40.82	43.38	−13.65
	2	0.66	0.25	97.98	15.80	17.72	1.97	48.99	50.51	−10.83
Lindau	1	0.79	0.41	1.54	0.49	0.55	3.04	38.14	43.90	−10.19
	2	0.69	0.28	98.52	18.96	20.17	1.88	46.52	49.16	−5.99

Table IV (contd.)

Station	β	L_{ap}	S_{ap}	$\bar{A}(\times 10^8)$	$A_{ap}(\times 10^8)$	$A_{ex}(\times 10^8)$	G	$\lvert\bar{\lambda}\rvert$	$\bar{\Phi}$	E
London	1	0.78	0.41	1.53	0.49	0.54	2.97	38.73	44.01	−10.75
	2	0.68	0.27	98.26	18.00	19.21	1.72	46.96	49.62	−6.33
McMurdo	1	0.31	0.32	1.53	0.15	0.10	7.26	72.11	47.51	64.93
	2	0.36	0.30	97.93	10.78	7.03	7.67	68.83	48.16	63.50
Mt. Wellington	1	0.84	0.52	1.53	0.66	0.70	2.27	32.82	39.21	−5.41
	2	0.77	0.43	97.93	31.99	31.31	1.36	40.04	43.15	2.16
Munich	1	0.81	0.36	1.56	0.45	0.49	3.17	35.46	46.00	−7.14
	2	0.72	0.31	100.10	22.39	22.07	1.77	43.59	48.01	1.44
Ottawa	1	0.82	0.53	1.53	0.67	0.71	2.03	34.63	38.50	−6.20
	2	0.75	0.40	97.93	28.93	30.32	1.29	41.64	44.47	−4.59
Oulu	1	0.64	0.41	1.53	0.40	0.50	2.52	50.50	43.81	−20.16
	2	0.54	0.17	97.93	9.08	12.52	2.09	57.00	53.46	−27.47
Resolute	1	0.41	0.17	1.53	0.10	0.13	0.21	65.98	53.63	−19.47
	2	0.42	0.09	97.93	3.63	5.97	0.86	65.36	56.60	−39.31
Rome	1	0.86	0.23	1.62	0.32	0.30	2.96	31.19	51.09	6.77
	2	0.78	0.35	105.20	28.60	25.90	1.54	38.44	46.46	10.42
Thule	1	0.36	0.23	1.53	0.13	0.11	2.06	86.67	51.23	10.62
	2	0.39	0.15	97.93	5.53	4.45	2.74	67.19	54.41	24.41
Uppsala	1	0.70	0.42	1.53	0.45	0.55	2.67	45.39	43.50	−18.58
	2	0.60	0.21	97.93	12.35	15.42	1.91	53.22	51.89	−19.88

Table V

Tridiurnal variation, $n = 2$
$R_0 = 50$ GV

Station	β	L_{ap}	S_{ap}	$\bar{A}(\times 10^3)$	$A_{ap}(\times 10^3)$	$A_{ez}(\times 10^3)$	G	$\lvert\bar{\lambda}\rvert$	$\bar{\Phi}$	E
Ahmadabad	1	0.92	0.21	1.14	0.22	0.20	2.98	16.84	51.79	12.18
	2	0 86	0.34	59.66	17.75	16.18	2.07	20.69	46.74	9.69
Alert	1	0.10	0.16	0.98	0.01	0.00	2.48	71.83	54.81	399.97
	2	0.14	0.20	41.12	1.11	0.13	0.39	68.43	52.31	751.05
Berkeley	1	0.82	0.51	1.01	0.42	0.46	2.44	25.24	39.57	−7.92
	2	0.78	0.49	42.43	16.01	17.45	1.79	28.15	40.64	−8.24
Cairo	1	0.88	0.19	1.12	0.19	0.17	2.93	20.27	52.77	10.03
	2	0.82	0.33	54.06	14.59	13.44	2.02	24.96	47.21	8.57
Calgary	1	0.76	0.68	0.98	0.51	0.57	1.42	29.65	31.21	−10.56
	2	0.63	0.48	40.95	12.21	15.20	1.25	37.74	41.01	−19.66
Chicago	1	0.82	0.65	0.98	0.52	0.56	2.15	25.21	32.92	−7.03
	2	0.71	0.50	40.95	14.73	16.34	1.67	32.32	39.82	−9.83
Churchill	1	0.53	0.56	0.98	0.29	0.35	1.28	43.46	37.11	−16.94
	2	0.44	0.32	40.95	5.84	8.54	1.12	48.32	47.44	−21.56
Dallas	1	0.84	0.46	1.00	0.39	0.41	2.75	23.69	41.64	−5.87
	2	0.61	0.45	42.16	15.37	16.04	1.90	26.13	42.08	−4.16
Deep River	1	0.75	0.63	0.98	0.46	0.52	2.16	29.81	33.93	−10.60
	2	0.63	0.45	40.95	11.57	13.47	1.73	37.31	42.30	−14.05
Denver	1	0.83	0.64	0.98	0.52	0.55	2.17	24.11	33.64	−5.76
	2	0.76	0.53	41.13	16.44	17.71	1.68	29.58	38.71	−7.15
Goose Bay	1	0.61	0.56	0.98	0.33	0.40	2.40	38.69	37.29	−16.78
	2	0.50	0.33	40.95	6.66	9.14	1.94	45.27	47.22	−27.12
Inuvik	1	0.42	0.53	0.98	0.22	0.27	0.76	49.35	38.44	−16.72
	2	0.35	0.32	40.95	4.61	6.15	0.75	53.69	47.52	−25.07
Kampala	1	0.95	0.24	1.14	0.26	0.25	2.20	13.03	50.55	6.84
	2	0.94	0.39	58.39	21.48	20.26	1.64	14.40	44.60	6.05
Kiel	1	0.69	0.54	0.98	0.37	0.44	3.15	33.66	38.09	−15.57
	2	0.54	0.35	40.97	7.84	9.83	2.60	42.55	46.23	−20.19
Kiruna	1	0.43	0.51	0.98	0.21	0.28	2.55	48.87	39.74	−22.23
	2	0.34	0.26	40.95	3.53	5.40	2.40	54.46	50.14	−34.58
Leeds	1	0.69	0.54	0.98	0.36	0.43	3.22	34.08	38.38	−18.33
	2	0.54	0.33	40.97	7.37	9.48	2.67	42.85	46.96	−22.22
Lindau	1	0.73	0.52	0.98	0.37	0.42	3.33	31.48	39.32	−13.29
	2	0.58	0.36	41.19	8.51	9.96	2.66	40.34	46.11	−14.51

Table V (contd.)

Station	β	L_{ap}	S_{ap}	$\bar{A}(\times 10^3)$	$A_{ap}(\times 10^3)$	$A_{ex}(\times 10^3)$	G	$\lvert\bar{\lambda}\rvert$	$\bar{\Phi}$	E
London	1	0.72	0.52	0.98	0.36	0.42	3.20	32.10	39.25	—13.80
	2	0.57	0.35	41.09	8.12	9.64	2.46	40.90	46.50	—15.72
McMurdo	1	0.10	0.34	0.98	0.03	0.01	7.07	71.54	46.86	112.05
	2	0.14	0.31	40.95	1.72	0.56	7.37	68.19	48.16	205.28
Mt. Wellington	1	0.79	0.61	0.98	0.47	0.51	2.47	27.42	35.04	—8.92
	2	0.67	0.47	40.95	12.94	13.85	1.89	35.09	41.21	—6.55
Munich	1	0.76	0.45	1.00	0.34	0.39	3.56	29.24	42.11	—11.42
	2	0.63	0.35	41.88	9.26	9.83	2.68	37.68	46.21	—5.77
Ottawa	1	0.76	0.63	0.98	0.46	0.51	2.24	29.34	34.19	—9.70
	2	0.64	0.45	40.95	11.72	13.34	1.75	36.86	42.28	—12.15
Oulu	1	0.50	0.53	0.98	0.26	0.34	2.59	44.78	38.68	—22.45
	2	0.39	0.29	40.95	4.60	6.96	2.40	51.51	48.76	—33.89
Resolute	1	0.18	0.24	0.98	0.04	0.05	0.44	64.53	50.85	—15.67
	2	0.20	0.06	40.95	0.53	1.14	0.46	63.46	57.53	—53.91
Rome	1	0.81	0.25	1.03	0.21	0.22	3.70	25.93	50.18	—2.94
	2	0.70	0.32	43.94	9.87	8.81	2.46	33.21	47.52	12.01
Thule	1	0.15	0.27	0.98	0.04	0.03	2.01	67.59	49.42	25.67
	2	0.17	0.17	40.95	1.21	0.69	2.10	65.68	53.33	74.12
Uppsala	1	0.61	0.54	0.98	0.32	0.40	2.82	38.77	38.27	—20.86
	2	0.47	0.29	40.95	5.58	8.42	2.46	46.97	48.65	—33.72

Table V (contd.)

Tridiurnal variation, $n = 2$
$R_0 = 90$ GV

Station	β	L_{ap}	S_{ap}	$\bar{A}(\times 10^3)$	$A_{ap}(\times 10^3)$	$A_{ez}(\times 10^3)$	G	$\lvert\bar{\lambda}\rvert$	$\bar{\varphi}$	E
Ahmadabad	1	0.89	0.25	1.96	0.44	0.39	2.27	19.16	50.22	13.17
	2	0.85	0.42	148.40	52.42	48.26	1.45	22.96	43.58	8.62
Alert	1	0.11	0.16	1.53	0.03	0.00	1.49	70.25	53.90	625.42
	2	0.15	0.27	98.42	3.94	0.59	0.69	67.20	49.68	564.02
Berkeley	1	0.79	0.46	1.57	0.58	0.64	2.15	26.95	41.62	−9.02
	2	0.73	0.46	101.50	34.19	36.58	1.34	31.04	41.79	−6.51
Cairo	1	0.85	0.24	1.86	0.37	0.32	2.24	22.88	50.91	14.56
	2	0.79	0.40	131.90	41.33	38.54	1.40	27.53	44.34	7.22
Calgary	1	0.70	0.59	1.53	0.62	0.74	1.36	33.50	36.12	15.60
	2	0.56	0.37	97.93	20.59	27.71	1.04	41.31	45.41	−25.70
Chicago	1	0.77	0.57	1.53	0.67	0.74	1.97	28.60	36.88	−9.05
	2	0.67	0.45	97.93	29.54	32.98	1.28	35.19	42.09	−10.42
Churchill	1	0.49	0.45	1.53	0.34	0.45	1.22	45.61	41.96	−43.74
	2	0.41	0.23	97.93	9.37	15.62	0.92	50.18	51.00	−40.01
Dallas	1	0.82	0.41	1.57	0.53	0.56	2.37	25.12	43.88	−6.28
	2	0.77	0.45	100.90	34.95	35.46	1.34	28.57	42.21	−1.45
Deep River	1	0.70	0.54	1.53	0.57	0.66	2.02	33.27	38.29	−12.91
	2	0.58	0.39	97.93	22.34	25.26	1.33	40.13	44.68	−11.53
Denver	1	0.79	0.57	1.53	0.69	0.74	1.98	26.93	36.99	−6.98
	2	0.71	0.48	98.36	32.98	35.11	1.29	32.87	41.07	−6.06
Goose Bay	1	0.56	0.45	1.53	0.39	0.49	2.26	41.55	42.14	−21.37
	2	0.46	0.26	97.93	11.72	16.25	1.45	47.36	49.91	−27.87
Inuvik	1	0.39	0.44	1.53	0.26	0.33	0.76	51.29	42.66	−21.67
	2	0.32	0.23	97.93	7.22	10.38	0.76	55.61	51.09	−20.52
Kampala	1	0.94	0.31	1.94	0.56	0.53	1.73	13.81	48.09	6.19
	2	0.93	0.47	144.50	63.79	60.73	1.15	15.16	41.14	5.03
Kiel	1	0.63	0.43	1.53	0.41	0.52	2.99	37.70	42.87	−20.47
	2	0.48	0.26	97.98	12.38	15.42	2.04	45.89	49.91	−19.66
Kiruna	1	0.39	0.38	1.53	0.23	0.33	2.51	51.29	44.98	−30.11
	2	0.30	0.10	97.93	3.13	7.32	2.17	46.50	55.99	−57.30
Leeds	1	0.62	0.42	1.53	0.40	0.51	3.07	38.04	43.38	−22.03
	2	0.48	0.25	97.98	11.60	14.50	2.10	46.03	50.51	−19.98
Lindau	1	0.66	0.41	1.54	0.42	0.51	3.14	35.57	43.90	−17.81
	2	0.52	0.28	98.52	14.38	16.14	2.02	43.76	49.16	−10.89

Table V (contd.)

Station	β	L_{ap}	S_{ap}	$\bar{A}(\times 10^3)$	$A_{ap}(\times 10^3)$	$A_{ex}(\times 10^3)$	G	$\lvert\bar{\lambda}\rvert$	$\bar{\Phi}$	E
London	1	0.65	0.41	1.53	0.41	0.50	2.97	36.13	44.01	—18.63
	2	0.51	0.27	98.26	13.56	15.36	1.72	44.18	49.62	—11.69
McMurdo	1	0.12	0.32	1.53	0.06	0.02	7.26	69.92	47.15	172.92
	2	0.16	0.30	97.93	4.69	1.73	7.67	66.64	48.16	171.20
Mt. Wellington	1	0.73	0.52	1.53	0.58	0.64	2.27	31.01	39.21	—9.66
	2	0.62	0.43	97.93	25.94	25.66	1.36	38.02	43.15	1.07
Munich	1	0.70	0.36	1.56	0.39	0.45	3.30	33.22	46.00	—13.97
	2	0.57	0.31	100.10	17.55	17.42	1.91	41.10	48.01	0.79
Ottawa	1	0.71	0.53	1.53	0.58	0.65	2.07	32.81	38.50	—11.44
	2	0.59	0.40	97.93	22.93	25.26	1.31	39.68	44.47	—9.22
Oulu	1	0.45	0.41	1.53	0.28	0.41	2.54	47.72	43.81	—29.91
	2	0.35	0.17	97.93	5.76	10.07	2.15	54.02	53.46	—42.88
Resolute	1	0.19	0.17	1.53	0.05	0.06	0.27	64.05	53.63	—24.42
	2	0.21	0.09	97.93	1.79	2.84	0.88	63.03	56.60	—37.04
Rome	1	0.76	0.23	1.62	0.28	0.27	3.16	29.49	51.08	5.91
	2	0.65	0.35	105.20	23.63	20.44	1.63	36.44	46.46	15.57
Thule	1	0.16	0.23	1.53	0.05	0.04	2.05	66.70	51.23	41.11
	2	0.18	0.15	97.93	2.58	1.15	2.40	64.84	54.41	124.54
Uppsala	1	0.54	0.42	1.53	0.35	0.48	2.73	42.42	43.50	—27.93
	2	0.41	0.21	97.93	8.51	12.44	2.04	50.03	51.89	—31.60

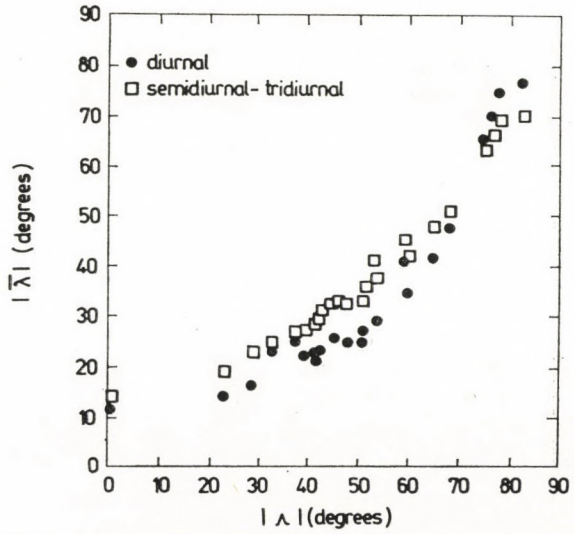

Fig. 1. Relation between the absolute value of the mean latitude $|\bar{\lambda}|$ and the absolute value of the geographic latitude $|\Lambda|$ for the diurnal variation ($n = 1$, $\beta = 1$, $R = \infty$) and for the semidiurnal and tridiurnal variations ($n = 2$, $\beta = 1$, $R_0 = 90$ GV)

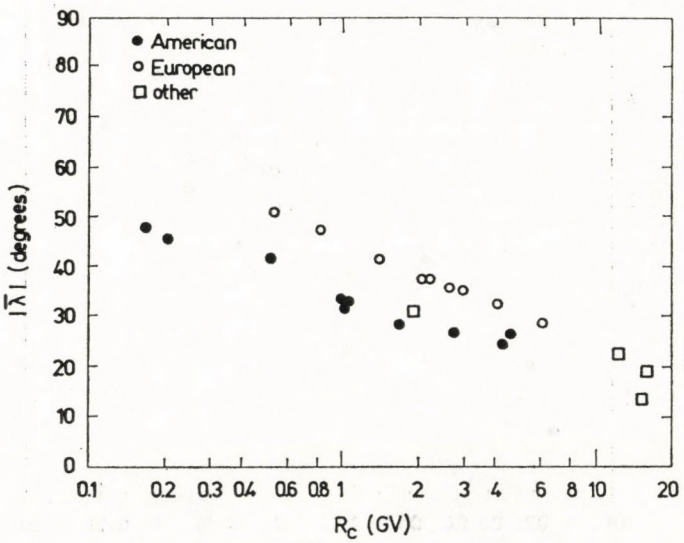

Fig. 2. Relation between the absolute value of the mean latitude $|\bar{\lambda}|$ and the minimum cutoff rigidity R_c for the semidiurnal and tridiurnal variations

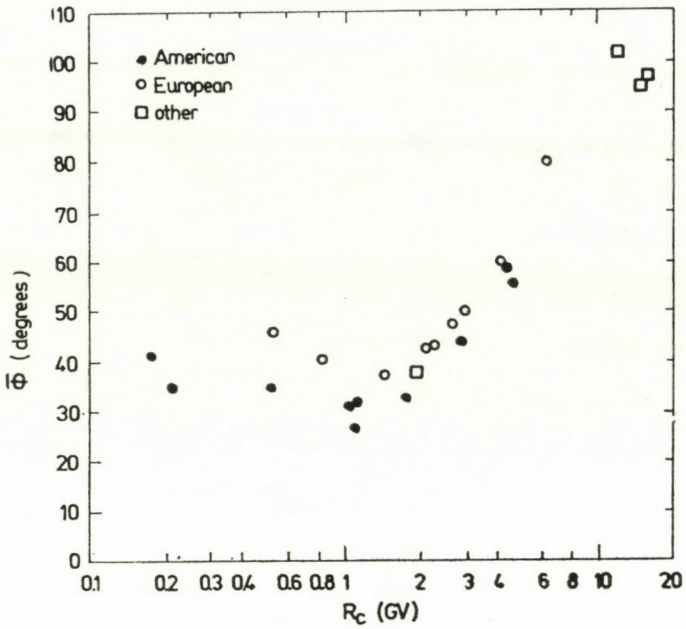

Fig. 3. Relation between the mean cone broadening $\overline{\Phi}$ for the diurnal variation, and the minimum cutoff rigidity R_c

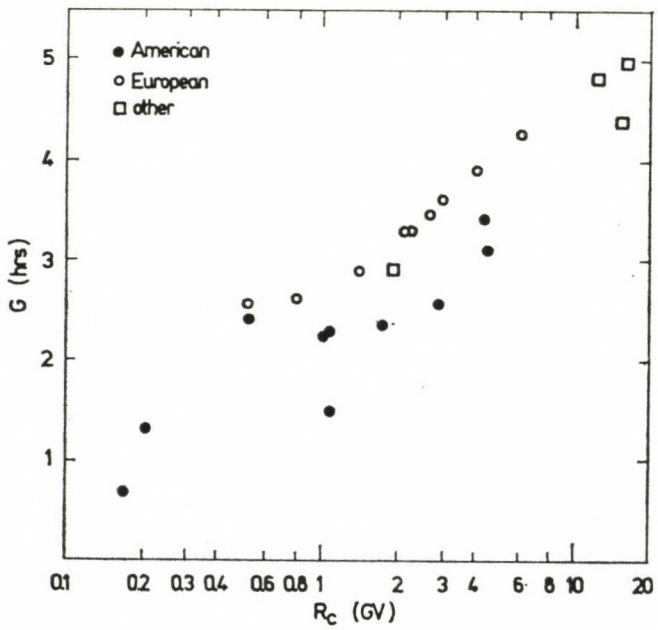

Fig. 4. The geomagnetic bending G(hrs) for the diurnal variation against R_c

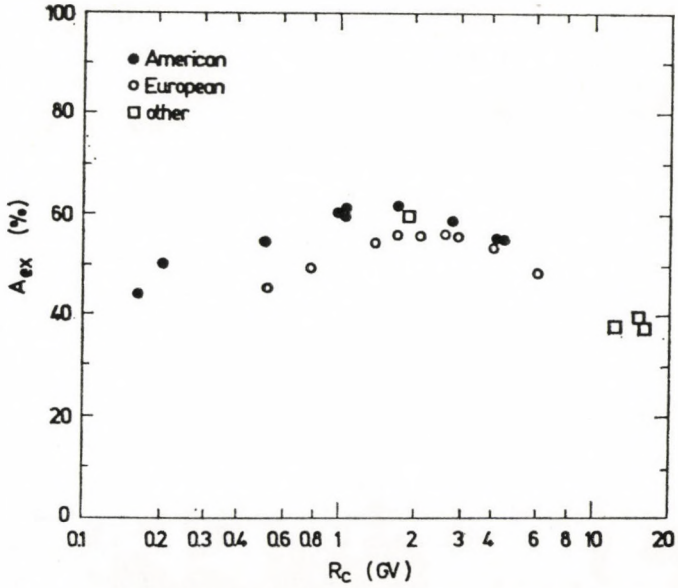

Fig. 5. The expected amplitude A_{ex} (%) of the diurnal variation against R_c

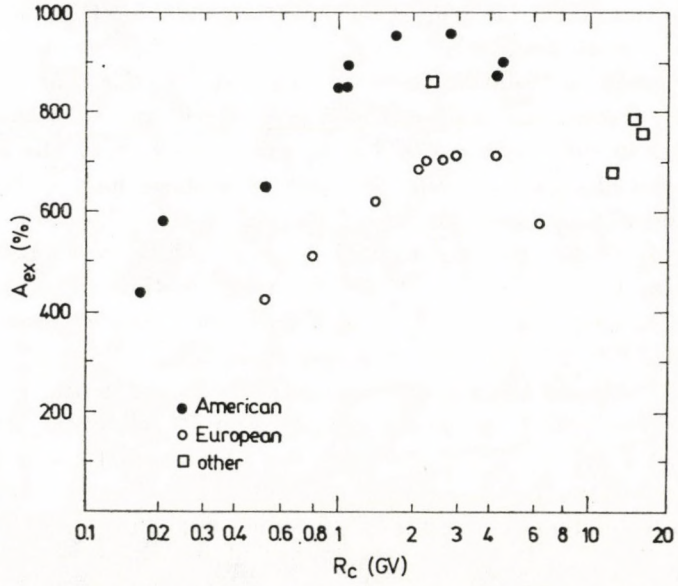

Fig. 6. The expected amplitude A_{ex}(%) of the semidiurnal variation ($n = 2$, $\beta = 1$, $R_0 = 90$ GV) against R_c

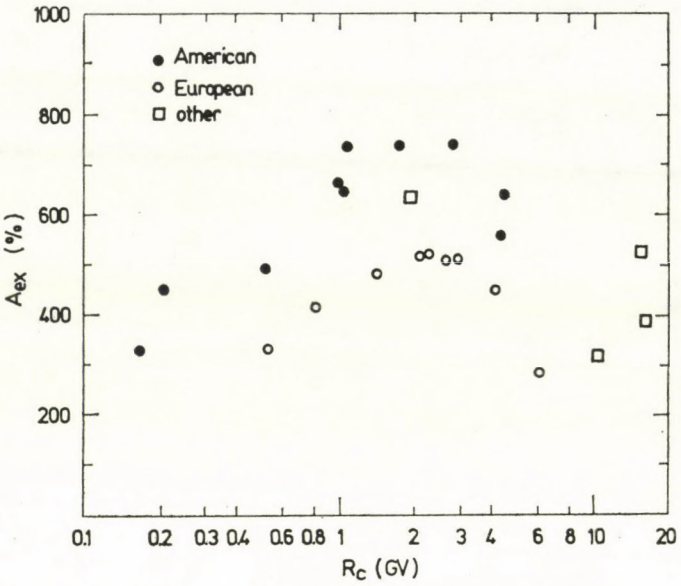

Fig. 7. The expected amplitude $A_{ex}(\%)$ of the tridiurnal variation ($n = 2$, $\beta = 1$ $R_0 = 90$ GV) against R_c

any station is, certainly, dependent on the station's geomagnetic rather than on geographic coordinates. Therefore, the difference in the response between any two stations having the same geographic latitude, to any anisotropy, is attributed to their different geographic longitudes which reflects their different geomagnetic coordinates.

Fig. 1 gives the relation between $|\bar{\lambda}|$ and $|\Lambda|$ for diurnal anisotropy with latitude dependence function cos λ and $\beta = 0$, and for semidiurnal and tridiurnal anisotropies with $\cos^2 \lambda$, $\beta = 1$, and $R_0 = 90$ GV. The irregularities in the represented points are expected since all stations have different geographic longitudes. The value of the error E has significantly large values as shown from Tables I—V for the polar stations (e.g. Alert and McMurdo). For semidiurnal and tridiurnal variations, for these stations, E is greater than 100% and, therefore, one has to be careful in using the corresponding values of L_{ap}, but for diurnal variation E is less than 20%.

Fig. 2 gives $|\bar{\lambda}|$ for tridiurnal and semidiurnal variations, for $n =$, $\beta = 1$, and $R_0 = 90$ GV against the minimum cutoff rigidity R_c with differentiation between the American and European stations. This classification has an advantage of grouping the stations with almost near geographic longitudes, where smooth relations are obtained for both the European and American stations. For the diurnal variation, this relation has nearly a similar shape.

The relation between the mean cone broadening $\bar{\Phi}$, of the diurnal variation, and R_c are given in Fig. 3 for the same groups. The represented points

show that the asymptotic cones for low cutoff rigidity stations have a wide longitudinal broadening which decreases with rigidity to reach its minimum value between 1 and 2 GV and then increases again. The wide broadening of the asymptotic cones for the low and high cutoff rigidity is explained according to the way of deflection of cosmic ray trajectories in the geomagnetic field. For low cutoff rigidity stations, the cosmic ray particles move almost parallel to the geomagnetic lines of force, and therefore it will be less controlled by the field where the station can accept particles from a wide longitude range. For high cutoff rigidity stations, the broadening is attributed to the ability of the geomagnetic field to resolve the cosmic ray trajectories according to their rigidities, since the particles move almost perpendicularly to the field lines. It can be seen from the Figure that $\bar{\Phi}$, as expected, is always smaller than 180°. The relations of $\bar{\Phi}$ for semidiurnal and tridiurnal variation show almost the same behaviour, but $\bar{\Phi} < 90°$ and $< 60°$ for semidiurnal and tridiurnal variation, respectively.

In Fig. 4 the value of the geomagnetic bending G (hrs) for diurnal variation increases with the cutoff rigidity R_c. The same relations for the other diurnal components give almost a similar shape but with more scattering of the represented points. The increase of G with R_c is attributed to the perpendicular motion, and hence a great deflection of cosmic ray trajectories in the earth's field.

Figs. 5, 6 and 7 represent the expected amplitudes A_{ex} for diurnal ($n = 1$, $\beta = 0$, $R_0 = \infty$) semidiurnal ($n = 2$, $\beta = 1$, $R_0 = 90$ GV) and tridiurnal ($n = 2$, $\beta = 1$, $R_0 = 90$ GV) variations, respectively. For diurnal variation, the present amplitudes are significantly smaller than those calculated by McCRACKEN et al due to the careful selection of the used parameters. A considerable increase is found in the time shift G, in the present calculation, for wide cone stations (e.g. Ahmedabad, Cairo, Kampala), while for the other stations G changes slightly. This arises from the effect of neglecting the asymptotic directions with high rigidity which have small deflections in the geomagnetic field.

REFERENCES

1. U. R. RAO, K. G. McCRACKEN and D. VENKATESAN, J. Geophys. Res., **68,** 345, 1963.
2. K. G. McCRACKEN, U. R. RAO, B. C. FOWLER, M. A. SHEA and D. F. SMART, IQSY Instruction Manual No. 10, 1965.
3. S. MORI, Nuovo Cimento, **53B,** 1—57, 1958.
4. S. MORI and S. YASUE, J. Fac. Sci., Shinshu Univ., **6,** 37, 1979.
5. Z. FUJII, K. FUJIMOTO, H. UENO, I. KONDO and K. NAGASHIMA, Acta Phys. Hung., **29,** Suppl. 2, 83, 1970.
6. K. NAGASHIMA, K. FUJIMOTO, Z. FUJII, H. UENO and I. KONDO, Reprint DPNU- 10, Nagoya, 1971.
7. B. LIETTI and J. J. QUENBY, Canad. J. Phys., **46,** S 942, 1968.
8. U. R. RAO and S. P. AGRAWAL, J. Geophy. Res., **75,** 2391, 1970.
9. G. SUBRAMANIAN, J. Geophys. Res., **76,** 1093, 1971.

10. S. Mori, S. Yasue and M. Ichinose, Proc. 12th Int. Conf. Cosmic Rays, Hobart, **2**, 673, 1971.
11. K. Fujimoto, K. Nagashima, Z. Fujii, H. Ueno and I. Kondo, Proc. 12th Int. Conf. Cosmic Rays, Hobart, **2**, 672, 1971.
12. S. Kudo and M. Wada, Proc. 12th Int. Conf. Cosmic Rays, Hobart, **2**, 679, 1971.
13. A. H. Girgis, M. F. Tolba, S. Abdel-Wahab and A. M. Salem, Planet. Space Sci., **25**, 39, 1977.
14. L. I. Dorman, Cosmic Ray Variations, State Publishing House for Technical and Theoretical Literature, Moscow, 1957.
15. M. F. Tolba and S. T. Lindgren, Scientific Report, UU/CRG 71-6, Uppsala University, 1971.
16. F. El-Bedewi, A. Goned and M. F. Tolba, Planet. Space Sci., **22**, 1185, 1974.
17. A. Goned and A. M. Salem, 3rd Conf. on Scientific Computations, Ain Shams University, 1976.

Acta Physica Academiae Scientiarum Hungaricae, Tomus 45 (3), pp. 275—279 (1978)

COMMUNICATIO BREVIS

COLLISION CASCADES AND THE DISTURBED ZONE DURING SPUTTERING PROCESSES (MODEL COMPUTATION)

By

J. GIBER, J. KAZSOKI and L. KOBLINGER

INSTITUTE OF PHYSICS, TECHNICAL UNIVERSITY, BUDAPEST

(Received 12. IX. 1978)

Although the cascades and the damage effect arising during ion sputtering of solid crystalline targets have been studied by many workers (see e.g. [1—3], and the references in their publications), no systematic numerical examination concerning the problem has been published so far.

For our investigations a computer model simulating the sputtering process has been developed [4]. In the computations Ar ions of 0.5 to 5 keV energy are incident perpendicularly to the (100) surface of an ideal bcc Cu-crystal. Both the bombarding ions and the target atoms were approximated by hard spheres, and the parameters of the collisions were calculated by the tools of classical mechanics. There was no memory in the program, i.e. the lattice points emptied by collision were assumed to be occupied again by the time a next interaction took place on that side.

Similar results were obtained [4] in the above mentioned energy interval by the application of the Bohr-type potential, taking the interaction of pairs into account. However, for the sake of the illustrative treatment very important for the problem examined, it appeared desirable to use the classical methods below, especially because the results obtained by two different treatments were nearly identical.

To illustrate the result of our investigations concerning the spread of the cascades Fig. 1 shows one of our representative results obtained from a run on a two-dimensional model.

In the three-dimensional examinations, the cascades have similar properties as those of the Figure. Based on the studies of many cascades, the radius of the disturbed region was estimated to be 140 to 600 Å in the primary ion energy interval of 0.5 to 5 keV. This is in agreement with the assumption of WERNER [5]. The numbers of the particles displaced in each layer upon the impact of a single primary ion, as a characteristic case with the energy of the primary ion, is shown in Fig. 2.

If the depth of the disturbed zone is defined as the depth of the layer where the average number of atoms liberated per primary ion is just one, then the average depth values in the investigated primary ion energy interval are those shown in Table I.

Table I

E_p [keV]	0.5	1	3	5
d [Å]	40	85	140	160

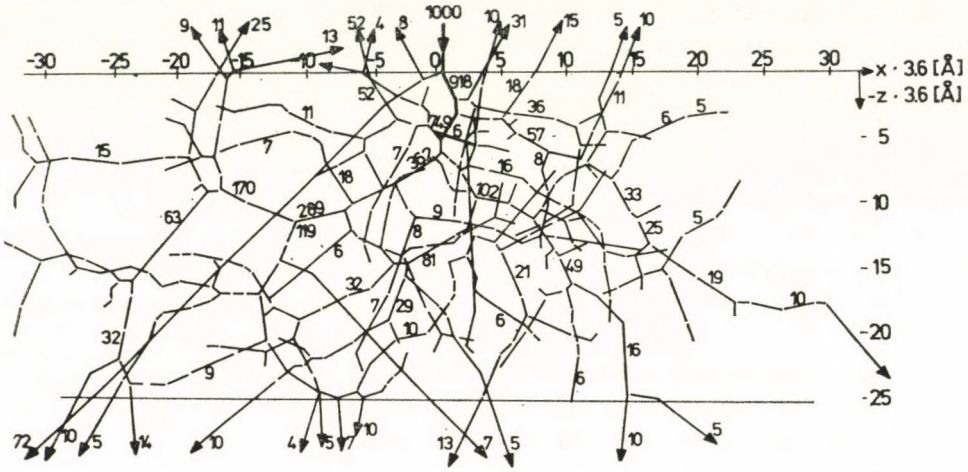

Fig. 1. Cascades caused by a primary ion incident on a two-dimensional lattice. Primary ion energy is 1 keV. (The figures on the lines are particle energies in eV)

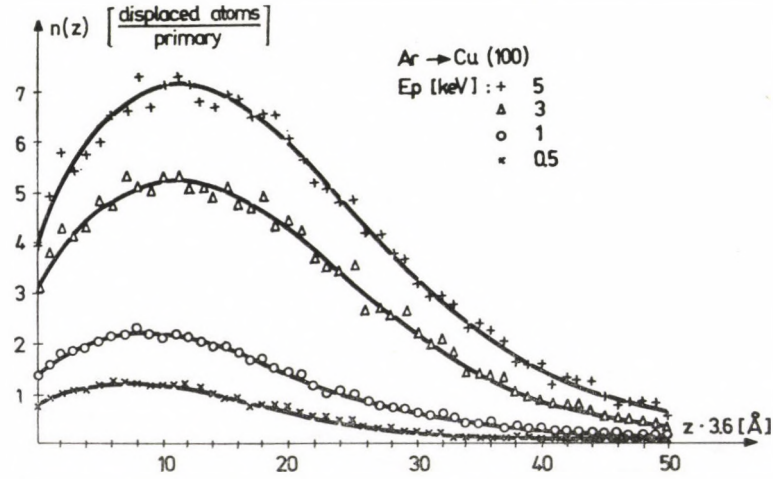

Fig 2. Number of target atoms knocked out from different layers

From the investigation of many cascades the following conclusions can be drawn:

— The moving particles cover relatively small distances (10 to 15 Å) with the exception of those moving in open directions (channeling).
— The probability of more than one collision occurring at the same crystal site during the cascade of one primary ion is negligible: thus the omission of the memory from the computer model is a reasonable approximation.
— The sputtered particles escape from the surface area around the point of incidence of the primary ion. The radius of this surface area is approximately equal to the radius of the disturbed zone.
— The characteristic running time of the cascades induced by one primary ion was found to be of an order of 10^{-11} s.

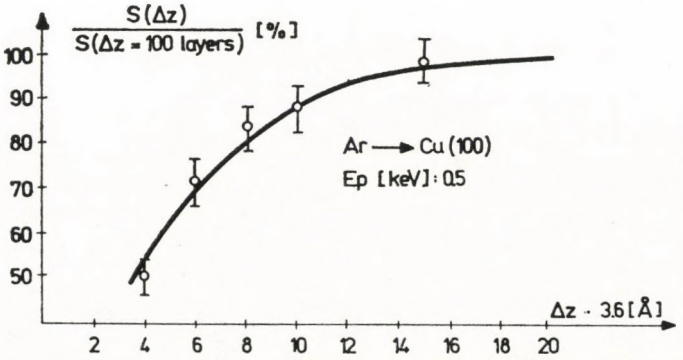

Fig. 3. The sputtering yield vs target model thickness curves for different primary ion energies

Since, upon the effect of one primary ion with $E_p = 5$ keV, about 7 atoms escape, one can draw at the same time the conclusion that with energies of this order one cannot speak of a "collapse" of the target lattice. This is supported also by the observation that in monocrystals the dependence of the sputtering efficiency on the incidence angle characteristic for the lattice structure remains unchanged also during the process of sputtering.

It was relevant to examine which are those deepest layers depending on the primary ion energy which, in our model, contribute to the sputtering efficiency. The data obtained from the average of many runs are shown in Fig. 3. It can be seen that the depth where the particles are not only displaced from their sites but from where they also escape is much smaller than the depth of the disturbed zone.

REFERENCES

1. M. T. Robinson, Phil. Mag., **12**, 741, 1965. Phil. Mag., **17**, 639, 1968.
2. P. Sigmund, Appl. Phys. Lett., **17**, 117, 1969.
3. P. Sigmund, Phys. Rev., **184**, 383, 1969.
4. J. Giber, J. Kazsoki and L. Koblinger, Acty Phys. Hung., **44**, 227, 1978.
5. M. W. Werner, Vacuum, **24**, 493, 1974.

RECENSIONES

DANIEL D. JOSEPH: **Stability of Fluid Motions I, II.**

Springer Verlag, Berlin, Heidelberg, New York 1976, 282 + 274 pages

These two volumes constitute Volumes 27 and 28 of Springer Tracts in Natural Philosophy edited by B. D. Coleman. The theory of stability of fluid motions has undergone a rapid development in the last decade to which the author of the book reviewed has made important contributions. So it is not surprising that this book represents a most authentic and up-to-date account of the theory of stability of flows satisfying equations of Navier-Stokes type. Even some of the results presented in it have not been published before. By applying "global" analysis the author discusses the problem of stability in most general terms without restriction to the case of small disturbances. Each chapter is supplied with a short introduction to set out its purpose. Bibliographical notes at the end of the chapters help the reader to follow the history of development of the field. Although the subject is treated with a high degree of mathematical rigour, the book is readable also for students knowing calculus and parts of the theory of differential equations. Especially, some appendices are prepared to help beginners. The book is carefully written with a clear exposition of the problems. It is supplied with an extensive list of references. The subject is covered under the following chapter headings:

Global Stability and Uniqueness; Instability and Bifurcation; Poiseuille Flow; The Form of the Disturbance whose Energy Increases Initially at the Largest Value of ν; Friction Factor Response Curves for Flow through Annular Ducts; Global Stability of Couette Flow between Rotating Cylinders; Global Stability of Spiral Couette—Poiseuille Flows; Global Stability of the Flow between Concentric Rotating Spheres; The Oberbeck—Boussinesq Equations. The Stability of Constant Gradient Solutions of the Oberbeck—Boussinesq Equations; Global Stability of Constant Temperature-Gradient and Concentration-Gradient States of a Motionless Heterogeneous Fluid; Two-Sided Bifurcation into Convection; Stability of Supercritical Convection-Wave Number Selection Through Stability; The Variational Theory of Turbulence Applied to Convection in Porous Material Heated from below; Stability Problems for Viscoelastic Fluids; Interfacial Stability.

P. SZÉPFALUSY

SERGIO A. ALBEVERIO and RAPHAEL J. HØEGH-KROHN: **Mathematical Theory of Feynman Path Integrals**

Lecture Notes in Mathematics Vol. 523
Springer-Verlag, Berlin, Heidelberg, New York, 1976 IV, 139 pages

Since their introduction by Feynman about thirty years ago path integrals have extensively been used in the physical literature. Simultaneously with their applications in different fields of physics considerable work has also been done as to their mathematical foundation to which the present book is an important contribution. The authors' approach is based on a general theory of oscillatory integrals on a separable real Hilbert space. Besides giving in this framework a mathematical justification of Feynman's heuristic formulation, the book contains applications to non-relativistic quantum mechanics, statistical mechanics and quantum field theory.

P. SZÉPFALUSY

D. TER HAAR: Lectures on Selected Topics in Statistical Mechanics

International Series in Natural Philosophy Volume 92
Pergamon Press, Oxford, New York, Toronto, Sydney, Paris, Frankfurt, 1977

The book represents the 92nd volume of the International Series in Natural Philosophy started in the sixties and published by Pergamon Press. The text consists of lecture notes prepared for a set of lectures given by the author at the 1971 Simla Summer School of Statistical Mechanics. The subject is covered under 8 chapter headings and includes a short introduction to some standard techniques (as e.g. Green's function method) with simple illustrative applications. A chapter is devoted to fluctuations in a perfect Bose gas which clarifies problems not adequately discussed in textbooks. The chapter on the statistical mechanics of stellar systems is an excellent summary of the field. The whole book is well written and easy to follow.

P. SZÉPFALUSY

Many Degrees of Freedom in Field Theory

Nato Advanced Study Institutes Series, Series B: Physics, Volume 30,
Editor: L. Streit, Plenum Publishing Corporation, New York and London, 1978, p. 248

Volume 30 contains the papers in modern field theory delivered at the International Summer Institute of Theoretical Physics, Bielefeld, 1976. Recently, field theory has provided several important ideas to the unified description of the interactions of elementary particles. A cluster of such ideas is presented in the Volume written at the highest level.

The topics of the papers can be divided into two groups: classical non-linear wave equations, solitons, and axiomatic quantum field theory.

In the first group the classical soliton physics and sine Gordon equation are treated in a comprehensive way (K. POHLMEYER), followed by classical static gauge-field solitons in three space dimensions (L. O'RAIFEARTAIGH). Unsolved problems of non-linear wave equations are discussed by M. REED.

In the axiomatic approach an introduction to some topics in constructive quantum field theory is given by J. FRÖHLICH, while R. F. STREATER formulates standard results for spontaneously broken symmetries in a rigorous way.

Two papers on statistical mechanics (strong mixing and dynamics of a thermodynamic system) are included in the Volume (M. CASSANDRO—G. JONA-LASINIO and D. W. ROBINSON's talks). The last paper is J. TARSKI's short introduction to nonstandard analysis and its physical applications.

Both the authors and the Volume are excellent.

G. PÓCSIK

Many Degrees of Freedom in Particle Theory

Nato Advanced Study Institutes Series, Series B: Physics, Volume 31
Editor: H. Satz, Plenum Publishing Corporation, New York and London, 1978, p. 566

This Volume, together with its companion volume (Volume 30) dealing with field theory contains the Proceedings of the International Summer Institute of Theoretical Physics, Bielefeld, 1976. 16 papers are included into the Volume written for experts on various topics of high energy physics. The majority of the topics belongs to five trends: 1. QCD related problems, weak gauge groups, complete unification (H. FRITZSCH); MIT bag (K. JONHSON); Lattice gauge theories (J. B. KOGUT). 2. Phenomenological implications of quark partons (P. V. LANDSHOFF, K. KAJANTIE). 3. Many papers deal with the various aspects of dual models such as string models (P. DI VECCHIA, L. C. BIEDENHARN—H. VAN DAM), unitarisation (CHAN HONG MO—TSOU SHEUNG TSUN), bootstrap (Y. ZARMI). 4. High energy interactions with nuclei (G. EILAM, A. H. MUELLER). 5. Particle clusters at high energy (A. KRZYWICKI, M. ANSELMINO et al). A good experimental comparison is given by G. H. THOMAS.

M. LE BELLAC discusses the reggeon field theory; V. CANUTO and J. LODENQUAI treat topics related to the high density matter in the Universe.

The receptive reader can learn much from this Volume. No doubt, the original purpose of the organizers was not to cover QCD and quark-parton physics, instead, more conventional pictures motivated by the Regge theory gain a larger ground in this excellent Volume. Nowadays, these belong to the life in high energy physics.

G. PÓCSIK

Optical Information Processing Vol. 2.

Edited by Euval S. Barrekette, George W. Stroke, Yu. E. Nesterikhin and Winston E. Kock
Plenum Publishing Corporation, New York, 1978

This volume is the second in a series which contains the notes of lectures given at joint Soviet and United States seminars on optical information processing. It is well known that both countries are carrying out high level research in this field and the articles presented give some insight into this work.

Some special problems of holography, principal questions of data processing by coherent optical methods, spatial modulation, image detection and the effect of fluctuations of light intensity on photoreception quality are discussed, as are some of the problems concerning optical processors such as the addressing by electro optical methods. We are provided with details on the solution of well defined tasks in radio-physics, laser interferometry, and optical feedback.

A few lectures are devoted to problems of optical data storage. High capacity and bulk holographic memories, character memories and memory organization questions are the subjects of this part of the volume.

Some topics of more general interest including integrated optics and X-ray holography by synchrotron radiation, are also discussed.

The general conclusion of the seminar seems to be that optical methods have limited chances of entering the storage market place in the next ten years, as opposed to the likelihood of their finding an opportunity for success in communication. They have already proved to be successful in the field of input-output devices.

N. KROÓ

Fluid Dynamics — Les Houches 1973

Editors: R. Balian—J. -L. Peube, Gordon and Breach Science Publishers
London, New York, Paris, 1977

The volume collects the most important lectures delivered at the Les Houches Summer School on Fluid Dynamics in the year 1973. The contributions in the volume are the following: P. GERMAIN: Asymptotic Methods in Fluid Mechanics, H. K. MOFFATT: Six Lectures on General Fluid Dynamics and two on Hydromagnetic Dynamo Theory, S. A. ORSZÁG: Lectures on the Statistical Theory of Turbulence, J.-L. PEUBE: Transport Properties in Flows. Besides, ten seminar lectures are included on experimental and numerical methods, hydrodynamic instabilities, electrohydrodynamics, "physical objects with fractional dimension: seacoasts, galaxy clusters, turbulence and soap" (MANDELBROT) turbulence, polymers, nematic liquid crystals, superfluid helium and dynamic meteorology.

The structure of the volume, due to the very interesting, sometimes extraordinary, presentation of the actual views of the subjects made by eminent researchers reflects adequately, and contributes to the realization of the aims of the directors of the Summer School, the Editors of this volume. Namely: they intended to show the importance, need and perspective possibility of theoretical understanding in this rapidly growing field of science, which, due to its special situation for the past few decades, seemed to be abandoned because of its profound and heavy problems and less elegant and fashionable specialities. The interaction between the modern methods of statistical mechanics, computer sciences and many other branches with fluid dynamics has been and will be able to open up new ways for further development. — A very interesting and useful book, but not only fluid physicists can profit from reading it!

I. ABONYI

75 Jahre Quantentheorie

Festband zum 75. Jahrestag der Entdeckung der Planck'schen Energiequanten.
Herausgegeben von W. Brauer, H. W. Streitwolf, K. Werner.
Akademie der Wissenschaften der DDR, Akademie-Verlag Berlin, 1977.

Im Rahmen der Veranstaltungen zum 275-jährigen Bestehen der Berliner Akademie der Wissenschaften führte die Akademie der Wissenschaften der DDR am 15. und 16. Dezember 1975 in Berlin ein Festkolloquium durch unter dem Titel: «75 Jahre Quantentheorie«. Das Kolloquium, zu dem die 75. Wiederkehr jenes Tages Anlass gab, an dem MAX PLANCK vor der Berliner Physikalischen Gesellschaft erstmals über seine Entdeckung, die Energiequanten, berichtete, führte eine Reihe international bekannter Physiker in Berlin zusammen. In diesem Jahrhundert befand sich eine völlig neue Epoche der Physik in Vorbereitung, wurde aber auch in vieler Hinsicht bereits weiterentwickelt und vollendet. Den entscheidenden Wendepunkt dieser neuen Phase in der Geschichte der Physik, die in ihrer Bedeutung nur mit der Zeit von GALILEI bis NEWTON verglichen werden kann, stellt der 14. Dezember des Jahres 1900 dar. An diesem Tag konzipierte MAX PLANCK das elementare Wirkungsquantum. Die Vorträge im 1. Teil des Buches (ROMPE, HUND, FUCHS, FRÖHLICH, BASOV, PRIGOGINE, GRECOS, KASCHLUHN, PONTECORVO, BRAUER, AUTH, KÜRTI, EBELING, HÖRZ) würdigen die Leistung MAX PLANCKS und die Bedeutung der Quantentheorie für Naturwissenschaft und Technik in aktueller, historischer und erkenntnistheoretischer Sicht.

Weitere Beiträge von Physikern aus der DDR, die aus zeitlichen Gründen nicht auf dem Festkolloquium vorgetragen werden konnten wurden im II. Teil veröffentlicht.

I. KOVÁCS
Lehrstuhl für Atomphysik an der
Technischen Universität Budapest

Printed in Hungary

A kiadásért felel az Akadémiai Kiadó igazgatója — Műszaki szerkesztő: Botyánszky Pál
A kézirat a kiadóba érkezett: 1978. XI. 3. — A kézirat nyomdába érkezett: 1978. XI. 9. — Terjedelem: 11,75 (A/5) ív

79.6476 Akadémiai Nyomda, Budapest — Felelős vezető: Bernát György

NOTES TO CONTRIBUTORS

I. PAPERS will be considered for publication in Acta Physica Hungarica, only if they have not previously been published or submitted for publication elsewhere. They may be written in English, French, German or Russian.

Papers should be submitted to

Prof. I. Kovács, Editor
Department of Atomic Physics, Technical University
1521 Budapest, Budafoki út 8, Hungary

Papers may be either articles with abstracts or short communications. Both should be as concise as possible, articles in general not exceeding 25 typed pages, short communications 8 typed pages.

II. MANUSCRIPTS

1. Papers should be submitted in five copies.

2. The text of papers must be of high stylistic standard, requiring minor corrections only.

3. Manuscripts should be typed in double spacing on good quality paper, with generous margins.

4. The name of the author(s) and of the institutes where the work was carried out should appear on the first page of the manuscript.

5. Particular care should be taken with mathematical expressions. The following should be clearly distinguished, e.g. by underlining in different colours: special founts (italics, script, bold type, Greek, Gothic, etc.); capital and small letters; subscripts and superscripts, e.g. x_2, x^3; small l and 1; zero and capital O; in expressions written by hand: e and l, n and u, v and v, etc.

6. References should be numbered serially and listed at the end of the paper in the following form: J. Ise and W. D. Fretter, Phys. Rev., *76*, 933, 1949.

For books, please give the initials and family name of the author(s), title, name of publisher, place and year of publication, e.g.: J. C. Slater, Quantum Theory of Atomic Structures, I. McGraw-Hill Book Company, Inc., New York, 1960.

References should be given in the text in the following forms: Heisenberg [5] or [5].

7. Captions to illustrations should be listed on a separate sheet, not inserted in the text.

III. ILLUSTRATIONS AND TABLES

1. Each paper should be accompanied by five sets of illustrations, one of which must be ready for the blockmaker. The other sets attached to the copies of the manuscript may be rough drawings in pencil or photocopies.

2. Illustrations must not be inserted in the text.

3. All illustrations should be identified in blue pencil by the author's name, abbreviated title of the paper and figure number.

4. Tables should be typed on separate pages and have captions describing their content. Clear wording of column heads is advisable. Tables should be numbered in Roman numerals (I, II, III, etc.).

IV. MANUSCRIPTS not in conformity with the above Notes will immediately be returned to authors for revision. The date of receipt to be shown on the paper will in such cases be that of the receipt of the revised manuscript.

Reviews of the Hungarian Academy of Sciences are obtainable at the following addresses:

AUSTRALIA
C.B.D. LIBRARY AND SUBSCRIPTION SERVICE, Box 4886, G.P.O., *Sydney N.S.W.2001*
COSMOS BOOKSHOP, 145 Ackland Street, *St. Kilda (Melbourne), Victoria 3182*

AUSTRIA
GLOBUS, Höchstädtplatz 3, *1200 Wien XX*

BELGIUM
OFFICE INTERNATIONAL DE LIBRAIRIE, 30 Avenue Marnix, *1050 Bruxelles*
LIBRAIRIE DU MONDE ENTIER, 162 Rue du Midi, *1000 Bruxelles*

BULGARIA
HEMUS, Bulvar Ruszki 6, *Sofia*

CANADA
PANNONIA BOOKS, P.O. Box 1017, Postal Station "B", *Toronto, Ontario M5T 2T8*

CHINA
CNPICOR, Periodical Department, P.O. Box 50, *Peking*

CZECHOSLOVAKIA
MAD'ARSKÁ KULTURA, Národní třida 22, *115 66 Praha*
PNS DOVOZ TISKU, Vinohradská 46, *Praha 2*
PNS DOVOZ TLAČE, *Bratislava 2*

DENMARK
EJNAR MUNKSGAARD, Norregade 6, *1165 Copenhagen*

FINLAND
AKATEEMINEN KIRJAKAUPPA, P.O. Box 128, *SF-00101 Helsinki 10*

FRANCE
EUROPERIODIQUES S. A., 31 Avenue de Versailles, *78170 La Celle St.-Cloud*
LIBRAIRIE LAVOISIER, 11 rue Lavoisier, *75008 Paris*
OFFICE INTERNATIONAL DE DOCUMENTATION ET LIBRAIRIE, 48 rue Gay-Lussac, *75240 Paris Cedex 05*

GERMAN DEMOCRATIC REPUBLIC
HAUS DER UNGARISCHEN KULTUR, Karl-Liebknecht-Strasse 9, *DDR-102 Berlin*
DEUTSCHE POST ZEITUNGSVERTRIEBSAMT, Strasse der Pariser Kommüne 3—4, *DDR-104 Berlin*

GERMAN FEDERAL REPUBLIC
KUNST UND WISSEN ERICH BIEBER, Postfach 46, *7000 Stuttgart 1*

GREAT BRITAIN
BLACKWELL'S PERIODICALS DIVISION, Hythe Bridge Street, *Oxford OX1 2ET*
BUMPUS, HALDANE AND MAXWELL LTD., Cowper Works, *Olney, Bucks MK46 4BN*
COLLET'S HOLDINGS LTD., Denington Estate, *Wellingborough, Northants NN8 2QT*
W.M. DAWSON AND SONS LTD., Cannon House, *Folkestone, Kent CT19 5EE*
H. K. LEWIS AND CO., 136 Gower Street, *London WC1E 6BS*

GREECE
KOSTARAKIS BROTHERS, International Booksellers, 2 Hippokratous Street, *Athens-143*

HOLLAND
MEULENHOFF-BRUNA B.V., Beulingstraat 2, *Amsterdam*
MARTINUS NIJHOFF B.V., Lange Voorhout 9—11, *Den Haag*
SWETS SUBSCRIPTION SERVICE, 347b Heereweg, *Lisse*

INDIA
ALLIED PUBLISHING PRIVATE LTD., 13/14 Asaf Ali Road, *New Delhi 110001*
150 B-6 Mount Road, *Madras 600002*
INTERNATIONAL BOOK HOUSE PVT. LTD., Madame Cama Road, *Bombay 400039*
THE STATE TRADING CORPORATION OF INDIA LTD., Books Import Division, Chandralok, 36 Janpath, *New Delhi 110001*

ITALY
EUGENIO CARLUCCI, P.O. Box 252, *70100 Bari*
INTERSCIENTIA, Via Mazzé 28, *10149 Torino*
LIBRERIA COMMISSIONARIA SANSONI, Via Lamarmora 45, *50121 Firenze*
SANTO VANASIA, Via M. Macchi 58, *20124 Milano*
D. E. A., Via Lima 28, *00198 Roma*

JAPAN
KINOKUNIYA BOOK-STORE CO. LTD., 17-7 Shinjuku-ku 3 chome, Shinjuku-ku, *Tokyo 160-91*
MARUZEN COMPANY LTD., Book Department, P.O. Box 5050 Tokyo International, *Tokyo 100-31*
NAUKA LTD. IMPORT DEPARTMENT, 2-30-19 Minami Ikebukuro, Toshima-ku, *Tokyo 171*

KOREA
CHULPANMUL, *Phenjan*

NORWAY
TANUM-CAMMERMEYER, Karl Johansgatan 41—43, *1000 Oslo*

POLAND
WĘGIERSKI INSTYTUT KULTURY, Marszalkowska 80, *Warszawa*
CKP I W ul. Towarowa 28 *00-958 Warsaw*

ROMANIA
D. E. P., *Bucureşti*
ROMLIBRI, Str. Biserica Amzei 7, *Bucureşti*

SOVIET UNION
SOJUZPETCHATI — IMPORT, *Moscow* and the post offices in each town
MEZHDUNARODNAYA KNIGA, *Moscow G-200*

SPAIN
DIAZ DE SANTOS, Lagasca 95, *Madrid 6*

SWEDEN
ALMQVIST AND WIKSELL, Gamla Brogatan 26, *101 20 Stockholm*
GUMPERTS UNIVERSITETSBOKHANDEL AB, Box 346, *401 25 Göteborg 1*

SWITZERLAND
KARGER LIBRI AG, Petersgraben 31, *4011 Basel*

USA
EBSCO SUBSCRIPTION SERVICES, P.O. Box 1943, *Birmingham*, Alabama 35201
F. W. FAXON COMPANY, INC., 15 Southwest Park, *Westwood*, Mass. 02090
THE MOORE-COTTRELL SUBSCRIPTION AGENCIES, *North Cohocton, N. Y. 14868*
READ-MORE PUBLICATIONS, INC., 140 Cedar Street, *New York, N. Y. 10006*
STECHERT-MACMILLAN, INC., 7250 Westfield Avenue, *Pennsauken* N. J. 08110

VIETNAM
XUNHASABA, 32, Hai Ba Trung, *Hanoi*

YUGOSLAVIA
JUGOSLAVENSKA KNJIGA, Terazije 27, *Beograd*
FORUM, Vojvode Mišiča 1, *21000 Novi Sad*

Index: 26.025
Acta Phys. Hung. Tom. 45. No. 3. Budapest, 10. V. 1979 HU-ISSN 0001-6705

ACTA PHYSICA

ACADEMIAE SCIENTIARUM HUNGARICAE

TOMUS XLV FASCICULUS 4

AKADÉMIAI KIADÓ, BUDAPEST
1978

ACTA PHYS. HUNG. APAHAQ 45 (4) 283–376 (1978)

ACTA PHYSICA

ACADEMIAE SCIENTIARUM HUNGARICAE

SZERKESZTI
KOVÁCS ISTVÁN

Az *Acta Physica* angol, német, francia vagy orosz nyelven közöl értekezéseket. Évente két kötetben, kötetenként 4—4 füzetben jelenik meg. Kéziratok a szerkesztőség címére (1521 Budapest XI., Budafoki út 8.) küldendők.

Megrendelhető a belföld számára az Akadémiai Kiadónál (1363 Budapest Pf. 24. Bankszámla 215-11488), a külföld számára pedig a „Kultura" Külkereskedelmi Vállalatnál (1389 Budapest 62, P.O.B. 149. Bankszámla 217-10990), vagy annak külföldi képviseleteinél.

The *Acta Physica* publish papers on physics in English, German, French or Russian, in issues making up two volumes per year. Subscription: $ 36.00 per volume. Distributor: "Kultura" Foreign Trading Company (1389 Budapest 62, P.O. Box 149) or its representatives abroad.

Die *Acta Physica* veröffentlichen Abhandlungen aus dem Bereich der Physik in deutscher, englischer, französischer oder russischer Sprache, in Heften, die jährlich zwei Bände bilden.

Abonnementspreis pro Band: $ 36.00. Bestellbar bei »Kultura« Außenhandelsunternehmen (1389 Budapest 62, Postfach 149) oder seinen Auslandsvertretungen.

Les *Acta Physica* publient des travaux du domaine de la physique en français, anglais, allemand ou russe, en fascicules qui forment deux volumes par an.

Prix de l'abonnement: $ 36.00 par volume. On peut s'abonner à l'Entreprise du Commerce Extérieur «Kultura» (1389 Budapest 62, P.O.B. 149) ou chez représentants à l'étranger.

«*Acta Physica*» публикуют трактаты из области физических наук на русском, немецком, английском и французском языках.

«*Acta Physica*» выходят отдельными выпусками, составляющими два тома в год.

Подписная цена — $ 36.00 за том. Заказы принимает предприятие по внешней орговле «Kultura» (1389 Budapest 62, P.O.B. 149) или его заграничные представительства.

ACTA PHYSICA

ACADEMIAE SCIENTIARUM HUNGARICAE

TOMUS XLV FASCICULUS 4

AKADÉMIAI KIADÓ, BUDAPEST
1978

ACTA PHYS. HUNG.

INDEX

PROF. SÁNDOR SZALAY 70 YEARS

Professor SZALAY (A. SZALAY), Ordinary Member of the Hungarian Academy of Sciences, celebrates his 70th birthday on 4th October 1979.

Professor SZALAY has achieved numerous outstanding scientific results in nuclear physics and in the very broad field of the applications of nuclear methods. Let us mention here only the evidence for the neutrino recoil effect in a cloud chamber, the discovery of uranium enrichment in some Hungarian coals and as a generalization of the latter, the clarification of the role of humic acids in Nature in the retention of uranium and other cations. These results

Acta Physica Academiae Scientiarum Hungaricae 45, 1978

led to the discovery of the uranium deposit in Hungary. Professor SZALAY played an important role in the introduction of isotope application into biomedical research and practice in Hungary. He initiated the study of the environment from the point of view of radioactive pollution, the application of the techniques of mass spectroscopy in the geochronological investigation of Hungarian rocks. The construction of many nuclear instruments and techniques in Debrecen were also prompted by him, e.g. Van de Graaff generators and other accelerators, scintillation and semiconductor detectors, alpha-, beta- and mass-spectrometers, etc.

His interest and activities cover very broad fields. He has never restricted himself to any individual branch of science. All his scientific activities have had a real inter- and multidisciplinary character from the very beginning. Every time he considered the phenomena of Nature, he followed the logic of Nature, regardless of the risk of eventually exceeding the boundaries of physics and entering e.g. the area of chemistry, geology, biology or medicine. His starting point was always experimental in all fields, confessing that the only solid basis in all branches of science was experiments and empirical evidence. Similarly, he has always been interested in the practical applications of his scientific results.

Most of his scientific work was carried out in cooperation with his numerous collaborators. As a result of his careful selection of talented young research associates, Professor SZALAY founded a scientific school. This school is characterized by the same main features as Professor SZALAY's own research activities: an experimental and interdisciplinary approach to the understanding of natural phenomena and a keen interest in the application of the fundamental results obtained. The staff of the Institute of Nuclear Research of the Hungarian Academy of Sciences has actually derived from this research community.

Professor SZALAY is highly active in research work at this Institute still to date. He is much interested in microelement research in plants and foods and in investigating the primordial atmosphere of the Earth by means of quadrupole mass spectroscopy.

His colleagues and all Hungarian physicists as well as the whole Hungarian scientific community wish him many more years and further success in his scientific and private life.

D. BERÉNYI

Acta Physica Academiae Scientiarum Hungaricae, Tomus 45 (4), pp. 285—291 (1978)

A CLASS OF STATIC WEYL SOLUTIONS FOR THE BRANS—DICKE MAXWELL FIELDS

By

P. P. RAO and R. N. TIWARI

DEPARTMENT OF MATHEMATICS, INDIAN INSTITUTE OF TECHNOLOGY, KHARAGPUR-721302, INDIA

(Received 7. IX. 1978)

Considering the static axially symmetric metric of WEYL and then using a result obtained by PERJÉS, a generalized relation between the g_{44} component of the metric tensor, the electrostatic (or magnetostatic in view of PERJÉS result) potential and the Brans—Dicke (BD) scalar field has been obtained for the BD Maxwell fields when both electric and magnetic fields are present. Further, using this relation, a theorem has been given at the end which enables one to generate the BD Maxwell solutions from the known solutions of the BD vacuum fields.

1. Introduction

In Einstein's theory for static fields the problem of generating Einstein—Maxwell solutions from the already known solutions has been tackled by various workers like WEYL [1], MAJUMDAR [2], PAPAPETROU [3], BONNOR [4] etc. While the work of WEYL and BONNOR are mainly concerned with static axially symmetric metric, MAJUMDAR and PAPAPETROU have solved the problem in general without imposing any symmetric restrictions. They have shown that in the presence of electrostatic field with the static metric

$$ds^2 = g_{ab}(\bar{x})\, dx^a\, dx^b + g_{44} dt^2, \qquad (a, b = 1, 2, 3,\ g_{44} < 0) \tag{i}$$

the g_{44} component of the metric tensor and electrostatic potential are related as

$$-g_{44} = 4\pi\psi^2 + A\psi + B. \tag{ii}$$

(A, B are arbitrary constants). This when further specialized to the form

$$-g_{44} = 4\pi(\psi \pm \sqrt{2})^2 \tag{iii}$$

reduces the source-free Einstein—Maxwell equations to a single Laplace equation. Thus to every solution of the Laplace equation there corresponds a unique solution of Einstein—Maxwell fields. It may be mentioned that in the general case, without any specialization of functional form (iii), Einstein—Maxwell fields for static WEYL's metric go over to the Einstein vacuum fields.

This class of solutions, widely known as WEYL—MAJUMDAR—PAPAPETROU (WMP) class, according to HARTLE and HAWKING [5], has a distinct astrophysical role and can be interpreted to describe a system of charged black holes held in equilibrium under their gravitational and electrostatic forces. They have further observed that the black holes belonging to this class are quite different from the already known black holes (Schwarzschild and Reissner—Nordström black holes).

In the Brans—Dicke theory the corresponding problem of finding the WMP class of solutions has been studied by NAYAK [6], TIWARI and NAYAK [7] and TIWARI and RAO [8].

None of the above authors [1]—[8], however, have considered the problem when both electric as well as magnetic fields are simultaneously present. Recently DAS [9], using a remarkable result of PERJÉS [10] obtained for static cylindrically symmetric field, has generalized the result of WEYL to the case when both the electric and magnetic fields are simultaneously present. WEYL's result, obviously, is obtained as a particular case of the result of DAS when the magnetic field is switched off.

In this paper, we have extended the work of DAS [9], to the source-free BD Maxwell fields for the static axially symmetric WEYL's metric. In doing so, we have first proved that the result of PERJÉS, which states that in a continuous field the relation, if any, between electric and magnetic field must always be linear, holds in the case of the static BD Maxwell fields also. The WMP relation so obtained when substituted back in the field equations as usual reduces the BD Maxwell field to BD vacuum equations. This finally gives a theorem which enables one to generate the solutions of the BD Maxwell fields from those of BD vacuum fields.

The WMP relation obtained here, however, cannot be said to be the only relation obtained from the field equations. The single differential equation used for getting the said relation contains more than one independent variables. There is no standard method of solving such an equation. The problem, therefore may be divided into various classes depending on whether the electromagnetic and the BD scalar potentials are null, non-null and mutually orthogonal. The case studied here, however, is in a sense more general as it does not involve any such restriction. In another sense it is less general since to avoid any such restriction on the physical fields the number of mathematical equations is to be increased. It is thus apparent that the WMP relation obtained here is not a unique one. There may be a relation or relations more general than the one obtained here.

2. Field equations

The source-free BD Maxwell field equations are:

$$R^i_j = -\frac{8\pi}{\varphi} T^i_j - \frac{\omega}{\varphi^2} \varphi^{,i} \varphi_{,j} - \frac{1}{\varphi} \varphi^{;i}_{;j}, \tag{1}$$

$$(3 + 2\omega)\, \varphi^{;s}_{;s} = 0, \tag{2}$$

$$T^i_j = -\frac{1}{4\pi}\left[F^{is}F_{js} - \frac{1}{4}\delta^i_j F^{sp}F_{sp}\right], \tag{3}$$

$$F^{ij}_{;j} = 0, \tag{4}$$

where F_{ij} are generated from the two potentials ξ and η as:

$$F_{4s} = \xi_{,s}, \tag{5}$$

$$F^{sp} = e^{2\beta}\gamma^{-1/2}\varepsilon^{spv}\eta_{,v}. \tag{6}$$

Here γ is the three dimensional metric given by $\gamma = \varrho^2 e^{4\alpha}$ and $\varepsilon^{spv} = \pm 1$ or 0. Hereafter a subscript comma or a semicolon will denote partial differentiation or covariant differentiation, respectively.

We now solve the field equations (1)—(4) for the axially symmetric static WEYL's metric, given by

$$ds^2 = e^{2\beta}dt^2 - e^{-2\beta}[e^{2\alpha}(d\varrho^2 + dz^2) + \varrho^2 d\Phi^2], \tag{7}$$

where α and β are functions of ϱ and z only, and ϱ, z, Φ, t correspond to x^1, x^2, x^3, x^4 co-ordinates, respectively. The final surviving BD Maxwell field equations (1)—(4) w.r.t. the metric (7) are:

$$\alpha_{,1}\left(\frac{1}{\varrho^2} + \frac{\varphi_{,2}^2}{\varphi^2}\right) = \frac{1}{\varrho}(\beta_{,1}^2 - \beta_{,2}^2) + 2\beta_{,1}\beta_{,2}\frac{\varphi_{,2}}{\varphi} + \frac{e^{-2\beta}}{\varrho\varphi}[(\eta_{,2}^2 - \eta_{,1}^2) + (\xi_{,2}^2 - \xi_{,1}^2)] -$$
$$- 2e^{-2\beta}\frac{\varphi_{,2}}{\varphi^2}(\eta_{,1}\eta_{,2} + \xi_{,1}\xi_{,2}) - \frac{\omega}{2}\frac{\varphi_{,2}^2}{\varrho\varphi^2} - \frac{\varphi_{,2}}{\varphi}\left(\frac{\beta_{,2}}{\varrho} - \beta_{,1}\frac{\varphi_{,2}}{\varphi}\right), \tag{8}$$

$$\alpha_{,2}\left(\frac{1}{\varrho^2} + \frac{\varphi_{,2}^2}{\varphi^2}\right) = -(\beta_{,1}^2 - \beta_{,2}^2)\frac{\varphi_{,2}}{\varphi} + \frac{2\beta_{,1}\beta_{,2}}{\varrho} - e^{-2\beta}\frac{\varphi_{,2}}{\varphi^2}[(\eta_{,2}^2 - \eta_{,1}^2) + (\xi_{,2}^2 - \xi_{,1}^2)] -$$
$$- \frac{2}{\varphi\varrho}e^{-2\beta}(\eta_{,1}\eta_{,2} + \xi_{,1}\xi_{,2}) + \frac{\omega}{2}\frac{\varphi_{,2}^3}{\varphi^3} + \frac{\varphi_{,2}}{\varphi}\left(\frac{\beta_{,2}\varphi_{,2}}{\varphi} + \frac{\beta_{,1}}{\varrho}\right), \tag{9}$$

$$\beta_{,11} + \beta_{,22} + \frac{\beta_{,1}}{\varrho} = \frac{e^{-2\beta}}{\varphi}[(\eta_{,1}^2 + \eta_{,2}^2) + (\xi_{,1}^2 + \xi_{,2}^2)] - \frac{\beta_{,2}\varphi_{,2}}{\varphi}, \tag{10}$$

$$\eta_{,11} + \eta_{,22} + \frac{\eta_{,1}}{\varrho} = 2\beta_{,1}\eta_{,1} + 2\beta_{,2}\eta_{,2}\,, \tag{11}$$

$$\xi_{,11} + \xi_{,22} + \frac{\xi_1}{\varrho} = 2\beta_{,1}\xi_{,1} + 2\beta_{,2}\xi_{,2}\,, \tag{12}$$

$$\varphi = mz + n, \text{ (}m \text{ and } n \text{ are arbitrary constants)}, \tag{13}$$

$$\eta_{,2}\xi_1 - \eta_{,1}\xi_{,2} = 0. \tag{14}$$

We now assume η to be dependent on ξ, i.e.

$$\eta = \eta(\xi). \tag{15}$$

In view of (15), Eq. (14) is identically satisfied and the Eqs. (11) and (12) together give the condition

$$\eta = a\xi + b, \text{ (}a \text{ and } b \text{ are arbitrary constants)}. \tag{16}$$

This relation is same as that obtained by PERJÉS [10]. Further assuming β to be functionally dependent on ξ and φ, viz.,

$$\beta = \beta(\xi, \varphi), \tag{17}$$

where ξ and φ are independent of each other (since, in the BD assumption, the Lagrange density of matter is not a function of φ), and making use of (16) and (17) in (10), (12) and (13), we get

$$\left\{\beta_{,\xi\xi} + 2\beta_{,\xi}^2 - \frac{e^{-2\beta}}{\varphi}(1 + a^2)\right\}(\xi_{,1}^2 + \xi_{,2}^2) + \beta_{,\xi}\xi_{,2}\varphi_{,2}\left(2\beta_{,\varphi} + \frac{1}{\varphi}\right) + \\ + \varphi_{,2}^2\left(\beta_{,\varphi\varphi} + \frac{\beta_{,\varphi}}{\varphi}\right) = 0. \tag{18}$$

Besides a general solution, which in this case is quite difficult to obtain, there are various possibilities to satisfy the equation (18). One such possibility, leading to the desired result, is to choose the coefficients of $(\xi_{,1}^2 + \xi_{,2}^2)$, $\xi_{,2}\varphi_{,2}$ and $\varphi_{,2}^2$ equal to zero. This gives a set of differential equations as follows:

$$\left.\begin{aligned} \beta_{,\xi\xi} + 2\beta_{,\xi}^2 - \frac{e^{-2\beta}}{\varphi}(1 + a^2) &= 0, \\ 2\beta_{,\varphi} + \frac{1}{\varphi} &= 0, \\ \beta_{,\varphi\varphi} + \frac{\beta_{,\varphi}}{\varphi} &= 0. \end{aligned}\right\} \tag{19}$$

It may be mentioned that Eq. (18) can be satisfied even by choosing $\xi_{,1}^2 + \xi_{,2}^2$, $\xi_{,2}\varphi_{,2}$ and $\varphi_{,2}^2$ to be vanishing. Physically this amounts to the magnitude of the gradient vector of the electromagnetic and the BD scalar fields being null, non-null and mutually orthogonal. (In fact, in this particular case $\varphi_{,2}^2$ being zero implies the BD scalar field being constant, leaving thereby only ordinary Einstein—Maxwell fields). In such a situation there may or may not exist any WMP relation. We would, however, like to avoid such a restricted physical situation to include non-null and non-orthogonal force fields also. The other possibilities will be studied later.

The set of equation (19) has a consistent solution

$$e^{2\beta} = \frac{1}{\varphi}\left[(1 + a^2)\,\xi^2 + c\xi + d\right], \tag{20}$$

where a, c, d are arbitrary constants.

The relation (20) is a generalized form of MAJUMDAR—PAPAPETROU relation for static axially symmetric BD Maxwell fields which, when BD scalar φ is constant, reduces to that obtained by DAS [9]. Obviously, when φ = constant and $a = 0$, Eq. (20) goes over to the well known relation obtained by MAJUMDAR and PAPAPETROU.

Using (16) and (20) in (10) and (12), we get a single equation,

$$\xi_{,11} + \xi_{,22} + \frac{\xi_{,1}}{\varrho} = \frac{\{c + (1 + a^2)\,2\xi\}\,(\xi_{,1}^2 + \xi_{,2}^2)}{(1 + a^2)\,\xi^2 + c\xi + d} - \frac{\xi_{,2}\varphi_{,2}}{\varphi}. \tag{21}$$

We now consider the substitution

$$\int \frac{d\xi}{(1 + a^2)\,\xi^2 + c\xi + d} = \frac{2}{\sqrt{c^2 - 4d(1 + a^2)}}\left(x + \frac{1}{2}\log\varphi\right), \tag{22}$$

x being the new variable. Eq. (22) integrates as

$$\xi = -\frac{c}{2(1 + a^2)} - \frac{\sqrt{c^2 - 4d(1 + a^2)}}{2(1 + a^2)}\coth\left(x + \frac{1}{2}\log\varphi\right). \tag{23}$$

This, when substituted in (20), gives β as

$$e^{2\beta} = \frac{1}{\varphi}\left[\frac{c^2 - 4d(1 + a^2)}{(1 + a^2)} \cdot \frac{e^{2x}\varphi}{(e^{2x}\varphi - 1)^2}\right]. \tag{24}$$

Again substituting (16), (20) and (22) in (8), (9) and (21) we get:

$$\begin{aligned} \alpha_{,1}\left(\frac{1}{\varrho^2} + \frac{\varphi_{,2}^2}{\varphi^2}\right) = {} & \frac{1}{\varrho}\left(x_{,1}^2 - x_{,2}^2\right) + 2x_{,1}x_{,2}\frac{\varphi_{,2}}{\varphi} - \frac{\omega}{2}\frac{\varphi_{,2}^2}{\varrho\varphi^2} - \\ & - \frac{\varphi_{,2}}{\varphi}\left(\frac{x_{,2}}{\varrho} - x_{,1}\frac{\varphi_{,2}}{\varphi}\right), \end{aligned} \tag{25}$$

$$\alpha_{,2}\left(\frac{1}{\varrho^2}+\frac{\varphi_{,2}^2}{\varphi^2}\right)=-(x_{,1}^2-x_{,2}^2)\frac{\varphi_{,2}}{\varphi}+\frac{2x_{,1}x_{,2}}{\varrho}+\frac{\omega}{2}\frac{\varphi_{,2}^3}{\varphi^3}+$$
$$+\frac{\varphi_{,2}}{\varphi}\left(\frac{x_{,2}\varphi_{,2}}{\varphi}+\frac{x_{,1}}{\varrho}\right), \tag{26}$$

$$x_{,11}x_{,22}+\frac{x_{,1}}{\varrho}=-\frac{x_{,2}\varphi_{,2}}{\varphi}. \tag{27}$$

It can be seen that Eqs. (25)—(27) are the BD vacuum equations for the static axially symmetric WEYL's metric;

$$ds^2=e^{2\chi}dt^2-e^{-2\chi}[e^{2\alpha}(d\varrho^2+dz^2)+\varrho^2d\Phi^2], \tag{28}$$

the solutions of which are known (see Appendix).

Thus the BD Maxwell fields for the metric (7), under the condition (23) and (24), are equivalent to BD vacuum fields for the metric (28) and vice-versa. This equivalence can always be used to generate BD vacuum fields for the metric (28) from the already known BD vacuum solutions for the metric

$$ds^2=e^{2\chi_0}dt^2-e^{-2\chi_0}[e^{2\alpha_0}(d\varrho^2+dz^2)+\varrho^2d\Phi^2]. \tag{29}$$

Hence the following theorem:

Theorem

Given any $(\alpha_0, x_0, \varphi_0)$ as the BD vacuum solution for the metric (29), one can always generate the corresponding BD Maxwell solution $(\alpha, x, \varphi, \xi, \eta)$, where

$$\alpha=\alpha_0,$$
$$x=\frac{1}{2}\log\left[\frac{c^2-4d(1+a^2)}{(1+a^2)\varphi_0}\cdot\frac{\varphi_0e^{2\chi_0}}{(\Phi_0e^{2\chi_0}-1)^2}\right],$$
$$\xi=-\frac{c}{2(1+a^2)}-\frac{\sqrt{c^2-4d(1+a^2)}}{2(1+a^2)}\coth\left(x_0+\frac{1}{2}\log\varphi_0\right),$$
$$\eta=a\xi+b,$$
$$\varphi=\varphi_0.$$

3. Appendix

The solutions for the metric (28) are:

$$\alpha=-\frac{k^2}{2}\log\left[\frac{1}{\varrho^2}+\frac{m^2}{(mz+n)^2}\right]+\frac{1}{2}(2k^2-k^2m+mk)\log[(mz+n)^2+m^2\varrho^2]+e,$$

$$x=k\log\varrho+\frac{k}{m}\log(mz+n),$$

$$\varphi=mz+n.$$

Acknowledgement

The authors would like to thank Prof. G. BANDOPADHYAY and Prof. J. R. RAO for their valuable discussions.

REFERENCES

1. H. WEYL, Ann. d. Physik, **54,** 117, 1917.
2. S. D. MAJUMDAR, Phys. Rev., **72,** 390, 1947.
3. A. PAPAPETROU, Proc. Roy. Irish. Acad., A **51,** 191, 1947.
4. W. BONNOR, Proc. Phys. Soc. (London), A **67,** 225, 1954.
5. J. B. HARTLE and S. W. HAWKING, Commun. Math. Phys., **26,** 87, 1972.
6. B. K. NAYAK, Aust. J. Phys., **28,** 585, 1975.
7. R. N. TIWARI and B. K. NAYAK, Phys. Rev., D **14,** 2502, 1976.
8. R. N. TIWARI and P. P. RAO, to appear in GRG (Switzerland), 1979.
9. K. C. DAS, To appear "Seminar on Recent Advances in Applied Mathematics and Applications" I.I.T., Kharagpur (1978).
10. Z. PERJÉS, Acta Phys. Hung. **25,** 393, 1968.

Acta Physica Academiae Scientiarum Hungaricae, Tomus 45 (4), pp. 293—298 (1978)

ON STATIC AXIALLY SYMMETRIC ELECTROVAC UNIVERSES

By

J. N. S. KASHYAP

DEPARTMENT OF MATHEMATICS, BANARAS HINDU UNIVERSITY, VARANASI-221005, INDIA

(Received 14. IX. 1978)

In this paper we consider an axially symmetric metric and obtain some exact static solutions of Einstein—Maxwell field equations in vacuo. In two cases the metric represents uniform electromagnetic field.

1. Introduction

According to the electronic structure of matter there is a possibility of the existence of electromagnetic and other fields besides its gravitational field. In this context consider the simplest atom of hydrogen which is associated with a magnetic field and effects the gravitational field due to its mass. The field so obtained is axially symmetric. The field of all heavenly bodies in the state of stationary rotation about their axes is also axially symmetric. So, from all these physical observations, the axially symmetric relativistic study of the universe and its constituents seems to be more realistic. In this direction several attempts have been made. The external gravitational field of the simplest model of a non-rotating sphere filled with matter of constant density has been obtained from the axially symmetric metric [1]:

$$dS^2 = -e^{2(\alpha-\beta)}(d\varrho^2 + dz^2) - \varrho^2 e^{-2\beta} d\varphi^2 + e^{2\beta} dt^2,$$

where α and β are functions of ϱ and z only. Making use of a metric of this type and successive approximations the gravitational field of hydrogen atom has been obtained in Einstein's unified field theory (1953) [2]. In the present investigation we consider the same metric and obtain some exact static solutions of Einstein—Maxwell field equations in vacuo. In two cases it is found that the metric represents a uniform electromagnetic field.

2. The field equations

The Einstein—Maxwell field equations in vacuo are

$$R_{\lambda\mu} = -8\pi E_{\lambda\mu}, \tag{2.1}$$

$$(v - gF^{\lambda\mu})_{,\mu} = 0, \tag{2.2}$$

where

$$E_{\lambda\mu} = -F_{\mu\alpha}F^{\alpha}_{\lambda} + \frac{1}{4}g_{\lambda\mu}F_{\alpha\beta}F^{\alpha\beta}, \tag{2.3}$$

$$F_{\lambda\mu} = A_{\lambda_1\mu} - A_{\mu_1\lambda}. \tag{2.4}$$

$R_{\lambda\mu}$ is the contracted curvature tensor, $E_{\lambda\mu}$ the electromagnetic energy tensor, $F_{\lambda\mu}$ the electromagnetic field tensor and A_{α} the 4-potential. A comma followed by a lower suffix denotes partial differentiation with respect to the corresponding variable.

The non-vanishing components of the contracted curvature tensor for the given metric are given as follows:

$$\begin{aligned}
R_{11} &= \alpha_{11} + \alpha_{33} - \beta_{11} - \beta_{33} + 2\beta_1^2 - \frac{1}{\varrho}(\alpha_1 + \beta_1),\\
R_{22} &= -\varrho^2 e^{-2\alpha}\left((\beta_{11} + \beta_{33} + \frac{\beta_1}{\varrho}\right),\\
R_{33} &= \alpha_{11} + \alpha_{33} - \beta_{11} - \beta_{33} + 2\beta_3^2 + \frac{1}{\varrho}(\alpha_1 - \beta_1),\\
R_{44} &= \frac{e^{4\beta}}{\varrho^2}R_{22}, \qquad R_{13} = 2\beta_1\beta_3 - \frac{\alpha_3}{\varrho}.
\end{aligned} \tag{2.5}$$

The lower suffixes 1 and 3 after a function indicate a partial differentiation with respect to ϱ and z respectively. Also we have

$$R_{12} = R_{14} = R_{23} = R_{24} = R_{34} = 0,$$

which in view of (2.1) provide:

$$F_{13} = F_{24} = 0; \quad F_{14}F_{14} - F_{23}F_{34} = 0. \tag{2.6}$$

The non-vanishing components of $F_{\alpha\beta}$ can, by virtue of (2.4), be derived from only two components A_2 and A_4 of the 4-potential A_{α}. Let us take

$$A_2 = \varphi, \quad A_4 = \psi. \tag{2.7}$$

Therefore, from (2.4), we have

$$\begin{aligned}
F_{12} &= -\varphi_1, & F_{14} &= -\psi_1,\\
F_{23} &= \varphi_3, & F_{3} &= -\psi_3,
\end{aligned} \tag{2.8}$$

From (2.3), (2.6) and (2.8) the non-vanishing independent components of the electromagnetic energy tensor are found to be

$$E_{11} = \frac{\varphi_1^2 - \varphi_3^2}{2\varrho^2 e^{-2\beta}} - \frac{\psi_1^2 - \psi_3^2}{2e^{2\beta}},$$

$$E_{22} = \frac{\varphi_1^2 + \varphi_3^2}{2e^{2\alpha-2\beta}} - \frac{\psi_1^2 + \psi_3^2}{2e^{2\alpha+2\beta}},$$

$$E_{33} = -\frac{\varphi_1^2 - \varphi_3^2}{2\varrho^2 e^{-2\beta}} + \frac{\psi_1^2 - \psi_3^2}{2e^{2\beta}}, \tag{2.9}$$

$$E_{44} = \frac{\varphi_1^2 + \varphi_3^2}{2e^{2\alpha-6\beta}} + \frac{\psi_1^2 + \psi_3^2}{2e^{2\alpha-2\beta}},$$

$$E_{13} = \frac{\varphi_1\varphi_3}{\varrho^2 e^{-2\beta}} - \frac{\psi_1\psi_3}{e^{2\beta}}.$$

Now the field equations (2.1) with the help of (2.5) (2.6) and (2.9) can be recast in the form as follows:

$$\alpha_{11} + \alpha_{33} - \beta_{11} - \beta_{33} + 2\beta_1^2 - \frac{1}{\varrho}(\alpha_1 + \beta_1) = -4\pi\left(\frac{\varphi_1^2 - \varphi_3^2}{\varrho^2 e^{-2\beta}} - \frac{\psi_1^2 - \psi_3^2}{e^{2\beta}}\right), \tag{2.10}$$

$$\beta_{11} + \beta_{33} + \frac{\beta_1}{\varrho} = 4\pi\left(\frac{\varphi_1^2 + \varphi_3^2}{\varrho^2 e^{-2\beta}} + \frac{\psi_1^2 + \psi_3^2}{e^{2\beta}}\right), \tag{2.11}$$

$$\frac{\alpha_1}{\varrho} = \beta_1^2 - \beta_3^2 + 4\pi\left(\frac{\varphi_1^2 - \varphi_3^2}{\varrho^2 e^{-2\beta}} - \frac{\psi_1^2 - \psi_3^2}{e^{2\beta}}\right), \tag{2.12}$$

$$\frac{\alpha_3}{\varrho} = 2\beta_1\beta_3 + 8\pi\left(\frac{\varphi_1\varphi_3}{\varrho^2 e^{-2\beta}} - \frac{\psi_1\psi_3}{e^{2\beta}}\right). \tag{2.13}$$

Also from (2.2), (2.6) and (2.8) we get

$$\varphi_{11} + \varphi_{33} - \frac{\varphi_1}{\varrho} = -2(\beta_1\varphi_1 + \beta_3\varphi_3), \tag{2.14}$$

$$\psi_{11} + \psi_{33} + \frac{\psi_1}{\varrho} = 2(\beta_1\psi_1 + \beta_3\psi_3), \tag{2.15}$$

$$\varphi_1\psi_1 + \varphi_3\psi_3 = 0. \tag{2.16}$$

3. Solutions of the field equations

Due to the non-linearity of the field equations taken into consideration it is difficult to find their exact solutions in general. In the present paper we, therefore, solve them in particular cases. Eq. (2.16) is identically satisfied in the following cases:

(i) $\psi_1 = \psi_3 = \varphi_3 = 0,$

(ii) $\psi_1 = \psi_3 = \varphi_1 = 0,$

(iii) $\varphi_1 = \varphi_3 = \psi_3 = 0,$

(iv) $\varphi_1 = \varphi_3 = \psi_1 = 0,$

(v) $\varphi_1 = \psi_3 = 0,$

(vi) $\varphi_3 = \psi_1 = 0.$

In these particular cases we now solve the field equations to determine α, β, φ and ψ. The method of obtaining solution in all cases is as in case i).

Case (i)

In this case ψ is constant and φ is a function of ϱ. Therefore the field equations (2.10)—(2.15) reduce to

$$\alpha_{11} + \alpha_{33} - \beta_{11} - \beta_{33} + 2\beta_1^2 - \frac{1}{\varrho}(\alpha_1 + \beta_1) = -4\pi\left(\frac{\varphi_1}{\varrho}e^{\beta}\right)^2, \tag{3.1}$$

$$\beta_{11} + \beta_{33} + \frac{\beta_1}{\varrho} = 4\pi\left(\frac{\varphi_1}{\varrho}e^{\beta}\right)^2, \tag{3.2}$$

$$\frac{\alpha_1}{\varrho} = \beta_1^2 - \beta_3^2 + 4\pi\left(\frac{\varphi_1}{\varrho}e^{\beta}\right)^2, \tag{3.3}$$

$$\frac{\alpha_3}{\varrho} = 2\beta_1\beta_3, \tag{3.4}$$

$$\varphi_{11} - \frac{\varphi_1}{\varrho} = -2\beta_1\varphi_1. \tag{3.5}$$

The Eq. (3.5) gives by integration

$$e^{2\beta} = \frac{\varrho}{\varphi_1}e^{Z}, \tag{3.6}$$

where Z is an arbitrary function of z only. Substituting for β from (3.6) in (3.2), we get

$$\left(\log\frac{\varrho}{\varphi_1}\right)_{11} + \frac{1}{\varrho}\left(\log\frac{\varrho}{\varphi_1}\right)_1 + Z_{33} = 8\pi\frac{\varphi_1}{\varrho}e^{z}. \tag{3.7}$$

Since φ is function of ϱ only and Z is function of z only, it follows that (3.7) will hold only if $\frac{\varphi_1}{\varrho}$ be a constant for e^z be a constant. Let us take

$$\varphi_1 = \frac{a}{4\pi}\varrho, \tag{3.8}$$

where a is an arbitrary constant. Then Eq. (3.7) reduces to

$$Z_{33} = 2ae^z. \tag{3.9}$$

The corresponding solution is

$$e^z = \frac{1}{a}\operatorname{cosech}^2 z. \tag{3.10}$$

Therefore, from (3.6), (3.8) and (3.10) we have

$$e^\beta = \frac{2\sqrt{\pi}}{a}\operatorname{cosech} z, \tag{3.11}$$

$$\varphi = \frac{a}{8\pi}\varrho^2 + b. \tag{3.12}$$

For the values of β and φ as given in (3.11) and (3.12) the Eqs. (3.3) and (3.4) provide

$$\alpha = \frac{1}{2}(c - \varrho^2). \tag{3.13}$$

In (3.12) and (3.13) b and c are arbitrary constants. For the values of α, β and φ so obtained Eq. (3.1) is identically satisfied.

Case (ii)

In this case ψ is constant and φ is a function of z. The corresponding solution is

$$\varphi = \frac{a}{4\pi}z + b,$$

$$e^\beta = \frac{2\sqrt{\pi}}{a}\operatorname{cosech}\log\varrho, \tag{3.14}$$

$$e = c\varrho.$$

Case (iii)

In this case φ is constant and ψ is a function of ϱ. The corresponding solution is

$$\psi = \frac{a}{8\pi}\varrho^2 + b,$$

$$e^\beta = \frac{a}{2\sqrt{\pi}}\varrho\cosh z, \tag{3.15}$$

$$e^\alpha = c\varrho\cosh^2 z\, e^{-\varrho^2/2}.$$

Case (iv)

In this case φ is constant and ψ is a function of z. The corresponding solution is

$$\psi = \frac{a}{4\pi} z + b,$$

$$e^{\beta} = \frac{a}{2\sqrt{\pi}} z \cosh \log \varrho, \tag{3.16}$$

$$e^{\alpha} = c\varrho^2 \cosh^2 \log \varrho.$$

Case (v)

In this case φ is a function of z and ψ is a function of ϱ only. The corresponding solution is

$$\varphi = \frac{1}{2a\sqrt{\pi}} \tanh z + d, \qquad \psi = \frac{a}{8\sqrt{\pi}} \varrho^2 + e,$$

$$e^{\beta} = \frac{a}{\sqrt{2}} \varrho \cosh z, \qquad e^{\alpha} = c\varrho \cosh^2 z \, e^{\varrho^2/2}. \tag{3.17}$$

Case (vi)

In this case φ is a function of ϱ and ψ is a function of z only. The corresponding solution is

$$\varphi = \frac{a}{8\sqrt{\pi}} \varrho^2 + d, \qquad \psi = -\frac{1}{2a\sqrt{\pi}} \coth z + e,$$

$$e^{\beta} = \frac{\sqrt{2}}{a} \operatorname{cosech} z, \qquad \alpha = \frac{1}{2}(c - \varrho^2). \tag{3.18}$$

Imposing the BERTOTTI conditions [3]

$$F_{\lambda\mu;\nu} = 0,$$

where semicolon denotes covariant derivative, it has been verified that in cases (ii) and (iv) the electromagnetic field is uniform.

Acknowledgement

The author is grateful to Dr. R. TIWARI for his interest in the preparation of this paper.

REFERENCES

1. J. L. SYNGE, Relativity — The General Theory, North Holland Publishing Co. Amsterdam, 312, 1960.
2. J. N. S. KASHYAP, Proc. Ind. Nat. Sc. Acad. **43A** No. 5, 352, 1977.
3. B. BERTOTTI, Phys. Rev., **116** (5), 1331, 1959.

Acta Physica Academiae Scientiarum Hungaricae, Tomus 45 (4), pp. 299—308 (1978)

SPATIALLY HOMOGENEOUS AND ANISOTROPIC EXPANDING UNIVERSE

By

V. B. JOHRI, G. K. GOSWAMI

and

I. J. SINGH

DEPARTMENT OF MATHEMATICS, UNIVERSITY OF GORAKHPUR, GORAKHPUR-273001, INDIA

(Received 21. IX. 1978)

We have studied Heckmann—Schucking models containing perfect fluids. In this way we have derived perfect fluid models of anisotropic universe corresponding to $\nu = 1$, $\frac{4}{3}$ and 2. The fate of density perturbations in a superdense model universe has been investigated.

1. Introduction

This work is a continuation of the study of the non-rotating cosmological models of the spatially homogeneous and anisotropic universe discussed by many authors [1—13].

In this paper, we investigate Heckmann—Schücking solutions of Einstein field equations with an energy momentum tensor corresponding to perfect fluid, assuming ν-law equation of state

$$p = (\nu - 1)\varrho.$$

In this way, we derive perfect fluid models of the universe corresponding to $\nu = 1, \frac{4}{3}$ and 2 that is for dust-filled, radiation-dominated and superdense stages of the universe. Moreover, we investigate the growth of the density perturbation in an unperturbed Heckmann—Schücking model. Various physical and geometrical properties of the background model have been also discussed, taking $8\pi G = C^4 = 1$.

2. The field equations

The Heckmann—Schüking metric is given by

$$ds^2 = dt^2 - A^2dx^2 - B^2dy^2 - C^2dz^2, \tag{1}$$

where A, B, C are the function of time only. We consider the energy momentum tensor of a perfect fluid, that is

$$T^{ij} = (p + \varrho)\, u^i u^j - p g^{ij}, \tag{2}$$

with

$$g_{ij}\ u^i u^j = 1, \tag{3}$$

u^i being 4-velocity vector of the fluid normalised to unity. Choosing comoving coordinates, we have

$$u_1 = u_2 = u_3 = 0.$$

The Einstein's field equations are

$$R_{ij} - \frac{1}{2} R g_{ij} + \lambda g_{ij} = -T_{ij}. \tag{4}$$

The field equations (4) in terms of line element (1) with the cosmological constant $\lambda = 0$ are given by

$$-\left(\frac{B_{44}}{B} + \frac{C_{44}}{C} + \frac{B_4 C_4}{BC}\right) = p, \tag{5}$$

$$-\left(\frac{A_{44}}{A} + \frac{C_{44}}{C} + \frac{A_4 C_4}{AC}\right) = p, \tag{6}$$

$$-\left(\frac{A_{44}}{A} + \frac{B_{44}}{B} + \frac{A_4 B_4}{AB}\right) = p, \tag{7}$$

$$\left(\frac{A_4 B_4}{AB} + \frac{B_4 C_4}{BC} + \frac{A_4 C_4}{AC}\right) = \varrho, \tag{8}$$

where A_4, B_4, C_4 stand for time derivatives of A, B, C, respectively. Subtracting Eq. (6) from (5), (7) from (6) and (5) from (7), we get

$$\frac{A_{44}}{A} - \frac{B_{44}}{B} + \frac{A_4 C_4}{AC} - \frac{B_4 C_4}{BC} = 0, \tag{9}$$

$$\frac{B_{44}}{B} - \frac{C_{44}}{C} + \frac{B_4 A_4}{BA} - \frac{C_4 A_4}{CA} = 0, \tag{10}$$

$$\frac{C_{44}}{C} - \frac{A_{44}}{A} + \frac{C_4 B_4}{CB} - \frac{A_4 B_4}{AB} = 0. \tag{11}$$

Further subtracting (11) from (9), we get

$$\frac{B_{44}}{B} + \frac{C_{44}}{C} + \frac{2 B_4 C_4}{BC} = \frac{2 A_{44}}{A} + \frac{A_4 C_4}{AC} + \frac{A_4 B_4}{AB}. \tag{12}$$

This equation can be written in the following form

$$\left(\frac{(BC)_4}{BC}\right)_4 + \left(\frac{(BC)_4}{BC}\right)^2 = 2\left(\frac{A_4}{A}\right)_4 + 2\left(\frac{A_4}{A}\right)^2 + \frac{A_4}{A}\left(\frac{(BC)_4}{BC}\right). \tag{13}$$

Integrating this equation, we get the following relation among A, B and C:

$$BC = A^2. \tag{14}$$

Therefore, we can assume

$$B = AD, \tag{15}$$

$$C = AD^{-1}, \tag{16}$$

where

$$D = D(t). \tag{17}$$

Simplifying (5) and (8) with the help of (15), (16), we get the equation in p and ϱ

$$p = -\left(\frac{2A_{44}}{A} + \frac{A_4^2}{A^2} + \frac{D_4^2}{D^2}\right), \tag{18}$$

$$\varrho = 3\left(\frac{A_4}{A}\right)^2 - \frac{D_4^2}{D^2}. \tag{19}$$

Further integrating equation (10),we get the first integral

$$\frac{D_4}{D} = \frac{K}{A^3}, \tag{20}$$

where K is an arbitrary constant of integration.

In general, the pressure p and density ϱ are independent thermodynamical quantities and the equation of state can be used to define the temperature

$$T = T(\varrho, p). \tag{21}$$

However, for barotropic fluids, we can assume the equation of state

$$p = (\nu - 1)\varrho. \tag{22}$$

We have obtained below the perfect fluid models corresponding to $\nu = 1$, 4/3 and 2, which represent the chronological history of the universe from the present day backwards.

3. Case I: Dust-filled universe

In this case $\nu = 1$ that is $p = 0$. Therefore from Eqs. (19) and (18), we get

$$\frac{2A_{44}}{A} + \frac{A_4^2}{A^2} + \frac{K^2}{A^6} = 0. \tag{23}$$

The substitution $\alpha = A^{3/2}$ reduces the above equation to the following form

$$\alpha^3\alpha_{44} = -\frac{3}{4}K^2, \tag{24}$$

which has the first integral

$$\alpha_4 = \left(\frac{3K^2}{4\alpha^2} + L\right)^{1/2},$$

where L is an arbitrary constant of integration. Further integration of this equation yields

$$\alpha^2 = L\left\{(t+M)^2 - \frac{3K^2}{4L^2}\right\},$$

where M is an arbitrary constant of integration, or

$$A^3 = L\left\{(t+M)^2 - \frac{3K^2}{4L^2}\right\}. \tag{25}$$

Therefore, from Eq., (19)

$$\varrho = \frac{4}{3\left\{(t+M)^2 - \frac{3K^2}{4L^2}\right\}}.$$

Now as $t \to 0$, $\varrho \to \infty$, therefore

$$M^2 = \frac{3K^2}{4L^2}.$$

Inserting the value of M^2 in the above equation we get

$$\varrho = \frac{4}{3(t^2+2Mt)}. \tag{26}$$

JOHRI and LAL [13] arrive at the same result by using tetrad techniques.

Inserting the value of M^2 in (25), we get

$$A^3 = \frac{\sqrt{3}K}{2M}\{(t^2+2Mt)\} \tag{27}$$

and from Eq. (20)

$$D = D_0\left(\frac{t}{t+2M}\right)^{1/\sqrt{3}}. \tag{28}$$

Thus, the Heckmann—Schücking model corresponding to dust-filled universe has the metric

$$ds^2 = dt^2 - (t^2+2Mt)^{2/3}\left[dx^2 + \left\{\frac{t}{t+2M}\right\}^{2/\sqrt{3}}dy^2 + \left\{\frac{t}{(t+2M)}\right\}^{-2/\sqrt{3}}dz^2\right]. \tag{29}$$

This model is characterised by the following properties

(i) The expansion scalar is given by

$$\theta = \frac{1}{3}u^{\lambda}_{;\lambda} = \frac{2}{3}\frac{(t+m)}{(t^2+2Mt)}.$$

This shows that the expansion scalar goes on decreasing with time more rapidly as compared to Friedmann model.

(ii) The shear scalar

$$\sigma^2 = \frac{1}{2}\sigma_{ij}\sigma^{ij}$$

where

$$\sigma_{ij} = u_{i;j} - \theta(g_{ij} - u_i u_j) = 3\frac{D_4^2}{D^2} \tag{30}$$

or

$$\sigma^2 = \frac{4M^2}{(t^2 + 2Mt)^2}.$$

(iii) It is obvious from Eq. (26) that the density of matter decreases more rapidly in the Heckmann—Schücking case than the density $\varrho = \frac{K}{t^2}$ in the Friedmann model.

(iv) The relative anisotropy can be obtained with the help of (26) and (30). We get

$$\frac{\sigma^2}{\varrho} = \frac{3M^2}{(t^2 + 2Mt)}$$

which is the ratio of the anisotropic energy for the matter to the total energy.

This shows that in a dust filled universe, the anisotropic energy density decreases rapidly with time in comparison with the total energy density of the universe.

4. Case II — Radiation-filled universe

In this case $v = 4/3$. This implies $p = \varrho/3$. This value of v corresponds to a radiation-dominated epoch of the universe.

We have from Eqs. (19) and (18)

$$\frac{A_{44}}{A} + \frac{A_4^2}{A^2} + \frac{1}{3}\frac{D_4^2}{D^2} = 0. \tag{31}$$

Inserting the value of $\frac{D_4}{D}$ in this equation and putting $A^2 = X$ we have

$$X^2 X_{44} = -\frac{2}{3}K^2,$$

which has the first integral

$$X_4 = \left(\frac{4K^2}{3X} + L\right)^{1/2},$$

where L is an arbitrary constant of integration. Further integration yields

$$\int \frac{dx}{\sqrt{\frac{4K^2}{3X}+L}} = t + M,$$

where M is an arbitrary constant of integration or

$$\frac{4K^2}{3L^{3/2}}[A' + A'^3 - \log(A' + A'^2 + 1)] = t + M, \tag{32}$$

where

$$A' = \frac{3L}{4K^2}A.$$

From Eq. (19) we get

$$\varrho = \alpha/A'^4,$$

where α is an arbitrary constant of integration.

Inserting the value of A' in Eq. (32), we have

$$\frac{4K^2}{3L^{3/2}}\left[\left(\frac{\alpha}{\varrho}\right)^{1/4} + \left(\frac{\alpha}{\varrho}\right)^{3/4} - \log\left(1 + \left(\frac{\alpha}{\varrho}\right)^{1/4} + \left(\frac{\alpha}{\varrho}\right)^{1/2}\right)\right] = t + M, \tag{33}$$

Now as we go back to primordial singularity

$$\varrho \to \infty \quad \text{as} \quad t \to 0.$$

Therefore

$$\alpha/\varrho \to 0 \quad \text{as} \quad t \to 0.$$

Hence $M = 0$.

Inserting the value of M in Eq. (33), we get

$$\frac{4K^2}{3L^{3/2}}\left[\left(\frac{\alpha}{\varrho}\right)^{1/4} + \left(\frac{\alpha}{\varrho}\right)^{3/4} - \log\left(1 + \left(\frac{\alpha}{\varrho}\right)^{1/4} + \left(\frac{\alpha}{\varrho}\right)^{1/2}\right)\right] = t. \tag{34}$$

This model is characterised by the following properties

(i) The density ϱ is given by Eq. (34).

(ii) The expansion scalar is given by

$$\theta = K'\left(\frac{\alpha}{\varrho}\right)^{-3/4}\left\{K'' + \left(\frac{\alpha}{\varrho}\right)^{1/2}\right\}^{1/2},$$

where K', K'' are arbitrary constants. This shows that expansion goes on decreasing with time more rapidly as compared to the Friedmann model.

(iii) The shear scalar is given by

$$\sigma^2 = \frac{3K^2}{A^6} = K'''\left(\frac{\alpha}{\varrho}\right)^{-3/2},$$

where K''' is an arbitrary constant.

(iv) The relative anisotropy is given by

$$\frac{\sigma^2}{\varrho} = K_1 \left(\frac{\alpha}{\varrho}\right)^{-1/2},$$

where K_1 is an arbitrary constant.

This shows that in this case, the anisotropic energy density decreases more rapidly with time than the total energy density of the universe.

5. Case III — Superdense universe

ZELDOVICH gave the equation of state for stiff matter by choosing $v = 2$, that is $p = \varrho$.

From Eq. (19), (20) and (18) we get

$$\frac{A_{44}}{A} + 2\left(\frac{A_4}{A}\right)^2 = 0 \tag{35}$$

which has the first integral

$$A^2 A_4 = a',$$

where a' is an arbitrary constant of integration.

Further integration yields

$$A^3 = (a_1 t + b), \tag{36}$$

where a_1, b are arbitrary constants of integration.

Inserting the value of A in Eq. (20) and integrating we get

$$D = D_0(a_1 t + b)^K, \tag{37}$$

where D_0 is an arbitrary constant of integration.

Inserting the value of A and D in Eq. (19), we have

$$\varrho = \frac{\alpha}{(a_1 t + b)^2}, \tag{38}$$

where α is an arbitrary constant.

Thus we get the following metric for the superdense spatially homogeneous and anisotropic universe

$$ds^2 = d\tau^2 - a_1^2(\tau^{2p_1} dx^2 + \tau^{2p_2} dy^2 + \tau^{2p_3} dz^2), \tag{39}$$

where $\tau = (a_1 t + b)$ and p_1, p_2, p_3 are arbitrary constants and

$$\begin{aligned} \Sigma p_i &= p_1 + p_2 + p_3 = 1, \\ \Sigma p_i^2 &= p_1^2 + p_2^2 + p_3^2 = \frac{1}{3} + 2K^2 \geq \frac{1}{3}. \end{aligned} \tag{40}$$

Moreover from Eq. (8), (38) and (40), we have

$$\Sigma p_i^2 = 1 - \frac{2\alpha}{a_1^2},$$

which implies $\Sigma p_i^2 \leq 1$, since α is a positive constant. Thus $1 \geq \Sigma p_i^2 \geq \frac{1}{3}$.

This is obviously a generalisation of the Kasner model for empty universe

$$ds^2 = dt^2 - t^{2p_1}dx^2 - t^{2p_2}dy^2 - t^{2p_3}dz^2,$$

where

$$\Sigma p_i = 1, \quad \Sigma p_i^2 = 1.$$

The limits of Σp_i^2 obtained above obey the restrictions prescribed by LAL [14] for non-empty universe.

This shows that the Kasner's metric can also represent the superdense stage of universe provided the indices p_i satisfy (39).

Moreover the above metric (39) is transformable to the metric obtained by ROY and SINGH [11]

$$ds^2 = L^2T^{1-a^2}(dT^2 - dx^2) - T^{(1+a)}dy^2 - T^{(1-a)}dz^2.$$

By using the following transformation

$$a_1 dT \to \tau^{-p_1} d\tau,$$

$$a_1\{a_1(1-p_1)\}\frac{p_2}{(1-p_1)}dy \to dy,$$

$$a_1\{a_1(1-p_1)\}\frac{p_3}{(1-p_1)}dz \to dZ,$$

where $$L = \{a_1^{\frac{1}{p_1}}(1-p)\}\frac{p_1}{(1-p_1)}, \quad a^2 = \frac{(3p_1-1)}{(p_1-1)},$$

$$p_2 = \frac{1}{2}(1-p_1)\left\{1 + \sqrt{\frac{3p_1-1}{p_1-1}}\right\}, \quad p_3 = \frac{1}{2}(1-p_1)\left\{1 - \sqrt{\frac{3p_1-1}{p_1-1}}\right\}.$$

This model is characterised by the following properties.

(i) The density σ is given by Eq. (38).

(ii) The expansion scalar is given by

$$\theta = \frac{a_1}{3(a_1 t + b)}.$$

This shows that the expansion goes on decreasing with time.

(iii) The shear scalar is

$$\sigma^2 = 3\left(\frac{D_4}{D}\right)^2$$

or

$$\sigma^2 = \frac{3K^2}{(a_1 t + b)^2}.$$

(iv) The relative anisotropy in this model is given by

$$\frac{\sigma^2}{\varrho} = K', \tag{41}$$

where K' is an arbitrary constant. This shows that unlike the cases of the dust-filled and radiation-dominated universe, the anisotropic energy density in this case is proportional to the total energy density of the universe.

6. Perturbation in superdense universe

The density perturbation in the universe has been discussed by many authors [15—23]. We have also derived linear density perturbation in a superdense universe taking (1) as the background model.

The mass conservation equation is given by

$$\varrho_4 = -(p + \varrho)\theta. \tag{42}$$

In a perturbed universe, we assume that the line element takes the form

$$ds^2 = dt^2 + 2g_{i4}\, dt\, dx^i + g_{ik}\, dx^i\, dx^k, \qquad (i = 1, 2, 3),$$

where the g_{4i} terms make allowance for the presence of vorticity and/or a translational velocity relative to the frame of isotropy of the unperturbed universe.

For the unperturbed model, we have to our order of approximation

$$\omega = 0,$$
$$3\sigma^2 = \theta^2 - 3(\theta_{11}\theta_{22} + \theta_{22}\theta_{33} + \theta_{33}\theta_{11}). \tag{43}$$

We introduce the condensation parameter S by

$$\varrho = \varrho_0(1 + S) \tag{44}$$

and using Eqs. (41), (42), (43), in the variation of the Raychaudhuri equation for the superdense stage of universe,

$$\delta\theta_4 + \frac{1}{3}\delta\theta^2 + 2\delta\sigma^2 + 2\delta\varrho = 0, \tag{45}$$

we get

$$S_{44} - \frac{2}{3}\frac{\varrho_4}{\varrho} S_4 - (4K'\varrho + 2\varrho)\, S = 0. \tag{46}$$

Inserting the value of ϱ from Eq. (28) and putting $(a_1 t + b) = T$ in (46), we have

$$T^2 S_{TT} - \frac{2}{3} T S_T - K_1 S = 0,$$

where K_1 is an arbitrary constant and S_T, S_{TT} stand for derivatives of S with respect to T, which yields the solution

$$S = C_1 T^{(5+\sqrt{25+36K_1})/6} + C_2 T^{(5-\sqrt{25+36K_1})/6}.$$

The first term on the right hand side represents a growing mode of the density perturbation but the second term decays with time.

REFERENCES

1. A. G. Doroshkevich, Ya. B. Zeldovich and I. D. Novikov, Zh. Eksp. Theor. Fiz. Pisma, **5**, 119, 1967; Sov. Phys. JETP Letters, **5**, 96, 1967.
2. C. W. Misner, Phys. Rev. Letters, **19,** 533, 1967; Astrophys. J. **151,** 431, 1968.
3. R. Kantowski, Thesis, Univ. of Texas, Austin, Texas, 1966.
4. J. Peter Vajk and Peter Gelgroth, J. Math. Phys., **71,** 2212, 1970.
5. K. S. Jacobs, Astrophys. J., **155,** 399, 1969.
6. G. R. R. Ellis and M. A. H. Maccallum, Comm. Math. Phys., **12,** 108, 1969.
7. R. A. Matzner, Astrophys. J., **157,** 1085, 1969.
8. K. P.Singh and Abdus Sattar, J. Phys. A. Math. Nucl. Gen., **6,** 1090, 1973.
9. K. P. Singh and D. N. Singh, Mon. Not. Royal Astron. Soc., **140,** 453, 1968.
10. O. Heckmann and E. Schucking, Gravitation, — An Introduction to Current Research, ed. L. Witten, Chap. XI., 1962.
11. S. R. Roy and P. N. Singh, J. Phys. A. Math. Gen., **9,** 255, 1977.
12. S. R. Roy and P. N. Singh, J. Phys. A. Math. Gen., **10,** 49, 1977.
13. V. B. Johri and B. K. Lal, Proc. of International Symposium on Relativity and Unified Field Theory, p. 187, 1975.
14. B. K. Lal, Ph. D. thesis, Univ. of Gorakhpur, India, 1977.
15. B. L. Hu and T. Regge, Phys. Rev. Letter, **29,** 1616, 1972.
16. T. E. Perko, F. A. Matzner and L. C. Shepley, Phys. Rev. D., **59,** 69,1972.
17. V. B. Johri, Tensor, New. Ser., **25,** 241, 1972.
18. N. Bandyopadhyay, J. Phys. A. Math. Gen., **10,** 189, 1977.
19. W. B. Bonnor, Mon. Not. Royal Astron. Soc., **117,** 104, 1957.
20. J. Silk and K. Breacher, Astrophys. J., **158,** 91, 1969.
21. W. Irvine, Ann. Phys. No. **32,** 322, 1965.
22. G. Field and L. C. Sheply, Astrophys. Space Sci., **1,** 309, 1968.
23. E. P. Liang, Astrophys. J., **204,** 235, 1976.

Acta Physica Academiae Scientiarum Hungaricae, Tomus 45 (4), pp. 309—315 (1978)

COUPLED ELECTROMAGNETIC AND SCALAR FIELDS IN A CYLINDRICALLY SYMMETRIC SPACE-TIME

By

J. N. S. KASHYAP

DEPARTMENT OF MATHEMATICS, BANARAS HINDU UNIVERSITY, VARANASI—221005, INDIA

(Received in revised form 17. X. 1978)

A class of exact non-static solutions of the relativistic field equations for coupled electromagnetic and zero rest mass scalar fields is obtained for the space-time defined by the most general cylindrically symmetric metric of MARDER.

1. Introduction

The study of electromagnetic fields coupled with meson fields has assumed considerable importance in the field of high energy particle physics. Often source-free electromagnetic fields are considered with meson fields (viz., zero rest mass scalar field, massive scalar field). The zero rest mass scalar field describes long-range interactions whereas the massive scalar field represents short-range interactions. At present we consider the zero rest mass scalar field coupled with electromagnetic field for a cylindrically symmetric space-time defined by the metric:

$$ds^2 = e^{2(\alpha-\beta)}(dt^2 - d\varrho^2) - \varrho^2 e^{-2\beta} d\varphi^2 - e^{2(\beta+\gamma)} dz^2. \tag{1.1}$$

For the metric given by (1.1) the components of Ricci tensor are:

$$R_{12} = R_{13} = R_{23} = R_{24} = R_{34} = 0.$$

Therefore, from the well-known Einstein—Maxwell equations, the components of electromagnetic energy momentum tensor are

$$E_{12} = E_{13} = E_{23} = E_{24} = E_{34} = 0,$$

which leads to the following restrictions on the electromagnetic field tensor $F_{\lambda\mu}$:

$$F_{14} = F_{23} = 0, \quad F_{12}F_{13} - F_{24}F_{34} = 0. \tag{1.2}$$

Imposing this set of restrictions on the electromagnetic field a class of exact non-static solutions of the Einstein—Maxwell equations for regions containing an electromagnetic field but no matter has already been obtained [1].

In the present investigation we consider a zero rest mass scalar field coupled with electromagnetic fields characterized by (1.2) and obtain a class of exact non-static solutions for the MARDER metric (1.1) [2] in the following cases:

(i) $F_{13} = F_{24} = 0$, (ii) $F_{12} = F_{34} = 0$,

(iii) $F_{13} = F_{24} = F_{34} = 0$, (iv) $F_{12} = F_{13} = F_{34} = 0$,

(v) $F_{12} = F_{24} = F_{34} = 0$, (vi) $F_{12} = F_{13} = F_{24} = 0$.

It is found that the solutions in the cases from (iii) to (vi) correspond either to the solutions of case (i) or to those of case (ii). An exact non-static solution of the field equations of general relativity containing only zero rest mass scalar field has also been obtained.

2. Field equations

In the presence of coupled electromagnetic and zero rest mass scalar fields, the general relativistic field equations are:

$$R_{\lambda\mu} - \frac{1}{2} R g_{\lambda\mu} = -8\pi(E_{\lambda\mu} + T_{\lambda\mu}). \tag{2.1}$$

The energy-momentum tensors $E_{\lambda\mu}$ and $T_{\lambda\mu}$ correspond to the source-free electromagnetic and scalar field, respectively, and are given as

$$E_{\lambda\mu} = -F_{\lambda\alpha}F^{\alpha}_{\mu} + \frac{1}{4} g_{\lambda\mu} F_{\alpha\beta}F^{\alpha\beta}, \tag{2.2}$$

and

$$T_{\lambda\mu} = V_{,\lambda}V_{,\mu} - \frac{1}{2} g_{\lambda\mu} V_{,\alpha}V_{,\beta}g^{\alpha\beta}, \tag{2.3}$$

where the electromagnetic field tensor $F_{\lambda\mu}$ and the scalar field V satisfy the relations:

$$F_{\lambda\mu} = A_{\lambda,\mu} - A_{\mu,\lambda}, \tag{2.4}$$

$$F^{\lambda\mu}_{\ ,\mu} = 0, \tag{2.5}$$

$$g^{\lambda\mu}V_{;\lambda\mu} = 0. \tag{2.6}$$

Here comma and semicolon denote partial and covariant differentiations, respectively.

Under the restrictions given by (1.2), the non-vanishing components of the field tensor $F_{\lambda\mu}$ can be derived only from the two components, A_2 and A_3, of the 4-potential A_μ. For convenience we take

$$A_2 = \varphi, \qquad A_3 = \psi, \tag{2.7}$$

and hence we have

$$F_{12} = -\varphi_1, \quad F_{13} = -\psi_1, \quad F_{24} = \varphi_4, \quad F_{34} = \psi_4. \tag{2.8}$$

Here and hereafter the lower suffixes 1 and 4 after a function indicate a partial differentiation with respect to ϱ and t respectively. Taking all field variables as functions of ϱ and t alone, it is found that the field equations (2.1), (2.5) and (2.6), therefore, reduce to the following:

$$\gamma_{44} - \gamma_1\alpha_1 - \gamma_4\alpha_4 + 2\beta_1\gamma_1 + 2\beta_4\gamma_4 + \beta_1^2 + \beta_4^2 + \gamma_4^2 - \frac{\alpha_1 + \gamma_1}{\varrho} = \\ = -4\pi\left[\frac{\varphi_1^2 + \varphi_4^2}{\varrho^2 e^{-2\beta}} + \frac{\psi_1^2 + \psi_4^2}{e^{2(\beta+\gamma)}} + V_1^2 + V_4^2\right], \tag{2.9}$$

$$\gamma_{14} - \gamma_4\alpha_1 - \gamma_1\alpha_4 + 2\beta_1\gamma_4 + 2\beta_4\gamma_1 + 2\beta_1\beta_4 + \gamma_1\gamma_4 - \frac{\alpha_4}{\varrho} = \\ = -8\pi\left[\frac{\varphi_1\varphi_4}{\varrho^2 e^{-2\beta}} + \frac{\psi_1\psi_4}{e^{2(\beta+\gamma)}} + V_1V_4\right], \tag{2.10}$$

$$-\alpha_{11} + \alpha_{44} - \gamma_{11} + \gamma_{44} - 2\beta_1\gamma_1 + 2\beta_4\gamma_4 - \beta_1^2 + \beta_4^2 - \gamma_1^2 + \gamma_4^2 = \\ = -4\pi\left[\frac{\varphi_1^2 - \varphi_4^2}{\varrho^2 e^{-2\beta}} - \frac{\psi_1^2 - \psi_4^2}{e^{2(\beta+\gamma)}} - V_1^2 + V_4^2\right], \tag{2.11}$$

$$-\alpha_{11} + \alpha_{44} + 2\beta_{11} - 2\beta_{44} - \beta_1^2 + \beta_4^2 + \frac{2\beta_1}{\varrho} = \\ = 4\pi\left[\frac{\varphi_1^2 - \varphi_4^2}{\varrho^2 e^{-2\beta}} - \frac{\psi_1^2 - \psi_4^2}{e^{2(\beta+\gamma)}} + V_1^2 - V_4^2\right], \tag{2.12}$$

$$\gamma_{11} - \gamma_1\alpha_1 - \gamma_4\alpha_4 + 2\beta_1\gamma_1 + 2\beta_4\gamma_4 + \beta_1^2 + \beta_4^2 + \gamma_1^2 - \frac{\alpha_1 - \gamma_1}{\varrho} = \\ = -4\pi\left[\frac{\varphi_1^2 + \varphi_4^2}{\varrho^2 e^{-2\beta}} + \frac{\psi_1^2 + \psi_4^2}{e^{2(\beta+\gamma)}} + V_1^2 + V_4^2\right], \tag{2.13}$$

$$\varphi_{11} - \varphi_{44} - \frac{\varphi_1}{\varrho} = -(2\beta_1 + \gamma_1)\varphi_1 + (2\beta_4 + \gamma_4)\varphi_4, \tag{2.14}$$

$$\psi_{11} - \psi_{44} + \frac{\psi_1}{\varrho} = (2\beta_1 + \gamma_1)\psi_1 - (2\beta_4 + \gamma_4)\psi_4, \tag{2.15}$$

$$V_{11} - V_{44} + \gamma_1 V_1 - \gamma_4 V_4 + \frac{V_1}{\varrho} = 0. \tag{2.16}$$

3. Solutions of the field equations

Subtracting (2.9) from (2.13) we obtain

$$\gamma_{11} - \gamma_{44} + \gamma_1^2 - \gamma_4^2 + \frac{2\gamma_1}{\varrho} = 0. \tag{3.1}$$

Also, subtracting (2.11) from (2.12) and making use of (3.1) we have

$$\beta_{11} - \beta_{44} + \beta_1\gamma_1 - \beta_4\gamma_4 + \frac{\beta_1 - \gamma_1}{\varrho} = 4\pi\left[\frac{\varphi_1^2 - \varphi_4^2}{\varrho^2 e^{-2\beta}} - \frac{\psi_1^2 - \psi_4^2}{e^{2(\beta+\gamma)}}\right]. \tag{3.2}$$

Therefore, the problem of solving the Eqs. (2.9)—(2.16) reduces to the problem of solving the Eqs. (2.9), (2.10), (2.11), (2.14), (2.15), (2.16), (3.1) and (3.2). The Eq. (3.1) corresponds to the wave equation in cylindrical coordinates for the function e^{γ} and has a solution

$$e^{\gamma} = \frac{A}{\varrho} \sin P \cos Q, \tag{3.3}$$

where $P = w\varrho + p$, $Q = wt + q$ and A, w, p, q are arbitrary constants. The solution (3.3) avoids the occurrence of singularity at $\varrho = t = 0$. For this solution of γ the Eq. (2.16) provides a solution for scalar field as follows:

$$e^{V} = B \operatorname{cosec} P \sec Q, \tag{3.4}$$

where B is also an arbitrary constant. Further, it is difficult to solve in general the remaining equations taken into consideration due to their non-linearity. In the present paper we, therefore, solve them in particular cases.

From (1.2) and (2.8) we obtain

$$\varphi_1\psi_1 = \varphi_4\psi_4, \tag{3.5}$$

which is identically satisfied in the following cases:

(i) $\psi_1 = \varphi_4 = 0,$

(ii) $\psi_4 = \varphi_1 = 0,$

(iii) $\psi_1 = \psi_4 = \varphi_4 = 0,$

(iv) $\psi_1 = \psi_4 = \varphi_1 = 0,$

(v) $\varphi_1 = \varphi_4 = \psi_4 = 0,$

(vi) $\varphi_1 = \varphi_4 = \psi_1 = 0.$

In these particular cases we now solve the remaining equations to determine α, β, φ and ψ.

Case (i)

In this case φ is a function of ϱ and ψ a function of t. It we take

$$\varphi = \frac{1}{2\sqrt{2\pi a}} \cos P, \tag{3.6}$$

$$\psi = \frac{aA}{2\sqrt{2\pi}} \sin Q, \tag{3.7}$$

then from (2.14), (2.15) and (3.2) we get

$$e^{\beta} = a\varrho \operatorname{cosec} P, \tag{3.8}$$

where a is another arbitrary constant. For the known values of $V, \beta, \gamma, \varphi$ and ψ as above, the Eqs. (2.9) and (2.10) take the form

$$\alpha_1 = (4\pi - 1)\,\omega \cot P + \frac{1}{\varrho},$$

$$\alpha_4 = -4\pi\omega \tan Q,$$

from which we have the solution

$$e^{\alpha} = b\varrho \operatorname{cosec} P\,(\sin P \cos Q)^{4\pi}, \tag{3.9}$$

where b is also an arbitrary constant. For α given by (3.9) the Eq. (2.11) is identically satisfied.

Case (ii)

In this case φ is a function of t and ψ a function of ϱ. If we take

$$\varphi = \frac{1}{2\sqrt{2\pi a}} \sin Q, \tag{3.10}$$

$$\psi = \frac{aA}{2\sqrt{2\pi}} \cos P, \tag{3.11}$$

then from the given equations we have

$$e^{\beta} = a\varrho \sec Q, \tag{3.12}$$

$$e^{\alpha} = b\varrho \sec Q(\sin P \cos Q)^{4\pi}. \tag{3.13}$$

Case (iii)

In this case φ is a function of ϱ. It we take

$$\varphi = \frac{1}{2\sqrt{\pi a}} \cos P, \tag{3.14}$$

then β and α are given by (3.8) and (3.9), respectively.

Case (iv)

In this case φ is a function of t. If we take

$$\varphi = \frac{1}{2\sqrt{\pi a}} \sin Q, \tag{3.15}$$

then β and α are given by (3.12) and (3.13), respectively.

Case (v)

In this case ψ is a function of ϱ. If we take

$$\psi = \frac{aA}{2\sqrt{\pi}} \cos P, \tag{3.16}$$

then β and α are given by (3.12) and (3.13), respectively.

Case (vi)

In this case ψ is a function of t. If we take

$$\psi = \frac{aA}{2\sqrt{\pi}} \sin Q, \tag{3.17}$$

then β and α are given by (3.8) and (3.9), respectively.

In the absence of the electromagnetic fields we take

$$\varphi = \psi = 0, \tag{3.18}$$

and Eq. (3.2) reduces to

$$\beta_{11} - \beta_{44} + \beta_1\gamma_1 - \beta_4\gamma_4 + \frac{\beta_1 - \gamma_1}{\varrho} = 0. \tag{3.19}$$

After making use of (3.3), it can be recast in the form

$$\beta_{11} - \beta_{44} + \beta_1\omega \cot P + \beta_4\omega \tan Q = \frac{\omega}{\varrho} \cot P - \frac{1}{\varrho^2}, \tag{3.20}$$

which provides the solution

$$e^{\beta} = c\varrho \operatorname{cosec} P \sec Q. \tag{3.21}$$

For the known values of γ, V and β given by (3.3), (3.4) and (3.21), respectively, the field equations (2.9), (2.10) and (2.11) under the condition (3.18) reduce to

$$\alpha_1 = 4\pi\omega \cot P - \frac{\omega \cot P \operatorname{cosec}^2 P}{\cot^2 P - \tan^2 Q} + \frac{1}{\varrho}, \tag{3.22}$$

$$\alpha_4 = -4\pi\omega \tan Q - \frac{\omega \tan Q \sec^2 Q}{\cot^2 P - \tan^2 Q}, \tag{3.23}$$

$$\alpha_{11} - \alpha_{44} = (1 - 4\pi)\,\omega^2(\cot^2 P - \tan^2 Q) - \frac{1}{\varrho^2}. \tag{3.24}$$

From (3.22) and (3.23) we have the solution

$$e^{\alpha} = E\varrho(\cot^2 P - \tan^2 Q)\,(\sin P \cos Q)^{4\pi}, \tag{3.25}$$

where E is an arbitrary constant. For α given by (3.25) the Eq. (3.24) is identically satisfied.

In the absence of the zero rest mass scalar field the non-static solutions [1] of the field equations represent uniform electromagnetic fields which are the transforms of the "homogeneous" electric or magnetic field of LEVI-CIVITA [3]. As the solutions of γ and β in (3.3), (3.8) and (3.12) are the same as given in [1], the only solutions (3.9) and (3.13) for α give a picture of the interaction between electromagnetic and zero rest mass scalar fields.

Acknowledgement

The author wishes to express his gratitude to Dr. R. TIWARI for his encouragement and interest in this work. His thanks are also due to the referee for his useful suggestions.

REFERENCES

1. L. RADHAKRISHNA, Proc. Nat. Inst. Sci. India, **29A**(5), 588, 1963.
2. L. MARDER, Proc. Roy. Soc., **244**, 524, 1958.
3. T. LEVI-CIVITA, R. C. Accad. Lincei. (5), **26**, 519, 1917.

Acta Physica Academiae Scientiarum Hungaricae, Tomus 45 (4), pp. 317—326 (1978)

THERMODYNAMIC CONCEPTS FOR A CLASS OF ONE-PORTS

By

H. FARKAS

INSTITUTE OF PHYSICS, TECHNICAL UNIVERSITY, BUDAPEST

(Received in revised form 21. XI. 1978)

The paper deals with one-ports represented by an equation involving two conjugated variables and their derivatives. The consideration does not require the a priori knowledge of thermodynamical concepts; energy, dissipation and reversibility are treated in terms of directly measurable input-output variables. A passivity concept is established on cyclic processes. A generalized energy function using a theorem on boundedness of the work in constructed. The work is partitioned into two terms: a reversible and an irreversible one. The laws of thermodynamics are reformulated for these systems. The results are applied to special cases.

1. Preliminaries

Rational thermodynamics

Criticizing the conventional thermodynamical treatments, TRUESDELL [1] developed another treatment which was intended to give "exact meaning" to the laws of thermodynamics by using the formalism of modern continuum mechanics. In that treatment the constitutive axioms play the role of the material equations of thermodynamics: they determine the dependence of the momentaneous values of dependent variables in the history of independent variables. The relations are given in functional form.

TRUESDELL's treatment induces some remarks. Obviously, the laws of thermodynamics are universally valid in every case, even though their mathematical formulation may depend on the constitutive equations of the model considered. Below we demonstrate the applicability of the laws of thermodynamics to rather general, nonlinear, nonideal systems.

Practical drawbacks of the rational thermodynamics arise from the difficulties accompanying the use of functionals. In special cases one must restrict oneself to constitutive relations involving functions alone.

To describe irreversibility, TRUESDELL introduces the "heating bound" as a primitive concept: "The irreversibility of natural processes is represented by the existence of an a priori least upper bound B for the heating Q". ([1], page 9). Using these concepts the second law is written in the form

$$Q \leq B. \tag{1}$$

The notion "heating" is used here in the meaning of heat current (heating power).

Finally, note that the role of independent variables and that of dependent variables are not equivalent: the history of the former determines the value of the latter at a moment. This asymmetry is rather unjustified. For example, in electrotechnics one deals not only with capacities but also with inductivities.

Network thermodynamics

The theory developed in recent years adapts the language and formalism of electrical network to general physical systems. Concepts originating from thermodynamics as well as from control theory are also introduced [2, 3]. In the literature of network thermodynamics local formulation is preferred (with respect to time).

In this paper some ideas from both of these theories will be used. Consideration will be focussed on the behaviour of the system as a whole: composition will not be taken into acount. The treatment is based on global formulation (in time).

2. A general model of one-port

The investigated system is represented by a one-port that is a black box with two simultaneously measurable quantities: e and U. These quantities may depend upon time: $e(t)$, $U(t)$, and they are conjugated to each other. That means that the elementary work done on the system is: $U\,\mathrm{d}e$, while the work from time t_0 to time t_1:

$$W = \int_{t_0}^{t_1} U(t)\,\frac{\mathrm{d}e}{\mathrm{d}t}\,\mathrm{d}t. \tag{2}$$

This relation is assumed to be valied for arbitrary processes and not only for "quasistatic" ones. The quasistatic or nonstatic character of processes will be mentioned later.

An equation of the type

$$U^{(m)} = f(U, \dot{U}, \ldots, U^{(m-1)};\ e, \dot{e}, \ldots, e^{(n)}) \tag{3}$$

is assumed to be valid for the system. This equation will be referred to as *the equation of motion of the system*. In addition, assume that:

i) it thoroughly characterizes the system;
ii) it has the simplest possible form;
iii) the function f is continuous.

iv) $$\frac{\partial f}{\partial e^{(n)}} = 0.$$

Examples

A) Let the system be an electrical one-port with two poles. Then U is the voltage between the two poles, whle e is the charge carried to the positive pole.

B) Let the system be a rod along the x axis and be fixed at one of its terminals. Then U is the force exerted on the free terminal, while e is the coordinate of the free terminal, provided that both the force and the displacement are in the direction x.

Note that any electric one-port consisting of arbitrarily connected simple two-poles (capacities, inductivities, resistances) of finite number leads to an equation of the type (3.). A similar statement is true for mechanical one-ports consisting of usual simple viscoelastic models.

Now thermodynamic ideas will be applied to our system. Particular account will be paid to the problem of reversibility — irreversibility.

Due to the equation of motion (3), it is reasonable to define the *state* of the system as a vector $\mathbf{r}$ with the coordinates

$$r_i = \begin{cases} U^{(i)} & \text{for} \quad i = 0, 1, \ldots, m-1, \\ e^{(i-m)} & \text{for} \quad i = m, m+1, \ldots, m+n \end{cases} \tag{4}$$

($e^{(i)}$, $U^{(i)}$ denote time derivatives of i-th order.) The *state space* R^{m+n+1} has $m + n + 1$ dimensions.

A *process* taking place from time t_1 to time t_2 is an ordered pair of functions $\{U(t), e(t)\}$ continuously differentiable up to m-th and n-th order, respectively, such that the equation of motion is satisfied. A continuous curve $\mathbf{r} = \mathbf{r}(t)$ in the state space is associated to any process with the *initial state* $\mathbf{r}_1 = \mathbf{r}(t_1)$ and the *end state* $\mathbf{r}_2 = \mathbf{r}(t_2)$. Let $g = \{U(t), e(t)\}$ be a process during the time interval $[t_1, t_2]$. For this process we will use the following short notations:

$$U_g = U(t); \quad e_g = e(t); \tag{5}$$

$$(\mathbf{r}_1, t_1) \xrightarrow{g} (\mathbf{r}_2, t_2). \tag{6}$$

A *cycle* is a process for which the end state is identical to the initial state: $(\mathbf{r}_0, t_1) \xrightarrow{g} (\mathbf{r}_0, t_2)$. A nullprocess is a process during which the state remains constant: $\mathbf{r}(t) =$ constant. Obviously such a state r must be an *equilibrium state* that is $U =$ constant, $e =$ constant.

If $(\mathbf{r}_1, t_1) \xrightarrow{g} (\mathbf{r}_2, t_2)$ and $(\mathbf{r}_2, t_2) \xrightarrow{h} (\mathbf{r}_3, t_3)$ are two processes, then their *union* $l = g \cup h$ is also a process: $(\mathbf{r}_1, t_1) \xrightarrow{l} (\mathbf{r}_3, t_3)$, where

$$U_l = \begin{cases} U_g & \text{for} \quad t_1 \leq t \leq t_2, \\ U_h & \text{for} \quad t_2 \leq t \leq t_3, \end{cases}$$

$$e_l = \begin{cases} e_g & \text{for} \quad t_1 \leq t \leq t_2, \\ e_h & \text{for} \quad t_2 \leq t \leq t_3. \end{cases} \tag{7}$$

This statement can easily be proved using the continuity conditions.

There are continuous curves in the state space to which no process belongs. For example, any coordinate axis is such a line in case of $n > 0$ and $m > 1$.

Processes induce a classification of the states; putting two states **r** and **s** into the same class if there exists a process with initial state **r** and end state **s** as well as another process with initial state **s** and end state **r**. In this case we say that the two states are *accessible from each other*. A subset B of the state space will be called *connected set with respect to processes* if for any two points **r**, **s** in B there exists a process g with initial state **r** and end state **s** as well as another process g^* with initial state **r** and end state **s** so that all the states involved by g or g^* are in B. Obviously, if B is connected, then any two points in it are accessible from each other. The whole state space is not necessarily connected as it is easily seen from the famous example of MEIXNER [4]; in this case there is a damping, not reexcitable internal degree of freedom.

On physical backgrounds it is plausible to postulate that

A) Given a function $U(t)$ continuously differentiable m times, there exists a process g so that

$$U_g = U(t).$$

B) Given a function $e(t)$ continuously differentiable n times, there exists a process g^* so that

$$e_{g^*} = e(t).$$

These postulates represent a symmetry of certain kind between the variables e and U: anyone of them can be regarded as *input* and the other as *output*.

Our system will be called *passive* if the inequality

$$W_g \geq 0 \tag{8}$$

is valid for any cycle g. If the inequality

$$W_g > 0 \tag{9}$$

is valid for all the cycles but nullprocesses, we shall say that our system is *dissipative*.

This definition of passivity has a global character with respect to time: it refers to processes, while there is a definition of passivity in network thermodynamics having local meaning referred to a point of time [2]. The consideration below will elucidate the relationship between the two definitions of passivity.

Theorem 1. The system is passive if and only if for any fixed states **r**, **s** accessible from each other the work has a lower bound over all the processes starting from **r** and ending at **s**, that is to $\{\mathbf{r}, \mathbf{s}\}$ there exists a constant K so that

$K < W_g$ for all processes of the type

$$(\mathbf{r}, t_1) \xrightarrow{g} (\mathbf{s}, t_2) \tag{10}$$

(t_1, t_2 are arbitrary, not fixed).

Proof I. If the system is not passive, then

$$W_g < 0$$

holds for a cycle g. Let $\mathbf{r}$ and $\mathbf{s}$ be states contained in g. Let h be the process consisting of a process of the type $(\mathbf{r}, t_0) \xrightarrow{g_0} (\mathbf{s}, t_1)$ and N cycles arising from g by a proper translation of time so that

$$(\mathbf{s}, t_i) \xrightarrow{g_i} (\mathbf{s}, t_{i+1}) \qquad i = 1, 2, \ldots, N.$$

$t_{i+1} - t_i = T$: duration belonging to the cycle g. Such a process g_0 exists because $\mathbf{r}$ and $\mathbf{s}$ are states accessible from each other, while the existence of $g_i (i = 1, 2, \ldots, N)$ follows from the fact that our system is an *autonomous* one that is the equation of motion (3) does not involve time t explicitly. The work during the process $(\mathbf{r}, t_0) \xrightarrow{h} (\mathbf{s}, t_{N+1})$ constructed in such a manner is:

$$W_h = W_{g_0} + N \cdot W_g$$

because the work is invariant under translation of time. Since N may be an arbitrarily large integer, the work W_h cannot have a lower bound.

Proof II. Let $\mathbf{r}$, $\mathbf{s}$ be states accessible from each other such that the work W_h during the processes of the type $(\mathbf{r}, t_1) \xrightarrow{h} (\mathbf{s}, t_2)$ does not have a lower bound. Then there is a process $(\mathbf{r}, t_0) \xrightarrow{g} (\mathbf{r}, t_1)$ and a process $(\mathbf{r}, t_1) \xrightarrow{h} (\mathbf{s}, t_2)$ so that

$$W_h < -2\,|W_g|$$

holds. The union of these two processes $(\mathbf{s}, t_0) \xrightarrow{l} (\mathbf{s}, t_2)$ is a cycle, and the work associated with it is negative:

$$W_l = W_g + W_h < 0,$$

therefore the system cannot be passive.

Theorem 1 permits us to introduce the *potential function* ("energy") by the following definition. Let $\mathbf{s}$ be a fixed state of a passive system. Let us define the potential function $E_s(\mathbf{r})$ referring to the state $\mathbf{s}$ as follows:

$$E_s(\mathbf{r}) = \inf_g W_g, \tag{11}$$

where g is any process of the type $(\mathbf{s}, t_1) \xrightarrow{g} (\mathbf{r}, t_2)$ ($t_1 < t_2$ but otherwise arbitrary quantities). By Theorem 1, $E_s(\mathbf{r})$ exists in case if $\mathbf{r}$ and $\mathbf{s}$ are accessible from each other.

It follows immediately from the definition (11) that if g is a process with initial point $\mathbf{s}$ and end point $\mathbf{u}$, then the inequalities

$$E_s(\mathbf{r}) \leq E_u(\mathbf{r}) + W_g, \tag{12}$$

$$E_r(\mathbf{u}) \leq E_r(\mathbf{s}) + W_g \tag{13}$$

are valid provided all the quantities exist.

The potential function $E_s(\mathbf{r})$ is defined over H_s, where H_s is a set connected with respect to processes and $\mathbf{s} \in H_s$. From the physical point of view the most important case is when $\mathbf{s}$ is a state reached by the system after very long time (aged system). In this case H_s consists of states reproducibly realizable starting from that reference state $\mathbf{s}$. Restricting ourselves to that case, we will say that our system is *regular* if $E_s(\mathbf{r})$ does not depend on the coordinate r_{m+n+1} that is on $e^{(n)}$ provided that $n > 0$. Regularity is not a strict requirement: it follows, for example, from the continuity of $E_s(\mathbf{r})$ and the assumption that the value of $e^{(n)}$ can be changed by a finite amount during an arbitrary small time interval. Simple special systems turn out to be regular in this sense.

For a regular system we defined the function D_s called *dissipation* as

$$D_s(\mathbf{r}) = U\dot{e} + \frac{\mathrm{d}E}{\mathrm{d}\mathbf{r}} \cdot \frac{\mathrm{d}\mathbf{r}}{\mathrm{d}t}, \tag{14}$$

where in the right-hand side the term $U^{(m)}$ must be eliminated by the equation of motion (3). If D_s is continuous at a point $\mathbf{r} \in H_s$, then the inequality

$$D_s \geq 0 \tag{15}$$

holds at that point. To see this let us suppose for a moment that $D_s < 0$. From this hypothesis we conclude the existence of a neighbourhood H of $\mathbf{r}$ in which $D_s < 0$, and taking a process through $\mathbf{r}$ within this neighbourhood H, the desired contradiction yields after integrating D_s with respect to time for this process.

Theorem 2. If a state function $E(\mathbf{r})$ as well as the quantity

$$\begin{aligned} D = U\dot{e} + \frac{\mathrm{d}E}{\mathrm{d}\mathbf{r}} \cdot \frac{\mathrm{d}\mathbf{r}}{\mathrm{d}t} = U\dot{e} + \sum_{i=0}^{m-2} \frac{\partial E}{\partial U^{(i)}} U^{(i+1)} + \\ + \frac{\partial E}{\partial U^{(m-1)}} \cdot f(U, \ldots, U^{(m-1)}; e, \ldots, e^{(n)}) + \sum_{i=0}^{n} \frac{\partial E}{\partial e^{(i)}} e^{(i+1)} \end{aligned} \tag{16}$$

exists for all $U^{(i)}$, $e^{(j)}$, and furthermore, if the quantity D is nonnegative definite, then the system is passive.

Proof. It immediately follows from the conditions that D is integrable with respect to time for every cycle g, and

$$\int_g D \, \mathrm{d}t \geq 0, \qquad \text{for every cycle } g.$$

Since

$$\int_g \frac{\mathrm{d}E}{\mathrm{d}\mathbf{r}} \cdot \frac{\mathrm{d}\mathbf{r}}{\mathrm{d}t}\,\mathrm{d}t = 0 \quad \text{for every cycle } g,$$

it follows that the work during any cycle cannot be negative, that is the system is passive.

Local definition of passivity is based on the requirement that the quantity D is nonnegative definite [2]. From the above statements it follows that that passivity in the global sense is not so strict a requirement as passivity in the local sense, nevertheless for systems of physically simple behaviour (e.g. regular systems) the two definitions are essentially equivalent to each other.

A process $(\mathbf{r}, t_1) \xrightarrow{g} (\mathbf{s}, t_2)$ is called *reversible* if another process $(\mathbf{s}, t_2) \xrightarrow{g^*} (\mathbf{r}, t_3)$ so that

$$W_g + W_{g^*} = 0.$$

Obviously, g is also reversible, and

$$E_s(\mathbf{r}) = W_{g^*} = -W_g$$

holds for any passive system.

3. Remarks and problems

1. The systems investigated above are "mechanical", that is not thermodynamical. Thermal variables were abandoned. This is justified for example in the case of the electrical network whose parameters do not depend on temperature. To introduce thermal variables, it is necessary to deal with models of multi-ports.

2. The potential function defined above can be regarded as a generalization of mechanical energy for nonconservative passive systems.

3. With the aid of the above notions thermodynamical laws can easily be formulated for the considered systems. For instance, the statement: "Every adiabatically isolated one-port is passive." is equivalent to the statement about the nonexistence of a perpetuum mobile of first kind. Similarly, the second law (the statement about the nonexistence of a perpetuum mobile of second kind) is formulated as follows: "Every one-port placed under isotherm conditions is passive." In that case the potential function can be regarded as free energy.

4. Using the stricter condition of dissipativity, the results remain valid with some modifications. For example, the inequality (15) reduces to equality only in the trivial case $\frac{\mathrm{d}\mathbf{r}}{\mathrm{d}t} = 0$ for dissipative systems. It would be reasonable to formulate the statements about the nonexistence of perpetuum

mobiles in their stricter form; allowing the case $W = 0$ for nullprocesses alone.

5. By the relation (14) the power ($P = U\dot{e}$) is written as a sum of a "reversible" term ($-\dot{E}$, total time derivative) and an "irreversible" term (D, dissipation, nonnegative definite):

$$P = -\dot{E} + D. \tag{17}$$

Partition of the same type occurs in a construction of sufficient conditions for the minimum of the functional

$$I[y] = \int_{x_1}^{x_2} F(x, y, y')\, dx. \tag{18}$$

It is proved [5] — under some conditions — $F(x, y, y')$ can be given as a sum:

$$F(x, y, y') = -F^*(x, y, y') + E(x, y, y'), \tag{19}$$

where F is an "invariant basic function" (that is total derivative):

$$F^*(y, x, y') = -F\big(x, y, p(x, y)\big) - \big(y' - p(x, y)\big) F\big(x, y, p(x, y)\big) \tag{20}$$

and E is the Weierstrass function; it is nonnegative definite:

$$E(x, y, y') \geq 0. \tag{21}$$

For the function $p(x, y)$ a partial differential equation is given (Eq. 10.35 in [5]):

$$F_{y'y'}(x, y, p)\,(p_x + pp_y) + F_{yy'}(x, y, p)\, p - F_{xy'}(x, y, p) - F_y(x, y, p). \tag{22}$$

These formulas can be applied to our system in case of the equation of motion

$$U = f(e, \dot{e}). \tag{23}$$

In this case

$$p(x, y) = 0$$

is a solution of Eq. (22). Substituting this solution into (20) we get

$$F^* = -\dot{e} f(e, 0) \tag{24}$$

and hence

$$E = \big(f(e, \dot{e}) - f(e, 0)\big)\dot{e}. \tag{25}$$

6. Some further problems are suggested as follows.

Is it possible to deduce conditions of simple form for the existence and unicity of the potential function?

How can we find the potential function by systematic mathematical method for cases more general than (23)?

When is the partition (17) unique)?

4. Special cases

In the following simple special cases the potential function can be determined easily.

A) "Capacitive" system. The equation of motion:

$$U = f(e).$$

Systems of that type are passive. The potential function is:

$$E(e) = \int f(e)\, de.$$

Hence the dissipation equals zero. Since

$$W_g = \Delta E$$

for every process g, all the processes are reversible.

B) "Resistive" system:

$$U = f(\dot{e}).$$

It is passive if the inequality

$$f(x)\, x \geq 0$$

is valid for every real x. In this case $E = 0$, and

$$D = f(\dot{e})\, \dot{e}.$$

C) Systems with equation of motion of the type

$$U = f(e, \dot{e}).$$

In this case the state variables are: e, $\dot{e}$. The system is passive if

$$\big(f(x, y) - f(x, 0)\big) y \geq 0$$

holds for every real x, y. Then the potential function

$$E = \int f(e, 0)\, de$$

and the dissipation:

$$D = \big(f(e, \dot{e}) - f(e, 0)\big)\, \dot{e}.$$

It is seen that all the state space is connected with respect to processes, and the system is regular. Work minimum is reached in the limit case $e = 0$ (infinitely slow process, quasistatic process).

D) Let us consider, finally, the systems with equation of motion

$$\dot{U} = f(e).$$

The work during the process $(e_1, U_1; t_1) \xrightarrow{g} (e_2, U_2; t_2)$ is:

$$W_g = \int_1^2 Ue\, \mathrm{d}t = [Ue]_1^2 - \int_1^2 ef(e)\, \mathrm{d}t.$$

Using Theorem 1, we can see that this system is passive if

$$ef(e) \leq 0.$$

Then the potential function is

$$E = Ue,$$

while the dissipation

$$D = -\dot{U}e = -f(e)\, e.$$

Notice that work minimum is reached in the limit case of infinitely quick processes: such processes are reversible in this case.

Acknowledgement

The author wishes to thank Prof. I. GYARMATI and Dr. F. SZIGETI for their valuable remarks and criticism.

REFERENCES

1. C. TRUESDELL, Rational Thermodynamics, McGraw-Hill, 1969.
2. G. F. OSTER and A. S. PERELSON, Israel J. Chem., **11**, 445, 1973.
3. G. F. OSTER and A. S. PERELSON, Arch. Rat. Mech. Anal., **55**, 230, 1975.
4. J. MEIXNER, Rheol. Acta, **12**, 465, 1973.
5. A. KÓSA, Calculus of Variations, Tankönyvkiadó, Budapest, 1973 (in Hungarian).
6. E. B. LEE and L. MARCUS, Foundations of Optimal Control Theory, John Wiley New York, 1968.

Acta Physica Academiae Scientiarum Hungaricae, Tomus 45 (4), pp. 327—362 (1978)

CONTRIBUTION TO THE INTENSITY DISTRIBUTIONS OF THE MULTIPLET BANDS IN DIATOMIC MOLECULES III

By

I. KOVÁCS, I. PÉCZELI and A. GRANDPIERRE

DEPARTMENT OF ATOMIC PHYSICS, TECHNICAL UNIVERSITY, BUDAPEST

(Received 23. XI. 1978)

Explicit expressions are obtained for the intensity distributions in the branches of septet transitions of any type with $\Delta\Lambda = 0$ and $\Delta\Lambda = \pm 1$ where the upper and lower electronic states may belong to one of the limiting Hund's cases a) or b). Moreover the intensity scattering of the main branches of the (a)–(a) transitions over the main and satellite branches of the (a)–(b) transitions from quartet to septet cases are given.

In the first [1] and second [2] part of this paper the formulae of the intensity distribution of the quartet, quintet, sextet transitions and of the transitions of any type and any multiplicity in the limiting Hund's cases have been treated. In the third part general formulae of the line strengths are given for all branches of the septet transitions of any type with $\Delta\Lambda = 0$ and $\Delta\Lambda = \pm 1$ where the upper and lower terms may belong to one of the limiting Hund's cases a) or b). These formulae give after substitution of the proper Λ values (0, 1, 2, . . .) the line strengths of all branches for $\Sigma - \Sigma$, $\Pi - \Pi$, $\Delta - \Delta$ . . . and $\Pi - \Sigma$, $\Delta - \Pi$, $\Phi - \Delta$, . . . transitions completed with the line strengths of the lacking branches of the $\Pi - \Sigma$ transitions already published [3]. Algebraic expressions where both states may belong to a coupling case intermediate between Hund's cases a) and b) in general form would be very complicated but for a given transition with the known value of the coupling constant Y numerical values of the line strengths for each value of the rotational quantum number can be calculated by the numerical diagonalization of the Hamiltonian with the aid of an electronic computer.

The procedure applied for the production of the line strengths in the limiting Hund's cases has been described in the first part of this paper [1]. The elements of the transformation matrix of septet terms of any type for case b) required for the application are the following:

$^7X(b)$ *transformation matrix*

$$S_{\Lambda-3,\,J-3}=\sqrt{\frac{v_2^- v_3^- v_4^- v_5^- v_6^- v_7^-}{C_{J-3}(J)}}\,,\qquad S_{\Lambda-2,\,J-3}=-\sqrt{\frac{6v_2^- v_3^- v_4^- v_5^- v_6^- v_2^+}{C_{J-3}(J)}}\,,$$

$$S_{\Lambda-1,\,J-3}=\sqrt{\frac{15v_2^- v_3^- v_4^- v_5^- v_2^+ v_3^+}{C_{J-3}(J)}}\,,\qquad S_{\Lambda,\,J-3}=-\sqrt{\frac{20v_2^- v_3^- v_4^- v_2^+ v_3^+ v_4^+}{C_{J-3}(J)}}\,,$$

$$S_{\Lambda+1,\,J-3}=\sqrt{\frac{15v_2^- v_3^- v_2^+ v_3^+ v_4^+ v_5^+}{C_{J-3}(J)}}\,,\qquad S_{\Lambda+2,\,J-3}=-\sqrt{\frac{6v_2^- v_2^+ v_3^+ v_4^+ v_5^+ v_6^+}{C_{J-3}(J)}}\,,$$

$$S_{\Lambda+3,\,J-3}=\sqrt{\frac{v_2^+ v_3^+ v_4^+ v_5^+ v_6^+ v_7^+}{C_{J-3}(J)}}\,;$$

$$S_{\Lambda-3,\,J-2}=\sqrt{\frac{3v_3^- v_4^- v_5^- v_6^- v_7^- v_2^+}{C_{J-2}(J)}}\,,\qquad S_{\Lambda-2,\,J-2}=-\sqrt{\frac{2v_3^- v_4^- v_5^- v_6^- [2v_2^+ +\Lambda]^2}{C_{J-2}(J)}}\,,$$

$$S_{\Lambda-1,\,J-2}=\sqrt{\frac{5v_3^- v_4^- v_5^- v_3^+ [v_2^+ +2\Lambda]^2}{C_{J-2}(J)}}\,,\quad S_{\Lambda,\,J-2}=-\Lambda\sqrt{\frac{60v_3^- v_4^- v_3^+ v_4^+}{C_{J-2}(J)}}\,,$$

$$S_{\Lambda+1,\,J-2}=-\sqrt{\frac{5v_3^- v_3^+ v_4^+ v_5^+ [v_2^- -2\Lambda]^2}{C_{J-2}(J)}}\,,\quad S_{\Lambda+2,\,J-2}=\sqrt{\frac{2v_3^+ v_4^+ v_5^+ v_6^+ [2v_2^+ -\Lambda]^2}{C_{J-2}(J)}}\,,$$

$$S_{\Lambda+3,\,J-2}=-\sqrt{\frac{3v_2^- v_3^+ v_4^+ v_5^+ v_6^+ v_7^+}{C_{J-2}(J)}}\,;$$

$$S_{\Lambda-3,\,J-1}=\sqrt{\frac{15v_4^- v_5^- v_6^- v_7^- v_2^+ v_3^+}{C_{J-1}(J)}}\,,\qquad S_{\Lambda-2,\,J-1}=-\sqrt{\frac{10v_4^- v_5^- v_6^- v_3^+ (v_1^+ +2\Lambda)^2}{C_{J-1}(J)}}\,,$$

$$S_{\Lambda-1,\,J-1}=-\sqrt{\frac{v_4^- v_5^- [v_3^- v_6^- -4(v_3^+ +\Lambda)(2\Lambda-1)]^2}{C_{J-1}(J)}}\,,$$

$$S_{\Lambda,\,J-1}=\sqrt{\frac{12v_4^- v_4^+ [v_3^- v_5^+ -2\Lambda(2\Lambda-1)]^2}{C_{J-1}(J)}}\,,$$

$$S_{\Lambda+1,\,J-1}=-\sqrt{\frac{v_4^+ v_5^+ [v_3^+ v_6^+ +4(v_3^- -\Lambda)(2\Lambda+1)]^2}{C_{J-1}(J)}}\,,$$

$$S_{\Lambda+2,\,J-1}=-\sqrt{\frac{10v_3^- v_4^+ v_5^+ v_6^+ (v_1^- -2\Lambda)^2}{C_{J-1}(J)}}\,,\qquad S_{\Lambda+3,\,J-1}=\sqrt{\frac{15v_2^- v_3^- v_4^+ v_5^+ v_6^+ v_7^+}{C_{J-1}(J)}}\,;$$

$$S_{\Lambda-3,J}=\sqrt{\frac{5v_5^-v_6^-v_7^-v_2^+v_3^+v_4^+}{C_J(J)}},\qquad S_{\Lambda-2,J}=-(\Lambda-1)\sqrt{\frac{30v_5^-v_6^-v_3^+v_4^+}{C_J(J)}},$$

$$S_{\Lambda-1,J}=-\sqrt{\frac{3v_5^-v_4^+[v_6^-v_3^+-2\Lambda(2\Lambda-1)]^2}{C_J(J)}},$$

$$S_{\Lambda,J}=\Lambda\sqrt{\frac{4[3v_3^-v_6^+-(\Lambda-5)(2\Lambda+1)]^2}{C_J(J)}},$$

$$S_{\Lambda+1,J}=\sqrt{\frac{3v_4^-v_5^+[v_3^-v_6^+-2\Lambda(2\Lambda+1)]^2}{C_J(J)}},\quad S_{\Lambda+2,J}=-(\Lambda+1)\sqrt{\frac{30v_3^-v_4^-v_5^+v_6^+}{C_J(J)}},$$

$$S_{\Lambda+3,J}=-\sqrt{\frac{5v_2^-v_3^-v_4^-v_5^+v_6^+v_7^+}{C_J(J)}};$$

$$S_{\Lambda-3,J+1}=\sqrt{\frac{15v_6^-v_7^-v_2^+v_3^+v_4^+v_5^+}{C_{J+1}(J)}},\qquad S_{\Lambda-2,J+1}=\sqrt{\frac{10v_6^-v_3^+v_4^+v_5^+[v_8^--2\Lambda)^2}{C_{J+1}(J)}},$$

$$S_{\Lambda-1,J+1}=-\sqrt{\frac{v_4^+v_5^+[v_3^+v_6^++4(v_6^--\Lambda)(2\Lambda-1)]^2}{C_{J+1}(J)}},$$

$$S_{\Lambda,J+1}=-\sqrt{\frac{12v_5^-v_5^+[v_4^-v_6^+-2\Lambda(2\Lambda-1)]^2}{C_{J+1}(J)}},$$

$$S_{\Lambda+1,J+1}=-\sqrt{\frac{v_4^-v_5^-[v_3^-v_6^--4(v_6^++\Lambda)(2\Lambda+1)]^2}{C_{J+1}(J)}},$$

$$S_{\Lambda+2,J+1}=\sqrt{\frac{10v_3^-v_4^-v_5^-v_6^+[v_8^++2\Lambda]^2}{C_{J+1}(J)}},\qquad S_{\Lambda+3,J+1}=\sqrt{\frac{15v_2^-v_3^-v_4^-v_5^-v_6^+v_7^+}{C_{J+1}(J)}};$$

$$S_{\Lambda-3,J+2}=\sqrt{\frac{3v_7^-v_2^+v_3^+v_4^+v_5^+v_6^+}{C_{J+2}(J)}},\qquad S_{\Lambda-2,J+2}=\sqrt{\frac{2v_3^+v_4^+v_5^+v_6^+[2v_7^--\Lambda])^2}{C_{J+2}(J)}},$$

$$S_{\Lambda-1,J+2}=\sqrt{\frac{5v_6^-v_4^+v_5^+v_6^+[v_7^--2\Lambda]^2}{C_{J+2}(J)}},\quad S_{\Lambda,J+2}=-\Lambda\sqrt{\frac{60v_5^-v_6^-v_5^+v_6^+}{C_{J+2}(J)}},$$

$$S_{\Lambda+1,J+2}=-\sqrt{\frac{5v_4^-v_5^-v_6^-v_6^+[v_7^++2\Lambda]^2}{C_{J+2}(J)}},\quad S_{\Lambda+2,J+2}=-\sqrt{\frac{2v_3^-v_4^-v_5^-v_6^-[2v_7^++\Lambda]^2}{C_{J+2}(J)}},$$

$$S_{\Lambda+3,J+2}=\sqrt{\frac{3v_2^-v_3^-v_4^-v_5^-v_6^-v_7^+}{C_{J+2}(J)}};$$

$$S_{\Lambda-3,J+3}=\sqrt{\frac{v_2^+v_3^+v_4^+v_5^+v_6^+v_7^+}{C_{J+3}(J)}},\qquad S_{\Lambda-2,J+3}=\sqrt{\frac{6v_7^-v_3^+v_4^+v_5^+v_6^+v_7^+}{C_{J+3}(J)}},$$

$$S_{\Lambda-1,J+3}=\sqrt{\frac{15v_6^-v_7^-v_4^+v_5^+v_6^+v_7^+}{C_{J+3}(J)}},\qquad S_{\Lambda,J+3}=\sqrt{\frac{20v_5^-v_6^-v_7^-v_5^+v_6^+v_7^+}{C_{J+3}(J)}},$$

$$S_{\Lambda+1,J+3}=\sqrt{\frac{15v_4^-v_5^-v_6^-v_7^-v_6^+v_7^+}{C_{J+3}(J)}},\qquad S_{\Lambda+2,J+3}=\sqrt{\frac{6v_3^-v_4^-v_5^-v_6^-v_7^-v_7^+}{C_{J+3}(J)}},$$

$$S_{\Lambda+3,J+3}=\sqrt{\frac{v_2^-v_3^-v_4^-v_5^-v_6^-v_7^-}{C_{J+3}(J)}}\,; \tag{1}$$

where $v_{n+1}^{\pm}=v_n^{\pm}+1$ and $v_0^{\pm}=J\pm\Lambda-4$

$$\begin{aligned}
C_{J-3}(J)&=8(J-2)(J-1)J(2J-3)(2J-1)(2J+1),\\
C_{J-2}(J)&=8(J-2)(J-1)J(J+1)(2J-1)(2J+1),\\
C_{J-1}(J)&=8(J-1)J(J+1)(2J-3)(2J+1)(2J+3),\\
C_J(J)&=4(J-1)J(J+1)(J+2)(2J-1)(2J+3),\\
C_{J+1}(J)&=8J(J+1)(J+2)(2J-1)(2J+1)(2J+5),\\
C_{J+2}(J)&=8J(J+1)(J+2)(J+3)(2J+1)(2J+3),\\
C_{J+3}(J)&=8(J+1)(J+2)(J+3)(2J+1)(2J+3)(2J+5).
\end{aligned}\tag{2}$$

After substitution of $0, 1, 2, \ldots$ for the value Λ these formulae give the transformation matrix elements for the ${}^7\Sigma$, ${}^7\Pi$, ${}^7\Delta$, ... terms. (For the ${}^7\Sigma$ and ${}^7\Pi$ terms see [1].)

The line strengths for the transitions ${}^7X_\Lambda(a)-{}^7X_\Lambda(a)$, ${}^7X_\Lambda(a)-{}^7X_\Lambda(b)$, ${}^7X_\Lambda(b)-{}^7X_\Lambda(a)$, ${}^7X_\Lambda(b)-{}^7X_\Lambda(b)$ that is for the septet transitions of any type with $\Delta\Lambda=0$ can be found in the second, third, fourth and fifth column, respectively, of Table I. The line strengths for the transitions ${}^7X_{\Lambda+1}(a)-{}^7Y_\Lambda(a)$, ${}^7X_{\Lambda+1}(a)-{}^7Y_\Lambda(b)$, ${}^7X_{\Lambda+1}(b)-{}^7Y_\Lambda(a)$, ${}^7X_{\Lambda+1}(b)-{}^7Y_\Lambda(b)$ that is for the septet transitions of any type with $\Delta\Lambda=\pm1$ are included in the third, fourth, fifth and sixth column, respectively, of Table II.

In the Tables

$$C_i^-(P)=JC_k(J-1),\qquad C_i(R)=(J+1)C_k(J),$$

$$C_i(Q)=\frac{J(J+1)}{J+1/2}C_k(J),$$

$$C_i(P)=JC_k(J),\qquad C_i^+(R)=(J+1)C_k(J+1), \tag{3}$$

where $i = 1, 2, \ldots, 7$ and $k = J - 3, J - 2, \ldots J + 3$, respectively. For all Tables the terms of case a) were assumed to be normal. If an inverted term occurs instead of a normal one then the suffixes corresponding to the inverted terms in the branch symbols have to be changed on the basis of the above correlation according to the pattern $1 \to 7$, $2 \to 6$, $3 \to 5$, $4 \to 4$, $5 \to 3$, $6 \to 2$, $7 \to 1$ wherever the inverted term occurs.

Finally, we give the scattering of the intensities of the main branches of the (a)—(a) transitions over the main and satellite branches of the (a)—(b) transitions only in the first approximation from quartet to septet cases in Tables III, IV, V and VI, respectively. In the Tables $A = P$ or R for $\Delta\Lambda = 0$ and P, Q, R for $\Delta\Lambda = \pm 1$. Namely, the intensity of the Q-branches for $\Delta\Lambda = 0$ in this approximation is zero.

REFERENCES

1. I. Kovács and I. Péczeli, Acta Phys. Hung., **43**, 293, 1977.
2. I. Kovács and A. Grandpierre, Acta Phys. Hung., **43**, 319, 1977.
3. I. Kovács, Rotational Structure in the Spectra of Diatomic Molecules, Akadémiai Kiadó, Budapest and Adam Hilger Ltd. London. 1969. pp. 169—192.

Table I

Line strengths for $^7X_A - {}^7X_A$ transitions

Branches	Line strengths			
	$^7X(a) - {}^7X(a)$	$^7X(a) - {}^7X(b)$	$^7X(b) - {}^7X(a)$	$^7X(b) - {}^7X(b)$
$P_1(J)$	$\frac{v_1^+ v_7^+}{J}$	$\frac{v_2^- v_3^- v_4^- v_5^- v_6^- v_7^{-2} v_1^+}{C_1(P)}$	$R_1(J-1)$	$\frac{v_1^- v_1^+ (2J+1)}{(J-3)(2J-5)}$
$Q_1(J)$	$\frac{(A-3)^2(2J+1)}{J(J+1)}$	$(A-3)^2 \frac{2v_2^- v_3^- v_4^- v_5^- v_6^- v_7^-}{C_1(Q)}$	$Q_1(J)$	$A^2 \frac{(J+1)(2J+1)}{(J-2)^2 J}$
$R_1(J)$	$\frac{v_2^+ v_8^-}{J+1}$	$\frac{v_2^- v_3^- v_4^- v_5^- v_6^- v_7^- v_8^- v_2^+}{C_1(R)}$	$P_1(J+1)$	$\frac{v_2^- v_2^+ (2J-5)(2J+3)}{(J-2)(2J-5)(2J-3)}$
$^QP_{21}(J)$	0	$\frac{6v_2^- v_3^- v_4^- v_5^- v_6^{-2} v_2^{+2}}{C_1(P)}$	$^QR_{12}(J-1)$	$A^2 \frac{3(2J+1)}{(J-3)(J-2)^2 J}$
$^RQ_{21}(J)$	0	$(A-2)^2 \frac{12v_2^- v_3^- v_4^- v_5^- v_6^- v_2^+}{C_1(Q)}$	$^PQ_{12}(J)$	$\frac{3v_2^- v_2^+ (2J+1)}{(J-2)^2 J(2J-3)}$
$^SR_{21}(J)$	0	$\frac{6v_2^- v_3^- v_4^- v_5^- v_6^- v_7^- v_2^+ v_3^+}{C_1(R)}$	$^OP_{12}(J+1)$	0
$^RP_{31}(J)$	0	$\frac{15v_2^- v_3^- v_4^- v_5^{-2} v_2^+ v_3^{+2}}{C_1(P)}$	$^PR_{13}(J-1)$	$\frac{15v_2^- v_2^+}{(J-2)^2 J(2J-5)(2J-3)}$
$^SQ_{31}(J)$	0	$(A-1)^2 \frac{30v_2^- v_3^- v_4^- v_5^- v_2^+ v_3^+}{C_1(Q)}$	$^OQ_{13}(J)$	0
$^TR_{31}(J)$	0	$\frac{15v_2^- v_3^- v_4^- v_5^- v_6^- v_2^+ v_3^+ v_4^+}{C_1(R)}$	$^NP_{13}(J+1)$	0
$^SP_{41}(J)$	0	$\frac{20v_2^- v_3^- v_4^{-2} v_2^+ v_3^+ v_4^{+2}}{C_1(P)}$	$^OR_{14}(J-1)$	0
$^TQ_{41}(J)$	0	$A^2 \frac{40v_2^- v_3^- v_4^- v_2^+ v_3^+ v_4^+}{C_1(Q)}$	$^NQ_{14}(J)$	0

${}^{U}R_{41}(J)$	0	$\frac{20v_2^-v_3^-v_4^-v_5^-v_2^+v_3^+v_4^+v_5^+}{C_1(R)}$	${}^{M}P_{14}(J+1)$	0
${}^{T}P_{51}(J)$	0	$\frac{15v_2^-v_3^{-2}v_2^+v_3^+v_4^+v_5^{+2}}{C_1(P)}$	${}^{N}R_{15}(J-1)$	0
${}^{U}Q_{51}(J)$	0	$(\Lambda+1)^2\,\frac{30v_2^-v_3^-v_2^+v_3^+v_4^+v_5^+}{C_1(Q)}$	${}^{M}Q_{15}(J)$	0
${}^{V}R_{51}(J)$	0	$\frac{15v_2^-v_3^-v_4^-v_2^+v_3^+v_4^+v_5^+v_6^+}{C_1(R)}$	${}^{L}P_{15}(J+1)$	0
${}^{U}P_{61}(J)$	0	$\frac{6v_2^{-2}v_2^+v_3^+v_4^+v_5^+v_6^{+2}}{C_1(P)}$	${}^{M}R_{16}(J-1)$	0
${}^{V}Q_{61}(J)$	0	$(\Lambda+2)^2\,\frac{12v_2^-v_2^+v_3^+v_4^+v_5^+v_6^+}{C_1(Q)}$	${}^{L}Q_{16}(J)$	0
${}^{W}R_{61}(J)$	0	$\frac{6v_2^-v_3^-v_2^+v_3^+v_4^+v_5^+v_6^+v_7^+}{C_1(R)}$	${}^{K}P_{16}(J+1)$	0
${}^{V}P_{71}(J)$	0	$\frac{v_1^-v_2^+v_3^+v_4^+v_5^+v_6^+v_7^{+2}}{C_1(P)}$	${}^{L}R_{17}(J-1)$	0
${}^{W}Q_{71}(J)$	0	$(\Lambda+3)^2\,\frac{2v_2^+v_3^+v_4^+v_5^+v_6^+v_7^+}{C_1(Q)}$	${}^{K}Q_{17}(J)$	0
${}^{Z}R_{71}(J)$	0	$\frac{v_2^-v_2^+v_3^+v_4^+v_5^+v_6^+v_7^+v_8^+}{C_1(R)}$	${}^{J}P_{17}(J+1)$	0
${}^{O}P_{12}(J)$	0	$\frac{3v_3^-v_4^-v_5^-v_6^-v_7^{-2}v_1^+v_2^+}{C_2(P)}$	${}^{S}R_{21}(J-1)$	0
${}^{P}Q_{12}(J)$	0	$(\Lambda-3)^2\,\frac{6v_3^-v_4^-v_5^-v_6^-v_7^-v_2^+}{C_2(Q)}$	${}^{R}Q_{21}(J)$	$\frac{3v_2^-v_2^+(2J+1)}{(J-2)^2\,J(2J-3)}$
${}^{Q}R_{12}(J)$	0	$\frac{3v_3^-v_4^-v_5^-v_6^-v_7^-v_8^-v_2^{+2}}{C_2(R)}$	${}^{Q}P_{21}(J+1)$	$\Lambda^2\,\frac{3(J-2)\,(2J+3)}{(J-2)^2(J-1)^2(J+1)}$
$P_2(J)$	$\frac{v_2^+v_6^-}{J}$	$\frac{2[2v_2^+ + \Lambda]^2v_3^-v_4^-v_5^-v_6^{-2}v_2^+}{C_2(P)}$	$R_2(J-1)$	$\frac{(J-3)(J+1)\,v_2^-v_2^+(2J+1)}{(J-2)^2\,J(2J-3)}$

Table I (continued)

Branches	Line strengths			
	$^{7}X(a) - {}^{7}X(a)$	$^{7}X(a) - {}^{7}X(b)$	$^{7}X(b) - {}^{7}X(a)$	$^{7}X(b) - {}^{7}X(b)$
$Q_2(J)$	$(\Lambda-2)^2 \dfrac{2J+1}{J(J+1)}$	$(\Lambda-2)^2 \dfrac{4(2v_2^+ + \Lambda)^2 v_3^- v_4^- v_5^- v_6^-}{C_2(Q)}$	$Q_2(J)$	$\Lambda^2 \dfrac{(J^2-J-5)^2(2J+1)}{(J-2)^2(J-1)^2 J(J+1)}$
$R_2(J)$	$\dfrac{v_3^+ v_7^-}{J+1}$	$\dfrac{2(2v_2^+ + \Lambda)^2 v_3^- v_4^- v_5^- v_6^- v_7^- v_3^+}{C_2(R)}$	$P_2(J+1)$	$\dfrac{(J-2)(J+2)\, v_3^- v_3^+ (2J+3)}{(J-1)^2(J+1)(2J-1)}$
${}^{Q}P_{32}(J)$	0	$\dfrac{5(v_2^+ + 2\Lambda)^2 v_3^- v_4^- v_5^{-2} v_3^{+2}}{C_2(P)}$	${}^{Q}R_{23}(J-1)$	$\Lambda^2 \dfrac{5(J+1)(2J-5)}{(J-2)^2(J-1)^2 J}$
${}^{R}Q_{32}(J)$	0	$(\Lambda-1)^2 \dfrac{10(v_2^+ + 2\Lambda)^2 v_3^- v_4^- v_5^- v_3^+}{C_2(Q)}$	${}^{P}Q_{23}(J)$	$\dfrac{5(J-2)\, v_3^- v_3^+ (2J+1)(2J+3)}{(J-1)^2 J(J+1)(2J-3)(2J-1)}$
${}^{S}R_{32}(J)$	0	$\dfrac{5(v_2^+ + 2\Lambda)^2 v_3^- v_4^- v_5^- v_6^- v_3^+ v_4^+}{C_2(R)}$	${}^{O}P_{23}(J+1)$	0
${}^{R}P_{42}(J)$	0	$\Lambda^2 \dfrac{60 v_3^- v_4^{-2} v_3^+ v_4^{+2}}{C_2(P)}$	${}^{P}R_{24}(J-1)$	0
${}^{S}Q_{42}(J)$	0	$\Lambda^4 \dfrac{120 v_3^- v_4^- v_3^+ v_4^+}{C_2(Q)}$	${}^{O}Q_{24}(J)$	0
${}^{T}R_{42}(J)$	0	$\Lambda^2 \dfrac{60 v_3^- v_4^- v_5^- v_3^+ v_4^+ v_5^+}{C_2(R)}$	${}^{N}P_{24}(J+1)$	0
${}^{S}P_{52}(J)$	0	$\dfrac{5(v_2^- - 2\Lambda)^2 v_3^{-2} v_3^+ v_4^+ v_5^{+2}}{C_2(P)}$	${}^{O}R_{25}(J-1)$	0
${}^{T}Q_{52}(J)$	0	$(\Lambda+1)^2 \dfrac{10(v_2^- - 2\Lambda)^2 v_3^- v_3^+ v_4^+ v_5^+}{C_2(Q)}$	${}^{N}Q_{25}(J)$	0
${}^{U}R_{52}(J)$	0	$\dfrac{5(v_2^- - 2\Lambda)^2 v_3^- v_4^- v_3^+ v_4^+ v_5^+ v_6^+}{C_2(R)}$	${}^{M}P_{25}(J+1)$	0
${}^{T}P_{62}(J)$	0	$\dfrac{2(2v_2^+ - \Lambda)^2 v_2^- v_3^+ v_4^+ v_5^+ v_6^{+2}}{C_2(P)}$	${}^{N}R_{26}(J-1)$	0

${}^{U}Q_{62}(J)$	0	$(\Lambda+2)^2\,\dfrac{4(2v_2^+-\Lambda)^2v_3^+v_4^+v_5^+v_6^+}{C_2(Q)}$	${}^{M}Q_{26}(J)$	0
${}^{V}R_{62}(J)$	0	$\dfrac{2(2v_2^+-\Lambda)^2v_3^-v_3^+v_4^+v_5^+v_6^+v_7^+}{C_2(R)}$	${}^{L}P_{26}(J+1)$	0
${}^{U}P_{72}(J)$	0	$\dfrac{3v_1^-v_2^-v_3^+v_4^+v_5^+v_6^+v_7^{+\,2}}{C_2(P)}$	${}^{M}R_{27}(J-1)$	0
${}^{V}Q_{72}(J)$	0	$(\Lambda+3)^2\,\dfrac{6v_2^-v_3^+v_4^+v_5^+v_6^+v_7^+}{C_2(Q)}$	${}^{L}Q_{27}(J)$	0
${}^{W}R_{72}(J)$	0	$\dfrac{3v_2^{-\,2}v_3^+v_4^+v_5^+v_6^+v_7^+v_8^+}{C_2(R)}$	${}^{K}P_{27}(J+1)$	0
${}^{N}P_{13}(J)$	0	$\dfrac{15v_4^-v_5^-v_6^-v_7^{-\,2}v_1^+v_2^+v_3^+}{C_3(P)}$	${}^{T}R_{31}(J-1)$	0
${}^{O}Q_{13}(J)$	0	$(\Lambda-3)^2\,\dfrac{30v_4^-v_5^-v_6^-v_7^-v_2^+v_3^+}{C_3(Q)}$	${}^{S}Q_{31}(J)$	0
${}^{P}R_{13}(J)$	0	$\dfrac{15v_4^-v_5^-v_6^-v_7^-v_8^-v_2^{+\,2}v_3^+}{C_3(R)}$	${}^{R}P_{31}(J+1)$	$\dfrac{15v_3^-v_3^+}{(J-1)^2(J+1)(2J-3)(2J-1)}$
${}^{O}P_{23}(J)$	0	$\dfrac{10(v_1^++2\Lambda)^2v_4^-v_5^-v_6^{-\,2}v_2^+v_3^+}{C_3(P)}$	${}^{S}R_{32}(J-1)$	0
${}^{P}Q_{23}(J)$	0	$(\Lambda-2)^2\,\dfrac{20(v_1^++2\Lambda)^2v_4^-v_5^-v_6^-v_3^+}{C_3(Q)}$	${}^{R}Q_{32}(J)$	$\dfrac{5(J-2)v_3^-v_3^+(2J+1)(2J+3)}{(J-1)^2J(J+1)(2J-3)(2J-1)}$
${}^{Q}R_{23}(J)$	0	$\dfrac{10(v_1^++2\Lambda)^2v_4^-v_5^-v_6^-v_7^-v_3^{+\,2}}{C_3(R)}$	${}^{Q}P_{32}(J+1)$	$\Lambda^2\,\dfrac{3(J+2)(2J-3)}{(J-1)^2J^2(J+1)}$
$P_3(J)$	$\dfrac{v_3^+v_5^-}{J}$	$\dfrac{[v_3^-v_6^- - 4(2\Lambda-1)(v_3^++\Lambda)]^2v_4^-v_5^{-\,2}v_3^+}{C_3(P)}$	$R_3(J-1)$	$\dfrac{(J-2)(J+1)v_3^-v_3^+(2J-5)(2J+3)}{(J-1)^2J(2J-1)(2J-3)}$
$Q_3(J)$	$(\Lambda-1)^2\,\dfrac{(2J+1)}{J(J+1)}$	$(\Lambda-1)^2\,\dfrac{2[v_3^-v_6^- - 4(2\Lambda-1)(v_3^++\Lambda)]^2v_4^-v_5^-}{C_3(Q)}$	$Q_3(J)$	$\Lambda^2\,\dfrac{(J^2-6)^2(2J+1)}{(J-1)^2J^3(J+1)}$
$R_3(J)$	$\dfrac{v_4^+v_6^-}{J+1}$	$\dfrac{[v_3^-v_6^- - 4(2\Lambda-1)(v_3^++\Lambda)^2]v_4^-v_5^-v_6^-v_4^+}{C_3(R)}$	$P_3(J+1)$	$\dfrac{(J-1)(J+2)v_4^-v_4^+(2J-3)(2J+5)}{J^2(J+1)(2J-1)(2J+1)}$

Table I (continued)

Branches	Line strengths			
	$^{7}X(a) - {}^{7}X(a)$	$^{7}X(a) - {}^{7}X(b)$	$^{7}X(b) - {}^{7}X(a)$	$^{7}X(b) - {}^{7}X(b)$
$^{Q}P_{43}(J)$	0	$\frac{12[v_3^- v_5^+ - 2\Lambda(2\Lambda-1)]^2 v_4^{-2} v_5^{+2}}{C_3(P)}$	$^{Q}R_{34}(J-1)$	$\Lambda^2 \frac{6(J-2)(2J+3)}{(J-1)^2 J^3}$
$^{R}Q_{43}(J)$	0	$\Lambda^2 \frac{24[v_3^- v_5^+ - 2\Lambda(2\Lambda-1)]^2 v_4^- v_4^+}{C_3(Q)}$	$^{P}Q_{34}(J)$	$\frac{6(J+2)v_4^- v_4^+(2J-3)}{J^3(J+1)(2J-1)}$
$^{S}R_{43}(J)$	0	$\frac{12[v_3^- v_5^+ - 2\Lambda(2\Lambda-1)]^2 v_4^- v_5^- v_4^+ v_5^+}{C_3(R)}$	$^{O}P_{34}(J+1)$	0
$^{R}P_{53}(J)$	0	$\frac{[v_3^+ v_6^+ + 4(2\Lambda+1)(v_3^- - \Lambda)]^2 v_3^- v_4^+ v_5^{+2}}{C_3(P)}$	$^{P}R_{35}(J-1)$	$\frac{36 v_4^- v_4^+}{J^3(2J-1)(2J+1)}$
$^{S}Q_{53}(J)$	0	$(\Lambda+1)^2 \frac{2[v_3^+ v_6^+ + 4(2\Lambda+1)(v_3^- - \Lambda)]^2 v_4^+ v_5^+}{C_3(Q)}$	$^{O}Q_{35}(J)$	0
$^{T}R_{53}(J)$	0	$\frac{[v_3^+ v_6^+ + 4(2\Lambda+1)(v_3^- - \Lambda)]^2 v_4^- v_4^+ v_5^+ v_6^+}{C_3(R)}$	$^{N}P_{35}(J+1)$	0
$^{S}P_{63}(J)$	0	$\frac{10(v_1^- - 2\Lambda)^2 v_2^- v_3^- v_4^+ v_5^+ v_6^{+2}}{C_3(P)}$	$^{O}R_{36}(J-1)$	0
$^{T}Q_{63}(J)$	0	$(\Lambda+2)^2 \frac{20(v_1^- - 2\Lambda)^2 v_3^- v_4^+ v_5^+ v_6^+}{C_3(Q)}$	$^{N}Q_{36}(J)$	0
$^{U}R_{63}(J)$	0	$\frac{10(v_1^- - 2\Lambda)^2 v_3^{-2} v_4^+ v_5^+ v_6^+ v_7^+}{C_3(R)}$	$^{M}P_{36}(J+1)$	0
$^{T}P_{73}(J)$	0	$\frac{15 v_1^- v_2^- v_3^- v_4^+ v_5^+ v_6^+ v_7^{+2}}{C_3(P)}$	$^{N}R_{37}(J-1)$	0
$^{U}Q_{73}(J)$	0	$(\Lambda+3)^2 \frac{30 v_2^- v_3^- v_4^+ v_5^+ v_6^+ v_7^+}{C_3(Q)}$	$^{M}Q_{37}(J)$	0
$^{V}R_{73}(J)$	0	$\frac{15 v_2^{-2} v_3^- v_4^+ v_5^+ v_6^+ v_7^+ v_8^+}{C_3(Q)}$	$^{L}P_{37}(J+1)$	0

${}^{M}P_{14}(J)$	0	$\dfrac{5v_5^-v_6^-v_7^{-2}v_1^+v_2^+v_3^+v_4^+}{C_4(P)}$	${}^{U}R_{41}(J-1)$	0
${}^{N}Q_{14}(J)$	0	$(\Lambda-3)^2\,\dfrac{10v_5^-v_6^-v_7^-v_2^+v_3^+v_4^+}{C_4(Q)}$	${}^{T}Q_{41}(J)$	0
${}^{O}R_{14}(J)$	0	$\dfrac{5v_5^-v_6^-v_7^-v_8^-v_2^{+2}v_3^+v_4^+}{C_4(R)}$	${}^{S}P_{41}(J+1)$	0
${}^{N}P_{24}(J)$	0	$(\Lambda-1)^2\,\dfrac{30v_5^-v_6^{-2}v_2^+v_3^+v_4^+}{C_4(P)}$	${}^{T}R_{42}(J-1)$	0
${}^{O}Q_{24}(J)$	0	$(\Lambda-2)^2(\Lambda-1)^2\,\dfrac{60v_5^-v_6^-v_3^+v_4^+}{C_4(Q)}$	${}^{S}Q_{42}(J)$	0
${}^{P}R_{24}(J)$	0	$(\Lambda-1)^2\,\dfrac{30v_5^-v_6^-v_7^-v_3^{+2}v_4^+}{C_4(R)}$	${}^{R}P_{42}(J+1)$	$\dfrac{30v_4^-v_4^+}{J^2(J+1)(2J-1)(2J+1)}$
${}^{O}P_{34}(J)$	0	$\dfrac{3[v_6^-v_3^+-2\Lambda(2\Lambda-1)]^2v_5^{-2}v_3^+v_4^+}{C_4(P)}$	${}^{S}R_{43}(J-1)$	0
${}^{P}Q_{34}(J)$	0	$(\Lambda-1)^2\,\dfrac{6[v_6^-v_3^+-2\Lambda(2\Lambda-1)]^2v_5^-v_4^+}{C_4(Q)}$	${}^{R}Q_{43}(J)$	$\dfrac{6(J+2)v_4^-v_4^+(2J-3)}{J^3(J+1)(2J-1)}$
${}^{Q}R_{34}(J)$	0	$\dfrac{3[v_6^-v_3^+-2\Lambda(2\Lambda-1)]^2v_5^-v_6^{-}v_4^{+2}}{C_4(R)}$	${}^{Q}P_{43}(J+1)$	$\Lambda^2\,\dfrac{6(2J-5)}{J^2(J+1)^2}$
$P_4(J)$	$\dfrac{v_4^-v_4^+}{J}$	$\Lambda^2\,\dfrac{4[3v_3^-v_6^+-(\Lambda-5)(2\Lambda+1)]^2v_4^-v_4^+}{C_4(P)}$	$R_4(J-1)$	$\dfrac{(J+1)(J+2)v_4^-v_4^+(2J-5)(2J-3)}{4J^3(2J-1)(2J+1)}$
$Q_4(J)$	$\Lambda^2\,\dfrac{2J+1}{J(J+1)}$	$\Lambda^4\,\dfrac{8[3v_3^-v_6^+-(\Lambda-5)(2\Lambda+1)]^2}{C_4(Q)}$	$Q_4(J)$	$\Lambda^2\,\dfrac{(J-2)^2(J+3)^2(2J+1)}{J^3(J+1)^3}$
$R_4(J)$	$\dfrac{v_5^-v_5^+}{J+1}$	$\Lambda^2\,\dfrac{4[3v_3^-v_6^+-(\Lambda-5)(2\Lambda+1)]^2v_5^-v_5^+}{C_4(R)}$	$P_4(J+1)$	$\dfrac{(J-1)(J+3)v_5^-v_5^+(2J-1)(2J+5)}{(J+1)^3(2J+1)(2J+3)}$
${}^{Q}P_{54}(J)$	0	$\dfrac{3[v_3^-v_6^+-2\Lambda(2\Lambda+1)]^2v_3^-v_4^-v_5^{+2}}{C_4(P)}$	${}^{Q}R_{45}(J-1)$	$\Lambda^2\,\dfrac{6(J+2)(2J-3)}{J^3(J+1)^2}$
${}^{R}Q_{54}(J)$	0	$(\Lambda+1)^2\,\dfrac{6[v_3^-v_6^+-2\Lambda(2\Lambda+1)]^2v_4^-v_5^+}{C_4(Q)}$	${}^{P}Q_{45}(J)$	$\dfrac{6(J-1)v_5^-v_5^+(2J+5)}{J(J+1)^3(2J+3)}$

Table I (continued)

Branches	Line strengths			
	$^{7}X(a) - {}^{7}X(a)$	$^{7}X(a) - {}^{7}X(b)$	$^{7}X(b) - {}^{7}X(a)$	$^{7}X(b) - {}^{7}X(b)$
$^{S}R_{54}(J)$	0	$\frac{3[v_3^- v_6^+ - 2\Lambda(2\Lambda+1)]^2 v_4^{-2} v_5^+ v_6^+}{C_4(R)}$	$^{O}P_{45}(J+1)$	0
$^{R}P_{64}(J)$	0	$(\Lambda+1)^2 \frac{30 v_2^- v_3^- v_4^- v_5^+ v_6^{+2}}{C_4(P)}$	$^{P}R_{46}(J-1)$	$\frac{30 v_5^- v_5^+}{J(J+1)^2(2J+1)(2J+3)}$
$^{S}Q_{64}(J)$	0	$(\Lambda+1)^2(\Lambda+2)^2 \frac{60 v_3^- v_4^- v_5^+ v_6^+}{C_4(Q)}$	$^{O}Q_{46}(J)$	0
$^{T}R_{64}(J)$	0	$(\Lambda+1)^2 \frac{30 v_3^{-2} v_4^- v_5^+ v_6^+ v_7^+}{C_4(R)}$	$^{N}P_{46}(J+1)$	0
$^{S}P_{74}(J)$	0	$\frac{5 v_1^- v_2^- v_3^- v_4^- v_5^+ v_6^+ v_7^{+2}}{C_4(P)}$	$^{O}R_{47}(J-1)$	0
$^{T}Q_{74}(J)$	0	$(\Lambda+3)^2 \frac{10 v_2^- v_3^- v_4^- v_5^+ v_6^+ v_7^+}{C_4(R)}$	$^{N}Q_{47}(J)$	0
$^{U}R_{74}(J)$	0	$\frac{5 v_2^{-2} v_3^- v_4^- v_5^+ v_6^+ v_7^+ v_8^+}{C_4(R)}$	$^{M}P_{47}(J+1)$	0
$^{L}P_{15}(J)$	0	$\frac{15 v_6^- v_7^{-2} v_1^+ v_2^+ v_3^+ v_4^+ v_5^+}{C_5(P)}$	$^{V}R_{51}(J-1)$	0
$^{M}Q_{15}(J)$	0	$(\Lambda-3)^2 \frac{30 v_6^- v_7^- v_2^+ v_3^+ v_4^+ v_5^+}{C_5(Q)}$	$^{U}Q_{51}(J)$	0
$^{N}R_{15}(J)$	0	$\frac{15 v_6^- v_7^- v_8^- v_2^{+2} v_3^+ v_4^+ v_5^+}{C_5(R)}$	$^{T}P_{51}(J+1)$	0
$^{M}P_{25}(J)$	0	$\frac{10(v_8^- - 2\Lambda)^2 v_6^{-2} v_2^+ v_3^+ v_4^+ v_5^+}{C_5(P)}$	$^{U}R_{52}(J-1)$	0
$^{N}Q_{25}(J)$	0	$(\Lambda-2)^2 \frac{20(v_8^- - 2\Lambda)^2 v_6^- v_3^+ v_4^+ v_5^+}{C_5(Q)}$	$^{T}Q_{52}(J)$	0

${}^{O}R_{25}(J)$	0	$\dfrac{10(v_8^- - 2\Lambda)^2 v_6^- v_7^- v_3^{+2} v_4^+ v_5^+}{C_5(R)}$	${}^{S}P_{52}(J+1)$	0
${}^{N}P_{35}(J)$	0	$\dfrac{[v_3^+ v_6^+ + 4(v_6^- - \Lambda)(2\Lambda - 1)]^2 v_5^- v_3^+ v_4^+ v_5^+}{C_5(P)}$	${}^{T}R_{53}(J-1)$	0
${}^{O}Q_{35}(J)$	0	$(\Lambda-1)^2 \dfrac{2[v_3^+ v_6^+ + 4(v_6^- - \Lambda)(2\Lambda-1)]^2 v_4^+ v_5^+}{C_5(Q)}$	${}^{S}Q_{53}(J)$	0
${}^{P}R_{35}(J)$	0	$\dfrac{[v_3^+ v_6^+ + 4(v_6^- - \Lambda)(2\Lambda - 1)]^2 v_6^- v_4^{+2} v_5^+}{C_5(R)}$	${}^{R}P_{53}(J+1)$	$\dfrac{36 v_5^- v_5^+}{(J+1)^3(2J+1)(2J+3)}$
${}^{O}P_{45}(J)$	0	$\dfrac{12[v_4^- v_6^+ - 2\Lambda(2\Lambda - 1)]^2 v_4^- v_5^- v_4^+ v_5^+}{C_5(P)}$	${}^{S}R_{54}(J-1)$	0
${}^{P}Q_{45}(J)$	0	$\Lambda^2 \dfrac{24[v_4^- v_6^+ - 2\Lambda(2\Lambda-1)]^2 v_5^- v_5^+}{C_5(Q)}$	${}^{R}Q_{54}(J)$	$\dfrac{6(J-1)v_5^- v_5^+(2J+5)}{J(J+1)^3(2J+3)}$
${}^{Q}R_{45}(J)$	0	$\dfrac{12[v_4^- v_6^+ - 2\Lambda(2\Lambda-1)]^2 v_5^{-2} v_5^{+2}}{C_5(R)}$	${}^{Q}P_{54}(J+1)$	$\Lambda^2 \dfrac{6(J+3)(2J-1)}{(J+1)^3(J+2)^2}$
$P_5(J)$	$\dfrac{v_3^- v_5^+}{J}$	$\dfrac{[v_3^- v_6^- - 4(v_6^+ + \Lambda)(2\Lambda+1)]^2 v_3^- v_4^- v_5^- v_5^+}{C_5(P)}$	$R_5(J-1)$	$\dfrac{(J-1)(J+1)v_5^- v_5^+(2J-5)(2J+5)}{J(J+1)^2(2J+1)(2J+3)}$
$Q_5(J)$	$(\Lambda+1)^2 \dfrac{2J+1}{J(J+1)}$	$(\Lambda+1)^2 \dfrac{2[v_3^- v_6^- - 4(v_6^+ + \Lambda)(2\Lambda+1)]^2 v_4^- v_5^-}{C_5(Q)}$	$Q_5(J)$	$\Lambda^2 \dfrac{(J^2+2J-5)^2(2J+1)}{J(J+1)^3(J+2)^2}$
$R_5(J)$	$\dfrac{v_6^+ v_4^-}{J+1}$	$\dfrac{[v_3^- v_6^- - 4(v_6^+ + \Lambda)(2\Lambda+1)]^2 v_4^{-2} v_5^- v_6^+}{C_5(R)}$	$P_5(J+1)$	$\dfrac{J(J+3)v_6^- v_6^+(2J-1)(2J+7)}{(J+1)(J+2)^2(2J+3)(2J+5)}$
${}^{Q}P_{65}(J)$	0	$\dfrac{10(v_8^+ + 2\Lambda)^2 v_2^- v_3^- v_4^- v_5^- v_6^{+2}}{C_5(P)}$	${}^{Q}R_{56}(J-1)$	$\Lambda^2 \dfrac{5(J-1)(2J+5)}{J(J+1)^2(J+2)^2}$
${}^{R}Q_{65}(J)$	0	$(\Lambda+2)^2 \dfrac{20(v_8^+ + 2\Lambda)^2 v_3^- v_4^- v_5^- v_6^+}{C_5(Q)}$	${}^{P}Q_{56}(J)$	$\dfrac{3(J+3)v_6^- v_6^+(2J-1)(2J+1)}{J(J+1)(J+2)^2(2J+3)(2J+5)}$
${}^{S}R_{65}(J)$	0	$\dfrac{10(v_8^+ + 2\Lambda)^2 v_3^{-2} v_4^- v_5^- v_6^+ v_7^+}{C_5(R)}$	${}^{O}P_{56}(J+1)$	0
${}^{R}P_{75}(J)$	0	$\dfrac{15 v_1^- v_2^- v_3^- v_4^- v_5^- v_6^+ v_7^{+2}}{C_5(P)}$	${}^{P}R_{57}(J-1)$	$\dfrac{15 v_6^- v_6^+}{J(J+2)^2(2J+3)(2J+5)}$

Table I (continued)

Branches	Line strengths			
	$^7X(a) - {}^7X(a)$	$^7X(a) - {}^7X(b)$	$^7X(b) - {}^7X(a)$	$^7X(b) - {}^7X(b)$
$^SQ_{75}(J)$	0	$(\Lambda+3)^2 \dfrac{30v_2^-v_3^-v_4^-v_5^-v_6^+v_7^+}{C_5(Q)}$	$^OQ_{57}(J)$	0
$^TR_{75}(J)$	0	$\dfrac{15v_2^{-2}v_3^-v_4^-v_5^-v_6^+v_7^+v_8^+}{C_5(R)}$	$^NP_{57}(J+1)$	0
$^KP_{16}(J)$	0	$\dfrac{3v_7^{-2}v_1^+v_2^+v_3^+v_4^+v_5^+v_6^+}{C_6(P)}$	$^WR_{61}(J-1)$	0
$^LQ_{16}(J)$	0	$(\Lambda-3)^2 \dfrac{6v_7^-v_2^+v_3^+v_4^+v_5^+v_6^+}{C_6(Q)}$	$^VQ_{61}(J)$	0
$^MR_{16}(J)$	0	$\dfrac{3v_7^-v_8^-v_2^{+2}v_3^+v_4^+v_5^+v_6^+}{C_6(R)}$	$^UP_{61}(J+1)$	0
$^LP_{26}(J)$	0	$\dfrac{2(2v_7^- - \Lambda)^2v_6^-v_2^+v_3^+v_4^+v_5^+v_6^+}{C_6(P)}$	$^VR_{62}(J-1)$	0
$^MQ_{62}(J)$	0	$(\Lambda-2)^2 \dfrac{4(2v_7^- - \Lambda)^2v_3^+v_4^+v_5^+v_6^+}{C_6(Q)}$	$^UQ_{62}(J)$	0
$^NR_{26}(J)$	0	$\dfrac{2(2v_7^- - \Lambda)^2v_7^-v_3^{+2}v_4^+v_5^+v_6^+}{C_6(R)}$	$^TP_{62}(J+1)$	0
$^MP_{36}(J)$	0	$\dfrac{5(v_7^- - 2\Lambda)^2v_5^-v_6^-v_3^+v_4^+v_5^+v_6^+}{C_6(P)}$	$^UR_{63}(J-1)$	0
$^NQ_{36}(J)$	0	$(\Lambda-1)^2 \dfrac{10(v_7^- - 2\Lambda)^2v_6^-v_4^+v_5^+v_6^+}{C_6(Q)}$	$^TQ_{63}(J)$	0
$^OR_{36}(J)$	0	$\dfrac{5(v_7^- - 2\Lambda)^2v_6^{-2}v_4^{+2}v_5^+v_6^+}{C_6(R)}$	$^SP_{63}(J+1)$	0
$^NP_{46}(J)$	0	$\Lambda^2 \dfrac{60v_4^-v_5^-v_6^-v_4^+v_5^+v_6^+}{C_6(P)}$	$^TR_{64}(J-1)$	0

${}^{O}Q_{46}(J)$	0	$\Lambda^4 \dfrac{120 v_5^- v_6^- v_5^+ v_6^+}{C_6(Q)}$	${}^{S}Q_{64}(J)$	0
${}^{P}R_{46}(J)$	0	$\Lambda^2 \dfrac{60 v_5^{-2} v_6^- v_5^{+2} v_6^+}{C_6(R)}$	${}^{R}P_{64}(J+1)$	$\dfrac{30 v_6^- v_6^+}{(J+1)(J+2)^2(2J+3)(2J+5)}$
${}^{O}P_{56}(J)$	0	$\dfrac{5(v_7^+ + 2\Lambda)^2 v_3^- v_4^- v_5^- v_6^{+2}}{C_6(P)}$	${}^{S}R_{65}(J-1)$	0
${}^{P}Q_{56}(J)$	0	$(\Lambda+1)^2 \dfrac{10(v_7^+ + 2\Lambda)^2 v_4^- v_5^- v_6^- v_6^+}{C_6(Q)}$	${}^{R}Q_{65}(J)$	$\dfrac{3(J+3) v_6^- v_6^+ (2J-1)}{J(J+1)(J+2)^3(2J+3)(2J+5)}$
${}^{Q}R_{56}(J)$	0	$\dfrac{5(v_7^+ + 2\Lambda)^2 v_4^{-2} v_5^- v_6^- v_6^{+2}}{C_6(R)}$	${}^{Q}P_{65}(J+1)$	$\Lambda^2 \dfrac{3J(2J+7)}{(J+1)(J+2)^2(J+3)^2}$
$P_6(J)$	$\dfrac{v_2^- v_6^+}{J}$	$\dfrac{2(2v_7^+ + \Lambda)^2 v_2^- v_3^- v_4^- v_5^- v_6^- v_6^+}{C_6(P)}$	$R_6(J-1)$	$\dfrac{(J-1)(J+3) v_6^- v_6^+ (2J-1)}{J(J+2)^2(2J+3)}$
$Q_6(J)$	$(\Lambda+2)^2 \dfrac{2J+1}{J(J+1)}$	$(\Lambda+2)^2 \dfrac{4(2v_7^+ + \Lambda)^2 v_3^- v_4^- v_5^- v_6^-}{C_6(Q)}$	$Q_6(J)$	$\Lambda^2 \dfrac{(J^2+3J-3)^2(2J+1)}{J(J+1)(J+2)^2(J+3)^2}$
$R_6(J)$	$\dfrac{v_7^+ v_3^-}{J+1}$	$\dfrac{2(2v_7^+ + \Lambda)^2 v_3^{-2} v_4^- v_5^- v_6^- v_7^+}{C_6(R)}$	$P_6(J+1)$	$\dfrac{J(J+4) v_7^- v_7^+ (2J+1)}{(J+1)(J+3)^2(2J+5)}$
${}^{Q}P_{76}(J)$	0	$\dfrac{3 v_1^- v_2^- v_3^- v_4^- v_5^- v_6^- v_7^{+2}}{C_6(P)}$	${}^{Q}R_{67}(J-1)$	$\Lambda^2 \dfrac{3(J-3)(2J+1)}{J(J+2)^2(J+3)^2}$
${}^{R}Q_{76}(J)$	0	$(\Lambda+3)^2 \dfrac{6 v_2^- v_3^- v_4^- v_5^- v_6^- v_7^+}{C_6(Q)}$	${}^{P}Q_{67}(J)$	$\dfrac{3 v_7^- v_7^+ (2J+1)}{J(J+1)(J+3)^2(2J+5)}$
${}^{S}R_{76}(J)$	0	$\dfrac{3 v_2^{-2} v_3^- v_4^- v_5^- v_6^- v_7^+ v_8^+}{C_6(R)}$	${}^{O}P_{67}(J+1)$	0
${}^{J}P_{17}(J)$	0	$\dfrac{v_7^- v_1^+ v_2^+ v_3^+ v_4^+ v_5^+ v_6^+ v_7^+}{C_7(P)}$	${}^{Z}R_{71}(J-1)$	0
${}^{K}Q_{17}(J)$	0	$(\Lambda-3)^2 \dfrac{2 v_2^+ v_3^+ v_4^+ v_5^+ v_6^+ v_7^+}{C_7(Q)}$	${}^{W}Q_{71}(J)$	0
${}^{L}R_{17}(J)$	0	$\dfrac{v_8^- v_2^{+2} v_3^+ v_4^+ v_5^+ v_6^+ v_7^+}{C_7(R)}$	${}^{V}P_{71}(J+1)$	0

Table I (continued)

Branches	Line strengths			
	$^{7}X(a) - {}^{7}X(a)$	$^{7}X(a) - {}^{7}X(b)$	$^{7}X(b) - {}^{7}X(a)$	$^{7}X(b) - {}^{7}X(b)$
$^{K}P_{27}(J)$	0	$\frac{6v_6^- v_7^- v_2^+ v_3^+ v_4^+ v_5^+ v_6^+ v_7^+}{C_7(P)}$	$^{W}R_{72}(J-1)$	0
$^{L}Q_{27}(J)$	0	$(\Lambda-2)^2 \frac{12v_7^- v_3^+ v_4^+ v_5^+ v_6^+ v_7^+}{C_7(Q)}$	$^{V}Q_{72}(J)$	0
$^{M}R_{27}(J)$	0	$\frac{6v_7^{-2} v_3^{+2} v_4^+ v_5^+ v_6^+ v_7^+}{C_7(R)}$	$^{U}P_{72}(J+1)$	0
$^{L}P_{37}(J)$	0	$\frac{15v_5^- v_6^- v_7^- v_3^+ v_4^+ v_5^+ v_6^+ v_7^+}{C_7(P)}$	$^{V}R_{73}(J-1)$	0
$^{M}Q_{37}(J)$	0	$(\Lambda-1)^2 \frac{30v_6^- v_7^- v_4^+ v_5^+ v_6^+ v_7^+}{C_7(Q)}$	$^{U}Q_{73}(J)$	0
$^{N}R_{37}(J)$	0	$\frac{15v_6^{-2} v_7^- v_4^{+2} v_5^+ v_6^+ v_7^+}{C_7(R)}$	$^{T}P_{73}(J+1)$	0
$^{M}P_{47}(J)$	0	$\frac{20v_4^- v_5^- v_6^- v_7^- v_4^+ v_5^+ v_6^+ v_7^+}{C_7(P)}$	$^{U}R_{74}(J-1)$	0
$^{N}Q_{47}(J)$	0	$\Lambda^2 \frac{40v_5^- v_6^- v_7^- v_5^+ v_6^+ v_7^+}{C_7(Q)}$	$^{T}Q_{74}(J)$	0
$^{O}R_{47}(J)$	0	$\frac{20v_5^{-2} v_6^- v_7^- v_5^{+2} v_6^+ v_7^+}{C_7(R)}$	$^{S}P_{74}(J+1)$	0
$^{N}P_{57}(J)$	0	$\frac{15v_3^- v_4^- v_5^- v_6^- v_7^- v_5^+ v_6^+ v_7^+}{C_7(P)}$	$^{T}R_{75}(J-1)$	0
$^{O}Q_{57}(J)$	0	$(\Lambda+1)^2 \frac{30v_4^- v_5^- v_6^- v_7^- v_6^+ v_7^+}{C_7(Q)}$	$^{S}Q_{75}(J)$	0
$^{P}R_{57}(J)$	0	$\frac{15v_4^{-2} v_5^- v_6^- v_7^- v_6^{+2} v_7^+}{C_7(R)}$	$^{R}P_{75}(J+1)$	$\frac{15v_7^- v_7^+}{(J+1)(J+2)^2(2J+3)(2J+5)}$

${}^{O}P_{67}(J)$	0	$\dfrac{6v_2^-v_3^-v_4^-v_5^-v_6^-v_7^-v_6^+v_7^+}{C_7(P)}$	${}^{S}R_{76}(J-1)$	0
${}^{P}Q_{67}(J)$	0	$(\Lambda+2)^2\,\dfrac{12v_3^-v_4^-v_5^-v_6^-v_7^-v_7^+}{C_7(Q)}$	${}^{R}Q_{76}(J)$	$\dfrac{3v_7^-v_7^+(2J+1)}{(J+1)(J+3)^2(2J+5)}$
${}^{Q}R_{67}(J)$	0	$\dfrac{6v_3^{-2}v_4^-v_5^-v_6^-v_7^-v_7^{+2}}{C_7(R)}$	${}^{Q}P_{76}(J+1)$	$\Lambda^2\,\dfrac{3(2J+1)}{(J+1)(J+3)^2(J+4)}$
$P_7(J)$	$\dfrac{v_1^-v_7^+}{J}$	$\dfrac{v_1^-v_2^-v_3^-v_4^-v_5^-v_6^-v_7^-v_7^+}{C_7(P)}$	$R_7(J-1)$	$\dfrac{v_7^-v_7^+(2J-1)}{(J+3)(2J+5)}$
$Q_7(J)$	$(\Lambda+3)^2\,\dfrac{2J+1}{J(J+1)}$	$(\Lambda+3)^2\,\dfrac{2v_2^-v_3^-v_4^-v_5^-v_6^-v_7^-}{C_7(Q)}$	$Q_7(J)$	$\Lambda^2\,\dfrac{J(2J+1)}{(J+1)(J+3)^2}$
$R_7(J)$	$\dfrac{v_8^+v_2^-}{J+1}$	$\dfrac{v_2^{-2}v_3^-v_4^-v_5^-v_6^-v_7^-v_8^+}{C_7(R)}$	$P_7(J+1)$	$\dfrac{v_8^-v_8^+(2J+1)}{(J+4)(2J+7)}$

Table II

Line strengths for

Branches		Line	
$\Delta\Lambda = +1$	$\Delta\Lambda = -1$	${}^{7}X(a) - {}^{7}Y(a)$	${}^{7}X(a) - {}^{7}Y(b)$
$P_1(J)$	$R_1(J-1)$	$\frac{v_6^- v_7^-}{2J}$	$\frac{v_2^- v_3^- v_4^- v_5^- v_6^{-2} v_7^{-2}}{2C_1(P)}$
$Q_1(J)$	$Q_1(J)$	$\frac{v_2^+ v_7^- \left(J+\frac{1}{2}\right)}{J(J+1)}$	$\frac{v_2^- v_3^- v_4^- v_5^- v_6^- v_7^{-2} v_2^+}{C_1(Q)}$
$R_1(J)$	$P_1(J+1)$	$\frac{v_2^+ v_3^+}{2(J+1)}$	$\frac{v_2^- v_3^- v_4^- v_5^- v_6^- v_7^- v_2^+ v_3^+}{2C_1(R)}$
${}^{Q}P_{21}(J)$	${}^{Q}R_{12}(J-1)$	0	$\frac{3v_2^- v_3^- v_4^- v_5^{-2} v_6^{-2} v_2^+}{C_1(P)}$
${}^{R}Q_{21}(J)$	${}^{P}Q_{12}(J)$	0	$\frac{6v_2^- v_3^- v_4^- v_5^- v_6^{-2} v_2^+ v_3^+}{C_1(Q)}$
${}^{S}R_{21}(J)$	${}^{O}P_{12}(J+1)$	0	$\frac{3v_2^- v_3^- v_4^- v_5^- v_6^- v_2^+ v_3^+ v_4^+}{C_1(R)}$
${}^{R}P_{31}(J)$	${}^{P}R_{13}(J-1)$	0	$\frac{15v_2^- v_3^- v_4^{-2} v_5^{-2} v_2^+ v_3^+}{2C_1(P)}$
${}^{S}Q_{31}(J)$	${}^{O}Q_{31}(J)$	0	$\frac{15v_2^- v_3^- v_4^- v_5^{-2} v_2^+ v_3^+ v_4^+}{C_1(Q)}$
${}^{T}R_{31}(J)$	${}^{N}P_{13}(J+1)$	0	$\frac{15v_2^- v_3^- v_4^- v_5^- v_2^+ v_3^+ v_4^+ v_5^+}{2C_1(R)}$
${}^{S}P_{41}(J)$	${}^{O}R_{14}(J-1)$	0	$\frac{10v_2^- v_3^{-2} v_4^{-2} v_2^+ v_3^- v_4^+}{C_1(P)}$
${}^{T}Q_{41}(J)$	${}^{N}Q_{14}(J)$	0	$\frac{20v_2^- v_3^- v_4^{-2} v_2^+ v_3^+ v_4^+ v_5^+}{C_1(Q)}$
${}^{U}R_{41}(J)$	${}^{M}P_{14}(J+1)$	0	$\frac{10v_2^- v_3^- v_4^- v_2^+ v_3^+ v_4^+ v_5^+ v_6^+}{C_1(R)}$
${}^{T}P_{51}(J)$	${}^{N}R_{15}(J-1)$	0	$\frac{15v_2^{-2} v_3^{-2} v_2^+ v_3^+ v_4^+ v_5^+}{2C_1(P)}$
${}^{U}Q_{51}(J)$	${}^{M}Q_{15}(J)$	0	$\frac{15v_2^- v_3^{-2} v_2^+ v_3^+ v_4^+ v_5^+ v_6^+}{C_1(Q)}$
${}^{V}R_{51}(J)$	${}^{L}P_{15}(J+1)$	0	$\frac{15v_2^- v_3^- v_2^+ v_3^+ v_4^+ v_5^+ v_6^+ v_7^+}{2C_1(R)}$
${}^{U}P_{61}(J)$	${}^{M}R_{16}(J-1)$	0	$\frac{3v_1^- v_2^{-2} v_2^+ v_3^+ v_4^+ v_5^+ v_6^+}{C_1(P)}$
${}^{V}Q_{61}(J)$	${}^{L}Q_{16}(J)$	0	$\frac{6v_2^{-2} v_2^+ v_3^+ v_4^+ v_5^+ v_6^+ v_7^+}{C_1(Q)}$
${}^{W}R_{61}(J)$	${}^{K}P_{61}(J+1)$	0	$\frac{3v_2^- v_2^+ v_3^+ v_4^+ v_5^+ v_6^+ v_7^+ v_8^+}{C_1(R)}$
${}^{V}P_{71}(J)$	${}^{L}R_{17}(J-1)$	0	$\frac{v_0^- v_1^- v_2^+ v_3^+ v_4^+ v_5^+ v_6^+ v_7^+}{2C_1(P)}$

$^7X_{A+1} - {}^7Y_A$ transitions

strengths

$^7X(b) - {}^7Y(a)$	$^7X(b) - {}^7Y(b)$
$\frac{v_0^- v_1^- v_2^- v_3^- v_4^- v_5^- v_6^- v_7^-}{2C_1^-(P)}$	$\frac{v_0^- v_1^-(2J+1)}{2(J-3)(2J-5)}$
$\frac{v_2^- v_3^- v_4^- v_5^- v_6^- v_7^{-2} v_2^+}{C_1(Q)}$	$\frac{v_1^- v_2^+(J+1)(2J+1)}{2(J-2)^2 J}$
$\frac{v_2^- v_3^- v_4^- v_5^- v_6^- v_7^- v_2^+ v_3^+}{2C_1^+(R)}$	$\frac{v_2^+ v_3^+(2J+3)}{2(J-2)(2J-3)}$
$\frac{3v_1^- v_2^- v_3^- v_4^- v_5^- v_6^- v_7^- v_2^+}{2C_2^-(P)}$	$\frac{3v_1^- v_2^+(2J+1)}{2J(J-3)(J-2)^2}$
$\frac{3v_2^- v_3^- v_4^- v_5^- v_6^- v_7^- v_2^+ v_3^+}{C_2(Q)}$	$\frac{3v_2^+ v_3^+(J+1)(2J+1)}{2(J-2)^2 J(J+1)(2J-3)}$
$\frac{3v_3^- v_4^- v_5^- v_6^- v_7^- v_2^+ v_3^+ v_4^+}{2C_2^+(R)}$	0
$\frac{15v_2^- v_3^- v_4^- v_5^- v_6^- v_7^- v_2^+ v_3^+}{2C_3^-(P)}$	$\frac{15v_2^+ v_3^+}{2(J-2)^2 J(2J-5)(2J-3)}$
$\frac{15v_3^- v_4^- v_5^- v_6^- v_7^- v_2^+ v_3^+ v_4^+}{C_3(Q)}$	0
$\frac{15v_4^- v_5^- v_6^- v_7^- v_2^+ v_3^+ v_4^+ v_5^+}{2C_3^+(R)}$	0
$\frac{5v_3^- v_4^- v_5^- v_6^- v_7^- v_2^+ v_3^+ v_4^+}{2C_4^-(P)}$	0
$\frac{5v_4^- v_5^- v_6^- v_7^- v_2^+ v_3^+ v_4^+ v_5^+}{C_4(Q)}$	0
$\frac{5v_5^- v_6^- v_7^- v_2^+ v_3^+ v_4^+ v_5^+ v_6^+}{2C_4^+(R)}$	0
$\frac{15v_4^- v_5^- v_6^- v_7^- v_2^+ v_3^+ v_4^+ v_5^+}{2C_5^-(P)}$	0
$\frac{15v_5^- v_6^- v_7^- v_2^+ v_3^+ v_4^+ v_5^+ v_6^+}{C_5(Q)}$	0
$\frac{15v_6^- v_7^- v_2^+ v_3^+ v_4^+ v_5^+ v_6^+ v_7^+}{2C_5^+(R)}$	0
$\frac{3v_5^- v_6^- v_7^- v_2^+ v_3^+ v_4^+ v_5^+ v_6^+}{2C_6^-(P)}$	0
$\frac{3v_6^- v_7^- v_2^+ v_3^+ v_4^+ v_5^+ v_6^+ v_7^+}{C_6(Q)}$	0
$\frac{3v_7^- v_2^+ v_3^+ v_4^+ v_5^+ v_6^+ v_7^+ v_8^+}{2C_6^+(R)}$	0
$\frac{v_6^- v_7^- v_2^+ v_3^+ v_4^+ v_5^+ v_6^+ v_7^+}{2C_7^-(P)}$	0

Table II

Branches		Line	
$\Delta\Lambda = +1$	$\Delta\Lambda = -1$	${}^{?}X(a) - {}^{?}Y(a)$	${}^{?}X(a) - {}^{?}Y(b)$
${}^{W}Q_{71}(J)$	${}^{K}Q_{17}(J)$	0	$\dfrac{v_1^- v_2^+ v_3^+ v_4^+ v_5^+ v_6^+ v_7^+ v_8^+}{C_1(Q)}$
${}^{Z}R_{71}(J)$	${}^{J}P_{17}(J+1)$	0	$\dfrac{v_2^+ v_3^+ v_4^+ v_5^+ v_6^+ v_7^+ v_8^+ v_9^+}{2C_1(R)}$
${}^{O}P_{12}(J)$	${}^{S}R_{21}(J-1)$	0	$\dfrac{3v_3^- v_4^- v_5^- v_6^{-2} v_7^{-2} v_2^+}{2C_2(P)}$
${}^{P}Q_{12}(J)$	${}^{R}Q_{21}(J)$	0	$\dfrac{3v_3^- v_4^- v_5^- v_6^- v_7^{-2} v_2^{+2}}{C_2(Q)}$
${}^{Q}R_{12}(J)$	${}^{Q}P_{21}(J+1)$	0	$\dfrac{3v_3^- v_4^- v_5^- v_6^- v_7^- v_2^{+2} v_3^+}{2C_2(R)}$
$P_2(J)$	$R_2(J-1)$	$\dfrac{v_5^- v_6^-}{2J}$	$\dfrac{v_3^- v_4^- v_5^{-2} v_6^{-2}[2v_2^+ + \Lambda]^2}{C_2(P)}$
$Q_2(J)$	$Q_2(J)$	$\dfrac{v_3^+ v_6^- \left(J+\frac{1}{2}\right)}{J(J+1)}$	$\dfrac{2v_3^- v_4^- v_5^- v_6^{-2}[2v_2^+ + \Lambda]^2}{C_2(Q)}$
$R_2(J)$	$P_2(J+1)$	$\dfrac{v_3^+ v_4^+}{2J}$	$\dfrac{v_3^- v_4^- v_5^- v_6^- v_3^+ v_4^+ [2v_2^+ + \Lambda]^2}{C_2(R)}$
${}^{Q}P_{32}(J)$	${}^{Q}R_{23}(J-1)$	0	$\dfrac{5v_3^- v_4^- v_5^{-2} v_3^+ [v_2^+ + 2\Lambda]^2}{2C_2(P)}$
${}^{R}Q_{32}(J)$	${}^{P}Q_{23}(J)$	0	$\dfrac{5v_3^- v_4^- v_5^{-2} v_3^+ v_4^+ [v_2^+ + 2\Lambda]^2}{C_2(Q)}$
${}^{S}R_{32}(J)$	${}^{O}P_{23}(J+1)$	0	$\dfrac{5v_3^- v_4^- v_5^- v_3^+ v_4^+ v_5^+ [v_2^+ + 2\Lambda]^2}{2C_2(R)}$
${}^{R}P_{42}(J)$	${}^{P}R_{24}(J-1)$	0	$\Lambda^2 \dfrac{30v_3^{-2} v_4^{-2} v_3^+ v_4^+}{C_2(P)}$
${}^{S}Q_{42}(J)$	${}^{O}Q_{24}(J)$	0	$\Lambda^2 \dfrac{60v_3^- v_4^{-2} v_3^+ v_4^+ v_5^+}{C_2(Q)}$
${}^{T}R_{42}(J)$	${}^{N}P_{24}(J+1)$	0	$\Lambda^2 \dfrac{30v_3^- v_4^- v_3^+ v_4^+ v_5^+ v_6^+}{C_2(R)}$
${}^{S}P_{52}(J)$	${}^{O}R_{25}(J-1)$	0	$\dfrac{5v_2^- v_3^{-2} v_3^+ v_4^+ v_5^+ [v_2^- - 2\Lambda]^2}{2C_2(P)}$
${}^{T}Q_{52}(J)$	${}^{N}Q_{25}(J)$	0	$\dfrac{5v_2^{-2} v_3^+ v_4^+ v_5^+ v_6^+ [v_2^- - 2\Lambda]^2}{C_2(Q)}$
${}^{U}R_{52}(J)$	${}^{M}P_{25}(J+1)$	0	$\dfrac{5v_3^- v_3^+ v_4^+ v_5^+ v_6^+ v_7^+ [v_2^- - 2\Lambda]^2}{2C_2(R)}$
${}^{T}P_{62}(J)$	${}^{N}R_{26}(J-1)$	0	$\dfrac{v_1^- v_2^- v_3^+ v_4^+ v_5^+ v_6^+ [2v_2^+ - \Lambda]^2}{C_2(P)}$
${}^{U}Q_{62}(J)$	${}^{M}Q_{26}(J)$	0	$\dfrac{2v_2^- v_3^+ v_4^+ v_5^+ v_6^+ v_7^+ [2v_2^+ - \Lambda]^2}{C_2(Q)}$
${}^{V}R_{62}(J)$	${}^{L}P_{26}(J+1)$	0	$\dfrac{v_3^+ v_4^+ v_5^+ v_6^+ v_7^+ v_8^+ [2v_2^+ - \Lambda]^2}{C_2(R)}$

(continued)

strengths

${}^7X(b) - {}^7Y(a)$	${}^7X(b) - {}^7Y(b)$
$\dfrac{v_7^- v_2^+ v_3^+ v_4^+ v_5^+ v_6^+ v_7^+ v_8^+}{C_7(Q)}$	0
$\dfrac{v_2^+ v_3^+ v_4^+ v_5^+ v_6^+ v_7^+ v_8^+ v_9^+}{2C_7^+(R)}$	0
$\dfrac{3v_0^- v_1^- v_2^- v_3^- v_4^- v_5^- v_6^- v_2^+}{C_1^-(P)}$	0
$\dfrac{6v_1^- v_2^- v_3^- v_4^- v_5^- v_6^- v_3^{+2}}{C_1(Q)}$	$\dfrac{3v_1^- v_2^-(J+1)(2J+1)}{2(J-2)^2 J(J+1)(2J-3)}$
$\dfrac{3v_2^- v_3^- v_4^- v_5^- v_6^- v_3^+ v_4^{+2}}{C_1^+(R)}$	$\dfrac{3v_2^- v_3^+(J-2)(2J+3)}{2(J-2)^2(J-1)^2(J+1)}$
$\dfrac{v_1^- v_2^- v_3^- v_4^- v_5^- v_6^-[2v_2^+ + \Lambda + 1]^2}{C_2^-(P)}$	$\dfrac{v_1^- v_2^-(J-3)(J+1)(2J+1)}{2(J-2)^2 J(2J-3)}$
$\dfrac{2v_2^- v_3^- v_4^- v_5^- v_6^- v_3^+[2v_3^+ + \Lambda + 1]^2}{C_2(Q)}$	$\dfrac{v_2^- v_3^+(J^2-J-5)^2(2J+1)}{4(J-2)^2(J-1)^2 J(J+1)}$
$\dfrac{v_3^- v_4^- v_5^- v_6^- v_3^+ v_4^+[2v_4^+ + \Lambda + 1]^2}{C_2^+(R)}$	$\dfrac{v_3^+ v_4^+(J-2)(J+2)(2J+3)}{2(J-1)^2(J+1)(2J-1)}$
$\dfrac{5v_2^- v_3^- v_4^- v_5^- v_6^- v_3^+[v_3^+ + 2\Lambda]^2}{C_3^-(P)}$	$\dfrac{5v_2^- v_3^+(J+1)(2J-5)}{2(J-2)^2(J-1)^2 J}$
$\dfrac{10v_3^- v_4^- v_5^- v_6^- v_3^+ v_4^+[v_4^+ + 2\Lambda]^2}{C_3(Q)}$	$\dfrac{5v_3^+ v_4^+(J-2)(2J+1)(2J+3)}{2(J-1)^2 J(J+1)(2J-3)(2J-1)}$
$\dfrac{5v_4^- v_5^- v_6^- v_3^+ v_4^+ v_5^+[v_5^+ + 2\Lambda]^2}{C_3^+(R)}$	0
$\Lambda^2 \dfrac{15v_3^- v_4^- v_5^- v_6^- v_3^+ v_4^+}{C_4^-(P)}$	$\dfrac{15v_3^+ v_4^+}{(J-1)^2 J(2J-3)(2J-1)}$
$\Lambda^2 \dfrac{30v_4^- v_5^- v_6^- v_3^+ v_4^+ v_5^+}{C_4(Q)}$	0
$\Lambda^2 \dfrac{15v_5^- v_6^- v_3^+ v_4^+ v_5^+ v_6^+}{C_4^+(R)}$	0
$\dfrac{5v_4^- v_5^- v_6^- v_3^+ v_4^+ v_5^+[v_4^- - 2\Lambda]^2}{C_5^-(P)}$	0
$\dfrac{10v_5^- v_6^- v_3^+ v_4^+ v_5^+ v_6^+[v_5^+ - 2\Lambda]^2}{C_5(Q)}$	0
$\dfrac{5v_6^- v_3^+ v_4^+ v_5^+ v_6^+ v_7^+[v_6^- - 2\Lambda]^2}{C_5^+(R)}$	0
$\dfrac{v_5^- v_6^- v_3^+ v_4^+ v_5^+ v_6^+[2v_5^- - \Lambda - 1]^2}{C_6^-(P)}$	0
$\dfrac{v_6^- v_3^+ v_4^+ v_5^+ v_6^+ v_7^+[2v_6^- - \Lambda - 1]^2}{C_6(Q)}$	0
$\dfrac{v_3^+ v_4^+ v_5^+ v_6^+ v_7^+ v_8^+[2v_7^- - \Lambda - 1]^2}{C_6^+(R)}$	0

Table II

Branches		Line	
$\Delta\Lambda = +1$	$\Delta\Lambda = -1$	${}^7X(a) - {}^7Y(a)$	${}^7X(a) - {}^7Y(b)$
${}^UP_{72}(J)$	${}^MR_{27}(J-1)$	0	$\frac{3v_0^-v_1^-v_2^-v_3^+v_4^+v_5^+v_6^+v_7^+}{2C_2(P)}$
${}^VQ_{72}(J)$	${}^LQ_{27}(J)$	0	$\frac{3v_1^-v_2^-v_3^+v_4^+v_5^+v_6^+v_7^+v_8^+}{C_2(Q)}$
${}^WR_{72}(J)$	${}^KP_{27}(J+1)$	0	$\frac{3v_2^-v_3^+v_4^+v_5^+v_6^+v_7^+v_8^+v_9^+}{2C_2(R)}$
${}^NP_{13}(J)$	${}^TR_{31}(J-1)$	0	$\frac{15v_4^-v_5^-v_6^{-2}v_7^{-2}v_2^+v_3^+}{2C_3(P)}$
${}^OQ_{13}(J)$	${}^SQ_{31}(J)$	0	$\frac{15v_4^-v_5^-v_6^-v_7^{-2}v_2^{+2}v_3^+v_4^+}{C_3(Q)}$
${}^PR_{13}(J)$	${}^RP_{31}(J+1)$	0	$\frac{15v_4^-v_5^-v_6^-v_7^-v_2^{+2}v_3^{+2}}{2C_3(R)}$
${}^OP_{23}(J)$	${}^SR_{32}(J-1)$	0	$\frac{5v_4^-v_5^{-2}v_6^{-2}v_3^+[v_1^+ + 2\Lambda]^2}{C_3(P)}$
${}^PQ_{23}(J)$	${}^RQ_{32}(J)$	0	$\frac{10v_4^-v_5^-v_6^{-2}v_3^{+2}[v_1^+ + 2\Lambda]^2}{C_3(Q)}$
${}^QR_{23}(J)$	${}^QP_{32}(J+1)$	0	$\frac{5v_4^-v_5^-v_6^-v_3^{+2}v_4^+[v_1^+ + 2\Lambda]^2}{C_3(R)}$
$P_3(J)$	$R_3(J-1)$	$\frac{v_4^-v_5^-}{2J}$	$\frac{v_4^{-2}v_5^{-2}[v_3^-v_6^- - 4(v_3^+ + \Lambda)(2\Lambda-1)]^2}{2C_3(P)}$
$Q_3(J)$	$Q_3(J)$	$\frac{v_4^+v_5^-\left(J+\frac{1}{2}\right)}{J(J+1)}$	$\frac{v_4^-v_5^{-2}v_4^+[v_3^-v_6^- - 4(v_3^+ + \Lambda)(2\Lambda-1)]^2}{C_3(Q)}$
$R_3(J)$	$P_3(J+1)$	$\frac{v_4^+v_5^+}{2(J+1)}$	$\frac{v_4^-v_5^-v_4^+v_5^+[v_3^-v_6^- - 4(v_3^+ + \Lambda)(2\Lambda-1)]^2}{2C_3(R)}$
${}^QP_{43}(J)$	${}^QR_{34}(J-1)$	0	$\frac{6v_3^-v_4^{-2}v_4^+[v_3^-v_5^+ - 2\Lambda(2\Lambda-1)]^2}{C_3(P)}$
${}^RQ_{43}(J)$	${}^PQ_{34}(J)$	0	$\frac{12v_4^{-2}v_4^+v_5^+[v_3^-v_5^- - 2\Lambda(2\Lambda-1)]^2}{C_3(Q)}$
${}^SR_{43}(J)$	${}^OP_{34}(J+1)$	0	$\frac{6v_4^-v_4^+v_5^+v_6^+[v_3^-v_5^+ - 2\Lambda(2\Lambda-1)]^2}{C_3(R)}$
${}^RP_{53}(J)$	${}^PR_{35}(J-1)$	0	$\frac{v_2^-v_3^-v_4^+v_5^+[v_3^+v_6^+ + 4(v_3^- - \Lambda)(2\Lambda+1)]^2}{2C_3(P)}$
${}^SQ_{53}(J)$	${}^OQ_{35}(J)$	0	$\frac{v_3^-v_4^+v_5^+v_6^+[v_3^+v_6^+ + 4(v_3^- - \Lambda)(2\Lambda+1)]^2}{C_3(Q)}$
${}^TR_{53}(J)$	${}^NP_{35}(J+1)$	0	$\frac{v_4^+v_5^+v_6^+v_7^+[v_3^+v_6^+ + 4(v_3^- - \Lambda)(2\Lambda+1)]^2}{2C_3(R)}$
${}^SP_{63}(J)$	${}^OR_{36}(J-1)$	0	$\frac{5v_1^-v_2^-v_3^-v_4^+v_5^+v_6^+(v_1^- - 2\Lambda)^2}{C_3(P)}$
${}^TQ_{63}(J)$	${}^NQ_{36}(J)$	0	$\frac{10v_2^-v_3^-v_4^+v_5^+v_6^+v_7^+(v_1^- - 2\Lambda)^2}{C_3(Q)}$

(continued)

strengths

${}^7X(b) - {}^7Y(a)$	${}^7X(b) - {}^7Y(b)$
$\frac{3v_5^-{}^2v_6^-v_3^+v_4^+v_5^+v_6^+v_7^+}{C_7^-(P)}$	0
$\frac{6v_6^-{}^2v_3^+v_4^+v_5^+v_6^+v_7^+v_8^+}{C_7(Q)}$	0
$\frac{3v_7^-v_3^+v_4^+v_5^+v_6^+v_7^+v_8^+v_9^+}{C_7^+(R)}$	0
$\frac{15v_0^-v_1^-v_2^-v_3^-v_4^-v_5^-v_2^+v_3^+}{2C_1^-(P)}$	0
$\frac{15v_1^-v_2^-v_3^-v_4^-v_5^-v_3^+v_4^+{}^2}{C_1(Q)}$	0
$\frac{15v_2^-v_3^-v_4^-v_5^-v_4^+{}^2v_5^+{}^2}{2C_1^+(R)}$	$\frac{15v_2^-v_3^-}{2(J-1)^2(J+1)(2J-3)(2J-1)}$
$\frac{5v_1^-v_2^-v_3^-v_4^-v_5^-v_3^+[v_4^+ + 2\Lambda]^2}{2C_2^-(P)}$	0
$\frac{5v_2^-v_3^-v_4^-v_5^-v_4^+{}^2[v_5^+ + 2\Lambda]^2}{C_2(Q)}$	$\frac{5v_2^-v_3^-(J-2)(2J+1)(2J+3)}{2(J-1)^2J(J+1)(2J-3)(2J-1)}$
$\frac{5v_3^-v_4^-v_5^-v_4^+v_5^+{}^2[v_6^+ + 2\Lambda]^2}{2C_2^+(R)}$	$\frac{5v_3^-v_4^+(J+2)(2J-3)}{2(J-1)^2J^2(J+1)}$
$\frac{v_2^-v_3^-v_4^-v_5^-[v_1^-v_4^- - 4(v_4^+ + \Lambda)(2\Lambda+1)]^2}{2C_3^-(P)}$	$\frac{v_2^-v_3^-(J-2)(J+1)(J+3)(2J+5)}{2(J-1)^2J(2J-3)(2J-1)}$
$\frac{v_3^-v_4^-v_5^-v_4^+[v_2^-v_5^- - 4(v_5^+ + \Lambda)(2\Lambda+1)]^2}{C_3(Q)}$	$\frac{v_3^-v_4^+(J^2-6)^2(2J+1)}{4(J-1)^2J^3(J+1)}$
$\frac{v_4^-v_5^-v_4^+v_5^+[v_3^-v_6^- - 4(v_6^+ + \Lambda)(2\Lambda+1)]^2}{2C_3^+(R)}$	$\frac{v_4^+v_5^+(J-1)(J+2)(2J-3)(2J+5)}{2J^2(J+1)(2J-1)(2J+1)}$
$\frac{3v_3^-v_4^-v_5^-v_4^+[v_4^-v_3^+ - 2(\Lambda+1)(2\Lambda+1)]^2}{2C_4^-(P)}$	$\frac{3v_3^-v_4^+(2J-3)(J+1)}{J^3(J-1)^2}$
$\frac{3v_4^-v_5^-v_4^+v_5^+[v_5^-v_4^+ - 2(\Lambda+1)(2\Lambda+1)]^2}{C_4(Q)}$	$\frac{3v_4^+v_5^+(J+2)(2J+3)}{J^3(J+1)(2J-1)}$
$\frac{3v_5^-v_4^+v_5^+v_6^+[v_6^-v_5^+ - 2(\Lambda+1)(2\Lambda+1)]^2}{2C_4^+(R)}$	0
$\frac{v_4^-v_5^-v_4^+v_5^+[v_3^+v_6^+ + 4(v_3^- - \Lambda)(2\Lambda+1)]^2}{2C_5^-(P)}$	$\frac{18v_4^+v_5^+}{J^3(2J-1)(2J+1)}$
$\frac{v_5^-v_4^+v_5^+v_6^+[v_4^+v_7^+ + 4(v_4^- - \Lambda)(2\Lambda+1)]^2}{C_5(Q)}$	0
$\frac{v_4^+v_5^+v_6^+v_7^+[v_5^+v_8^+ + 4(v_5^- - \Lambda)(2\Lambda+1)]^2}{2C_5^+(R)}$	0
$\frac{5v_4^-{}^2v_5^-v_4^+v_5^+v_6^+[v_3^- - 2\Lambda]^2}{2C_6^-(P)}$	0
$\frac{5v_5^-{}^2v_4^+v_5^+v_6^+v_7^+[v_4^- - 2\Lambda]^2}{C_6(Q)}$	0

Table II

Branches		Line	
$\Delta\Lambda = +1$	$\Delta\Lambda = -1$	${}^{7}X(a) - {}^{7}Y(a)$	${}^{7}X(a) - {}^{7}Y(b)$
${}^{U}R_{63}(J)$	${}^{M}P_{36}(J+1)$	0	$\frac{5v_3^-v_4^+v_5^+v_6^+v_7^+v_8^+(v_1^+ - 2\Lambda)^2}{C_3(R)}$
${}^{T}P_{73}(J)$	${}^{N}R_{37}(J-1)$	0	$\frac{15v_0^-v_1^-v_2^-v_3^-v_4^+v_5^+v_6^+v_7^+}{2C_3(P)}$
${}^{U}Q_{73}(J)$	${}^{M}Q_{37}(J)$	0	$\frac{15v_1^-v_2^-v_3^-v_4^+v_5^+v_6^+v_7^+v_8^+}{C_3(Q)}$
${}^{V}R_{73}(J)$	${}^{L}P_{37}(J+1)$	0	$\frac{15v_2^-v_3^-v_4^+v_5^+v_6^+v_7^+v_8^+v_9^+}{2C_3(R)}$
${}^{M}P_{14}(J)$	${}^{U}R_{41}(J-1)$	0	$\frac{5v_5^-v_6^{-2}v_7^{-2}v_2^+v_3^+v_4^+}{2C_4(P)}$
${}^{N}Q_{14}(J)$	${}^{T}Q_{41}(J)$	0	$\frac{5v_5^-v_6^-v_7^{-2}v_2^+v_3^+v_4^+}{C_4(Q)}$
${}^{O}R_{14}(J)$	${}^{S}P_{41}(J+1)$	0	$\frac{5v_5^-v_6^-v_7^-v_2^{+2}v_3^{+2}v_4^+}{2C_4(R)}$
${}^{N}P_{24}(J)$	${}^{T}R_{42}(J-1)$	0	$(\Lambda-1)^2\,\frac{15v_5^{-2}v_6^{-2}v_3^+v_4^+}{C_4(P)}$
${}^{O}Q_{24}(J)$	${}^{S}Q_{42}(J)$	0	$(\Lambda-1)^2\,\frac{30v_5^-v_6^{-2}v_3^{+2}v_4^+}{C_4(Q)}$
${}^{P}R_{24}(J)$	${}^{R}P_{42}(J+1)$	0	$(\Lambda-1)^2\,\frac{15v_5^-v_6^-v_3^{+2}v_4^{+2}}{C_4(R)}$
${}^{O}P_{34}(J)$	${}^{S}R_{43}(J-1)$	0	$\frac{3v_4^-v_5^{-2}v_4^+[v_6^-v_3^+ - 2\Lambda(2\Lambda-1)]^2}{2C_4(P)}$
${}^{P}Q_{34}(J)$	${}^{R}Q_{43}(J)$	0	$\frac{3v_5^{-2}v_4^{+2}[v_6^-v_3^+ - 2\Lambda(2\Lambda-1)]^2}{C_4(Q)}$
${}^{Q}R_{34}(J)$	${}^{Q}P_{43}(J+1)$	0	$\frac{3v_5^-v_4^{+2}v_6^+[v_6^-v_3^+ - 2\Lambda(2\Lambda-1)]^2}{2C_4(R)}$
$P_4(J)$	$R_4(J-1)$	$\frac{v_3^-v_4^-}{2J}$	$\Lambda^2\,\frac{2[3v_3^-v_6^+ - (\Lambda-5)(2\Lambda+1)]^2v_3^-v_4^-}{C_4(P)}$
$Q_4(J)$	$Q_5(J)$	$\frac{v_5^+v_4^-\left(J+\frac{1}{2}\right)}{J(J+1)}$	$\Lambda^2\,\frac{4[3v_3^-v_6^+ - (\Lambda-5)(2\Lambda+1)]^2v_4^-v_5^+}{C_4(Q)}$
$R_4(J)$	$P_4(J+1)$	$\frac{v_5^+v_6^+}{2(J+1)}$	$\Lambda^2\,\frac{2v_5^+v_6^+[3v_3^-v_6^+ - (\Lambda-5)(2\Lambda+1)]^2}{C_4(R)}$
${}^{Q}P_{54}(J)$	${}^{Q}R_{45}(J-1)$	0	$\frac{3v_2^-v_3^-v_4^-v_5^+[v_3^-v_6^+ - 2\Lambda(2\Lambda+1)]^2}{2C_4(P)}$
${}^{R}Q_{54}(J)$	${}^{P}W_{45}(J)$	0	$\frac{3v_3^-v_4^-v_5^+v_6^+[v_3^-v_6^+ - 2\Lambda(2\Lambda+1)]^2}{C_4(Q)}$
${}^{S}R_{54}(J)$	${}^{O}P_{45}(J+1)$	0	$\frac{3v_4^-v_5^+v_6^+v_7^+[v_3^-v_6^+ - 2\Lambda(2\Lambda+1)]^2}{2C_4(R)}$
${}^{R}P_{44}(J)$	${}^{P}R_{46}(J-1)$	0	$(\Lambda+1)^2\,\frac{15v_1^-v_2^-v_3^-v_4^-v_5^+v_6^+}{C_4(P)}$

(continued)

strengths

$^7X(b) - {}^7Y(a)$	$^7X(b) - {}^7Y(b)$
$\frac{5v_6^-v_4^+v_5^+v_6^+v_7^+v_8^+[v_5^- - 2\Lambda]^2}{2C_6^+(R)}$	0
$\frac{15v_4^{-2}v_5^{-2}v_4^+v_5^+v_6^+v_7^+}{2C_7^-(P)}$	0
$\frac{15v_5^{-2}v_6^-v_4^+v_5^+v_6^+v_7^+v_8^+}{C_7(Q)}$	0
$\frac{15v_6^-v_7^-v_4^+v_5^+v_6^+v_7^+v_8^+v_9^+}{2C_7^+(R)}$	0
$\frac{10v_0^-v_1^-v_2^-v_3^-v_4^-v_2^+v_3^+v_4^+}{C_1^-(P)}$	0
$\frac{20v_1^-v_2^-v_3^-v_4^-v_3^+v_4^+v_5^{+2}}{C_1(Q)}$	0
$\frac{10v_2^-v_3^-v_4^-v_4^+v_5^{+2}v_6^{+2}}{C_1^+(R)}$	0
$(\Lambda+1)^2\frac{30v_1^-v_2^-v_3^-v_4^-v_3^+v_4^+}{C_2^-(P)}$	0
$(\Lambda+1)^2\frac{60v_2^-v_3^-v_4^-v_4^+v_5^{+2}}{C_2(Q)}$	0
$(\Lambda+1)^2\frac{30v_3^-v_4^-v_5^{+2}v_6^{+2}}{C_2^+(R)}$	$\frac{15v_3^-v_4^-}{J^2(J+1)(2J-1)(2J+1)}$
$\frac{6v_2^-v_3^-v_4^-v_4^+[v_1^-v_5^+ - 2(\Lambda+1)(2\Lambda+1)]^2}{C_3^-(P)}$	0
$\frac{12v_3^-v_4^-v_5^{+2}[v_2^-v_6^+ - 2(\Lambda+1)(2\Lambda+1)]^2}{C_3(Q)}$	$\frac{3v_3^-v_4^-(J+2)(2J-3)}{J(J+1)^2(2J+3)}$
$\frac{6v_4^-v_5^+v_6^{+2}[v_3^-v_7^+ - 2(\Lambda+1)(2\Lambda+1)]^2}{C_3^+(R)}$	$\frac{3v_4^-v_5^+(J-1)(2J+5)}{J^2(J+1)^3}$
$(\Lambda+1)^2\frac{2v_3^-v_4^-[3v_1^-v_6^+ - (\Lambda-4)(2\Lambda+3)]^2}{C_4^-(P)}$	$\frac{v_3^-v_4^-(J-1)(J+1)(2J-3)(2J+3)}{2J^3(2J-1)(2J+1)}$
$\frac{4v_4^-v_5^+[3v_2^-v_7^+ - (\Lambda-4)(2\Lambda+3)]^2}{C_4(Q)}$	$\frac{v_4^-v_5^+(J-2)^2(J+3)^2(2J+1)}{4J^3(J+1)^3}$
$(\Lambda+1)^2\frac{2v_5^+v_6^+[3v_3^-v_8^+ - (\Lambda-4)(2\Lambda+3)]^2}{C_4^+(R)}$	$\frac{v_5^+v_6^+(J-1)(J+3)(2J-1)(2J+5)}{2(J+1)^3(2J+1)(2J+3)}$
$\frac{6v_3^{-2}v_4^-v_5^+[v_2^-v_6^+ - 2(\Lambda+1)(2\Lambda+1)]^2}{C_5^-(P)}$	$\frac{3v_4^-v_5^+(J+2)(2J-3)}{J^3(J+1)^2}$
$\frac{12v_4^{-2}v_5^+v_6^+[v_3^-v_7^+ - 2(\Lambda+1)(2\Lambda+1)]^2}{C_5(Q)}$	$\frac{3v_5^+v_6^+(J-1)(2J+5)}{8J(J+1)^3(2J+3)}$
$\frac{6v_5^-v_5^+v_6^+v_7^+[v_4^-v_8^+ - 2(\Lambda+1)(2\Lambda+1)]^2}{C_5^+(R)}$	0
$(\Lambda+1)^2\frac{30v_3^{-2}v_4^{-2}v_5^+v_6^+}{C_6^-(P)}$	$\frac{15v_5^+v_6^+}{J(J+1)^2(2J+1)(2J+3)}$

Table II

Branches		Line	
$\Delta\Lambda = +1$	$\Delta\Lambda = -1$	${}^{7}X(a) - {}^{7}Y(a)$	${}^{7}X(a) - {}^{7}Y(b)$
${}^{S}Q_{64}(J)$	${}^{O}Q_{46}(J)$	0	$(\Lambda+1)^2 \dfrac{30v_2^-v_3^-v_4^-v_5^+v_6^+v_7^+}{C_4(Q)}$
${}^{T}R_{64}(J)$	${}^{N}P_{46}(J+1)$	0	$(\Lambda+1)^2 \dfrac{15v_3^-v_4^-v_5^+v_6^+v_7^+v_8^+}{C_4(R)}$
${}^{S}P_{74}(J)$	${}^{O}R_{47}(J-1)$	0	$\dfrac{5v_0^-v_1^-v_2^-v_3^-v_4^-v_5^+v_6^+v_7^+}{2C_4(P)}$
${}^{T}Q_{74}(J)$	${}^{N}Q_{47}(J)$	0	$\dfrac{5v_1^-v_2^-v_3^-v_4^-v_5^+v_6^+v_7^+v_8^+}{C_4(Q)}$
${}^{U}R_{74}(J)$	${}^{M}P_{47}(J+1)$	0	$\dfrac{5v_2^-v_3^-v_4^-v_5^+v_6^+v_7^+v_8^+v_9^+}{2C_4(R)}$
${}^{L}P_{15}(J)$	${}^{V}R_{51}(J-1)$	0	$\dfrac{15v_6^{-2}v_7^{-2}v_2^+v_3^+v_4^+v_5^+}{2C_5(P)}$
${}^{M}Q_{15}(J)$	${}^{U}Q_{51}(J)$	0	$\dfrac{15v_6^-v_7^{-2}v_2^{+2}v_3^+v_4^+v_5^+}{C_5(Q)}$
${}^{N}R_{15}(J)$	${}^{T}P_{51}(J+1)$	0	$\dfrac{15v_6^-v_7^-v_2^{+2}v_3^{+2}v_4^+v_5^+}{2C_5(R)}$
${}^{M}P_{25}(J)$	${}^{U}R_{52}(J-1)$	0	$\dfrac{5v_5^-v_6^{-2}v_3^+v_4^+v_5^+(v_8^- - 2\Lambda)^2}{C_5(P)}$
${}^{N}Q_{25}(J)$	${}^{T}Q_{52}(J)$	0	$\dfrac{10v_6^{-2}v_3^+v_4^+v_5^+(v_6^- - 2\Lambda)^2}{C_5(Q)}$
${}^{O}R_{25}(J)$	${}^{S}P_{52}(J+1)$	0	$\dfrac{5v_6^-v_3^{+2}v_4^{+2}v_5^+(v_8^- - 2\Lambda)^2}{C_5(R)}$
${}^{N}P_{35}(J)$	${}^{T}R_{53}(J-1)$	0	$\dfrac{v_4^-v_5^-v_4^+v_5^+[v_3^+v_6^+ + 4(v_6^- - \Lambda)(2\Lambda-1)]^2}{2C_5(P)}$
${}^{O}Q_{35}(J)$	${}^{S}Q_{53}(J)$	0	$\dfrac{v_5^-v_4^{+2}v_5^+[v_3^+v_6^+ + 4(v_6^- - \Lambda)(2\Lambda-1)]^2}{C_5(Q)}$
${}^{P}R_{35}(J)$	${}^{R}P_{53}(J+1)$	0	$\dfrac{v_4^{+2}v_5^{+2}[v_3^+v_6^+ + 4(v_6^- - \Lambda)(2\Lambda-1)]^2}{2C_5(R)}$
${}^{O}P_{45}(J)$	${}^{S}R_{54}(J-1)$	0	$\dfrac{6v_3^-v_4^-v_5^-v_5^+[v_4^-v_6^+ - 2\Lambda(2\Lambda-1)]^2}{C_5(P)}$
${}^{P}Q_{45}(J)$	${}^{R}Q_{54}(J)$	0	$\dfrac{12v_4^-v_5^-v_5^{+2}[v_4^-v_6^+ - 2\Lambda(2\Lambda-1)]^2}{C_5(Q)}$
${}^{Q}R_{45}(J)$	${}^{Q}P_{54}(J+1)$	0	$\dfrac{6v_5^-v_5^{+2}v_6^+[v_4^-v_6^+ - 2\Lambda(2\Lambda-1)]^2}{C_5(R)}$
$P_5(J)$	$R_5(J-1)$	$\dfrac{v_2^-v_3^-}{2J}$	$\dfrac{v_2^-v_3^-v_4^-v_5^-[v_3^-v_6^- - 4(v_6^+ + \Lambda)(2\Lambda+1)]}{2C_5(P)}$
$Q_5(J)$	$Q_5(J)$	$\dfrac{v_6^+v_3^-\left(J+\frac{1}{2}\right)}{J(J+1)}$	$\dfrac{v_3^-v_4^-v_5^-v_6^+[v_3^-v_6^- - 4(v_6^+ + \Lambda)(2\Lambda+1)]}{C_5(Q)}$
$R_5(J)$	$P_5(J+1)$	$\dfrac{v_6^+v_7^+}{2(J+1)}$	$\dfrac{v_4^-v_5^-v_6^+v_7^+[v_3^-v_6^- - 4(v_6^+ + \Lambda)(2\Lambda+1)]^2}{2C_5(R)}$

(continued)

strengths

${}^{7}X(b) - {}^{7}Y(a)$	${}^{7}X(b) - {}^{6}Y(b)$
$(\Lambda+1)^2 \dfrac{60v_4^{-2}v_5^-v_5^+v_6^+v_7^+}{C_6(Q)}$	0
$(\Lambda+1)^2 \dfrac{30v_5^-v_6^-v_5^+v_6^+v_7^+v_8^+}{C_6^+(R)}$	0
$\dfrac{10v_3^{-2}v_4^{-2}v_5^-v_5^+v_6^+v_7^+}{C_7^-(P)}$	0
$\dfrac{20v_4^{-2}v_5^-v_6^-v_5^+v_6^+v_7^+v_8^+}{C_7(Q)}$	0
$\dfrac{10v_5^-v_6^-v_7^-v_5^+v_6^+v_7^+v_8^+v_9^+}{C_7^+(R)}$	0
$\dfrac{15v_0^-v_1^-v_2^-v_3^-v_2^+v_3^+v_4^+v_5^+}{2C_1^-(P)}$	0
$\dfrac{15v_1^-v_2^-v_3^-v_3^+v_4^+v_5^+v_6^{+2}}{C_1(Q)}$	0
$\dfrac{15v_2^-v_3^-v_4^+v_5^+v_6^{+2}v_7^{+2}}{2C_1^+(R)}$	0
$\dfrac{5v_1^-v_2^-v_3^-v_3^+v_4^+v_5^+(v_{-2}^- - 2\Lambda)^2}{2C_2^-(P)}$	0
$\dfrac{5v_2^-v_3^-v_4^+v_5^+v_6^{+2}(v_{-1}^- - 2\Lambda)^2}{C_2(Q)}$	0
$\dfrac{5v_3^-v_5^+v_6^{+2}v_7^{+2}[v_0^- - 2\Lambda]^2}{2C_2^+(R)}$	0
$\dfrac{v_2^-v_3^-v_4^+v_5^+[v_3^+v_6^+ + 4(v_0^- - \Lambda)(2\Lambda+3)]^2}{2C_3^-(P)}$	0
$\dfrac{v_3^-v_5^+v_6^{+2}[v_4^+v_7^+ + 4(v_1^- - \Lambda)(2\Lambda+3)]^2}{C_3(Q)}$	0
$\dfrac{v_6^{+2}v_7^{+2}[v_5^+v_8^+ + 4(v_2^- - \Lambda)(2\Lambda+3)]^2}{2C_3^+(R)}$	$\dfrac{18v_4^-v_5^-}{(J+1)^3(2J+1)(2J+3)}$
$\dfrac{3v_2^{-2}v_3^-v_5^+[v_1^-v_6^+ - 2(\Lambda+1)(2\Lambda+3)]^2}{2C_4^-(P)}$	0
$\dfrac{3v_3^{-2}v_6^{+2}[v_2^-v_7^+ - 2(\Lambda+1)(2\Lambda+3)]^2}{C_4(Q)}$	$\dfrac{3v_4^-v_5^-(J-1)(2J+5)}{J(J+1)^3(2J+3)}$
$\dfrac{3v_4^-v_6^+v_7^{+2}[v_3^-v_8^+ - 2(\Lambda+1)(2\Lambda+3)]^2}{2C_4^+(R)}$	$\dfrac{3v_5^-v_6^+(2J-1)}{(J+1)^2(J+2)}$
$\dfrac{v_2^{-2}v_3^{-2}[v_1^-v_4^- - 4(v_7^+ + \Lambda)(2\Lambda+3)]^2}{2C_5^-(P)}$	$\dfrac{v_4^-v_5^-(J-1)(J+2)(2J-3)(2J+5)}{2J(J+1)^2(2J+1)(2J+3)}$
$\dfrac{v_3^{-2}v_4^-v_6^+[v_2^-v_5^- - 4(v_8^+ + \Lambda)(2\Lambda+3)]^2}{C_5(Q)}$	$\dfrac{v_5^-v_6^+(J^2+2J-5)^2(2J+1)}{4J(J+1)^3(J+2)}$
$\dfrac{v_4^-v_5^-v_6^+v_7^+[v_3^-v_6^- - 4(v_9^+ + \Lambda)(2\Lambda+3)]^2}{2C_5^+(R)}$	$\dfrac{v_6^+v_7^+J(J+3)(2J+1)(2J+7)}{2(J+1)(J+2)^2(2J-3)(2J+5)}$

Table II

Branches		Line	
$\Delta\Lambda = +1$	$\Delta\Lambda = -1$	${}^{7}X(a) - {}^{7}Y(a)$	${}^{7}X(a) - {}^{7}Y(b)$
${}^{Q}P_{65}(J)$	${}^{Q}R_{56}(J-1)$	0	$\frac{5v_1^-v_2^-v_3^-v_4^-v_5^-v_6^+[v_8^+ + 2\Lambda]^2}{C_5(P)}$
${}^{R}Q_{65}(J)$	${}^{P}Q_{56}(J)$	0	$\frac{10v_2^-v_3^-v_4^-v_5^-v_6^+v_7^+[v_8^+ + 2\Lambda]^2}{C_5(Q)}$
${}^{S}R_{65}(J)$	${}^{O}P_{56}(J+1)$	0	$\frac{5v_3^-v_4^-v_5^-v_6^+v_7^+v_8^+[v_8^+ + 2\Lambda]^2}{C_5(R)}$
${}^{R}P_{75}(J)$	${}^{P}R_{57}(J-1)$	0	$\frac{15v_0^-v_1^-v_2^-v_3^-v_4^-v_5^-v_6^+v_7^+}{2C_5(P)}$
${}^{S}Q_{75}(J)$	${}^{O}Q_{57}(J)$	0	$\frac{15v_1^-v_2^-v_3^-v_4^-v_5^-v_6^+v_7^+v_8^+}{C_5(Q)}$
${}^{T}R_{75}(J)$	${}^{N}P_{57}(J+1)$	0	$\frac{15v_2^-v_3^-v_4^-v_5^-v_6^+v_7^+v_8^+v_9^+}{2C_5(R)}$
${}^{K}P_{16}(J)$	${}^{W}R_{61}(J-1)$	0	$\frac{3v_6^-v_7^{-2}v_2^+v_3^+v_4^+v_5^+v_6^+}{2C_6(P)}$
${}^{L}Q_{16}(J)$	${}^{V}Q_{61}(J)$	0	$\frac{3v_7^{-2}v_2^{+2}v_3^+v_4^+v_5^+v_6^+}{C_6(Q)}$
${}^{M}R_{16}(J)$	${}^{U}P_{61}(J+1)$	0	$\frac{3v_7^-v_2^{+2}v_3^{+2}v_4^+v_5^+v_6^+}{2C_6(R)}$
${}^{L}P_{26}(J)$	${}^{V}R_{62}(J-1)$	0	$\frac{v_5^-v_6^-v_3^+v_4^+v_5^+v_6^+[2v_7^- - \Lambda]^2}{C_6(P)}$
${}^{M}Q_{26}(J)$	${}^{U}Q_{62}(J)$	0	$\frac{2v_6^-v_3^+v_4^+v_5^+v_6^+[2v_7^- - \Lambda]^2}{C_6(Q)}$
${}^{N}R_{26}(J)$	${}^{T}P_{62}(J+1)$	0	$\frac{v_3^{+2}v_4^{+2}v_5^+v_6^+[2v_7^- - \Lambda]^2}{C_6(R)}$
${}^{M}P_{36}(J)$	${}^{U}R_{63}(J-1)$	0	$\frac{5v_4^-v_5^-v_6^-v_4^+v_5^+v_6^+[v_7^- - 2\Lambda]^2}{2C_6(P)}$
${}^{N}Q_{36}(J)$	${}^{T}Q_{63}(J)$	0	$\frac{5v_5^-v_6^-v_4^{+2}v_5^+v_6^+[v_7^- - 2\Lambda]^2}{C_6(Q)}$
${}^{O}R_{36}(J)$	${}^{S}P_{63}(J+1)$	0	$\frac{5v_6^-v_4^{+2}v_5^{+2}v_6^+[v_7^- - 2\Lambda]^2}{2C_6(R)}$
${}^{N}P_{46}(J)$	${}^{T}R_{64}(J-1)$	0	$\Lambda^2\,\frac{30v_3^-v_4^-v_5^-v_6^-v_5^+v_6^+}{C_6(P)}$
${}^{O}Q_{46}(J)$	${}^{S}Q_{64}(J)$	0	$\Lambda^2\,\frac{60v_4^-v_5^-v_6^-v_5^{+2}v_6^+}{C_6(Q)}$
${}^{P}R_{46}(J)$	${}^{R}P_{64}(J+1)$	0	$\Lambda^2\,\frac{30v_5^-v_6^-v_5^{+2}v_6^{+2}}{C_6(R)}$
${}^{O}P_{56}(J)$	${}^{S}R_{65}(J-1)$	0	$\frac{5v_2^-v_3^-v_4^-v_5^-v_6^-v_6^+[v_7^+ + 2\Lambda]^2}{2C_6(P)}$
${}^{P}Q_{56}(J)$	${}^{R}Q_{65}(J)$	0	$\frac{5v_3^-v_4^-v_5^-v_6^-v_6^{+2}[v_7^+ + 2\Lambda]^2}{C_6(Q)}$

(continued)

strengths

${}^7X(b)-{}^7Y(a)$	${}^7X(b)-{}^7Y(b)$
$\frac{5v_2^-{}^2v_3^-{}^2v_4^-v_6^+[v_9^+ + 2\Lambda]^2}{2C_6^-(P)}$	$\frac{2v_5^-v_6^+(J-1)(2J+5)}{2J(J+1)^2(J+2)^2}$
$\frac{5v_3^-{}^2v_4^-v_5^-v_6^+v_7^+[v_{10}^+ + 2\Lambda]^2}{C_6(Q)}$	$\frac{5v_6^+v_7^+(J+3)(2J-1)(2J+1)}{2J(J+1)(J+2)^2(2J+3)(2J+5)}$
$\frac{5v_4^-v_5^-v_6^-v_6^+v_7^+v_8^+[v_{11}^+ + 2\Lambda]^2}{2C_6^+(R)}$	0
$\frac{15v_2^-{}^2v_3^-{}^2v_4^-v_5^-v_6^+v_7^+}{2C_7^-(P)}$	$\frac{15v_6^+v_7^+}{2J(J+2)^2(2J+3)(2J+5)}$
$\frac{15v_3^-{}^2v_4^-v_5^-v_6^-v_6^+v_7^+v_8^+}{C_7(Q)}$	0
$\frac{15v_4^-v_5^-v_6^-v_7^-v_6^+v_7^+v_8^+v_9^+}{2C_7^+(R)}$	0
$\frac{3v_0^-v_1^-v_2^-v_2^+v_3^+v_4^+v_5^+v_6^+}{C_1^-(P)}$	0
$\frac{6v_1^-v_2^-v_3^+v_4^+v_5^+v_6^+v_7^+{}^2}{C_1(Q)}$	0
$\frac{3v_2^-v_4^+v_5^+v_6^+v_7^+{}^2v_8^+{}^2}{C_1^+(R)}$	0
$\frac{v_1^-v_2^-v_3^+v_4^+v_5^+v_6^+[2v_2^+ - \Lambda - 1]^2}{C_2^-(P)}$	0
$\frac{2v_2^-v_4^+v_5^+v_6^+v_7^+{}^2[2v_3^+ - \Lambda - 1]^2}{C_2(Q)}$	0
$\frac{v_5^+v_6^+v_7^+{}^2v_8^+{}^2[2v_4^+ - \Lambda - 1]^2}{C_2^+(R)}$	0
$\frac{5v_1^-{}^2v_2^-v_4^+v_5^+v_6^+[v_{-3}^- - 2\Lambda]^2}{C_3^-(P)}$	0
$\frac{10v_2^-{}^2v_5^+v_6^+v_7^+{}^2[v_{-2}^- - 2\Lambda]^2}{C_3(Q)}$	0
$\frac{5v_3^-v_6^+v_7^+{}^2v_8^+{}^2(v_{-1}^- - 2\Lambda)^2}{C_3^+(R)}$	0
$(\Lambda+2)^2\,\frac{15v_1^-{}^2v_2^-{}^2v_5^+v_6^+}{C_4^-(P)}$	0
$(\Lambda+2)^2\,\frac{30v_2^-{}^2v_3^-v_6^+v_7^+{}^2}{C_4(Q)}$	0
$(\Lambda+2)^2\,\frac{15v_3^-v_4^-v_7^+{}^2v_8^+{}^2}{C_4^+(R)}$	$\frac{15v_5^-v_6^-}{(J+1)(J+2)^2(2J+3)(2J+5)}$
$\frac{5v_1^-{}^2v_2^-{}^2v_3^-v_6^+[v_{10}^+ + 2\Lambda]^2}{C_5^-(P)}$	0
$\frac{10v_2^-{}^2v_3^-v_4^-v_7^+{}^2[v_{11}^+ + 2\Lambda]^2}{C_5(Q)}$	$\frac{5v_5^-v_6^-(J+3)(2J-1)(2J+1)}{2J(J+1)(J+2)^2(2J+3)(2J+5)}$

Table II

Branches		Line	
$\Delta\Lambda = +1$	$\Delta\Lambda = -1$	${}^{\nu}X(a) - {}^{\nu}Y(a)$	${}^{\nu}X(a) - {}^{\nu}X(b)$
${}^{Q}R_{56}(J)$	${}^{P}P_{65}(J+1)$	0	$\frac{5v_4^- v_5^- v_6^- v_6^{+2} v_7^+ [v_7^+ + 2\Lambda]^2}{2C_6(R)}$
$P_6(J)$	$R_6(J-1)$	$\frac{v_1^- v_2^-}{2J}$	$\frac{v_1^- v_2^- v_3^- v_4^- v_5^- v_6^- [2v_7^+ + \Lambda]^2}{C_6(P)}$
$Q_6(J)$	$Q_6(J)$	$\frac{v_7^+ v_2^- \left(J + \frac{1}{2}\right)}{J(J+1)}$	$\frac{2v_2^- v_3^- v_4^- v_5^- v_6^- v_7^+ [2v_7^+ + \Lambda]^2}{C_6(Q)}$
$R_6(J)$	$P_6(J+1)$	$\frac{v_7^+ v_8^+}{2(J+1)}$	$\frac{v_3^- v_4^- v_5^- v_6^- v_7^+ v_8^+ [2v_7^+ + \Lambda]^2}{C_6(R)}$
${}^{Q}P_{76}(J)$	${}^{Q}R_{67}(J-1)$	0	$\frac{3v_0^- v_1^- v_2^- v_3^- v_4^- v_5^- v_6^- v_7^+}{2C_6(P)}$
${}^{R}Q_{76}(J)$	${}^{P}Q_{67}(J)$	0	$\frac{3v_1^- v_2^- v_3^- v_4^- v_5^- v_6^- v_7^+ v_8^+}{C_6(Q)}$
${}^{S}R_{76}(J)$	${}^{O}P_{67}(J+1)$	0	$\frac{3v_2^- v_3^- v_4^- v_5^- v_6^- v_7^+ v_8^+ v_9^+}{2C_6(R)}$
${}^{J}P_{17}(J)$	${}^{Z}R_{71}(J-1)$	0	$\frac{v_6^- v_7^- v_2^+ v_3^+ v_4^+ v_5^+ v_6^+ v_7^+}{2C_7(P)}$
${}^{K}Q_{17}(J)$	${}^{W}Q_{71}(J)$	0	$\frac{v_7^- v_2^{+2} v_3^+ v_4^+ v_5^+ v_6^+ v_7^+}{C_7(Q)}$
${}^{L}R_{17}(J)$	${}^{V}P_{71}(J+1)$	0	$\frac{v_2^{+2} v_3^{+2} v_4^+ v_5^+ v_6^+ v_7^+}{2C_7(R)}$
${}^{K}P_{27}(J)$	${}^{W}R_{72}(J-1)$	0	$\frac{3v_5^- v_6^- v_7^- v_3^+ v_4^+ v_5^+ v_6^+ v_7^+}{C_7(P)}$
${}^{L}Q_{27}(J)$	${}^{V}Q_{72}(J)$	0	$\frac{6v_6^- v_7^- v_3^{+2} v_4^+ v_5^+ v_6^+ v_7^+}{C_7(Q)}$
${}^{M}R_{27}(J)$	${}^{U}P_{72}(J+1)$	0	$\frac{3v_7^- v_3^{+2} v_4^{+2} v_5^+ v_6^+ v_7^+}{C_7(R)}$
${}^{L}P_{37}(J)$	${}^{V}R_{73}(J-1)$	0	$\frac{15v_4^- v_5^- v_6^- v_7^- v_4^+ v_5^+ v_6^+ v_7^+}{2C_7(P)}$
${}^{M}Q_{37}(J)$	${}^{U}Q_{73}(J)$	0	$\frac{15v_5^- v_6^- v_7^- v_4^{+2} v_5^+ v_6^+ v_7^+}{C_7(Q)}$
${}^{N}R_{37}(J)$	${}^{T}P_{73}(J+1)$	0	$\frac{15v_6^- v_7^- v_4^{+2} v_5^{+2} v_6^+ v_7^+}{2C_7(R)}$
${}^{M}P_{47}(J)$	${}^{U}R_{74}(J-1)$	0	$\frac{10v_3^- v_4^- v_5^- v_6^- v_7^- v_5^+ v_6^+ v_7^+}{C_7(P)}$
${}^{N}Q_{47}(J)$	${}^{T}Q_{74}(J)$	0	$\frac{20v_4^- v_5^- v_6^- v_7^- v_5^{+2} v_6^+ v_7^+}{C_7(Q)}$
${}^{O}R_{47}(J)$	${}^{S}P_{74}(J+1)$	0	$\frac{10v_5^- v_6^- v_7^- v_5^{+2} v_6^{+2} v_7^+}{C_7(R)}$
${}^{N}P_{57}(J)$	${}^{T}R_{75}(J-1)$	0	$\frac{15v_2^- v_3^- v_4^- v_5^- v_6^- v_7^- v_6^+ v_7^+}{2C_7(P)}$

(continued)

strengths

$^7X(b) - {}^7Y(a)$	$^7X(b) - {}^7Y(b)$
$\frac{5v_3^- v_4^- v_7^+ v_8^{+2}[v_{12}^+ + 2\Lambda]^2}{C_5^+(R)}$	$\frac{5v_6^- v_7^+ J(2J+7)}{2(J+1)(J+2)^2(J+3)^3}$
$\frac{v_1^{-2} v_2^{-2} v_3^- v_4^-[2v_7^+ + \Lambda + 1]^2}{C_6^-(P)}$	$\frac{v_5^- v_6^-(J-1)(J+3)(2J-1)}{2J(J+2)^2(2J+3)}$
$\frac{2v_2^{-2} v_3^- v_4^- v_5^- v_7^+[2v_8^+ + \Lambda + 1]^2}{C_6(Q)}$	$\frac{v_6^- v_7^+(J^2+3J-3)^2(2J+1)}{4J(J+1)(J+2)^2(J+3)^2}$
$\frac{v_3^- v_4^- v_5^- v_6^- v_7^+ v_8^+[2v_9^+ + \Lambda + 1]^2}{C_6^+(R)}$	$\frac{v_7^+ v_8^+ J(J+4)(2J+1)}{2(J+1)(J+3)^2(2J+5)}$
$\frac{3v_1^{-2} v_2^{-2} v_3^- v_4^- v_5^- v_7^+}{C_7^-(P)}$	$\frac{3v_6^- v_7^+(2J+1)}{2J(J+2)^2(J+3)}$
$\frac{6v_2^{-2} v_3^- v_4^- v_5^- v_6^- v_7^+ v_8^+}{C_7(Q)}$	$\frac{3v_7^+ v_8^+}{2(J+1)(J+3)^2(2J+5)}$
$\frac{3v_3^- v_4^- v_5^- v_6^- v_7^- v_8^+ v_9^+}{C_7^+(R)}$	0
$\frac{v_0^- v_1^- v_2^+ v_3^+ v_4^+ v_5^+ v_6^+ v_7^+}{2C_1^-(P)}$	0
$\frac{v_1^- v_3^+ v_4^+ v_5^+ v_6^+ v_7^+ v_8^{+2}}{C_1(Q)}$	0
$\frac{v_4^+ v_5^+ v_6^+ v_7^+ v_8^{+2} v_9^{+2}}{2C_1^+(R)}$	0
$\frac{3v_0^{-2} v_1^- v_3^+ v_4^+ v_5^+ v_6^+ v_7^+}{2C_2^-(P)}$	0
$\frac{3v_1^{-2} v_4^+ v_5^+ v_6^+ v_7^+ v_8^{+2}}{C_2(Q)}$	0
$\frac{3v_2^- v_5^+ v_6^+ v_7^+ v_8^{+2} v_9^{+2}}{2C_2^+(R)}$	0
$\frac{15v_0^{\ 2} v_1^{-2} v_4^+ v_5^+ v_6^+ v_7^+}{2C_3^-(P)}$	0
$\frac{15v_1^{-2} v_2^- v_5^+ v_6^+ v_7^+ v_8^{+2}}{C_3(Q)}$	0
$\frac{15v_2^- v_3^- v_6^+ v_7^+ v_8^{+2} v_9^{+2}}{2C_3^+(R)}$	0
$\frac{5v_0^{-2} v_1^{-2} v_2^- v_5^+ v_6^+ v_7^+}{2C_4^-(P)}$	0
$\frac{5v_1^{-2} v_2^- v_3^- v_6^+ v_7^+ v_8^{+2}}{C_4(Q)}$	0
$\frac{5v_2^- v_3^- v_4^- v_7^+ v_8^{+2} v_9^{+2}}{2C_4^+(R)}$	0
$\frac{15v_0^{-2} v_1^{-2} v_2^- v_3^- v_6^+ v_7^+}{2C_5^-(P)}$	0

Table II

Branches		Line	
$\Delta\Lambda = +1$	$\Delta\Lambda = -1$	${}^{7}X(a) - {}^{7}Y(a)$	${}^{7}X(a) - {}^{7}Y(b)$
${}^{O}Q_{57}(J)$	${}^{S}Q_{75}(J)$	0	$\frac{15v_3^- v_4^- v_5^- v_6^- v_7^- v_6^{+2} v_7^+}{C_7(Q)}$
${}^{P}R_{57}(J)$	${}^{R}P_{75}(J+1)$	0	$\frac{15v_4^- v_5^- v_6^- v_7^- v_6^{+2} v_7^{+2}}{2C_7(R)}$
${}^{O}P_{67}(J)$	${}^{S}R_{76}(J-1)$	0	$\frac{3v_1^- v_2^- v_3^- v_4^- v_5^- v_6^- v_7^- v_7^+}{C_7(P)}$
${}^{P}Q_{67}(J)$	${}^{R}Q_{76}(J)$	0	$\frac{6v_2^- v_3^- v_4^- v_5^- v_6^- v_7^- v_7^{+2}}{C_7(Q)}$
${}^{Q}R_{67}(J)$	${}^{Q}P_{76}(J+1)$	0	$\frac{3v_3^- v_4^- v_5^- v_6^- v_7^- v_7^{+2} v_8^+}{C_7(R)}$
$P_7(J)$	$R_7(J-1)$	$\frac{v_0^- v_1^-}{2J}$	$\frac{v_0^- v_1^- v_2^- v_3^- v_4^- v_5^- v_6^- v_7^-}{2C_7(P)}$
$Q_7(J)$	$Q_7(J)$	$\frac{v_1^- v_8^+ \left(J+\frac{1}{2}\right)}{J(J+1)}$	$\frac{v_1^- v_2^- v_3^- v_4^- v_5^- v_6^- v_7^- v_8^+}{C_7(Q)}$
$R_7(J)$	$P_7(J+1)$	$\frac{v_8^+ v_9^+}{2(J+1)}$	$\frac{v_2^- v_3^- v_4^- v_5^- v_6^- v_7^- v_8^+ v_9^+}{2C_7(R)}$

(continued)

strengths

${}^{?}X(b) - {}^{?}Y(a)$	${}^{?}X(b) - {}^{?}Y(b)$
$\frac{15v_1^{-2}v_2^-v_3^-v_4^-v_7^+v_8^{+2}}{C_5(Q)}$	0
$\frac{15v_2^-v_3^-v_4^-v_5^-v_8^{+2}v_9^{+2}}{2C_5^+(R)}$	$\frac{15v_6^-v_7^-}{2(J+1)(J+3)^2(2J+5)(2J+7)}$
$\frac{3v_0^{-2}v_1^{-2}v_2^-v_3^-v_4^-v_7^+}{2C_6^-(P)}$	0
$\frac{3v_1^{-2}v_2^-v_3^-v_4^-v_5^-v_8^{+2}}{C_6(Q)}$	$\frac{3v_6^-v_7^-(2J+1)}{2(J+1)(J+3)^2}$
$\frac{3v_2^-v_3^-v_4^-v_5^-v_6^-v_8^+v_9^{+2}}{2C_6^+(R)}$	$\frac{3v_7^-v_8^+(2J+1)}{2(J+1)(J+3)^2(J+4)}$
$\frac{v_0^{-2}v_1^{-2}v_2^-v_3^-v_4^-v_5^-}{2C_7^-(P)}$	$\frac{v_6^-v_7^-(2J-1)}{2(J+3)(2J+5)}$
$\frac{v_1^{-2}v_2^-v_3^-v_4^-v_5^-v_6^-v_8^+}{C_7(Q)}$	$\frac{v_7^-v_8^-J(2J+1)}{4(J+1)(J+3)^2}$
$\frac{v_2^-v_3^-v_4^-v_5^-v_6^-v_7^-v_8^+v_9^+}{2C_7^+(R)}$	$\frac{v_8^+v_9^+(2J+1)}{2(J+4)(2J+7)}$

Table III

Intensity scattering of the main branches of the (a) — (a) quartet transition over the main and satellite branches of the (a) — (b) transition

(a) — (a)	(a) — (b)			
$S_1^A(a)$	S_1^A	S_{21}^A	S_{31}^A	S_{41}^A
	$\frac{1}{8}S_1^A(a)$	$\frac{3}{8}S_1^A(a)$	$\frac{3}{8}S_1^A(a)$	$\frac{1}{8}S_1^A(a)$
$S_2^A(a)$	S_{12}^A	S_2^A	S_{32}^A	S_{42}^A
	$\frac{3}{8}S_2^A(a)$	$\frac{1}{8}S_2^A(a)$	$\frac{1}{8}S_2^A(a)$	$\frac{3}{8}S_2^A(a)$
$S_3^A(a)$	S_{13}^A	S_{23}^A	S_3^A	S_{43}^A
	$\frac{3}{8}S_3^A(a)$	$\frac{1}{8}S_3^A(a)$	$\frac{1}{8}S_3^A(a)$	$\frac{3}{8}S_3^A(a)$
$S_4^A(a)$	S_{14}^A	S_{24}^A	S_{34}^A	S_4^A
	$\frac{1}{8}S_4^A(a)$	$\frac{3}{8}S_4^A(a)$	$\frac{3}{8}S_4^A(a)$	$\frac{1}{8}S_4^A(a)$

Table IV

Intensity scattering of the main branches of the (a) — (a) quintet transition over the main and satellite branches of the (a) — (b) transition

(a) — (a)	(a) — (b)				
$S_1^A(a)$	S_1^A	S_{21}^A	S_{31}^A	S_{41}^A	S_{51}^A
	$\frac{1}{16} S_1^A(a)$	$\frac{4}{16} S_1^A(a)$	$\frac{6}{16} S_1^A(a)$	$\frac{4}{16} S_1^A(a)$	$\frac{1}{16} S_1^A(a)$
$S_2^A(a)$	S_{12}^A	S_2^A	S_{32}^A	S_{42}^A	S_{52}^A
	$\frac{4}{16} S_2^A(a)$	$\frac{4}{16} S_2^A(a)$	0	$\frac{4}{16} S_2^A(a)$	$\frac{4}{16} S_2^A(a)$
$S_3^A(a)$	S_{13}^A	S_{23}^A	S_3^A	S_{43}^A	S_{53}^A
	$\frac{6}{16} S_3^A(a)$	0	$\frac{4}{16} S_3^A(a)$	0	$\frac{6}{16} S_3^A(a)$
$S_4^A(a)$	S_{14}^A	S_{24}^A	S_{34}^A	S_4^A	S_{54}^A
	$\frac{4}{16} S_4^A(a)$	$\frac{4}{16} S_4^A(a)$	0	$\frac{4}{16} S_4^A(a)$	$\frac{4}{16} S_4^A(a)$
$S_5^A(a)$	S_{15}^A	S_{25}^A	S_{35}^A	S_{45}^A	S_5^A
	$\frac{1}{16} S_5^A(a)$	$\frac{4}{16} S_5^A(a)$	$\frac{6}{16} S_5^A(a)$	$\frac{4}{16} S_5^A(a)$	$\frac{1}{16} S_5^A(a)$

Table V

Intensity scattering of the main branches of the (*a*) — (*a*) sextet transition over the main and satellite branches of the (*a*) — (*b*) transition

(*a*) — (*a*)	(*a*) — (*b*)					
$S_1^A(a)$	S_1^A	S_{21}^A	S_{31}^A	S_{41}^A	S_{51}^A	S_{61}^A
	$\frac{1}{32} S_1^A(a)$	$\frac{5}{32} S_1^A(a)$	$\frac{10}{32} S_1^A(a)$	$\frac{10}{32} S_1^A(a)$	$\frac{5}{32} S_1^A(a)$	$\frac{1}{32} S_1^A(a)$
$S_2^A(a)$	S_{12}^A	S_2^A	S_{32}^A	S_{42}^A	S_{52}^A	S_{62}^A
	$\frac{5}{32} S_2^A(a)$	$\frac{9}{32} S_2^A(a)$	$\frac{2}{32} S_2^A(a)$	$\frac{2}{32} S_2^A(a)$	$\frac{9}{32} S_2^A(a)$	$\frac{5}{32} S_2^A(a)$
$S_3^A(a)$	S_{13}^A	S_{23}^A	S_3^A	S_{43}^A	S_{53}^A	S_{63}^A
	$\frac{10}{32} S_3^A(a)$	$\frac{2}{32} S_3^A(a)$	$\frac{4}{32} S_3^A(a)$	$\frac{4}{32} S_3^A(a)$	$\frac{2}{32} S_3^A(S)$	$\frac{10}{32} S_3^A(a)$
$S_4^A(a)$	S_{14}^A	S_{24}^A	S_{34}^A	S_4^A	S_{54}^A	S_{64}^A
	$\frac{10}{32} S_4^A(a)$	$\frac{2}{32} S_4^A(a)$	$\frac{4}{32} S_4^A(a)$	$\frac{4}{32} S_4^A(a)$	$\frac{2}{32} S_4^A(a)$	$\frac{10}{32} S_4^A(a)$
$S_5^A(a)$	S_{15}^A	S_{25}^A	S_{35}^A	S_{45}^A	S_5^A	S_{65}^A
	$\frac{5}{32} S_5^A(a)$	$\frac{9}{32} S_5^A(a)$	$\frac{2}{32} S_5^A(a)$	$\frac{2}{32} S_5^A(a)$	$\frac{9}{32} S_5^A(a)$	$\frac{5}{32} S_5^A(a)$
$S_6^A(a)$	S_{16}^A	S_{26}^A	S_{36}^A	S_{46}^A	S_{56}^A	S_6^A
	$\frac{1}{32} S_6^A(a)$	$\frac{5}{32} S_6^{A\prime}a)$	$\frac{10}{32} S_6^A(a)$	$\frac{10}{32} S_6^A(a)$	$\frac{5}{32} S_6^A(a)$	$\frac{1}{32} S_6^A(a)$

Table VI

Intensity scattering of the main branches of the $(a) - (a)$ septet transition over the main and satellite branches of the $(a) - (b)$ transition

$(a) - (a)$	$(a) - (b)$						
$S_1^A(a)$	S_1^A	S_{21}^A	S_{31}^A	S_{41}^A	S_{51}^A	S_{61}^A	S_{71}^A
	$\frac{1}{64} S_1^A(a)$	$\frac{6}{64} S_1^A(a)$	$\frac{15}{64} S_1^A(a)$	$\frac{20}{64} S_1^A(a)$	$\frac{15}{64} S_1^A(a)$	$\frac{6}{64} S_1^A(a)$	$\frac{1}{64} S_1^A(a)$
$S_2^A(a)$	S_{12}^A	S_2^A	S_{32}^A	S_{42}^A	S_{52}^A	S_{62}^A	S_{72}^A
	$\frac{6}{64} S_2^A(a)$	$\frac{16}{46} S_2^A(a)$	$\frac{10}{64} S_2^A(a)$	0	$\frac{10}{64} S_2^A(a)$	$\frac{16}{46} S_2^A(a)$	$\frac{6}{64} S_2^A(a)$
$S_3^A(a)$	S_{13}^A	S_{23}^A	S_3^A	S_{43}^A	S_{53}^A	S_{63}^A	S_{73}^A
	$\frac{15}{64} S_3^A(a)$	$\frac{10}{64} S_3^A(a)$	$\frac{1}{64} S_3^A(a)$	$\frac{12}{64} S_3^A(a)$	$\frac{1}{64} S_3^A(a)$	$\frac{10}{64} S_3^A(a)$	$\frac{15}{64} S_3^A(a)$
$S_4^A(a)$	S_{14}^A	S_{24}^A	S_{34}^A	S_4^A	S_{54}^A	S_{64}^A	S_{74}^A
	$\frac{20}{64} S_4^A(a)$	0	$\frac{12}{64} S_4^A(a)$	0	$\frac{12}{64} S_4^A(a)$	0	$\frac{20}{64} S_4^A(a)$
$S_5^A(a)$	S_{15}^A	S_{25}^A	S_{35}^A	S_{45}^A	S_5^A	S_{65}^A	S_{75}^A
	$\frac{15}{64} S_5^A(a)$	$\frac{10}{64} S_5^A(a)$	$\frac{1}{64} S_5^A(a)$	$\frac{12}{64} S_5^A(a)$	$\frac{1}{64} S_5^A(a)$	$\frac{10}{64} S_5^A(a)$	$\frac{15}{64} S_5^A(a)$
$S_6^A(a)$	S_{16}^A	S_{26}^A	S_{36}^A	S_{46}^A	S_{56}^A	S_6^A	S_{76}^A
	$\frac{6}{64} S_6^A(a)$	$\frac{16}{64} S_6^A(a)$	$\frac{10}{64} S_6^A(a)$	0	$\frac{10}{64} S_6^A(a)$	$\frac{16}{64} S_6^A(a)$	$\frac{6}{64} S_6^A(a)$
$S_7^A(a)$	S_{17}^A	S_{27}^A	S_{37}^A	S_{47}^A	S_{57}^A	S_{67}^A	S_7^A
	$\frac{1}{64} S_7^A(a)$	$\frac{6}{64} S_7^A(a)$	$\frac{15}{64} S_7^A(a)$	$\frac{20}{64} S_7^A(a)$	$\frac{15}{64} S_7^A(a)$	$\frac{6}{64} S_7^A(a)$	$\frac{1}{64} S_7^A(a)$

Acta Physica Academiae Scientiarum Hungaricae, Tomus 45 (4), pp. 363—369 (1978)

THE EFFECT OF ROTATION-VIBRATIONAL INTERACTION ON THE LINE INTENSITIES IN THE OPTICAL SPECTRA OF DIATOMIC MOLECULES

By

A. I. KOBYLANSKY

INSTITUTE FOR HIGH TEMPERATURES, MOSCOW, USSR

(Received 28. XI. 1978)

Using perturbation calculation simple relations have been received that make possible to evaluate the appearance of rotation-vibrational interaction in the line intensity of gaseous diatomic molecules from a sufficient number of experimental data. The connection between the rotational temperature determined from the optical spectra neglecting rotation-vibrational interaction and the real rotational temperature of the gas has been found.

Introduction

In many practical applications of spectroscopy, especially in those that make it possibile to determine the temperature of a gas from the optical spectra of diatomic molecules it is necessary to know the intensity distribution in the rotational structure of electro-vibrational bands both in emission and in absorption. Generally, in the "0-th order" approximation the relative intensity of lines within the bands is determined by the product of Hönl–London and Boltzman population factors [1], the appearance of centrifugal distortion of the molecule in the vibrational wave function (the rotation-vibrational interaction, RVI) is not considered.

The best example, when the 0-th order approximation is not appropriate to describe line intensities is the UV spectra of OH radical. As it can be seen from the calculation of Franck–Condon factors the effect of RVI on the line intensities at different J quantum numbers corresponds to that of the expected and the same is found even in the spectra of heavier molecules e.g. LaO [2].

In principle, there is no difficulty in calculating the relative intensities of rotational lines considering RVI, using computers. But direct calculation cannot be applied is most cases since that $R_e(r)$ dipole-moment matrix elements and the interaction potential $U(r)$ is unknown in a broad interval of internuclear distance for most molecules.

In the present work a method is suggested for the analysis of the appearance of RVI in the intensity distribution of electro-vibrational spectra of diatomic molecules that is based upon considering the effective rotational potential as a perturbation of $U(r)$. Using the first order of perturbation

calculation the relation to the 0-th order is received and it is possible to determine the corrections. The corrected factors are connected to experimental data, namely to the relative intensities of neighbouring electro-vibrational bands.

Theory

The integral coefficient of absorption or emission for the lines of electro-vibrational transitions in Born–Oppenheimer approximation is

$$S_{if} = A_{if} \nu_{if}^n H(J_i J_f) |\langle v_i J_i | \operatorname{Re} | v_f J_f \rangle|^2 \exp(-c_2 F_i/T); \tag{1}$$

here the subscripts i and f belong to initial and final states correspondingly, A_{if} is constant for a given electro-vibrational transition, ν_{if} is the frequency of the transition, $n = 1$ for absorption, $n = 4$ for emission, $H(J_i, J_f)$ are Hönl–London factors, c_2 is the second radiation constant, F_i is the rotational term, T is the temperature of gas. The functions $|vJ\rangle$ are eigenfunctions of the radial part of the Hamiltonian of the molecule

$$\hat{H}_r = B \frac{d^2}{dr^2} + u(r) + \frac{BQ(J)}{r^2}, \tag{2}$$

where $B = \hbar/4\pi mc$, m is the reduced mass of the molecule, energy is expressed in units of cm^{-1}. The third term corresponds to the effective rotational potential, the function $Q(J)$ is determined by the coupling of angular moments in the specific state of the molecule (in Hund's case a) and c))

$$Q(J) = J(J+1) - \Omega^2,$$

where Ω is the projection of angular momentum to the axis of the molecule). Substituting $Q(J) = 0$ in to Eq. (2), the radial part of the Hamiltonian is received for non-rotating molecule. Let the eigenfunctions of this operator be denoted by $|v\rangle$ and by E_v the corresponding eigenvalues (vibrational levels of a non-rotating molecule).

The effect of RVI on line intensities appears in the dependence of the dipole-moment of the electro-vibrational transition from J_i and J_f. Substituting $\langle v_i J_i | \operatorname{Re} | v_f J_f \rangle$ by $\langle v_i | \operatorname{Re} | v_f \rangle$ in Eq. (1) the 0-th order approximation is received, the line intensities calculated this way in 0-th order are denoted by S_{if}^0.

In order to find the approximated dependence of the radial wave function from J, the effective rotational potential in the operator of Eq. (2) is considered as perturbation. In first approximation the radial wavefunction is

$$|vJ\rangle = |v\rangle + BQ(J) \sum_{u \neq v} \frac{\langle v | r^{-2} | u \rangle}{E_v - E_u}. \tag{3}$$

Typical molecular spectra will be examined having transitions between low vibrational states and the vibrational term is much smaller than disso-

ciation energy. In these states the relative deviations compared to the average internuclear distance are small, thus introducing $x = r - \langle v\,|\,r^{-2}\,|\,v\rangle^{-1/2}$ and keeping only the first two terms in the expansion of r^{-2}

$$r^{-2} = \langle v\,|\,r^{-2}\,|\,v\rangle\,(1 - 2x\langle v\,|\,r^{-2}\,|\,v\rangle^{1/2}) \tag{4}$$

is received.

Substituting Eq. (4) into Eq. (3)

$$|\,vJ\rangle = |\,v\rangle - 2\langle v\,|\,r^{-2}\,|\,v\rangle^{3/2}\,BQ(J)\sum_{u\neq v}\frac{\langle v\,|\,x\,|\,u\rangle}{E_v - E_u}\,. \tag{5}$$

The vibrations of the molecule can be considered harmonic in its lower states therefore it can be assumed that the matrix elements $\langle v\,|\,x\,|\,u\rangle$ are the same as for the harmonic oscillator, that is they differ from 0 only for $u = v \pm 1$.

The error of this approximation can be extimated by Eq. (3) using Morse oscillator. For typical anharmonicity value the factors left in Eq. (5) do not exceed a few percent.

For Morse oscillator just as for harmonic oscillator

$$\langle v\,|\,x\,|\,v+1\rangle = \langle v+1\,|\,x\,|\,v\rangle = \sqrt{\frac{(v+1)\,B}{E_{v+1} - E_v}}\,. \tag{6}$$

Introducing the following notation $\omega = E_v - E_{v-1} \approx E_{v+1} - E_v$, $B\langle v\,|\,r^{-2}\,|\,v\rangle = B_v$ and substituting (6) into (5)

$$|\,vJ\rangle = |\,v\rangle - 2\left(\frac{B_v}{\omega}\right)^{3/2} Q(J)\,(\sqrt{v}\,|\,v-1\,|\rangle - \sqrt{v+1}\,|\,v+1\rangle). \tag{7}$$

The condition of applicability of perturbation calculation is

$$||\,|\,vJ\rangle - |\,v\rangle\,||^2 = 4(2v+1)\left(\frac{Bv}{\omega}\right)^3 Q^2(J) \ll 1 \tag{8}$$

that is satisfied for most of the diatomic molecules (not considering hydrogen and its isotopes) in low vibrational states for values of some hundred of J. Applying Eq. (7)

$$S_{if}/S_{if}^0 = \frac{|\langle v_i J_i\,|\,\mathrm{Re}\,|\,v_f J_f\rangle|^2}{|\langle v_i\,|\,\mathrm{Re}\,|\,v_f\rangle|^2} = [1 - p_i Q(J_i) - p_f Q(J_f)]^2, \tag{9}$$

where

$$p_i = 2\left(\frac{B_i}{\omega_i}\right)^{3/2}\left(\sqrt{v_i}\,\frac{\langle v_i - 1\,|\,\mathrm{Re}\,|\,v_f\rangle}{\langle v_i\,|\,\mathrm{Re}\,|\,v_f\rangle} - \sqrt{v_i+1}\,\frac{\langle v_i + 1\,|\,\mathrm{Re}\,|\,v_f\rangle}{\langle v_i\,|\,\mathrm{Re}\,|\,v_f\rangle}\right), \tag{9a}$$

$$p_f = 2\left(\frac{B_f}{\omega_f}\right)^{3/2}\left(\sqrt{v_f}\,\frac{\langle v_i\,|\,\mathrm{Re}\,|\,v_f - 1\rangle}{\langle v_i\,|\,\mathrm{Re}\,|\,v_f\rangle} - \sqrt{v_f+1}\,\frac{\langle v_i\,|\,\mathrm{Re}\,|\,v_f + 1\rangle}{\langle v_i\,|\,\mathrm{Re}\,|\,v_f\rangle}\right). \tag{9b}$$

In order to determine the effect of RVI on line intensity on the basis of Eq. (9) it is necessary to know the rotational and vibrational constants in both states and four kinds of dipole-moment matrix element. (Especially for 0 — 1 or 1 — 0 band three, for 0 — 0 bands two.)

The square of these matrix elements can be calculated from the relative intensities of the adjoining bands by Delandrés table.

The signs of the dipole-moment matrix elements are given usually by the signs of the overlap integrals of the corresponding harmonic oscillator wavefunctions but the real vibrational functions do not differ significantly from the Hermite polynomials, thus the overlap integrals do not change sign in case they significantly differ from zero.

The relative sign of the Hermite functions are determined by the condition $\langle v \mid x \mid v+1 \rangle \geq 0$ corresponding to the choice of sign in Eq. (6).

Applying Eq. (9) the error in determining the rotational temperature from the spectra of diatomic molecules originating from neglecting the effect of RVI on the nonlinearities can be evaluated. As p_i and p_f are usually much smaller than 1, the appearance of RVI becomes significant only for $J \gg 1$.

Therefore considering selection rules $|J_i - J_f| \leq 1$ $Q(J_f) \approx Q(J_i)$ can be taken.

Denoting

$$\tau(v_i, v_f) = 2(p_i + p_f)/c_2 B_i \tag{10}$$

and assuming that values of J with that Eq. (9) is close to 1 are interesting Eq. (9) is rewritten in the following form:

$$|\langle v_i J_i| \operatorname{Re} |v_f J_f\rangle|^2 / |\langle v_i| \operatorname{Re} |v_f\rangle|^2 \approx$$
$$\approx 1 - c_2 B_i Q(J_i)\, \tau(v_i, v_f) \approx \exp\left[-c_2 F_i \tau(v_i, v_f)\right]. \tag{11}$$

Substituting (11) in to Eq. (1)

$$S_{if} = A_{if} \nu_{if}^h H(J_i J_f)\, |\langle v_i| \operatorname{Re} |v_f\rangle|^2 \exp\left(-c_2 F_i / T_r\right), \tag{12}$$

where

$$\frac{1}{T_r} = \frac{1}{T} + \tau(v_i, v_f). \tag{13}$$

From Eq. (12) it can be seen that the application of 0-th order approximation in the determination of the rotational temperature leads to the determination of T_r the relation of which to the real temperature of the gas is given by Eq. (13).

Discussion

Eq. (9) can be demonstrated on the results of a calculation on the line intensities of a model molecule where the potential of the interatomic interaction is for example in the form of $U(r) = A/r^2 - B/r$ that makes an analyti-

cal solution possible for the vibrational problem for different J-s. The constants A and B of the upper and lower electronic states were fitted to receive the equilibrium internuclear distance and first vibrational quantum for the $A^2\Pi$ and $X^2\Sigma$ states of the OH molecule.

The function $R_e(r)$ was chosen $R_e(r) = r^{-3.5}$ that gives back the intensity distribution in the 0 — 0, 1 — 0 and 0 — 1 bands in the spectra of 0-th. In Fig. 1 the results are shown and the line intensities from the 0-th order and from Eq. (9) can be compared.

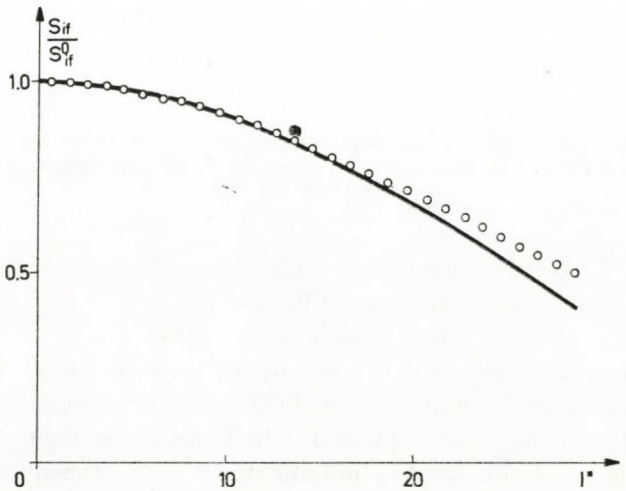

Fig. 1. The effect of RVI on the line intensity in the spectra of LaO in the R and P branch that practically coincide. The results of direct calculation are denoted by circles in the 0 — 0 band, triangles in the 0 — 1 band and continuous lines are calculated from Eq. (9)

For $J \gtrsim 20$ a significant difference comes up between the direct and the approximate calculations. This can be explained by the non-satisfactory nature of the first approximation of perturbation theory beside not fulfilling the condition in Eq. (8) that occurs for light molecules like OH already for $J \approx 20$.

Fig. 2 illustrates the effect of RVI on the line intensities in the 2 bands of the $B^2\Sigma - X^2\Sigma$ system of LaO assuming $R_e(r) = \text{const}$. In Eq. (9) instead of the line intensities of the band Franck–Condon factors were used.

It was shown by KLEIN, based on measurements of UV line intensities in a dense plasma of OH molecules, that in a wide range of temperature, T_r rotational temperature calculated in 0-th order differs from the one by the formula $1/T_r = 1/T + \text{const}\ (v_i\, v_f)$ thus Eq. (3) was contradicted experimentally.

Using the results of KLEIN [4] and LEARNER [5] for the square of the matrix elements in the case of 0 — 0, 1 — 0 and 0 — 1 bands of OH $\tau(0, 0) =$

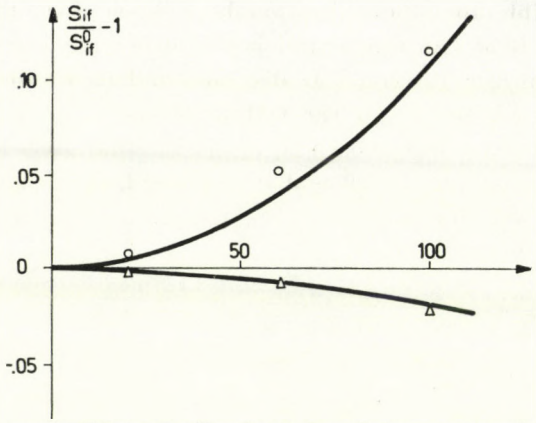

Fig. 2. The appearance of RVI in the line intensity of the spectra of the model molecule: R branch of 0 — 0 band. Circles denote the results of direct calculation, continuous line is the result of Eq. (9)

$= 2{,}25 \cdot 10^{-5}$ degree^{-1} is received, vhile from the experimental data by KLEIN the corresponding constant $\tau(0, 0) = 2.5 \cdot 10^{-5}$ degree^{-1}.

In the 0 — 0 band for $J \gtrsim 25$ and in other bands for smaller J-s as well KLEIN points out the difference of the dependence of ln S_{if} from F_i from linear attributed by him to a result of possible predissociation effects.

But as it was noted above for molecules like OH the first approximation of perturbation calculation for J values like this is not sufficient. Second approximation leads to terms in Eq. (11) that depend on the second power of $Q(J)$ that gives the deviation from the general intensity distribution, given in Eq. (12) without assuming predissociation effects.

The spectra of OH radical is a special case and it is well known that the effect of RVI on line intensity can be successfully calculated and measured for the transitions between lower vibrational states. There are cases known, when 0-th order approximation adequately describes line intensities like e.g. the 0 — 0 band of the Swan system of C_2 or the 0 — 1 violet band of CN.

In the first case p_i and p_f, the correction coefficients of the 0 — 1 and 1 — 0 bands are small because the dipole-moment matrix elements are small. In the second case $p_i + p_f$ is close to zero, therefore the appearance of RVI in the line intensity can be neglected.

Conclusions

An appropriate method of calculation was shown for the effect of RVI on the line intensities in the spectra of diatomic molecules and the value of possible error in determining rotational temperature not considering these effects was given.

Evaluating Eq. (9) some approximations were made, like assuming close to harmonic vibration and smallness of rotational quantum compared to vibrational quantum (Eq. (8)).

Because of lack of experimental data no final conclusions can be drawn about the applicability of the method used but still some experimental data are known that do not contradict the theory above.

Beside quantitative evaluation a correction was found between the effect of RVI and the relative intensities of bands that make some qualitative suggestions possible as well. Temperature measurement from 0 — 0 band in 0-th approximation gives correct results if 0 — 1 and 1 — 0 bands have sufficiently small and nearly equal intensities (like e.g. 0 — 0 Swan band).

The author acknowledges valuable criticism and comments from Professor L. V. GURVICH and Candidate V. V. VEITS.

REFERENCES

1. I. KOVÁCS, Rotational Structure in the Spectra of Diatomic Molecules, Akadémiai Kiadó, Budapest, 1969.
2. J. MARANON and C. B. SUAREZ, Spectrosc. Lett., **7**, 303, 1974.
3. H. S. HEAPS and G. HERZBERG, Z. Phys., **133**, 48, 1952.
4. L. KLEIN, Jqsrt, **13**, 581, 1973
5. R. C. T. LEARNER, Proc. Roy. Soc., A**269**, 311, 1962.

Acta Physica Academiae Scientiarum Hungaricae, Tomus 45 (4), pp. 371—374 (1978)

COMMUNICATIO BREVIS

EINSTEIN UNIVERSE WITH A SOURCE-FREE ELECTROMAGNETIC FIELD

By

L. K. PATEL

DEPARTMENT OF MATHEMATICS, GUJARAT UNIVERSITY, AHMEDABAD 380 009, INDIA

(Received 14. IX. 1978)

PATEL and BHATT [1] have obtained an electrovac universe whose metric is similar to the well-known NUT metric [2]. This electrovac universe is described under the flat background (i.e. when the electromagnetic field disappears, the geometry of this universe becomes Minkowskian). The purpose of the present note is to obtain an exact solution of the Einstein—Maxwell equations which, in the absence of the electromagnetic field, reduces to the well-known Einstein's universe.

We shall use the following field equations corresponding to the perfect fluid distribution plus source-free electromagnetic fields

$$R_{ik} - \frac{1}{2} g_{ik} R - = 8\pi[(p + \varrho) v_i v_k - p g_{ik} + E_{ik}] + \lambda g_{ik}, \; v_i v^i = 1, \tag{1}$$

$$E_{ik} = - g^{jm} F_{ij} F_{km} + \frac{1}{4} g_{ik} F_{jm} F^{jm}, \tag{2}$$

$$F_{ik} = A_{i,k} - A_{k,i}, \tag{3}$$

$$F^{ik}; \quad k = 0; \tag{4}$$

the notations being usual. Here λ is a cosmological constant.

We know that the geometry of the Einstein universe is described by the line-element

$$ds^2 = dt^2 - dx^2 - dy^2 - dz^2 - \frac{(x dx + y dy + z dz)^2}{R^2 - (x^2 + y^2 + z^2)}, \tag{5}$$

where R is a constant. We carry out the following transformation from the co-ordinates (x, y, z, t) to the coordinates (u, α, β, r).

$$\begin{aligned} x &= R \sin \frac{r}{R} \sin \alpha \cos \beta, \quad y = R \sin \frac{r}{R} \sin \alpha \sin \beta, \\ z &= R \sin \frac{r}{R} \cos \alpha, \qquad t - r = u. \end{aligned} \tag{6}$$

Under the transformation (6) the Einstein's metric (5) transforms to the form

$$ds^2 = 2dudr + du^2 - R^2 \sin^2 \frac{r}{R}(d\alpha^2 + \sin^2 \alpha d\beta^2). \tag{7}$$

We shall use (7) as the metric of the Einstein's universe.

For the brief description of our new solution of Einstein—Maxwell equations we consider the space-time given by the line element

$$\begin{aligned} ds^2 = {} & 2(du - 2b \cos \alpha d\beta)dr - M^2(d\alpha^2 + \sin^2 \alpha d\beta^2) \\ & + R^2(b^2 + R^2)^{-1}(du - 2b \cos \alpha d\beta)^2, \end{aligned} \tag{8}$$

where b is a constant, M^2 is given by

$$M^2 = (R^2 - b^2) \sin^2 \frac{r}{R} + b^2 \tag{9}$$

and the coordinates are named as $x^1 = u$, $x^2 = \alpha$, $x^3 = \beta$, $x^4 = r$. Introducing the basic differential 1-forms,

$$\theta^{(1)} = du - 2b \cos \alpha d\beta, \quad \theta^{(2)} = Md\alpha, \tag{10}$$

$$\theta^{(3)} = M \sin \alpha d\beta, \qquad \theta^{(4)} = dr + \frac{1}{2} R^2(R^2 + b^2)^{-1}\theta^{(1)}$$

the metric (8) becomes

$$ds^2 = 2\theta^{(1)}\theta^{(4)} - (\theta^{(2)})^2 - (\theta^{(3)})^2 = g_{(ab)}\theta^{(a)}\theta^{(b)}. \tag{11}$$

Using Cartan's equations of structure and the exterior calculus of differential forms one can get the tetrad components $R_{(ab)}$ of Ricci tensor R_{ik}. A metric, more general than the metric (8), has been considered by PATEL and AKABARI [3], in connection with an Einstein-NUT metric. They have given the details regarding the computation of the tetrad components of Ricci tensor. Therefore we shall not go into the details here. The non-vanishing components of $R_{(ab)}$ for the metric with tetrad (10) are given by

$$\begin{aligned} & R_{(44)} = -2/R^2, \; 4R_{(11)} = R^4(b^2 + R^2)^{-2}R_{(44)}, \\ & R_{(14)} = -M^{-4}(b^2 + R^2)^{-1}[2b^2R^2 - M^4], \\ & R_{(22)} = R_{(33)} = -M^{-2} + R^2(b^2 + R^2)^{-1}[M_{rr}/M + M_r^2/M^2 - 2b^2/M^4]. \end{aligned} \tag{12}$$

Here and in what follows M^2 is given by (9) and a suffix indicates the derivative, e.g. $M_r = \partial M/\partial_r$ etc.

It is verified that the electromagnetic 4-potential A_i given by

$$A_i = \frac{eR}{M^2} \sin \frac{r}{R} \cos \frac{r}{R}(1, 0, -2b \cos \alpha, 0) \tag{13}$$

satisfies the Maxwell equations (4) identically.

Here e is a constant. The non-zero components of the field tensor F_{ik} can be computed with the help of (3). They are given by

$$\left.\begin{aligned} F_{14} &= -F_{34}/2b\cos\alpha = e\left(b^2\cos^2\frac{r}{R} - R^2\sin^2 r/R\right)\Big/M^2, \\ F_{23} &= -2eb\cos\alpha\sin\frac{r}{R}\cos\frac{r}{R}\Big/M^2. \end{aligned}\right\} \tag{14}$$

The non-zero components of the electromagnetic energy tensor E_{ik} can be obtained from (2). They are given by

$$\begin{aligned} M^{-2}E_{22} &= -(2b\cos\alpha)^{-1}E_{34} = E_{11}(b^2+R^2)R^{-2} = E_{14} \\ &= [M^2\sin^2\alpha + 4b^2R^2\cos^2\alpha(b^2+R^2)^{-1}]^{-1}E_{33} \\ &= (b^2+R^2)\,(2b\cos\alpha R^2)^{-1}\,E_{13} = e^2/M^4. \end{aligned} \tag{15}$$

The tetrad components of E_{ik} can be obtained from the relations

$$E_{(ab)} = e^i_{(a)}e^k_{(b)}\,E_{ik}, \quad dx^i = e^i_{(a)}\theta^{(a)}. \tag{16}$$

For the metric (8) and the tetrads (10) we have

$$\begin{aligned} e^1_{(a)} &= (1,\ 0,\ 2b\cot\alpha/M,\ 0), \\ e^2_{(a)} &= (0,\ 1/M,\ 0,\ 0), \\ e^3_{(a)} &= (0,\ 0,\ \operatorname{cosec}\alpha/M,\ 0), \\ e^4_{(a)} &= \left(-\frac{R^2}{2}(b^2+R^2)^{-1}.\ 0,\ 0,\ 1\right). \end{aligned} \tag{17}$$

With the aid of the results (15) (16) and (17) we obtain the following non-zero components of $E_{(ab)}$.

$$E_{(14)} = E_{(22)} = E_{(33)} = e^2/2M^4. \tag{18}$$

The field equations (1) can be expressed in the tetrad form as

$$R_{(ab)} = -8\pi[(p+\varrho)\,v_{(a)}v_{(b)} - \frac{1}{2}(\varrho - p)\,g_{(ab)} + E_{(ab)}] + \lambda g_{(ab)},\ v_{(a)}v^{(a)} = 1. \tag{19}$$

We shall assume the following form of the tetrad components $v_{(a)}$ of the flow vector v_i of the perfect fluid

$$v_{(a)} = (1/2\,x,\ 0,\ 0,\ x), \tag{20}$$

where x is a parameter to be determined from the field equations.

From the results (12), (18), (19) and (20) we have

$$x^2 = (b^2+R^2)\,R^{-2}, \tag{21}$$

$$2\pi e^2 = R^2b^2(b^2+R^2)^{-1}, \tag{22}$$

$$8\pi p = \lambda - (R^2+b^2)^{-1}, \tag{23}$$

and

$$8\pi\varrho = -\lambda + 3(R^2 + b^2)^{-1}. \tag{24}$$

Thus the metric (8) alongwith (9) describes the Einstein's universe with a source-free electromagnetic field. The pressure p and the density ϱ of the perfect fluid filling the universe are given by (23) and (24) and the electromagnetic charge e is related to the constants b and R by Eq. (22).

When $b = 0$, we get $e = 0$ from (22) and, consequently, the electromagnetic field disappears. In this case the metric (8) alongwith (9) reduces to the Einstein's metric (7).

When R tends to infinity we have $2\pi e^2 = b^2$. In this case the line element (8) alongwith (9) takes the form

$$ds^2 = 2(du - 2b\cos\alpha d\beta)dr - (r^2 + b^2)(d\alpha^2 + \sin^2\alpha d\beta^2) + (du - 2b\cos\alpha d\beta)^2. \tag{25}$$

The metric (25) is discussed by PATEL and BHATT [1] in connection with a NUT-type electrovac universe.

REFERENCES

1. L. K. PATEL and P. V. BHATT, A NUT-type Electrovac Universe, to apper in 'Vidya', the Journal of Gujarat University.
2. E. NEWMAN, L. TAMBURINO and T. UNTI, J. Math. Phys., **4**, 915, 1963.
3. L. K. PATEL and R. S. AKABARI, Acta Phys. Hung., **44**, 181, 1979.

RECENSIONES

CLIFFORD H. EDWARDS and ROBERT L. FISHER:

Teaching Elementary School Science: A Competency-Based Approach

Praeger Publishers, New York, 1977, p. 464

Teaching science in comprehensive schools is an important goal of the new curricula prepared in the last two decades. Many projects were constructed throughout the world and the main feature of them was to provide much more facilities for personal observations of nature and phenomena of the everyday life and performing pupil experiments than before. This competency-based approach to teacher education helps the prospective science teachers in developing instructional skills through many excercises given in the book.

In Ch. 1 the basis for professional development is outlined after specifying teacher competencies. The connection between scientific literacy and elementary school science has been unfolded in Ch. 2 formulating the goals of instruction in science. In Ch. 3 viable instructional objectives in science are given with many examples in well-ordered structure. An appropriate preassessment (Ch. 4) of children (also of different ethnic groups) permit the instructional designer to prepare more efficient and effective objectives. The main steps of children learning and development (Ch. 5) is sketched supported by psychology and classification of Piaget. In Chs. 6—11 the organization of subject matter (also spiral curriculum), science teaching methods and their use (demonstrations, experimentation, field trips among others), strategies in science education (feedback, individualizing instruction, affective and psychomotor goals), planning learning experiences in science (levels of planning, developing lesson plans, samples), evaluation (criterion-referenced forms of), and teaching stimulation (interaction models for teaching concepts and principles, inquiry and effective lesson) are discussed extensively and supported by many examples. The contemporary programs of science are shown in Ch. 12 with interesting remarks.

At the end of each chapter many references to textbooks and articles are given. The actual classroom situation and the exploring pupil in natural environment is shown in many nice photographs supporting the text. The book could help the methodology of general school teacher education.

F. J. KEDVES

B. KUCHOWICZ:

Nuclear and Relativistic Astrophysics and Nuclidic Cosmochemistry: 1963—1967

Vol. I. Gordon and Breach Science Publishers, Ltd. London, 1976, pp. 366.

In the last two decades there has been a great increase in our knowledge of astrophysics and cosmology. We have witnessed some very fundamental discoveries, among which are the quasars, the X-ray sources, the microwave background and most recently the pulsars. Especially this fact makes it necessary to have a bibliographical survey which systematically covers the achievements of the past and serves as a guide to the literature.

Nowadays the compilation of a compendium must be a far more tedious undertaking than it was a few decades ago, because of the acceleration of scientific progress and the nearly exponential growth of the number of publications to be surveyed. Little wonder that there is a delay in publishing this kind of books. In the case of the present volume, for example,

which reviews the literature for the years 1963—67, the delay has been almost ten years. Such a delay, while regrettable, does not mean that the effort devoted to publishing this book is not worth while, in fact it contains a vast material of permanent value especially for reference purposes.

Dr. KUCHOWICZ published his first bibliographical survey on nuclear astrophysics in 1967. Slightly over two thousand references from all areas of research related to nuclear astrophysics or some borderline research up to the beginnings of 1964 were given there. Therefore the present publication may be regarded as a continuation of the preceding one mentioned. The present book covering the years 1963—67, however, had to be published in three volumes because of the immense increase in literature. The first volume contains the survey part with 5690 references. The two subsequent volumes give the bibliography.

The survey is divided into three main parts. Part I covers the field called nuclidic cosmochemistry. The problems of abundances of chemical elements and their isotopes in various celestial bodies, in cosmic radiation and in space are briefly surveyed. In this part references to X- and γ-ray astronomy are also given.

Part II deals with the most essential problems of nuclear astrophysics: 1) nuclear energy generation and synthesis of chemical elements in stars 2) stellar structure, stellar models and pulsation 3) cosmogony of stars and planetary systems 4) neutrino astrophysics and 5) laboratory research motivated by, and related to astrophysics. Special attention is paid to novae and supernovae.

In Part III mainly the compendium of theoretical researches on relativistic astrophysics and cosmology is presented. This part deals with the galaxies, radio sources and quasars, the gravitational collapse, superdense matter and other applications of general relativity to astrophysics, the problem of antimatter as well as cosmology. Of course, the experimental results on galaxies, radio sources and quasars which have a direct importance for the objective of this book have also been referenced.

This book is well structured. The author certainly has a very broad understanding of astrophysics. He writes extremely clearly and concisely. I am sure that he achieved his principal aim in preparing the present publication.

The book has been written in a very condensed, systematic way and is almost perfectly complete.

There are really very few books which can serve as a systematic bibliographical survey for research workers. Therefore I recommend this book to all professionals working in the vastly developing areas of nuclear and relativistic astrophysics.

B. SZEIDL

Printed in Hungary

A kiadásért felel az Akadémiai Kiadó igazgatója Műszaki szerkesztő: Botyánszky Pál

A kézirat a kiadóba érkezett: 1978. XII. 7. — A kézirat nyomdába érkezett: 1978. XII. 14. — Terjedelem: 8,25 (A/5) ív, 3 ábra

79.6591 Akadémiai Nyomda, Budapest — Felelős vezető: Bernát György

NOTES TO CONTRIBUTORS

I. PAPERS will be considered for publication in Acta Physica Hungarica, only if they have not previously been published or submitted for publication elsewhere. They may be written in English, French, German or Russian.

Papers should be submitted to

Prof. I. Kovács, Editor
Department of Atomic Physics, Technical University
1521 Budapest, Budafoki út 8, Hungary

Papers may be either articles with abstracts or short communications. Both should be as concise as possible, articles in general not exceeding 25 typed pages, short communications 8 typed pages.

II. MANUSCRIPTS

1. Papers should be submitted in five copies.

2. The text of papers must be of high stylistic standard, requiring minor corrections only.

3. Manuscripts should be typed in double spacing on good quality paper, with generous margins.

4. The name of the author(s) and of the institutes where the work was carried out should appear on the first page of the manuscript.

5. Particular care should be taken with mathematical expressions. The following should be clearly distinguished, e.g. by underlining in different colours: special founts (italics, script, bold type, Greek, Gothic, etc.); capital and small letters; subscripts and superscripts, e.g. x_2, x^3; small *l* and 1; zero and capital O; in expressions written by hand: *e* and *l*, *n* and *u*, *v* and *v*, etc.

6. References should be numbered serially and listed at the end of the paper in the following form: J. Ise and W. D. Fretter, Phys. Rev., *76*, 933, 1949.

For books, please give the initials and family name of the author(s), title, name of publisher, place and year of publication, e.g.: J. C. Slater, Quantum Theory of Atomic Structures, I. McGraw-Hill Book Company, Inc., New York, 1960.

References should be given in the text in the following forms: Heisenberg [5] or [5].

7. Captions to illustrations should be listed on a separate sheet, not inserted in the text.

III. ILLUSTRATIONS AND TABLES

1. Each paper should be accompanied by five sets of illustrations, one of which must be ready for the blockmaker. The other sets attached to the copies of the manuscript may be rough drawings in pencil or photocopies.

2. Illustrations must not be inserted in the text.

3. All illustrations should be identified in blue pencil by the author's name, abbreviated title of the paper and figure number.

4. Tables should be typed on separate pages and have captions describing their content. Clear wording of column heads is advisable. Tables should be numbered in Roman numerals (I, II, III, etc.).

IV. MANUSCRIPTS not in conformity with the above Notes will immediately be returned to authors for revision. The date of receipt to be shown on the paper will in such cases be that of the receipt of the revised manuscript.

Reviews of the Hungarian Academy of Sciences are obtainable at the following addresses:

AUSTRALIA
C.B.D. LIBRARY AND SUBSCRIPTION SERVICE, Box 4886, G.P.O., *Sydney N.S.W.2001*
COSMOS BOOKSHOP, 145 Ackland Street, *St. Kilda (Melbourne), Victoria 3182*

AUSTRIA
GLOBUS, Höchstädtplatz 3, *1200 Wien XX*

BELGIUM
OFFICE INTERNATIONAL DE LIBRAIRIE, 30 Avenue Marnix, *1050 Bruxelles*
LIBRAIRIE DU MONDE ENTIER, 162 Rue du Midi, *1000 Bruxelles*

BULGARIA
HEMUS, Bulvar Ruszki 6, *Sofia*

CANADA
PANNONIA BOOKS, P.O. Box 1017, Postal Station "B", *Toronto, Ontario M5T 2T8*

CHINA
CNPICOR, Periodical Department, P.O. Box 50, *Peking*

CZECHOSLOVAKIA
MAD'ARSKÁ KULTURA, Národní třida 22, *115 66 Praha*
PNS DOVOZ TISKU, Vinohradská 46, *Praha 2*
PNS DOVOZ TLAČE, *Bratislava 2*

DENMARK
EJNAR MUNKSGAARD, Norregade 6, *1165 Copenhagen*

FINLAND
AKATEEMINEN KIRJAKAUPPA, P.O. Box 128, *SF-00101 Helsinki 10*

FRANCE
EUROPERIODIQUES S. A., 31 Avenue de Versailles, *78170 La Celle St.-Cloud*
LIBRAIRIE LAVOISIER, 11 rue Lavoisier, *75008 Paris*
OFFICE INTERNATIONAL DE DOCUMENTATION ET LIBRAIRIE, 48 rue Gay-Lussac, *75240 Paris Cedex 05*

GERMAN DEMOCRATIC REPUBLIC
HAUS DER UNGARISCHEN KULTUR, Karl-Liebknecht-Strasse 9, *DDR-102 Berlin*
DEUTSCHE POST ZEITUNGSVERTRIEBSAMT, Strasse der Pariser Kommüne 3—4, *DDR-104 Berlin*

GERMAN FEDERAL REPUBLIC
KUNST UND WISSEN ERICH BIEBER, Postfach 46, *7000 Stuttgart 1*

GREAT BRITAIN
BLACKWELL'S PERIODICALS DIVISION, Hythe Bridge Street, *Oxford OX1 2ET*
BUMPUS, HALDANE AND MAXWELL LTD., Cowper Works, *Olney, Bucks MK46 4BN*
COLLET'S HOLDINGS LTD., Denington Estate, *Wellingborough, Northants NN8 2QT*
W.M. DAWSON AND SONS LTD., Cannon House, *Folkestone, Kent CT19 5EE*
H. K. LEWIS AND CO., 136 Gower Street, *London WC1E 6BS*

GREECE
KOSTARAKIS BROTHERS, International Booksellers, 2 Hippokratous Street, *Athens-143*

HOLLAND
MEULENHOFF-BRUNA B.V., Beulingstraat 2, *Amsterdam*
MARTINUS NIJHOFF B.V., Lange Voorhout 9—11, *Den Haag*
SWETS SUBSCRIPTION SERVICE, 347b Heereweg, *Lisse*

INDIA
ALLIED PUBLISHING PRIVATE LTD., 13/14 Asaf Ali Road, *New Delhi 110001*
150 B-6 Mount Road, *Madras 600002*
INTERNATIONAL BOOK HOUSE PVT. LTD., Madame Cama Road, *Bombay 400039*
THE STATE TRADING CORPORATION OF INDIA LTD., Books Import Division, Chandralok, 36 Janpath, *New Delhi 110001*

ITALY
EUGENIO CARLUCCI, P.O. Box 252, *70100 Bari*
INTERSCIENTIA, Via Mazzé 28, *10149 Torino*
LIBRERIA COMMISSIONARIA SANSONI, Via Lamarmora 45, *50121 Firenze*
SANTO VANASIA, Via M. Macchi 58, *20124 Milano*
D. E. A., Via Lima 28, *00198 Roma*

JAPAN
KINOKUNIYA BOOK-STORE CO. LTD., 17-7 Shinjuku-ku 3 chome, Shinjuku-ku, *Tokyo 160-91*
MARUZEN COMPANY LTD., Book Department, P.O. Box 5050 Tokyo International, *Tokyo 100-31*
NAUKA LTD. IMPORT DEPARTMENT, 2-30-19 Minami Ikebukuro, Toshima-ku, *Tokyo 171*

KOREA
CHULPANMUL, *Phenjan*

NORWAY
TANUM-CAMMERMEYER, Karl Johansgatan 41—43, *1000 Oslo*

POLAND
WĘGIERSKI INSTYTUT KULTURY, Marszalkowska 80, *Warszawa*
CKP I W ul. Towarowa 28 *00-958 Warsaw*

ROMANIA
D. E. P., *Bucureşti*
ROMLIBRI, Str. Biserica Amzei 7, *Bucureşti*

SOVIET UNION
SOJUZPETCHATI — IMPORT, *Moscow* and the post offices in each town
MEZHDUNARODNAYA KNIGA, *Moscow G-200*

SPAIN
DIAZ DE SANTOS, Lagasca 95, *Madrid 6*

SWEDEN
ALMQVIST AND WIKSELL, Gamla Brogatan 26, *101 20 Stockholm*
GUMPERTS UNIVERSITETSBOKHANDEL AB, Box 346, *401 25 Göteborg 1*

SWITZERLAND
KARGER LIBRI AG, Petersgraben 31, *4011 Basel*

USA
EBSCO SUBSCRIPTION SERVICES, P.O. Box 1943, *Birmingham*, Alabama 35201
F. W. FAXON COMPANY, INC., 15 Southwest Park, *Westwood*, Mass. 02090
THE MOORE-COTTRELL SUBSCRIPTION AGENCIES, *North Cohocton, N. Y. 14868*
READ-MORE PUBLICATIONS, INC., 140 Cedar Street, *New York, N. Y. 10006*
STECHERT-MACMILLAN, INC., 7250 Westfield Avenue, *Pennsauken* N. J. 08110

VIETNAM
XUNHASABA, 32, Hai Ba Trung, *Hanoi*

YUGOSLAVIA
JUGOSLAVENSKA KNJIGA, Terazije 27, *Beograd*
FORUM, Vojvode Mišiča 1, *21000 Novi Sad*

Index: 26.025
Acta Phys. Hung. Tom. 45. No. 4. Budapest, 10. VI. 1979 HU-ISSN 0001-6705